

DOE/SF 11570-2

Bill Delamater

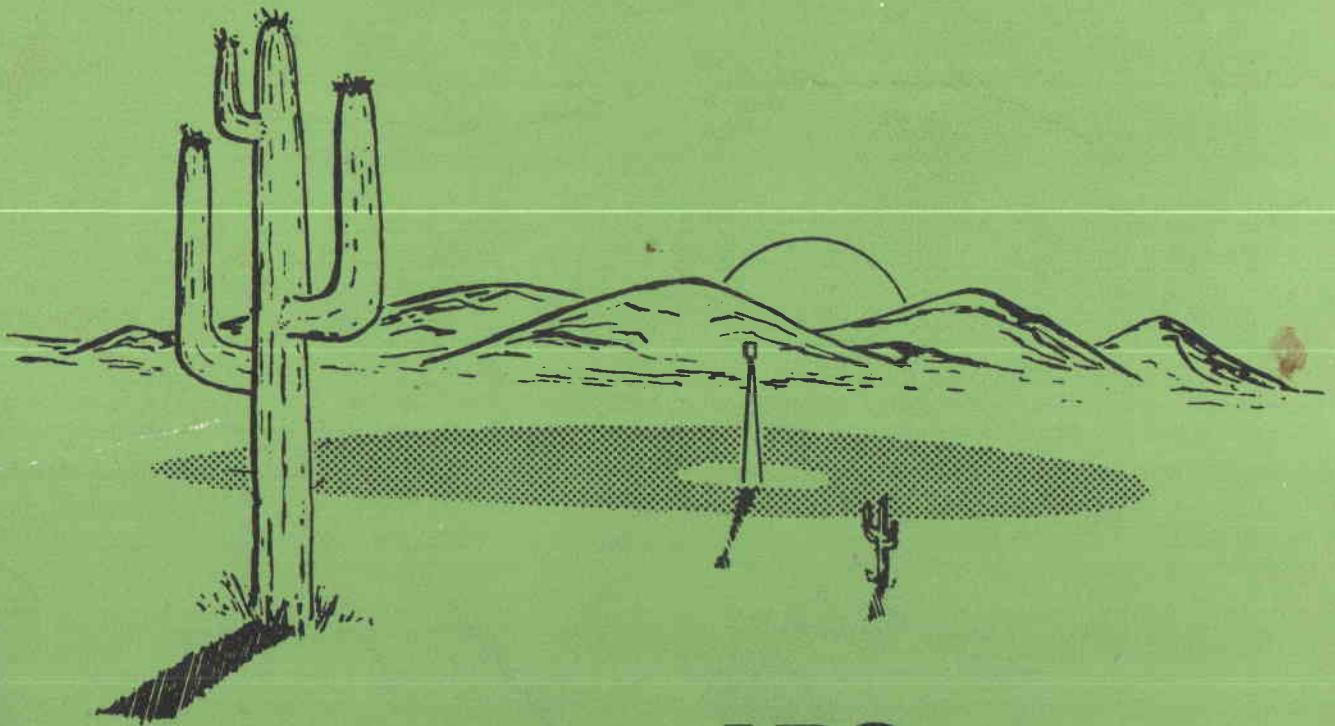
Final
Technical
Report

April 1982

Volume I

Advanced
Conceptual
Design

Advanced Conceptual Design for Solar Repowering of the Saguaro Power Plant



APS.

MARTIN MARIETTA

Babcock & Wilcox

a McDermott company

Gibbs & Hill Inc.

Contract DE-AC03-81SF11570
Report No. DOE/SF 11570-2

Volume I

Final
Technical
Report

April 1982

Advanced Conceptual
Design

**ADVANCED CONCEPTUAL
DESIGN FOR SOLAR REPOWERING
OF THE SAGUARO POWER PLANT**

Sponsored By:

San Francisco Operations Office
Department of Energy

Period Covered:

October 1981—April 1982

Author:

Eric R. Weber

This report was prepared as an account of work sponsored by the United States Government. Neither the United States nor the United States Department of Energy, nor any of their employees, nor any of their contractors, subcontractors, or their employees, makes any warranty, express or implied or assumes any legal liability or responsibility for the accuracy, completeness or usefulness of any information, apparatus, product or process disclosed, or represents that its use would not infringe on privately-owned rights.

ARIZONA PUBLIC SERVICE COMPANY
Phoenix, Arizona 85036

FOREWORD

This report is submitted by the Arizona Public Service Company to the Department of Energy in accordance with provisions of contract DE-AC03-81SF-11570. This final technical report summarizes the work related to the conceptual design, cost and performance of the Advanced Conceptual Design for Solar Repowering of the Saguaro Power Plant that was performed during the period from September 30, 1981 through April 30, 1982. The final technical report is published in three volumes

Executive Summary

Volume I - Advanced Conceptual Design

Volume II - Appendices

This contract was under the direction of Mr. Keith A. Rose of the Department of Energy, San Francisco Operations Office, Oakland, CA. Mr. Harold F. Norris of Sandia National Laboratories, Livermore, CA was the Technical Manager.

The efforts performed by the Arizona Public Service team were as follows:

- 1) Arizona Public Service Company - Site Owner; Overall Program Management; Program Plan; Fossil Subsystems, EPGS, and Interfaces.
- 2) Martin Marietta Corporation - Lead on Selection of System Configuration; Solar System Conceptual Design, Analysis, Performance Estimates, and Optimization of the Collector Subsystem, Receiver, and Thermal Storage; Cost Collection and System Economic Analysis; Reproduction of Major Study Documentation.
- 3) Babcock and Wilcox Company - Lead on Solar Steam Generator; and Review of Receiver Design.
- 4) Gibbs and Hill, Inc. - Conceptual Design, Analysis, Optimization, and Cost Data for the Solar/Fossil Interfaces, Site and Site Facilities, and Tower; Recommendation for Upgrading Existing Fossil Steam Generator and EPGS Control Systems.

This document was edited and reproduced by the Martin Marietta Corporation

ACKNOWLEDGMENTS

This report has been prepared by Arizona Public Service Company for the Department of Energy with the written contributions of the following personnel:

Arizona Public Service Company

Eric R. Weber, Program Manager
Dale L. Thornburg, Senior Consulting Engineer
Lester L. Daviet, II, System Planning

Martin Marietta Denver Aerospace

Wilfred L. DeRocher, Jr., Program Manager
John E. Montague, Economics Analyst
Thomas H. Oliver, Engineer, Receiver
Richard H. Sterrett, Engineer, Energy Storage
Phillip R. Lukens, Design Engineer, Receiver
Thomas G. Hills, Cost Analyst

Babcock and Wilcox Company

Daniel B. Young, Program Manager

Gibbs and Hill, Inc.

Lloyd Winsor, Program Manager
Dorel J. Damsker, Ph.D., Control System Analyst

CONTENTS

		<u>Page</u>
1.0	EXECUTIVE SUMMARY	1-1
1.1	Background.	1-2
1.2	Site Description	1-6
1.2.1	Plant Features.	1-6
1.2.2	Climate and Geography	1-8
1.3	Project Summary	1-9
1.4	Conceptual Design Description	1-13
1.4.1	Collector Subsystem	1-15
1.4.2	Receiver Subsystem.	1-15
1.4.3	Thermal Energy Storage Subsystem.	1-17
1.4.4	Solar Steam Generator	1-18
1.4.5	Plant Interfaces.	1-19
1.4.6	Master Control Subsystem	1-19
1.4.7	Operating Modes	1-20
1.5	System Performance.	1-21
1.6	Economic Findings	1-24
1.7	Development Plan.	1-30
1.8	Site Owner's Assessment	1-33
2.0	INTRODUCTION.	2-1
2.1	Study Objectives and Approach	2-1
2.2	Technical Selection and Generation Unit Selection	2-3
2.2.1	Solar Technology Selection.	2-3
2.2.2	Generation Unit Selected for Repowering	2-5
2.2.3	Primary Solar Subsystem Characteristic Selection.	2-6
2.3	Site Location	2-9
2.4	Site Geography.	2-9
2.5	Climate	2-12
2.6	Existing Plant Description.	2-14
2.7	Existing Plant Performance Summary	2-14
3.0	SELECTION OF PREFERRED SYSTEM	3-1
3.1	Trade Studies	3-4
3.1.1	Turbine Steam Inlet Temperature	3-4
3.1.2	Optimization of Receiver Outlet Temperature	3-5
3.1.3	Fossil-to-Solar Ratio	3-6
3.1.4	Type and Number of Energy Storage Tanks	3-6
3.1.5	Location of Salt/Steam Heat Exchangers and Storage Tanks.	3-7
3.1.6	Cavity vs External Receiver	3-10
3.1.7	Use of Solar Energy During Annual Boiler Shutdown	3-10
3.1.8	Allowable Receiver Absorber Surface Temperature Cycles.	3-11
3.1.9	Collector Field Shape	3-13
3.2	System Size Selection	3-14
3.3	Technology Selection.	3-18
3.4	Value of Energy Storage	3-20

	<u>Page</u>
4.0	CONCEPTUAL DESIGN 4-1
4.1	System Description. 4-3
4.2	System Functional Requirements. 4-10
4.3	System Design and Operating Characteristics 4-15
4.3.1	Operating Modes 4-21
4.3.2	Instrumentation and Controls. 4-25
4.4	Site Requirements 4-27
4.5	System Performance. 4-32
4.5.1	Design Day Performance. 4-32
4.5.2	Annual Performance Using STEAEC 4-32
4.5.3	Annual Performance Using SOLTES 4-37
4.6	Project Capital Cost Summary. 4-39
4.6.1	Cost Estimates - Approach and Groundrules 4-39
4.6.2	Engineering Design Costs. 4-40
4.6.3	Construction Costs. 4-43
4.6.4	Owner's Cost Estimate 4-45
4.6.5	Summation of Capital Costs. 4-46
4.6.6	Project Cost at Year of Commercial Operation. 4-46
4.7	Operating and Maintenance Costs and Considerations. 4-48
5.0	SUBSYSTEM CHARACTERISTICS 5-1
5.1	Collector Subsystem 5-2
5.1.1	Collector Subsystem Requirements 5-2
5.1.2	Collector Subsystem Design Description. 5-3
5.1.3	Collector Field Subsystem Performance 5-13
5.1.4	Collector Subsystem Cost. 5-14
5.2	Receiver Subsystem 5-15
5.2.1	Receiver Subsystem Requirements 5-15
5.2.2	Structural Design 5-17
5.2.3	Receiver Thermal Analyses 5-43
5.2.4	Receiver Supply and Return Piping 5-65
5.2.5	Receiver Tower Design 5-72
5.2.6	Receiver Cost Summary 5-74
5.3	Master Control Subsystem 5-75
5.3.1	Master Control Subsystem Requirements 5-77
5.3.2	Design Description. 5-80
5.3.3	Performance and Cost 5-107
5.4	Fossil Energy Subsystem 5-109
5.5	Energy Storage Subsystem. 5-110
5.5.1	Energy Storage Subsystem Requirements 5-110
5.5.2	Thermal Energy Storage Subsystem Design Description 5-111
5.5.3	Thermal Energy Storage Subsystem Performance and Cost Estimate. 5-119
5.6	Electric Power Generating Subsystem 5-120
5.6.1	EPGS Requirements 5-120
5.6.2	EPGS Design Description 5-120
5.6.3	EPGS Performance. 5-121
5.6.4	EPGS to Solar Interfaces 5-122
5.6.5	EPGS Cyclic Performance 5-122
5.6.6	EPGS Control System Upgrading Recommendation. 5-126
5.6.7	EPGS Modification Costs 5-140

		<u>Page</u>
5.7	Solar Steam Generator Subsystem	5-141
5.7.1	Subsystem Requirements.	5-141
5.7.2	Subsystem Design Description.	5-143
5.7.3	Subsystem Performance	5-150
5.7.4	Subsystem Cost Estimate	5-153
6.0	ECONOMIC ANALYSIS	6-1
6.1	Economic Analysis Assumptions	6-1
6.2	Saguaro Solar Repowering Project Cost	6-3
6.3	Fuel Displacement Analysis.	6-5
6.3.1	Fuel Displacement Analysis Methodology.	6-5
6.3.2	Plant and System Simulation Models.	6-7
6.3.3	Fuel Displacement Analysis Results.	6-9
6.3.4	Fuel Displacement Economics Summary	6-13
6.4	Demonstration Value Analysis.	6-13
6.5	Economic Analysis Summary	6-21
7.0	REFERENCES.	7-1

FIGURE

	<u>Page</u>
1.0-1	Saguaro Repowering Station (Artists Concept) 1-1
1.1-1	Repowered System Diagram 1-3
1.2-1	Saguaro Power Plant 1-6
1.2-2	Saguaro Heat Balance at 100% Power 1-7
1.3-1	Repowering System Schematic 1-9
1.3-2	Collector Field Location. 1-11
1.4-1	Solar Equipment Location. 1-13
1.4-2	Martin Marietta Second Generation Heliostat 1-16
1.4-3	Receiver General Configuration. 1-16
1.4-4	Hot Salt Storage Tank Configuration 1-17
1.4-5	Evaporator Configuration Arrangement. 1-18
1.4-6	Clear Day Scenario. 1-20
1.5-1	Design Point Efficiency For 60 MWe Solar Plant (SM = 1.05). 1-21
1.5-2	Annual Efficiency For 60 MWe Solar Plant. 1-23
1.6-1	Saguaro Solar Repowering Project Implementation Cost (1982 \$ x 1000). 1-24
1.6-2	Total Escalated Project Implementation Cost 1-25
1.6-3	Cumulative Present Worth of Fuel Displaced March 6, 1981 Forecast (1987 \$) 1-27
1.7-1	Development Plan Schedule 1-32
1.7-2	Project Organization Chart. 1-32
2.2-1	Repowering System Schematic 2-8
2.3-1	APS Repowering - Saguaro Station Location 2-10
2.4-1	Collector Field Location. 2-11
2.5-1	Saguaro Average Temperature 2-13
2.5-2	Saguaro Average Monthly Precipitation 2-13
2.6-1	Saguaro Power Plant 2-15
2.6-2	Saguaro Station Plot Plan 2-16
3.1-1	Storage Tank/Heat Exchanger Location Options. 3-8
4.1-1	Repowered System Diagram. 4-4
4.1-2	Collector Field Location. 4-7
4.1-3	Solar Equipment Location. 4-8
4.2-1	Peak Solar Profile at Summer Solstice 4-13
4.3-1	Saguaro Heat Balance at 100% Power. 4-19
4.3-2	Clear Day Scenario Solar Alone. 4-22
4.3-3	Operating Mode Transition Matrix. 4-24
4.4-1	Alternative Auxiliary Power Sources 4-29
4.4-2	Solar System Auxiliary Power Distribution 4-30
4.5-1	Design Point Efficiency For 60 MWe Solar Plant (SM = 1.05). 4-33
4.5-2	Annual Efficiency of 60 MWe Solar Plant 4-35
4.5-3	SOLTES Model. 4-38
4.6-1	Geographic Identification of Cost Accounts. 4-41
4.6-2	Solar Subsystem Equipment and Piping Cost Accounts. 4-42
4.6-3	Saguaro Solar Repowering Construction Cost Estimate (1982 \$). 4-45
4.6-4	Construction Spend Plan 4-47

	<u>Page</u>	
5.1-1	Second Generation Heliostat-Front View.	5-5
5.1-2	Heliostat Assembly.	5-6
5.1-3	Heliostat Dimensions.	5-9
5.1-4	Tower Height Optimization and Performance Analysis Approach . .	5-10
5.1-5	Heliostat Locations	5-11
5.1-6	Heliostat Distribution.	5-12
5.2-1	Receiver General Configuration.	5-18
5.2-2	Receiver Panel Interconnection Piping	5-19
5.2-3	Receiver Support and Side Wall Structure.	5-21
5.2-4	Receiver North Cavity Door.	5-22
5.2-5	Door Closure Trajectory	5-23
5.2-6	Absorber Panel Arrangement.	5-25
5.2-7	Receiver Absorber Panel Supports.	5-26
5.2-8	Interfaces Between Absorber Tubes and Lateral Support Pipes . .	5-27
5.2-9	Receiver Surge Tank Location.	5-29
5.2-10	Outboard Lateral Support Attachment	5-31
5.2-11	North Aperture Size Optimization.	5-44
5.2-12	Receiver North Aperture	5-46
5.2-13	Receiver South Aperture	5-46
5.2-14	Receiver East Aperture.	5-47
5.2-15	Effect of Heliostat Aiming on Peak Flux	5-48
5.2-16	Absorbed Flux-North Cavity-Design Point	5-50
5.2-17	Absorbed Flux-East Cavity-Design Point.	5-51
5.2-18	Absorbed Flux-South Cavity-Design Point	5-52
5.2-19	Repowering Salt Flow Schematic.	5-54
5.2-20	Typical Tube Segment in MITAS Model	5-57
5.2-21	Absorber Tube MITAS Model Node Diagram.	5-58
5.2-22	Bulk Salt Temperature Rise Across Receiver Panels	5-60
5.2-23	Receiver Maximum Tube Temperatures.	5-61
5.2-24	Absorber Tube Heat Transfer Coefficient and Salt Velocity Profiles.	5-62
5.2-25	Temperature Profile For Lateral Support Pipe, °C (°F)	5-64
5.2-26	Receiver Design Point Losses.	5-66
5.2-27	Receiver Supply and Return Piping	5-68
5.2-28	Tower Area Piping	5-70
5.2-29	Salt Piping General Plot Plan	5-71
5.2-30	Receiver Tower.	5-73
5.3-1	Master Control Subsystem Elements	5-76
5.3-2	Master Control Subsystem Hierachy	5-83
5.3-3	Control Room Layout	5-85
5.3-4	Example of Steam Generation Proportioning	5-90
5.3-5	Control Diagram for Receiver Salt Supply and Return	5-93
5.3-6	Repowering Salt Flow Schematic.	5-96
5.3-7	Energy Storage Control Subsystem Diagram.	5-99
5.3-8	Saguaro Combustion Control.	5-101
5.3-9	Solar Steam Generator Control Subsystem	5-104
5.5-1	Energy Storage Area Flow Diagram.	5-113
5.5-2	Salt Melting System	5-114
5.5-3	Initial Processing of Salt.	5-115
5.5-4	Energy Storage Plot Plan.	5-118
5.6-1	Integration Control Schematic	5-132

	<u>Page</u>
5.6-2	Distributed Control Arrangement 5-138
5.7-1	Solar Steam Generator Schematic 5-142
5.7-2	Solar Steam Generator Piping Plan View. 5-144
5.7-3	Solar Steam Generator Piping Elevation View 5-145
5.7-4	Preheater Sectional Arrangement 5-146
5.7-5	Evaporator Sectional Arrangement. 5-147
5.7-6	Superheater Sectional Arrangement 5-148
5.7-7	Steam Drum Sectional Arrangement. 5-149
5.7-8	Fluid Temperature Distribution - 100% Power 5-152
5.7-9	Fluid Temperature Distribution - 50% Power. 5-153
6.2-1	Total Escalated Project Implementation Cost 6-4
6.3-1	Fuel Displacement Analysis Method 6-6
6.3-2	Peak Demand Day Load Demand and Resource Dispatch 6-8
6.3-3	APS Load Resource Forecast, 1990, March 6, 1981 Forecast. 6-10
6.3-4	Yearly Fuel Displacement, March 6, 1981 Loads and Resources Forecast. 6-11
6.3-5	Cumulative Present Worth of Fuel Displaced, March 6, 1981 Forecast. 6-12
6.4-1	Expected BBEC, Market Scenario A. 6-18
6.4-2	Expected BBEC, Market Scenario E. 6-19
6.4-3	Expected BBEC, With and Without Repowering Demonstration. (1991 Plant Start-Up) 6-20

TABLE

	<u>Page</u>
1.1-1	Team Members and Responsibilities 1-4
1.1-2	Utility Advisory Council Members. 1-5
1.4-1	Conceptual Design Summary 1-14
1.6-1	Saguaro Repowering Economics For 10 Years of Operation (1987 \$). 1-28
1.6-2	Saguaro Solar Repowering Project Economics Summary (1987 \$) . . 1-29
2.2-1	Advantages of Molten Salt Central Receiver Systems. 2-5
3-1	Tradeoff Study Summary. 3-3
3.1-1	Reference 1-2 Trade Study Basis 3-4
3.1-2	Reference 1-2 Storage Configuration Study Assumptions 3-6
3.1-3	Solar Plant Description for Heat Exchanger/Storage Location Trades. 3-8
3.1-4	Typical Insolation Scenario Summary 3-12
3.2-1	Benefit to Cost Ratio 3-17
3.2-2	Incremental Benefit to Cost Evaluation. 3-17
3.3-1	Advantages of Molten Salt 3-18
3.4.1	Typical Weeks for Dispatch Analysis 3-20
3.4-2	Solar Dispatch Strategies 3-21
3.4-3	EBCOST Results - Summer Week 7/14/85-7/20/85(1985\$) 3-22
3.4-4	Value of Storage Analysis - Summary (1982\$) 3-22
4.2-1	Functional Environmental Requirements 4-11
4.3-1	System Design Description at Design Point 4-16
4.3-2	Properties of Molten Salt 4-20
4.5.1	STEAEC-Derived Annual Energy Production (Solar Operation Only) 4-36
4.6-1	Construction Cost Accounts. 4-39
4.6-2	Engineering Design Cost Breakdown (1982 \$). 4-40
4.6-3	Saguaro Repowering Construction Cost Breakdown (1982 \$) 4-43
4.6-4	Saguaro Power Plant Solar Repowering Project Construction Cost Estimates, 1982 \$ 4-44
4.6-5	Owner's Cost Estimate 4-45
4.6-6	Total Capital Investment. 4-46
4.7-1	Solar Repowering Annual Operating and Maintenance Cost Estimate (1982 \$) 4-48
5.1-1	Performance Summary of Second Generation Heliostat. 5-4
5.1-2	Collector Subsystem Field Efficiency Matrix 5-13
5.1-3	Collector Subsystem Design Point Performance. 5-14
5.2-1	Receiver Air Supply System Characteristics. 5-30
5.2-2	Receiver Pressure Drop Summary. 5-32
5.2-3	Material Properties of Martin Marietta ESA-3560 Ablator 5-35
5.2-4	Receiver Weight Summary 5-41
5.2-5	Heliostat Aiming Strategy 5-49
5.2-6	Tube Lengths Used for Receiver Pressure Drop Calculations 5-56
5.2-7	Receiver Subsystem Engineering and Construction Costs (1982 \$ x 10 ⁻³) 5-74
5.3-1	Master Control Subsystem Characteristics. 5-81
5.3-2	Operational Control Subsystem Characteristics 5-87
5.3-3	Collector Control Subsystem Characteristics 5-91

	<u>Page</u>
5.5-1	Thermal Storage Tank Materials. 5-112
5.6-1	Gross EPGS Heat Rate (Fossil Steam), MW_t/MW_e (Btu/kWh). . . 5-121
5.6-2	Auxiliary Electrical Loads (Fossil Steam), MW_e 5-121
5.6-3	Gross EPGS Heat Rate (Solar Steam) at 6.77 kPa (2.0 in. Hga) Backpressure 5-122
5.6-4	EPGS Elements That Require Changes. 5-123
5.6-5	EPGS Elements That Do Not Require Changes 5-124
5.7-1	Heat Exchanger Characteristics. 5-151
6.1-1	Economic Parameters 6-1
6.1-2	APS Fuel Cost and Escalation Data (1982 \$). 6-3
6.3-1	Simplified Fuel Displacement Results, Present Worth Savings . . (1987 \$). 6-9
6.3-2	Repowering Economics, 10 Year Operation (1987 \$). 6-13
6.4-1	1991 STCR Market Scenarios. 6-14
6.4-2	Standalone 100MWe-3hr Plant Costs (1982 \$). 6-16
6.4-3	Probability Assessments For 100 MWe-3hr Standalone STCR Plants. 6-16
6.5-1	Saguaro Solar Repowering Project Economics Summary (1987 \$) . . 6-21

The Arizona Public Service Company (APS), in association with Martin Marietta Corporation, Babcock and Wilcox, Inc., and Gibbs and Hill, Inc., has completed an advanced conceptual design of a solar thermal central receiver repowered gas/oil fired steam-Rankine electrical power generation plant. This work was performed under sponsorship of the U.S. Department of Energy as specified in Contract DE-AC03-81SF-11570, Advanced Conceptual Design for Solar Repowering of the Saguaro Power Plant. The conceptual design is based on a central receiver technology which uses molten salt (60% NaNO_3 , 40% KNO_3 , by wt) for the heat transport and thermal storage fluid. Unit One of APS's Saguaro power plant is to be repowered. The plant is located 43 km (27 mi) north of Tucson, Arizona. The selection of both the site and the molten salt central receiver promotes a near-term feasibility demonstration and cost-effective power production from an advanced solar thermal technology. The recommended system concept is to repower the existing electric power generating system at the minimum useful level (60 MW_e net) using a field of 5000 Martin Marietta second-generation (57.4 m^2) heliostats and a storage capacity of 4.0 hours to be used for optimum dispatch of power to the utility system. An artist's concept of the repowered plant is shown in Figure 1.0-1. The total project construction cost is estimated to be 127 million in 1982 dollars. The plant will be capable of displacing fossil energy equivalent to 2.7 million barrels of No. 6 oil in its first 10 years of operation.

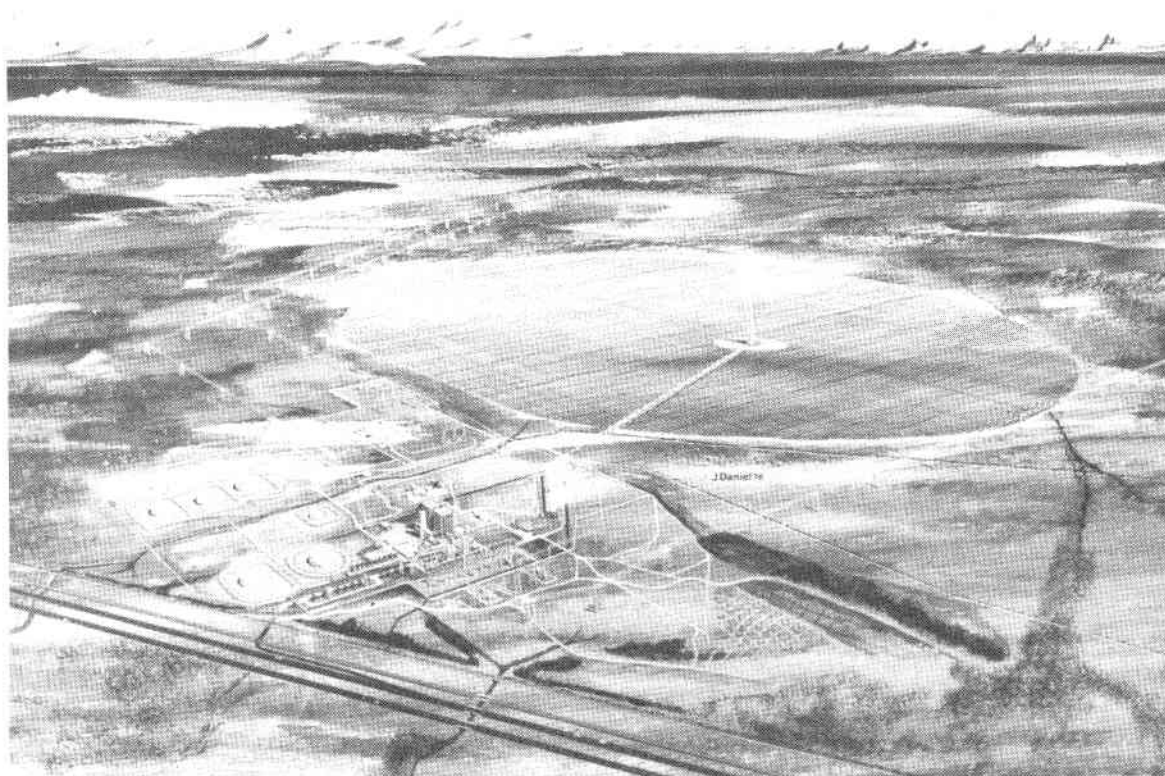


Figure 1.0-1 Saguaro Repowering Station (Artist Concept)

1.1 BACKGROUND

Solar thermal central receivers can be considered as an emerging alternative renewable energy source. As such they must overcome both engineering and economic challenges. The events of the last few years have shown that solar thermal central receivers in both standalone and hybrid versions, are technically feasible. Additionally the use of molten salt as a heat transport and thermal storage fluid promises electrical power generation that is independent of the minute to minute variations in sunlight due to partial cloud cover. There have been many studies that show this technology is economically viable, even when competing with coal, providing heliostat cost goals can be approached. The use of third party financing and existing tax incentives increases the economic acceptability of the technology. However, the number of solar thermal central receivers to be built will be severely limited until a valid demonstration plant has been built and operated. The subject of this study is the site-specific character of an excellent demonstration plant.

This study builds on and updates the work of the prior Saguaro repowering study--Saguaro Power Plant Solar Repowering Project--as presented in References 1-1,-2,-3, and -4.* The objectives of these studies were to develop a site-specific advanced conceptual design that (1) provides a practical and effective use of solar energy by repowering the Saguaro power plant of APS, (2) has the potential for construction and operation by 1985, (3) uses molten salt technology for the receiver and energy storage subsystems, (4) provides the best possible economics for the overall plant application, (5) incorporates the most recent technical developments of solar central receiver components, subsystems, and other elements into the conceptual designs; and (6) ensures that performance estimates for the advanced conceptual design are based, to the maximum extent possible, on performance characteristics of commercially available equipment. The advanced concept presented here satisfies all of these objectives and can result in a near-term demonstration of a very economically attractive solar-derived power production technology. This demonstration will provide a viable basis for significant market penetration of solar thermal repowering and new solar thermal standalone and solar hybrid power plants beginning in the early 1990s. It will also resolve any current operational and dispatch uncertainties associated with central station solar thermal power.

The solar repowered system concept is shown in Figure 1.1-1 where the solar-related equipment is above the horizontal dashed line and the existing equipment is below that line. Interfaces between the solar system and the existing plant involve the boiler feedwater line, superheated steam line, and control system. The use of molten salt, as shown in Figure 1.1-1, provides much higher plant efficiency when operating from storage than does the water/steam technology, and has many other operating advantages when compared with sodium. After evaluation, we consider molten salt to be much safer than sodium as a heat transfer fluid in this application and find that the cost and overall efficiencies favor the use of molten salt.

* See Chapter 7.0 for list of References.

Figure 1.1-1

1-3

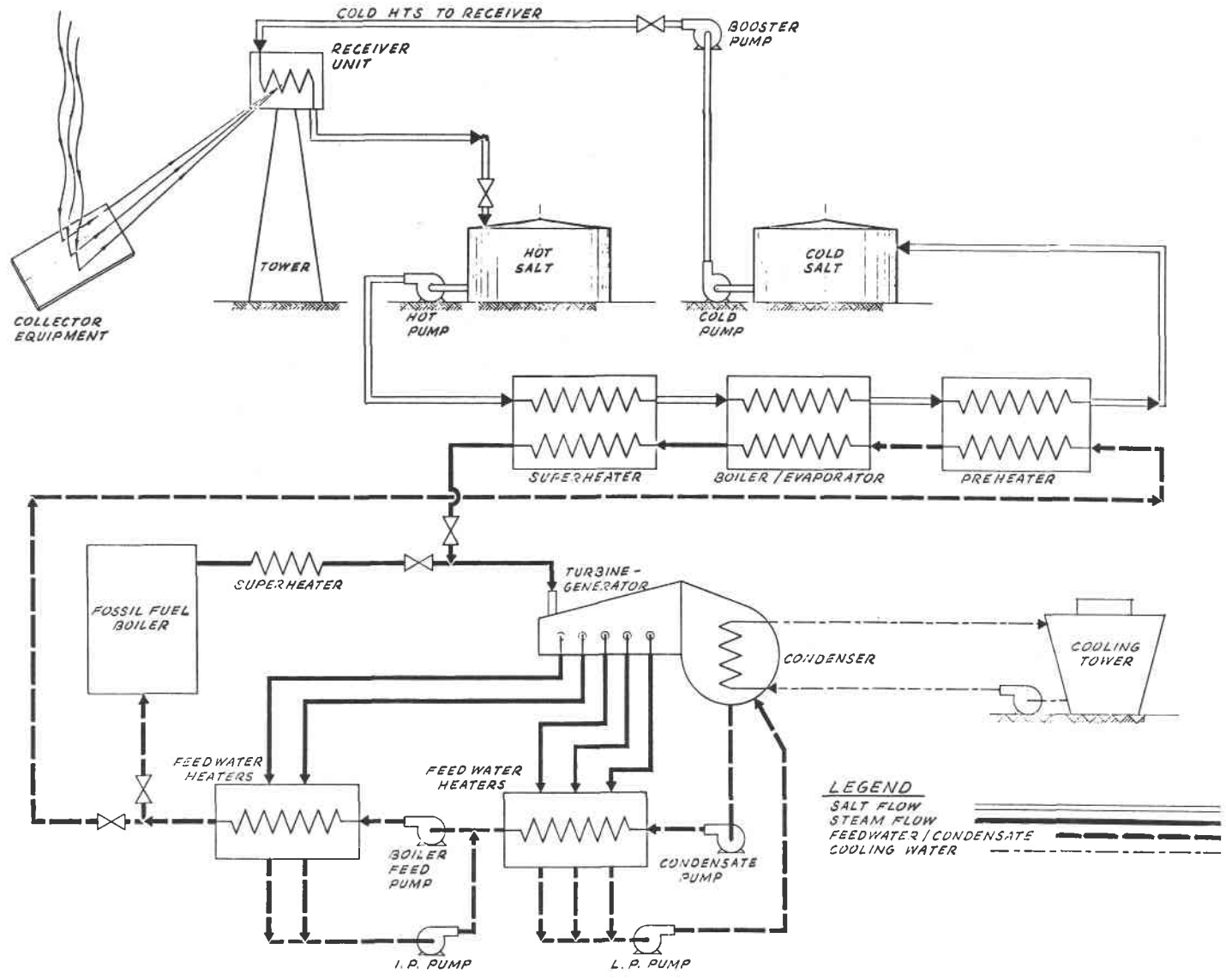


Figure 1.1-1 Repowered System Diagram

Provision of isolation valves between the new and existing systems means that either the solar or fossil system can be operated alone. They can also be operated together where the total steam flow is proportioned between the two sources. The fossil boiler fuel flow rate will be set to produce the desired fossil steam rate. Similarly, the solar steam generator's salt flow rate will be set to produce the desired solar steam rate.

The primary areas of responsibility of the team members involved in this repowering conceptual design study are shown in Table 1.1-1. The combined team, using each member's area of expertise developed and performed the design analyses discussed in this report. Table 1.1-2 lists the members of the Utility Advisory Council that were involved in the prior Saguaro study. The council members reviewed the Saguaro repowering concept and its major design features in terms of application to their own situations. While some recognized that solar repowering will not be economically attractive in the early 1980's for their utilities, they all emphasized the need for solar thermal central receiver repowering demonstrations to be conducted soon. They also stated that the molten salt technology could be adapted to their needs when the concept had been adequately demonstrated.

Table 1.1-1 Team Members and Responsibilities

Organization	Responsibility
Arizona Public Service Company	Site Owner; Overall Program Management; Program Plan; Fossil Subsystems, EPGS, and Interfaces
Martin Marietta Corporation	Lead on Selection of System Configuration; Solar System Conceptual Design, Analysis, Performance Estimates, and Optimization of the Collector Subsystem, Receiver and Thermal Storage; Cost Collection and System Economic Analysis; Reproduction of Major Study Documentation.
Babcock and Wilcox	Lead on Solar Steam Generator; and Review of Receiver Design.
Gibbs and Hill, Inc.	Conceptual Design, Analysis; Optimization, and Cost Data for the Solar Fossil Interfaces, Site and Site Facilities, and Tower; Recommendation for Upgradng Existing Fossil Steam Generator and EPGS Control Systems.

Table 1.1-2 Utility Advisory Council Members

Joseph Kitchen	United States Department of Interior, Las Vegas, Nevada
Stan Hightower, Harry Remmers, and Robert Zelenka	Water and Power Resources Service, Denver, Colorado
Harold Franson	Colorado-Ute Electric Association, Montrose, Colorado
Jeffery Wright	Kansas Gas and Electric Company, Wichita, Kansas
Richard Bell	Hawaiian Electric Company, Honolulu, Hawaii
Patrick McCarter	Public Service Company of Colorado, Denver, Colorado
Donald Squire and Steven Chalmers	Salt River Project, Phoenix, Arizona
Harold Seielstad	Pacific Gas and Electric Company, San Francisco, California
R. C. Kuether	Kansas City Power and Light Company, Kansas City, Missouri

1.2 SITE DESCRIPTION

The Saguaro station is located 46 km (27 mi) north of Tucson, Arizona, on Interstate 10. A picture of the station is shown in Figure 1.2-1.

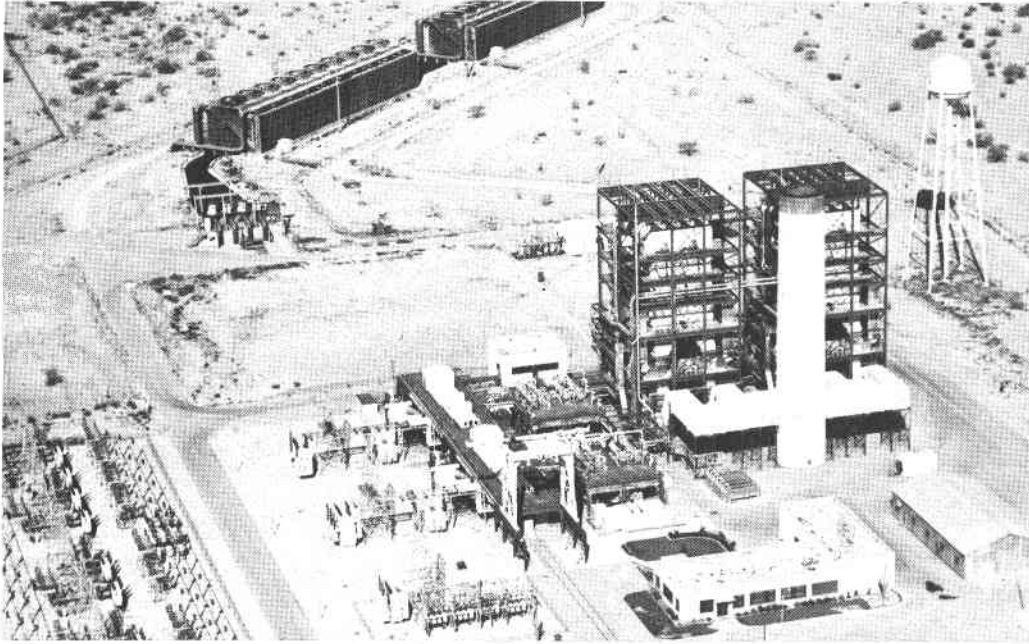


Figure 1.2-1 Saguaro Power Plant

The thermal energy storage subsystem and the solar steam generator will be located in the area between the boilers and the cooling towers while the collector field (not shown) will be located in the area above the figure.

1.2.1 Plant Features

The site was chosen for repowering based on the following features:

- 1) Plant site is not physically constrained for a solar collector field;
- 2) Site has high solar insolation (6.9 to 7.6 kWh/m² - day);
- 3) Steam cycle thermal requirements are matched by the molten salt's capabilities;
- 4) Typical of non-reheat turbines that are solar repowerable;
- 5) Site is easily accessible and close to major metropolitan areas;
- 6) Fossil steam generator burns natural gas and/or No. 6 fuel oil;
- 7) Potential exists for high cost fuel displacement during solar operation;
- 8) Low seismic risk site.

The section of land immediately east of the plant is owned by APS, and is available for the collector field. It is surrounded by three sections of state-owned land. The State of Arizona has placed this land in a reserve category pending consideration for use in this repowering program. The high insolation level, low seismic risk, non-reheat steam turbine, and general plant layout type all increase the probability of a successful operation.

An important characteristic of the existing plant is that it does not include reheat. This means that this first demonstration of the molten salt central receiver technology need not include the requirement for controlling two reheat superheaters in parallel (fossil and solar) as would be necessary for a reheat cycle. Unit No. One was originally constructed in 1954 but the high-pressure casing was replaced in 1975. Both the turbine and boiler can be operated in a load following mode and their power level is controlled by an automatic dispatch system from the APS dispatch center in Phoenix, AZ. A heat balance for Unit No. One at 100% load and 6.7 kPa (2.0 in. Hg) condenser pressure is shown in Figure 1.2-2. The gross electrical output from the unit is 120.2 MW_e with a steam flow of 4.54 x 10⁵ kg/hr (1.00 x 10⁶ lb/hr). The boiler thermal efficiency is 83%. The turbine was built by General Electric, the boiler by Combustion Engineering, and the cooling towers by Marley Co.

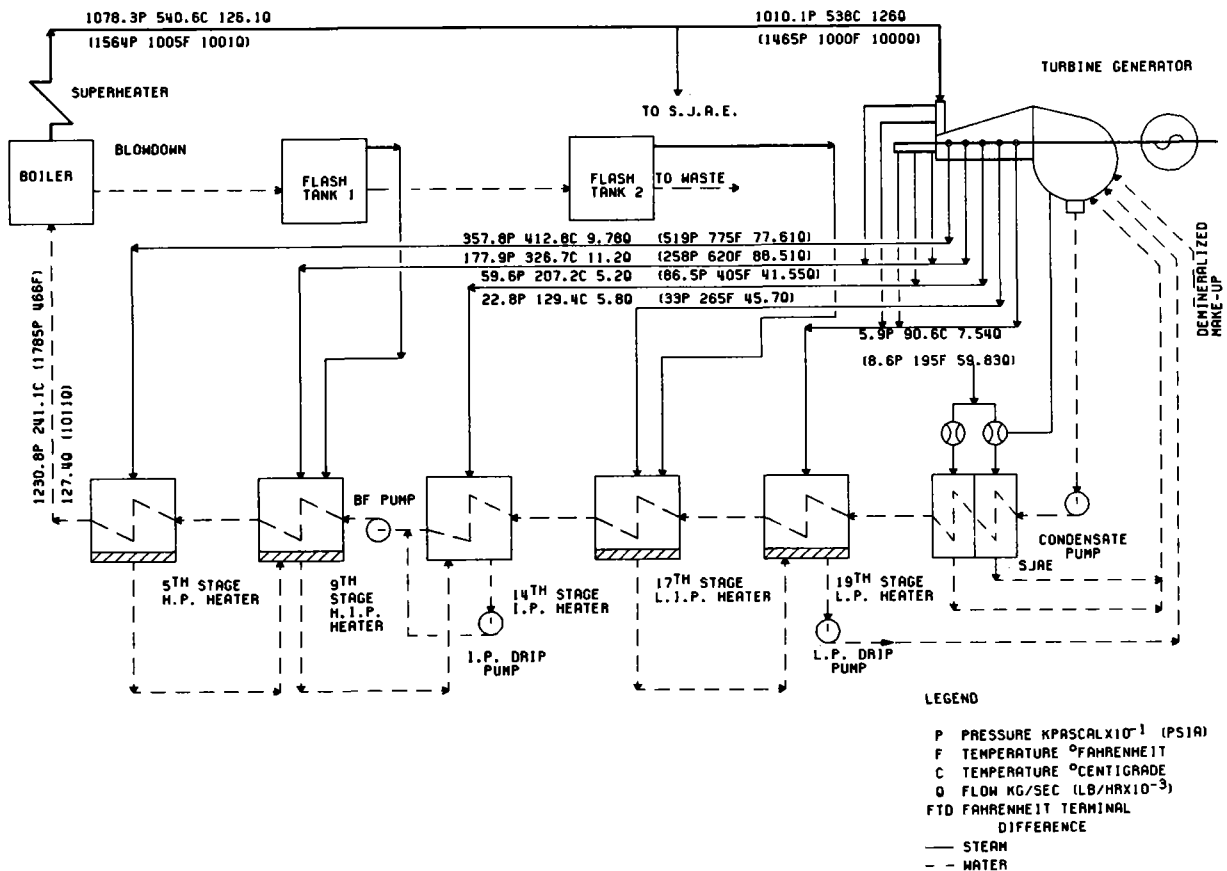


Figure 1.2-2 Saguaro Heat Balance at 100% Power

1.2.2 Climate and Geography

The Saguaro site terrain is ideally suited for a solar thermal central receiver plant. It is basically flat desert land that slopes up slightly to the east and a little to the north toward the Tortolita mountains. The existing vegetation is low and sparse and there are a few shallow washes for drainage. The existing vegetation is brush and cacti. There is no free ground water and the soil moisture is very low. Average yearly rainfall is 0.28 m (11.1 in.) and relative humidity ranges from 25 to 52%. The soils underlying the site consist of a surface stratum of clayey sand, and sandy and silty clay of low to medium plasticity with a maximum safe soil bearing pressure of 192 kPa (4000 psf).

1.3 PROJECT SUMMARY

The Arizona Public Service Company team has prepared an effective conceptual design for repowering Unit One of the APS Saguaro Station using the solar thermal central receiver technology with molten salt as the heat transport and thermal storage fluid. Molten salt has been judged by the various APS engineering, legal, and operating divisions to be an ideal application because of its system performance, compatibility with Saguaro, cost, prior industrial experience and its safety when used as recommended here. A schematic of the repowered system is presented in Figure 1.3-1 where the existing non-reheat steam turbine and electric generator are shown toward the center of the figure.

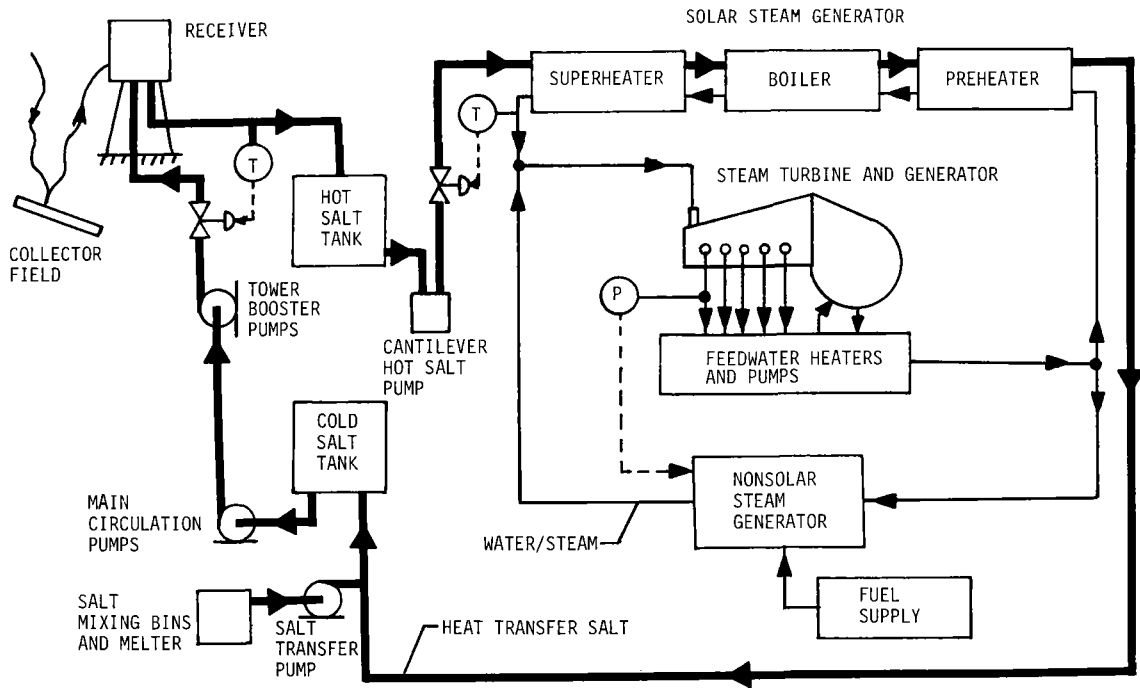


Figure 1.3-1 Repowering System Schematic

This 120 MW_e gross unit is operated with five feedwater heaters, a split-tee condenser, and wet cooling towers. Cooling water is obtained from three on-site wells. The existing fossil steam generator includes an economizer and superheater, and can be fired with natural gas, No. 6 fuel oil, or a combination of the two. This 1954 system was upgraded to the current power level in 1975 by replacement of the high pressure turbine shell. The turbine cycle efficiency of 39.37% is representative of current design practice.

The solar repowering system can be thought of as an alternative steam supply that is in parallel with the existing fossil steam generator as shown in Figure 1.3-1. Interfaces between the solar and existing systems have been kept very simple. Existing boiler feedwater pumps and heaters are used for both solar and fossil operation. The repowering concept provides for fully rated turbine generator operation from fossil-generated steam alone, up to 60 MWe net from solar-generated steam alone, or fossil and solar-generated steam in selectable proportions. This feature will permit APS to use the repowered Saguaro Unit One in those ways that are most beneficial to the demonstration program and to APS. The capacity credit for this unit is not lost, as Unit One can be operated at any time. Also, since the addition of a renewable energy source (solar) will satisfy the requirements of the 1978 Fuel Use Act (which severely restricts the generation of electric power from oil or gas after 1990) the useful lifetime of this unit can be extended well past 1990.

A single surrounding collector field consisting of 5000 Martin Marietta improved second generation heliostats will be located just to the east of the Saguaro Station on APS owned land that will be supplemented by a small amount of leased land. The quad-cavity receiver is mounted on a 120 m (394 ft) tall conical reinforced concrete tower. The molten salt for the receiver is pumped from cold salt storage at 277°C (530°F) by the main circulation and booster pumps to the receiver where it is heated to 566°C (1050°F) by the solar energy reflected from the heliostats. The salt remains a liquid during the addition of solar energy, which means that the receiver design is simpler and less subject to creep-fatigue damage than two phase systems, such as water/steam, would be. The hot salt is returned to the hot salt storage tank located near the station cooling towers along with the cold salt storage tanks, as shown in Figure 1.3-2.

The use of molten salt storage gives this solar thermal central receiver concept a number of advantages. First, energy storage is at a high temperature so that system efficiency does not degrade when operating from storage. Next, all thermal energy goes directly to storage so it is unnecessary to run the turbine when solar energy is being collected. This decoupling of the collection of energy from the use of solar energy greatly simplifies the control system design. It also gives the plant operators significant freedom as to when the stored energy will be used. Our analyses found that collecting energy in the morning, and using it in the afternoon and evening when the APS system load is high, makes an economically effective system.

The hot salt from storage is pumped through a set of three counterflow heat exchangers when it is desired to generate steam from solar energy. The feedwater from the turbine feedwater heaters is pumped through the preheater and into the boiler. The steam then flows through the superheater to the turbine. The solar steam generator is sized to provide the steam necessary for operation at 66 MW_e gross. The thermal energy storage subsystem was sized for 4.0 hours of

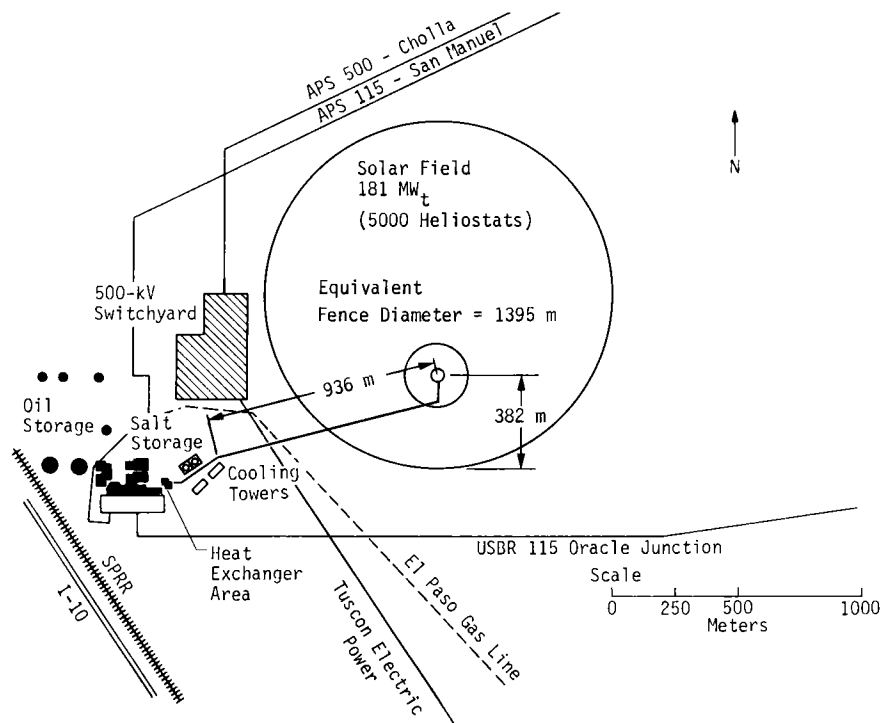


Figure 1.3-2 Collector Field Location

operation at 60 MWe net. The collector and receiver were sized to provide 5% more power than required at the repowering level (solar multiple of 1.05) at the solar design point of noon on summer solstice. This set of sizes results in the best combination of investment and value for a solar repowering demonstration project.

The repowered system performance was evaluated using typical meteorological year insolation data from the Phoenix, AZ airport. This resulted in 150 GWh_e being available to the APS grid if there were no outages. This amount of energy corresponds to the combustion of 2.7 million barrels of oil in 10 years. Construction costs have been estimated at \$126.8 million in 1982 dollars using a cost basis of \$263/m² for the collector field that represents 60% of the total construction cost. Other costs range from \$1.29 million (1%) for site preparation to \$9.8 million (7.7%) for the thermal storage subsystem. Owner's costs are estimated at \$7.12 million. No allowance has been made for interest on funds used during construction. The solar-related operating and maintenance costs (estimated at \$1.44 million for the n-th year of operation in 1982 dollars) must also be added to the owner's costs.

The value of the fuel to be displaced in the APS grid by solar energy was determined using an APS production cost computer model. Solar energy was dispatched to displace the highest value fuel expected to be used on each day. The results are dependent on the specific

load/resources forecast (updated each 6 months), the projected cost of fuel, and the number of operating years. Using the March 6, 1981 forecast of load demand and generation resources, the APS 1981 long range fuel cost forecast, and 14 years of operation as a specific case; the levelized annual fuel and O&M savings are TBD million in 1987 dollars. The fuel savings range from 3.5 to 20.2 million in 1987 dollars over the range of parameters investigated. The first value corresponds to displacement of all coal for 10 years using APS projections of coal costs, while the second value corresponds to displacement of all oil for 10 years using the APS projections of oil costs.

A project development plan was prepared that leads to initial repowered plant operation at the beginning of 1987. This plan provides for phased procurement and review milestones, with a hardware procurement and construction phase of 3 years. The critical path includes heliostat procurement and installation, with the receiver also having a long critical path. APS feels that the schedule is realistic if APS is permitted to manage the project as it now does on other similar-sized generation construction projects.

Arizona Public Service's evaluation of the recommended repowering concept is that it will be an excellent demonstration of the molten salt solar thermal central receiver technology. This demonstration must be conducted soon if solar thermal central receiver systems are to become a useful part of the solution to our nation's energy needs in the 1990's. APS is a progressive solar-oriented utility that sees the Saguaro repowering project as a necessary precursor to larger solar standalone and solar hybrid systems. Saguaro Station is a near-ideal location with excellent sunshine and sufficient land available for the collector field. The turbine and generator are representative of many existing systems that can be adapted to repowering, it has simple interfaces with the solar system, and requires little retrofit. Use of molten salt as a heat transport medium means inexpensive energy storage, decoupling of the collection of solar energy from use of that energy in the turbine, daily delay of solar energy use until the peak demand occurs on the APS grid, and highly efficient operation from storage.

A number of improvements were made as part of this advanced conceptual design effort. The solar system was designed to have a net power output of 60MWe at noon on the summer solstice with a solar insolation of 950 W/m² (desing paint). The system has 5000 Martin Marietta improved second generation heliostat, that provide a solar multiple of 1.05. The solar conetral receiver was modified to reduce weight and improve performance. The solar stream generator subsystem incorporates the U-tube configuration developed during the Babcock and Wilcox steam generator contract with Sandia National Laboratories Livermore. The solar system is designed to be operational by January of 1987.

In summary, the actual repowering of Saguaro Unit One will demonstrate a solar thermal central receiver power generation system using molten salt for both heat transfer and storage. It will also demonstrate the daily dispatching of a solar power system into a utility grid in an optimum manner. In this way it can provide the basis for an industry funded expansion of solar thermal central receivers into a viable part of our nation's energy supply.

1.4 CONCEPTUAL DESIGN DESCRIPTION

The selected system characteristics, shown in Table 1.4-1, were developed based on the functional requirements determined early in the study. This configuration uses a quad-cavity receiver on a single tower surrounded by 5000 heliostats. As shown in Figure 1.3-2, the tower and heliostat field are located to the east of the existing plant. The tower is located to the south of the field center. Salt storage is located near the cooling towers. The solar steam generator is located just to the east of boiler No. One to minimize the high pressure feedwater and steam line distance to the interface location. Shown in more detail in Figure 1.4-1, these high pressure lines are more expensive than comparable lengths of salt piping. The solar-to-fossil interconnections are between the No. One boiler and the feedwater heater deck. A salt drain tank is located next to the solar steam generator since this is the lowest point in the system.

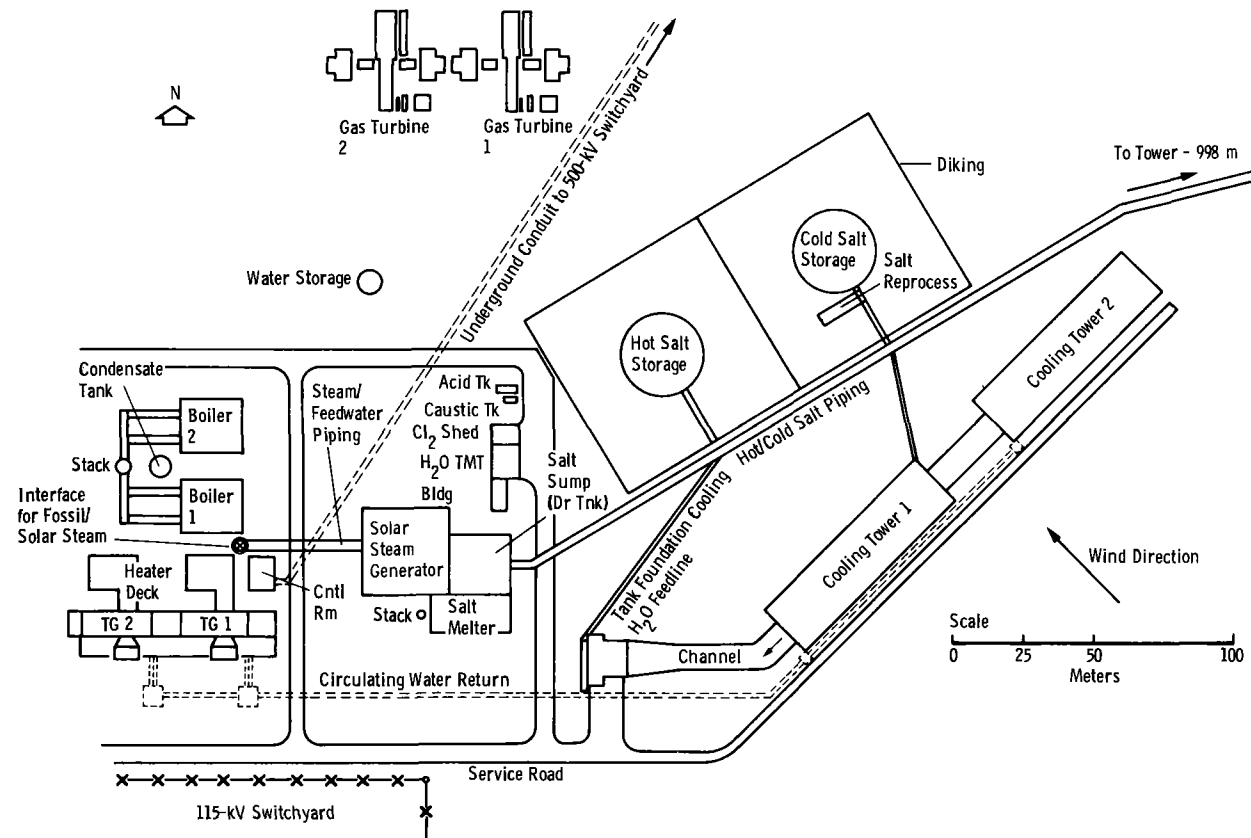


Figure 1.4-1 Solar Equipment Location

Table 1.4-1 Conceptual Design Summary

Table 1.4-1

1. Prime Contractor:	Arizona Public Service Company
2. Major Subcontractors:	Martin Marietta Corporation Babcock and Wilcox Company Gibbs and Hill, Inc.
3. Site Process:	
Turbine Manufacturer:	General Electric
Date of Manufacture:	1954
Turbine Type:	Non Reheat
Gross Electrical Power:	120.2 MWe
Net Electric Power (Design Point)	
Receiver + Storage Operation + EPGS:	60.0 MWe
Storage + EPGS Operation:	62.1 MWe
Fossil * + Receiver + Storage + EPGS:	110.7 MWe
Fossil * + Storage + EPGS:	112.8 MWe
Fossil Only + EPGS:	113.2 MWe
* Fossil at 54.2 MWe Gross	
Steam Temperature:	538°C (1000°F)
Steam Pressure:	10.0 MPag (1450 psig)
Feedwater Temperature (66 MWe Gross):	216°C (420.4°F)
Steam Flowrate (66 MWe Gross):	67.9 kg/sec (538.7 x 10 ³ lb/hr)
Condenser Pressure:	6.7 kPa (2 in. Hg)
Gross Heat Rate (66 MWe Gross):	9382 kJ/kWhe (8892 Btu/kWhe)
Gross Cycle Efficiency (66 MWe Gross):	38.4%
4. Site Location:	Saguaro Station 43 km (27 mi) north of Tucson, Arizona on Interstate 10.
Longitude:	111° 17' 50" West
Latitude:	32° 33' 22" North
Elevation:	589 m (1931 ft) above mean sea level
5. Design Point:	Noon, Summer Solstice
6. Receiver	
Receiver Fluid:	Molten Salt (60% NaNO ₃ , 40% KNO ₃ by weight)
Configuration:	Quad-cavity
Type:	Once through, two zone, 10 passes/zone
Elements:	46 tubes/panel, 10 panels per zone
Solar Multiple:	1.05
Nominal Thermal Power at Tower Base:	181 MWt (6.176 x 10 ⁸ Btu/hr)
Maximum Thermal Power at Tower Base:	199 MWt (6.790 x 10 ⁸ Btu/hr)
Nominal Salt Flow Rate:	409 kg/sec (3.245 x 10 ⁶ lb/hr)
Salt Temperature - In:	277°C (530°F)
Salt Temperature - Out:	566°C (1050°F)
Efficiency: (Design Point)	90.5%
7. Heliostats	
Number:	5000
Individual Mirror Area:	57.41 m ²
Cost (installed including foundations, wiring, etc):	\$263/m ²
Type:	Martin Marietta improved second generation
Field Configuration	Surrounding Field
Total Mirror Area	2.8705 x 10 ⁵ m ² (3.090 x 10 ⁶ ft ²)
Total Collected Energy to Receiver	191.3 MWt
Field Efficiency: (Design Point)	71.6%
8. Thermal Energy Storage	
Duration:	4.0 hr @ 172 MWt discharge
Media:	Molten Salt (60% NaNO ₃ , 40% KNO ₃)
Type:	Hot/Cold Tank Pair
Capacity:	688 MWht
Cold Salt Temperature:	277°C (530°F)
Hot Salt Temperature:	566°C (1050°F)
Maximum Charge Rate:	199 MWt
Maximum Discharge Rate:	172 MWt
9. Solar Steam Generator	
Preheater Type:	U-tube, straight shell
Evaporator Type:	U-tube, straight shell
Superheater Type:	U-tube, U-shell
Duty:	172 MWt (5.869 x 10 ³ Btu/hr)
Inlet Salt Temperature:	566°C (1050°F)
Outlet Salt Temperature:	277°C (530°F)
Salt Flowrate:	388.5 kg/sec (3.084 x 10 ⁶ lb/hr)
Steam Flowrate:	67.8 kg/sec (5.380 x 10 ⁵ lb/hr)
10. Total Project Construction Cost (\$263/m ² heliostat cost):	126.8 x 10 ⁶ (1982 \$)
11. Construction Time:	3 Years
12. Solar Plant Contribution at Design Point:	60.0 MWe (net)
13. Solar Fraction - Annual:	0.285
14. Annual Fossil Energy Saved:	0.27 x 10 ⁶ barrels of oil equivalent
15. Types of Fuel Displaced in 1987:	52% Oil and Purchases 48% Coal
16. Annual Energy Produced:	149.7 GWhe
17. Ratio of $\frac{\text{Annual Energy Produced}}{\text{Total Heliostat Mirror Area}}$:	1.447 $\frac{\text{MWht}}{\text{m}^2}$
18. Ratio of $\frac{\text{Project Construction Cost}}{\text{Annual Fuel Displaced}}$:	253 \$/MWht
19. Site Insolation (direct normal)	
Annual Average:	2.519 - 2.774 MWh/m ²
Source:	SOLMET, Phoenix, AZ, TMY - Watts Engineering Data

The two molten salt storage tanks were located at a convenient point close to the solar steam generators along the horizontal salt piping to the receiver tower. These tanks, and all major salt-containing elements, are diked to contain any salt that might leak. A salt melter, to initially melt the granular salt and to provide a source of heat if the receiver should be shut down for an extended period, is located next to the solar steam generators. The hot salt pumps are located just outside the hot salt dike and the cold salt main circulation pumps are located just outside the cold salt dike. The receiver booster pumps are located inside the receiver tower just above ground level. Water for cooling the various tank foundations will be taken from the EPGS cooling water makeup system. After use, it will be returned to the cooling tower return lines.

The selected 60 MW_e net solar configuration will provide minimum interface requirements on the existing plant. To maximize the displacement of oil and gas use in the APS utility system, the equipment will be designed to promote operational flexibility. To enhance this flexibility, 4.0 hours of storage capacity (688 MWh_t) will be installed to aid chiefly in the daily delay of the start of the turbine. The storage may also be used to provide operation of the EPGS at some part load condition for longer times. Therefore, the solar steam generator will be designed to provide quality steam at part load.

1.4.1 Collector Subsystem

The collector subsystem is composed of 5000 Martin Marietta improved second-generation heliostats, each with 57.41 m² of mirror area and 93% reflectivity. This heliostat is shown in Figure 1.4-2. The Martin Marietta second generation heliostat has been improved by replacing the paper honeycomb core with a light weight aluminum honeycomb core. Not only is the mirror assembly lighter, but it is also less sensitive to trapped moisture. The corners and edge frame have been redesigned to provide a better rain barrier. The bar joist to elevation beam interface has been stiffened and the overall structure is now designed for optimum strength and reduced weight. A new stowlock design that is operationally simpler has been incorporated. These and other redesigns make the improved heliostat an excellent choice for repowering applications. The collector subsystem with the improved heliostat has a design point efficiency of 71.6%, redirecting 195.2 MW_t of solar energy into the four apertures of the quad-cavity receiver.

1.4.2 Receiver Subsystem

A quad-cavity receiver was shown to be more efficient than an external receiver for this application. As shown in Figure 1.4-3, each of the cavities has a door that can be closed to reduce thermal losses when the receiver is not operating. These doors are covered with an ablative material to protect the receiver absorber tubes and door structure in the event of a total power loss to the solar system when the heliostats are focused on the receiver. Booster pumps provide the fluid head to move the salt up the tower and through the receiver. A cold salt surge tank is used at the receiver inlet and a passive

system composed of morning glory spillways and plunge pools are used at the receiver outlet. These devices decouple receiver salt flow transients from transients in the long supply and return piping. After being heated from 277°C (530°F) to 566°C (1050°F) in the receiver, the salt exits into the downcomer. A morning glory spillway

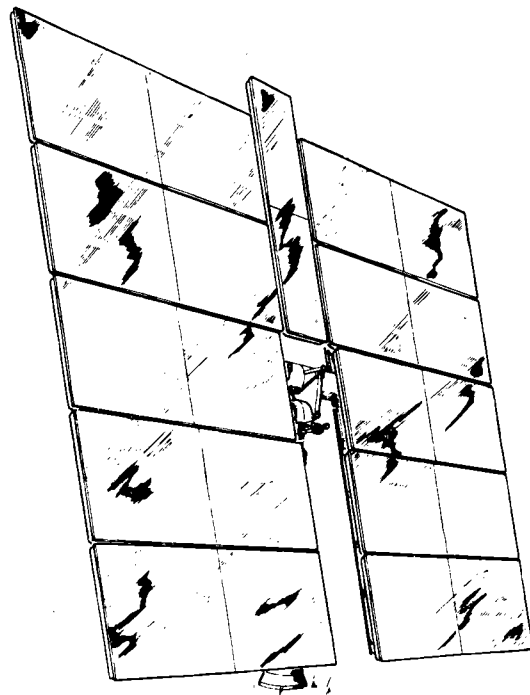


Figure 1.4-2

Martin Marietta
Second Generation
Heliostat

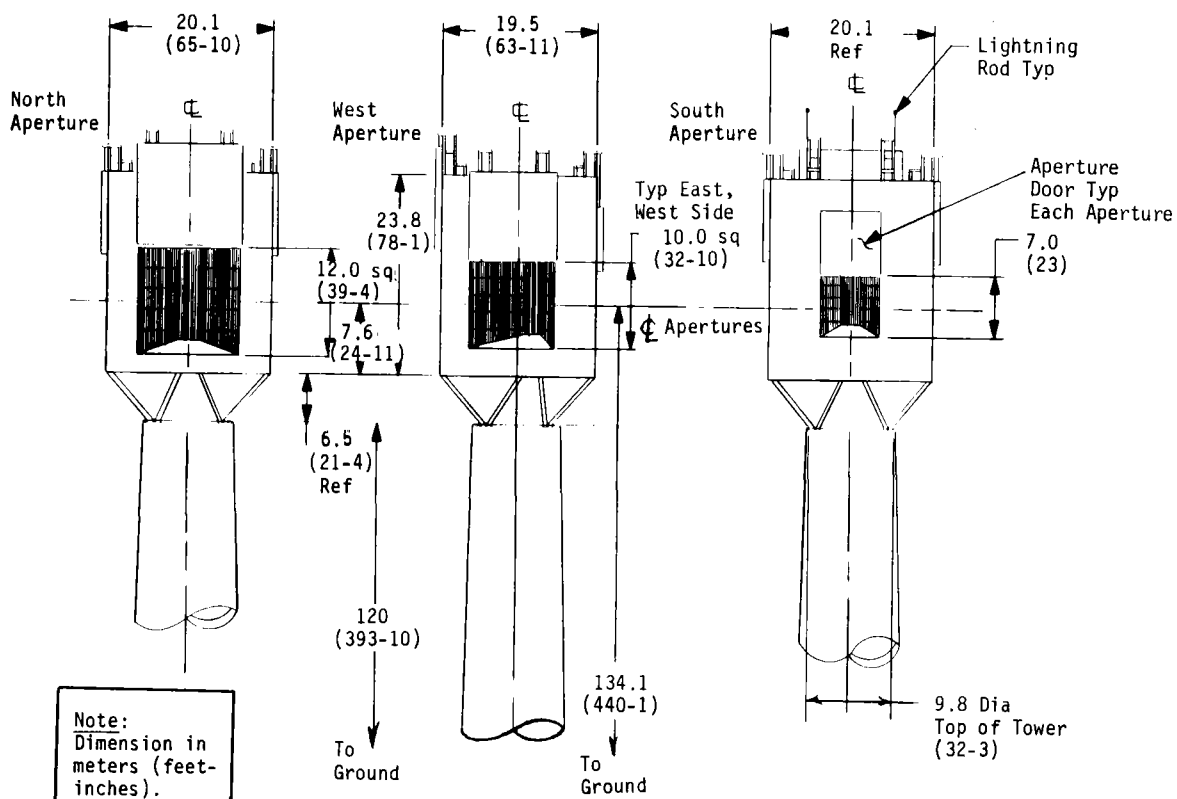


Figure 1.4-3 Receiver General Configuration

design maintains the desired pressure head at the receiver outlet. The hot salt then flows to the storage area where it is sent to the hot storage tank (or to the cold or drain tanks during startup).

1.4.3 Thermal Energy Storage Subsystem

The use of a relatively large storage system effectively decouples the collection of solar energy from the use of that energy in the turbine generator. Ample storage capacity results in much simpler operation since the turbine never sees the immediate effect of cloud passage. Molten salt leaves the cold storage tank at 277°C (530°F) and is pumped via the main circulation pumps (cold pump) through approximately 1.1 km (0.70 mi) of horizontal piping to the receiver tower and booster pumps. The cold salt storage tank is made of carbon steel to the same general requirements as oil or hot asphalt storage tanks with the exception of thicker external insulation requirements for salt thermal storage systems. The recommended form of the hot salt storage tank (see Fig. 1.4-4) is to again use a carbon steel shell for the tank and external insulation. There will also be a significant amount of internal insulation. A special, thin, Incoloy 800 liner is used to keep the hot salt from contacting the insulation. The liner has a wafflelike configuration that accommodates thermal expansion and contraction as well as transmitting the pressure loads through the internal insulation to the carbon steel shell of the tank. An internally insulated hot salt tank is recommended because it promises to be significantly cheaper than an all stainless steel tank in the larger sizes appropriate to larger solar systems.

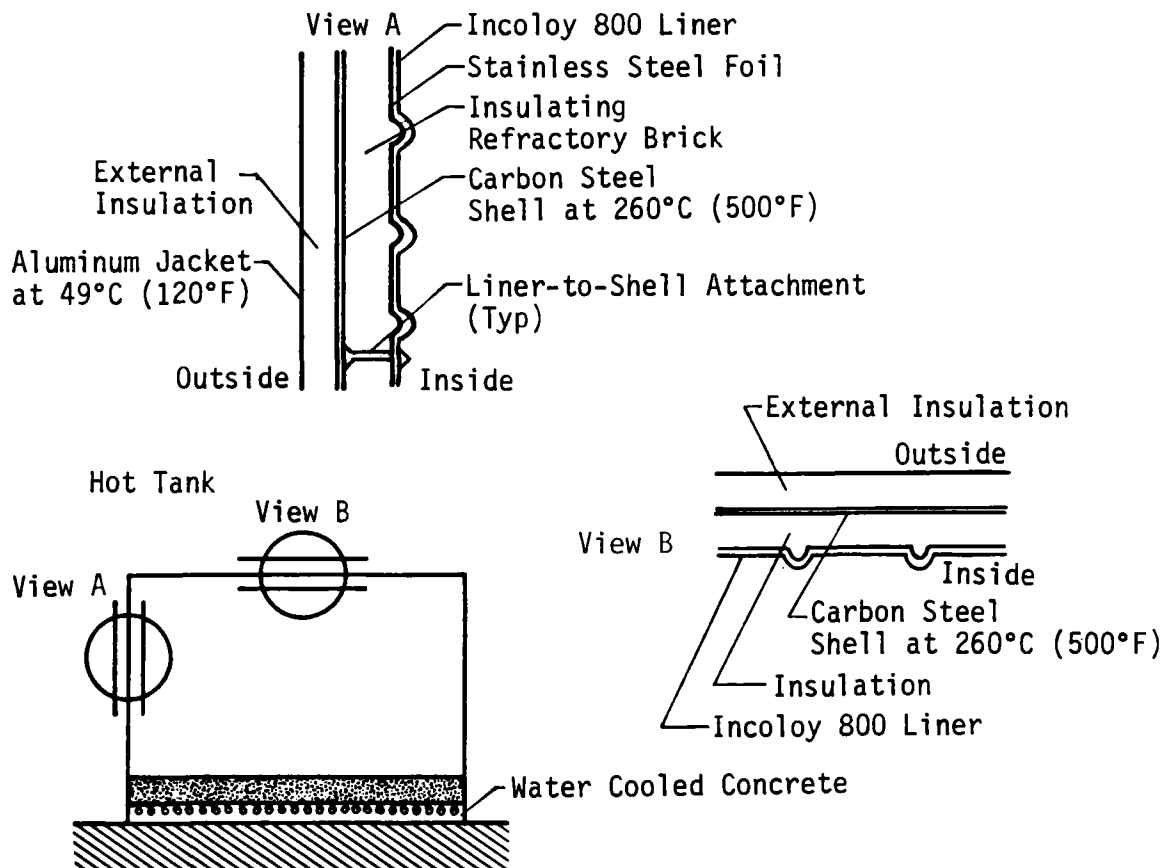


Figure 1.4-4 Hot Salt Storage Tank Configuration

1.4.4 Solar Steam Generator

The solar steam generator consists of three separate counter-flow heat exchangers (superheater, boiler/evaporator, and preheater). A set of hot salt pumps is used to maintain salt flow from the hot salt storage tank, through the heat exchangers and back to the cold salt tank. The solar steam generator takes pressurized water from the existing feedwater system (heaters and pumps) and converts it to steam at the same conditions as the existing fossil-fired boiler. A pair of forced recirculation water pumps is used to recirculate water from the steam drum through the evaporator and back to the steam drum. These same pumps also provide water from the steam drum to mix with the feedwater to ensure that the preheater inlet water temperatures are high enough to prevent salt from freezing in the preheater. A salt recirculation pump is used to maintain the desired salt temperature into the boiler/evaporator during steady state operation and transients.

The configuration arrangement of the evaporator is shown in Figure 1.4-5. A similar U-tube, straight shell arrangement is used for the preheater. However, the superheater uses a U-tube, U-shell configuration to provide the necessary insensitivity to thermal transients due to the daily startup and shutdown of these heat exchangers. The forced recirculation system used with the evaporator permits smaller heat exchangers to be used that can be started more rapidly than a natural circulation evaporator.

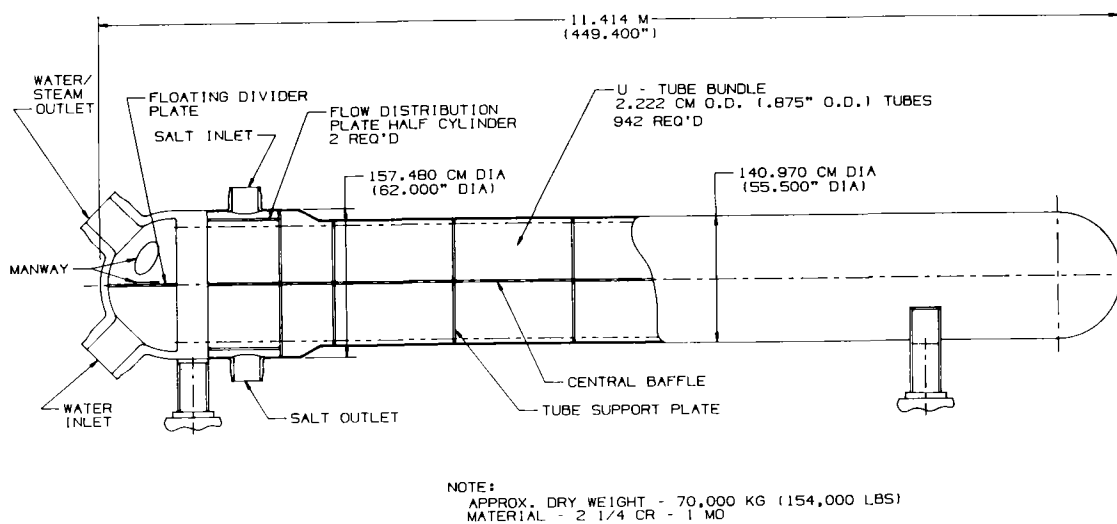


Figure 1.4-5 Evaporator Configuration Arrangement

1.4.5 Plant Interfaces

The physical interfaces will simply occur as pipe tees in the feedwater and steam lines. The equipment and control interfaces between the solar and fossil system are configured so that either system can be used alone, or the two systems can generate the same quality of steam at the same time in selectable proportions. This approach includes the ability to automatically control the power level of either or both systems from the APS dispatch center. Because the fossil system can be operated alone, there is no change in the availability of Saguaro Unit One as part of the APS generation capability, thus, capacity credit is retained for the solar repowered Saguaro Unit One.

1.4.6 Master Control Subsystem

The entire repowered electrical power generation facility will be monitored and controlled by a master control subsystem that consists of six functional subsystems, a red-line unit element, and a data acquisition system. The actions of six subsystems are coordinated by an operational control subsystem that also interfaces with APS central dispatch and processes and responds to all emergencies. The red-line units are completely independent of the basic control and data acquisition subsystems. They are used to warn the operator of existing or impending emergencies. Corrective actions are taken through normal control channels. The controlled subsystems are:

- | | |
|---------------------|-------------------------------|
| 1) Collector field; | 4) Receiver; |
| 2) Fossil boiler; | 5) Electric power generation; |
| 3) Energy storage; | 6) Solar steam generator. |

Of these six controlled subsystems, the fossil boiler and electric power generation subsystems currently exist at Saguaro and their control hardware is established and operating. It is recommended that APS upgrade the fossil steam generator and EPGS control systems to be compatible with the approach and specific equipment type used for the solar systems. This upgrading is not included as part of the repowering costs. The report assumes that APS will accept the recommendation and upgrade the two control systems.

The general design approach for the master control subsystem uses the supervisory control concept. That is, the six plant digital control systems are responsible for first level control functions while the supervisory computer of the operational control subsystem prescribes the proper operating instructions (e.g., set points) so that desired operational objectives can be met. Normal plant control is completely automatic and the human operator intervenes only for emergencies or gross operational conditions.

1.4.7 Operating Modes

Basic operating modes for the solar and fossil systems and the transitions between these modes were assessed. The results of this assessment show that the number of operational modes for the repowered Saguaro plant is low because the large storage capacity effectively decouples the solar energy collection process from the use of solar energy in the EPGs. Five basic steady state operating modes can be logically arranged into three combination modes, where two of the basic modes operate at the same time. By judicious ordering, the number of valid transitions between the steady state operating modes has also been kept low. There are ten such transitions when the direction of transition is counted separately. The result is a relatively simple set of modes and transitions. The clear day scenario of Figure 1.4-6 illustrates the few operating modes that are required as well as the decoupling of the collection from the use of solar energy. The lower two parts of the figure show how the energy collection is coordinated with insolation. The upper two parts of the figure show how energy can be dispatched to suit the load. The center part of the figure shows how storage is filled in the morning and emptied in the evening and thus provides the decoupling feature. Operating procedures for the receiver, solar steam generator, and storage subsystems were developed to aid in the conceptual design effort. The procedures aided in the selection of piping, control valves, and control systems.

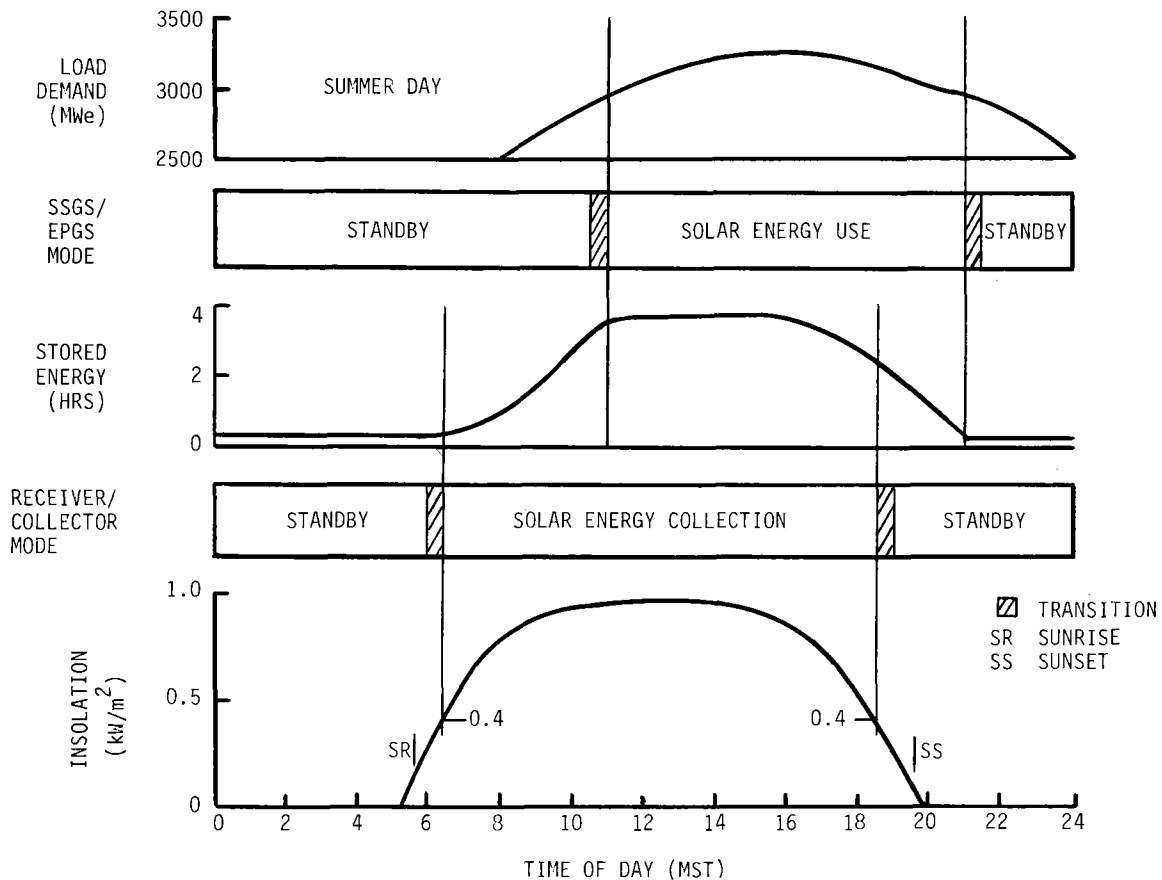


Figure 1.4-6 Clear Day Scenario

1.5 SYSTEM PERFORMANCE

The design point and annual performance of the selected Saguaro repowering conceptual design has been evaluated using three computer models--DELSOL II, TRASYS and STEAEC. The individual solar subsystem performances were modeled separately, with the results input into the STEAEC system simulation program, together with solar insolation and weather data, to model the annual performance of the system.

The collector subsystem performance was evaluated using the DELSOL II computer program. The collector field performance, as defined by the ratio of solar radiation inside the apertures over the total available radiation incident on the collector area, was calculated as 71.6% at the design point. Receiver losses were evaluated using the TRASYS thermal radiation analysis model, again for the design point and off-design cases. Thermal losses in the salt vertical and horizontal piping, and the storage subsystem, were also determined. The resulting design point system performance staircase is shown in Figure 1.5-1. Assuming a reference direct normal insolation value of 950 W/m², the total system efficiency at the design point is 23.2%. The design point staircase shows an overall field/receiver efficiency of 66.5% (including heliostat reliability, cosine, reflectivity, shading and blocking, tower shadow, attenuation, spillage, absorptivity, and receiver radiation losses). At design point the tower shadow does not extend into the collector field.

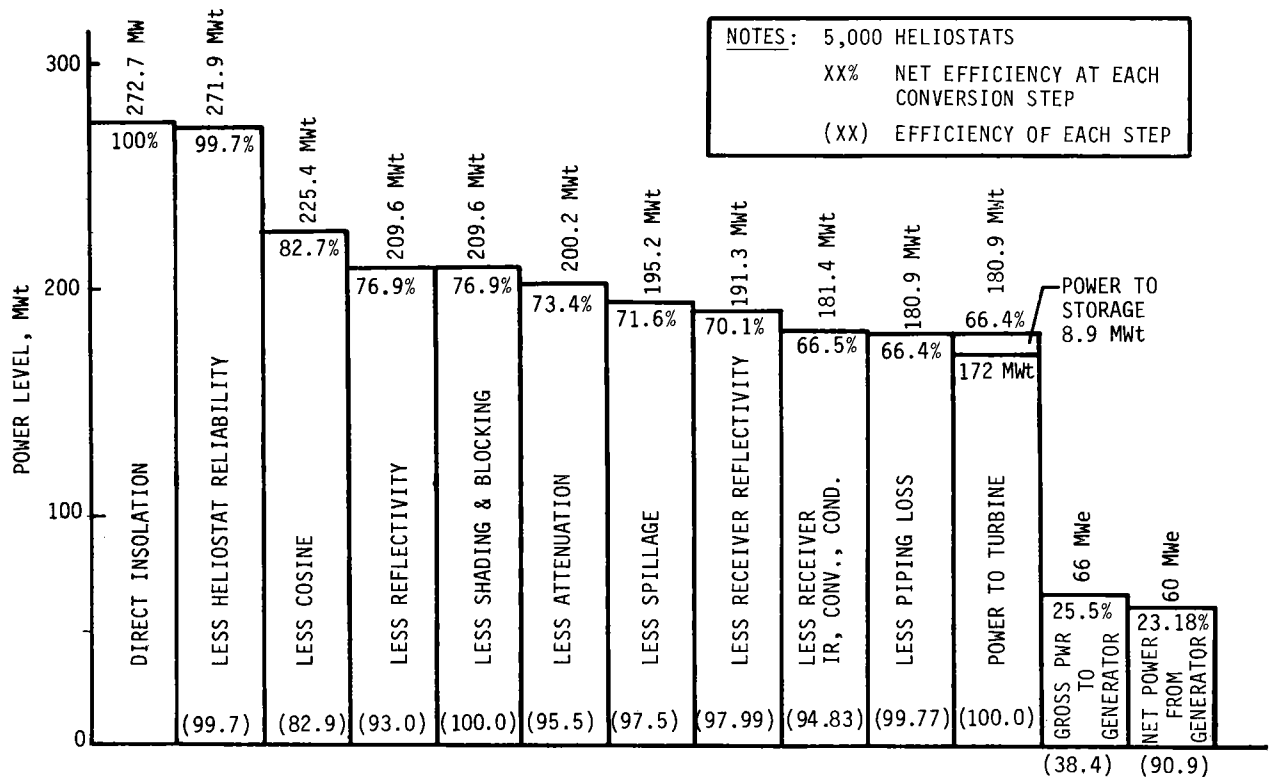


Figure 1.5-1 Design Point Efficiency for 60 MWe Solar Plant (SM = 1.05)

The EPGS gross cycle efficiency of 38.4% at 66 MWe gross was determined for the selected steam conditions of 538°C (1000°F), 10.0 MPa (1450 psig) and 6.75 kPa (2 in. Hg) backpressure. An additional 6.0 MWe is required for auxiliaries to operate solar subsystem components and miscellaneous support buildings and equipment. This design point staircase does not include operation of the fossil energy source, which requires some energy for induced and forced draft fans, and fuel pumps. The net power output from the system at the design point with a total of 5000 heliostats gives 60 MWe net, with 8.9 MW_t going to the storage system.

The annual system performance was evaluated using the STEAEC computer model, which simulates the performance of the system using 15 minute time steps and a site weather data tape. For the site weather data (insolation, wind speed and direction, temperature and pressure), the SOLMET Typical Meteorological Year (TMY) weather data base was chosen. As no TMY exists for the Saguaro site area, the TMY data tape for Phoenix, AZ was used. Phoenix, AZ is approximately 143 km (89 mi) northwest of the Saguaro site. This SOLMET data yields an average daily direct normal insolation value of 6.9 kWh/m²-day. Other data indicate 30-year averages as high as 7.6 kWh/m²-day. Actually, because of the higher site elevation, lower pollution levels, and lower humidity levels, the insolation at Saguaro should be slightly greater than that of Phoenix.

The STEAEC computer model simulated annual performance is shown in Figure 1.5-2 and provided predictions of various solar subsystem losses under hourly operation. The predicted annual energy produced from the solar plant of 149708 MWh_e (not including scheduled or forced outages) results in a solar plant capacity factor of 0.285. The annual average efficiency of converting solar insolation to net electrical energy is 20.6%. As currently coded, the STEAEC computer model discharges storage immediately for power production (immediate dispatch). Therefore, in the annual energy staircase, only 10154 MWh is directed to storage resulting in low usage (15 fillings/yr) of the 688 MWh_t of thermal storage capacity. In our proposed dispatch scenario more energy would be directed to storage due to the daily delay in the start of the turbine with respect to the start of collection of solar energy. Thus, in a daily start delay operating mode, the yearly energy to storage will be higher than Figure 1.5-2 indicates.

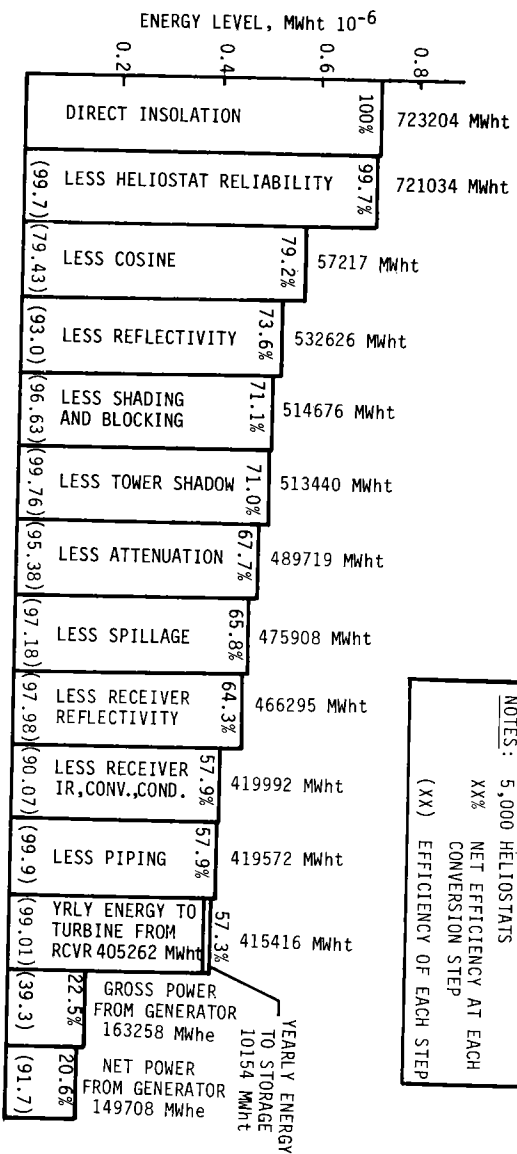
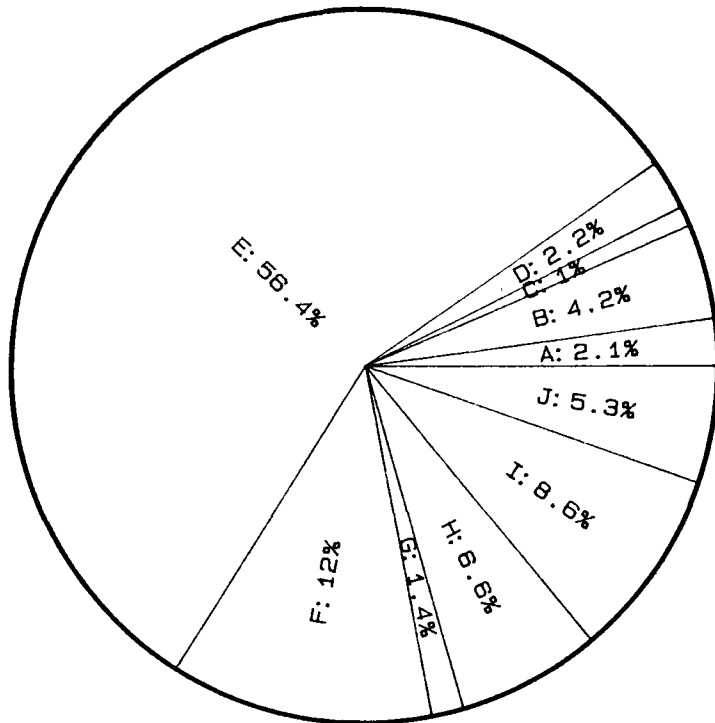


Figure 1.5-2 Annual Efficiency for 60 MWe Solar Plant

1.6 ECONOMIC FINDINGS

The Advanced Conceptual Design for Solar Repowering of the Saguaro Power Plant costs were estimated in four discrete elements: preliminary and detail design engineering costs, construction costs, owner's costs, and operating and maintenance costs. For engineering, construction, and operating and maintenance costs, estimates were made for each subsystem comprising the total repowering system including all necessary interfaces with the existing fossil unit. In as many cases as practical, estimates were developed by obtaining vendor quotations for major components commercially available; costs incurred on solar-related hardware procurements for past and on-going Subsystem Research Experiments (receiver, thermal storage) and the Barstow Pilot Plant (heliostats) were used as a basis for solar components. Figure 1.6-1 summarizes the project implementation costs, in 1982 dollars, where project implementation costs are defined as all costs expended up to and including system checkout.



A=PREL. ENGRG.	- \$2856
B=FINAL ENGRG.	- \$5724
<hr/>	
C=SITE PREP.	- \$1214
D=SITE FACILITIES	- \$3044
E=COLLECTOR S/S	- \$75540
F=RECEIVER S/S	- \$16124
G=MASTER CONTROL	- \$1968
H=THERMAL STORAGE	- \$8794
I=EPGS/HEAT EXCH.	- \$11506
<hr/>	
J=OWNER'S COSTS	- \$7115
TOTAL	= \$ 133885

Figure 1.6-1
Saguaro Solar Repowering Project Implementation Cost (1982 \$x 1000)

As shown in the figure, the design engineering effort accounts for 6.3% of the total project cost, or \$8,580,000. The total construction cost estimate, accounts C through I in the figure, is \$118,190,000. Of this cost 64% is in the collector subsystem, which is comprised of 5000 Martin Marietta improved second generation heliostats. Detailed cost estimates for each component of the heliostat and collector subsystem were developed from production process plans and heliostat component lists for a 4000 per year production rate, yielding an installed heliostat cost of \$263/m², or \$75,540,000 for the collector subsystem. The owner's cost of \$7,115,000 includes land rights, environmental studies and permits, utility project management, and taxes and insurance during construction. Allowance for funds used during construction is not included in these estimates.

The annual operating and maintenance expense associated with the solar repowering system is estimated to be \$1,441,000 per year (1982 \$). Of this cost, 33% is due to additional operators (13 total personnel) at the Saguaro plant for solar operations; 31% is maintenance personnel expenses associated with the solar repowering plant. The remainder of the estimate is materials and spare parts for the solar subsystems.

To convert these cost estimates to an appropriate measure of the solar repowering project cost for use in economic analyses, each component of the project cost was escalated at 8% per year to the period of expenditure as set forth in the development plan schedule. This is shown in Figure 1.6-2, where the appropriate escalated cost estimate by major task is shown. The total project implementation cost is the sum of the escalated yearly expenditures, or \$171,126,000, which is used in the following economic analyses.

COSTS IN THEN YEAR DOLLARS (\$000)

	1982	1983	1984	1985	1986	TOTAL
Preliminary Design	\$756	2,359				3,115
Detailed Design		1,637	5,105			6,742
Permits	\$320	327				647
Construction *			27,608	121,866	9,107	158,581
Checkout					2,041	2,041
TOTAL YEARLY OUTLAYS	\$1,076	4,323	32,713	121,866	11,148	\$171,126

* Not Including AFUDC

Figure 1.6-2 Total Escalated Project Implementation Cost
(Then-Year Dollars x 1000)

The economic analysis of the Saguaro repowering project examined the value of the project in comparison with the total project costs (implementation and operation). The value of the project is based on two discrete benefits: predicted fuel displacement on the APS system over the project demonstration period; and the value associated with demonstrating a cost-effective future utility generation alternative--Solar Thermal Central Receiver technology.

The value of fuel displacement on the APS system was quantified utilizing standard utility production cost computer programs. These programs model the dispatch of the various generation units in the system to meet the projected load demand. The fuel savings resulting from repowering were determined by taking the difference in annual fuel expenses incurred to meet the projected load demand without repowering and the annual fuel expenses incurred with Saguaro Unit One repowered by solar. In this analysis, the solar contribution was based on projected solar output from the STEAEC simulation program using Phoenix insolation data, yielding hourly net electrical output, which was then shifted to maximize fuel displacement value through the use of the solar storage capacity. This solar energy contribution to the system was then modeled in the production cost program by a decrease in the hourly load demand.

The result of this analysis was that, on the APS System in the 1987-1996 time frame, the solar repowering project displaces a yearly average of 131 GWHe of fossil-fired generation and purchased power. The repowering plant did not displace its full 144 GWHe annual electric output due to system reserve requirements necessitated greater utilization of pumped storage, averaging 13 GWHe/yr, or 9.4% of the possible energy displacement due to solar. Of the fossil-generated energy displaced, 47.6% was coal generation (62 GWHe/yr) and 52.4% oil-fired generation (69 GWHe/yr).

In order to compare the fuel displacement value of the repowering system in relation to the project cost, the yearly fuel displacements were discounted to 1987 (year of first operation of the project), using the current cost of capital for APS of 14.5% as the discount rate. The results of this calculation, which yields cumulative present worth of fuel displaced as a function of number of years of solar operation, are shown in Figure 1.6-3. As shown in the figure, approximately half of the fuel displacement value is due to displacing coal. Over the assumed 10 year solar demonstration period, the total present worth of the fuel displaced is \$33.0 M, in 1987 \$.

With the present worth of fuel displaced according to APS dispatch analysis, the project implementation cost in 1987 \$, and calculating the present worth of 10 years of solar operating and maintenance expenses escalating at 8% per year, the direct economics of repowering Saguaro at 60 MWe can be assessed. A summary of this assessment is presented in Table 1.6-1.

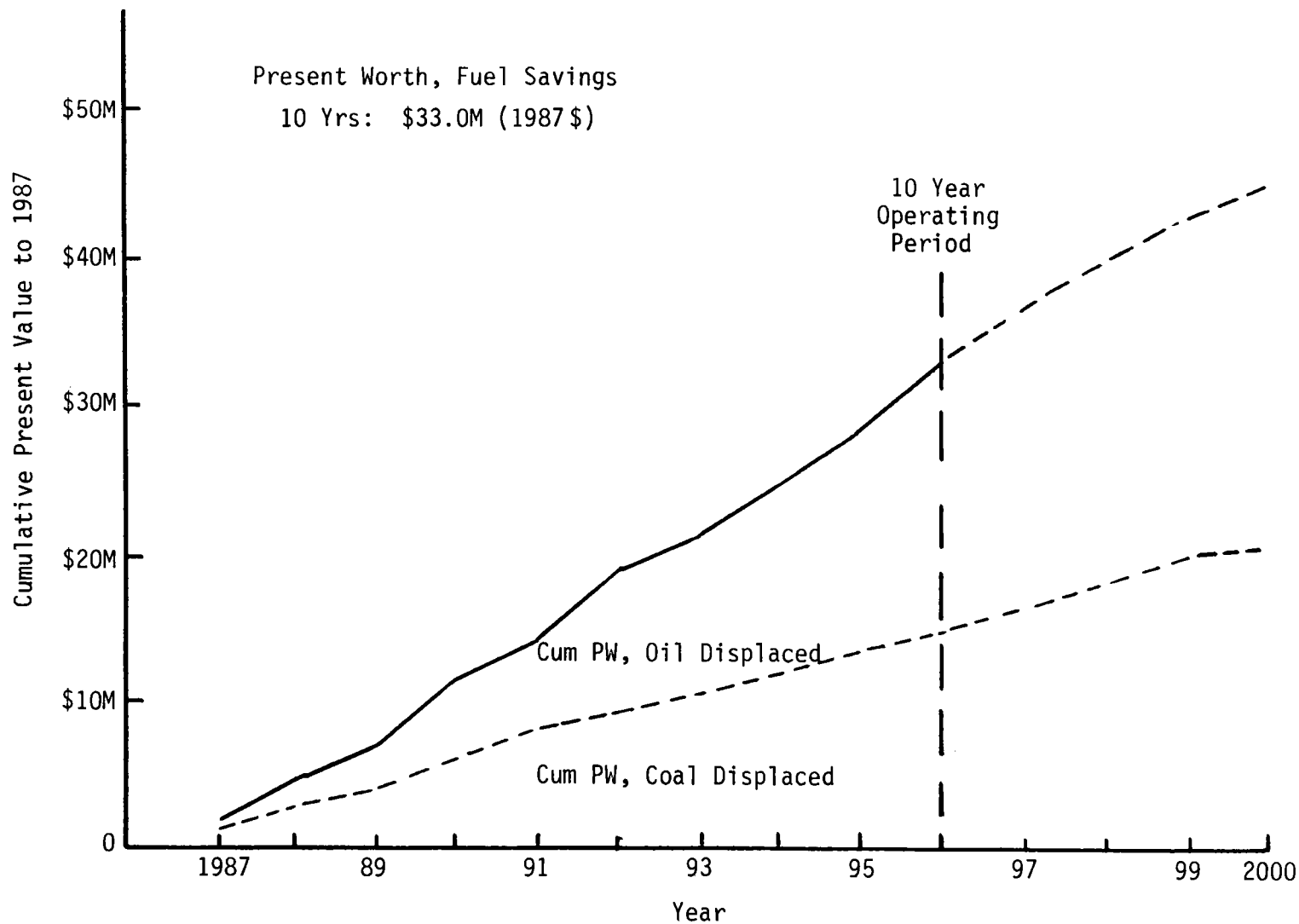


Figure 1.6-3 Cumulative Present Worth of Fuel Displaced, March 6, 1981 Forecast (1987 \$)

Table 1.6-1 *Saguaro Solar Repowering Economics - 10 Year Operation (1987 \$)*

SAGUARO REPOWERING PROJECT COST	
Construction Cost (Excluding AFUDC)	\$171.1M
Present Worth, O&M Expenses	15.7M
TOTAL PROJECT COST	<u>\$186.8M</u>
SAGUARO REPOWERING PROJECT FUEL DISPLACEMENT	
Present Worth, Assuming 100% Oil Displacement	\$ 92.2M
Present Worth, APS Dispatch Analysis	\$ 33.0M
Present Worth, Assuming 100% Coal Displacement	\$ 17.8M
NET SAGUARO REPOWERING PRESENT WORTH	
100% Oil Displacement	(\$ 94.6M)
APS Dispatch Analysis	(\$153.8M)
100% Coal Displacement	(\$169.0M)

As shown in the table, the net present worth of the Saguaro Repowering Project, defined as project cost less fuel savings, is \$-153.8M (1987 \$) using the fuel displacement predictions based on APS system modeling. Also shown in the Table are upper and lower limits on possible fuel savings. The upper limit was assumed to be a 100% oil displacement case, using oil cost of \$5.19/MBTU (1982 \$) escalating at 9%. This case reduces the net project present worth cost approximately \$59M. The 100% coal case, the lower bound on fuel displacement value, utilizing \$1.00/MBTU coal escalating at 8%, increases the net project cost by about \$15M.

However, as mentioned earlier, the Saguaro Repowering Project will have value in terms of the overall solar thermal central receiver program -- demonstrating large-scale technical feasibility of STCR technology in a utility environment, thereby reducing technical and economic uncertainty (risk) to utilities, and providing a renewable central-station generation alternative for future utility expansion. As part of the economic analysis of the Saguaro project, an approach utilizing risk analysis and probability assessment was formulated and implemented to quantify, in present worth terms, the value associated with demonstrating STCR technology.

Basically, this demonstration value assessment considered seven market scenarios for 100 MWe-3 hr storage standalone STCR plants coming on line in 1991. Three of the scenarios dealt with the costs and number of STCR plants assuming a successful Saguaro repowering demonstration. The remaining four scenarios looked at the possible STCR market without repowering. One of the scenarios was a 100% fossil-fired alternative. The market, in each case, was limited from 1 to 4 STCR plants, with associated heliostat costs based on market size. The total potential market is much larger, but only the first increment was considered in these scenarios.

After defining the market, expected levelized busbar energy costs (BBEC) were determined for each scenario, where the relevant parameters for the cost and performance of the STCR plants (construction costs, O&M expenses, annual output and plant life) were varied and assigned probabilities commensurate with the uncertainty level with and without repowering.

By combining the expected BBEC for each scenario with the scenario probability, expected costs of electricity with and without repowering were obtained, as well as an expected amount of solar-generated electricity. The difference between the two costs of electricity times the net solar generation can be thought of as the expected value of the repowering demonstration. Specifically, the expected BBEC of the "with repowering" scenarios was 13.1 cents/kWh (1982 \$), with 934,000 MWh annual solar generation; without repowering, the expected BBEC was calculated as 16.2 cents/kWh. Over the life of these plants, the net present worth in 1987 of ratepayer savings is \$230M (1987 \$).

The overall economics of the Saguaro repowering project, considering both the fuel displaced and a "demonstration value" are summarized in Table 1.6-2. Thus it can be seen that, for the "middle-of-the-road" set of probability assumptions used, the Saguaro repowering demonstration has a significant positive value to the people in the United States. The value extends beyond APS's service area as APS will not be the only builder of STCR systems in the 1990's and beyond.

Table 1.6-2 Saguaro Solar Repowering Project Economics Summary (1987 \$)

Saguaro Repowering Project Cost	(\$190M)
Present Worth, APS Fuel Displacement	\$ 30M
Net Present Worth, Saguaro Project	(\$160M)
Present Worth, Future Ratepayer Savings	\$230M
Net Present Worth, Repowering	\$ 70M

1.7 DEVELOPMENT PLAN

The Arizona Public Service Company approach to a development plan for a solar repowering of its oil/gas fired Saguaro Power Plant, includes all activities in the process from this advanced conceptual design study to completion of checkout and evaluation and through operational experience. The major objective of the development plan is successful completion of a demonstration plant, which incorporates in its design the results of directly associated development activities. The development plan presents six programmatic activities, each of which can be related to a distinct project phase occurring in chronological order. These activities are identified as:

- 1) Design Phase,
- 2) Final Engineering,
- 3) Construction Phase,
- 4) System Checkout and Startup Phase,
- 5) System Performance Validation Phase,
- 6) Joint User/DOE Operations Phase.

Recognizing that a first-of-a kind demonstration plant requires design input from on-going, planned, and recommended development activities, the prior study (Ref 1-2 and -4) itemized a set of development activities. Most of those activities have been, or soon will be complete, only a few remain to be done. First is the need to develop bearings and seals for horizontal shaft pumps. This type of pump will be used for the main circulation and booster pumps. The materials development work must be continued in order to reduce inconsistencies in the current data and to identify a cheaper material for the evaporator. The Molten Salt Electric Experiment which is proposed for the CRTF is highly desirable, but is not mandatory. It will reduce uncertainties concerning design and operation of the master control subsystem. It would be helpful to do some mirror assembly exposure and cleaning tests at the Saguaro site. However, the mirror assembly tests are not necessary. Some of these development activities could be made a part of the Saguaro design phases.

It was determined that the critical construction path included heliostat procurement in terms of supporting subsystems design, procurement, and construction activities. Consideration of these scheduling factors led to a detailed project schedule with overlapping activities in the prior study (Ref 1-2). The plan is a phased program, with distinct milestones such as preliminary and critical design reviews identified. These review points constituted decision points prior to the start of major construction activities. The plan, as now conceived, does provide for the start of site preparation and procurement of heliostats prior to the design reviews. Delay of these activities until after the design reviews will result in lengthening the overall schedule. These programmatic risks must be assessed prior to finalizing a schedule and initiating construction.

Figure 1.7-1 shows a schedule and milestone chart that embodies the details given in the prior study project master control network but which has been rescheduled based on our current estimate of a likely start date. This network will serve as a framework for a project critical path method, which was developed for construction management. All items that impact program schedule have been identified. Inputs to the development plan from all team members were factored into the subsystem schedule in terms of design, procurement, and construction.

Finally, the development plan discussed a suggested framework for project organization, and the respective responsibilities of the user and DOE. Figure 1.7-2 shows the suggested organizational framework from the prior study.

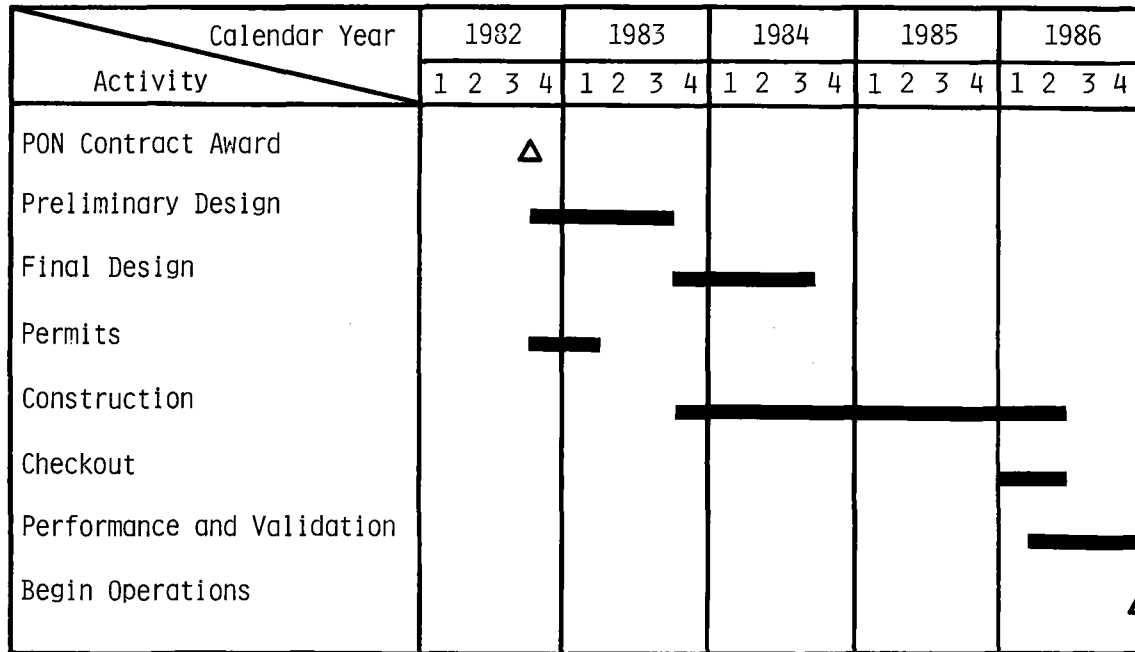


Figure 1.7-1 Development Plan Schedule

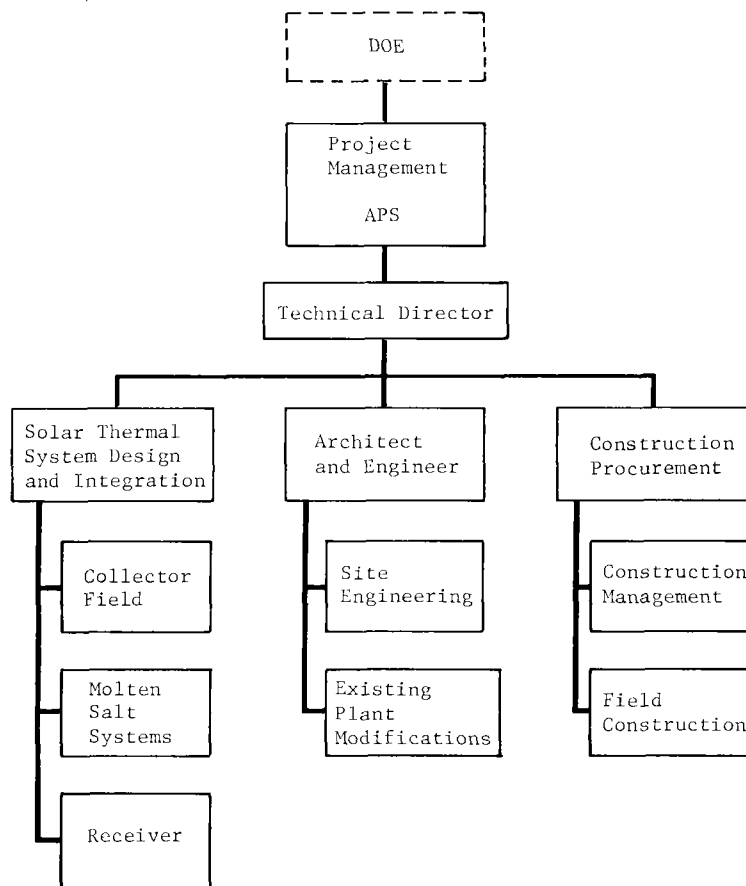


Figure 1.7-2 Project Organization Chart

Arizona Public Service Company undertook the prior conceptual design study with the objectives specified in the contract scope-of-work; namely, maximize fuel savings with minimum capital cost. Recognizing that these requirements are normally opposed to each other, study methodologies were directed towards determining the optimum level of repowering Saguaro with storage on the APS system that would result in a meaningful demonstration. At the outset of the study, a minimum 40 MW_e net repowering level was to be the lower bound for the analyses; however, after analysis of the operating system and the objectives of the repowering project, a minimum repowering level of 60 MW_e was determined. This size was judged to be the lowest practical repowering level that would have any measurable impact on the system, and produce cost and operating data for designing a commercial plant. The current advanced conceptual design study has emphasized the minimization of investment risk while maintaining a capability to demonstrate all significant parts of the molten salt technology as applied to standalone and hybrid solar thermal central receiver power systems.

Engineering design and investment risk were optimized at a repowering level of 60 MW_e net with 4 hours of thermal energy storage. All demonstration objectives can be satisfied and fuel displacement is greater than estimated operating and maintenance costs with this level of repowering. APS has concluded that these findings fully satisfy the project objectives. A solar module of the 60 MW_e size would be of great benefit since it would demonstrate a large solar power module directly scaleable to commercial sized solar thermal central receiver power plants. Economic considerations will govern the final design and size of the demonstration project. The following assessment refers to the selected plant size for repowering the Saguaro Plant and is the minimum size in terms of funding a demonstration to establish technical feasibility.

At the 60 MW_e solar repowering level, with 4 hours of thermal storage, fossil fuel displacement was maximized for an present worth fuel savings value of \$22.5 million in 1982 dollars, based upon ten years of operation on the APS system. The repowered Saguaro system design takes advantage of the excellent site characteristics and the manner in which the repowered unit is used in the APS utility grid. Using molten salt as a heat transfer and storage medium is shown to be very cost effective on the APS system as exhibited by the amount of fuel oil displacement. Maximum value of electrical power generated by the solar thermal system can be realized through economic dispatching in the APS grid when inexpensive molten salt sensible heat storage is incorporated into the design.

A relatively simple solar to non-solar interface has been designed so as to not impact the Saguaro Plant fossil-fired operations nor to reduce its future availability. All interfaces with the plant will be accomplished when Saguaro is down for its major overhaul, which coincides with the construction schedule developed for the solar repowering plant.

The solar repowering conceptual design provides operational flexibility to meet changing APS requirements. Our study indicates that if APS load demands increase at a rate greater than forecasted, the solar repowered plant will have a corresponding increase in the value of fuel displacement. In any case, the system design provides the flexibility through optimum plant dispatch to continue maximizing fuel displacement. Of primary importance is the fact that the demonstration plant size must be large enough to impact system dispatch strategy (e.g., approximately 1 percent of total system capacity). Smaller demonstrations have considerably reduced value and would not satisfy the national objective for a demonstration repowering project. It is for these reasons that a 60 MWe (or 1.4% of the total system capacity) repowering level was selected.

The concept in this design is applicable to many repowering applications in the Southwest where the majority of the candidate turbines are non-reheat systems. In addition, the concept can be extended to reheat applications using the same molten salt technology. The use of molten salt has been demonstrated to be safe and relatively free of operating problems when compared with a water/steam system.

The Saguaro Power Plant site was selected primarily because of land availability and secondarily because the plant offers the opportunity to demonstrate the feasibility of repowering oil fired units at a minimum first cost. If, as projected, heliostat costs approach the \$100 to \$120 per square meter level, Unit Two of the Saguaro station would become a candidate for solar repowering and a second collector field could be built to bring the solar repowering level of Unit One up to its rated capacity of 111 MWe net. More important is the fact that APS views the demonstration of repowering as a stepping stone to commercial solar standalone plants on its systems. The Saguaro site, and the Bouse site (located 177 km (110 mi) west of Phoenix), because of land availability and excellent solar insolation offer good potential for solar standalone plants.

In the 1990-2000 time period APS and other utilities will have to draw more heavily upon coal and nuclear as energy sources, provided that environmental and economic conditions do not eliminate them from consideration. Solar thermal electric plants can offer a good alternative; provided that economics and solar plant feasibility are demonstrated in the 1980 decade. Alternatives to solar repowering are considered to be synthetic fuels, which are assumed to be on a faster development demonstration course than solar. The same market conditions (the uncertainty in the cost of fossil fuels) are influencing synthetic fuels as well as solar. It is impossible to predict future world market fuel costs with precision. However, considering only the need for generating resources for the southwest region, solar thermal electric power plants have a high probability of being economically competitive. The higher initial cost of the solar system remains a first cost which can be recovered without the impact of escalation of world market fuel costs.

The economics of repowering can be realized only if the institutional and regulatory considerations are properly applied. This issue can only be resolved by submittal of a financial plan to the proper State Regulatory Commission. For the Saguaro project, APS must detail the degree of financial exposure, and the benefits expected to be gained by its customers and shareholder-owners. Other than this major issue, all other issues such as environmental impact assessment, and the obtaining of required construction permits are considered to be solvable within reasonable limits of time and effort.

In summary, APS believes that the results of this advanced conceptual design study are strong evidence that solar repowering can be successfully and economically utilized in our power generation system.

Proceeding with a vigorous solar repowering demonstration program will be convincing evidence of the merits of solar repowering as a vital step toward achieving solar standalone plants. Furthermore, this study, because of specific data, has established a reference of plant costs and economics, which when proven by actual construction, will be a sound basis for further plans for solar plants.

Study Title: Advanced Conceptual Design for Solar Repowering of the Saguaro Power Plant.

Contract Number: DE-AC03-81SF11570

Contract Cost: \$239,214

Period of Performance: September 30, 1981 through April 30, 1982

Prime Contractor: Arizona Public Service Company

Principal Investigator: Eric R. Weber

Mailing Address: P. O. Box 21666
Phoenix, AZ 85036

2.1

STUDY OBJECTIVES AND APPROACH

The solar thermal technology, site, and specific unit for repowering were selected in prior analyses and studies. The objectives of this advanced conceptual design study were to: (1) incorporate the most recent technical developments of solar central receiver components, subsystems, and other elements into the conceptual designs; and (2) ensure that performance estimates for the advanced conceptual design are based, to the maximum extent possible, on performance characteristics of commercially available equipment. We have satisfied both of these objectives and, through our approach of using low cost thermal energy storage, we will provide the electric power dispatch flexibility needed to maximize the value of the fossil energy that can be displaced. Additionally, a significant consideration throughout the study was the desire to maximize the probability of successful operation of the repowered system. Whenever there was a choice between a risky advanced technology and a more conservative approach, the conservative approach was taken. A failure in the repowering program that could result in a serious setback for this solar thermal technology that can contribute so much to relieving our nation's energy crisis must be avoided. The resulting conceptual design is technically achievable by 1986.

The overall approach taken in this advanced conceptual design study was to start with the concept from the prior Saguaro repowering study (Ref 1-1, 1-2, 1-3, 1-4), reduce the repowering level to 60 MWe, incorporate the results of work done between the two studies, and refine the subsystem designs. The result is an economically attractive and operationally viable solar thermal repowering system concept for the Saguaro power plant. This approach drew on the full talents of the APS team to develop an optimized design according to the following progression of effort:

- 1) Refine performance and design requirements;
- 2) Incorporate the results of new work;
- 3) Refine the conceptual design;
- 4) Identify interface requirements with Saguaro Unit One;
- 5) Evaluate the concept for operability in the APS grid;
- 6) Prepare plant performance estimates;
- 7) Generate detailed costs for the repowered plant.

For those parts of the concept that involve molten salt and the solar systems, we were able to draw heavily on prior and concurrent work by the various team members (see Chapter 7.0 References). This work provided a base on which to build and a reference for evaluation of the elements of the repowering concept as the design progressed.

The above steps provided a systematic method for development of a best site-specific design based on minimum cost, operational viability, and construction by 1986. The specific end-products developed and documented in this study are:

- 1) A definition of the repowered system requirements (Subsystem Requirements of Chapter 5.0);
- 2) A series of trade studies that led to the selection of the Saguaro-specific system configuration (Chapter 3.0);
- 3) A site-specific conceptual design with performance and cost estimates (Chapter 4.0);
- 4) Documentation in the form of monthly and final reports.

The analyses and conceptual designs presented in this final report satisfy the objectives stated in section 2.1. The result is a Saguaro-specific conceptual design that will provide an excellent

demonstration of advanced solar thermal central receiver technologies. That demonstration can help United States utilities to accept and promote solar thermal central receiver technology as a part of their planning starting in the 1990s.

The study was performed in two tasks. Task 1 - Refined Baseline Conceptual Design--included all of the technical analyses and Task 2 - Program Management--involved management, coordination, planning, travel, preparation, reproduction, and distribution of the study reports. The trade studies of Task 1 resulted in our selection of a 60 MWe net repowering level for detailed analysis and justified the value of storage for dispatch. The functional requirements of the prior study (Ref 1-2) were reviewed and updated to suit the 60 MWe repowering level. Generally net power level is used in this report except when gross power level is explicitly stated.

The system configuration was also updated as part of the Task 1 effort along with a definition of the subsystem interfaces. Conceptual designs were prepared for five of the seven major subsystems. No new work was done on the fossil energy or electric power generation subsystems as they have not changed. A recommendation for the upgrading of their control systems to use equipment compatible with the rest of the master control subsystem was proposed. Plant performance was established both at the design point of noon summer solstice and on an annual basis. The annual performance was calculated using the STEAEC computer program. Data for the repowered plant was entered into the SOLTES computer program for later evaluation. Cost estimates for the total plant including engineering, construction, owner's and operating and maintenance costs were also prepared. The economic assessment of plant value was determined in terms of 100% coal and 100% oil displacement and computer simulation of energy displaced on the APS system using forecasts of APS loads and generation resources. An estimate of the value of using Saguario to demonstrate a commercial sized solar thermal central receiver power plant using molten salt technology was prepared.

2.2 TECHNOLOGY SELECTION AND GENERATION UNIT SELECTION

The technical approach and repowered unit were selected by APS well before the 1979 repowering RFP was issued. The molten salt technology potential was identified as part of the Martin Marietta Advanced Central Receiver Power System Phase I study (Ref 2-1)*. The Saguario Unit One was identified as a strong candidate during the Public Service of New Mexico Technical and Economic Assessment of Solar Hybrid Repowering study (Ref 2-2). These two selections were combined into the excellent repowering project described here.

2.2.1 Solar Technology Selections

The basic solar technology to be selected from within the various solar thermal central receiver alternatives involved the receiver heat transport fluid. Four fluids were considered--water/steam, molten salt, sodium, and air, or a combination of air and water/steam. These four technologies have been addressed by DOE contractors in the Solar Central Receiver Hybrid Power System studies (Ref 2-3, -4) and in the Advanced Water/Steam Receiver studies (Ref 2-5). Our team members were involved in both of these study programs. As a result, the molten salt technology was selected for the reasons emphasized below.

Water/steam technology has the major advantage of being a fluid familiar to utility people. However, its thermal energy cannot be conveniently stored, system thermal efficiency is lower for the stored energy, it is more susceptible to cloud cover transients, and it requires special considerations for reheat turbines. Sodium has good thermal conductivity, which reduces receiver size. There is a large body of material data and equipment designs from various nuclear programs. However, sodium presents serious safety concerns and appropriate precautions must be taken. Unfortunately,

*See Chapter 7 for references.

these precautions and the related equipment are expensive. Also, sodium has a high cost per megawatt-hour of thermal energy stored. The use of air at high temperature as the working fluid in a combined cycle system promises the high thermal efficiency of the combined cycle and thus, lower collector field costs. However, demonstration of the high thermal efficiencies will not be achieved by 1986 due to unsolved receiver materials problems and because difficulties still remain in minimizing the effects of pressure losses in the interconnecting piping. As with the water/steam systems, the cost of storing energy is high and there is a loss in efficiency when operating from stored energy for hot air systems. Our evaluation of recent work on these competing technologies has not changed our basic commitment to the use a molten salt for the receiver heat transport and storage medium.

A number of occurrences since the first Saguaro repowering study have reinforced our decision to use molten salt as the receiver working fluid. A test version of a molten salt receiver was designed, built, and tested at the CRTF in Albuquerque, NM (Ref 2-6,2-7). The tests were very successful including the ability of the controlled receiver to operate satisfactorily through major cloud transients. A significant amount of work on materials compatibility with molten salt has been done, e.g. Ref 2-8 and 2-9, and this work is continuing. In particular 304SS has emerged as a useful material for containing hot salt and materials have been identified for gaskets, pump seals, and valve seats. A study, Molten Salt Steam Generator Subsystem Research Experiment, Phase I, is being conducted by Babcock and Wilcox that examines the design and fabricability of steam generators using molten salt as the heat transport fluid. The results of that study have been incorporated in this work. Another study, Molten Salt Receiver Subsystem Research Experiment, is being conducted by Babcock and Wilcox that examines the design and fabricability of molten salt quad cavity receivers. The ongoing analyses and considerations of that work were factored into our receiver design work. These activities plus other work by Sandia National Laboratories Livermore, Ca. and others indicate that molten salt is a preferred working fluid for solar thermal central receivers.

The receiver and energy storage fluid selected is a salt mixture consisting of 60% NaNO_3 and 40% KNO_3 by weight. This salt was chosen for the advantages listed in Table 2.2-1 and Ref 2-1. Molten salt is a key to solving a major problem of every solar system-- what to do when the sun goes down. Salt can be stored efficiently at a high enough temperature that the turbine does not know whether its thermal energy came directly from the receiver or through storage. The single phase use of salt--it is only used as a liquid--simplifies the receiver, storage, and piping system designs as there is no boiling in the receiver or freezing in storage. The salt has negligible vapor pressure, is basically safe, and has been used extensively for many years by the chemical industry (Ref 2-10). It must be treated with care, as one would treat any hot fluid. Any system leaks tend to result in the salt freezing quickly with minimum safety or environmental impact concerns.

Table 2.2-1 Advantages of Molten Salt Central Receiver Systems

Significantly Lower Cost Than Water/Steam Systems Because:

- Simple, Single Phase Receiver (Creep-Fatigue Effects on Receiver Are Minimized),
- Significantly Improved Performance from Storage (No Degradation of Steam Conditions),
- Very Compatible with Repowering,
- Low Cost Molten Salt Ingredients (\$0.412/kg),
- Excellent Heat Storage and Transport Media,
- Lighter, Lower Cost Piping
- Excellent Applicability to Reheat Turbines

Safety Considerations:

- Does Not React with Air or Water,
- Commonly Used in Open Baths for Heat Treatment.

Over 30 Years' Experience Using Molten Salt Heat Transfer Systems in the Chemical Industry

- High Reliability, Low Cost Components are Readily Available

2.2.2 Generation Unit Selected for Repowering

The major factors considered in the selection of an APS generation unit for solar repowering included:

- 1) Power level
- 2) Fuel type
- 3) Insolation level
- 4) Available land area
- 5) Unit age
- 6) Unit condition

Power level was considered from a number of different points of view. When one considers the repowering program as a demonstration for solar thermal standalone plants, then the upper limit of current generation unit practice--500 MW_e--should be considered. This level can be compared with the 10 MW_e solar pilot plant in Barstow, CA and it is recognized that a 50 to 1 scale up in plant size might be too large. However, if two steps are used, 7 to 1, then the steps are not too large. This implies an initial repowering size of 70 MW_e. Prior repowering studies have indicated that there is a large repowering market with most of the units being within a 3 to 1 ratio from the 70 MW_e level. With regard to the APS need, size can be considered with respect to the estimated APS peak load demand of 3731 MW_e in 1987. The APS dispatch center has estimated that for a unit to be properly considered for dispatch, the unit should be at least 2% of demand load. This would imply 60 MW_e for most days of the year. Combining these three considerations together resulted in a requirement for a unit that could be solar repowered to at least 60 MW_e.

The second factor considered was fuel type. The Powerplant and Industrial Fuel Use Act of 1978 requires that all oil/natural gas use by utilities be stopped by 1990 with certain exceptions. One of the exceptions is use of gas or oil in conjunction with a renewable energy source, such as solar. Thus the solar repowering of an oil/gas fueled unit would fit in with APS's response to the Fuel Use Act. So only units burning oil or natural gas were considered.

The third factor considered was insolation level. Solar insolation is excellent in the southern and western parts of the APS service area and is not as good in the higher northeastern region.

The fourth consideration was available land. The 60 MW_e repowering requirement implies a land area in excess of 1.3×10^6 m (0.5 sq. mi). When the above four requirements are applied to the APS generation units, the Saguaro generation station was found to be the only station with acceptable units. Fortunately, as will be seen in the remaining parts of this chapter, it is an excellent choice.

The Saguaro station has four oil or gas fired generation units, Units One and Two are steam-Rankine, and the other two units are combustion turbines. Unit One was built in 1954 and was upgraded in 1975 to 115 MW_e net (Ref 2-11). Unit Two was built in 1955 at a rating of 99 MW_e. Unit One was selected for repowering because of the 1975 upgrading and because the specific location of the steam and water piping makes its integration with the solar system simpler. Due to the desire for repowering simplicity, it is fortunate that Unit One does not have a reheat capability. However, reheat can be readily incorporated into the selected solar concept simply by the addition of a fourth heat exchanger, so the absence of reheat does not limit the application of the technology to reheat type turbines in the future. Thus, the absence of reheat simplifies the design, which is appropriate for a first demonstration system.

2.2.3 Primary Solar Subsystem Characteristic Selection

Our prior solar central receiver system studies have indicated that there are advantages to multiple collector fields for large solar standalone plants. These advantages are not as likely to exist for repowered plants where the existing geography and man-made objects must be accommodated.

Our preliminary analyses indicated that a single surrounding collector field of up to 15,000 second-generation heliostats could be fitted within the existing geography at Saguaro and that a single surrounding field would result in the shortest piping runs. While the length of piping depends on field size and tower location within the field, the piping is on the order of 1.6 km, (1 mi) long. This length indicates the need for a careful evaluation of costs, insulation effectiveness, pressure losses, thermal expansion, and drain provisions.

Martin Marietta's prior solar work has shown the advantages of cavity receivers as opposed to external receivers (Ref 2-1, 2-3, 2-4, 2-5). In addition to the thermal efficiency advantages, the ability to close the cavity doors and reduce heat leaks at night means that the receiver will not have to be drained as often as an exposed receiver would.

The combination of higher efficiencies and operational flexibility led to a primary choice of a quad-cavity configuration for the receiver. This choice was substantiated by a trade study in the first Saguaro study (Ref. 1-2).

Initially it was felt that a solar thermal energy system would be ideally suited to the APS load demand profile as that profile includes a great deal of air conditioner use that is time-coordinated with the solar energy resource. However, the air conditioning load lags the solar energy resource due to the thermal capacity of buildings, streets, etc. This meant that the concept should have an ability to store energy in the morning for later use in the evening. Thus the provision for a moderate amount of energy storage. Thermal energy storage has another major advantage, it decouples the collection of solar energy from its use in generating steam. This means that the turbine will not see cloud cover transients, the pumping systems can be decoupled, the control systems are decoupled, and the operations of solar energy collection and turbine power generation are almost independent.

The solar thermal energy steam generator approach parallels the fossil fuel steam generator except that hot salt is used as the heat source instead of fossil fuel. This is shown in the system schematic of Figure 2.2-1. The figure shows the collector field, receiver, salt circulation pumps and hot and cold salt storage tanks. The decoupling between receiver and solar steam generator can be readily seen in the figure. The solar steam generator takes the form of a superheater, boiler, and preheater in a counterflow configuration. This is a most effective way to transfer heat from the molten salt to the water and steam. Figure 2.2-1 also shows the existing steam turbine and generator as well as how the solar and fossil steam systems are interconnected at the main steam line and at the feedwater heater outlet.

To ensure the capacity credit for the existing plant is not lost, the system has been conceptualized so that the fossil system can continue to be operated as it was before the solar system was added. As our analyses progressed, it was found desirable to provide for solar alone and combinations of solar and fossil operation. The result is a concept that provides for steam generation by operation of fossil alone, solar alone, or a combination of solar and fossil in selectable proportions.

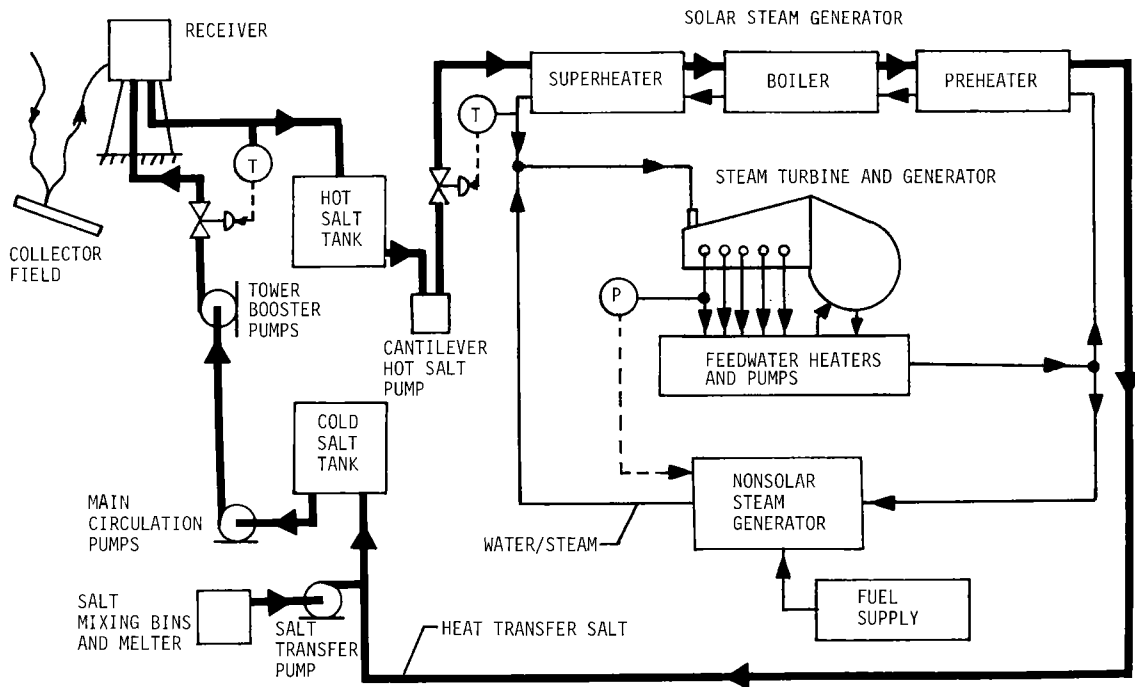


Figure 2.2-1 Repowering System Schematic

2.3 SITE LOCATION

The Saguaro Station is located in southeastern Arizona on Interstate 10 approximately 143 km (89 mi) southeast of Phoenix, AZ, and 43 km (27 mi) northwest of Tucson, AZ (see Fig 2.3-1). The nearest community to the Saguaro plant is Marana, AZ, which is 15 km (9.3 mi) to the southeast. The plant is located in Section 15 of Range 10 East, Township 10 South of the Red Rock, AZ quadrangle.

2.4 SITE GEOGRAPHY

Arizona Public Service Company owns 3.88×10^6 m² (960 acres) with the western 1.29×10^6 m² (320 acres) being presently occupied by the Saguaro station. The eastern section, 2.59×10^6 m², is unused. The solar system heat exchangers and energy storage tanks would be located adjacent to the existing Unit No. One fossil steam generator within the plant boundaries. The collector field would be predominantly located on the eastern section (14) of the APS property (see Fig. 2.4-1). However, there would be some overlap of the collector field onto section 11 of the Red Rock quadrangle. This section (11) is owned by the State of Arizona as State Trust Land and is leased for cattle grazing. A request was sent by APS to the Arizona State Land Department to reserve three sections of land (11,12 and 13) for APS lease and use. The State Land Commissioner has acknowledged and recorded the request. APS has leased land from the state before. Additionally, the State of Arizona is very active in promoting and using solar energy and is very responsive to solar energy projects.

The terrain is basically flat desert land that slopes up slightly to the east and a little to the north towards the Tortolita mountains. The existing vegetation is low and sparse brush and cacti. There are a few shallow washes for drainage. There is no free ground water and soil moisture is very low. The soils underlying the site consist of a surface stratum of clayey sand and sandy and silty clay of low to medium plasticity. Additional specific data on soil properties is given in Ref. 1-2. The control room of the existing plant is located at 111°17'50" west lon., 32°33'22" north lat., and 589 m (1931 ft) above mean sea level.

Figure 2.3-1

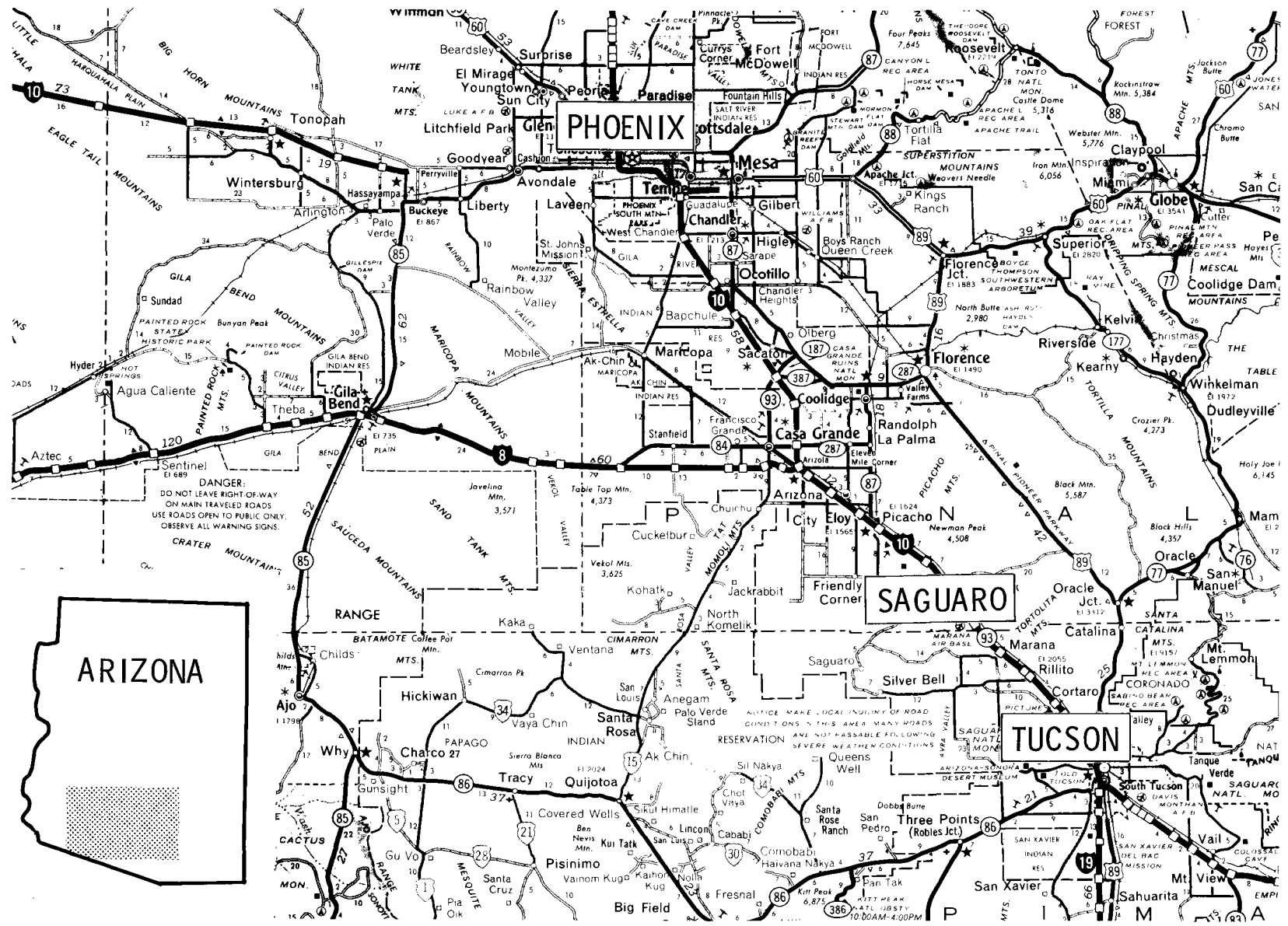


Figure 2.3-1 APS Repowering - Saguaro Station Location

Figure 2.4-1

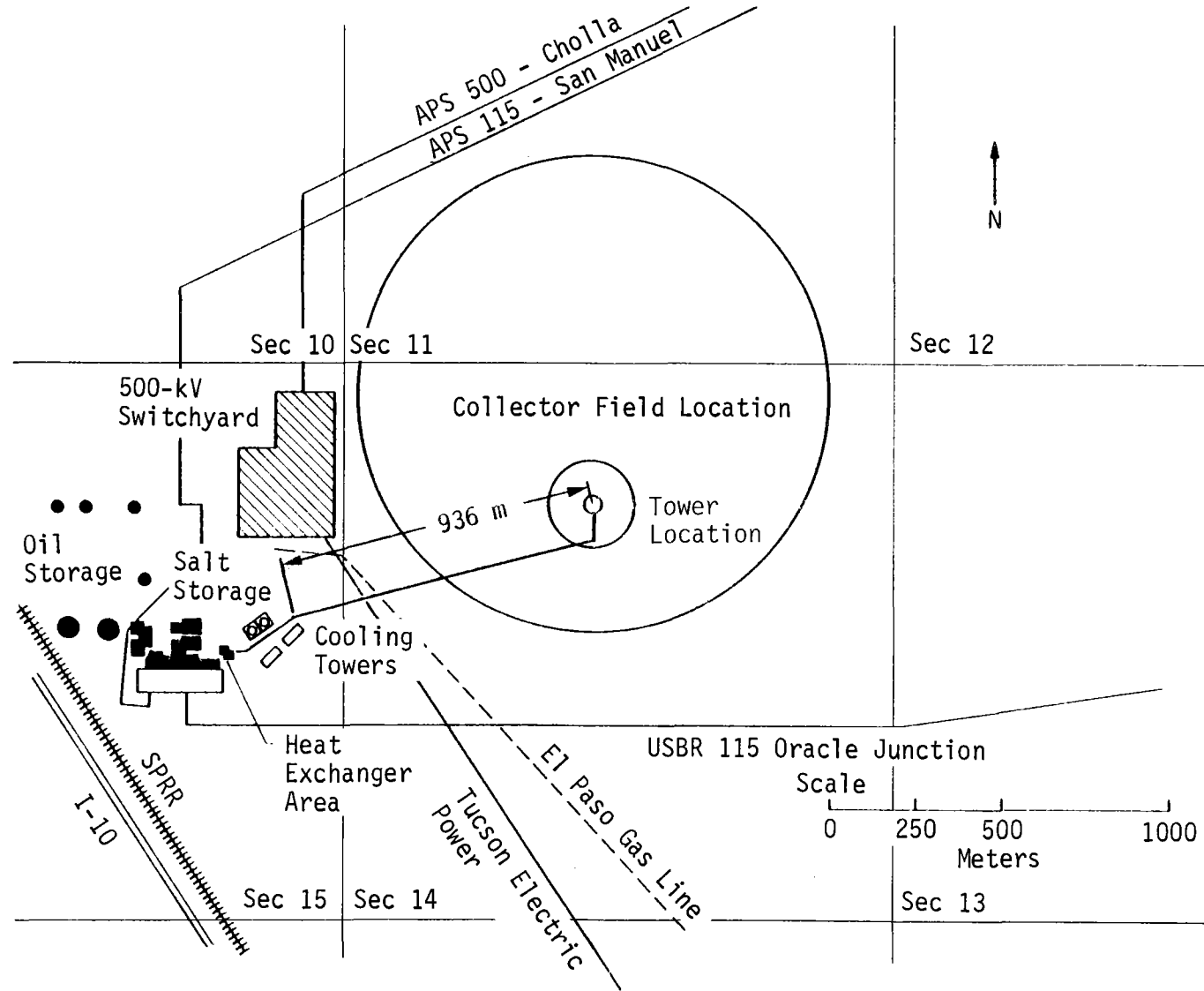


Figure 2.4-1 Collector Field Location

2-11

2.5 CLIMATE

The local climate is that of a southwestern desert with hot summers and cooler winters (See also appendix D). Figure 2.5-1 shows the range of average daily temperatures at Saguaro. Extreme temperature data for Coolidge, AZ, which is located near Saguaro but at a slightly lower elevation are summer dry bulb of 46°C (115°F), summer wet bulb of 25°C (77°F), and winter extreme of -8°C (18°F). The winter temperatures are seldom below freezing (21 days per average year) and only minimal protection is afforded otherwise uninsulated water lines.

The average monthly precipitation for Saguaro is shown in Figure 2.5-2 and has been taken for the Arizona state climatic division covering the southern and southeastern part of the state (Ref 2-12). Yearly average precipitation is 0.28 m (11.1 in.). An analysis of the flood potential at Saguaro was made by APS in June of 1971. The minor potential effects of flooding on the solar site is discussed in Ref. 1-2. Snow does fall at Saguaro, but the average yearly total is less than 0.025 m (1 in.).

Wind speeds at Saguaro are generally light. Data collected at Saguaro from June 1974 through June 1975 showed only one occurrence of a wind speed greater than 8 m/s (18 mph) and it was from the south. Winds are generally from the south or southeast. It was calm (1 m/s) for 3.6% of the year. The yearly average fastest wind speed for Tucson, AZ is 26.4 m/s (59 mph). The annual extreme fastest mile wind speed 10 m (30 ft) above the ground at a 100-year mean recurrence level is 33.5 m/s (75 mph) using American National Standard (A58.1-1972) data.

Moderate thunderstorms are associated with the summer rains. Hail seldom occurs and when it does appear, it is then in the 6 to 12 mm (1/4 to 1/2 in.) range.

There are more than 300 sunny days at Saguaro in most years. The average of 3850 hours of sunshine per year corresponds to 87% of the possible sunshine. The identification of the correct value for average daily direct normal insolation for the Saguaro site has not been possible. Data extracted from Watts Engineering studies indicated a value of $7.6 \text{ kWh/m}^2\text{-day}$. However the SOLMET Typical Meteorological Year (TMY) data prepared by SNLL for Phoenix, AZ gives a value of $6.93 \text{ kWh/m}^2\text{-day}$. The direct normal insolation data taken at Tucson, AZ, was not in a form for input into the system simulation models. Both the direct normal insolation data being collected at Saguaro and at Coolidge, AZ, have interruptions of data and have not been recorded long enough to get valid average data. The Phoenix, AZ, TMY insolation data were used for our performance runs. The resulting performance data are felt to be 5 to 10% low.

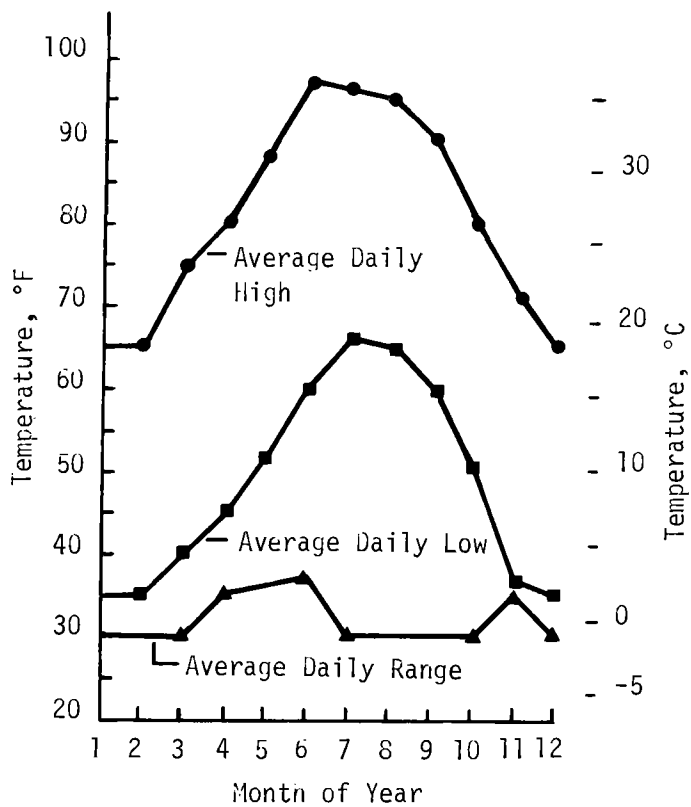


Figure 2.5-1 Saguaro Average Temperature

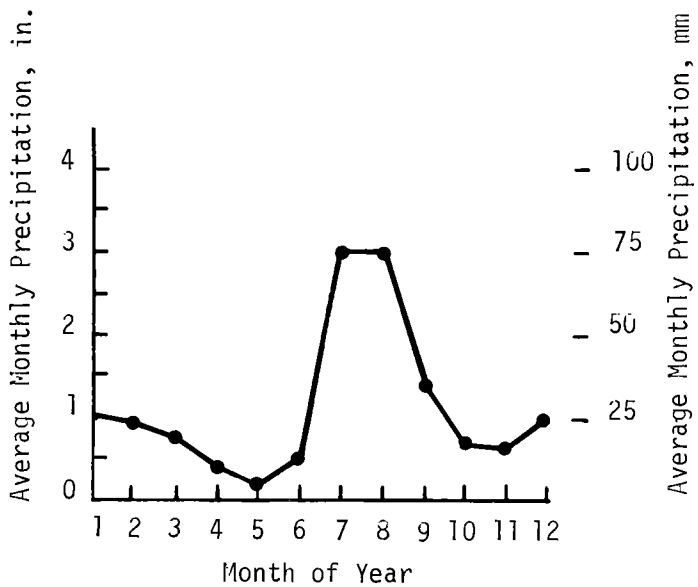


Figure 2.5-2 Saguaro Average Monthly Precipitation

2.6 EXISTING PLANT DESCRIPTION

Unit One of the APS Saguaro Station, which is to be repowered with solar energy, is a conventional non-reheat steam-Rankine turbine generator system for the generation of electrical power to be used on the APS grid (Ref 2-11). Steam for the turbine is generated by a gas/oil fired boiler with an economizer and superheater. The unit was the first APS generator to use outdoor construction. That is, there are no turbine or boiler buildings. Unit One was originally used as a baseload generator, but as the APS system has grown, it is now used for area protection.

Figure 2.6-1 shows an aerial view of the Saguaro station taken in 1955. The topography of the land area to be used for repowering has not changed much over the intervening time period. A plot plan of the station is shown in Figure 2.6-2. Further specifics on the existing plant can be found in Ref 1-2 and 1-4.

2.7 EXISTING PLANT PERFORMANCE SUMMARY

The two gas/oil fired electric generating units at Saguaro produced an average of 498,548,000 kWh_e net and 53,937,000 kWh_e auxiliary use each year over the 6 year period from 1975 to 1980. This annual energy source corresponds to a 6-year average capacity factor of 26.63%. Unit One or Unit Two is on the line 6000 to 7000 hours per year, on reserve shutdown (hot or cold standby) 800 to 1200 hours per year, and unavailable from 500 to 2000 hours per year due to forced, maintenance, and planned outages. The plant operates in an area protection mode since it is the largest station in the southeastern part of the APS system. As an area protection station, the units run at approximately 40 MWe net load for most of their operating hours.

The largest cause of unavailability at the Saguaro Plant is the planned outages. It is our present practice to schedule a 3-week outage (504 hours) on each unit annually and an 8-week outage (1344 hours) every 5 years. During the last 5 years, the Saguaro Plant has not experienced any large forced or unscheduled outages.

From published reports to the Federal Energy Regulatory Commission, the 6-year (1975-1980) average cost for operations was \$644,755; maintenance \$589,161; natural gas and oil boiler fuel \$12,879,111; for a total of \$14,113,027.

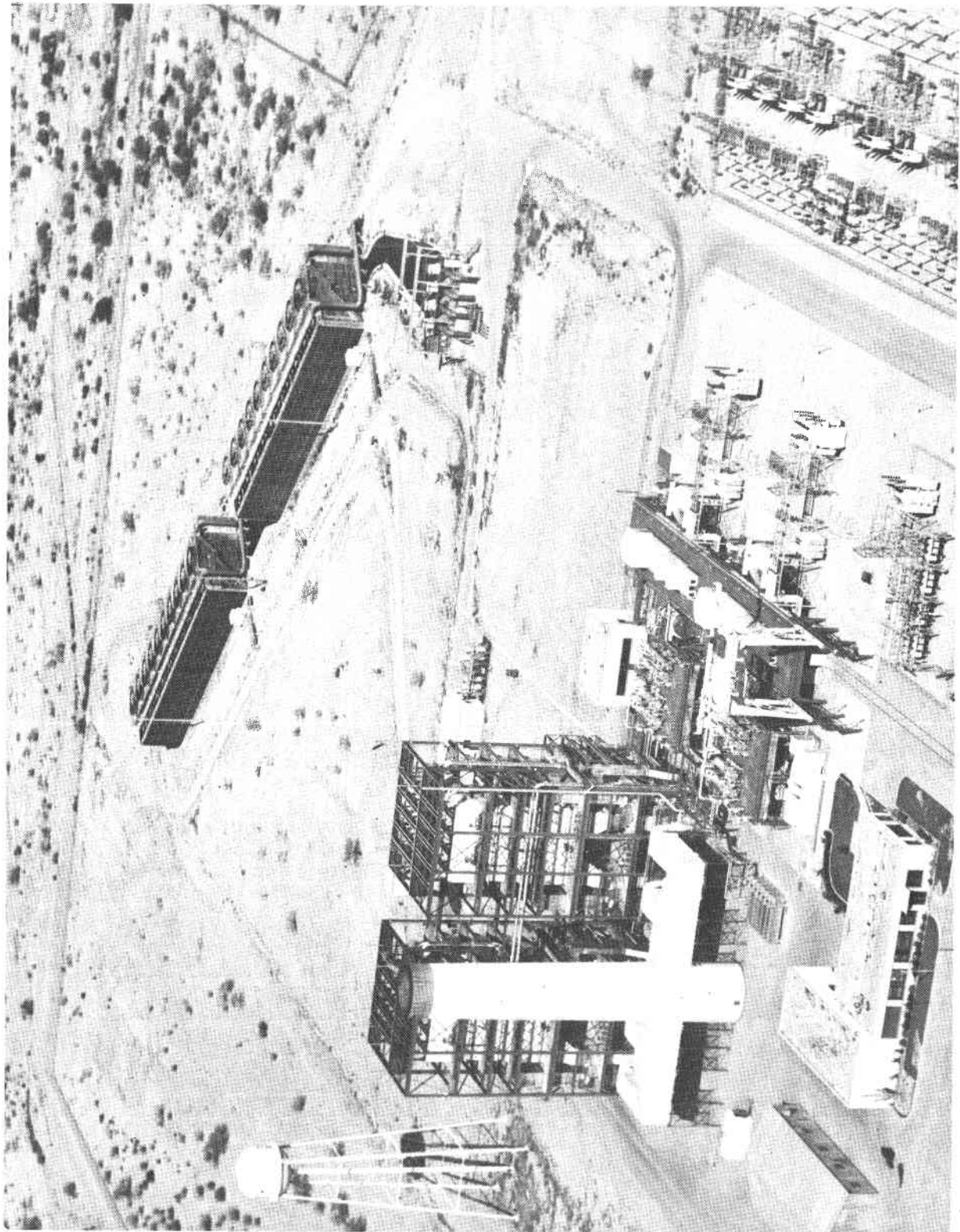


Figure 2.6-1

Figure 2.6-1 Saguaro Power Plant

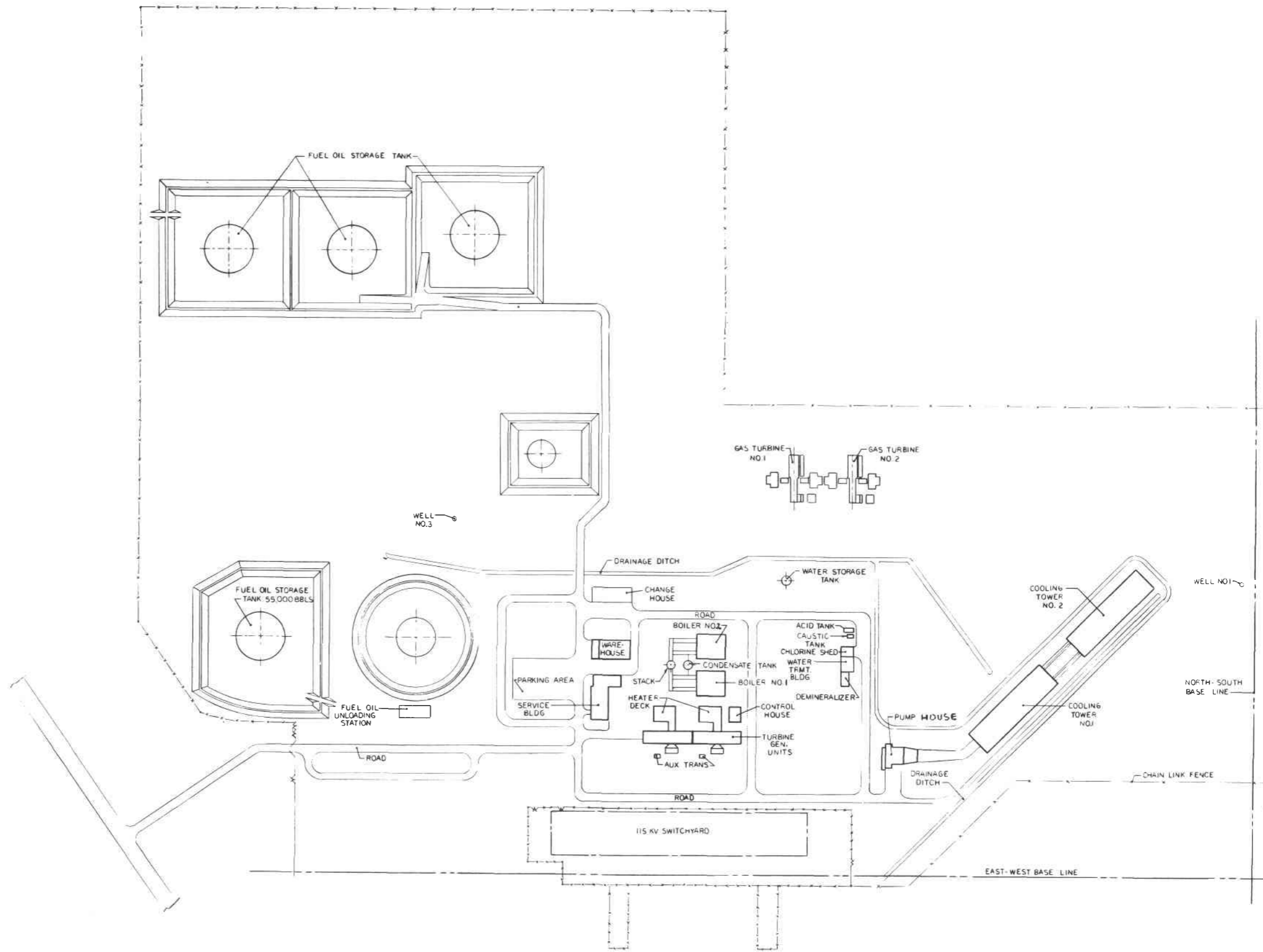


Figure 2.6-2 Saguaro Station Plot Plan

The objective of the configuration selection process for the advanced conceptual design for solar repowering of the Saguaro power plant is to identify an operationally attractive configuration that can be a valid solar thermal central receiver demonstration project while minimizing capital investment. A demonstration is needed that will be applicable to all solar thermal central receiver power system applications - repowering, standalone, hybrid, and cogeneration. The power level should be large enough so that all sizes of commercial systems are in a scaleable range. Not only should each individual subsystem be addressed but the integration of all the subsystems together must be included. For a demonstration to be representative of 3-500 MWe systems, it must be large. Yet it is desired to minimize capital investment. The approach is to recommend a solar system with the minimum repowering level (60 MWe) that can be validly dispatched on the APS system. Costs are further minimized by use of a solar multiple just above unity to reduce the collector field size.

Thermal storage is demonstrated by including four hours of storage that is used to effectively shift the solar resource to match the APS summer load demand. This use of thermal storage also increases the value of the solar system to APS. Additionally, we have emphasized development of a system with significant operational flexibility. This not only helps its acceptance by APS but will also aid in its acceptance by other utilities in the southwestern United States. It is also important to avoid technical, cost, and schedule risks that could jeopardize the project and thus delay the acceptance of solar thermal central receivers. A description of the preferred system is given in Section 4.1.

The advanced conceptual design solar system configuration evaluations were divided into four groups. In section 3.1, we: 1) summarize the configuration trade studies from the prior Saguaro repowering study (Ref 1-2), 2) identify specific subsystem trade studies in this volume, and 3) address two new subjects - number of receiver operational cycles and number of receiver cavities. Section 3.2 discusses the selection of system repowering level based on use of the solar repowered system in APS's projected load and resources mix in the 1987 to 2000 time frame. Section 3.3 restates the basis for selection of the molten salt technology. Section 3.4 presents an evaluation of the utility of thermal storage in the APS system using an electric power production costing model.

Figure 2.2-1 is a diagram of the repowering concept used in these analyses. The thermal storage system is based on molten salt, which means that thermal storage is relatively inexpensive. Thermal storage is also used to decouple collection of solar energy from use of solar energy. During the collection process, cold salt is taken from the cold salt tank and pumped to and up the tower to the receiver. This cold (277°C) salt is heated to 566°C in the receiver and returned to the hot salt tank. The collector/receiver can be operated whenever there is enough sunshine and the hot salt

tank is not full. During the usage process, hot salt is pumped through the heat exchanger string (superheater, boiler, and preheater) and returned to the cold salt tank. Concurrently water from the EPGS is heated and converted to superheated steam and fed back to the turbine. This use of solar energy can occur whenever there is hot salt in the hot salt tank. The system retains the use of the existing fossil steam generator and is configured so that solar can be used alone, fossil can be used alone, or solar and fossil can be used together in selectable proportions.

The trade studies were conducted in the usual way of establishing assumptions, limits, and criteria for selection, doing the analysis, and then selecting a configuration. The site-specific considerations were first established. The only unusual factor was the use of the Phoenix, AZ Typical Meteorological Year (TMY) insolation data. These data were prepared by Sandia National Laboratories-Albuquerque, using 23 years of SOLMET data collected by NOAA as its basis. These TMY data have an average annual insolation of $6.93 \text{ kWh/m}^2\text{-day}$ compared with the $7.6 \text{ kWh/m}^2\text{-day}$ indicated by the Watts Engineering Company data. While use of the TMY data means a more expensive solar system per unit of produced electrical energy, these are the best data available to us, and they correlate with the limited data taken at the Saguaro site. The trade study selection criteria can be grouped into categories of cost/value, confidence, and acceptance by the utilities. The specific criteria were derived from the prior Saguaro study, the contract statement of work and program objectives. The economic environment used in the trade studies was provided by the APS System Planning Department.

A summary of the tradeoff studies that have been addressed is shown in Table 3-1. The applicability of the trade study results from the prior Saguaro study is indicated as is the reference paragraph where a discussion of each specific trade study can be found. A summary of the applicable studies from Ref 2-1 is given in section 3.1.

Table 3-1 Tradeoff Study Summary

Trade Study	Prior Study Results Applicability	Approach	Reference Paragraphs
Level of Repowering	No	} Will be reevaluated in a unified dispatch analysis.	3.2
Number Hours of Storage	No		
Effect of APS Demand Profile on Amount of Storage	No		
Energy Load Profile	No		
Utility of Raising Turbine Inlet Steam Temperature to 538°C (1000°F)	Yes	No change in conclusion.	3.4.2 (Ref 1-2)
Optimization of Receiver Outlet Temperature	Yes	New data are limited to value used in baseline concept.	3.1
Collector Field Size	No	Change to 60 MWe net level and heliostat characteristics.	5.1.3
Fossil-to-Solar Ratio	Yes	Baseline concept permits varying ratio over wide range.	3.1
Type and Number of Energy Storage Tanks	Partly	Reevaluated based on Storage SRE data.	5.5.2 3.4.2 (Ref 1-2)
Location of Salt/Steam Heat Exchangers and Storage Tanks	Yes	No change in conclusion.	3.4.4 (Ref 1-2)
Cavity vs External Receiver	Yes	No change in conclusion.	3.4.5 (Ref 1-2)
Use of Solar Energy During Annual Boiler Shutdown	Yes	Baseline concept has this ability.	3.1

3.1 SUBSYSTEM TRADE STUDIES

The prior Saguaro tradeoff studies were performed in parallel with standalone and dispatch analyses. Ground rules for the configuration trades were established during the start of these analyses and were selected based on ranges of variables involved in the solar system sizing analyses. Ground rules for the configuration trade studies are listed in Table 3.1-1.

Table 3.1-1 Reference 1-2 Trade Study Basis

Solar Thermal Energy System Size - 370 MW _t Peak - Base of Tower (85 MW _e - 6 hours of storage)
Heliostat Costs: \$230/m ²
Land Costs: \$0.062/m ² (\$250/acre)
Tower Cost Model: Sandia National Laboratories-Livermore, Solar Utility Repowering/Industrial Retrofit Technical Information Memoranda Numbered 5 and 6, January 11, 1980 and January 18, 1980.
Heat Exchanger, Receiver, and Storage Cost Estimates Developed from Martin Marietta Alternate Central Receiver and Hybrid Contracts (Ref 2-1, -3, -4)
APS Economic Parameters (10- and 30-year System Life)
Annual Solar Energy Produced - 350,000 MWh _e (Capacity Factor 0.47)
Insolation - Phoenix (SOLMET - TMY)

Since the initial repowering concept considered the use of 30 MW_e of fossil fuel capacity at all times, these analyses assumed an 85-MW_e gross 6-hour storage solar plant. For a fully sized collector field (i.e., can charge total storage capacity on summer solstice day with immediate dispatch of solar power), this plant yields a solar plant annual capacity factor of 0.47. Although the final selected configuration is different than the capacities in Table 3.1-1 indicate, results of the configuration analyses are applicable for the selected configuration.

3.1.1 Turbine Steam Inlet Temperature

The prior Saguaro study configuration trade analysis concerning the economic benefit of raising the throttle steam temperature generated from the solar steam generator assessed the performance and cost impacts of changing the throttle temperature from 509°C (948°F) to 538°C (1000°F) for major equipment items. The analysis assumed the same gross electric output from the solar plant at 85

MW_e for each of the two cases. Parasitic power losses were assumed to be the same for each of the two cases. Performance values were calculated for the two configurations using 509°C (948°F) and 538°C (1000°F) throttle temperature. Gross cycle efficiencies were determined for each case based on actual operating data for the 509°C (948°F) case and estimated cycle efficiencies based on References 2-11 and 3-1 for the 538°C (1000°F) case.

Results of the analysis clearly indicated that the 538°C (1000°F) throttle steam temperature condition is the better of the two conditions considered. A cost reduction of over \$700,000 resulted from increasing the steam conditions to 538°C (1000°F). Operating and maintenance cost differences were assumed to be negligible between the two cases. Due to the slightly lower water and salt flowrates for the 538°C (1000°F) case, pumping power would be slightly less at 538°C (1000°F).

The use of 538°C (1000°F) steam also means that the selected configuration will have a wider applicability to other repowering opportunities. DeRienzo (Ref 3-2) has shown that the repowering market is more than tripled in going from a steam temperature of 510 C (950°F) to 538°C (1000°F).

3.1.2 Optimization of Receiver Outlet Temperature

A primary consideration regarding receiver outlet temperature is that it should be high enough to permit generation of 538°C (1000°F) steam. This is a widely used superheated steam temperature. When line losses are considered between the steam generator output and the turbine inlet, it is advisable to be able to generate steam at 543°C (1010°F). The large majority of applications can be satisfied with this temperature of steam. The hot salt temperature thus must exceed 560°C (1040°F) to provide an adequate temperature difference for the superheater heat exchanger if the area of the heat exchanger is to be reasonable.

With regard to thermal energy storage and pumping power, it is desirable to raise the receiver outlet temperature as high as possible. High salt temperatures decrease the quantity of salt in storage and the pumping power required. All of the recent materials work on metal corrosion when exposed to hot salt (Ref 2-8 and 2-9) indicate that 566°C (1050°F) is a valid upper limit. Recent unpublished SNLL results indicate that the inside wall of the absorber tubes should not exceed 600°C (1112°F) for extended periods. Other considerations are the loss of strength by the absorber tubes at elevated temperatures and the tendency of the salt to break down at temperatures above 600°C (1112°F). The receiver control system steady state and dynamic errors will require that some margins be established. All of these considerations indicate that the design receiver outlet salt temperature should be retained at 566°C (1050°F).

3.1.3 Fossil-to-Solar Ratio

In the prior Saguaro repowering study it was found to be uneconomic to require that the solar and fossil systems be operated in a fixed ratio. A preliminary analysis performed as part of the dispatch analysis showed that a fixed solar to fossil ratio would mean burning gas or oil at Saguaro in the winter to displace coal or nuclear generated power. It was thus decided to design the repowered system so that the ratio between solar and fossil could be varied from all solar to all fossil. The lower operating limits on the solar and fossil steam generators do limit the range of ratios of fossil to solar energy that can be obtained. The ability to operate all solar, all fossil, or the two together in selectable proportions has been retained in the advanced conceptual design.

3.1.4 Type and Number of Energy Storage Tanks

The purpose of the prior Saguaro study storage tank tradeoff analysis was to determine the most cost-effective storage tank configuration and type for a nominal storage capacity of 6 hours for a solar steam generator rated at 85 MW_e gross. The assumptions used in the analysis are shown in Table 3.1-2. The thermal capacity of the storage subsystem was based on an EPGS cycle conversion efficiency of 40%. The soil bearing load limit was based on Ref 3-3 for the Saguaro plant site. Cost correlations were based on work performed by Martin Marietta and reported in Ref 3-4.

Table 3.1-2 Reference 1-2 Storage Configuration Study Assumptions

Hot/cold storage system most economical for 1275 MWh _t size (Ref 3-4). Soil load bearing limit of 191.5 kPa (4000 psf). Maximum allowable hoop stress is 1.2066×10^5 kPa (17,500 psi) for 44.4mm (1.75 in.) shell thickness (API code). Hot salt temperature = 566°C (1050°F) and cold salt temperature = 277°C (530°F); ambient temperature = 28°C (83°F). Salt heat capacity = 1.549 J/kg°C (0.37 btu/lb.°F), Hot salt density = 1728.2 kg/m ³ (107.8 lb/ft ³), Cold salt density = 1909.3 kg/m ³ (119.1 lb/ft ³). Ullage volume = 2% of total tank volume. Maximum tank shell temperature = 343°C (650°F).

Results from Ref 3-4 were used initially in the study to determine the best configuration type (hot/cold, thermocline, cascade). The conclusions from Ref 3-4 were:

- 1) The optimum tank configuration for each system is the smallest number of large tanks possible within the mechanical constraints (soil bearing load, tank hoop stress).
- 2) For small storage systems where only one tank of each kind is needed, (<3000 MWh_t), the hot and cold-tank system is the most economical approach.

- 3) For intermediate storage systems (10,000 MWh_t), the hot and cold-tank system is recommended, since the cost advantages of the thermocline and cascade systems do not warrant the added technical risk.
- 4) For large storage systems (15,000 MWh_t), the cost advantage of the cascade system is attractive enough to encourage a solution to the thermal cycling problem. In light of the current information, though, a hot and cold-tank is still recommended.

The 1275 MWh_t storage capacity of the prior Saguaro study was classified as a small storage system and, therefore, the second conclusion (above) holds--the dual-tank system was the most economical. Based on the other conclusions, the dual tank system was also the most technically viable for near-term applications.

The selected configuration was the separate hot and cold tank configuration with the hot tank internally and externally insulated. An internal liner was used in the hot tank. Both tanks employed cooling coils in their foundations. The optimum tank dimensions and insulation thicknesses were determined by the Storage Parametric Analysis Model (SPAM) (Ref 3-4). The current study considered the use of an externally insulated hot salt tank made of Type 304 stainless steel (paragraph 5.5.2). While the externally insulated tank is cheaper, it was decided to use the internally insulated hot salt tank as it is representative of what will be used in the future and thus should be included in a demonstration program.

3.1.5 Location of Salt/Steam Heat Exchangers and Storage Tanks

The location tradeoff of the salt/steam heat exchanger and salt storage tanks in the prior Saguaro study considered cost estimates and pumping power costs for various location options. The four options considered were:

- 1) Heat exchanger located at base of tower, hot and cold tanks at base of tower;
- 2) Heat exchanger located near main plant, hot and cold tanks at base of tower;
- 3) Heat exchanger located near main plant, hot tank at base of tower, cold tank at plant;
- 4) Heat exchanger and hot and cold tanks near main plant.

The location options are shown schematically in Figure 3.1-1. Capital and operating costs were based on the system requirements shown in Table 3.1-3. Economic pipe diameters were determined based on the economic factors provided by APS and pump power costs of 35 mills/kWh_e escalating at 8%/yr. Two plant configurations were considered in this analysis. In the first case the fossil energy source at Saguaro would be operating continuously at 35 MW_e gross to supplement solar derived power. A second configuration (120 MW_e, 3.8 hr of storage, solar multiple = 1.04) was developed to increase the value of the solar thermal power installation. This configuration minimizes the use of the fossil-fired boiler.

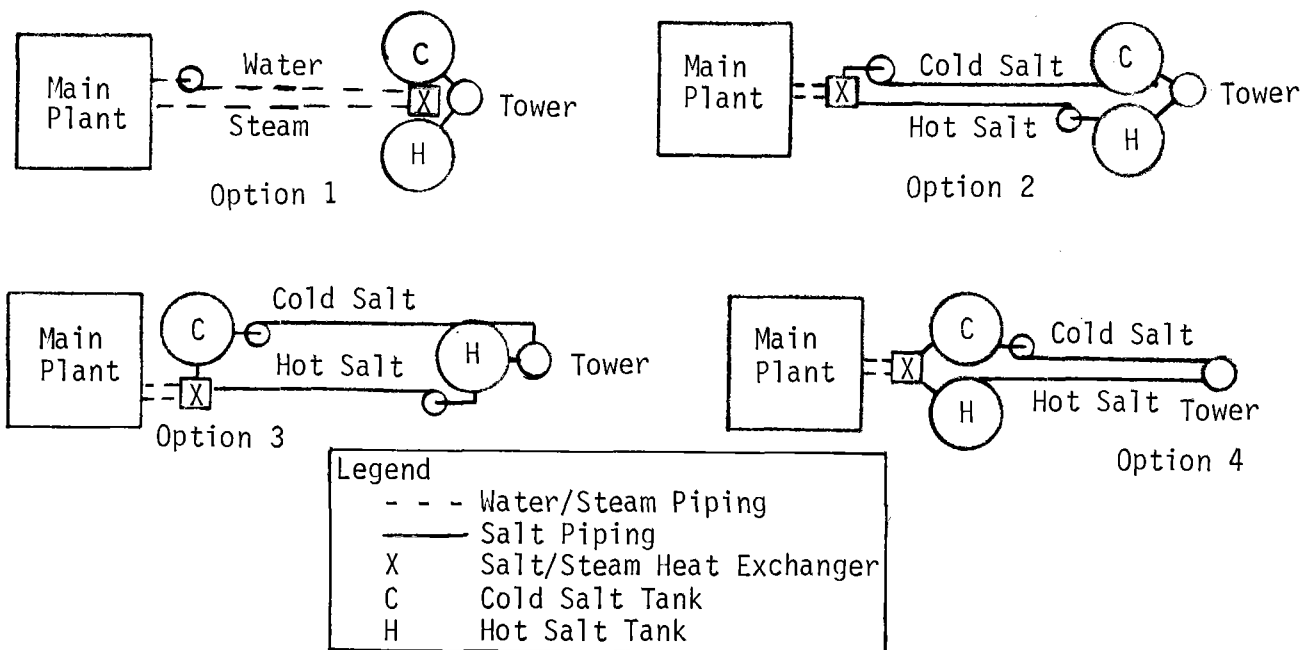


Figure 3.1-1 Storage Tank/Heat Exchanger Location Options

Table 3.1-4 Solar Plant Description for Heat Exchanger/Storage Location Trades

Level of Repowering	85 MW _e gross
EPGS Cycle Efficiency	40%
Storage Capacity	6 hours (1275 MWh _t)
Peak Power Base of Tower	370 MW _t
Turbine Throttle Conditions	538°C (1000°F) 10.0 MPa (1450 psig) 3468 kJ/kg (1491 Btu/lb)
Boiler Feedwater Conditions	229°C (445°F) 989 kJ/kg (425 Btu/lb)
Water/Steam Flowrate through Salt/ Steam Heat Exchanger	312,400 kg/hr (687,350 lb/hr)
Distance from Plant to Base of Tower	1340 m (4400 ft)
Salt Temperature	Hot 566°C (1050°F) Cold 288°C (550°F)
Salt Flowrates - Peak Flow through Receiver	3,083,000 kg/hr (6,781,700 lb/hr)
- Flow through Salt/ Steam Heat Exchanger	1,782,000 kg/hr (3,920,300 lb/hr)

A life cycle cost analysis was performed for the first configuration to assess which location option provided the lowest cost over 10- and 30-year periods. The results of the life cycle cost analysis involved levelized annual cost (annualized cost) for both capital and pump power cost. Based on total annualized cost, the Case 2 location option gave the lowest value. Therefore, the storage tanks at the base of the tower and the salt/steam heat exchanger at the main plant provided the lowest cost option for both the 10- and 30-year system lifetimes for the first configuration.

The second configuration (120 MW_e gross, 3.8-hour storage, solar multiple = 1.04) was developed to maximize the value (or benefit) of the solar capital investment for APS. This configuration was developed after the analysis had been performed on the original configuration as described in Table 3.1-3. In this new configuration, there is no difference between the peak flowrate requirements in the hot and cold salt piping in locations described by options 2,3, or 4. If the storage tanks are located at the base of the tower and the heat exchanger at the main plant, the flowrate of salt at 120 MW_e gross from the base of the tower to the main plant will occur for a longer period of time per day than if the storage tanks are located near the main plant. Storage tanks located near the main plant will result in a peak flowrate at 120MW_e gross for only one time (noon) in the day at summer solstice. Therefore, the total capital investment in the horizontal piping and pumps will be less for option 4 due to its lower average flowrate, and hence, pressure drop. The pump power costs will also be less for option 4 because the salt head in the tower can be used to overcome the horizontal hot salt pipe friction. Therefore, the storage tanks located near the main plant appears to be the optimum location for this configuration.

Other factors were considered in the heat exchanger/storage tank location study. Because the startup procedure for the salt/steam heat exchanger was envisioned as being dependent on fossil-derived steam from Unit One for startup, it would be advantageous to locate the salt/steam heat exchanger near the main plant. Storage tanks located near the main plant will also be easier to maintain and monitor. Any salt reprocessing equipment would have to be located near the storage tanks. This equipment would also be more easily monitored near the main plant. When salt is initially processed, processing will probably be done at the main plant. Transfer of processed salt to storage tanks located near the main plant may be easier. Because the base of tower elevation is higher than the main plant, the salt drain must be located near the main plant. A drain tank near the storage tanks is the best location, favoring storage tanks near the main plant. A single stage hot salt pump is all that is required for storage tanks located near the plant. Multistage hot salt pumps would be required if storage tanks are located near the tower. Fewer electrical lines (power or control) would be required to the base of the tower if storage tanks are located near the main plant. In a two-tank configuration, the ullage gas will be transferred between the tanks. Shorter gas transfer lines will result if the two tanks are located together. Tank foundation cooling requirements will be met with cooling tower water, favoring a main plant location for the tanks.

Some benefits are derived if storage tanks are located near the base of the tower. Such a location would be safer to personnel located at the main plant. Main plant operations would not be disrupted in the event of a tank leak or malfunction. Control of the receiver salt flowrate would involve shorter lag times (however, control of the salt/steam heat exchanger would have longer lag times). The cold storage tank can serve as a surge tank for the bypass recirculation line around the receiver booster pump which is required for flow control. If storage tanks are located near the main plant, air coolers on the receiver booster pump bypass will be needed.

Based on these economic, maintainability, and safety issues, salt/steam heat exchangers and storage tanks located near the main plant appear to be the best option for the selected solar system configuration.

3.1.6 Cavity vs External Receiver

An investigation was performed as part of the prior Saguaro study to compare quad-cavity collector/receiver modules with exposed collector/receiver modules of the same net thermal power output. To cover the expected range of the final receiver size selection, two module sizes were investigated at power levels of 370 and 215 MW_t at the base of the tower. A collector/receiver module of each type was designed to produce 370 MW_t, and the total cost of each was determined and compared. Then, the receiver dimensions, weights, costs, and thermal performance were scaled down from these results to produce the 215-MW_t designs. This information was used to calculate the total system cost of each module for this lower power level. In both cases, it was found that, although exposed receivers enjoy an advantage in terms of receiver and tower costs, the higher thermal efficiencies inherent in the cavity design allow for substantial savings in the cost of the collector field. This savings was such that, over the range of power levels investigated, the quad-cavity receiver was found to be the better choice.

3.1.7 Use of Solar Energy During Annual Boiler Shutdown

The approach used early in the prior Saguaro repowering study was to operate solar only when the fossil steam generator was also operating. However, the dispatch analysis showed that it was very uneconomic to run the fossil system for the whole year. Thus, it was decided to include the capability to operate the turbine on solar steam alone. With this capability included in the basic concept, it was no longer necessary to perform this trade study because the solar system could be used to provide steam to the turbine when the fossil steam generator was down for maintenance. It is planned to perform scheduled maintenance on the solar system when the electrical power generating subsystem is down for maintenance.

3.1.8 Allowable Receiver Absorber Surface Temperature Cycles

The prior Saguaro study used a design requirement of 27,000 temperature cycles induced by the application and removal of solar flux on the receiver absorbing panels. This corresponds to an average of 2.47 temperature cycles per day. The availability of specific insolation variation data from Ref 3-5 prompted an analysis to determine if more or fewer cycles were likely. Ref 3-5 presents data for eight representative partly cloudy days and gives direct normal insolation data at 16 sec intervals. The eight representative days are shown in Table 3.1-4 along with a number of cloudy days to bring the number of cloudy and partly cloudy days up to the average for the 15 month period. The relative importance of each of the eight different kinds of cloudy days has also been determined using Case 3 as the reference. Case 3 is the most important form of partly cloudy day in terms of total direct normal energy available on that kind of day.

The number of large insolation cycles was counted for each representative day and is listed along with the number that might be expected in the 15 month time period. A large insolation cycle was a swing from high insolation to less than 50 percent and back to the high level again. The relationship between insolation cycles and absorber tube temperature cycles is not at all clear. Even though insolation might drop over a large part of the field, if the frequency of the cycle is higher than the natural frequency (in a thermal capacity sense) of the absorber panel, then the tube temperature will not change much. Also the spatial variation of the clouds over the collector field will affect the temperature swings. On those days when the insolation variations are greatest, it is likely that the receiver will be shut down.

The total number of insolation cycles estimated for the 15 month period is 2408. This corresponds to 58,000 insolation cycles over thirty years. Case 3 accounts for 42% of the insolation reversals and 5.3% of the energy, while Case 4 accounts for 22% of the insolation reversals and 1.5% of the energy. Thus it can be seen that not trying to collect all of the energy on type 3 or 4 days can drastically reduce the number of insolation reversals at a low cost in lost energy. It was decided to raise the design number of temperature cycles from 27,000 to 60,000 over thirty years. The 60,000 cycles contains an adequate design margin when it is realized that the receiver will be shut down on the worst days and that an insolation cycle will not necessarily cause a temperature swing of the magnitude used in the fatigue analyses.

Table 3.1-4 Typical Insolation Scenario Summary

Number	Salient Characteristic	Number of Cases	Date	Total Energy for Day kWh/m ²	Relative* Importance	Number of Insolation Cycles	
						Reference Day	15 Month Period
1	Isolated sharp transition	7	26 April 1979	8.1	0.32	3	21
2	Very high frequency variations, does not go to zero	7	26 August 1978	9.4	0.37	21	147
3	High frequency fluctuations, does go to zero	25	8 August 1978	7.1	1	40	1000
4	Frequent sharp transitions between full off and full on	8	29 March 1979	6.1	0.27	65	520
5	Variations not going to zero, medium frequency	8	8 July 1979	7.3	0.33	20	160
6	Medium to low frequency variations, more off than on	13	15 October 1978	3.9	0.29	13	169
7	Slow variations, transmittance significantly affected	7	20 January 1979	5.3	0.21	2	14
8	Very slow variations bounded by clear conditions	7	9 December 1978	5.1	0.20	5	35
9	Cloudy days	32	---	0	0	0	0
10	Clear Days	342	---	8.25	15.90	1	342

Total (15 months)

456

2408

*Product of Number of Cases Times Total Energy for Day Normalized to Case 3.

3.1.9 Collector Field Shape

The decision to go from a 316MW_t to a 181MW_t receiver size raised the question of how many cavities should the receiver have and what should the corresponding collector field shape be. Preliminary results from a Martin Marietta in-house analysis were used to address this question. The value of a receiver/collector field configuration was defined in terms of annual energy absorbed by the receiver divided by an annualized capital cost. Operating and maintenance costs were not considered as they should be independent of configuration. Salt pumping costs were included because of the tower height effect.

The preliminary results of that study showed that two and three cavity receiver configurations had a value between the single cavity (north field) and the four cavity (surrounding field) values. The quad cavity configuration was better than the single cavity for the larger size fields. The degree of improvement was dependent on whether the single cavity was tipped and the cost basis of the receiver. The DELSOL II computer program was used in this analysis. The two and three cavity receiver configurations are applicable where the shape of the land available is constrained. As a result it was decided to retain the quad cavity surrounding field configuration and to place ten percent of the heliostats in the south field. It was felt that this configuration would be a better demonstration for the larger collector fields expected in the future. Further details of this analysis are contained in paragraph 5.1.2.

Through consideration of life-cycle costs, the prior study established optimum solar plant subsystem sizes (level of repowering, and storage capacity) and the amount and type of fuels displaced. That study (Ref 1-2 and -4) selected a full repowering (120 MWe gross), a near unity solar multiple, and 3.8 hours of energy storage for effective dispatch of the solar power. There have been a number of changes in non-technical factors in the interim. Changes in the national economic climate and the possible need to consider other than Federal Government means of financing plant construction required re-examination of the selected system repowering size. In the prior study, a 60 MWe repowering level was identified as a practical minimum, but it did not meet the objective of maximizing the value of fuel displacement. With this background information available, it then became necessary to determine if 60 MWe of repowering is a practical and economic minimum.

A new criterion was established for selecting the repowering level; namely, identify a minimum repowering level that results in a meaningful, cost-effective demonstration of the molten salt technology. The demonstration size should be such as to permit scaling to a commercial sized stand-alone plant.

Prior to the initiation of the analysis several additional assumptions were developed, since the APS System Planning Group had introduced new resource types into its forecast plan. The prior work had shown that fuel savings were very sensitive to the resource mix of the APS system. A utility's annual resource forecast reflects a continually evolving plan to satisfy updates of the changing system load demand. Because of this requirement the system generation resource mix changes from forecast to forecast as does the margin of resources over peak demand. The resource forecast normally covers a 10-year period and is reinforced by a long-term forecast covering a period of 20 years. The 10-year forecast reflects actual resource additions which are under construction as well as planned additions that can be brought on line within the forecast period. The long-term forecast reflects planned resource additions, which can either become actual resources or can be replaced by different resources which are more economically attractive.

The APS resource forecast plan to be used in the analysis of size selection showed a pumped storage unit coming on line in 1991. This new resource type competed with solar repowering since both are trying to satisfy the peak electrical power requirements that are part of the annual load demand. Peak load demands in the summer are met by combustion turbines or oil/gas fired Rankine units. Both the solar system and the pumped storage units attempt to increase their value by displacing as much of the expensive fuel as they can. The determination of the relative amounts of oil/gas fuel being displaced by each resource is difficult. To facilitate this analysis, the

General Electric Optimum Generation Program (OGP) and APS' detailed production costing model, PCOST, were used. The OGP program is used to model the pumped storage resource, which is a new forecasted resource on the APS system. OGP program runs define the amount of energy required for pumping and the amount of electrical energy that is generated on an hourly basis. These results are then used in the PCOST program.

The first step was to identify the range of solar sizes to be considered in the analysis. The upper limit on the repowering level was set by the nameplate rating of the Saguaro Unit One, which is 120 MWe gross, or approximately 115 MWe net. In the prior study a minimum 30 MWe repowering level was considered as a lower bound because automatic dispatch control does not go below this level. Discussions with the APS Operations Department suggested that a 40 MWe lower bound should be used for the repowering level. This bound was judged to be the lowest repowering level that could be seen, from a dispatch point of view, on the utility grid. Ideally the size should be at least 1 percent of the total planned generating capacity of the APS system in 1987. The 40 MWe value represents 1.3 percent of the planned capacity. Sizes for the analysis were selected to be 40, 60, 80 and 111 MWe net with the accompanying storage capacity of 3.8 hours.

After defining the range of system sizes to be considered, several economic assumptions were made to be consistent with financial and fuel cost factors used by the System Planning Department. These factors are give in Chapter 6.0, but specific economic factors will be identified for our discussion of the analysis. Cost of money is assumed as 14.4 percent, along with a 1987-2000 uniform annual equivalent fixed charge rate of 23 percent. A 30 year project life is assumed along with: no allowance for funds during construction (AFUDC); no capitalized property taxes; and no Ad Valorem taxes due to the extension of Arizona Solar Energy tax exemption.

Production costing runs were made to determine the potential operating cost benefits which APS may realize through a solar repowering of Saguaro Steam Unit One. Repowering levels of 40, 60, 80 and 111 MWe net were analyzed assuming a January 1, 1987 in-service date. The March 6, 1981 APS Loads and Resources Plan was modeled by reducing the 1987-2000 projected hourly loads by the rated solar project output according to a dispatch schedule developed in the prior study. Better dispatch algorithms have been identified in the interim and were used for the work reported in Chapter 6.0.

Rather than use a selection criteria based upon fuel savings, a benefit to cost evaluation was performed. Although finalized plant costs were not available, preliminary estimates for the respective repowering levels were made. Equivalent capital investment which can be supported by the 1987-2000 annual operating cost savings was used as the benefit parameter. The operating cost savings are the value of the fuel displaced plus the fossil plant operating and maintenance

costs saved less the solar plant operating and maintenance (O&M) costs incurred. The results of the benefit to cost analysis are given in Table 3.2-1. The 40 MWe repowering level was eliminated as its O&M costs exceeded the value of the fuel displaced. Table 3.2-1 shows an increase in benefit to cost ratio with increasing level of repowering. This seems to indicate that the maximum level of repowering should be used. Actually the relative change in ratio values are more important than the actual values given in Table 3.2-1. That is, will the increased value of fuel displaced be greater than the increased cost on an annualized basis? Table 3.2-2 shows the results of considering incremental costs and savings. For each case, it can be seen that the incremental capital investment supported by the savings is not as large as the incremental cost. This means that the smallest plant size (60 MWe) should be used.

A conclusion that can be drawn from the benefit to cost evaluation is that the benefit to cost ratios for the 60, 80 and 111 MWe repowering sizes are all less than one. This means that substantial financial subsidy will be required. These analyses used higher heliostats costs and a less effective dispatch strategy than were used in the Chapter 6.0 analyses. Thus the results are different in the two cases. Furthermore, the incremental benefit to cost ratio evaluation indicates that a departure from a 60 MWe solar repowering project to an 80 or 111 MWe size is not justified because the incremental cost savings to incremental capital cost increase ratios are substantially less than one. However, even if the incremental ratios had been greater than unity, the more than 130 million dollar increase in the amount of capital at risk must be considered. In light of today's capital markets, it is better to go with the smaller plant and lower capital exposure for a demonstration plant.

Table 3.2-1 Benefit to Cost Ratio

Repowering Size (MWe)	1987 Estimated Construction Cost (\$10 ⁶)	Equivalent Capital Investment Supported By 1987-2000 Annual Operating Cost Savings (\$10 ⁶)	Benefit To Cost Ratio
60	204.1	14.8	0.073
80	255.0	33.1	0.130
111	335.6	88.6	0.264

Table 3.2-2 Incremental Benefit to Cost Evaluation

Repowering Size (MWe)	Incremental 1987 Construction Cost (\$10 ⁶)	Incremental Capital Investment Supported By 1987-2000 Annual Operating Cost Savings (\$10 ⁶)	Incremental Benefit To Cost Ratio
<u>From</u> <u>To</u>			
60 80	50.9	18.3	0.360
60 111	131.5	73.8	0.561
80 111	80.6	55.5	0.689

Each of the three alternative central receiver technologies (water/steam, molten salt, molten sodium) were considered for use at Saguaro (see also section 2.2). The molten salt system was selected because of the advantages listed in Table 3.3-1. The sodium technology was considered but not selected because of concerns with the safety aspects and the lack of utility or industrial experience with liquid sodium. Sodium reacts violently with air and water and is toxic. Salt does not have these problems and has been used safely for nearly 40 years in the metals and chemical industries. Our evaluations show sodium and sodium hardware cost more than the salt equivalents and do not offer significant gains in efficiency to offset those disadvantages.

Table 3.3-1 Advantages of Molten Salt

<u>Over Water/Steam</u>
- Operation from Storage at Receiver Conditions
- More Cost Effective Thermal Storage
Higher Differential Temperature
Simplification or Elimination of Components
- Simpler Receiver - Single Phase Fluid
- Decoupled Turbine and Receiver
Cloud Transients Can Not Affect Turbine
- Lower Pressure Operation
Lower Construction Cost
- Cost Effective Incorporation of Reheat Turbine Systems
<u>Over Molten Sodium</u>
- Much Less Expensive
- No Violent Reaction with Air or Water
- Greater Heat Density Capacity
Smaller Piping and Storage
- Less Costly Components
No Nuclear Industry Standards
- Higher Expected Plant Capacity Factor

A fossil-augmented solar Brayton topping cycle was also considered because of its potential for high efficiency. There are two 55-MW_e combustion turbines at Saguaro. The high Brayton efficiencies promise a significant reduction in collector subsystem costs. It is felt, however, that the high efficiencies will not be achievable by 1986 because receiver materials will not be available and there are difficulties in minimizing pressure losses. Additionally, solar thermal energy for the Brayton cycle cannot be stored easily and the gas turbine exhaust temperatures are not high enough to produce the steam conditions required by Saguaro.

For all the above reasons, the molten salt technology was selected by APS as best for a 1986 application. The Martin Marietta Alternate Central Receiver Power System, Phase I (Ref 2-1), Phase II (Ref 2-7), the Hybrid (Ref 2-3,-4) studies, and the ongoing Molten Salt Storage SRE have examined all aspects of the molten salt technology. These studies also concluded that large solar standalone plants based on salt technology can be cost competitive in the late 1980's. A series of test programs have verified the practicality of using heat transfer salt up to 600°C (1112°F) in the heat transfer boundary layer and up to 566°C (1050°F) for the bulk salt, which is quite adequate for a 538°C (1000°F) steam supply. Similar results have been obtained by Sandia National Laboratories-Livermore under independent study. Vendors have been identified for every needed component. In many cases multiple vendors are available. Martin Marietta test work was performed under separate contracts related to molten salt central receivers and thermal storage subsystems. Subsystem research experiments (SREs) sponsored by DOE have been conducted for molten salt receivers, are being conducted for molten salt thermal storage, and are being considered for a full system electricity experiment. This program will ensure the use of proven technology for the Saguaro repowering installation.

This section describes a computer analysis performed to verify the simplified dispatch analysis performed during the previous study which resulted in a storage capacity of 4 hours (Appendix A, Ref 1-4). The purpose of this storage capacity is to delay use of the solar energy collected in the morning until late in the afternoon and evening to more closely match the peak load demand on the APS system, thereby maximizing displacement of higher cost oil-fired generation. This should result in maximizing the value of the repowering plant.

To verify the previous analysis, the Ernst and Whitney Embedded Cost computer program EBCOST was used to model the projected APS generation system in the 1985 time frame. This model operates under several dispatch strategies; for this analysis, the fixed commitment option was utilized. This mode accepts as input a set priority for generation unit commitment, and dispatches the units on the system according to that priority to meet the load demand, with fixed reserve requirements. The model operates on an hourly basis for one week at a time, providing as output hourly system generation and hourly system operating cost, as well as 12-hour totals.

In order to assess the value of storage, the following approach was used. First, the projected APS generation mix for the 1985 time frame was input to the program, based on the APS production mix and load demand forecast of July 20, 1979 to be consistent with the earlier analysis. For the load demand input, four "typical" weeks were chosen, representing a typical week for each season. Specifically, the periods used and the corresponding peak load demands are shown in Table 3.4-1.

Table 3.4-1 Typical Weeks for Dispatch Analysis

<u>Season</u>	<u>Date</u>	<u>Peak Load Demand</u>
Winter	12/13/85 - 12/19/85	2258 MWe
Spring	4/12/85 - 4/18/85	2293 MWe
Summer	7/14/85 - 7/20/85	3449 MWe
Fall	10/15/85 - 10/21/85	2597 MWe

Fuel costs, incremental heat rates, minimum and maximum generation levels, variable operating costs, and start-up costs were then input for each of the 35 plants projected to be on the APS system in the 1985 time frame. All costs were input in 1985 dollars.

After the above input development, a base case (no solar) was run for each of the typical weeks to provide a baseline against which to determine the value of storage. To evaluate the benefit of dispatch storage of 4 hours at 60 MWe, two additional cases were run for each of the typical weeks. In the first case, representing solar repowering without dispatch storage, the load demand was reduced by 60 MWe for the hours of the day where the repowering plant would be operating,

assuming a clear day. In other words, the demand was reduced by 60 MWe for the hours where insolation was above 400 W/m². By differencing the total system operating cost for the base case (no solar) and this case (solar - no storage), a value of solar was obtained.

The solar case was then rerun, where the solar output was shifted about the peak demands using the 4 hours of dispatch storage. The actual time periods for solar dispatch for both the no storage and 4 hour storage are shown in Table 3.4-2. Any additional operating savings over the solar, no storage case is a value that can be assigned to the dispatch storage.

Table 3.4-2 Solar Dispatch Strategies

Season	Hours Solar Oper.	Dispatch, No Storage	Dispatch, 4 Hr Storage
Winter	6	9 AM - 3 PM	8 AM - 11 AM; 6 PM - 9 PM
Spring	8	8 AM - 4 PM	11 AM - 7 PM
Summer	10	7 AM - 5 PM	12 PM - 10 PM
Fall	8	8 AM - 4 PM	Noon - 8 PM

The results of the three EBCOST runs for the summer week are given in Table 3.4-3. In the table, the first two columns are the system generation and total operating cost for the base (no solar) case. The following columns show the total operating savings for the solar - no storage and solar - 4 hr storage cases, respectively. By taking the difference between these operating costs, the daily and total week operating savings due to the dispatch storage was obtained, as shown in the last column. Finally, in order to be able to later assess the yearly value of storage, the weekly incremental savings due to storage is divided by the weekly output of the solar repowering project, or 4200 MWh, yielding \$17.15/MWh (approximately 1.7 cents/kWh), in 1985 dollars. Without storage, the value of the solar output is \$82.37/MWh (8.2 cents/kWh), so the addition of storage increases the value of the project during this time of the year by nearly 21%.

This analysis was performed for each of the four typical weeks of the year to obtain the incremental value due to storage for each season. The next computation was to determine the predicted solar output for each season, using the Phoenix TMY data input to the STEAEC program. In this analysis, the two week scheduled outage in January and February was taken into account. After de-escalating the incremental operating cost savings to 1982 dollars the yearly operating savings due to the dispatch storage was calculated, as shown in Table 3.4-4. As shown in the table, over half of the additional operating savings accrue during the summer months, when expensive peaking fuels can be displaced with the addition of storage. The final calculation is to convert this yearly savings into present worth savings over the 10 year operating period, using the average escalation of coal (8%) and oil (9%) and a 14.5% discount rate, yielding a present worth value of \$8.4M, in 1982 dollars.

Table 3.4-3 EBCOST Results - Summer Week (1985 \$)

	<u>MWHe</u>	<u>Base Case Operating Cost</u>	<u>60 MWe Solar No Storage (7 AM- 5 PM) Operating Savings</u>	<u>60 MWe Solar 4-hr Storage (12 PM- 10 PM) Operating Savings</u>	<u>Storage Value</u>
Sun	65,523	\$ 1,816,665	\$ 44,203	\$ 64,195	\$19,992
Mon	65,996	1,896,568	49,667	53,697	4,030
Tue	68,920	2,167,322	54,444	66,496	12,052
Wed	68,409	2,100,672	54,328	63,546	9,218
Thu	66,397	1,874,115	46,122	53,743	7,621
Fri	67,470	2,027,134	54,906	62,024	7,118
Sat	59,658	1,352,558	42,283	54,300	12,017
Week Total	462,373	\$13,235,034	\$345,953	\$418,271	\$72,048

Value of Storage = $\frac{\$72,048}{10\text{h} \times 7\text{d} \times 60 \text{ MWe}} = \$17.15/\text{MWHe} \text{ (1985\$)}$
--

Table 3.4-4 Value of Storage Analysis - Summary (1982 \$)

<u>Season</u>	<u>Storage Value, 1982 \$/MWHe</u>	<u>Seasonal Energy Output</u>	<u>Total Seasonal Storage Value</u>
Winter	\$2.63	x 21,044 MWH =	\$ 55,366
Spring	\$3.79	x 43,024 MWH =	\$ 163,257
Summer	\$13.61	x 43,065 MWH =	\$ 586,297
Fall	\$8.45	x 36,866 MWH =	\$ 311,407
Yearly Storage Value =			\$1,116,327
Present Worth Savings, 10 Years = (8.5% Fuel Escalation)			\$8,402,600 (1982 \$)

This present worth savings can then be compared to the cost of the additional 4 hrs storage for dispatch use. As tabulated in Section 4, the total cost of the storage subsystem is \$8,794,000. However, all of this cost would not be saved by going to a "no-storage" system, since a small amount (about 30 min) of storage is required in a molten salt system to decouple the receiver and the steam generator

for operational considerations. A review of the storage subsystem costs shows that a 30 minute storage subsystem would have a cost of approximately \$3,477,000, with a majority of this cost in the drain tank and hot salt pumps and sump included in the storage subsystem. Thus, the incremental cost of adding the additional 3.5 hours of storage capacity is \$5,317,000 (1982 \$).

With the present worth system operating savings of \$8.4M and a cost figure of \$5,317,000, it can be seen that the addition of storage capacity has a positive value of \$3,085,600. In other terms, the benefit-to-cost ratio for the additional storage can be calculated to be 1.58. Thus, the additional storage capacity for the Saguaro Repowering Project maximizes the value of the project, as well as demonstrating the molten salt storage technology for use in future commercial plants.

4.0 CONCEPTUAL DESIGN

Based on the sizes and configurations developed in the effort described in Chapter 3, the conceptual design activity added sufficient detail to the system concept to provide a basis for an assessment of technical feasibility, estimates of total system performance and installation costs, and an economic evaluation of the repowered system concept. In addition to the following, the potential limitations and risks which previously examined are summarized.

- 1) Detailed description of final system configuration, section 4.1;
- 2) Functional requirements, section 4.2;
- 3) System design and operating characteristics, section 4.3;
- 4) Site preparation, modification of existing facilities, and interface requirements; section 4.4;
- 5) Estimate of system performance, section 4.5;
- 6) Estimate of capital cost, section 4.6;
- 7) Operating and maintenance cost, section 4.7.

Potential limitations that could have an effect on the Saguaro repowering project are discussed in section 4.8 of Ref 1-2. It was found that adequate land is available which is either owned by APS or has been reserved with the State of Arizona Land Department. There were no environmental problems which could limit or prevent the construction and operation of the solar system. The proposed land was recently declared to be part of the Tucson Aquifer that the city of Tucson uses as a source of drinking water. This means that design provisions must be made to prevent contamination of the aquifer by construction or operation of the repowered plant. The effect of increasing the number of turbine starts and stops on equipment lifetime was addressed including the factors discussed in Ref 4-1. A summary of a General Electric Company report specifically defining the costs and risks involved is given in paragraph 5.6.5. Some new and replaced equipment will be required whose costs have been included. The fact that Saguaro Unit One is a non-reheat turbine is considered to be an advantage for a first demonstration program and not a limitation. No operational limitations were uncovered that can not be overcome by proper design practices.

Safety of the solar repowered system concept is discussed in Section 4.9 of Ref 1-2. Hazards to plant personnel and to the general public were addressed in terms of: 1) visual hazards of reflected solar energy, 2) releases of pressurized water and steam, 3) catastrophic failure of equipment including pressure vessels, and 4) releases of molten salt. Each of these potential hazards can be constrained to acceptable levels by a combination of design, test, and procedural approaches.

An estimate of the impact of the repowering project on the local environment was presented in section 4.10 of Ref 1-2. The topics addressed included: site and study plat, climate and air quality, land use, archaeology, geophysical factors, hydrology, ecology and microclimatic factors, and socioeconomic and demographic factors. Ref 4-2 through 4-14 provided relevant information. It was concluded that impact to the environment could be mitigated to an acceptable level.

Institutional and regulatory considerations were presented in section 4.11 of Ref 1-2. That section presented the utility perspective, and more specifically APS's perspective, of various institutional considerations along with specific regulatory issues. The term "institutional considerations" was defined, for the purposes of that study, as a relationship in which costs and risks are shared among participants. The participants considered were APS, manufacturers of solar components, and the Federal Government, that is, essentially the study team members and DOE.

There are potential risks involved with the application of a new technology, such as a solar thermal central receiver, to repowering of oil/gas-fired steam plants. The major ones for solar repowering that must be considered include:

- 1) Electricity rate considerations affecting the ability of APS to capitalize the plant cost into the existing rate base;
- 2) The scaling of solar hardware components without benefit of intermediate demonstration steps;
- 3) The reliability of the new technology;
- 4) Increased costs due to new components and subsystems;
- 5) Increased costs of operation and maintenance;
- 6) Changes in federal and state regulatory requirements as related to the application of renewable resources.

These risks ultimately relate to financial exposure, which must be evaluated and decided upon both by the APS Board of Directors and the regulating body, Arizona Corporation Commission. The identification of an acceptable institutional arrangement can only be on the basis of suggestions; with final selection reflecting the consideration of the aforementioned bodies.

Institutional considerations as they reflect a first-of-a-kind repowering application, must be on the basis wherein the government assumes the majority of the costs and risks, since the project has to be considered as an R&D effort leading to commercialization. The purpose of this section is to discuss considerations that can be used in evaluating institutional management alternatives. Available APS experience suggests that the ultimate success of an institutional arrangement, as applied to repowering, can be related to the:

- 1) Ease of cost of financing;
- 2) Degree of APS cost and risk sharing;
- 3) Degree of centralized project control;

- 4) Potential for effective reduction of uncertainties;
- 5) Financial resources of APS;
- 6) APS - vendor relationships.

Acceptable approaches to each of these considerations were identified and discussed.

Detailed descriptions of subsystems are included in Chapter 5 and the appendices. The appendices also contain detailed drawings, equipment specifications, operating procedures, performance data, and cost data. Contained in this chapter are the system level designs, performance, and cost data.

4.1 SYSTEM DESCRIPTION

The advanced conceptual design for solar repowering of the Saguaro power plant resulted from: 1) the Saguaro Power Plant Solar Repowering Project of 1979 and 1980, 2) the feasibility of considerations discussed in Chapter 2, and 3) the sizing and configuration trade studies described in Chapter 3. The Saguaro power plant was considered for repowering because it uses oil and gas, the insolation level is high, and there is plenty of suitable land available. Unit One was selected because its steam inlet conditions are representative of many turbines in the United States and it is in good condition having been reworked and upgraded in 1975. The other major item was selecting the use of molten salt as the receiver heat and transport fluid because it is safe, provides cost effective thermal storage, and maintains its high temperature in passing through storage. Molten salt is also compatible with Unit One steam conditions, and results in a simpler system because it is used only in a liquid phase.

A diagram of the repowered system is shown in Figure 4.1-1. Martin Marietta second generation heliostats (57.41 m^2) were selected for the collector field as they are appropriate to the time frame of interest. They also meet the same accuracy specifications as the first generation heliostats. The selected heliostats promise low cost in high production quantities, yet can be produced for reasonable cost in the quantities required for this project. Martin Marietta has more experience in producing heliostats than any other potential vendor and thus has a better knowledge of how to manufacture and deliver cost effective heliostats. Every heliostat delivered by Martin Marietta has met all of the required performance specifications.

The heliostats reflect solar energy into the four apertures of the cavity receiver that is mounted on a 120 m (393.7 ft) conical reinforced concrete tower. As part of the prior study, a quad-cavity receiver was shown to be more efficient than an exposed receiver for this application. Each of the cavities has a door that can be closed to reduce thermal losses when the receiver is not operating. These doors are covered with an ablative material that helps to protect the receiver absorber tubes and door structures in the event of a total electric power loss to the solar system.

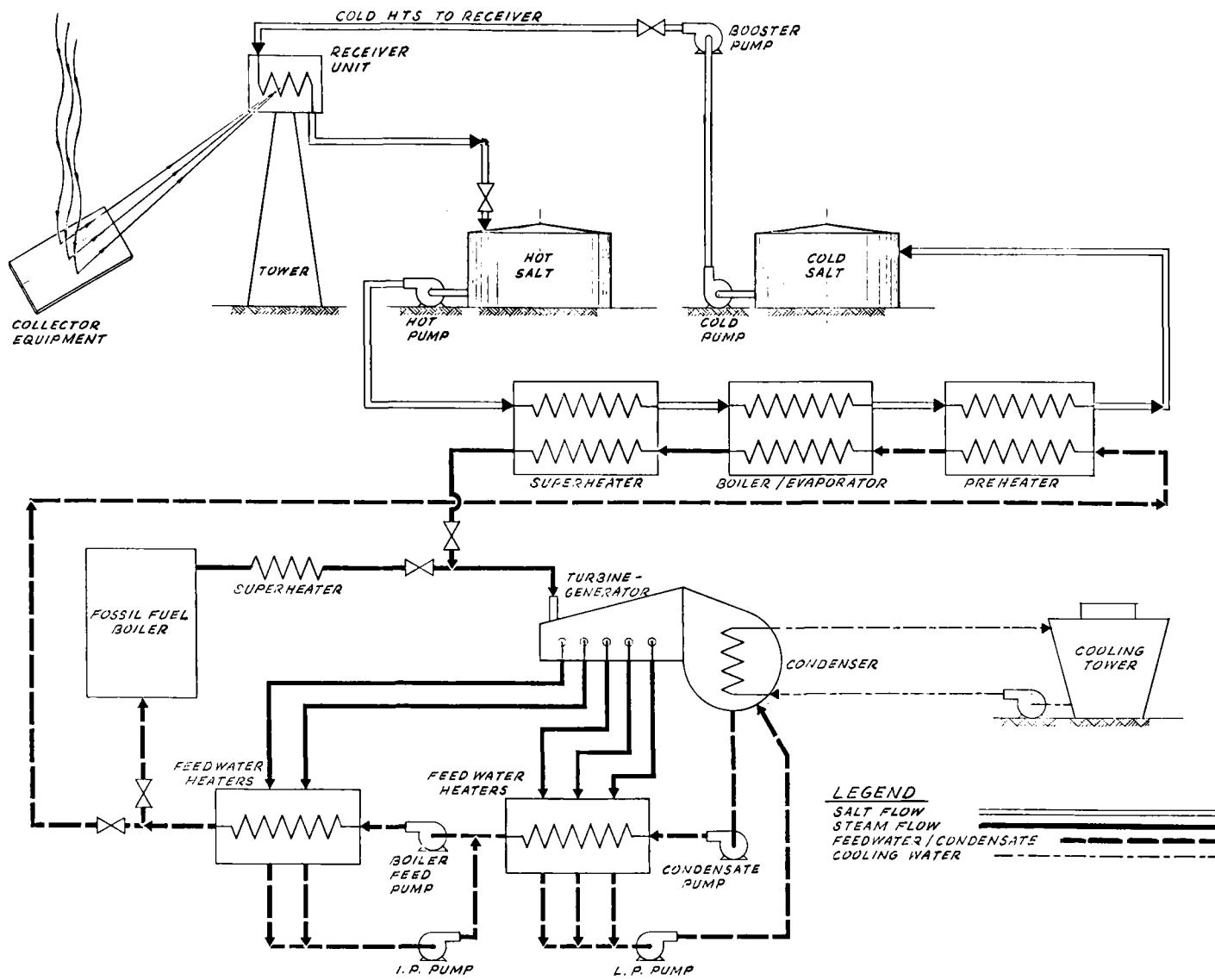


Figure 4.1-1 Repowered System Diagram

The use of a relatively large storage system decouples the collection of solar energy from the use of that energy by the turbine generator. This means a much simpler operation because the turbine never sees the immediate effect of cloud passage. Molten salt leaves the cold storage tank at 277°C (530°F) and is pumped via the main circulation pumps (cold pump) through approximately 1.13 km (0.70 mi) of horizontal piping to the receiver tower and booster pumps. The booster pumps provide the hydraulic head to move the salt up the tower and through the receiver. A surge tank is used at the inlet to the receiver and a special outlet device is used at the outlet of the receiver. These devices decouple receiver salt flow transients from transients in the long supply and return piping. After being heated to 566°C (1050°F) in the receiver, the salt exits into the downcomer. Maximum receiver absorber tube temperature at the design point of noon on the summer solstice is 589°C (1092°F). Salt level at the receiver outlet is maintained by a morning glory spillway. The salt flows over the edge of the spillway and then flows down the inside of the downcomer leaving the center area open. After reaching its limit velocity of approximately 12 m/sec (40 ft/sec), the salt falls into a plunge pool where most of its kinetic energy is absorbed. A series of five sets of morning glory spillways and plunge pools, called the receiver outlet works, are used to dissipate much of the salt's mechanical energy. The hot salt then flows to the storage area where it is sent to the hot storage tank (or to the cold or drain tanks during startup).

The cold salt storage tank is made of carbon steel to the same general requirements as oil or hot asphalt storage tanks except that it has thicker external insulation. The recommended form of the hot salt storage tank is to again use a carbon steel shell for the tank and some external insulation. However, there will be a significant amount of internal insulation. A special, thin, Incoloy 800 liner is used to keep the hot salt from contacting the insulation. The liner has a waffle-like configuration that accommodates thermal expansion and contraction as well as transmitting the pressure loads through the internal insulation to the carbon steel shell of the tank. An internally insulated hot salt tank is recommended because it promises to be significantly cheaper in the larger sizes appropriate to larger solar systems. However, if the DOE sponsored storage subsystem research experiment results do not support the internal liner, then the tank configuration selection may change to an externally insulated hot salt cylindrical tank made of 304 or 316 stainless steel.

The solar steam generator consists of three separate counterflow heat exchangers (superheater, boiler/evaporator, and preheater). A set of hot salt pumps is used to maintain salt flow from the hot salt storage tank, through the solar steam generator, and back to the cold salt tank. The solar steam generator takes pressurized water from the existing feedwater system (heaters and pumps) and converts it to steam at the same conditions as the existing fossil-fired boiler. A water recirculation pump is used to recirculate water from the steam drum to

mix with boiler feedwater to ensure that the preheater inlet water temperatures are high enough to prevent salt from freezing in the preheater. A salt recirculation pump is used to transfer cold salt from the preheater outlet back to the boiler inlet, and to maintain the desired salt temperature into the boiler/evaporator during steady state operation and transients.

The interfaces between the solar and fossil systems are configured so that fossil can be used alone, solar used alone, or the two systems can generate the same quality of steam at the same time in selectable proportions. This approach includes the ability to automatically change the power level of either, or both systems from the APS dispatch center. Because the fossil system can be operated alone, there is no change in the availability of Saguaro Unit One as part of the APS generation capability; or, the Saguaro Unit One capacity credit is retained.

The Unit One fossil steam generator is an outdoor unit with economizer, water wall boiler and superheater. The unit can burn oil, gas, or both. The turbine generator was fitted with a new high pressure steam shell in 1975 that upgraded its capacity to 120.2 MW_e gross. The EPGS cycle uses five feedwater heaters and a steam jet air ejector. The configuration of the condensate, boiler feed, and drip pumps (intermediate and low pressure) is shown in Figure 4.1-1. A conventional forced draft cooling tower is used for the condenser circulating water. Makeup water for both the boiler and cooling water system is obtained from a set of on-site deep wells.

The rationale for selection of a single collector field can be seen on Figure 4.1-2. Use of a single field results in shorter horizontal piping as compared to multiple fields. Additionally multiple near-circular fields would not pack as many heliostats into the available space. A second field could be located to the north and slightly west of the station. That location is sufficiently far from the cooling towers and has been reserved for a possible future repowering of Unit Two at Saguaro.

The receiver tower was located in the field on the basis of prior experience with the RCELL collector field optimization program. The DELSOL optimization program located too few heliostats in the south quadrant of the collector field to justify the presence of a south cavity. As discussed in Chapter 3, the storage tanks and solar steam generator are located near the main plant. This is shown more clearly in Figure 4.1-3. The solar steam generator is located close to the interconnection points so that the high pressure steam and feedwater piping can be kept short. These high pressure lines are more expensive than comparable lengths of salt piping. The solar to fossil interconnections are located between the No. One boiler and the feedwater heater deck. A salt drain tank is located next to the solar steam generator; this is the lowest point in the system.

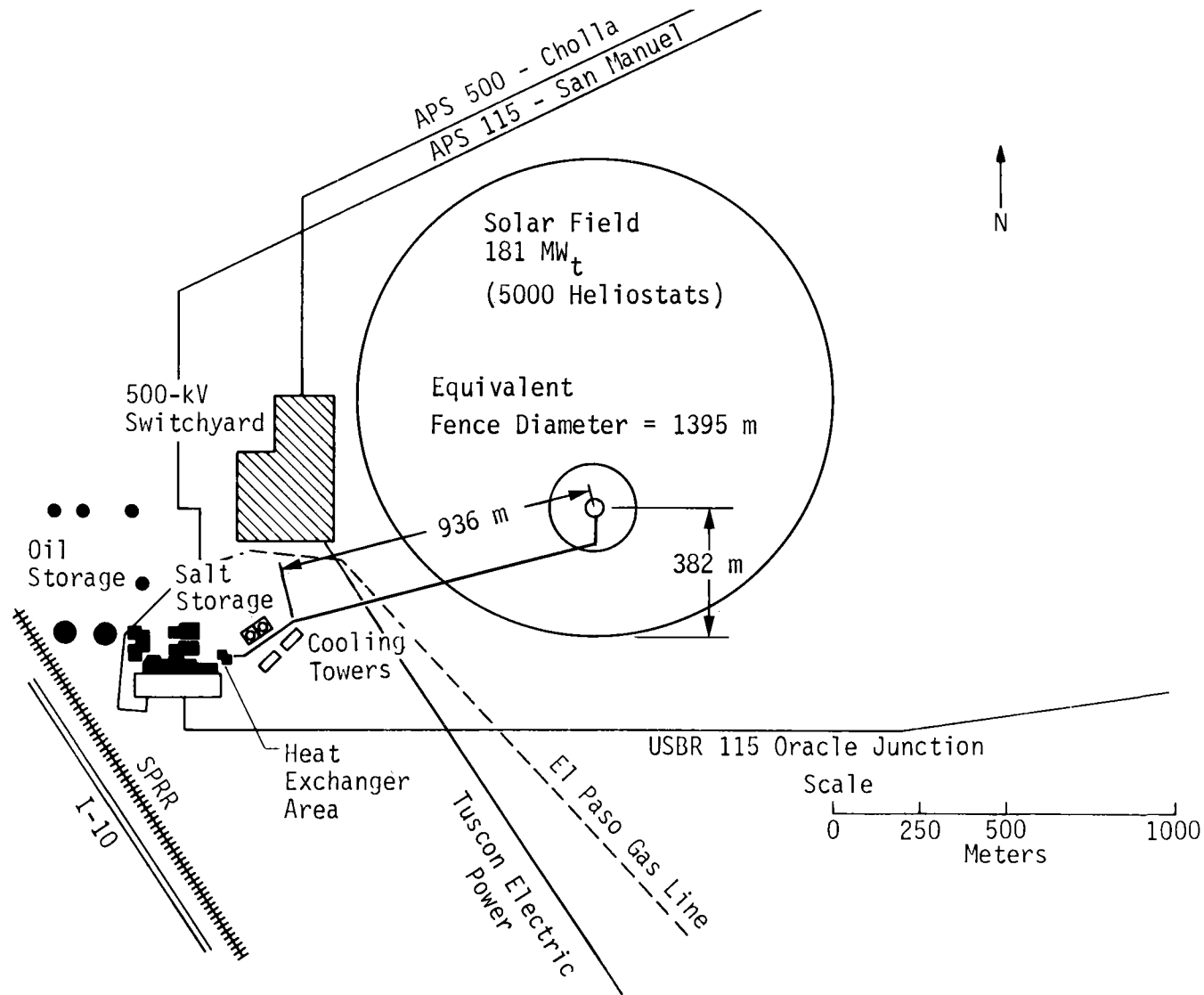


Figure 4.1-2 Collector Field Location

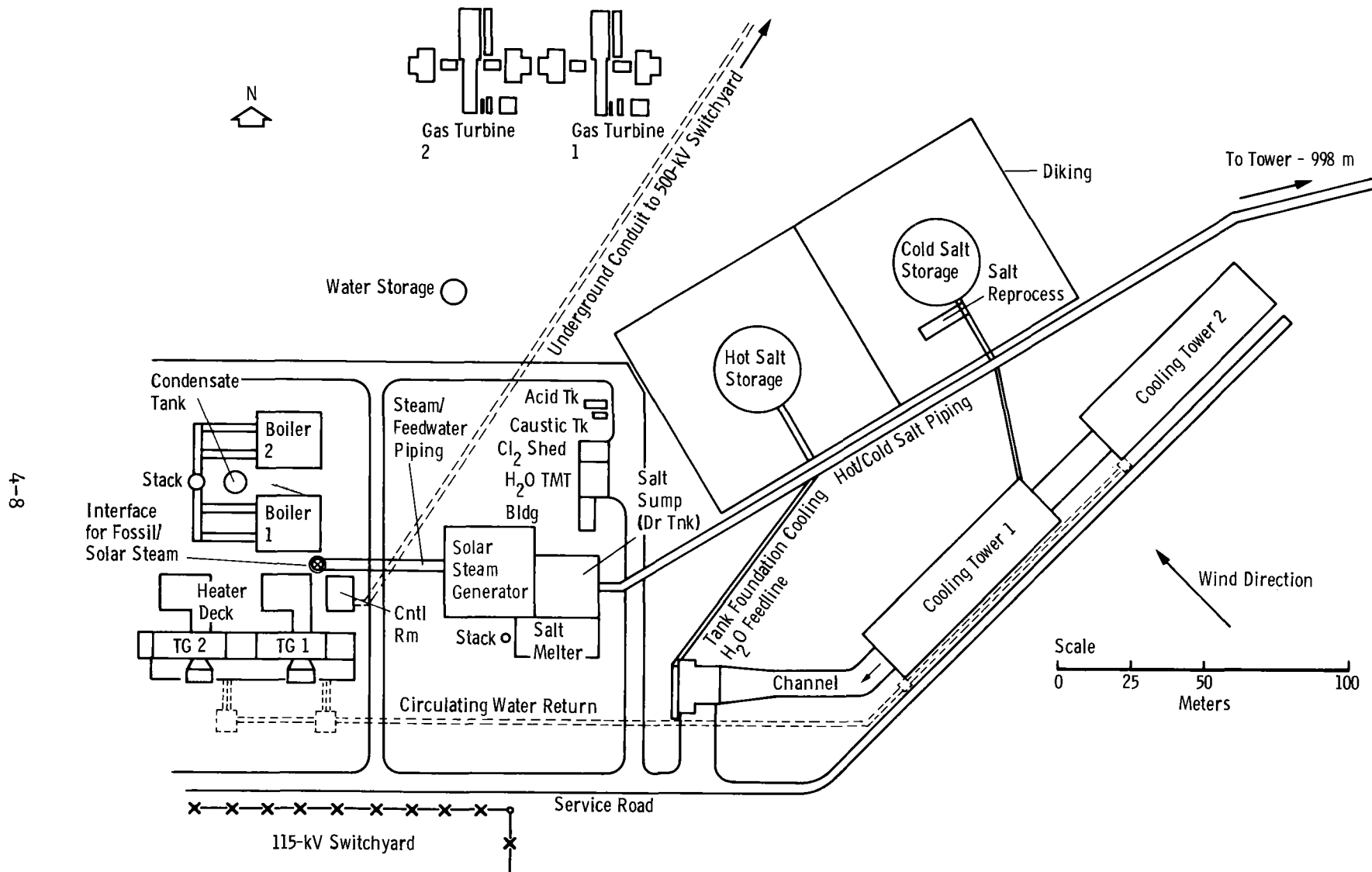


Figure 4.1-3 Solar Equipment Location

The two storage tanks were located at a convenient point close to the solar steam generator, along the horizontal salt piping to the receiver tower. These tanks, and all major salt containing elements, are diked to contain any salt that might leak. A salt melter, which will be used to initially melt the granular salt and to provide a source of heat if the receiver should be shut down for an extended period, is located next to the solar steam generator. The hot salt pumps are located just outside the hot salt dike, and the cold salt main circulation pumps are located just outside the cold salt dike. The receiver booster pumps are located inside the receiver tower above ground level. Water for cooling the various tank foundations will be taken from the circulating water makeup system. After use, it will be returned to the cooling tower return lines.

The selected 60 MW_e net solar configuration will provide minimum interface requirements on the existing plant. To maximize the displacement of oil and gas used in the APS utility system, the equipment will be designed to promote operational flexibility. To enhance this flexibility 4 hours of storage capacity (688 MWh_t) will be installed to aid in the daily delay of the start of the turbine and to provide operational flexibility to the solar plant. Also, the storage may be used to provide extended operation of the EPGS at some part load conditions. Therefore the solar steam generator will be designed to provide quality steam down to one half of its design rating. Further detailed description of the performance and design of the system is included in sections 4.3 and 4.5.

4.2 SYSTEM FUNCTIONAL REQUIREMENTS

The solar repowered plant configuration must meet the requirements of the utility as a safe, simple, and cost-effective method of electrical power generation. For the specific Saguaro site, this solar power system installation must also be configured within the physical constraints of the land area around the plant. Design point and operating environmental conditions used in this study are shown in Table 4.2-1. The solar plant must also be designed to be compatible with the existing plant equipment design and operating conditions. When installed, the plant should also be compatible with the existing and future generation resources of the APS total system, so as to maximize the benefit (i.e., fuel savings) and operating experience of the solar plant in actual utility dispatch.

The level of repowering with solar shall be at least 60 MW_e as established early in the program based on APS requirements (see section 2.2). The actual selected level of repowering is 60 MWe net which corresponds to 55% of the turbine generator's gross capacity. Storage capacity of 4 hours at full level of repowering (688 MWh_t) is selected to provide operational flexibility. Thermal storage will be used to either provide a delay in the start of the turbine in order to promote maximum displacement of oil and gas in the APS system, or to enhance continuous steam production from the solar steam generator. Based on these requirements, the resulting solar multiple is 1.05.

The general requirement of the solar thermal power system is to provide quality steam at 538°C (1000°F) and 10.0 MPa (1450 psig) for the steam Rankine thermal-to-electric power cycle. In addition to providing steam to the turbine, the repowered plant will have the capability to operate on fossil alone, solar alone, or combined in selectable proportions. Then the amount and quality of solar derived steam shall be regulated to provide smooth transitions between fossil and solar operation. A steam proportioning system consisting of control valves and water and steam piping will be provided to blend steam and divide feedwater between the fossil boiler, and the solar steam generator. Steam blending will be required for transitions between fossil and solar-derived steam to the turbine. The blending will minimize temperature excursions in the steam to the turbine to prevent thermal shock. The steam temperature at the turbine steam valve shall average not more than 538°C (1000°F) over any 12 month operating period. In maintaining this average, the temperature shall not exceed 546°C (1015°F), except during abnormal conditions resulting in temperatures not in excess of 552°C (1025°F) for operating periods not more than 400 hours per 12 month operating period, nor exceed 566°C (1050°F) for swings of 15 minutes or less, aggregating not more than 80 hours per 12 month operating period.

Table 4.2-1 Functional Environmental Requirements

Design Point	
Insolation	950 W/m ²
Time	Noon @ Summer Solstice
Environmental	
Dry Bulb Temperature	38.9°C (102.0°F)
Wet Bulb Temperature	20.6°C (69.0°F)
Atmospheric Pressure	94.20 kPa (27.82 in Hg)
Wind Speed	5.1 m/sec (11.4 mph)
Wind Direction	135° (Southeast)
Soil Bearing Strength	191.6 kPa (4000 psf)
Average Annual Daily Insolation	6.93 $\frac{\text{kWh}}{\text{m}^2 \text{ day}}$
Site Location	
Longitude	111° 17' 49.97" West
Latitude	32° 33' 22.28" North
Elevation	589 m (1931 ft) Above Mean Sea Level
Maximum Environmental Conditions	
Operating Wind Speed	15.6 m/sec (35 mph)
Survival Wind Speed	40.0 m/sec (90 mph)
Seismic Zone	UBC Zone II
Earthquake Ground Acceleration	0.10 g
Temperature Extremes	-7 to 46°C (20 to 115°F)

In the interest of achieving safe and simple operation of the solar thermal system, molten nitrate salt has been selected as a heat transport and thermal energy storage medium. The molten salt will be used in a liquid phase to cool the receiver, transport energy from the receiver to thermal storage, and store thermal energy in a single pair of hot and cold storage containment vessels. These vessels will store salt at 566°C (1050°F) and 277°C (530°F). Thermal energy will be accepted at 100% of the power provided by the collector/receiver subsystem. The maximum discharge rate of the thermal storage subsystem will correspond to the maximum thermal rating of the solar steam generator.

The solar collector/receiver subsystem will be able to collect solar energy according to the peak power profile in Figure 4.2-1. All receiver components will be designed to accept power levels of at least 10% above the nominal peak power of 181 MW_t. These high power conditions are possible during an exceptionally good solar insolation day. Salt will enter the receiver at a nominal temperature of 277°C (530°F) and exit at 566°C (1050°F). During the night the cavity receiver will be closed to the environment to minimize heat leakage and cavity cooldown.

The solar steam generator will consist of three separate heat exchangers - superheater, boiler, and preheater. Hot salt at 566°C (1050°F) will enter the superheater and exit the preheater at 277°C (530°F). Feedwater from the EPGs will enter the preheater at 227°C (440°F) and superheated steam will exit the superheater at 543°C (1010°F). The solar steam generator will be rated at a maximum power level of 172 MW_t and will be able to produce quality steam from 86 to 172 MW_t to enhance the operational flexibility of the power system. The 86 MW_t represents the thermal output requirement to produce a turbine generator gross electrical output of 30 MWe. This corresponds to the minimum rating of the fossil steam generator. With the storage fully charged, electrical energy can be produced for nearly 8 hours from storage at the minimum load condition and 4 hours at the repowered level conditions. Operation of the solar steam generator at lower duties will provide the same superheater outlet steam temperatures as at the full repowered level. When the solar steam generator is operating in parallel with the fossil steam generator, the solar steam will be attemperated to match the fossil steam temperature. A salt recirculation pump and loop will be incorporated from the cold salt line back to salt piping between the superheater and boiler (see section 5.7 for schematic of solar steam generator). This loop will serve to recirculate salt as needed to either prevent thermal shock to the heat exchangers, or to maintain salt temperatures to the boiler low enough to prevent corrosion. Two parallel feedwater pumps will be used to circulate water (forced circulation) from the steam disengaging drum through the evaporator. Also a water recirculation pump and loop will be installed from the steam disengaging drum to the preheater feedwater inlet to maintain a high enough temperature (238°C (460°F)) to prevent salt freezing.

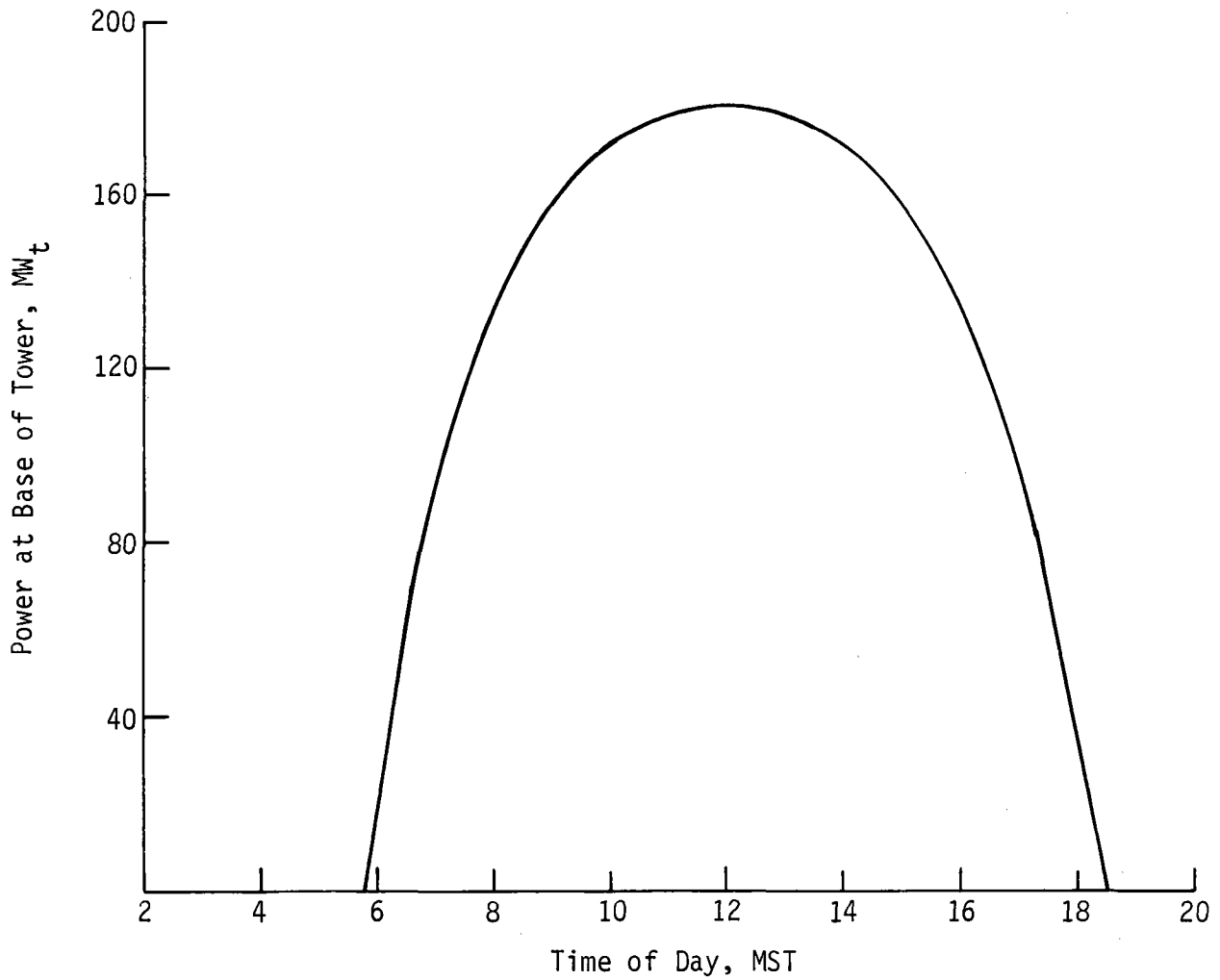


Figure 4.2-1 Peak Solar Profile at Summer Solstice

$$\frac{1}{2} \text{ hr storage} = 167 \text{ MW} \times \frac{1}{2} \text{ hr} = 83.5 \text{ MWh}$$

→ 7% increase in peak power
 would require
 $\eta \frac{40}{83.5} = 48\%$ increase in
 storage.

The design life of the plant is 30 years and construction materials have been selected to satisfy this requirement.

Materials of construction have been selected based on material compatibility tests conducted by Martin Marietta and SNLL. Salt piping and heat exchanger materials were selected based on operating temperatures according to the following:

Carbon Steel Plate (SA516 Gr70)	}	$\leq 343^{\circ}\text{C}$ (650 $^{\circ}\text{F}$)
Carbon Steel Pipe (A 106 Gr B)		
Chrome-Moly (A213 Grade T22)		343 - 468 $^{\circ}\text{C}$ (650 - 875 $^{\circ}\text{F}$)
Nickel Alloy (Incoloy 800) absorber tubes and hot salt storage tank liner	}	$\geq 468^{\circ}\text{C}$ (875 $^{\circ}\text{F}$)
Stainless Steel (304) all other applications		

High pressure water piping is A106 carbon steel and steam piping is A213, GrT22 low alloy (2.25 Cr - 1.0 Mo) steel.

The operational control system of the repowered plant will be structured to provide automatic power generation from APS central dispatch. A supervisory control scheme will be developed to control and monitor the various fossil, solar, and EPGS subsystems. The supervisory computer will accept commands from the APS central dispatch computer and will in turn direct the various first level plant analog and digital control systems. Normal plant control will be completely automatic and a human operator will intervene only for abnormal conditions.

Plant maintenance and repairs shall be conducted in safe working conditions. Personnel will be fully trained in safety and operating procedures to minimize any risk to the health and well being of plant crews.

4.3 SYSTEM DESIGN AND OPERATING CHARACTERISTICS

The selected system characteristics, shown in Table 4.3-1, were developed based on the functional requirements described in the previous section. This configuration utilizes a quad-cavity receiver on a single tower surrounded by 5000 heliostats. As shown in Figure 4.1-2, the tower and heliostat field are located to the east and slightly north of the existing plant. The tower is located to the south of the field center. Salt storage is located near the cooling towers. A simplified flow schematic of the system is shown in Figure 4.1-1. A design point EPGS heat balance is illustrated in Figure 4.3-1. Operating modes and instrumentation and control characteristics are included in the following discussion.

The properties of molten salt as used in the advanced conceptual design are given in Table 4.3-2. This set of data was established by Martin Marietta after a careful review of all available literature. It was decided to use a single set of salt properties so that all analyses in this report involving salt properties would be done on a consistent basis.

Table 4.3-1 System Design Description at Design Point

EPGS	
Type	Non Reheat
Gross Electrical Power (Repowered)	66.0 MWe
Net Electric Power	
Receiver + Storage Operation + EPGs	60.0 MWe
Storage Operation Only + EPGs	62.1 MWe
Fossil* + Receiver + Storage + EPGs	110.7 MWe
Fossil* + Storage + EPGs	112.8 MWe
Fossil Only + EPGs	113.2 MWe
*Fossil at 54.2 MWe gross	
Steam Temperature	538°C (1000°F)
Steam Pressure	10.0 MPa (1450 psig)
Steam Flowrate (66 MWe gross)	67.9 kg/sec (538.7x10 ³ lb/hr)
Feedwater Temperature (66 MWe gross)	216°C (420.4°F)
Heat Rejection	Wet Cooling
Condenser Pressure	6.7 kPa (2 in. Hg)
Gross Heat Rate (66 MWe gross)	9382 kJ/kWh (8892 Btu/kWh)
Gross Cycle Efficiency (66 MWe gross)	38.4%
Collector	
Heliostat Number	5000
Heliostat Size	57.41 m ² (618 ft ²)
Total Mirror Area	287,050 m ² (3.090x10 ⁶ ft ²)
Total Collected Energy to Receiver	191.3 MWt
Field Efficiency (Design Point)	71.6%
Receiver	
Type	Molten Salt Cooled Quad-Cavity
Number	1
Solar Multiple	1.05
Nominal Thermal Power at Tower Base	181 MWt (6.176 x 10 ⁸ Btu/hr)
Maximum Thermal Power at Tower Base	199 MWt (6.790 x 10 ⁸ Btu/hr)
Nominal Salt Flow Rate	409 Kg/sec (3.245 x 10 ⁶ lb/hr)
Salt Temperature - In	277°C (530°F)
Salt Temperature - Out	566°C (1050°F)
Efficiency	90.5%
Number of Absorber Panels	20
Number of Control Zones	2
Absorber Active Surface Area	632.5m ² (6808 ft ²)
Maximum Heat Flux on Absorber	631 kWt/m ² (200,000 Btu/hr-ft ²)

Table 4.3-1 System Design Description at Design Point (cont)

Receiver (cont)	
Maximum Tube Temperature	589°C (1092 °F)
Outer Dimensions	
Height	36.1 m (118.4 ft)
Depth (E/W)	20.1 m (65.8 ft)
Width	19.5 m (63.9 ft)
Total Wet Weight	704x10 ³ Kg (1.55x10 ⁶ lb)
Aperture Midpoint Elevation	134.1 m (440.1 ft)
Thermal Storage	
Type	Hot/Cold Tank Pair
Capacity	688 MWh _t
Salt Quantity	5.59x10 ⁶ Kg (12.33x10 ⁶ lb)
Cold Salt Tank Shell Height	10.19m (33.42ft)
Cold Salt Tank Shell Diameter	22.96m (75.33 ft)
Cold Tank Volume	4218m ³ (148.9x10 ³ ft ³)
Hot Salt Tank Shell Height	11.51m (37.75ft)
Hot Salt Tank Liner Diameter	22.66m (74.33ft)
Hot Tank Volume	4640m ³ (163.8x10 ³ ft ³)
Cold Salt Temperature	277°C (530°F)
Hot Salt Temperature	566°C (1050°F)
Maximum Charge Rate	199 MW _t
Maximum Discharge Rate	172 MW _t
Tower	
Type	Concrete/Conical
Number	1
Height	120 m (393.7 ft)
Base Dimensions	
Outside Diameter	16.8 m (55 ft)
Inside Diameter	16.0 m (52.3 ft)
Top Dimensions	
Outside Diameter	12.3 m (40.3 ft)
Inside Diameter	11.8 m (38.6 ft)
Solar Steam Generator	
Type	
Preheater	U-tube, Straight Shell
Evaporator	U-tube, Straight Shell
Superheater	U-tube, U-Shell
Evaporator Circulation Type	Forced
Duty	172 MW _t (5.869 x 10 ⁸ Btu/hr)
Inlet Salt Temperature	566°C (1050°F)
Outlet Salt Temperature	277°C (530°F)

Table 4.3-1 System Design Description at Design Point (concl)

Solar Steam Generator	
Salt Flow Rate	388.5 kg/sec (3.084 x 10 ⁶ lb/hr)
Steam Flow Rate	67.8 kg/sec (5.380 x 10 ⁵ lb/hr)
Steam Blowdown	0.678 kg/sec (5.327 x 10 ³ lb/hr)
Total Active Surface Area	2870 m ² (30.9x10 ³ ft ²)
Fossil Steam Generator	
Type	Combustion Engineering, Natural Circulation, Water Wall
Fuel	Gas/No. 6 Oil
Duty	316 MW _t (1.079 x 10 ⁹ Btu/hr)
Firing Rate	381 MW _t (1.3004 x 10 ⁶ Btu/hr)
Efficiency	83%
Steam Rate	126.1 kg/sec (1.00 x 10 ⁶ lb/hr)
Steam Temperature	541°C (1005°F)
Steam Pressure	10.7 x 10 ³ kPa (1550 psig)

Figure 4.3-1

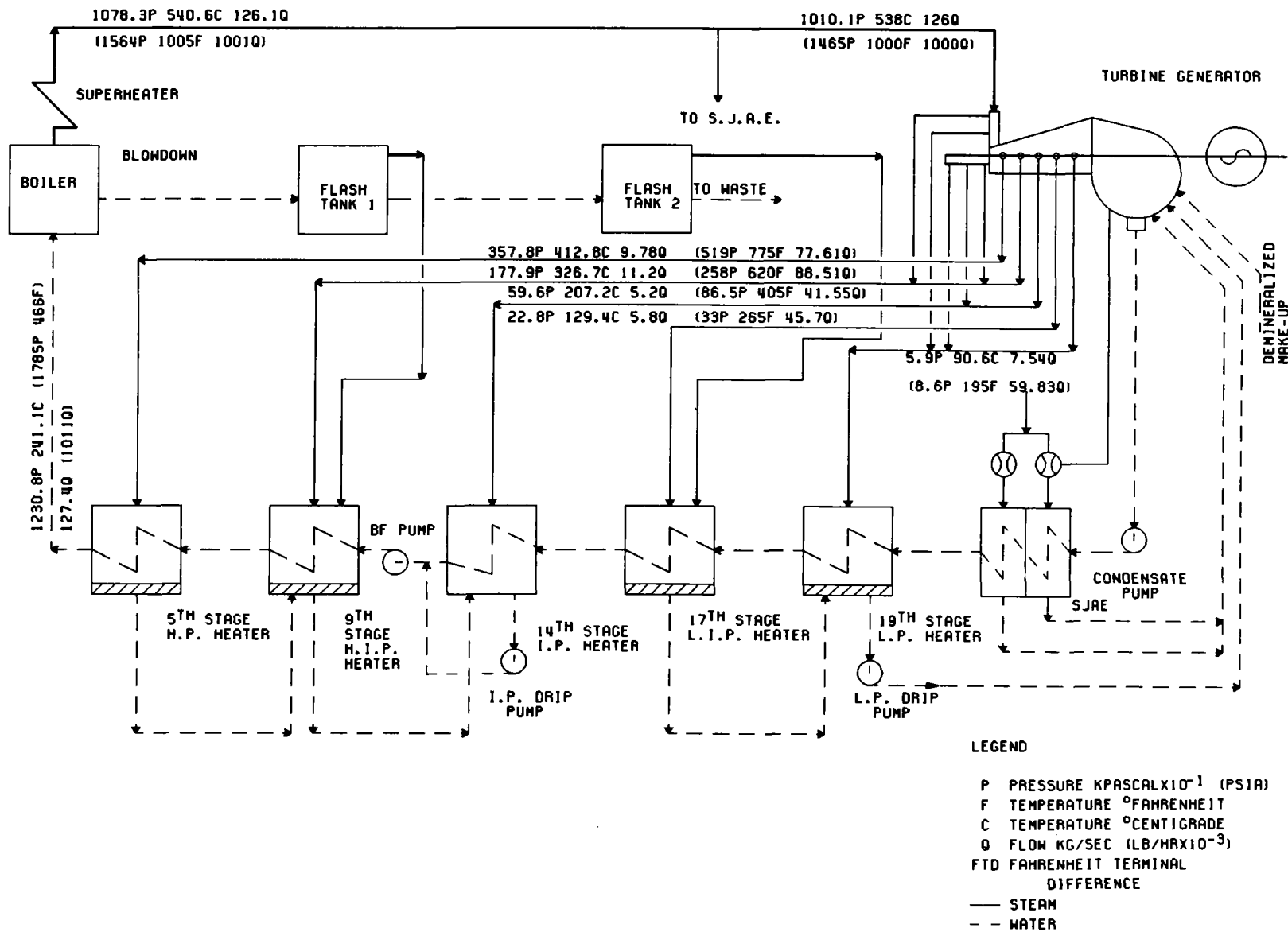


Figure 4.3-1 Saguaro Heat Balance at 100% Power

Table 4.3-2 Properties of Molten Salt

Composition: 60% NaNO ₃ , 40% KNO ₃ by weight
Heat Capacity $C_p = 1532 \text{ watt sec/kg } ^\circ\text{C}$ $C_p = 0.366 \text{ Btu/lb } ^\circ\text{F}$
Density $\rho = 2101.6 - 0.6684T \text{ kg/m}^3 \text{ for } T \text{ in } ^\circ\text{C}$ $\rho = 132.0 - 0.02318T \text{ lb/ft}^3 \text{ for } T \text{ in } ^\circ\text{F}$
Viscosity $\mu = 1.886 \times 10^{-2} - 9.610 \times 10^{-5}T + 1.799 \times 10^{-7} T^2$ $\quad - 1.155 \times 10^{-10} T^3 \text{ Pa sec, } T \text{ in } ^\circ\text{C}$ $\mu = 49.89 - 0.1379T + 1.389 \times 10^{-4} T^2 - 4.790 \times 10^{-8} T^3 \text{ lb/ft}$ $\quad \text{hr, } T \text{ in } ^\circ\text{F}$
Thermal Conductivity $K = 0.52 \text{ watts/m } ^\circ\text{C}$ $K = 0.30 \text{ Btu/hr ft } ^\circ\text{F}$
Melting/Freezing Temperature Range 221 to 245°C 429 to 473°F
Heat of Fusion $\Delta H_f = 1.089 \times 10^5 \text{ watt sec/kg}$ $\Delta H_f = 46.8 \text{ Btu/lb}$

4.3.1 Operating Modes

An assessment of the conceptual configuration was made to identify the basic operating modes for the solar and fossil systems as well as the transitions between these modes. The results of this assessment show the number of operational modes for the repowered Saguaro plant is low because the large storage capacity effectively decouples the solar energy collection process from the use of the solar energy in the EPGs.

By judicious ordering, the number of valid transitions between the steady state operating modes has also been kept low.

The elements involved in establishing the modes, and transitions between modes, are:

- CR - Collector and Receiver;
- SB - Standby;
- S - Storage;
- F - Fossil Boiler;
- E - EPGs.

Therefore, there are four subsystem elements and a standby mode. The standby mode indicates the time that the subsystem equipment is not in one of the other operating modes and that the equipment can be readily transitioned into another operating mode. It is defined differently for each of the modes, e.g., collector and receiver standby means the receiver is full of salt and warm with the heliostats stowed. Each of the elements goes through a standby mode when it is being started from a complete shutdown, or being shut down for an extended period from normal operation.

The basic steady state modes are:

- 1) Collector and receiver operating and filling storage with hot salt;
- 2) Standby;
- 3) The EPGs and solar steam generator operating and removing hot salt from storage;
- 4) The EPGs operating with steam properly proportioned from both the solar and fossil steam generators. The solar system is removing hot salt from storage;
- 5) The EPGs operating with steam only from the fossil steam generator.

One of the ways in which these modes can be used is shown in the solar alone clear day scenario of Figure 4.3-2. The bottom part of the figure shows the resource available--direct normal solar insolation as

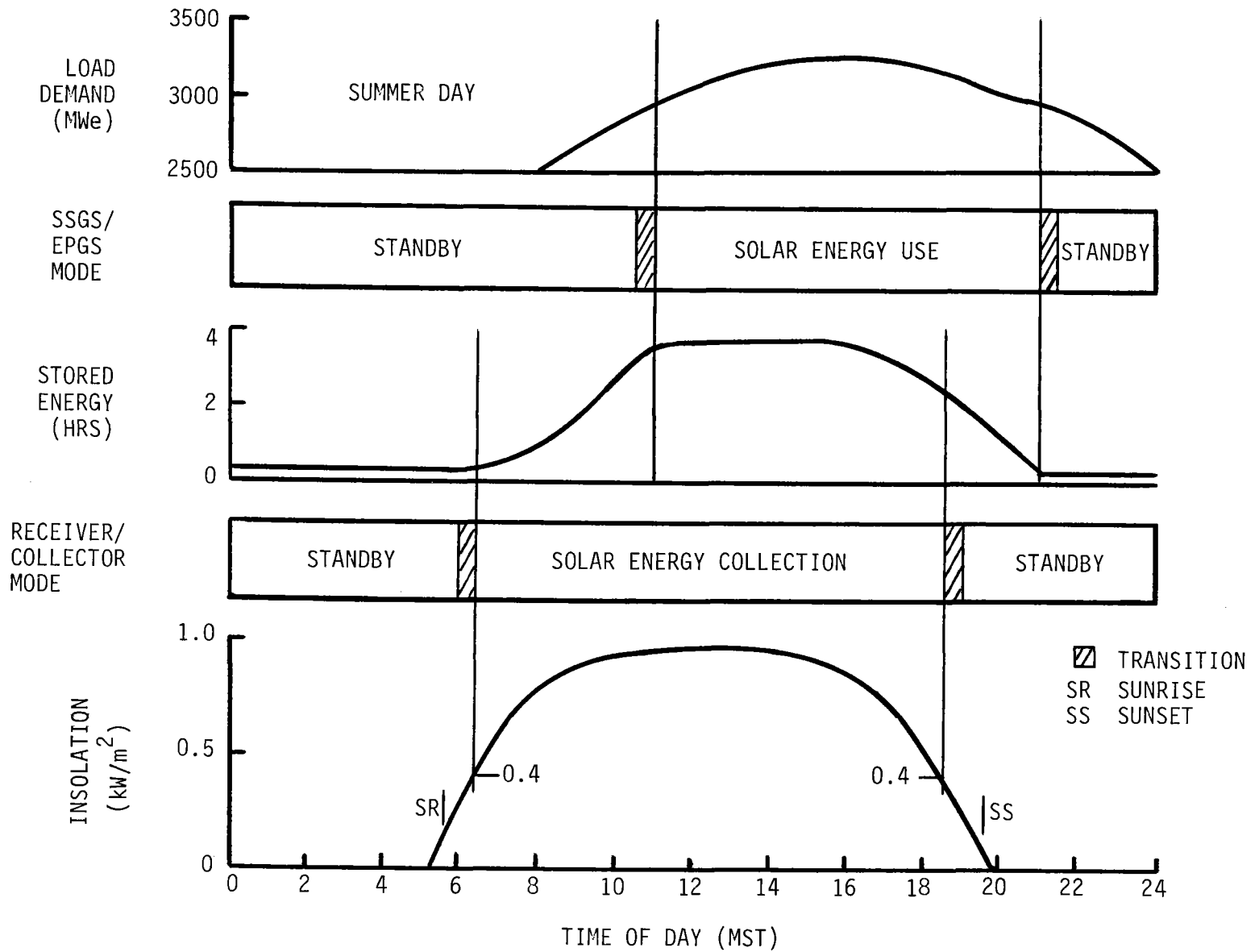


Figure 4.3-2 Clear Day Scenario - Solar Alone

a function of time of day which was taken from the Phoenix TMY tape for a summer day. The upper part of the figure shows the load to be satisfied-- the peak few hundred megawatts of load demand as it is forecast to be on a summer day in 1987 for the APS grid. The middle of the figure shows how our conceptual design can be used to match the resource and the load and how few modes and transitions are required. The receiver and collector are initially in standby. As the sun rises, the receiver and collector are transitioned to solar energy collection as the insolation reaches 0.4 Kw/m^2 . The receiver and collector route the thermal energy directly to storage continuously until the insolation drops below 0.4 Kw/m^2 at which time the receiver and collector are transitioned to standby.

During the morning, the APS dispatcher checks the weather and load forecasts for the day and decides that he wants power from Saguaro starting at 11 AM so he can shave the peak load. The solar steam generator subsystem (SSGS) and the electrical power generating subsystem (EPGS) are then transitioned from standby so full power will be generated starting at 11 AM. Power generation from stored solar energy then continues until storage is down to a minimum level of approximately 0.4 hours, at which time (9PM) the SSGS and EPGS are transitioned to standby to await the next availability of solar energy and a call for power from the dispatcher. If the solar energy had not been needed until later in the day, then it would have been necessary to put the receiver and collector into standby when thermal storage became full. Had solar energy been needed earlier, the dispatcher could have requested it at any time there was enough energy in storage. The small number of operating modes and transitions needed on a clear day is obvious from the figure as is the low level of interaction between the collection and use of solar energy.

Because the five basic modes are not mutually exclusive, certain derived steady state modes can be considered. These are when elements operate in parallel.

The derived steady state modes are:

- 1) and 3) Collector and receiver operating and filling storage while the solar steam generator removes heat from storage to generate steam for the EPGS. (Early afternoon on Figure 4.3-2).
- 1) and 4) As in the 1) and 3) combination except that steam for the EPGS is also being generated by the fossil steam generator in the desired proportion.
- 1) and 5) The collector and receiver operating and filling storage while the EPGS operates on steam from the fossil steam generator.

For none of the three derived modes are there significant interactions between the basic modes. Consideration of the various operating conditions during representative operating days, shows that the normal transitions only involve going between the basic modes even though the derived modes may exist for some parts of the day. The days considered include: all solar with immediate or smart dispatch (for the displacement of the most expensive fuel), all fossil, and combined solar and fossil. The result is that only five, two-way, transitions need be considered during normal operation. These are:

- 1) and 2) Collector and receiver operating to and from standby.
- 3) and 2) EPGS and solar steam generator operating to and from standby.
- 3) and 4) Steam generation by solar steam generator to and from steam generation by both solar and fossil systems.
- 5) and 2) EPGS and fossil steam generator operating to and from standby.
- 5) and 4) Steam generation by fossil steam generator to and from steam generation by both fossil and solar systems.

A matrix representation of these transitions, including the "to" and "from" effects, is shown in Figure 4.3-3. The matrix being symmetrical about its diagonal reflects the to/from aspects of the transitions. The result is a relatively simple set of modes and transitions.

FROM \ TO	I CR - S	II SB	III S - E	IV S - E F	V F - E
I CR - S	-	X			
II SB	X	-	X		X
III S - E		X	-	X	
IV S - E F			X	-	X
V F - E		X		X	-

Figure 4.3-3 Operating Mode Transition Matrix

The operating, standby and fully non-operational modes of the solar steam generator and the transitions between these modes have been examined in some detail. (See Appendix B). A method of warming the solar steam generator using feedwater and steam from the fossil system

was conceptualized and evaluated. The analysis identified the need for two additional interfaces to the existing system and additional ways of using the water and salt recirculation pumps. The result is a useful technique for transitioning the solar steam generator.

Similar steady state operating and standby modes and the transitions between these modes have been defined for the receiver and molten salt supply and return piping. These procedures are outlined in Appendix B. Development of the procedures aided in defining control parameters for the main circulation and receiver booster pumps, the need for a receiver surge tank, and the need for a method of handling intermediate temperature salt coming from the receiver during startup, shutdown and partly cloudy weather.

4.3.2 Instrumentation and Controls

The entire repowered electrical power generation facility will be monitored and controlled by a master control subsystem which consists of six functional subsystem control subsystems, an operational control subsystem that integrates the six control subsystems, a data acquisition system, and red-line units. The controlled subsystems are:

- 1) Collector field;
- 2) Receiver;
- 3) Energy Storage;
- 4) Fossil Steam Generator;
- 5) Electric Power Generation;
- 6) Solar Steam Generator.

Of these six controlled subsystems, the fossil steam generator and electric power generation subsystems currently exist at Saguaro and their control hardware is established and operating. A recommendation for upgrading the fossil steam generator and the EPGS control systems to be compatible with the controls on the solar system is described in paragraph 5.6.6. The operational control subsystem also provides the interfaces with the APS central dispatch center, the data acquisition subsystem, and the red-line units. The red-line units independently monitor all critical plant parameters and warn the operator of any emergencies. Caution and warning signals are also generated by the operational control subsystem, the data acquisition system and the distributed controllers for the various subsystems. Response to emergencies can be effected through the various control subsystems.

The general design approach for the master control subsystem utilizes the supervisory control concept. The six plant analog and digital control systems are responsible for first-level control functions while the supervisory computer of the operational control subsystem prescribes the proper operating instructions (i.e. set points) so that desired operational objectives can be met. Normal plant control is completely automatic and the human operator intervenes only for emergencies or gross operational conditions. A completely separate set of data collection, processing, and display equipment is used for warnings and emergencies. It is called a "red line" system. In addition to these emergency categories, the operator will be involved during start-up and shutdown and during transitions between steady-state operating modes (see section 4.3.1). When all the plant equipment is operating correctly, control will be from the main control room. However, when necessary, some control activity can take place from electronic control racks in various plant locations. Specific details on the instrumentation and control can be found in the Subsystem Conceptual Designs in Chapter 5 and the Master Control Subsystem discussion in section 5.3.

4.4 SITE REQUIREMENTS

Because the collector field site is relatively flat, and the location for the rest of the solar equipment is flat, relatively little site preparation is required. Site grading will involve the filling of a few washes, preparing the dikes around the energy storage tanks, and preparations for the installation of foundations, access roads, cable, conduit, and piping. A series of drainage trenches will be dug and backfilled with gravel to keep water away from the tower and other major equipment foundations. The solar steam generator and energy storage area of 6000 m² (1.6 acres) will require the removal of a minimum amount of desert scrub and grading for drainage since the land presently slopes to the southwest. In addition to a 7.6 m (25 ft) wide, heavy traffic, road from the heat exchanger area to the tower, aggregate base coarse (ABC) roads 0.1 to 0.15 m (4 to 6 in.) thick, will be provided for mirror access. Depending on additional evaluation of the grading and drainage requirements, the area under the heliostats will either be covered with ABC or left with the natural cover. As a security precaution, a 2.4 m (8ft) high chain link fence with barbed wire will be installed around the collector field and along the tower road to connect with the existing security fence.

The existing control house will be approximately tripled in size on both levels to provide space for the video consoles, computers, peripheral equipment and office space for control operators, auxiliary operators and water and salt analysts (see also paragraph 5.3.2). A new combined administration and instrument repair building of 372 m² (4000 ft²) will be built near the existing building. The administrative area consists of office space for the plant managing personnel, locker rooms for the operating and maintenance personnel, space for plant records and files, conference rooms, and rest rooms. The present plant administrative facilities do not have the space needed for the additional personnel associated with the solar repowering operations. A new building will be constructed for solar system repair, including the heliostats. This warehouse/machine shop will have a 9 m (30ft) clearance for a 4500 kg (5 t) bridge crane. This shop will be a 278.7 m² (3000 sq ft), rigid frame, insulated metal siding building located in the heat exchanger/storage tank area. This building will provide covered storage for salt and specific spare parts. In addition, it will provide additional work areas for the instrument repairmen, electricians, mechanics, and other maintenance personnel. This location has been selected since it is central to the proposed additional solar facilities. All other new building construction will be in a style to match the existing buildings.

The existing power plant has been designed to fail safely in that the loss of load will cause the turbine to disconnect from the transmission lines and to shut down the turbine safely. This results in the loss of most electrical power for auxiliaries. Concurrently the fossil boiler will shut off fuel flow and vent any over pressure in the steam drum. A similar situation, loss of electrical power to most auxiliaries, will occur for many on-site failures. Other than the temporary loss of generation, the situation is not serious and the boiler and turbine generator can be restarted when power can be brought to the unit from an external source or from Unit No. Two.

The loss of electric power is more serious for a solar thermal power system. When fluid flow through the receiver stops, the solar flux level must be quickly brought to near zero. This could be difficult if there is no electrical power for the heliostats. This situation is addressed in detail in section 5.2.2. For the purpose of this discussion it is considered desirable to increase the probability of having an adequate amount (6.5 MW_e) of auxiliary power available. The approach to obtaining this increase in reliability is shown in Figure 4.4-1. The Saguaro switchyard has two 115 kV buses (east and west) that are connected to separate transmission lines and that are not normally connected together. The preferred source of power (A) to the collector field and receiver salt pumps is the 12 kV transfer bus. The 12 kV transfer bus is connected to the 115 kV west main bus. However, upon loss of the west bus, the system can be immediately (less than 8 cycles) switched to the 115 kV east main bus through the alternate source (B).

The connections between the preferred and alternate sources and the solar system are shown in Figure 4.4-2, where the (A) and (B) connections are shown in the upper left hand part of the figure. Separate 12 kV/4160 V transformers are used for each source. Either source can feed all, or some, of the loads in the tower area. The major loads, such as the booster pumps, are run at 4160 V and the smaller loads, such as the heliostat field, are run at 480 V.

A 900 kW diesel generator has been provided as a backup for those cases where both the (A) and (B) power sources are lost for an extended period. If either, or both, of sources (A) and (B) are lost, then the diesel will be started automatically and can be ready to accept load in 25 s. The circuitry will be set up so that the diesel can power up to 900 kW of selectable loads at 480 V. This will permit stowing the heliostats a section of the field at a time, operating the salt transfer pump, operating control valves, or operating the tower elevator. The purpose of the diesel is not to respond to an emergency, but rather to help secure the system after an emergency and to avoid further damage. Emergency response of the solar system is discussed in section 5.2.2.

Figure 4.4-1

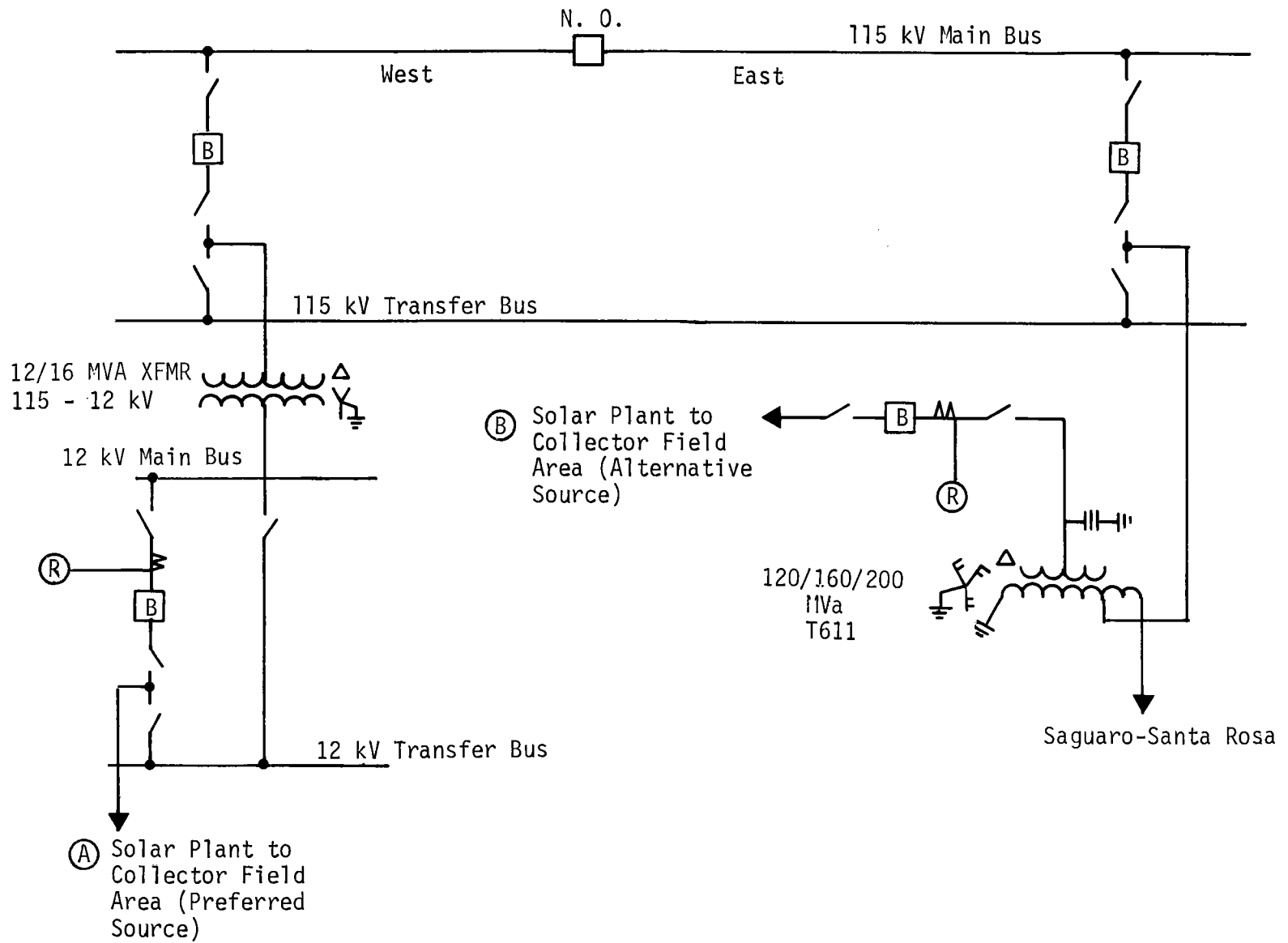


Figure 4.4-1 Alternative Auxiliary Power Sources

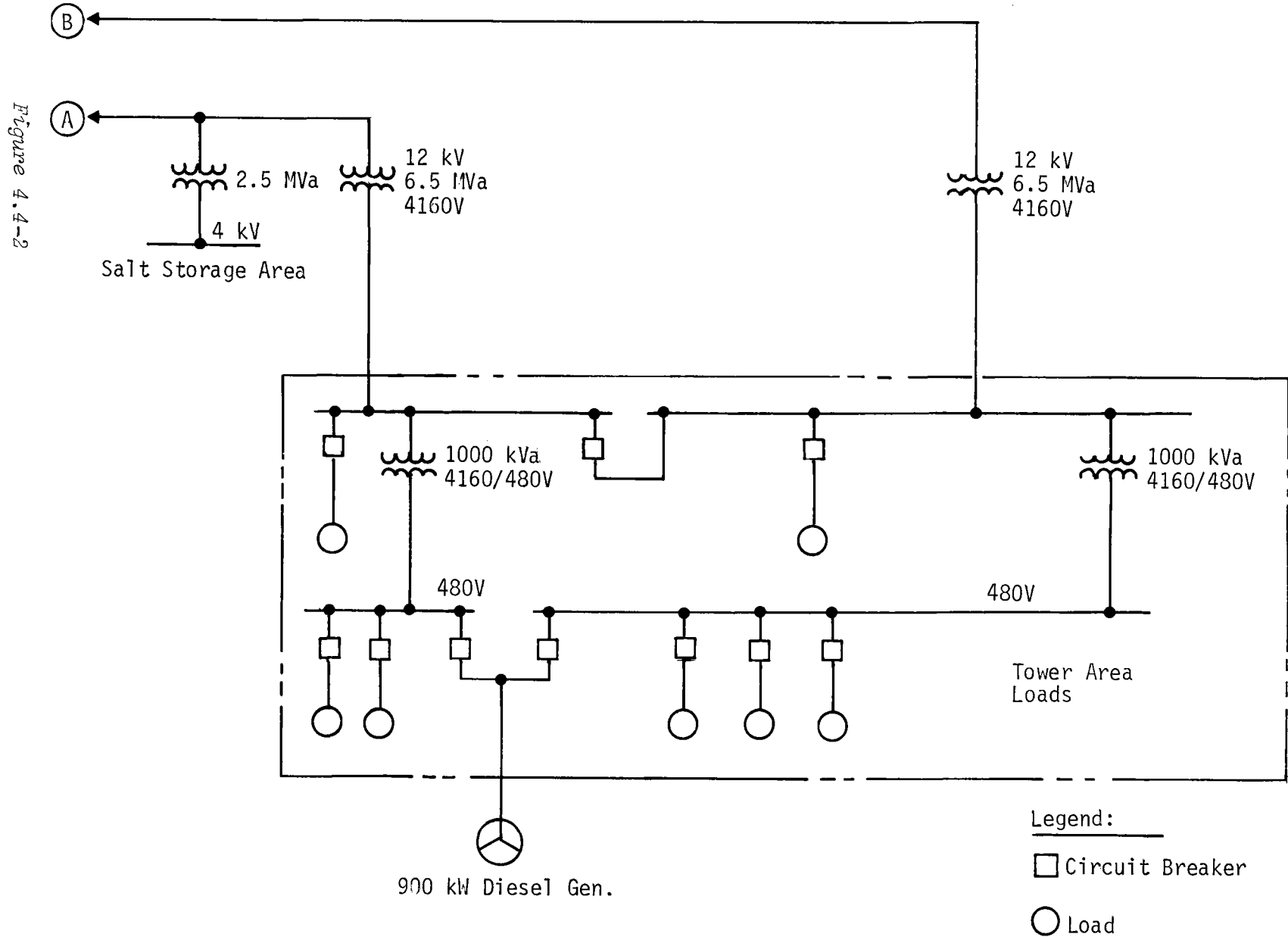


Figure 4.4-2 Solar System Auxiliary Power Distribution

The interfaces between the existing plant piping and the solar power additions have been kept to a minimum. Down time of the existing plant during cut-in of the solar system will be minimized because each connection will be valved, or relayed, so that the existing plant can be operated after the cut-ins have been completed. The cut-in work will be scheduled as part of a normal shutdown in 1984 so that connections to the solar system can be readily made. The interfaces between the solar parts of the system and the existing plant are such that nonoperation of the solar part will not inhibit operation of the existing plant in the manner customary, before the solar system was added. This feature is a reflection of the requirement for turbine operation from fossil generated steam alone, solar generated steam alone, or both together.

The specific interfaces are summarized as follows: (a more detailed listing is in section 3.8.3 of Ref 1-3), boiler feedwater and high pressure steam connections to the existing piping; start-up system attemperator and steam drum drain connection to the condenser; energy storage tank foundation cooling connection to cooling tower circulating water system; natural gas and fuel oil connection to salt melter; service water; fire protection; service and instrument air extensions to the new facilities; electronic to pneumatic conversions and connections to the existing boiler and turbine control system; two 12 kV electric connections to the existing 12 kV substation and the existing 230/115 kV autotransformer are required.

The repowered system plot plan, Figure 2.6-2 of section 2.6, indicates the existing two unit boilers, turbines and cooling towers, and the repowered system equipment. The repowered system equipment is located east of the present plant. The salt/steam heat exchangers are adjacent to the existing units, then the energy storage tanks and, approximately 1 km to the east and north, the receiver tower surrounded by the solar collectors. These facilities are interconnected with piping, controls, and wiring. The major site constraints are discussed in section 2.4 and shown in Figure 2.4-1. The location of the major solar system elements and plant interfaces are discussed in section 4.1 and shown in Figures 4.1-2 and -3.

The primary interface connections between the new solar and the existing systems are the feedwater and steam piping connections, which are located between the Unit One heater deck and fossil boiler as shown on the plot plan. Additional connections to the other support systems will be determined during the preliminary design.

The plot plan indicates that the repowering equipment has been located in such a manner that it does not create any constraints on the use of any existing, or proposed equipment. In addition, this arrangement does not create a situation where any of the existing facilities will require removal and/or reinstallation.

4.5 SYSTEM PERFORMANCE

The design point and annual performance of the selected Saguaro repowering advanced conceptual design has been evaluated, using three computer models--DELSOL II, TRASYS, and STEAEC. The performance of the individual solar subsystems were modeled separately, with the results input into the STEAEC system simulation program, together with solar insolation and weather data, to model the annual performance of the system.

4.5.1 Design Day Performance

As discussed further in 5.1, the collector subsystem performance was evaluated using the DELSOL II computer program. The collector field performance, as defined by the ratio of solar radiation inside the apertures over the total available radiation incident on the collector area, was calculated for a matrix of 7 sun azimuth angles and 6 sun elevation angles, as well as for the sun position at noon, day 172 for the site. As discussed further in 5.2, the receiver losses were evaluated using the TRASYS thermal radiation analysis model, again for the design point and off-design cases. Thermal losses in the salt vertical and horizontal piping were also estimated.

The resulting design point system performance staircase is shown in Figure 4.5-1. Design point is solar noon on summer solstice. Assuming a reference direct normal insolation value of 950 W/m^2 , the total system efficiency at the design point is 23.18%. The design point staircase shows an overall field/receiver efficiency of 66.5% (including heliostat reliability, cosine, reflectivity, shading and blocking, tower shadow, attenuation, spillage, absorbtivity, and receiver radiation losses).

The EPGS gross cycle efficiency of 38.4% was determined for the selected steam conditions of 538°C (1000°F), 10.0 MPa (1450 psig) and 6.75 kPa (2 in Hg) back pressure. An additional 6 MW_e is required for auxiliaries to operate solar subsystem components and miscellaneous support buildings and equipment. This design point staircase does not include operation of the fossil energy source, which requires some energy for induced and forced draft fans, and fuel pumps. The net power output from the system at the design point with a total of 5,000 heliostats gives 60 MW_e net, with 8.9 MW_t going to the storage system.

4.5.2 Annual Performance Using STEAEC

The annual system performance was evaluated using the STEAEC system model, which simulates the performance of the system using 15 minute time steps and a site weather data tape. For site weather data (insolation, wind speed and direction, temperature and pressure), the SOLMET Typical Meteorological Year (TMY) weather data base was chosen. Because no TMY data tape exists for the Saguaro site area, the TMY

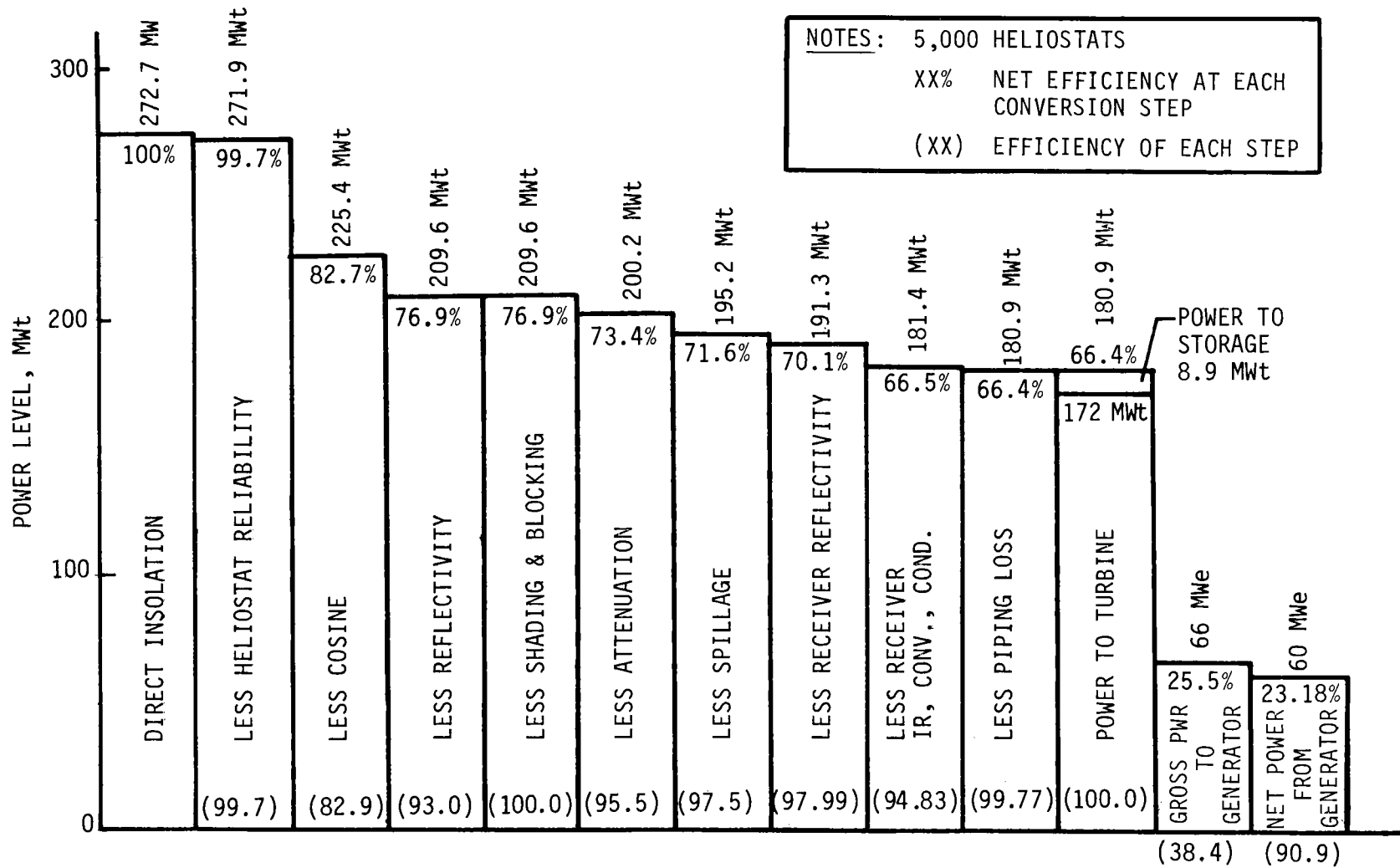
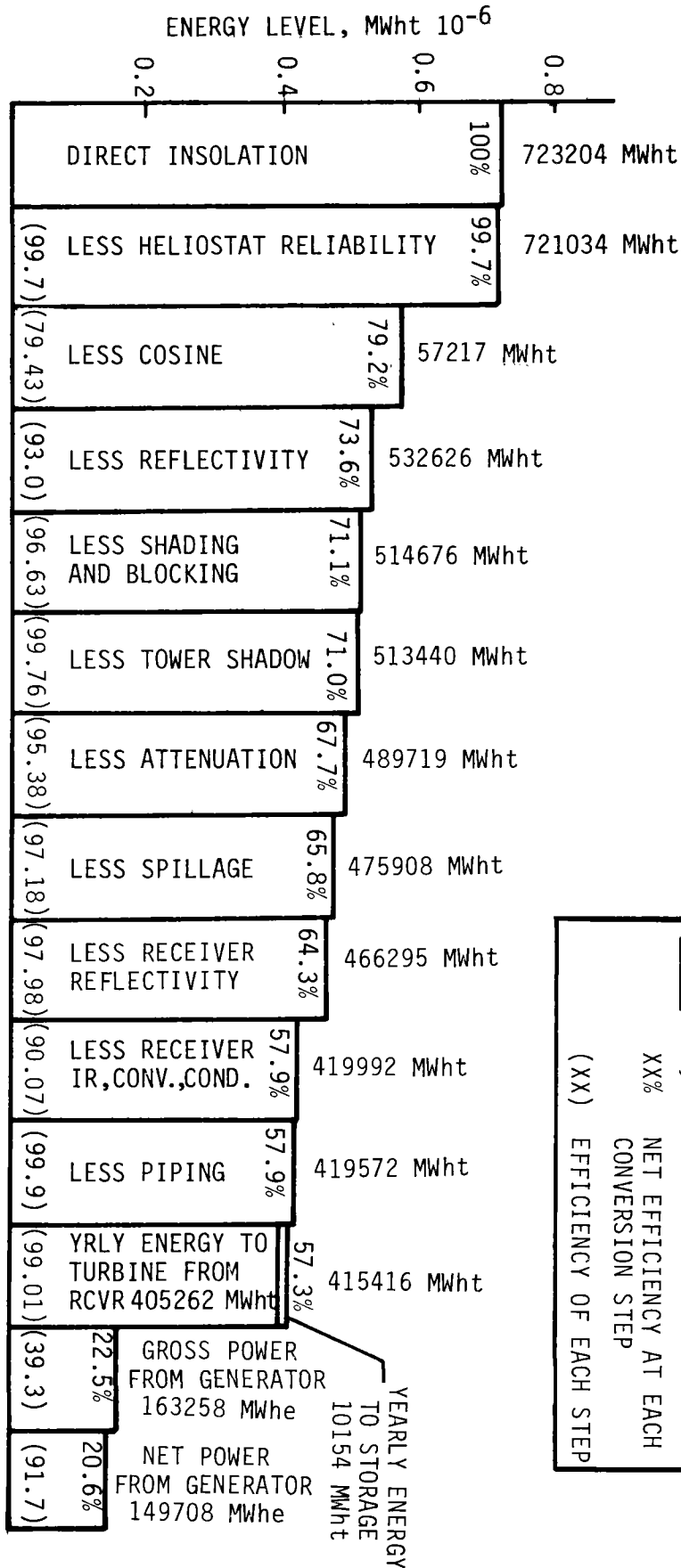


Figure 4.5-1 Design Point Efficiency for 60 MWe Solar Plant (SM = 1.05)

data tape for Phoenix, AZ was used. As discussed in section 2.5, Phoenix, AZ is approximately 143 km (89 mi) northwest of the Saguaro site. The higher site elevation and lower humidity levels of the Saguaro site should result in the insolation at Saguaro being slightly greater than that at Phoenix. The SOLMET data, recorded on the tape at 1 hour intervals, was converted to 15 minute interval data using linear interpolation techniques before input to the STEAEC model for a more realistic evaluation of the system performance. This SOLMET data yields an average daily direct normal insolation value of 6.93 kWh/m²-day.

The solar plant annual energy staircase is shown in Figure 4.5-2. This STEAEC derived data results in a solar annual capacity factor of 0.285 and an annual efficiency of converting solar insolation to net electrical energy of 20.6%. The 5,000 heliostat collector module will charge 0.26 hours of storage on the summer solstice day when the plant is operating at the maximum level of repowering--66 MW_e gross. However 4.0 hours of storage has been selected for this application to aid in the start delay of the turbine for cost-effective dispatch. In a start delay operating mode, therefore, the yearly energy to storage will be higher than Figure 4.5-2 indicates. The more probable use of storage is discussed in paragraph 4.3.1. The STEAEC computer model cannot model start delay operating sequences.

A tabulation of the yearly energy conversion and production throughout various solar plant locations is shown in Table 4.5-1. Total annual energy produced from the plant is 149,708 MWh_e, which is equivalent to the displacement of 2.7 x 10⁵ bbl of oil if all of this electrical energy was used to displace oil. In a coal and nuclear intensive utility, such as APS, fuels other than oil will be displaced. The dispatch analysis of section 3.2 and Appendix A of Refs 1-2 and 1-4 discusses how the recommended concept was configured to permit maximization of the oil displaced. Chapter 6 presents the anticipated types and quantities of fossil fuel that can be displaced in the APS system after 1987.



NOTES: 5,000 HELIOSTATS
 XX% NET EFFICIENCY AT EACH CONVERSION STEP
 (XX) EFFICIENCY OF EACH STEP

Figure 4.5-2 Annual Efficiency for 60 MWe Solar Plant

Table 4.5-1 STEAEC-Derived Annual Energy Production
(Solar Operation Only)

Yearly Auxiliary Energy Furnished Collector Field	=	180.94	MWh _e
Yearly Auxiliary Energy Furnished Receiver	=	30.56	MWh _e
Yearly Auxiliary Energy Furnished Turbine	=	2129.35	MWh _e
Yearly Auxiliary Energy Furnished Storage	=	2020.92	MWh _e
Yearly Energy to Collector Field	=	723204.48	MWh _t
Yearly Energy to Receiver	=	466295.31	MWh _t
Yearly Energy to Working Fluid	=	419991.89	MWh _t
Yearly Energy in Working Fluid	=	419571.90	MWh _t
Yearly Energy to Turbine from Receiver	=	405261.82	MWh _t
Yearly Energy to Storage	=	10153.54	MWh _t
Yearly Energy to Turbine from Storage	=	9843.59	MWh _t
Yearly Integral of Energy in Storage	=	19932.04	MWh _t
Yearly Surplus Energy to Receiver	=	0.00	MWh _t
Yearly Surplus Energy to Storage	=	0.00	MWh _t
Yearly Excess Charge Rate to Storage	=	0.00	MWh _t
Yearly Receiver Minimum Flow Losses	=	816.28	MWh _t
Yearly Turbine Minimum Flow Losses	=	197.85	MWh _t
Yearly Storage Minimum Flow Losses	=	69.50	MWh _t
Yearly Gross Electricity From Turbine	=	163258.49	MWh _e
Yearly Net Electricity from Turbine	=	149707.87	MWh _e
Yearly Auxiliary Energy Purchases from Net	=	4361.77	MWh _e

4.5.3

Annual Performance Using SOLTES

A SOLTES model of the Saguaro Repowering Plant was developed and inputs provided to the customer. Figure 4.5-3 is a block diagram of the proposed model. A central receiver and collector field component model was developed by Sandia National Laboratories, Albuquerque and is based upon the corresponding parts of the computer program STEAEC. Since the Electric Power Generation Subsystem of the Saguaro plant has been clearly defined, the individual components are lumped together into a single component model, EPGSM. The load management routine establishes the power demand and transfers this information to the EPGSM. Given the power required, the EPGSM calculates the necessary salt flowrate, the specific enthalpy of the steam and the parasitic power requirements. The load management routine then coordinates the components of the entire model in order to produce the power.

During the simulation of a typical day the following events occur. The insolation valve (INSVLV) monitors the TMY Weather Data Tape and starts the salt flow from the cold storage tank to the receiver when the direct insolation is greater than 400 watts per square meter. All of the information on the piping requirements are generated and recorded by the pump and pipe models of the system. The central receiver/collector field model (CRLIQS) determines the energy collected and establishes the flowrate required to produce the fixed outlet temperature. If the flowrate is below a specified minimum, the outlet temperature for that flowrate is calculated and used for the time step. The drag valve (DRGVLV) is used to recover the kinetic energy which the salt has gained by coming down from the tower. The flow is diverted from the normal path if the salt temperature is below 549°C (1020°F) and returned to the cold storage tank. The salt whose temperature is above the minimum is stored in the hot salt tank (STORE 5). This process is repeated through the day as long as there is cold salt available.

The electric power generation subsystem (EPGSM) is activated by the load management (LODMG) routine. Hot salt is pumped from the hot storage tank, through the EPGSM and into the cold tank. The electricity generated is used to meet the load demands. An energy accounting routine is used to get detailed information on the performance of the system.

While all input data was collected and most was input to the model, the model could not be operated because the EPGSM routine had not been coded. Thus no results were available.

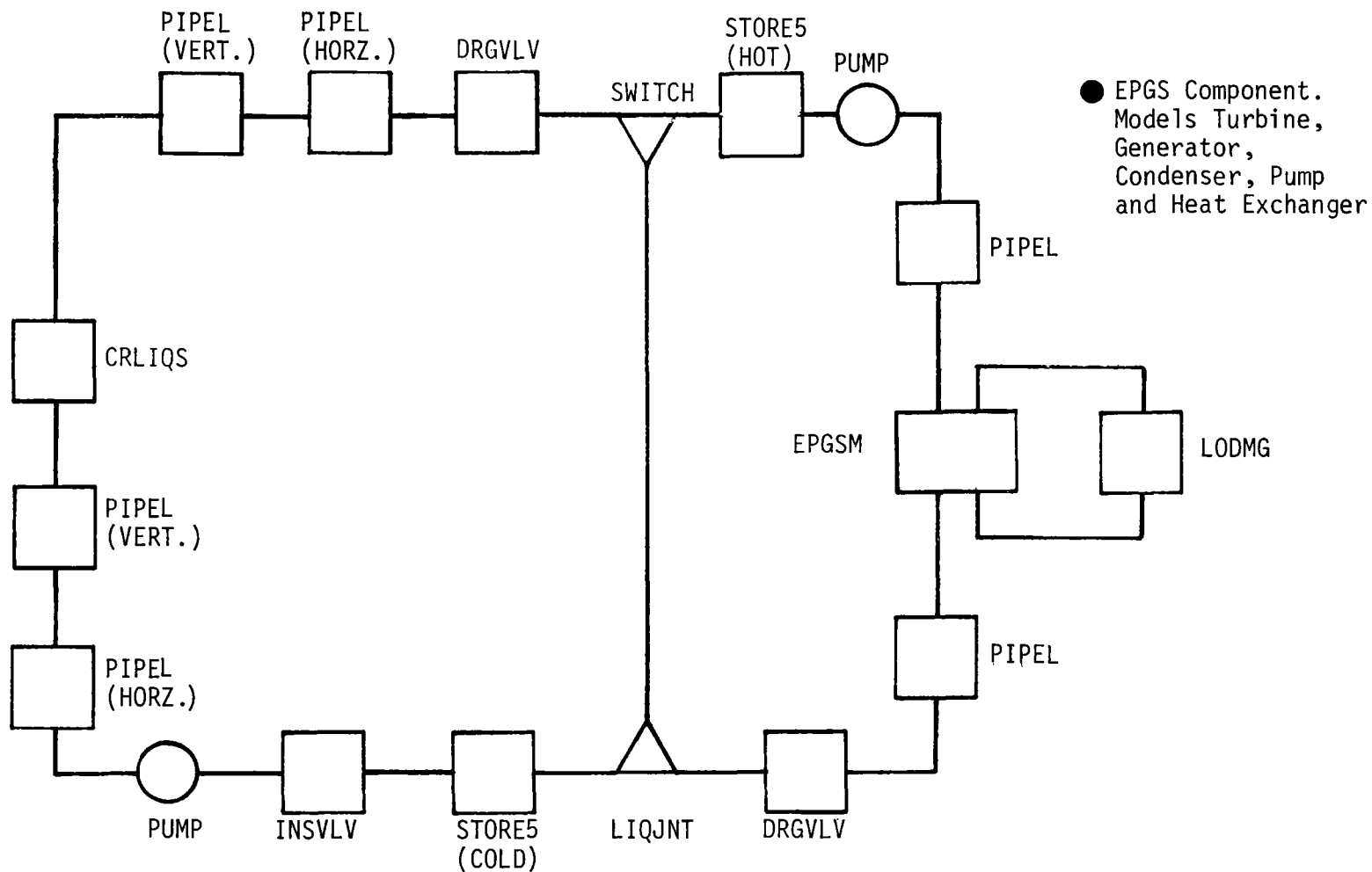


Figure 4.5-3 SOLTES Model

4.6 PROJECT CAPITAL COST SUMMARY

This section presents a summation of the capital cost estimates developed for the selected 60 MWe net Saguaro repowering design. The capital cost has been divided into three major components for discussion: engineering design costs, construction costs, and owner's costs.

4.6.1 Cost Estimates - Approach and Groundrules

A methodical step-by-step approach was used to estimate project capital costs. The steps taken were:

- 1) Identify costing groundrules.
- 2) Establish cost account categories and definitions.
- 3) Document the source, date, and account category of each cost estimate (when possible, vendor quotations for commercially available equipment were obtained).
- 4) Check estimates for consistency in labor rates, costing location, etc.
- 5) Summarize cost estimates and compile cost back-up sheets.

The groundrules identified for the capital cost estimates were:

- 1) All costs expressed in 1982 \$.
- 2) Material and labor priced to Saguaro site (Red Rocks, AZ).
- 3) Estimates include installation and check-out of equipment.
- 4) Estimates do not include design contingencies.
- 5) Owner's costs include all environmental costs associated with the site and sales tax, property tax, and insurance during construction.

The cost accounts defined in this study are the same as those used in the 1980 Saguaro Repowering study. The account structure was developed by Sandia National Laboratories, Livermore (SNLL) and is shown in Table 4.6-1.

Table 4.6-1 Construction Cost Accounts

5100	Site Modifications
5200	Site Facilities
5300	Collector Subsystem
5400	Receiver Subsystem
5500	Master Control Subsystem
5600	Fossil Energy Subsystem
5700	Energy Storage Subsystem
5800	Electric Power Generation Subsystem
	5890 Solar Steam Generator
5900	Process Heat Subsystem

Two of the SNLL accounts were not used due to the repowering design. Modifications to the existing fossil energy system were included in account 5800 (electric power generation subsystem) instead of account 5600 (fossil energy subsystem); therefore, account 5600 was not used in the study. Account 5900 (process heat subsystem) also was not included in the study since it was not applicable to the repowering design.

The top-level accounts were subdivided into second and third level subaccounts to provide greater visibility to major solar components. A complete tabulation of subaccounts and their definitions can be found in Appendix G.

A clearer picture of the many accounts and subaccounts is provided by Figures 4.6-1 and 4.6-2. Figure 4.6-1 illustrates the relationships of the major accounts to the existing plant and Figure 4.6-2 shows the assignment of piping and circulation equipment to the appropriate sub-accounts.

4.6.2 Engineering Design Costs

The design requirements were split into two categories: preliminary design and detailed design. Each account was analysed to determine the manmonths of remaining preliminary design and detailed design needed before construction of the repowering project could begin. The design manmonths were converted to dollars by applying a wraparound 1982 wage rate for engineering labor. The design breakdown is given in Table 4.6-2.

Table 4.6-2 Engineering Design Cost Breakdown (1982 \$)

Account	Preliminary Design	Detailed Design	Total Design
5100 - Site Preparation	36,000	36,000	72,000
5200 - Site Facilities	72,000	144,000	216,000
5300 - Collector Subsystem	252,000	432,000	684,000
5400 - Receiver Subsystem	900,000	1,656,000	2,556,000
5500 - Master Control Subsystem	360,000	1,368,000	1,728,000
5700 - Thermal Storage Subsystem	432,000	540,000	972,000
5800 - Electric Power Generation Subsystem	516,000	972,000	1,488,000
5000 - System Integration	288,000	576,000	864,000
Total Project Engineering	\$2,856,000	\$5,724,000	\$8,580,000

4-41

Figure 4.6-1

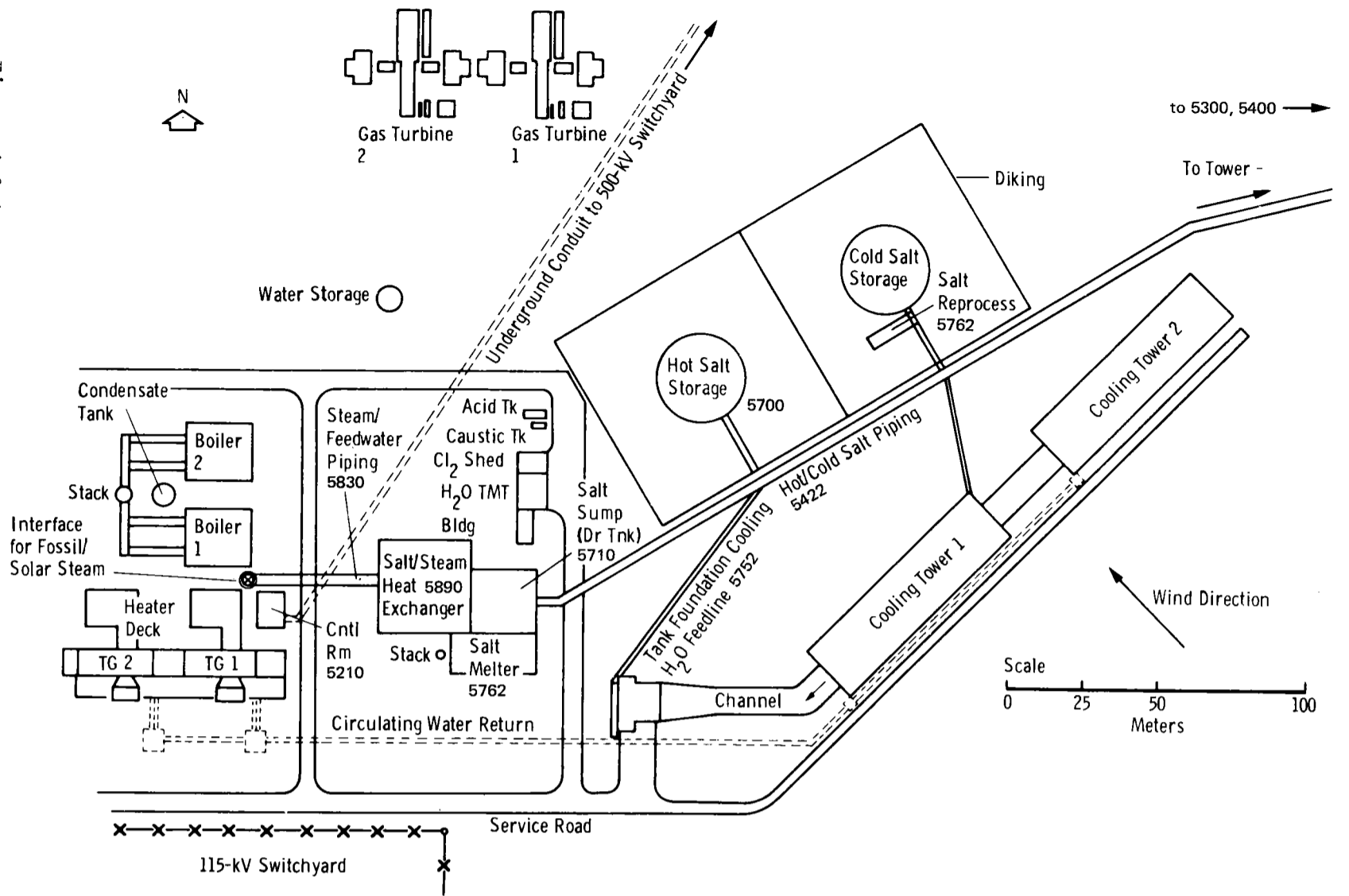


Figure 4.6-1 Geographic Identification of Cost Accounts

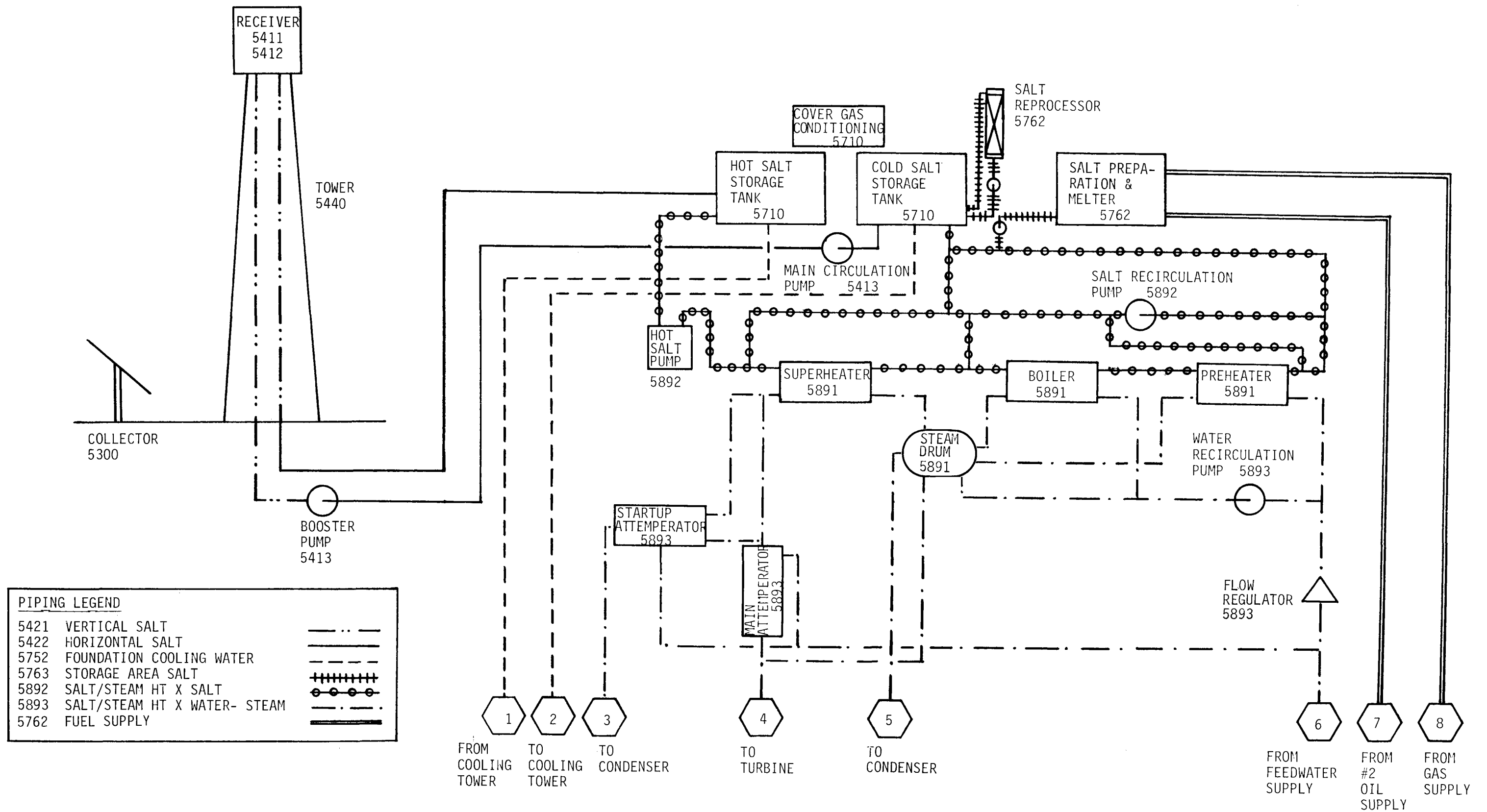


Figure 4.6-2 Solar Subsystems Equipment and Piping Cost Accounts

4.6.3 Construction Costs

The total construction cost estimate of the 60 MWe net repowering system is \$118.2 million (1982 \$). The breakdown by major cost account is shown in Table 4.6-3.

Table 4.6-3 Saguaro Repowering Construction Cost Breakdown (1982 \$)

Account	Cost
5100 Site Preparation	\$ 1,214,000
5200 Site Facilities	3,044,000
5300 Collector Subsystem (\$263.16/m ²)	75,540,000
5400 Receiver Subsystem	16,124,000
5500 Master Control Subsystem	1,968,000
5700 Thermal Storage Subsystem	8,794,000
5800 Electric Power Generation Subsystem	11,506,000
Total Construction Cost	\$118,190,000

The construction cost includes all direct and indirect field costs, construction management costs, contingencies, and fees. Design engineering costs are not included. Further cost detail is provided by the subaccount breakdown in Table 4.6-4 and by the cost account worksheets contained in Appendix G.

Figure 4.6-3 shows the system components that drive the construction cost. The collector subsystem is the major cost driver, contributing nearly two-thirds of the cost of the entire repowering project. A heliostat cost of \$263.16/m² was used in deriving the collector subsystem cost and represents a per heliostat cost of \$15,108. The collector cost includes all heliostat-related costs, i.e. wiring, installation, and foundation. This estimate has been based on detailed production process plans, manpower requirements and vendor quotes commensurate with a production level of 4000 Martin Marietta Improved Second Generation Heliostats per year. Of the remaining system components, the thermal storage subsystem, solar steam generator, and the receiver unit (including absorber, structure, and receiver circulation equipment) contribute the most to cost. The thermal storage subsystem cost is driven by the cost of the storage tanks and the 14.6 million pounds of salt contained in the subsystem. The solar steam generator cost and the receiver unit cost are driven by their complexity of design and construction.

Table 4.6-4 Saguaro Solar Repowering Construction Cost Estimate, 1982 \$

5100	Land, General Site Preparation			
5130	Yard Work (Collector Field)		1,214,000	1,214,000
5200	Site Facilities			3,044,000
5210	Operations		1,700,000	
5220	Security		413,000	
5230	Storage and Maintenance		931,000	
5300	Collector Subsystem (\$263.16/m ²)			75,540,000
5400	Receiver Subsystem			16,124,000
5410	Receiver Unit		7,517,000	
5411	Absorber Unit	3,213,000		
5412	Support Structure	2,814,000		
5413	Circulation Equipment	1,164,000		
5414	Instrumentation and Control	326,000		
5420	Riser, Downcomer, and Horizontal Piping		5,296,000	
5421	Vertical Piping	1,373,000		
5422	Horizontal Piping	3,923,000		
5430	Heat Transport Fluid		249,000	
5440	Tower		1,468,000	
5450	Tower Foundation		1,594,000	
5500	Master Control Subsystem			1,968,000
5510	Hardware		1,968,000	
5700	Energy Storage Subsystem			8,794,000
5710	Media Containment Equipment		2,568,000	
5720	Media Circulation Equipment		456,000	
5750	Foundations		569,000	
5760	Heat Transport Fluid		5,183,000	
5800	Electric Power Generation Subsystem			11,506,000
5820	Steam Turbine Modifications		629,000	
5860	Electric Plant Equipment		2,449,000	
5890	Salt/Steam Heat Exchangers		8,428,000	
5891	Heat Exchangers	3,851,000		
5892	Salt Circulation Equipment	2,533,000		
5893	Steam/Water Circulation Equipment	1,679,000		
5894	Heat Transport Fluid	208,000		
5895	Foundations	157,000		
TOTAL CONSTRUCTION COST				\$118,190,000

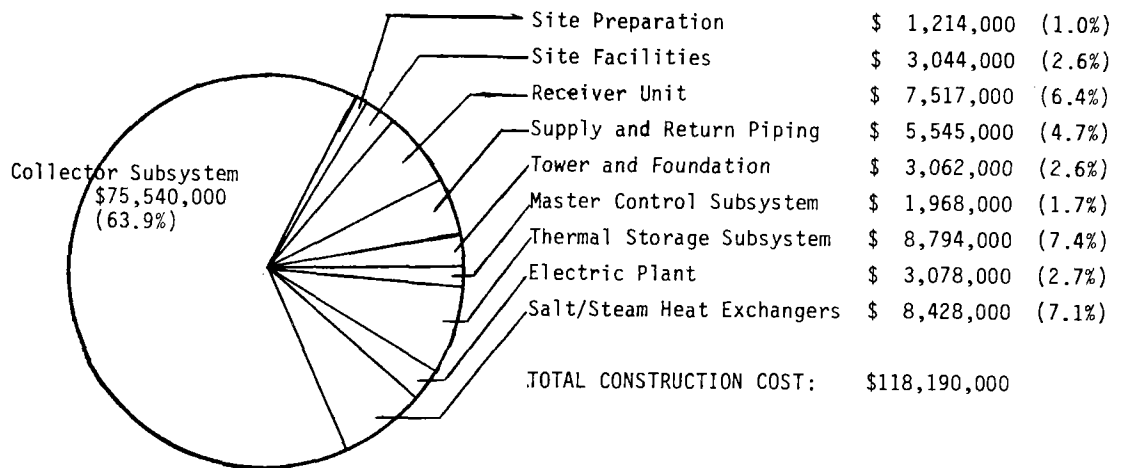


Figure 4.6-3 Saguaro Solar Repowering Construction Cost Estimate (1982 \$)

4.6.4 Owner's Cost Estimate

Owner's costs represent those costs over and above engineering and construction costs incurred by the owner. Owner's costs include land leasing and/or purchase costs, consulting costs for soil sampling and land surveys, cost of an archaeological search and other environmental studies, project management and engineering costs, consumable supplies and start-up costs, property taxes and insurance during construction, and sales tax. The owner's cost incurred prior to commercial operation of the repowered plant is estimated to be \$7.1 million (1982 \$). The basis for this estimate is detailed in Appendix G, and Table 4.6-5 shows a summary of the major owner's cost items.

Table 4.6-5 Owner's Cost Estimate*

	1982 \$
Land and land rights	\$ 150,000
Consulting services	90,000
Archaeological search	15,000
Environmental studies	350,000
Project management and engineering	3,000,000
Consumable supplies and start-up	1,500,000
Property tax and insurance	1,560,000
Sales tax	450,000
Total Owner's Cost	\$7,115,000

* Excludes Allowance for Funds Used During Construction (AFUDC).

Project management and engineering is the major owner's cost component (42% of the total). The project management cost represents coordination and engineering effort required of APS beyond that of the architect engineer and prime contractors done at the design and construction levels.

It has been recently identified that, due to a new Arizona State Law, this project will be exempted from state property taxes and state sales taxes. Currently, the owners cost estimate includes \$1,460,800 for property taxes during construction and \$450,000 for state sales taxes. Eliminating these costs would reduce the owner's costs estimate by \$1,910,000, resulting in an owner's cost of \$5,205,000. Due to the late identification of the exemption, this reduction is not considered in the cost summaries or economic analysis.

4.6.5 Summation of Capital Costs

Table 4.6-6 show a summation of design engineering, construction, and owner's costs for the 60 MWe net solar repowering project. Total capital investment is estimated at \$2230/kWe.

Table 4.6-6 Total Capital Investment

	<u>1982 \$</u>
Design Engineering	\$ 8,580,000
Construction Cost	118,190,000
Owner's Cost*	7,115,000
Total Cost Closed to Plant*	\$133,885,000
Total Capital Investment (\$/kWe)*	2,230

* Excludes Allowance for Funds Used During Construction (AFUDC).

4.6.6 Project Cost at Year of Commercial Operation

To obtain a realistic picture of the cost outlays required from the initiation of preliminary design work to the completion of construction of the project, the costs estimated in sections 4.6.2-4.6.4 were projected over the development plan schedule. The costs, in first quarter 1982 \$, were escalated at 8% annually to the period of their expenditure. Expected yearly costs are shown in Figure 4.6-4.

The costs for preliminary and detail design and the cost to obtain necessary permits and surveys were considered to occur as equal quarterly outlays during the time the design and permit work was scheduled to occur. Then year construction costs and related project management costs were calculated using a typical S-shaped spending plan over the construction period. The total cost of the project, in then-year dollars and excluding Allowance for Funds Used During Construction, is \$171,126,000. This figure is utilized in the economic analyses of Chapter 6.

COSTS IN THEN YEAR DOLLARS (\$000)

	1982	1983	1984	1985	1986	TOTAL
Preliminary Design	\$756	2,359				\$3,115
Detailed Design		\$1,637	5,105			6,742
Permits	\$320	327				647
Construction *			\$27,608	121,866	9,107	158,581
Checkout					\$2,041	2,041
TOTAL YEARLY OUTLAYS	\$1,076	4,323	32,713	121,866	11,148	\$171,126

* Not Including AFUDC

Figure 4.6-4 Construction Spend Plan

OPERATING AND MAINTENANCE COSTS AND CONSIDERATIONS

This section presents a summary of the annual operations and maintenance cost estimates associated with the repowered portion of Saguaro Unit One. As with the capital cost estimates, the validity of the economic analyses discussed in Chapter 6 depends to a large extent on the credibility of these estimates. To achieve accurate cost estimates, the required personnel for operating and maintaining the solar repowering hardware, as well as operating consumables and maintenance materials have been estimated and costed separately on the cost worksheets found in Appendix G.

A summary of the annual operating and maintenance cost estimates is shown in Table 4.7-1. Each of the major elements and considerations are discussed in the following paragraphs.

Table 4.7-1 Solar Repowering Annual Operating and Maintenance Cost Estimates (1982 \$)

OM100	Operations		\$1,001,000
	OM110 Operating and Maintenance Personnel	912,000	
	OM120 Operating Consumables	89,000	
OM200	Maintenance Materials		390,000
	OM210 Spare Parts and Materials	390,000	
OM300	Maintenance Labor		50,000
	OM310 Scheduled Maintenance	50,000	
	Yearly Solar Operating and Maintenance		\$1,441,000

A review of the new solar related equipment and the existing IBEW (International Boiler and Electrical Workers) classifications indicates that some equipment is similar to that presently in service (heat exchangers, pumps, computer, controls, instrumentation, heat tracing). The receiver appears to be similar to a fossil boiler, however, the heliostats are completely different. It would appear that in most cases new classifications will not be required. Some training to familiarize personnel with the new equipment and molten salt safety will be required.

The solar-dedicated operating personnel would consist of one control operator, two auxiliary operators (one salt systems, and one heliostat field) and a water and salt chemistry analyst. Based on a two shift operation, these manning requirements are equivalent to 12 manweeks of 40 hours. In addition, it is estimated that a results engineer would also be required for solar data compilation on a standard 40 hour workweek. The total operating requirement for the solar portion of the plant is 13 people.

The maintenance personnel requirements are difficult to determine since failure rates are not established. In addition, the amount of maintenance that can be performed at night will depend on the location and available lighting. It has been estimated that one computer technician, one instrument (electronics) repairman, one electrician, and three heliostat technicians will be required. The heliostat technicians will be required for 2 shifts, 5 day operation, the computer technician and instrument repairman will be required for 1 shift, 7 day operation, and the electrician will be required for 2 shifts, 7 day operation. Thus, a total of 13 maintenance personnel is estimated to be necessary for the solar portion of the plant, resulting in a total requirement for operations and maintenance of 26 equivalent people.

The control valves and pumps (mechanics), heat exchanger and receiver leaks (welders), and heat tracing and insulation (insulators) will also require maintenance. These requirements will depend on installed spares, redundant equipment, failure frequency, maintenance scheduling (cloudy days and weekends), and amount of lost generation (caused by equipment failures). It is anticipated that the existing plant maintenance personnel will be sufficient to cover any routine maintenance on these hardware elements.

The annual operating consumables identified for the solar portion of the plant consist of salt replenishment costs and heliostat washing costs. Assuming a 2.5% replenishment rate on the total salt volume of 15×10^6 pounds, the annual cost of replenishment is estimated to be \$75,000. Heliostat washing is assumed to occur 12 times a year at 80 hours per wash. Total annual washing cost is estimated at \$14,000.

The materials and spare parts necessary for repairs have been estimated as a percentage of the initial capital investment for the major subsystems. Although these estimates are based on reliability studies made on components such as heliostats, receivers and other salt studies, there exists no operational data for a commercial solar plant. For this study, maintenance materials for each year, were estimated at 0.1% of the collector subsystem capital cost, and 1% of all other solar subsystem capital costs.

At the present level of conceptual design, only one scheduled maintenance operation beyond the normal operating and maintenance personnel functions has been identified. The provision for computer maintenance services is estimated to be \$50,000 annually.

5.0 SUBSYSTEM CHARACTERISTICS

This chapter addresses each of the seven major subsystems in terms of components, requirements, design description, performance, and costs. The major subsystems addressed are;

- 1) Collector;
- 2) Receiver (including supply and return piping, tower);
- 3) Master Control;
- 4) Fossil Energy;
- 5) Energy Storage;
- 6) Electric Power Generation;
- 7) Solar Steam Generator;
- 8) Site Facilities (Section 4-4).

The subsystem requirements include those given with the System Requirements Specification (Ref 1-3), those that arose because of the general situation, those that were derived from the conceptual design of Chapter 4, and those that were derived in the course of the analysis.

In addition to the detailed subsystem information presented in this chapter, further information is contained in Appendices A, B, and C. Supporting information for the cost data is presented in Section 4.6 and Appendix G.

5.1 COLLECTOR SUBSYSTEM

This section details the key design and operational characteristics of the collector subsystem design developed for the Advanced Conceptual Design for Solar Repowering of the Saguaro Power Plant. The collector subsystem consists of:

- 1) Heliostats, including reflective surface, structural support, drive units, control sensors, pedestals, foundations, and cabling;
- 2) Controllers, including heliostat, heliostat array, line, and field controllers, interface electronics, and power supplies;
- 3) Support equipment for alignment, washing, operations and maintenance, and installation and removal.

The approach taken for the advanced conceptual design of the collector subsystem was to (1) select an improved version of the Martin Marietta second generation heliostat as a baseline, (2) optimize the collector field for the most cost effective field configuration to supply energy for the receiver, and then (3) analyze the design point and annual performance of the collector subsystem .

5.1.1 Collector Subsystem Requirements

The primary requirement for the collector subsystem is to direct solar radiation onto the receiver absorber surfaces during all solar insolation periods in a cost effective manner that satisfies the receiver incident heat flux requirements. Since results from the collector field parametric analyses dictated a unique approach to the collector field design--a fixed collector field size and a variable solar multiple to account for design performance refinements--there is no absolute requirement for design point power from the collector field. A requirement of a minimum of 181.0 MW_t redirected into the apertures from the collector field was derived, to ensure sufficient thermal input to the EPGS for 66.0 MW_e gross electric output.

In order to achieve the primary power requirement discussed above, the collector subsystem must respond to normal tracking mode control commands. The collector subsystem must also execute alternative drive modes in response to commands from the master control subsystem for emergency defocusing of the reflected energy, or to protect the heliostat array against environmental extremes. The heliostat must be properly positioned for repair or maintenance in response to either master control or local commands. Heliostat design must provide for a stowed or safe position for use at night, during periodic maintenance and during adverse weather conditions. The interface of the collector subsystem with the receiver subsystem (and thereby the balance of plant subsystems) is accomplished through the operational control subsystem as part of the master control subsystem.

The collector field design, operational, and survivability requirements are further defined in the Collector Subsystem Requirements Definition, A10772 (Issue D), as modified by the System Requirements Specification, Section 3.3.2, contained in Volume II of the prior report (see Ref 1-3).

5.1.2 Collector Subsystem Design Description

The collector subsystem conceptual design description has been divided into two components for discussion. The first component is the heliostat design, including wiring, control and support equipment. The second component is the final collector field configuration, which has been optimized using the heliostat design characteristics and collector field requirements that will provide a valid representation of a larger collector field.

5.1.2.1 Heliostat Design Description - The Martin Marietta second-generation heliostat design complies with the performance requirements defined by Sandia Laboratory's Requirements Specification A10772, Issue D, as summarized in Table 5.1-1. A number of improvements, discussed below, have been incorporated in the heliostat version used in this study as compared to the version tested at the CRTF in the spring of 1981.

The heliostat design, as shown in Figure 5.1-1, incorporates 11 flat or focused and individually canted mirror assemblies mounted on a rigid, lightweight rack assembly structure. The heliostat reflective surface is driven using a two-axis gear drive (azimuth and elevation), with individual two-speed dc motors for each axis. Each of the 10 full-size mirror assemblies is approximately 3.6 x 1.5 m (12 x 5 ft). The half size mirror assembly is the same length but only half width.

The mirror assemblies are designed to use 1.5 mm (0.060 in.) fusion glass second surface mirrors that will provide a reflectivity of up to 96%. The study used a reflectivity of 93%. The mirror-supporting structure is a steel/honeycomb/steel sandwich. To achieve an optimum low-cost design, the honeycomb material is aluminum. This provides a design with maximum rigidity and minimum weight. Improved resistance to the entrance of rain into the honeycomb has been effected by redesign of the corner and edge frame rain barriers. A new laminate is used between the mirror and the front steel sheet that will reduce stress in the glass. Additionally, better adhesives have been selected for building up the mirror assembly.

The mirror assemblies are arranged to allow the heliostat to be positioned in a mirror-face-down stow attitude. This important feature gives added protection to the mirrors from adverse weather, particularly frost and wind/rain/dust conditions that could easily dictate an unscheduled mirror washing operation prior to developing full plant power. In addition, although the mirror assemblies have not been tested beyond the 1 in. hail diameter requirements, the face-down mirror assemblies should be able to withstand much larger size hail without damage to the reflective surface because of the shock absorbing characteristics of the steel/honeycomb/steel support structure.

Figure 5.1-2 shows the rear view of the heliostat with the subassemblies and components identified. The reflective assembly consists of the rack assembly with the 11 mirror assemblies installed.

Table 5.1-1 Performance Summary of Second-Generation Heliostat

Item	Requirement	Baseline System	Remarks
Maximum Beam Pointing Error	1.5-mrad Standard Deviation Each Axis Reflected beam Sun 0.26 rad above horizon Gravity effect included No wind	≤ 1.5 mrad	Control system is baselined as the Phase I, 10-MWe system. Demonstrated by Sandia test to meet specified requirement.
Beam Quality	2.0-mrad Standard Deviation Each Axis Reflected beam	≤ 2.0 mrad	Design meets required error budget allocation
Reflective Surface	1.7 mrad (1σ) for Normal Operation 12 m/s (27 mph) Any position in field Gravity effect not included	≤ 1.7 mrad (1σ)	Allocation: 0.5 mrad for foundation 1.2 mrad for structure. Structural deflection analysis using NASTRAN shows design meets requirements.
Structural Strength	No Permanent Set When Subjected to: 12-m/s (27-mph) wind with 50 mm (2 in.) of ice on mirror surface 22-m/s (50-mph) wind with heliostat in any attitude and drives in operating mode 40-m/s (90-mph) wind with heliostat in stow position	Analysis shows that the design meets these requirements with standard safety factors.	At 12-m/s (27-mph) wind, uniformly distributed ice assumed.
Operational Requirements	Function as Appropriate for All Steady-State Modes of Plant Operation 15 min to stowage position No gimbal drift due to environmental loading 15 min over-the-shoulder resolution Heliostat computer control	Software and hardware meet requirements of all modes of operation < 15 min. Worm gear design for nonreversibility < 15 min. Computer control.	Demonstrated in previous heliostat programs. Nominal slew rate is $23^\circ/\text{min}$ in azimuth and elevation. All specification requirements are readily achievable with our open-loop control system design.
Safety	Emergency Defocussing to 3% Radiation Within 120 s Radiation on Normally Unirradiated Tower Surfaces Limited to 25 kW/m^2 ($78800 \text{ Btu/ft}^2/\text{h}$) Beam Control Strategy for Personnel/Property Protection	Design provides the capability. Design meets this requirements. Strategy is adequate.	All heliostats can be moving within 2 to 3 seconds. Baseline design includes corridor walk.
Maintainability	Automatic System Malfunction Detection Minimum Routine Field Maintenance	Mirror washing, visual inspection.	Control system includes self-test capability and status and alarm reporting. Environmentally sealed components, self-lubricating bearings, screened parts, all surfaces corrosion protected, etc.
Hail Survivability	Mirror Assemblies Must Survive Impact of 19-mm (0.75-in.) Diameter Hail at 20 m/s (65-fps) Velocity	Design meets the requirements.	Tests have shown survivability at velocities considerably higher than 20 m/s (65 fps).

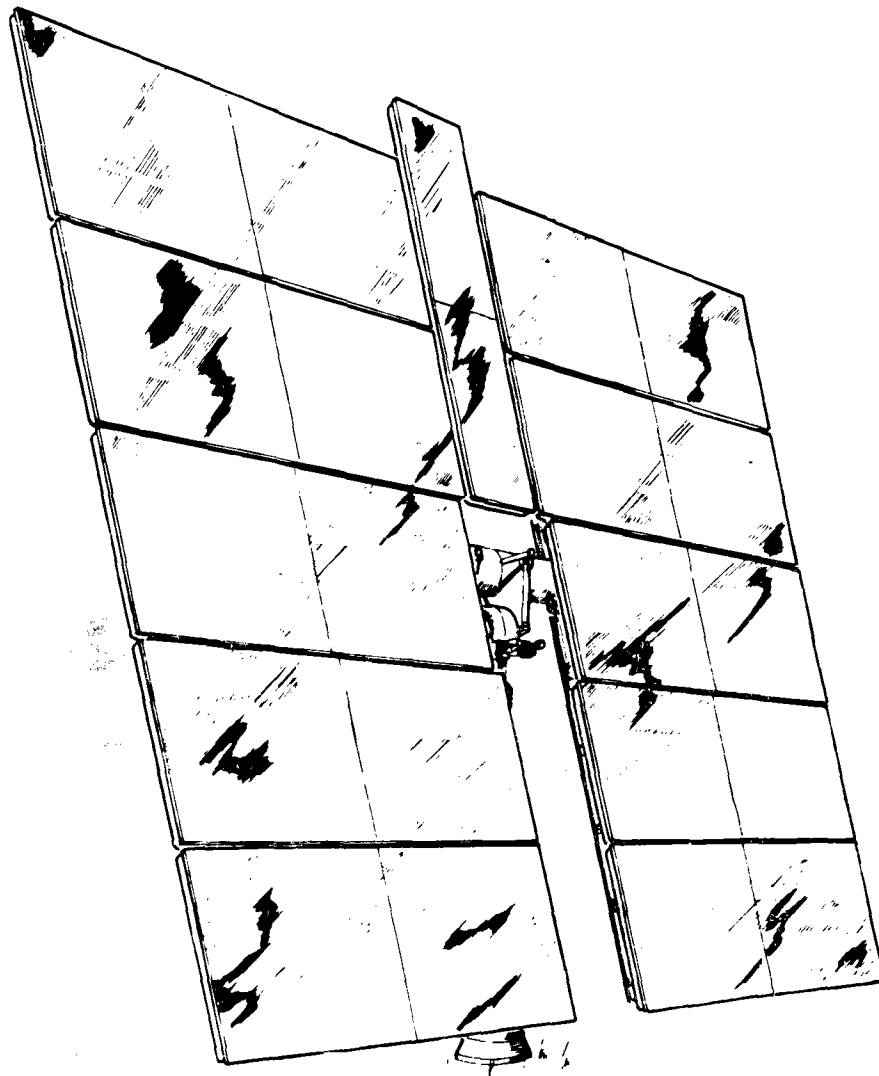
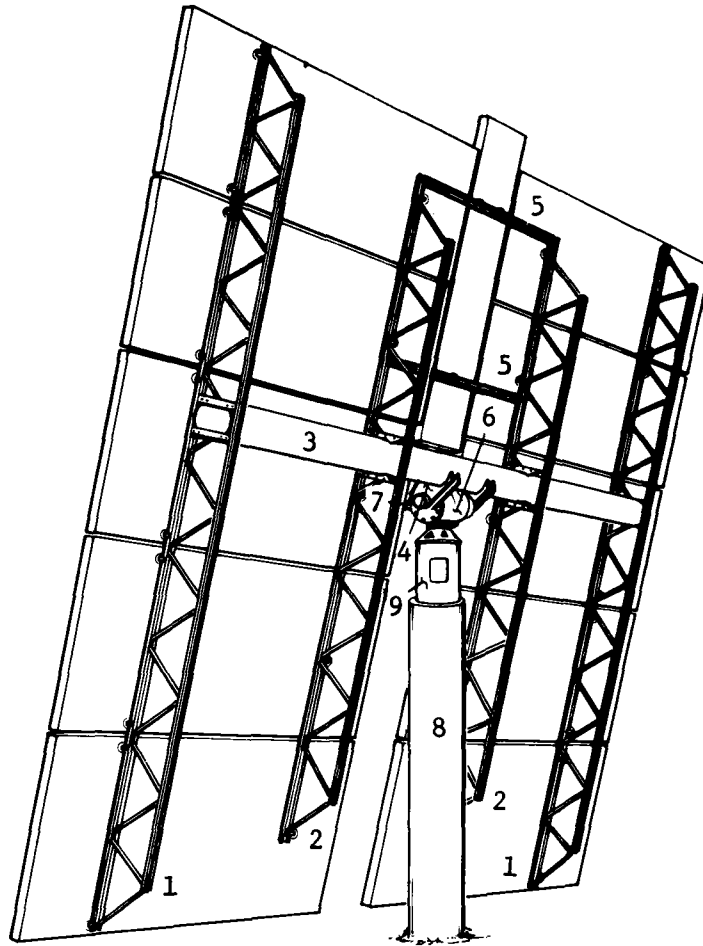


Figure 5.1-1 Second Generation Heliostat - Front View



Heliostat Assembly

Reflective Assembly

Mirror Assembly (11 Total)

Mirror Mounting Studs

Rack Assembly

1 - Long Bar Joist with Mirror Support Tabs

2 - Short Bar Joist with Mirror Support Tabs

3 - Elevation Beam

4 - Control Arms

5 - Mirror Support Stringer(s)

Drive Mechanism Assembly

6 - Drive Mechanism

7 - Drive Motors

Encoders

Encoder Couplers

Encoder & Limit Switch

Brackets

Pedestal/Foundation

8 - Pedestal/Foundation

9 - Pedestal Interface Tube

(Electronics Access Cover)

Figure 5.1-2 Heliostat Assembly

The rack assembly consists of five basic items--an elevation beam of large-diameter thin-wall tubing, and four open-web bar joists of proven design and economy. The rack assembly is attached to the drive mechanism through two control arms that are mechanically fastened to the elevation beam. The entire structure has been redesigned on the basis of strength, as opposed to stiffness, to reduce overall weight. The interfaces between the bar joists and the elevation beam have been made stiffer. Each mirror assembly is mounted to this rack assembly at three mounting points that provide for ease of canting without warpage of the reflective surface. Adjustments correct for all assembly tolerances and allow canting for slant ranges from 300 m to infinity.

The drive mechanism is mounted to the top of the pedestal/foundation. This drive is a conventional gear-drive unit with both azimuth and elevation drives combined into one integral, cast-iron housing for precise control of the relationship of the gimbal axes. Both elevation and azimuth drive trains are enclosed inside the drive housing and are submerged in an oil bath with dual seals on each output shaft. The result is a sealed drive with an anticipated 30 year life with no scheduled maintenance. The single, compact drive mechanism provides short load paths and thus very high rigidity with relatively low weight.

The heliostat design incorporates a "stow lock" mechanism that minimizes the size of the drive mechanism gears. The addition of this feature effectively isolates the drive mechanism's elevation gear train from wind loads in excess of 22 m/s (50 mph). The stow lock has been redesigned so that it is simpler to use.

The combined pedestal/foundation pier is a continuous, reinforced concrete column extending from below grade level to 3 m (10 ft) above grade. The poured-in-place feature allows the below grade portion to be readily varied to meet the soil conditions of the site.

An interface tube is embedded in the upper portion of the pedestal foundation to provide an economical interface with the drive mechanism. This tube has a thin wall and a large diameter to handle the bending loads associated with the large heliostat glass area and the design wind conditions. This interface tube is also used to house the field interface connections, the heliostat electronics, and the cabling. An electronic access door on the interface tube permits easy access to the azimuth encoder and the electronics for maintenance.

Individual heliostats are controlled by a microcomputer-based heliostat controller (HC), drive motors, encoders and an interconnecting cable harness. The microcomputer in the HC receives commands over a data bus, calculates the required gimbal angles, determines actual gimbal angles from the encoder outputs, and turns the drive motors on and off as required. The entire field of heliostats is controlled by a distributed computer control system consisting of a heliostat array controller (HAC) and heliostat line controllers (HLC) in the control room and heliostat field controllers (HFCs) and HCs located at the heliostat. The computers are interconnected by fiber optic data buses. Two heliostat line controllers are used to take over some HAC functions so that the system can handle the 5000 heliostats in the Saguaro collector field.

Features of the control system include an electronic package installed inside the interface adapter tube for environmental protection, low cost incremental encoders on the output axes, two-speed operation with a single motor per axis, a microcomputer that maximizes functions on a single chip and thereby reduces costs, very low energy consumption, fiber optic data buses, and "computer leveling," i.e., compensation in the control algorithm for pedestal tilt, thus relaxing the accuracy required in pedestal alignment and reducing installation costs. Better fiber optics equipment has been selected as part of the improvement program and the heliostat controller has been redesigned for more reliability. The heliostat averages 13 w for daily operation, 12 w in standby, and 210 w for slew with both motors operating. Additional characteristics of the heliostat control system are given in section 5.3.

Figure 5.1-3 shows a dimensional view of the heliostat. The total reflective area of the heliostat is 57.41 m^2 (618 ft^2). When allowance is made for the mirror edge strips, the total heliostat wind load area becomes 58.3 m^2 (628 ft^2).

5.1.2.2 Collector Field Design - The final collector field resulted from the use of the DELSOL II and RCELL computer programs. DELSOL II was used to optimize the tower height and RCELL was used to provide heliostat radial and azimuthal spacings. The overall approach to the collector field, tower height optimization is shown in Figure 5.1-4. The collector field for this demonstration is sized proportionally to a commercial sized system with 40 percent of the heliostats in the north quadrant of the field, 25 percent in each of the east and west quadrants and 10 percent in the south quadrant. Using these collector field constraints with DELSOL II, the tower height was optimized at 130m. This tower height is measured from the heliostats elevation axis to the centerline of the receiver apertures. This tower height was then used in the RCELL programs to provide the individual heliostat coordinates for the desired 5,000 heliostats. The resulting configuration is a surrounding field in the shape of a truncated ellipse, with a radial-stagger heliostat array, as shown in Figure 5.1-5.

The vacant strip in the southwest portion of the collector field is for the piping and access road. The heliostats that were removed for the access road were relocated so that the total number of heliostats remained the same. The resulting number of heliostats per quadrant is:

North:	1998
East:	1244
West:	1210
South:	548

The overall dimensions of the collector field to the heliostat foundation centerlines are 1370m (4496 ft) (north-south) by 1362m (4469 ft) (east-west), with a central exclusion radius of 123m (405 ft) around the tower. Figure 5.1-6 illustrates the location of the collector in relation to existing high voltage transmission lines and a buried natural gas line. The total land area inside the heliostat foundation boundary for the collector field and tower is 1.44 km^2 (355 acres), yielding a ground coverage fraction of 0.20 (heliostat reflective area/total land area).

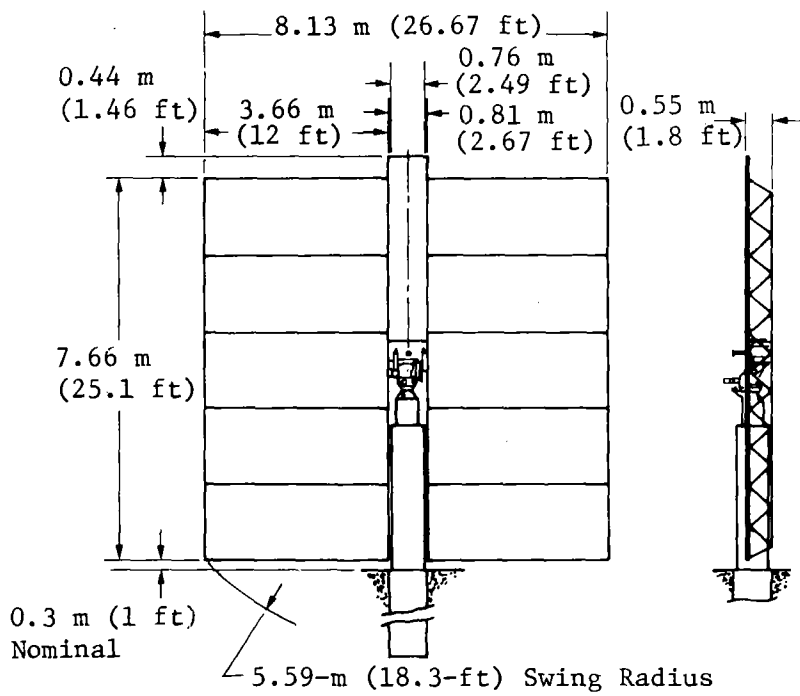


Figure 5.1-3 Heliostat Dimensions

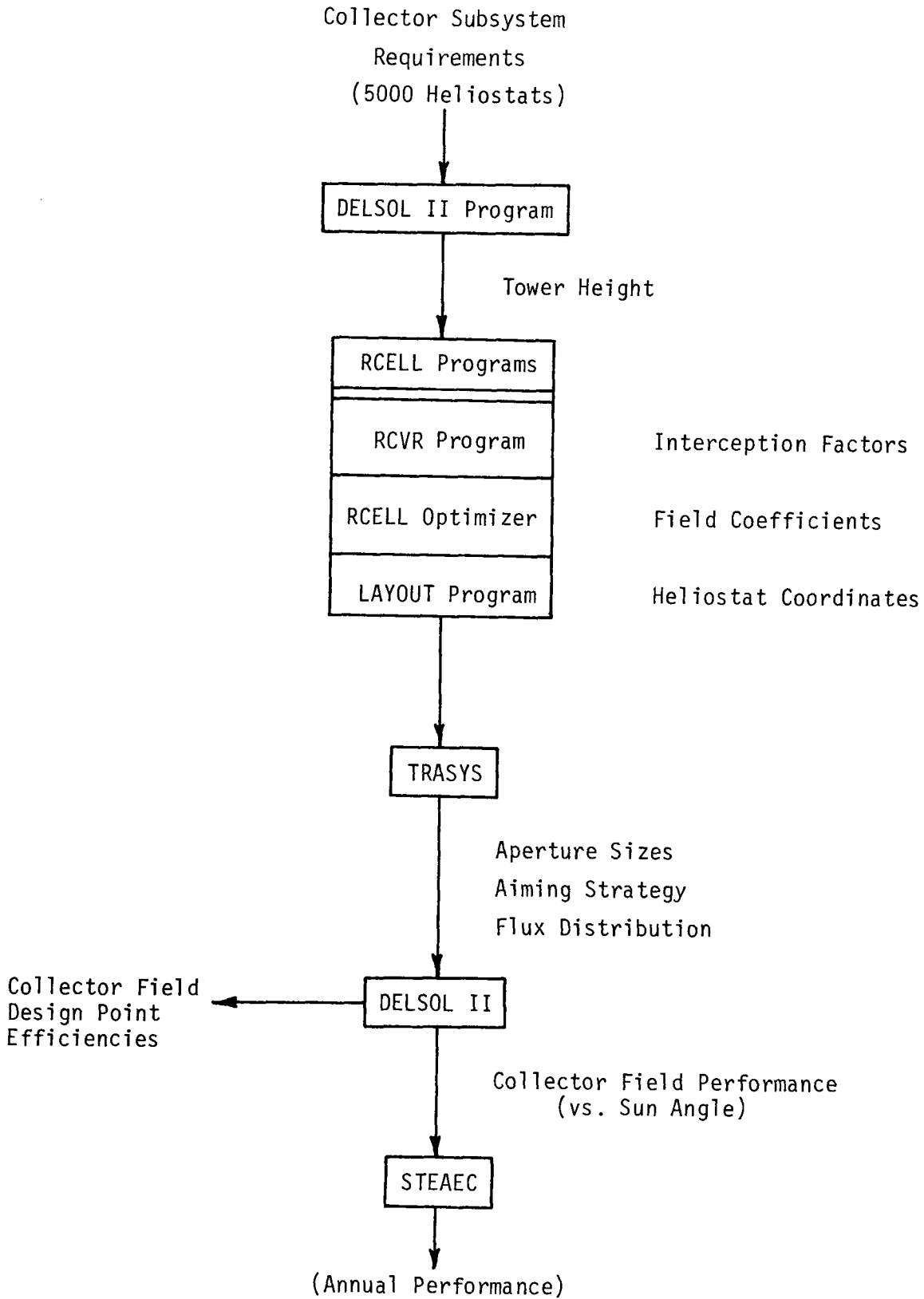


Figure 5.1-4 Tower Height Optimization and Performance Analysis Approach

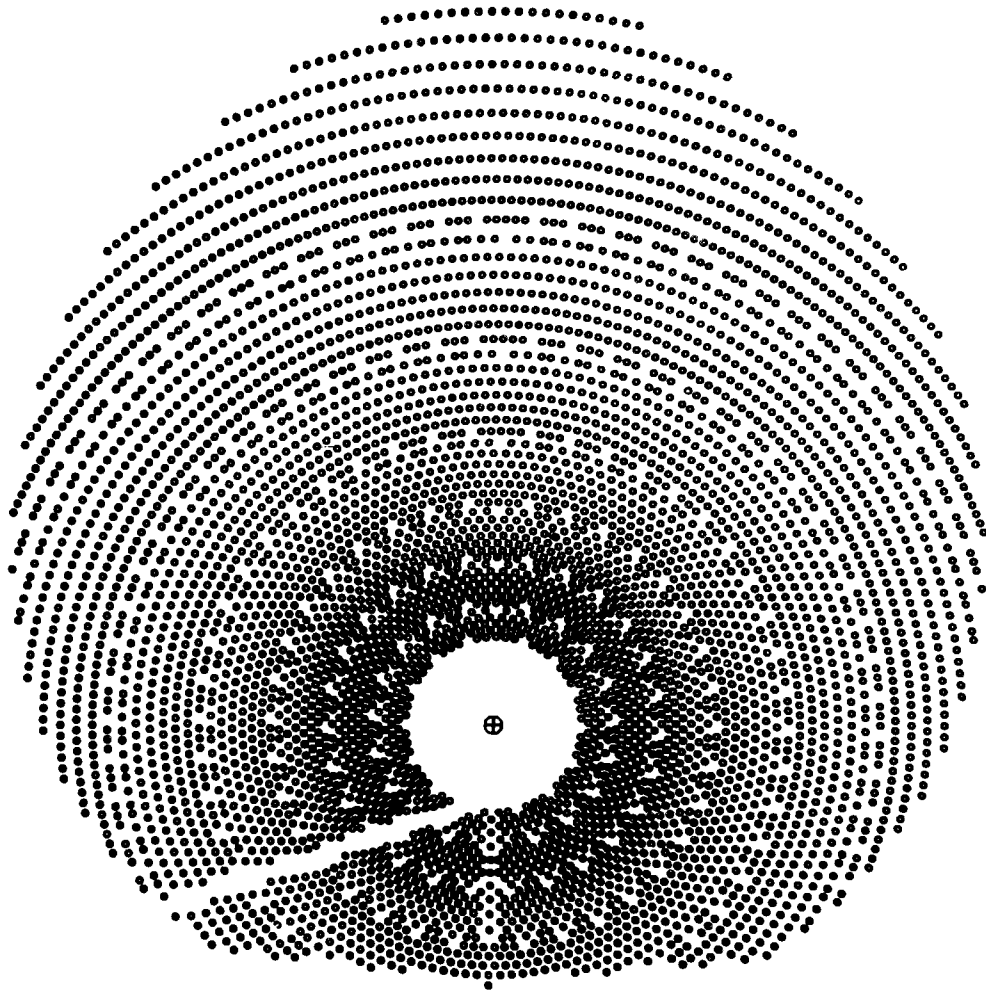


Figure 5.1-5 Heliostat Locations

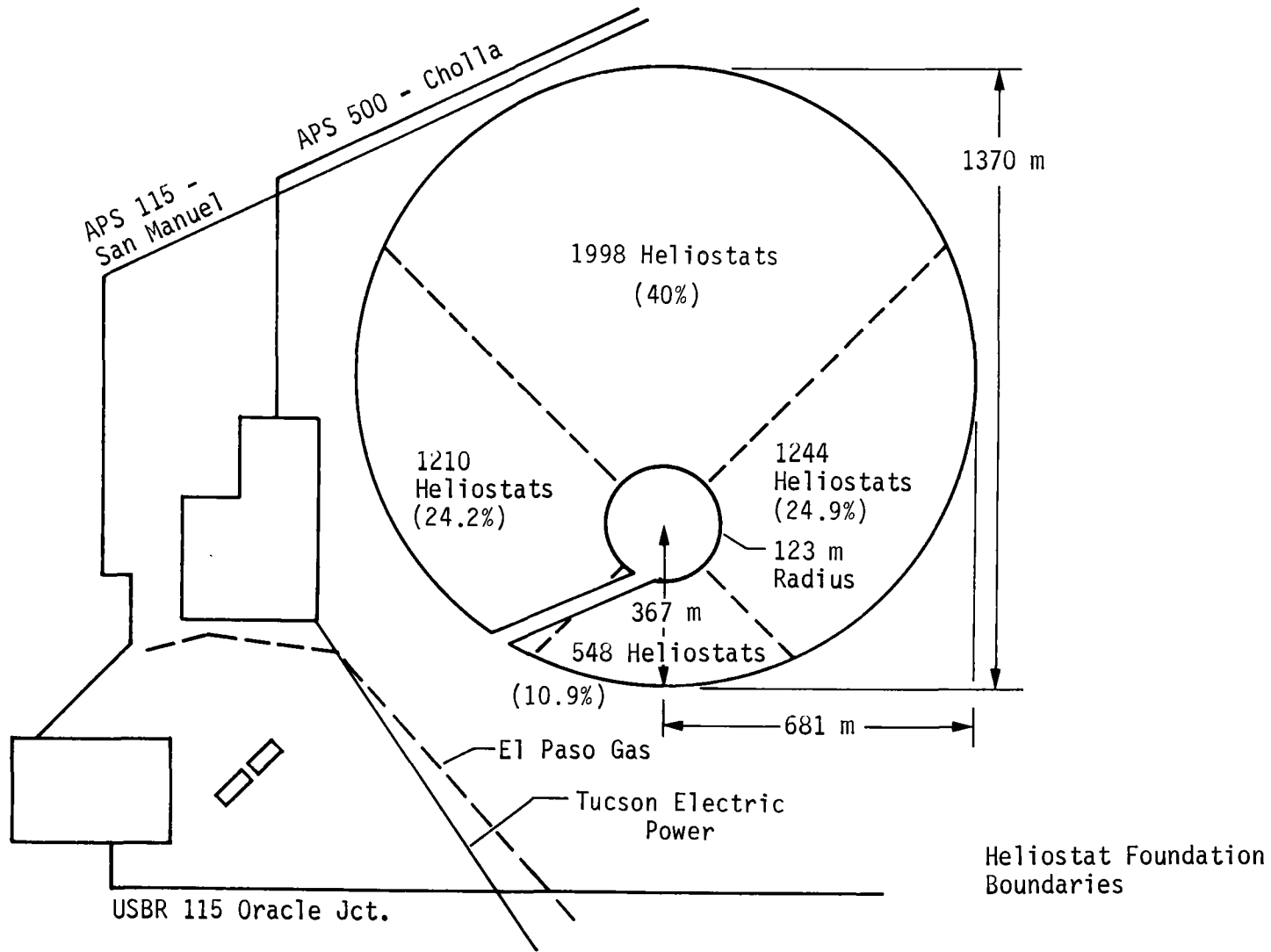


Figure 5.1-6 Heliostat Distribution

5.1.3 Collector Field Subsystem Performance

The performance of the collector field subsystem was analyzed using the DELSOL II computer code. Inputs to the code included: individual heliostat coordinates, heliostat design and performance parameters, receiver aperture sizes and aiming strategies, and site and atmospheric data. The receiver aperture sizes and aiming strategies used were the results of the receiver design task, discussed in detail in section 5.2. The collector field performance is measured as the product of the following efficiencies (losses): heliostat reliability, tower shadow, cosine losses, reflectivity (0.93), shading and blocking, atmospheric attenuation, and spillage around the apertures. Atmospheric attenuation was calculated using the Martin Marietta model developed from test data, which is of the form:

$$\% \text{ LOSS} = 100(1 - e^{-0.099931 \times \text{SR}})$$

where SR is the slant range in kilometers. At a 1 kilometer slant range, the loss due to atmospheric attenuation is approximately 9.51%. Spillage losses include any losses due to heliostat tracking errors and beam quality.

The collector field performance excluding heliostat reliability was first evaluated for a matrix of 7 sun azimuth angles and 6 elevation angles to generate the field efficiency matrix for input to the STEAEC system simulation model. The results of this analysis are given in Table 5.1-2. Using this efficiency matrix in STEAEC, with insolation data from the SOLMET TMY data tape for Phoenix, AZ, an annual average collector field efficiency of 65.8% was calculated, assuming a heliostat availability of 99.7%.

Table 5.1-2 Collector Subsystem Field Efficiency Matrix

Elevation Angle, rad rad (deg)	Azimuth Angle, rad (deg)						
	0.0 (0)	0.524 (30)	1.047 (60)	1.309 (75)	1.571 (90)	1.920 (110)	2.269 (130)
0.087 (5)	0.324	0.329	0.308	0.352	0.283	0.316	0.300
0.262 (15)	0.560	0.554	0.521	0.513	0.486	0.468	0.443
0.436 (25)	0.665	0.659	0.629	0.610	0.588	0.560	0.541
0.785 (45)	0.717	0.710	0.688	0.674	0.659	0.637	0.619
1.134 (65)	0.718	0.714	0.702	0.693	0.684	0.672	0.662
1.562 (89.5)	0.703	0.703	0.703	0.703	0.703	0.702	0.702

The collector field performance was also calculated for the noon, summer solstice design point, again using DELSOL II and the inputs previously discussed. The design point field efficiencies are given in Table 5.1-3.

Using a reference insolation level of 950 W/m^2 , the collector subsystem redirects 195.2 MW_t into the receiver apertures. This total power is divided among the four cavities in the following manner: north aperture, 78.2 MW_t (40.1%); east aperture, 48.4 MW_t (24.8%); west aperture, 47.1 MW_t (24.1%); south aperture, 21.5 MW_t (11.0%).

Table 5.1-3 Collector Subsystem Design Point Performance

Tower Shadow	1.00
Heliostat Reliability	0.997
Cosine	0.829
Reflectivity	0.93
Shading and Blocking	1.00
Atmospheric Attenuation	0.955
Spillage	<u>0.975</u>
Total Field Efficiency	71.6%

5.1.4 Collector Subsystem Cost

The collector subsystem, composed of 5000 Martin Marietta Improved Second Generation heliostats, has been estimated to have a construction cost of \$75,540,000, or $\$263.16/\text{m}^2$ (1982 \$). This estimate includes all costs associated with the collector subsystem - installed heliostats, field wiring, foundations, Heliostat Array Controller (HAC), and specialized heliostat installation equipment required for operations and maintenance. Design engineering cost for the Collector Subsystem is estimated at \$684,000, yielding a total installed collector subsystem cost of \$76,224,000 (1982 \$).

Each cost element of this estimate was developed from detailed production process plans and vendor quotes for materials, incorporating actual cost data from Martin Marietta's production of 1912 "First Generation" heliostats for the Barstow Pilot Plant and the IEA-SSPS field in 1981. A basic assumption impacting the cost estimate of $\$263.16/\text{m}^2$ was the assumed production rate of 4000 heliostats per year. This quantity was based on tooling only for providing heliostats for the Saguaro Project in the 1985 time frame, with a conservative market prediction of continuing production at the same rate for an additional 3.5 years. With a larger market prediction, higher production tooling would be utilized, as well as reduced material costs for higher quantity procurement, with heliostat costs of $\$200/\text{m}^2$ easily achievable at rates as low as 10,000 heliostats per year.

5.2 RECEIVER SUBSYSTEM

The receiver subsystem includes the receiver, supporting tower, horizontal and vertical piping, pumps, and valves. The basic function of this subsystem is to effectively intercept radiant solar flux directed from the collector subsystem and efficiently transfer as much of that thermal energy as possible into the molten salt working fluid for subsequent conversion to electric power. A cavity-type receiver on a conical concrete tower was determined to be the most cost effective receiver design during the prior Saguaro repowering study (see Section 3.4 of Ref 1-2).

5.2.1 Receiver Subsystem Requirements

Design requirements for the receiver are divided into two classifications--the general system requirements including those adapted from the System Requirements Specification of the prior Saguaro study (Ref 1-3) that are applicable to the receiver and the requirements derived during this study and the prior Saguaro study (Ref 1-2). All of the requirements have been met in our receiver design. Emphasis was placed on reducing receiver weight and thus reducing receiver and tower cost.

5.2.1.1 General Requirements - In the following discussion, the general requirements imposed on the receiver subsystem design by the general nature of the subsystem and by the Saguaro Power Plant Solar Repowering Project Systems Requirements Specification document (Ref 1-3) are summarized. The design shall:

- 1) Conform to the applicable codes and standards defined in Revision B of the System Requirements Specification (Ref 1-3);
- 2) Provide thermal control for safe, efficient operation, startup, shutdown, and standby modes;
- 3) Provide access for maintenance and inspection, provide for crew safety and be consistent with the intent of appropriate ASME boiler and other codes;
- 4) Be designed for a 30-yr operating life;
- 5) Be capable of operating in and surviving appropriate combinations of the environmental conditions summarized in Section 4.1.1 of Revision B of the System Requirements Specification (Ref 1-3), and shall be capable of surviving appropriate combinations of the environments specified in section 4.1.2 of the same document.

5.2.1.2 Derived Requirements - In addition to the general requirements mentioned above, we derived the following requirements for our receiver design:

- 1) The receiver shall be a quad cavity-type receiver with doors for survival protection and to decrease overnight cooldown.
- 2) The working fluid shall be a salt mixture, 60% NaNO_3 and 40% KNO_3 by weight. Salt properties are defined in section 4.3.

- 3) Salt shall enter the receiver at 277°C (530°F) and exit the receiver at 566°C (1050°F).
- 4) Apertures shall be sized for the best spillage vs thermal loss condition, see section 5.2.3.1.
- 5) The receiver absorbing panels shall be designed for 60,000 temperature cycles induced by application and removal of solar flux.
- 6) The maximum absorbed flux allowable in the absorber tubes (63. W/cm²) shall be determined by tube material strength at the maximum design mass flowrate and fluid temperatures.
- 7) The receiver shall be designed to provide base of tower solar power of 199 MW_t at noon on day 172 (summer solstice) from a surrounding field of 5000 heliostats, described in section 5.1.
- 8) The receiver shall be capable of transferring 181 MW_t of thermal power into the salt at a nominal peak mass flowrate of 409 kg/sec (3.245x10⁶ lb/hr) with the incident power defined above. At maximum conditions, the receiver shall be capable of transferring 199 MW_t into 450 kg/sec (3.570x10⁶ lb/hr) of salt.
- 9) The receiver shall have provisions for gravity draining.
- 10) The working fluid flow of the receiver shall be decoupled from the horizontal and vertical piping flow through the use of accumulators, surge tanks, or other flow decoupling devices.
- 11) In the event of a power failure, the receiver piping system shall be designed for a continuation of working fluid flow at more than 100% of design rate for a period of at least 60 sec.
- 12) The receiver shall be insulated to enhance its thermal efficiency and the cavity apertures shall be covered at night to reduce temperature degradation.
- 13) All salt lines, valves, pumps and tanks other than the absorber tubes within the cavities shall be heat traced.
- 14) The receiver shall be operable from 10 to 120% of design flowrate.
- 15) The receiver and associated piping equipment shall have provisions for salt fill and drain.
- 16) A salt supply and return piping system consisting of horizontal piping, vertical piping, main circulation pumps, and booster pumps and associated valving shall be provided.
- 17) The tower foundation shall be designed for a soil bearing strength of 191.6 kPa (4000 psf).
- 18) The tower shall be designed to support the receiver, riser, and downcomer under the applicable environmental conditions.

- 19) The tower shall be 120m (394 ft) high, shall be appropriately lighted, and shall include an elevator.

5.2.2 Structural Design

This section describes the repowering receiver design configuration and discusses the supporting analyses influencing the design.

- 5.2.2.1 Configuration Description - The Saguaro repowering solar receiver uses a beam column-type construction using standard AISC structural shapes and sizes. Major receiver loads are carried through eight columns on the outside perimeter of the receiver and a center section consisting of four columns and cross bracing. The loads are transmitted from the receiver columns to the tower thru a truss type super structure. Overall dimensions of the receiver can be obtained from Figure 5.2-1. The bulk of the construction is bolted using high-strength bolts that will resist wind, seismic and torsional loads.

The receiver structure encloses and supports four internal cavities with solar energy absorbing panels and apertures which can be closed by lowering overhead doors. The size and shape of each aperture was determined by the amount of solar flux directed from the collector field as described in section 5.2.3.

Maintenance and personnel safety were considered throughout the conceptual design. Piping and valves are located to allow access for maintenance and removal. Figure 5.2-2 shows the piping arrangement. Most of the lower piping and valves are located in the east, west, and south cavities below the lower radiation shields. These cavities are smaller than the north cavity and allow more working room between the floor and the lower radiation shield. Absorber panels have connections on both the upper and lower crossovers that allow for complete panel replacement as well as repair-in-place maintenance. Provisions are made for hoisting equipment to be installed in the top of the receiver structure for raising and lowering equipment, piping, valves, etc, and complete absorber panels. A crane can be installed early in the construction phase to support structural assembly of the receiver and removed when assembly is complete. Subsequent repair operations can be performed using portable hoists.

All platforms and openings are protected by rails or safety chains. The area under the receiver floor and above the tower top is open. The receiver has no siding and only the cavities are enclosed. The result of removing the siding is that the receiver has an "outdoor" appearance that is compatible with the turbine and boiler approach at Saguaro. More importantly there will be a freer movement of air and thus a cooler structure. The receiver floor and the top area of the receiver are covered with expanded metal to provide working surface while allowing free passage of air. Combined with a floor at the top of the tower, this provides a safe, well-ventilated, and daylighted work area for receiver maintenance operations. Lightning protection is provided by lightning rods installed at the high points on each door guide frame.

5-18

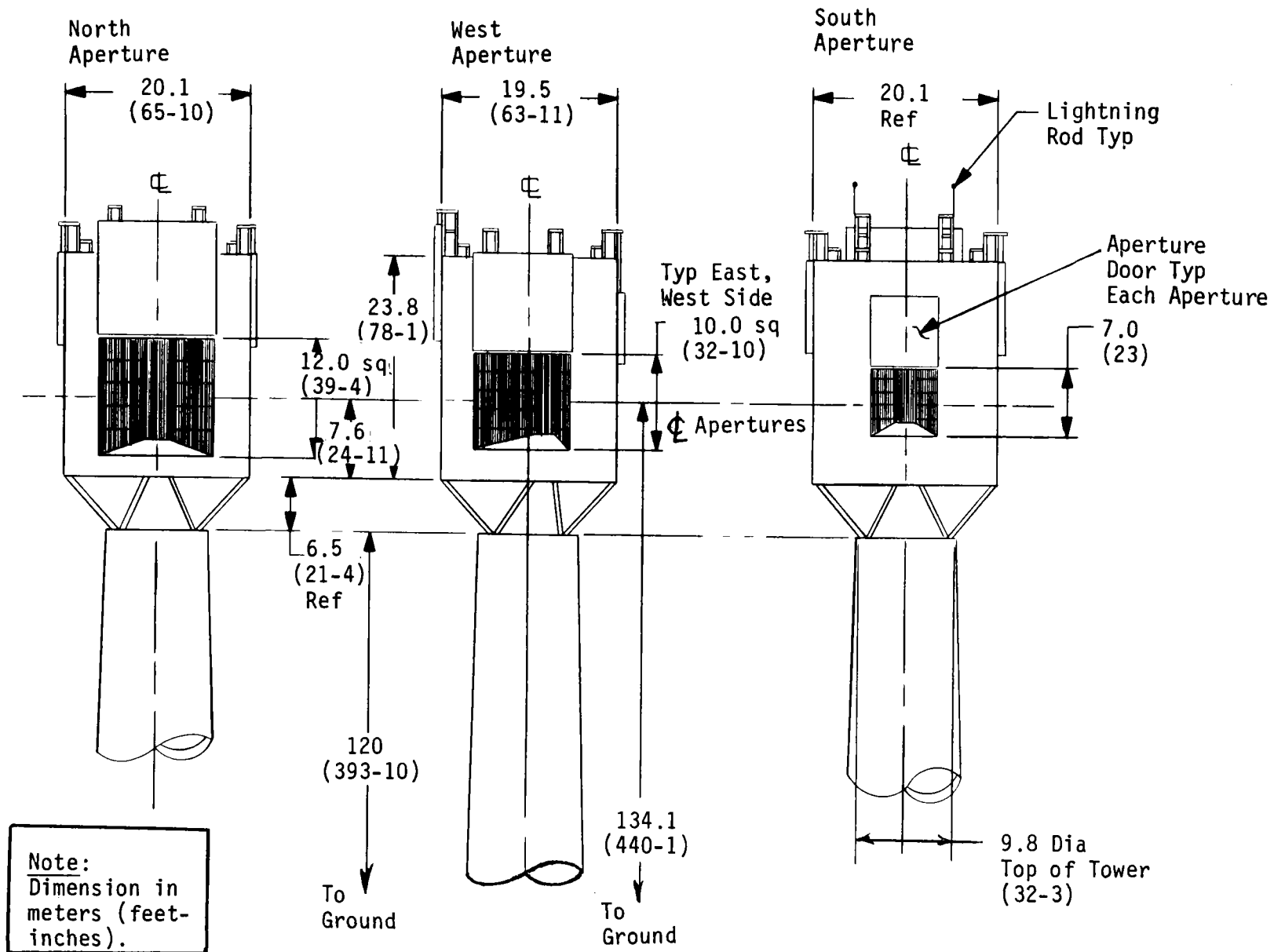
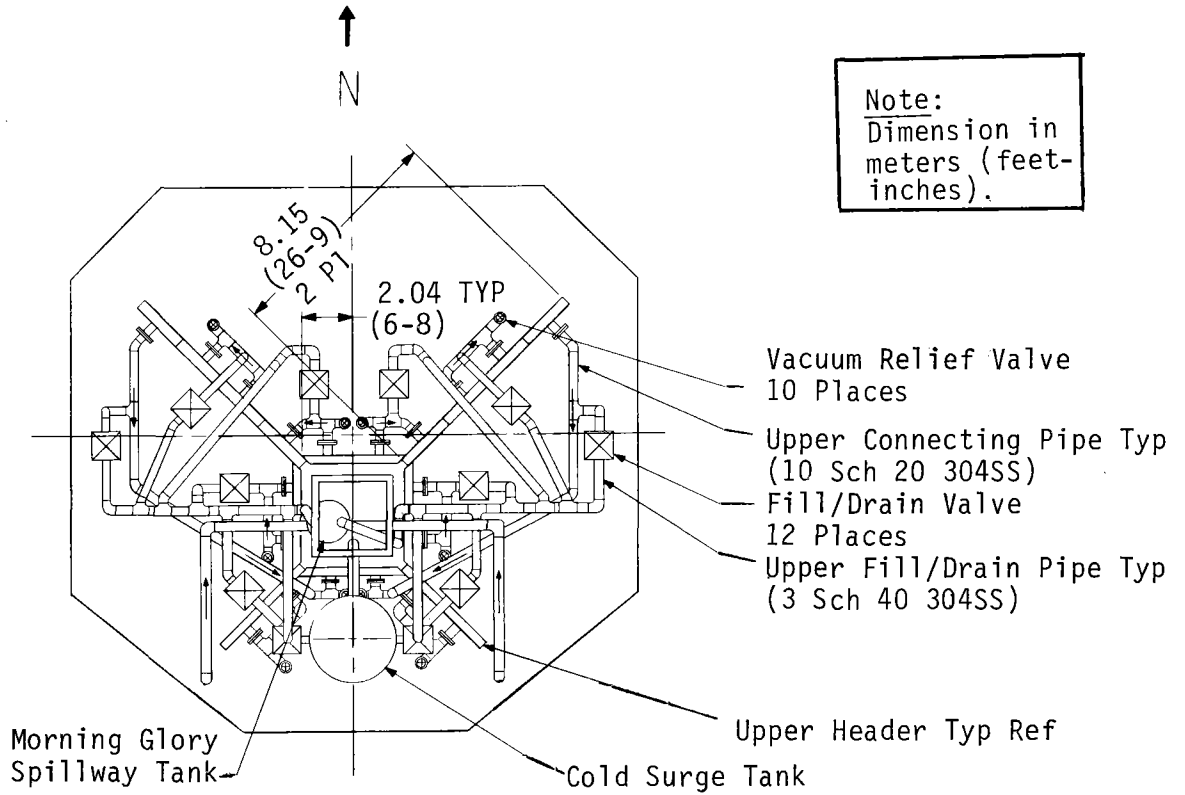
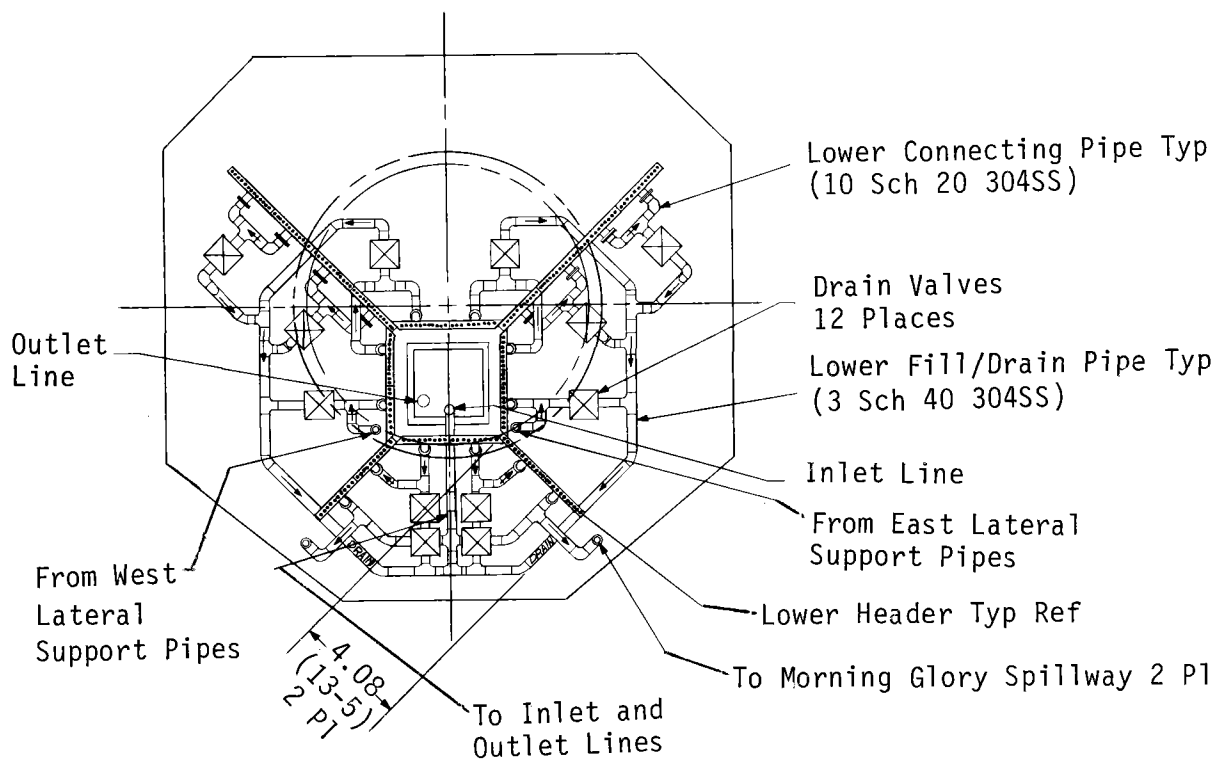


Figure 5.2-1 Receiver General Configuration



(a) Upper Crossover and Vent Piping



(b) Lower Crossover, Supply, Return and Drain Piping

Figure 5.2-2 Receiver Panel Interconnection Piping

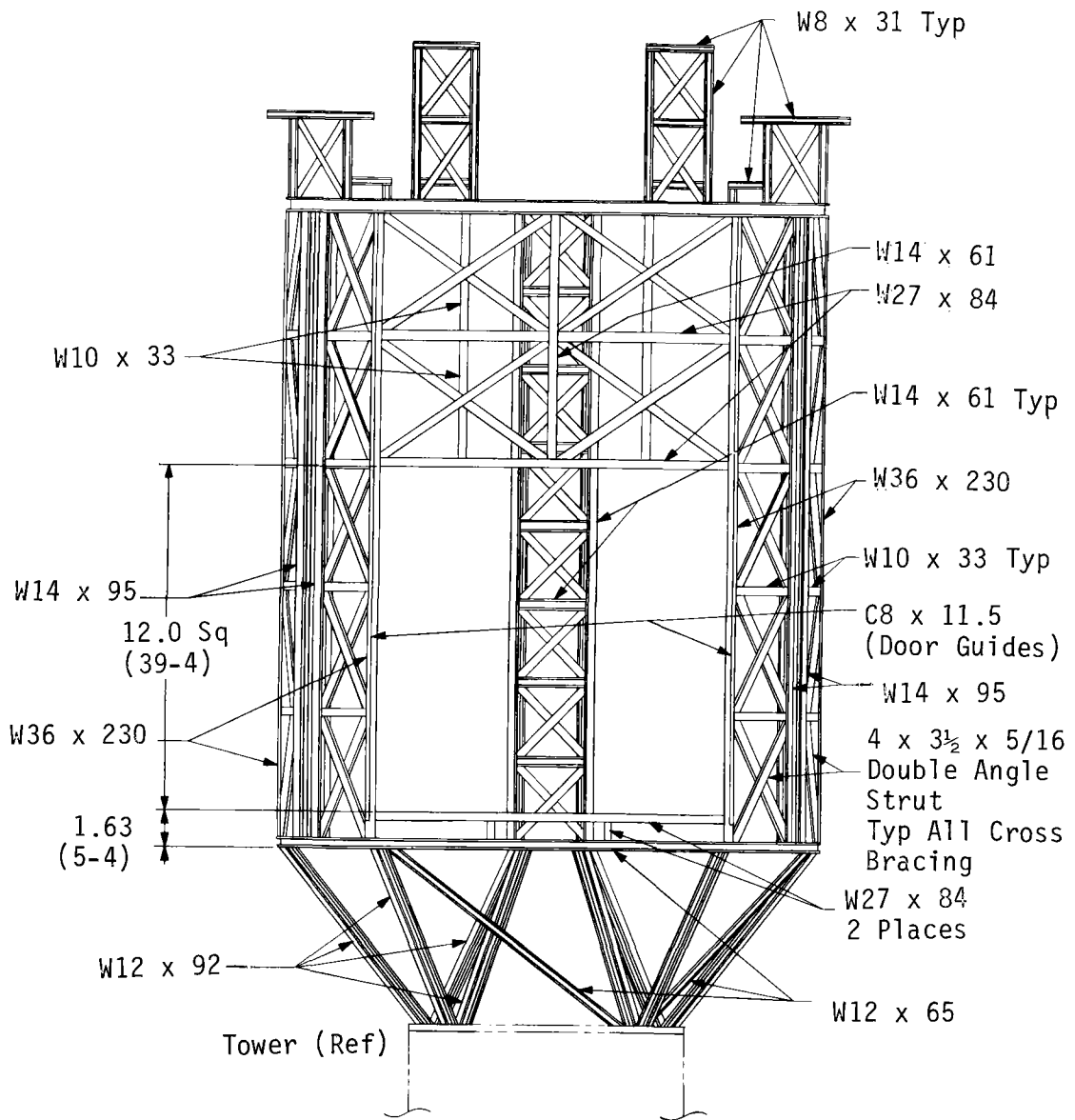
5.2.2.2 Structure - A complete set of structural drawings for the receiver conceptual design is given in Appendix A. Figures taken from those drawings are presented in this section to support the structural description.

The receiver is supported from the tower by I-beams formed into triangular or truss shapes (Fig. 5.2.3). These triangular shaped sections are tied together in the horizontal plane at the base of the receiver and form the supports for the floor joists. The receiver floor is covered with expanded metal designed to accommodate a live load of 488 kg/m^2 (100 lb/ft^2). Diagonal members connect the receiver floor structure to the tower top to provide support against torsional wind loads. This support structure provides a strong, rigid and light-weight system.

The receiver structure is assembled using eight columns placed at the outer edge of each aperture and four columns forming a center section. The columns are tied together with cross-braces to give the structure rigidity. All loads are transmitted through these columns to the support structure and into the tower. The receiver roof is supported with open-type joists and covered with expanded metal.

Each cavity has a door that can be closed during adverse weather conditions, or at night to reduce heat loss. The door can also be closed quickly during emergency conditions. Figure 5.2-4 shows the north cavity aperture door structure, which is typical of all doors. The side of the door facing outside the cavity is covered with 0.076 m (3 in.) of ablative material (see Paragraph 5.2.2.5). The ablative fills the cells of an aluminum honeycomb that is faced on each side with 0.8 mm (0.03 in.) aluminum sheet. The aluminum sheet is light weight and protects the ablative material from the weather. With the honeycomb, it also forms a rigid panel. These panels carry the ablative weight of 36.6 kg/m^2 (7.5 lb/ft^2) and the wind loads into the door primary structure. The cavity side of the door is formed of 0.10 m (4 in.) structural Tees on 1.8 m (6 ft) centers. The space between these steel T sections is filled with insulation. The insulation is faced with stainless steel sheet for protection.

The door, under normal operating conditions, is to be raised and lowered with a motor and gear box arrangement attached to a drum and cable mechanism. In case of a power failure the door will release into a free-fall condition. It is necessary to dissipate the kinetic energy acquired by the door in free-fall. This is accomplished by using a conical drum for the door cable and a counterweight with a constant diameter drum. When the door is in the raised position, the cable will be on the large end of the conical drum. When an emergency condition occurs, the door drum is released and the door will start to accelerate as the moment from the door is greater than from the counterweight. The diameter of the door drum is variable and as the diameter becomes smaller the moment also becomes smaller. As the

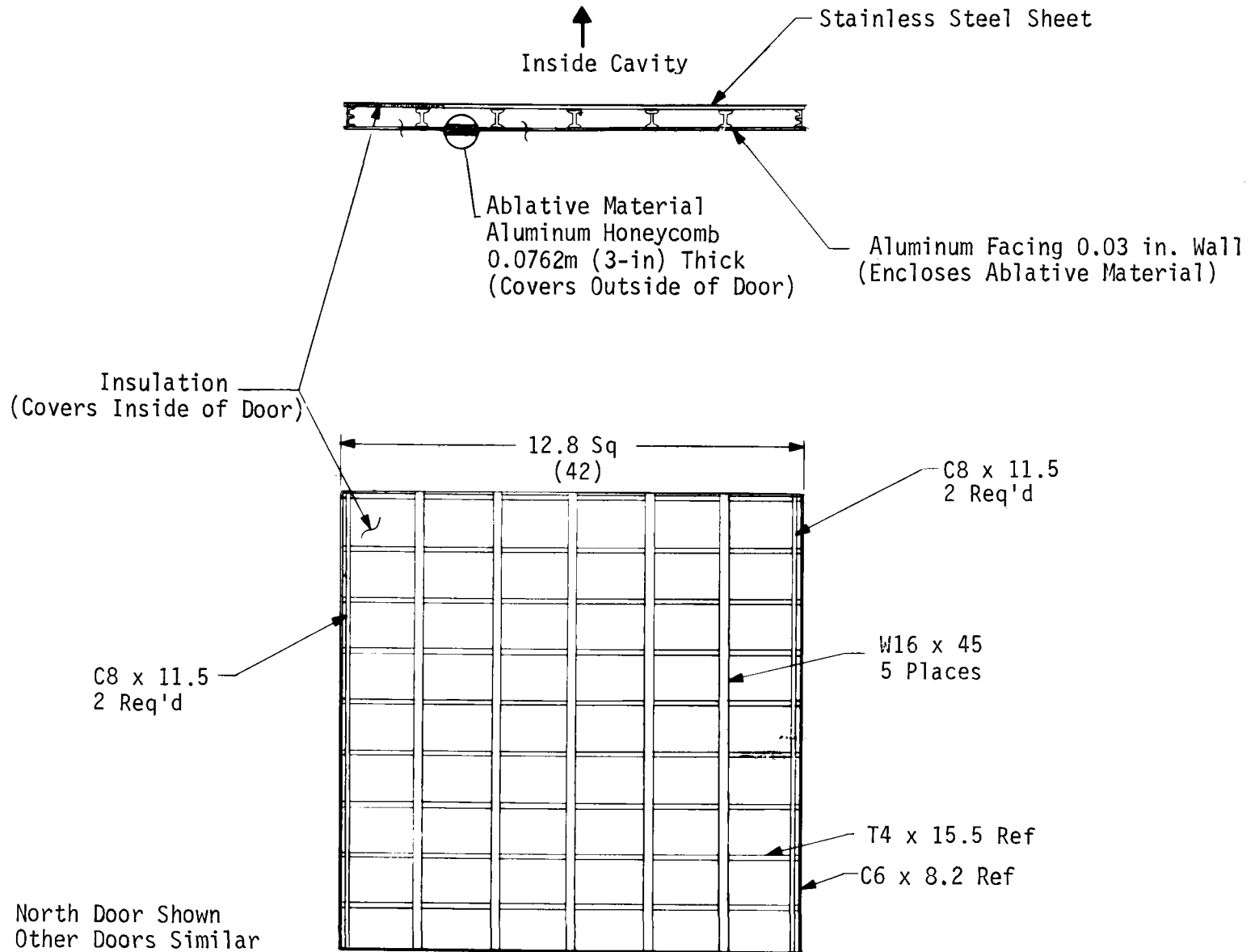


North Elevation View
(North Side Support
Structure Shown)

Note:
All Structural Steel
Sizes are in Inches
and Pounds.
1 Inch = 25.4×10^{-3} Meters
1 Pound = 0.45359 Kg
All Other Dimensions are in
Meters (Feet - Inches).

Figure 5.2-3 Receiver Support and Side Wall Structure

Figure 5.2-4



North Door Shown
Other Doors Similar

Figure 5.2-4 Receiver North Cavity Door

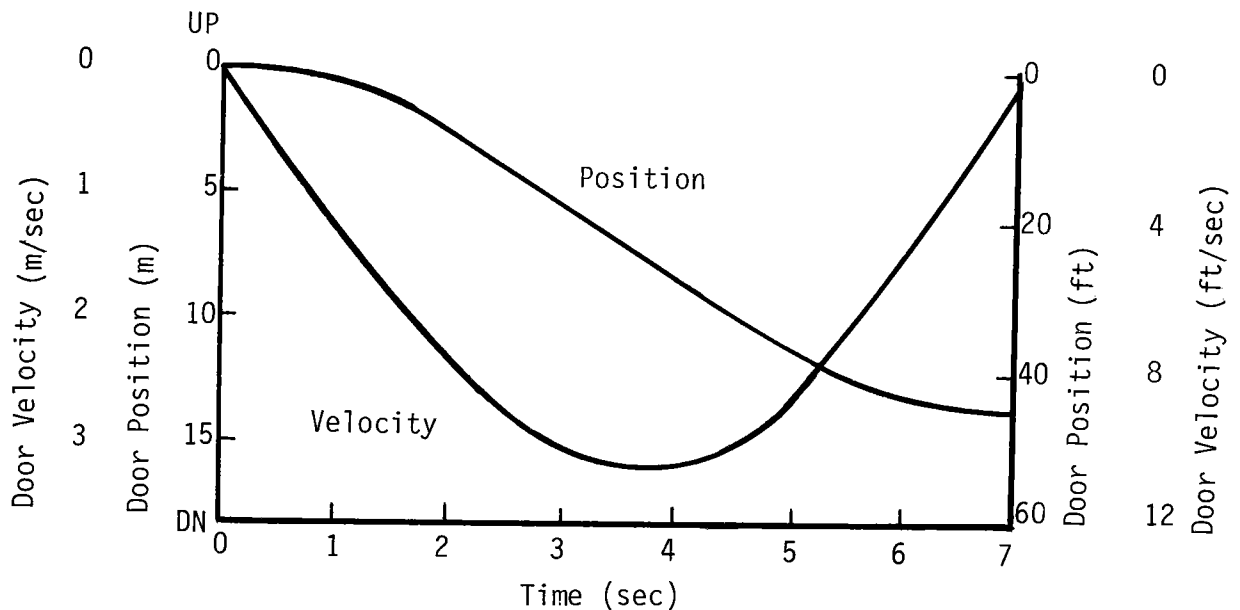


Figure 5.2-5 Door Closure Trajectory

counterweight moment becomes greater than the door moment, the door decelerates and stops falling in the closed position. The door is locked in place by a ratchet device, to keep it from rising to some intermediate position. This door mechanism has been evaluated in some detail. All of the ancillary functions have been identified and incorporated into the mechanism. Time histories have been calculated. Figure 5.2-5 is an example trajectory. These trajectories show that closing times on the order of 7 sec can be readily obtained with acceptable peak velocities. Design tolerances and friction variations can be easily compensated in the field. Two mechanisms are used for each door and they are located on the top of the receiver well out of the aperture flux spillage areas. The resulting mechanism is passive, simple, and inexpensive.

The inactive surfaces of each cavity are of stainless steel and painted with solar reflective white paint (Pyromark Series 2500, $\alpha_s = 0.32$, $E = 0.84$). The floor and ceilings of the cavities are thin gage stainless steel shields. These stainless steel shields are backed with 0.1 m (4 in.) of insulation to reduce heat conduction from the cavities to the receiver structure. On the outside of the insulation is 14 gauge galvanized corrugated steel siding. The shields protect the absorber panel headers and are supported from the receiver structure. The supports have minimum thermal conductance. Structural members within the cavities and around the edge of the apertures where solar flux impinges; are protected with stainless steel radiation shields, backed up with insulation. "Duraback"

ceramic fiber insulation in 0.10-m (4-in.) blankets is used in the receiver to reduce the heat loss and to protect the structural members from high temperature. The basic approach is to enclose and insulate the cavities and to allow the structural members to be exposed to the atmosphere. In this way, the temperature of the structural steel can be kept low. All piping, the surge tank, and the morning glory spillway tank are individually insulated to reduce heat loss and maintain a low temperature environment for valve controls, supports, etc. That part of the absorber panels and headers that are above and below the cavities are insulated and covered with 14 gauge galvanized corrugated steel siding.

5.2.2.3 Absorber Panels - The absorbing surfaces are divided into panels with 46 tubes per panel. As shown in Figure 5.2-6, the receiver is symmetrical with 10 absorbing panels on the east half (east pass) and 10 absorbing panels on the west half (west pass). Salt flow through the receiver starts from the cold surge tank and is divided into the two passes (east and west). The salt, in each pass, goes through a control valve, through the parallel lateral support pipes, through the 10 absorber panels (Fig. 5.2-6), to the morning glory spillway and then to the downcomer. Salt temperature is measured at the outlet of the various panels and used to set the inlet control valve position. Details on receiver control can be found in paragraph 5.3.2. The absorber tubes in each panel are 0.0381 m (1.50 in.) OD Incoloy 800 coated with black Pyromark Series 2500 paint ($\epsilon_s = 0.95$, $E = 0.90$). The tubes are connected at the top and bottom into headers that are made from 0.254-m (10-in.) diameter schedule 20S pipe of Incoloy 800 material. Panels are approximately 2.04 m (6.7 ft) wide and range in length from 10.77 m (35 ft 4 in.) to 17.88 m (58 ft 8 in.) measured from the top of the top header to the bottom of the bottom header. The individual tubes are separated by 6.4 x 3.1 mm (0.25 x 0.125 in.) spacers so that the tubes can be welded to each other along their full length.

The arrangement of the absorber tube panels results in two panels on the back wall of each cavity for a total of 368 tubes arranged in a square around the center structure. These tubes will only be heated on one side and are insulated from the center support structure. The radial absorbing sections (Fig. 5.2-6) on each side of the north cavity are made up of four panels each and absorb flux on both sides. Similar two-sided heating exists on the two panels that form each side of the south cavity. A total of 552 tubes are heated on both sides. The upper and lower headers are staggered in elevation (Fig. 5.2-7) to reduce the area of the panels not exposed to the solar flux.

The absorber tubes are parallel and attached to adjacent tubes with continuous webs or spacers for their entire length to form a solid panel. The tubes are attached to the headers by welding every other tube on the vertical centerline and alternate tubes at 30° off the vertical centerline. The panel upper headers of the radial panels are supported from built-up beams at the top of the receiver structure. The panel headers around the center section are supported vertically from beams around the center structure. The cavity back wall panels are supported laterally by buckstays to the center structure. The lower headers are guided to absorb loads perpendicular to the panel faces, but the headers can move up and down and parallel to the panel faces.

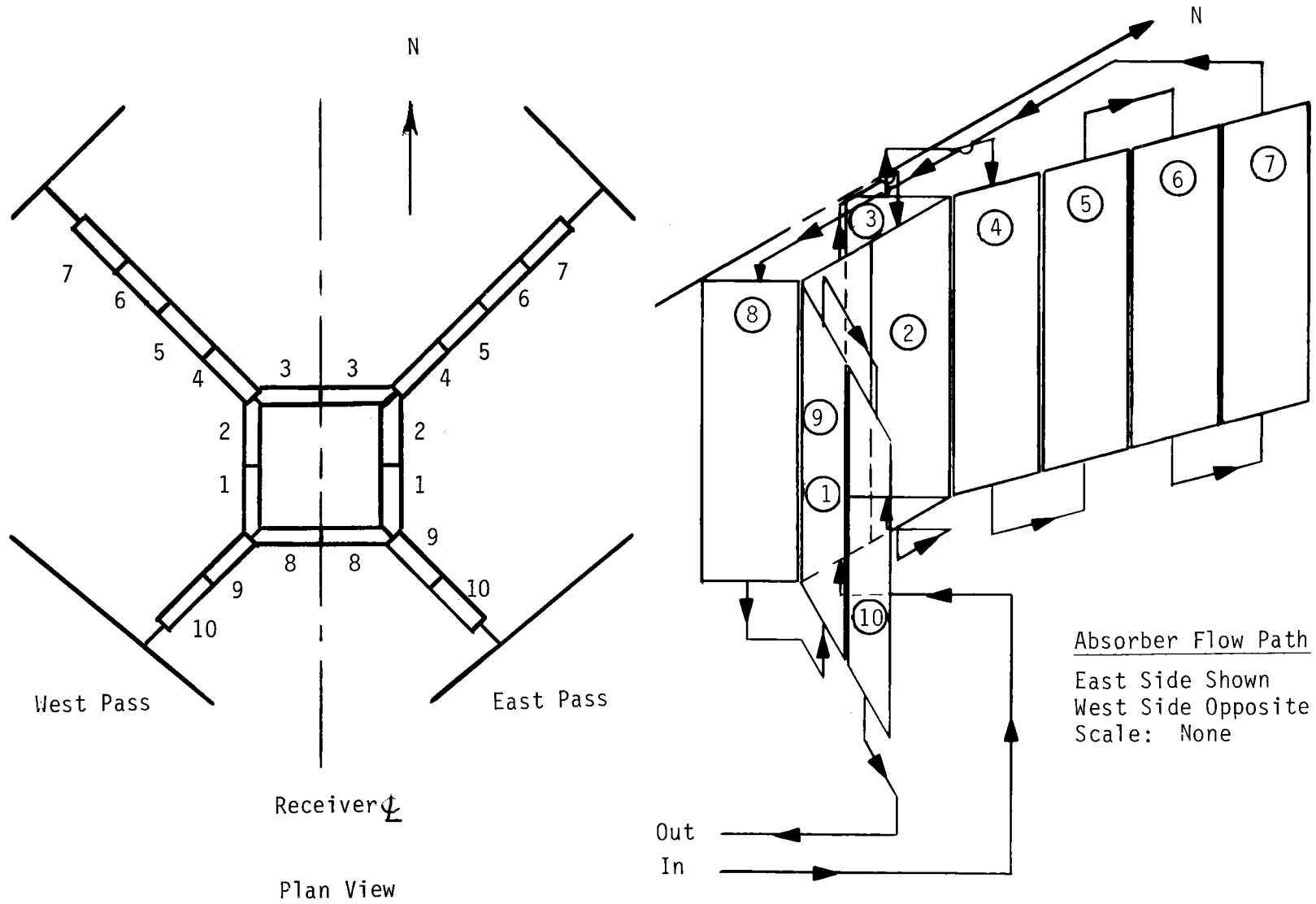


Figure 5.2-6 Absorber Panel Arrangement

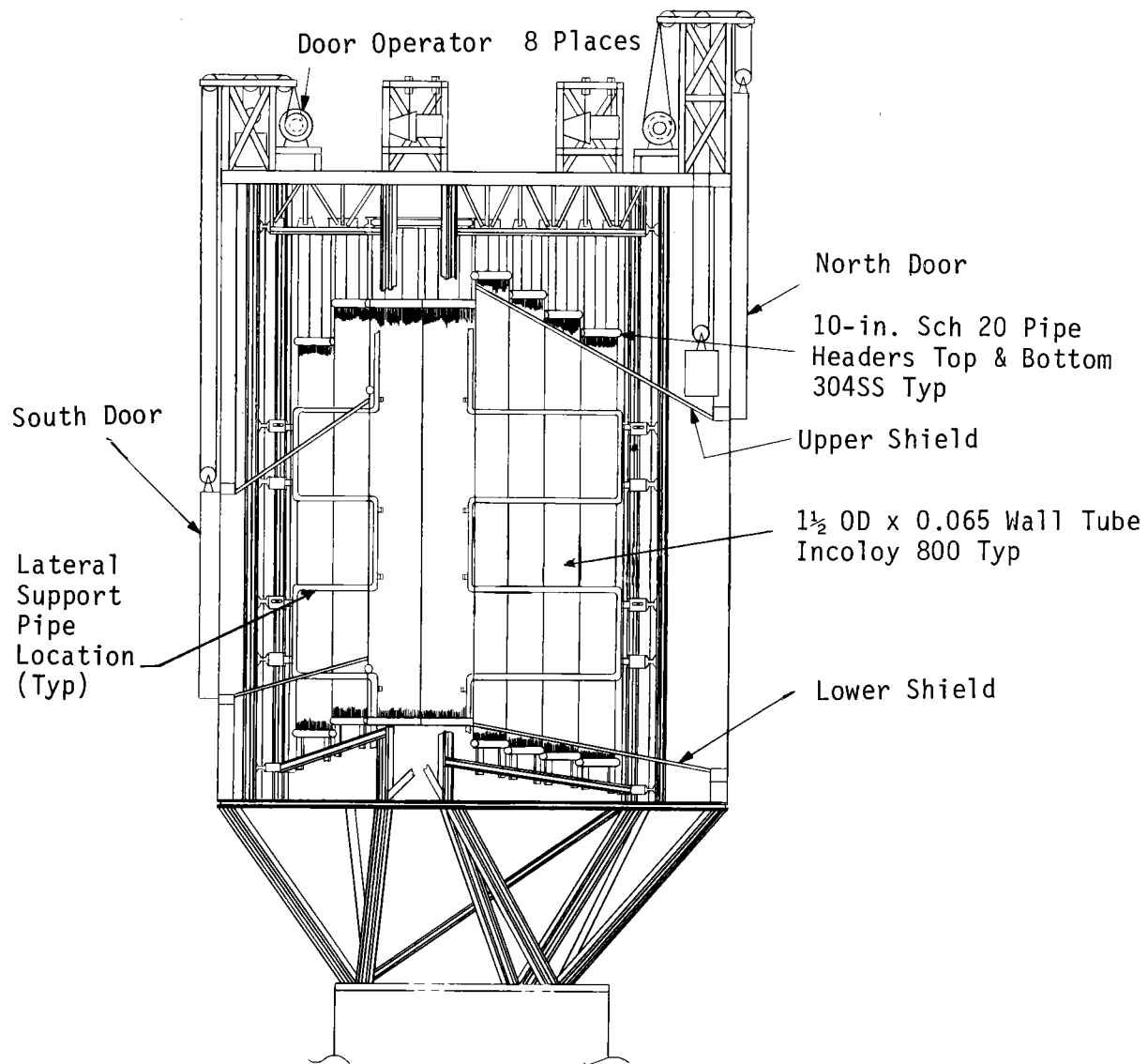


Figure 5.2-7 Receiver Absorber Panel Supports

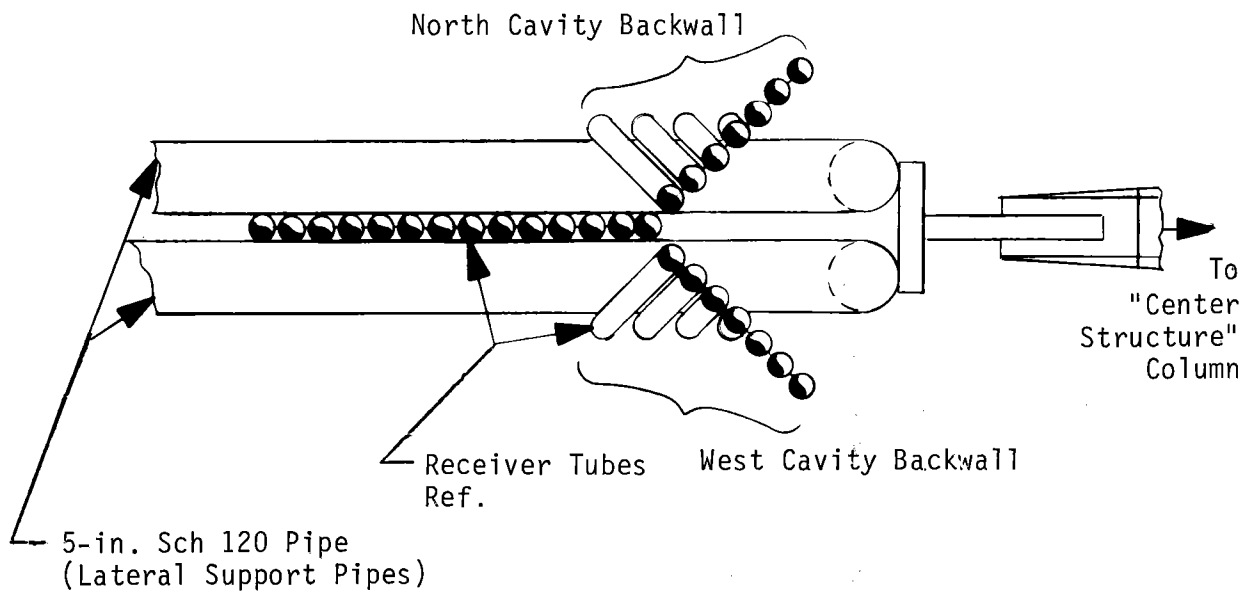


Figure 5.2-8 Interfaces Between Absorber Tubes and Lateral Support Pipes

The radial panels with two-sided heating are supported at 3.05 m (10 ft) intervals by two 0.13 m (5 in.) Schedule 120S lateral support pipes as shown in Figure 5.2-7 to prevent excess deflection due to wind loads. These stainless steel pipes go from the top of the receiver to the bottom in a zig-zag pattern with one pipe on each side of the panel to provide four pairs of panel support beams. The coolest heat transfer salt coming into the receiver is run through these pipes (see paragraph 5.2.3). Shown in Figure 5.2-8 is a detail of how the absorber tubes are bent where the lateral support pipes pass through the corners of the cavity back walls. The lateral support pipe horizontal sections are supported to permit both vertical and horizontal thermal expansion. The lateral support pipes can be removed by cutting the horizontal part of the pipe loose and then sliding it out through openings in the receiver structure. Both the back panel and radial support structures permit vertical and lateral (in the plane of the panel) movement to accommodate thermal expansion.

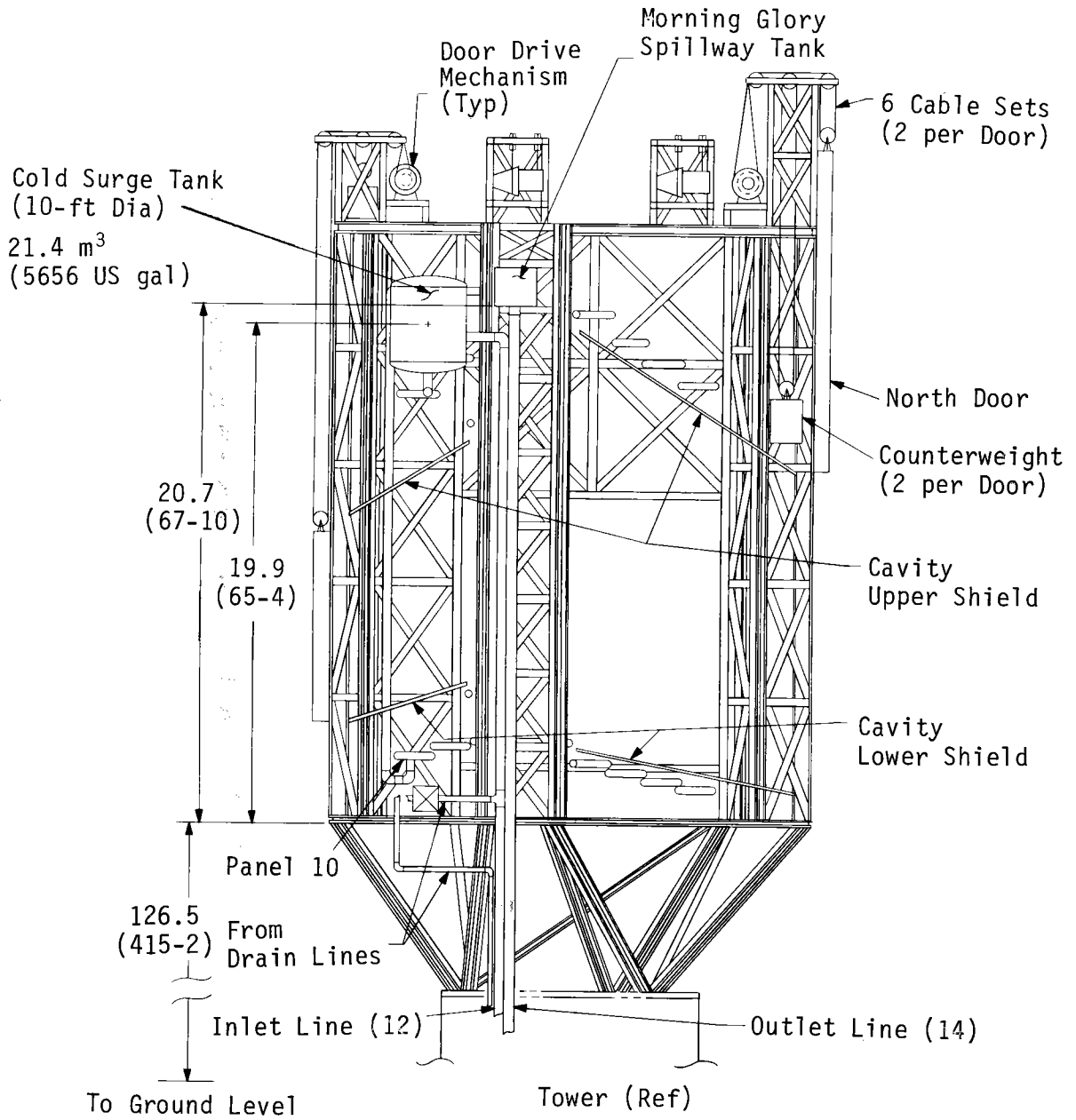
5.2.2.4 Piping - The receiver piping consists primarily of the riser and downcomer attachments, the upper and lower crossover supply, return, vent, and drain piping (Fig. 5.2-2), the surge tank, morning glory spillway, and the four lateral support pipes. Further piping details are included in Appendix A. The inlet pipes are made of A106 Gr B carbon steel and all other interconnecting piping, the lateral support pipes, and the downcomer are made of Type 304 stainless steel.

The drain lines are gathered and connected to the downcomer. Each (10) drain line has a normally closed, electrically powered, remotely controlled drain valve. The vent lines for the east and west passes are separately gathered and connected to the upper part of the morning glory spillway. Each (10) vent line has a normally closed, electrically powered, remotely controlled vent valve as well as a vacuum relief valve to help avoid absorber tube collapse should a vent valve fail to operate. The eight lateral support pipes are connected into an east and a west set. Each of the sets is fitted with an electrically powered, remotely controlled vent valve and a vacuum relief valve. The lateral support pipes can drain directly through the flow control valves to the riser and do not need separate drain valves.

The cold surge tank and morning glory spillway are shown in Figure 5.2-9 along with the inlet and outlet connections and the connections to the lateral support pipes. The morning glory spillway is mounted at the receiver top so that the free liquid level will be above the top of the highest headers. This will provide for positive filling of all of the absorber tubes and interconnecting piping. The inlet surge tank will be controlled to maintain its level at the half full point. The receiver inlet, or cold, surge tank is pressurized to 1.72 MPa (250 psig). The cold surge tank pressure was selected to provide the proper pressure drop through the receiver including the flow-control valves and a margin. The morning glory spillway tank is vented to the atmosphere.

The hot surge tank was deleted and replaced by the much smaller morning glory spillway tank. The cold surge tank was moved from the central area to over the south cavity. These two changes have opened up the center structure of the receiver. The only equipment in the center section is the riser, downcomer, and the morning glory spillway tank and its piping connections. It was desired to open up the center sections because of the difficulty in assembling receiver piping at Solar One.

The morning glory spillway, used to maintain the proper static head on the receiver outlet, is patterned after a spillway design used for medium head earth fill dams. The shape of the spillway (similar to the shape of a morning glory flower) is selected so that the salt will stick to the wall and flow smoothly into the outlet pipe and continue to flow along the downcomer wall. The center of the downcomer is not filled at any flow. The large circumference of the spillway crest means that a wide range of flows can be accommodated



East Elevation View

Note:
Dimensions
are in meters
(feet - inches).

Figure 5.2-9 Receiver Surge Tank Location

for only a slight change (less than 0.15 m or 6 in.) in salt height. The kinetic energy of the falling salt is absorbed in the salt when it falls into a 2.4 m (8 ft.) deep pool of salt. This plunge pool is adapted from small dam design approaches. The depth of salt is selected so that no scouring or erosion of the plunge pool tank will occur. The churning action of the salt in the plunge pool converts the salt's kinetic energy to thermal energy.

An air compressor system is provided to supply air to the cold surge tank. The air compressor will be located in a separate room in the top of the tower so it is not exposed to the higher temperatures in the receiver area and so that it can be readily serviced. The air storage tank will be located on the receiver floor under the south cavity. This location can be seen in Figure 5.2-7 just above the floor girders and just to the left of the center structure although the air storage tank is not shown.

The air supply system was sized to permit filling the cold surge tank from ambient pressure to its design value in 30 minutes using the compressor and stored air together. This resulted in the system characteristics shown in Table 5.2-1. The time to fill the air storage tank from ambient is under 1 hr. When the cold surge tank is being used to force salt through the receiver during an emergency, its air pressure will reduce as the air volume increases. During this process, the air storage tank will continue to supply air to the surge tank. The result is an average cold surge tank pressure above 1.41 MPa (205 psig) during the blowdown.

Table 5.2-1 Receiver Air Supply System Characteristics

Compressor	
Rating	0.047 Std m ³ /s (100 SCF/min)
Pressure	4.14 MPa (600 psig)
Motor Power	38 kW _e (50 hp)
Three Stages with Intercooling	
Weight	1600 kg (3500 lb)
Air Storage Tank	
Pressure	4.14 MPa (600 psig)
Volume	2.5 m ³ (88 ft ³)
Diameter	1.22 m (4 ft)
Shell Thickness	29 mm (1.125 in.)
Weight	2,700 kg (6,000 lb)

The absorber panel lateral support concept is shown in Figure 5.2-7. Two continuous 0.127-m (5-in.) diameter, schedule 120S stainless steel pipes were used to construct each of the four radial panel supports to meet the operating wind load requirements. Two pipes cross horizontally on each side of the absorber panels approximately every 3.05 m (10 ft) to provide lateral support for the absorber panels. The lateral support pipes are not attached directly to the absorber tubes so they are free to expand thermally with respect to each other. The support pipes are attached to the receiver structure on each side of the set of absorber panels in a manner that allows for thermal expansion of the support pipes, but transfers the absorber panel wind loads to the receiver structure. The form of attachment used at the outboard end of the receiver panel is shown in Figure 5.2-10. The inboard end supports are similar except that the receiver structure is a vertical W14x61 column.

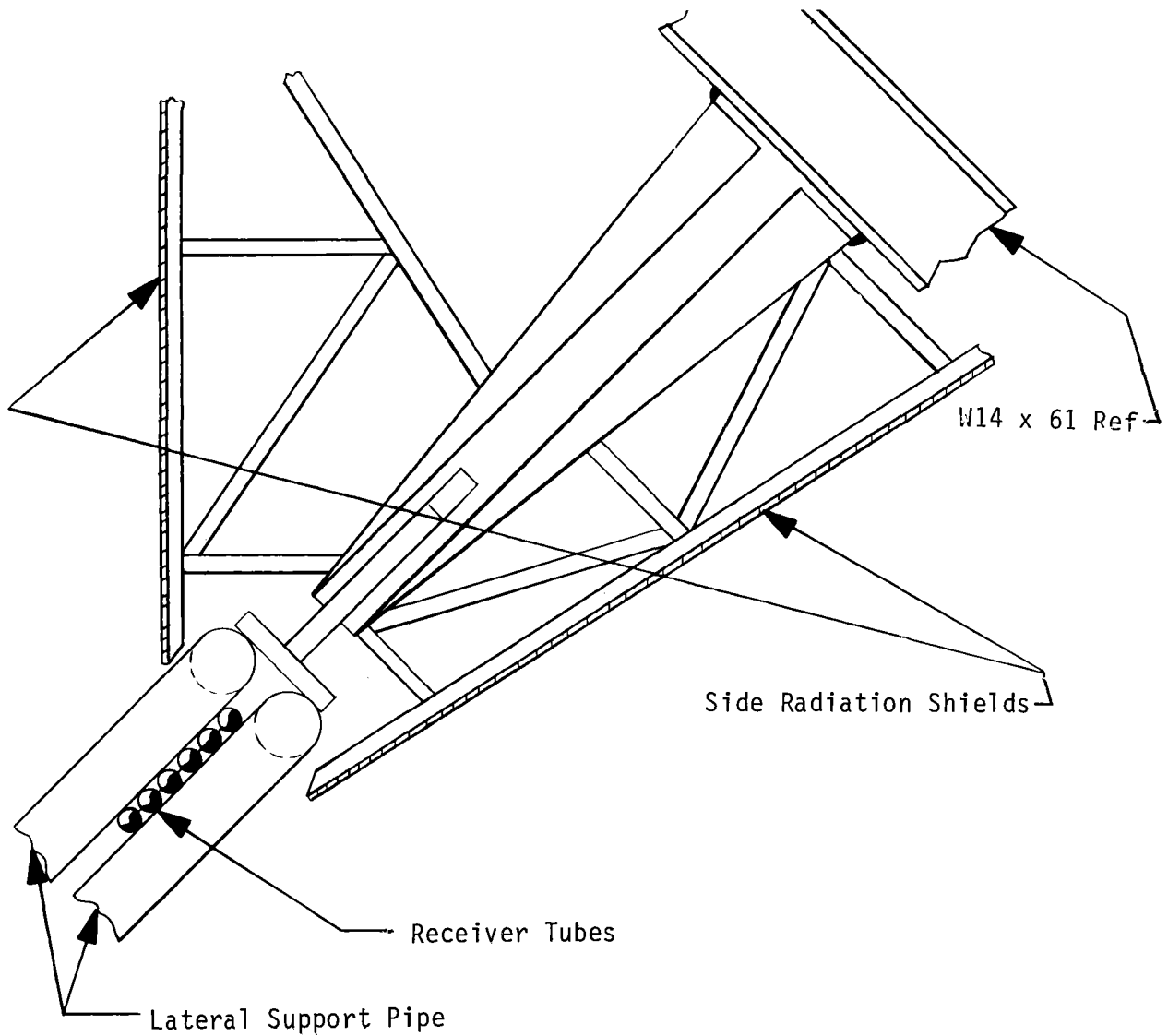


Figure 5.2-10 Outboard Lateral Support Attachment

For this support concept, cool salt flows through the support pipes to cool the pipe and to reduce the effect of the flux incident on its surface. A preliminary analysis of support pipe temperatures for the pipe supporting the north wall in the cavity is described in Paragraph 5.2.3.3. By painting the lateral support pipes white, the temperature increase in the salt was limited to less than 2.8°C (5 F) and the pipe external temperatures were less than 427°C (801°F). Four such pipe supports, e.g. one on each side of the northeast absorber and one on each side of the southeast absorber, are required in each symmetrical receiver half. Four pipes of this size are equivalent to a receiver panel in flow cross-sectional area. Because of the shorter length of the support pipes associated with the south cavity, restrictors will be provided to match flow rates, and thus salt velocities, in all eight support pipes. The connections to the lateral support pipes are shown in Figure 5.2-9.

An evaluation of pressure drops in the receiver at the design point was made with the results shown in Table 5.2-2. Most of the pressure drop can be seen to occur in the absorber tubes and the control valve. The control valve head was taken as a percentage of the dynamic head, and the margin was taken as a percentage of the first five items in Table 5.2-2.

Table 5.2-2 Receiver Pressure Drop Summary

Item	Equivalent Head of Salt, m (ft)
Absorber Tubes	49.4 (161.8)
Lateral Support Pipe	4.8 (15.7)
Tube Entrance/Exit	7.6 (24.8)
Connecting Pipe	3.7 (12.3)
Static Head (Morning Glory Spillway Crest over Cold Surge Tank)	1.7 (5.7)
Control Valve	22.6 (74.3)
Margin	6.7 (22.0)
Pressure in Morning Glory Spillway Tank	0 (0)
Total	96.5 (316.6)

5.2.2.5 Receiver Thermal Protection Considerations - Thermal protection methods were examined to (1) insulate the structure of the receiver from high temperatures, (2) minimize the cooldown of the receiver during overnight nonoperation, and (3) protect absorber tubes when a booster pump or power failure occurs with solar flux directed into the receiver. The first two items require the use of radiation shields within the receiver cavity to both redirect radiation within the receiver and also protect nonabsorber materials (structure, headers, instrumentation). The radiation shields are described in Section 5.2.2.2. Insulated doors on the receiver apertures are used to minimize cooldown during nonoperation. Protection of the absorber tubes during an unexpected salt flow stoppage required consideration of the potential causes of such a failure and methods to shield the absorber tubes from high energy flux.

Calculations were first performed to determine the absorber tube metal temperature rise rate with a salt flow stoppage and energy from the collector field into the receiver. Such an occurrence might happen due to one of the following:

- 1) Failure of the booster pumps;
- 2) Failure of the main circulation pumps;
- 3) Drag valve closure;
- 4) Salt piping blockage;
- 5) Receiver salt control valve failure in a closed position;
- 6) Electrical power failure;
- 7) Complete loss of high air pressure on the cold surge tank.

If such a salt flow stoppage should occur and power is available to the collector field, heliostats will be quickly defocused to reduce energy flux into the receiver. However a finite time period is involved in detecting the failure, deciding what action to take, and then acting. Therefore, in our evaluation the first step was to determine the time required to heat the absorber tubes to an upper temperature limit with complete salt flow stoppage. This temperature was determined to be approximately 927°C (1700°F) for Incoloy 800.

Results of these analyses, as given in Ref 1-2, clearly indicate that even a short-duration flow stoppage cannot be tolerated in a salt receiver with high solar flux levels on the receiver. Such an occurrence would lead to either absorber tube failure, tube warpage, or reduction of tube life. Therefore, in the receiver design, we have incorporated additional features that will ensure salt flow through the receiver (cold surge tank) and protection of absorber tube surfaces once salt flow through the receiver is exhausted (ablative covered door). A backup diesel generator will also be available that can provide 200 kW_e within 25 sec from start.

The primary approach for ensuring the availability of electric power is the provision of automatic power switching between the east and west 115-kV buses of the Saguaro switchyard. Upon loss of power on either bus, the solar system load would be immediately switched (within 8 cycles) to the other bus, and the diesel generator would be started. The solar system load is only switched to the diesel when both the east and west buses are lost. The worst case occurs when both the east and west 115-kV buses are lost at the same time, and then the diesel must be started. The diesel will be used to maintain power for the most important functions only. It does not have enough capacity to drive the salt booster pumps. However, it can be used to operate control valves, receiver doors, salt transfer pumps, or the collector field (only portions at any one time).

It is expected that any loss of cold salt surge tank pressure would be gradual. At the first sign of pressure loss, the heliostats would be quickly defocused. If salt flow dropped below a set limit before the cavity solar flux had dropped sufficiently, then the quick cavity door closing function would be exercised.

In case a booster pump stops due to a power failure, enough salt will be contained in the receiver cold salt surge tank to provide design flow through the receiver for at least 60 sec. During this time, the heliostats without power will be providing energy into the receiver. Even if power is available to the field, 1.1 MW_e is required to slew all 5,000 heliostats at the same time. Based on slew rates of 0.33r and 0.42r/min for the azimuthal and elevation directions, respectively, and heliostat control logic, 60 sec are required to get all heliostats off the receiver. Without power to the collector field, peak flux levels at the aperture higher than 315 kW_t/m² (100,000 Btu/hr-ft²) can last up to 4 min, and more than 6 min are required before all energy is off the receiver due to the apparent sun motion.

After a booster pump or power failure, the receiver door will be closed, with gravity assist, to shield incoming flux from the absorber tubes. The door mechanism discussed in paragraph 5.2.2.2 requires 7 sec to complete the cavity door closure. Once the door closes, the face of the door intercepts the incoming flux. Without thermal protection, the solar flux may damage the door by either creating thermal stresses that will warp it or burning a hole through the thin metal sheets. Therefore, various thermal protective systems were evaluated to protect the door.

Our evaluation of thermal protection methods considered the use of typical schemes for high-temperature applications. These methods included ablative, radiative, transpiration cooling, and heat-sink concepts. The concept selected for receiver door application was the use of an ablative material. The ablative provides the lowest cost and lowest weight of the options considered. The properties of the selected ablative material are given in Table 5.2-3.

Table 5.2-3 Material Properties of Martin Marietta ESA-3560 Ablator

Density	480 ₊₃₂ Kg/m ³ (30 ₊₂ lb/ft ³)
Thermal Conductivity	0.098 W/m-°C (0.68 Btu-in/hr-ft ² -°F)
Specific Heat at 24°C	1.55 J/Kg°C (0.37 Btu/lb-°F)
Emissivity	0.80
Ablation Temperature	443°C (830°F)
Effective Heat of Ablation	13491 kJ/kg (5800 Btu/lb) for 50 sec at 681 kW _t /m ² (60 Btu/ft ² -sec)
Storage Life	Indefinite below 66°C (150°F)

This ablative material has been used on flight test vehicles and the Viking spacecraft. A 0.076 m (3 in.) thickness of this ablative material was estimated to be sufficient to accept the peak solar flux and carry heat away from the receiver door as the material ablates. The material will be installed in small easily handled panels on the receiver door to minimize the expense of replacement. For design details, see Appendix A.

It now appears that such power failures leading to salt pump outages or collector field inoperation would occur infrequently, thus minimizing the need for replacement of ablative surfaces. However, the use of low cost thermal protection schemes alleviates the concern for absorber tube replacements due to excessive temperatures during potential failure modes.

5.2.2.6 Stress and Dynamic Analysis - The structural framework of the receiver module is designed to provide unobstructed entry for solar flux and protection for the absorber tube panels. The structure is symmetrical about the north-south axis and provides apertures of the following sizes:

- 1) North cavity - 12x12m (39 ft 4 in. by 39 ft 4 in.);
- 2) East-west cavities - 10x10m (32 ft 10 in. by 32 ft 10 in.);
- 3) South cavity - 7x7m (23 ft 0 in. by 23 ft 0 in.)

The most important receiver elements, the absorbing surfaces, are suspended from roof trusses in staggered "curtain" panels. Each panel consists of 46 tubes with 0.038-m (1-1/2-in.) OD of Incoloy 800 welded together with spacers between the tubes. Panel sizes are approximately 2.04 m (6.7 ft) wide and range from 10.8 m (35 ft 4 in.) to 17.9 m (58 ft 8 in.) long. The main structural framing offers no lateral or vertical restraint inhibiting thermal expansion and contraction of the tube panels; restraint systems of special design are discussed in Section 5.2.2.3.

The steel roof sections were designed to accommodate heavy-duty hoists for all cavity doors. Provisions were also made for a 9.1×10^3 kg (10-ton) lift crane on the central tower of the receiver. The lift crane can be used for hauling prefabricated panel sections into place. The construction crane will be removed when construction is complete. However, provisions have been made for rigging and supporting temporary hoists that can be used for component removal and replacement.

All structural elements of the receiver are standard A36 steel sections selected in accordance with AISC specifications (Ref 5-1). The siding is corrugated 14-gage steel siding and the roof is expanded metal. Standard long-span steel joists (18 LJ 02) are used on the roof. Open-web steel joists (J series) are used to carry the expanded metal floor deck.

Because of the heavy loads carried by the superstructure columns, the receiver loads were carried into the tower by a set of triangular trusses made up of standard I-beams. Diagonal I-beams were used to transfer torsional loads to the tower.

Loadings and design criteria have been cited in a number of reports and communications (Ref 2-1,5-2,5-3), in Section 5.2.1, and in the System Requirements Specification of the prior study (Ref 1-3). A brief summary of the design factors considered is useful.

- 1) Snow and ice - These conditions were assumed to include a layer of ice with a thickness of 25 mm (1 in.) and a snow cover with a weight of 240 Pa (5 lb/ft²).
- 2) Wind - For analysis a maximum wind condition that assumed winds up to 40 m/s (90 mph) with a gust factor of 1.05 at a reference height of 10 m (30 ft) was used. This value is used in the System Requirements Specification. However Reference 5-4 identifies a maximum wind speed at the 10-m (30-ft) level as being 33.5 m/s (75 mph) on a 100-yr recurrence level. The higher number was used as being conservative. The following model, as defined in the System Requirements Specification (Ref 1-3) was used for the extrapolation of wind speed to higher elevations.

$$V_H = V_1 (H/H_1)^c$$

where V_H = wind velocity at height H

V_1 = reference wind velocity

H_1 = reference height (10 m (30 ft))

$c = 0.15$

This formula results in a dynamic pressure of 2.50 kPa (52.3 psf) at the receiver centerline for a reference height velocity of 40 m/s (90 mph).

The location of Saguaro falls under Exposure C of ANSI A58.1-1972, which is defined as flat open country or flat coastal plains. When Exposure C data are taken from ANSI A58.1-1972, the resulting dynamic pressure at the receiver centerline is 2.50 kPa (52.3 psf) for a velocity of 40 m/s (90 mph). These two approaches give the same wind loading. However, the loads would be much lower if the 100-yr recurrence level of wind velocity had been used. A further discussion of wind loads is given as part of the analysis of lateral loads.

- 3) Earthquake conditions - Saguaro lies in Universal Building Code (UBC) Zone 2 that has low earthquake requirements (Ref 5-5). As the UBC requirements do not specify accelerations, another source is necessary. It is felt that the Nuclear Regulatory Commission requirements that were referenced in the prior study contract form of the System Requirements Specification were too stringent. Reference 5-6 gives an average survival value of $\ddot{X}_g = 0.07$ g for UBC seismic zone 2. During the design of the APS's Cholla station, a ground acceleration of 0.10 g was used. For the Saguaro design, \ddot{X}_g was taken as 0.10 g along with the methodology of Reference 5-6.

Lateral acceleration

$$(1) \quad \ddot{X}_{TT} = 1.05 \ddot{X}_g + \frac{1}{25} \left[H_t \sqrt{\frac{\ddot{X}_g}{W_R}} - 4.4 \right] \quad \text{and} \quad \ddot{X}_{TT} > \ddot{X}_g$$

where

\ddot{X}_{TT} = tower top acceleration,

\ddot{X}_g = ground acceleration,

H_t = height of tower, ft,

W_R = weight of tower, kips.

Vertical acceleration

$$(2) \quad \ddot{X}_{TT} = 3\ddot{X}_g$$

Peak accelerations for the top of the tower were obtained using these equations for both survival and operating conditions.

Survival

$$\ddot{X}_g = 0.10 \text{ g}$$

$$\text{Lateral acceleration } \ddot{X}_{TT} = 0.10 \text{ g,}$$

$$\text{Vertical acceleration } \ddot{X}_{TT} = 0.30 \text{ g.}$$

Operating

$$\ddot{X}_g = 0.07 \text{ g}$$

$$\text{Lateral acceleration } \ddot{X}_{TT} = 0.07 \text{ g,}$$

$$\text{Vertical acceleration } \ddot{X}_{TT} = 0.21 \text{ g.}$$

Structural design was based on maximum or survival conditions.

- 4) Live loads - In addition to the loading conditions outlined above, a live load of 4.8 kPa (100 psf) was used for sizing structural members for the receiver deck. This live load was used to represent special equipment loads or opening requirements for piping and auxiliary conduits that were not finalized during this conceptual design.
- 5) Combined loads - The following design criteria for combined loads were employed as a result of telephone conference communications with Sandia National Laboratories, Livermore (Ref 5-7).

Wind effects

$$(3) \quad 1.4 D + 1.7 W$$

Seismic effects

$$(4) \quad 1.0 D + 1.0 E, \text{ or}$$

$$(5) \quad 1.0 D - 1.0 E,$$

whichever is greater

where:

D refers to dead load,

W to wind load,

E to earthquake load.

These criteria are based on design procedures from ACI 318 (Ref 5-8). The wind and seismic loads of Equations (3) through (5) were not combined. Loading conditions obtained by using (3) were found to produce the most adverse set of loads on the receiver module.

A special analysis was performed for lateral loads (wind and seismic) acting against the receiver module to determine the most critical situation. This analysis was adapted from a similar analysis performed during the Martin Marietta Solar Central Receiver Hybrid Power System study. The four selected conditions were:

- 1) High wind at 40 m/s (90 mph) at 10 m (30 ft) reference height approaching the receiver from a direction 0.70 rad (40°) east of north, acting on the outside walls with all cavity doors closed;
- 2) Earthquake lateral forces acting against outside walls of receiver under same conditions as above;
- 3) High wind at 15.6 m/s (35 mph) again at a reference point of 10 m (30 ft), acting against the absorber tube panels with cavity doors open. Wind at an incident angle of 45° to north-south axis. This wind speed is used as it represents the speed at which heliostat stow must be initiated and the cavity doors closed.
- 4) Earthquake lateral forces acting on receiver absorber tube panels with conditions same as 3).

Condition 1) was found to superimpose the maximum loading condition and was used in conjunction with (3) previously mentioned.

Separate analyses were conducted on the strength of the receiver lateral support pipes and on the honeycomb-strengthened ablative material. In both cases, the structures were found to be conservatively designed.

Thermal stress and creep fatigue analyses were performed during the prior study (Ref 1-2) on the receiver absorber tubes and on the lateral support pipes. The design guidelines for creep-fatigue damage were based on the ASME Boiler Code, Code Case 1592. The results showed that the total projected damage due to creep and fatigue was 0.111 where the limit value is 1.0. The current design predicts more thermal cycles and thus more fatigue damage. It also predicts lower metal temperatures and thus less creep damage. When the large margin from the prior study is considered (0.111 vs 1.0) it is felt that an adequate creep-fatigue margin exists for the current design.

A combination of special factors served to offer a number of design constraints to obtaining the most effective and economical design for the receiver:

- 1) The geometry of the receiver offered symmetry only about the north-south axis. The north aperture was the largest opening; the east and west doors were 69% and the south door 34% as large as the north door. Additionally the depths of the cavities are different and the east and west apertures are not centered on the back wall. All of which means that the center support structure is not in the geometric center (north/south direction) of the receiver. Nor is the receiver center of gravity in the center of the receiver center structure. This loading is alleviated by the location of the heavy (when wet) cold surge tank over the south cavity. The morning glory spillway is not very heavy. The result is that the center structure loads introduce large moments into the receiver-to-tower supporting structure. A more careful consideration of this off-center loading could result in a decrease in weight of the receiver to tower supporting structure.
- 2) Limitations on deck space were imposed by the extensive number of pipes and tubes leading to and from the absorber panels.
- 3) Many factors remain unknown such as exact location of man-ways, personnel platforms, and elevator shaft openings. However, costs were estimated for such features.

During the design analysis, there were some concerns regarding the structural integrity of the steel in continuous contact with the high temperature environment within the receiver cavities. The operating temperatures of the molten salt within the tube panels will range from 277°C (530°F) to 566°C (1050°F). For ordinary structural steels such as the A36 used in this design at temperatures above 371°C (700°F), both yield and tensile strengths decrease with increasing temperatures (Ref 5-1). At 482°C (900°F), the modulus of elasticity for structural steel decreases to 172×10^6 kPa (25×10^6 psi) compared to a room temperature value of 200×10^6 kPa (29×10^6 psi). At 538°C (1000°F) the yield strength is approximately 70% of its room temperature value. The incorporation of "outdoor" construction into the design will provide better airflow patterns to cool the structure. The open structure will also be able to radiate its heat away to the earth and sky. The use of insulation and good airflow passages, however, will assure that temperatures of the structural steel sections will not rise more than 111°C (200°F) above ambient.

5.2.2.7 Weight - The results of the receiver weight study are summarized in Table 5.2-4. While the distribution of weights is somewhat different than prior quad-cavity molten salt receivers of comparable thermal capacity, the total weight on a per megawatt basis is comparable. Weight differences are due to (1) moving the insulation from the receiver outside wall to the cavity exterior, (2) smaller south cavity, (3) ablative material added to cavity doors, (4) redesign of the absorber tube lateral support structure, (5) addition of the cold surge tank, (6) replacement of floor structure with truss structure, (7) elimination of outside covering, and (8) addition of door counterbalances.

Table 5.2-4 Receiver Weight Summary

<u>Description</u>	<u>Weight</u>	
	<u>kg</u>	<u>lb</u>
Roof:		
Structure	42,928	94,640
Covering	<u>10,915</u>	<u>24,063</u>
	53,843	118,703
Walls:		
North Structure	42,284	93,220
South Structure	38,401	84,661
East Structure	42,739	94,224
West Structure	<u>42,739</u>	<u>94,224</u>
	166,163	366,329
Floor:		
Structure	25,437	56,080
Covering	<u>10,915</u>	<u>24,063</u>
	36,352	80,143
Support Structure:	27,612	60,874
Center Section:		
Structure	21,443	47,273
Insulation	<u>1,930</u>	<u>4,256</u>
	23,373	51,529
Radiation Shields:		
Structure and Facing		
Sides	7,643	16,849
Upper	24,854	54,794
Lower	21,192	46,720
Insulation		
Sides	3,099	6,832
Upper	3,549	7,825
Lower	<u>2,135</u>	<u>4,707</u>
	62,472	137,727
Doors:		
North		
Structure	10,380	22,885
Insulation	1,600	3,528
Ablative	6,001	13,230
Drive Mechanism	2,697	5,946
Counter Weight	21,656	47,743
Pulley Support Structure	7,163	15,791

Table 5.2-4 Receiver Weight Summary (cont)

<u>Description</u>	<u>Weight</u>	
	<u>kg</u>	<u>lb</u>
South		
Structure	4,189	9,236
Insulation	581	1,280
Ablative	2,178	4,801
Drive Mechanism	1,042	2,297
Counter Weight	5,684	12,532
Pulley Support Structure	4,259	9,390
East		
Structure	7,298	16,090
Insulation	1,111	2,450
Ablative	4,167	9,187
Drive Mechanism	1,886	4,159
Counter Weight	14,102	31,090
Pulley Support Structure	4,259	9,390
West		
Structure	7,298	16,090
Insulation	1,111	2,450
Ablative	4,167	9,187
Drive Mechanism	1,886	4,159
Counter Weight	14,102	31,090
Pulley Support Structure	4,259	9,390
	<u>133,080</u>	<u>293,391</u>
Piping:		
Absorber Tubes	26,944	59,401
Absorber Headers	3,434	7,571
Upper Interconnection Pipes w/Valves	5,147	11,347
Lower Interconnection Pipes w/Valves	4,211	9,284
Riser and Downcomer	3,186	7,024
Cold Surge Tank	20,342	44,847
Morning Glory Spillway	753	1,661
Lateral Support Pipes	11,284	24,877
	<u>75,301</u>	<u>166,012</u>
Piping Insulation:	30,210	66,602
Miscellaneous Insulation	3,039	6,700
Receiver Dry Weight:	<u>611,445</u>	<u>1,348,010</u>
Salt:		
Absorber Tubes and Headers	32,568	71,800
Upper Interconnection Piping	9,580	21,120
Lower Interconnection Piping	7,838	17,280
Riser and Downcomer	6,214	13,700
Cold Surge Tank	24,516	54,050
Morning Glory Spillway	3,674	8,100
Lateral Support Pipes	7,688	16,950
	<u>92,078</u>	<u>203,000</u>
Receiver Wet Weight:	<u>703,523</u>	<u>1,551,010</u>

5.2.3 Receiver Thermal Analyses

This section describes the receiver thermal analyses that were conducted and summarizes the resulting performance.

- 5.2.3.1 Aperture Sizing - Aperture size, shape, and cavity depth significantly influence the overall receiver size. The apertures must be large enough to allow the maximum amount of solar energy to enter the cavities (minimum spillage) while permitting a minimum amount of thermal losses. The aperture should be shaped so a good flux distribution can be achieved on the receiver absorbing surfaces. Depth and shape of the cavity also influence the absorber surface flux levels and distribution. Based on Phase I Advanced Water Steam Receiver (AWSR) work done by Martin Marietta, (Ref 2-4) square vertical apertures were selected for the repowering system receiver design. Tilted apertures show some reduced spillage advantage over vertical apertures but not a significant enough advantage to warrant the expected increased complexity and cost of receiver design. Square apertures were found to allow a heliostat aiming capability sufficient to provide reasonable flux distributions on the receiver absorbing walls. Heliostats are aimed (see Section 5.2.3.2) up and down at the aperture plane along its vertical centerline to distribute the solar flux within the cavity. Therefore the height of the aperture primarily depends on the desired peak flux. The width of the solar image from the heliostats in the corner of each cavity's collector field establishes the aperture width. Square apertures allow satisfactory peak flux limitations on the cavity absorbing surfaces for our collector field. If all heliostats were aimed at the center of each aperture and no limit were placed on peak flux values, a rectangular aperture with its long side horizontal would be optimum.

The apertures for the hybrid receiver were initially sized by an iterative approach using the Martin Marietta Thermal Radiation Analysis System (TRASYS) computer program. The spillage results as a percentage of the energy delivered to the aperture plane, were plotted against aperture size and summed with the corresponding cavity percentage thermal loss to indicate the optimum aperture sizes. The minimum point of the sum of the cavity losses and spillage losses determines the optimum aperture size. Figure 5.2-11 illustrates the sizing of the north aperture. As can be seen from the figure, the aperture size optimum is relatively flat near the selected cavity size. The east/west and south apertures were sized in the same manner. Thermal losses were calculated using correlations derived from detailed nodal computer models of solar cavities developed during the Martin Marietta Advanced Water/Steam Receiver Phase I project. These models were also used on the Martin Marietta Solar Central Receiver Hybrid Power System Phase I (Ref 2-3) study to determine the thermal losses from that receiver. For the north cavity, the optimum aperture size is 12x12 m (39.37x39.37 ft). The optimum aperture size for the east and west cavities is 10x10 m (32.81x32.81 ft), and that for the south cavity is 7x7 m (22.97x22.97 ft).

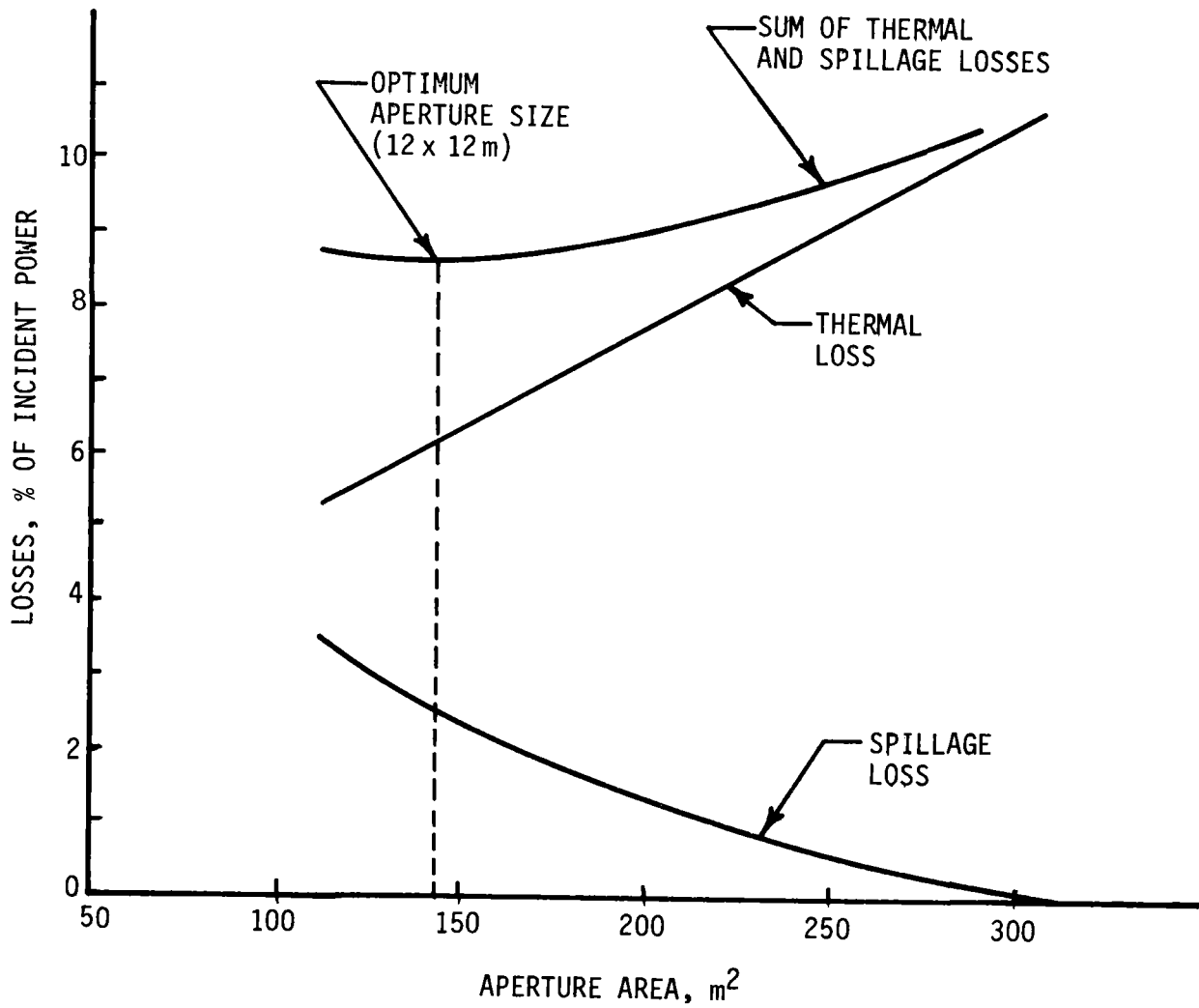


Figure 5.2-11 North Aperture Size Optimization

5.2.3.2 Flux Determination - Martin Marietta's TRASYS program was used to develop aiming strategies and flux distributions on the receiver surfaces. TRASYS is a computer program developed by Martin Marietta with the generalized capability to solve the radiation related aspects of thermal analysis problems. It has provided valuable, accurate data to support thermal analyses of a variety of space systems. The program has been expanded over several years to handle radiation problems associated with heliostat fields and solar central receivers by the addition of a "Mirror Field" library of subroutines. TRASYS-generated heliostat flux data have been compared with actual heliostat test data several times, most recently in the Martin Marietta Alternate Central Receiver Power System Phase II project (Ref 2-7). These comparisons indicated that TRASYS is fully capable of reproducing experimental measurements within a reasonable level of accuracy. Its particular advantage lies in its ability to determine radiant thermal interactions within a cavity receiver.

To calculate this information, TRASYS requires a geometric cavity surface description, along with the size and location of all the heliostats, the desired date, time, and solar beam strength. Each mirror on the heliostat is aimed directly at the aperture center unless otherwise specified, and the combined flux from all the heliostats is then totaled for each surface node.

The optimized collector field configuration described in Section 5.1 was used in the TRASYS model for repowering. The field was divided into north, south, east, and west quadrants, and separate TRASYS models were constructed for each quadrant. Figures 5.2-12 through 5.2-14 are computer generated plots of the north, east, and south cavities of the receiver, showing the nodal breakdown of the cavities. (Because of symmetry, it was not necessary to model the west cavity.)

Information calculated by TRASYS for each heliostat includes: the solar flux incident on that mirror, the flux reflected to the receiver (after allowing for atmospheric attenuation), the cosine of the half bounce angle, and the aperture and overall efficiencies. Results given for the entire field include the total power entering the aperture, the incident and absorbed fluxes on each receiver node, the field cosine of angle of incidence, aperture efficiency, and atmospheric attenuation.

An additional capability of the TRASYS program is the ability to simulate the effects of heliostat aiming. When the rows of heliostats are all aimed at the center of the aperture, their images strike the back wall of the receiver in a relatively tight group, resulting in a flux distribution with a sharp peak (Figure 5.2-15). Implementation of an aiming strategy to vertically spread the images from the various rows apart from each other can lower the maximum flux level as much as 32%, as shown in the figure.

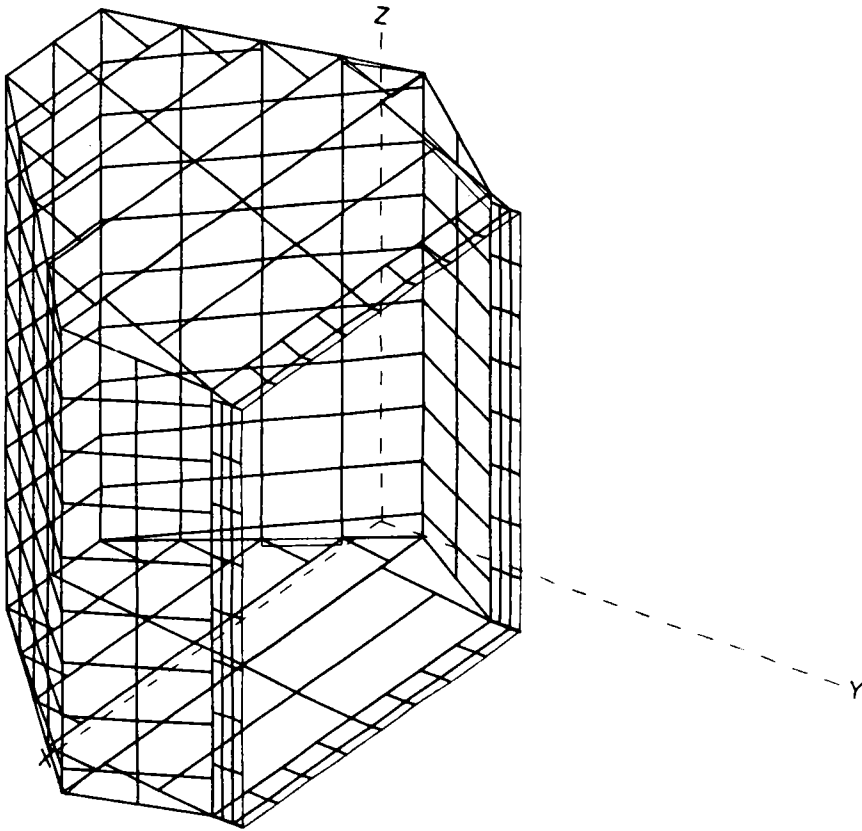


Figure 5.2-12 Receiver North Aperture

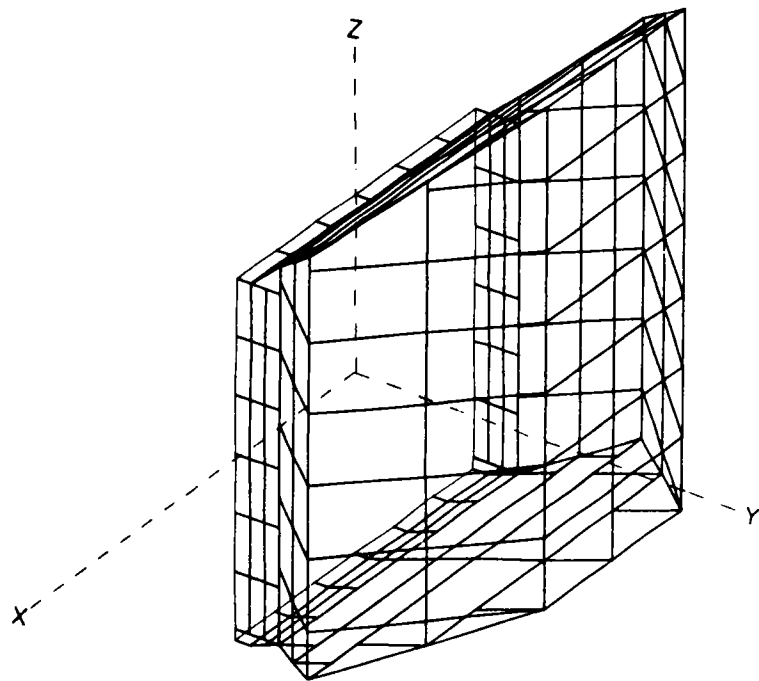


Figure 5.2-13 Receiver South Aperture

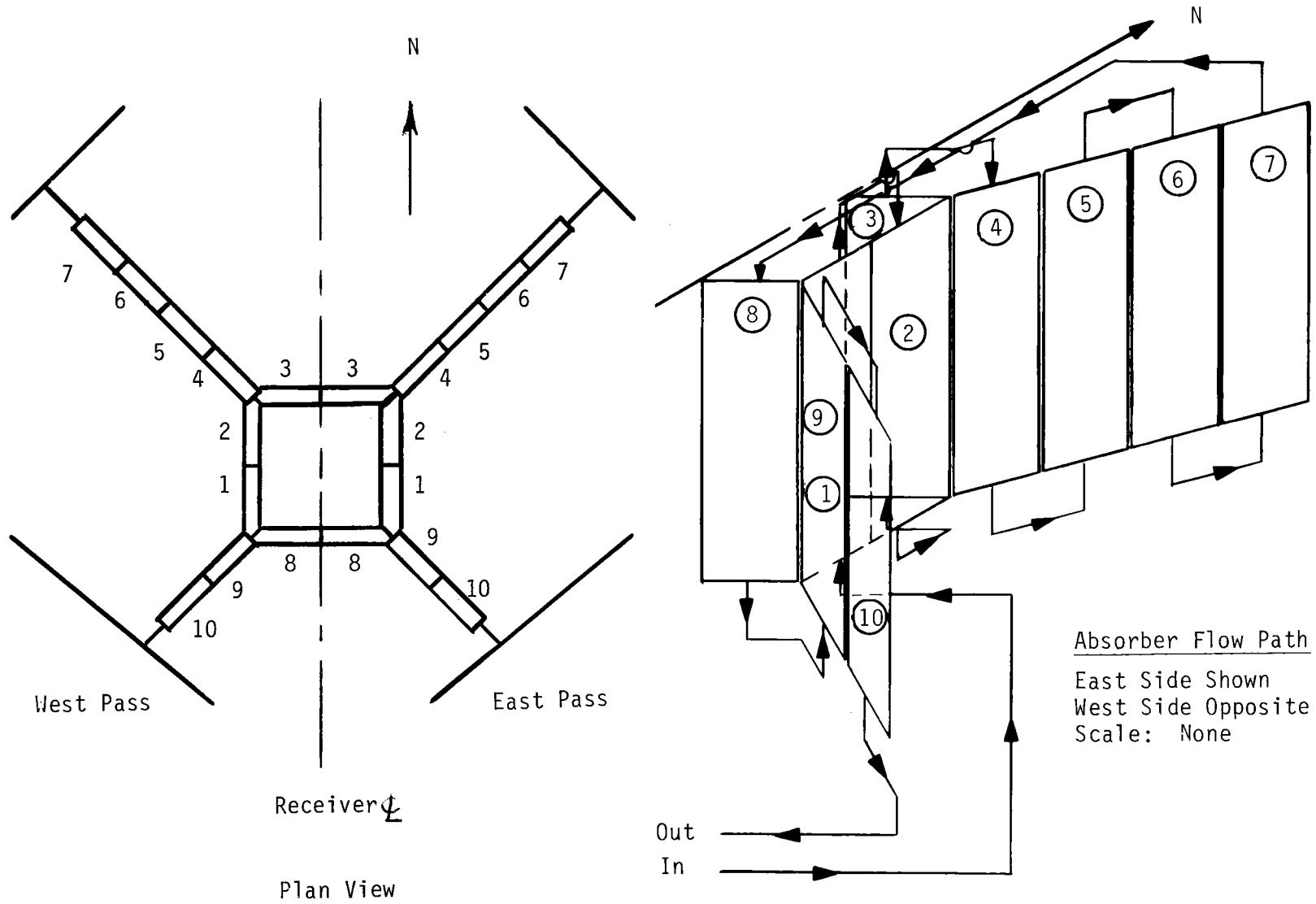


Figure 5.2-6 Absorber Panel Arrangement

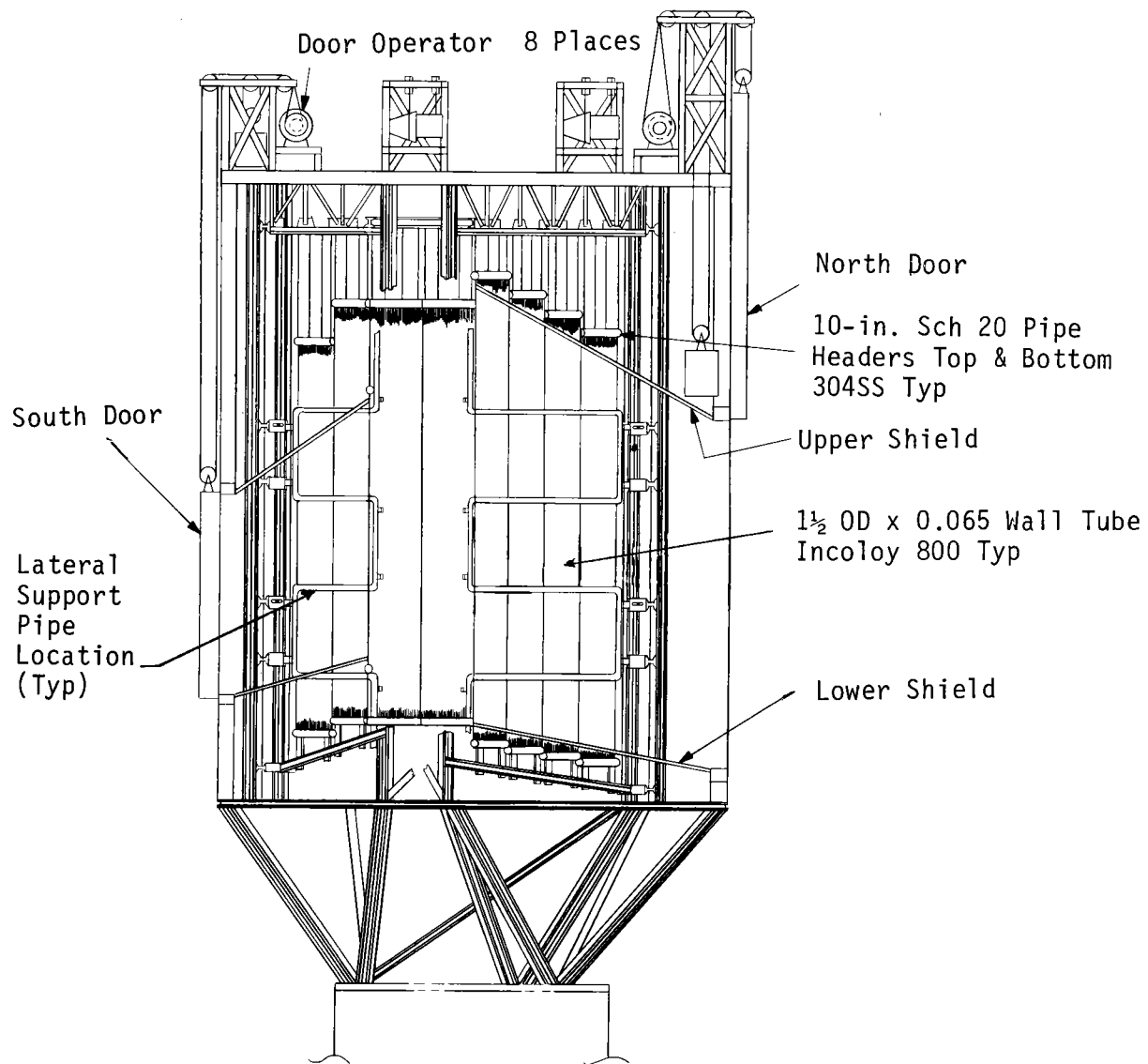


Figure 5.2-7 Receiver Absorber Panel Supports

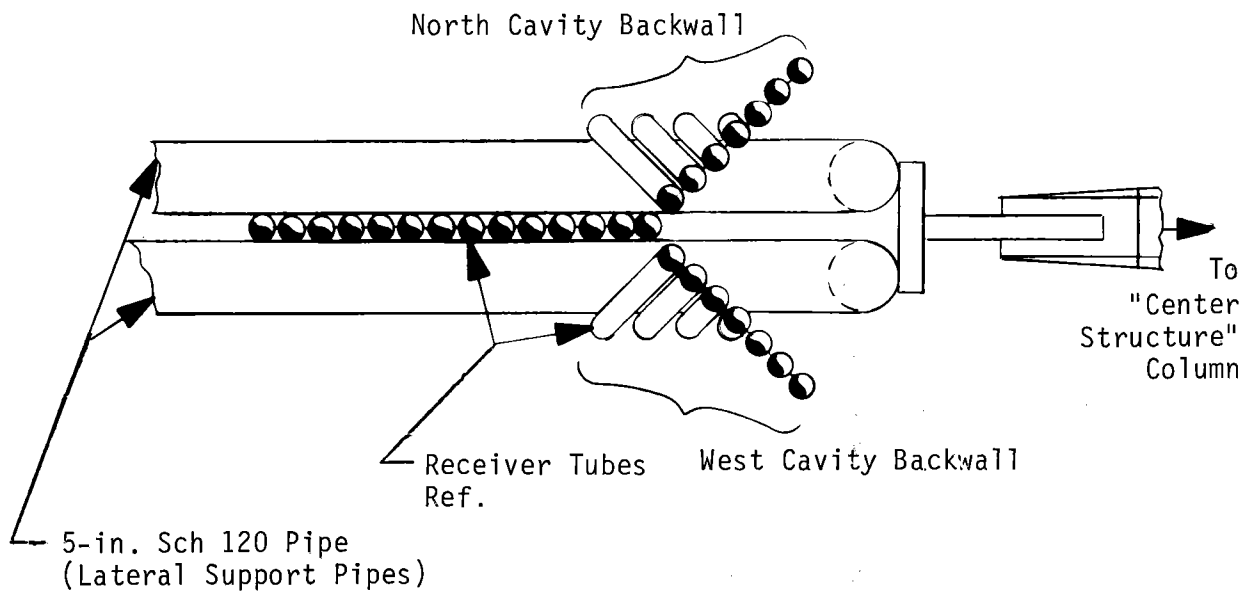


Figure 5.2-8 Interfaces Between Absorber Tubes and Lateral Support Pipes

The radial panels with two-sided heating are supported at 3.05 m (10 ft) intervals by two 0.13 m (5 in.) Schedule 120S lateral support pipes as shown in Figure 5.2-7 to prevent excess deflection due to wind loads. These stainless steel pipes go from the top of the receiver to the bottom in a zig-zag pattern with one pipe on each side of the panel to provide four pairs of panel support beams. The coolest heat transfer salt coming into the receiver is run through these pipes (see paragraph 5.2.3). Shown in Figure 5.2-8 is a detail of how the absorber tubes are bent where the lateral support pipes pass through the corners of the cavity back walls. The lateral support pipe horizontal sections are supported to permit both vertical and horizontal thermal expansion. The lateral support pipes can be removed by cutting the horizontal part of the pipe loose and then sliding it out through openings in the receiver structure. Both the back panel and radial support structures permit vertical and lateral (in the plane of the panel) movement to accommodate thermal expansion.

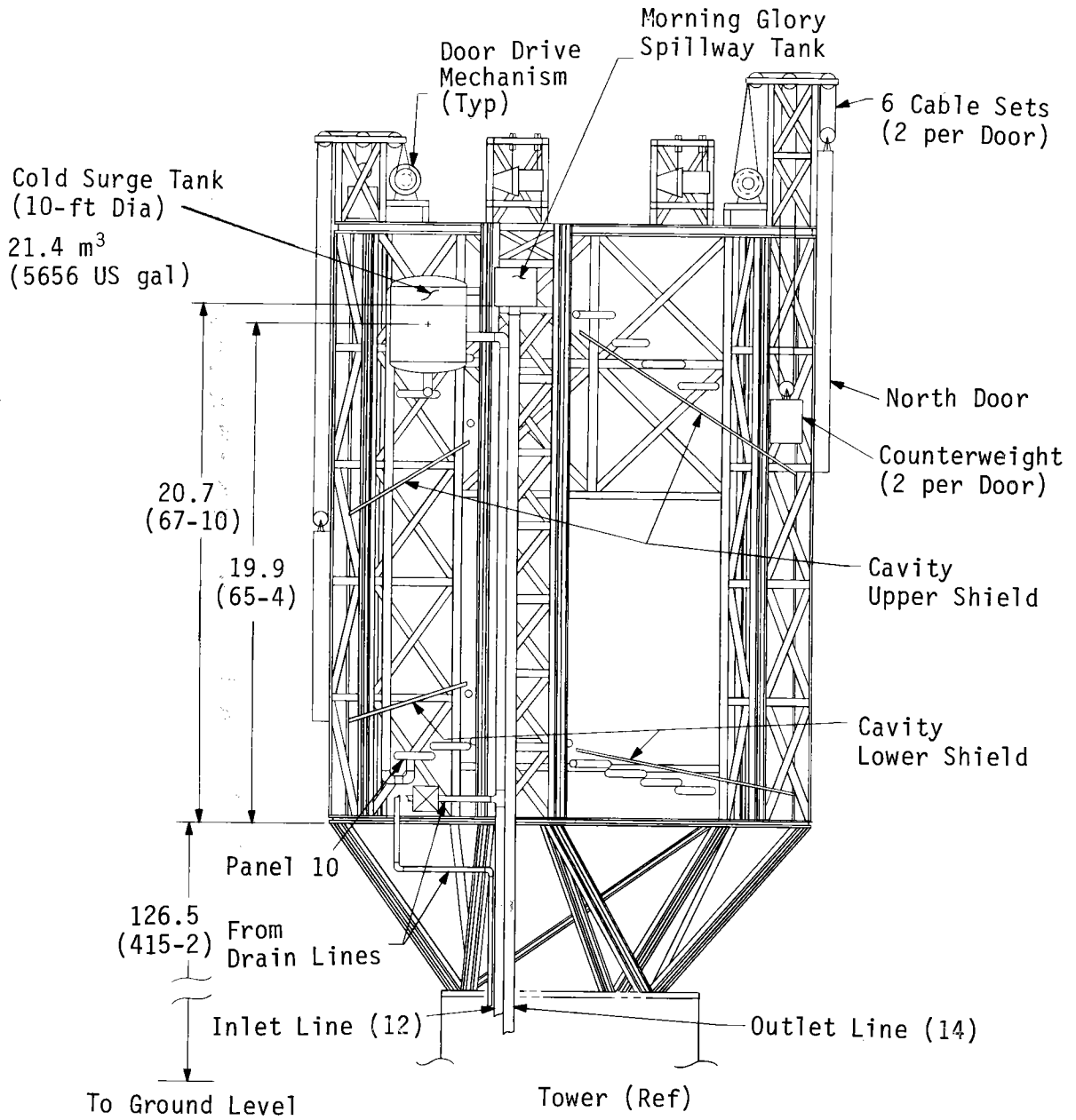
5.2.2.4 Piping - The receiver piping consists primarily of the riser and downcomer attachments, the upper and lower crossover supply, return, vent, and drain piping (Fig. 5.2-2), the surge tank, morning glory spillway, and the four lateral support pipes. Further piping details are included in Appendix A. The inlet pipes are made of A106 Gr B carbon steel and all other interconnecting piping, the lateral support pipes, and the downcomer are made of Type 304 stainless steel.

The drain lines are gathered and connected to the downcomer. Each (10) drain line has a normally closed, electrically powered, remotely controlled drain valve. The vent lines for the east and west passes are separately gathered and connected to the upper part of the morning glory spillway. Each (10) vent line has a normally closed, electrically powered, remotely controlled vent valve as well as a vacuum relief valve to help avoid absorber tube collapse should a vent valve fail to operate. The eight lateral support pipes are connected into an east and a west set. Each of the sets is fitted with an electrically powered, remotely controlled vent valve and a vacuum relief valve. The lateral support pipes can drain directly through the flow control valves to the riser and do not need separate drain valves.

The cold surge tank and morning glory spillway are shown in Figure 5.2-9 along with the inlet and outlet connections and the connections to the lateral support pipes. The morning glory spillway is mounted at the receiver top so that the free liquid level will be above the top of the highest headers. This will provide for positive filling of all of the absorber tubes and interconnecting piping. The inlet surge tank will be controlled to maintain its level at the half full point. The receiver inlet, or cold, surge tank is pressurized to 1.72 MPa (250 psig). The cold surge tank pressure was selected to provide the proper pressure drop through the receiver including the flow-control valves and a margin. The morning glory spillway tank is vented to the atmosphere.

The hot surge tank was deleted and replaced by the much smaller morning glory spillway tank. The cold surge tank was moved from the central area to over the south cavity. These two changes have opened up the center structure of the receiver. The only equipment in the center section is the riser, downcomer, and the morning glory spillway tank and its piping connections. It was desired to open up the center sections because of the difficulty in assembling receiver piping at Solar One.

The morning glory spillway, used to maintain the proper static head on the receiver outlet, is patterned after a spillway design used for medium head earth fill dams. The shape of the spillway (similar to the shape of a morning glory flower) is selected so that the salt will stick to the wall and flow smoothly into the outlet pipe and continue to flow along the downcomer wall. The center of the downcomer is not filled at any flow. The large circumference of the spillway crest means that a wide range of flows can be accommodated



East Elevation View

Note:
Dimensions
are in meters
(feet - inches).

Figure 5.2-9 Receiver Surge Tank Location

for only a slight change (less than 0.15 m or 6 in.) in salt height. The kinetic energy of the falling salt is absorbed in the salt when it falls into a 2.4 m (8 ft.) deep pool of salt. This plunge pool is adapted from small dam design approaches. The depth of salt is selected so that no scouring or erosion of the plunge pool tank will occur. The churning action of the salt in the plunge pool converts the salt's kinetic energy to thermal energy.

An air compressor system is provided to supply air to the cold surge tank. The air compressor will be located in a separate room in the top of the tower so it is not exposed to the higher temperatures in the receiver area and so that it can be readily serviced. The air storage tank will be located on the receiver floor under the south cavity. This location can be seen in Figure 5.2-7 just above the floor girders and just to the left of the center structure although the air storage tank is not shown.

The air supply system was sized to permit filling the cold surge tank from ambient pressure to its design value in 30 minutes using the compressor and stored air together. This resulted in the system characteristics shown in Table 5.2-1. The time to fill the air storage tank from ambient is under 1 hr. When the cold surge tank is being used to force salt through the receiver during an emergency, its air pressure will reduce as the air volume increases. During this process, the air storage tank will continue to supply air to the surge tank. The result is an average cold surge tank pressure above 1.41 MPa (205 psig) during the blowdown.

Table 5.2-1 Receiver Air Supply System Characteristics

Compressor	
Rating	0.047 Std m ³ /s (100 SCF/min)
Pressure	4.14 MPa (600 psig)
Motor Power	38 kW _e (50 hp)
Three Stages with Intercooling	
Weight	1600 kg (3500 lb)
Air Storage Tank	
Pressure	4.14 MPa (600 psig)
Volume	2.5 m ³ (88 ft ³)
Diameter	1.22 m (4 ft)
Shell Thickness	29 mm (1.125 in.)
Weight	2,700 kg (6,000 lb)

The absorber panel lateral support concept is shown in Figure 5.2-7. Two continuous 0.127-m (5-in.) diameter, schedule 120S stainless steel pipes were used to construct each of the four radial panel supports to meet the operating wind load requirements. Two pipes cross horizontally on each side of the absorber panels approximately every 3.05 m (10 ft) to provide lateral support for the absorber panels. The lateral support pipes are not attached directly to the absorber tubes so they are free to expand thermally with respect to each other. The support pipes are attached to the receiver structure on each side of the set of absorber panels in a manner that allows for thermal expansion of the support pipes, but transfers the absorber panel wind loads to the receiver structure. The form of attachment used at the outboard end of the receiver panel is shown in Figure 5.2-10. The inboard end supports are similar except that the receiver structure is a vertical W14x61 column.

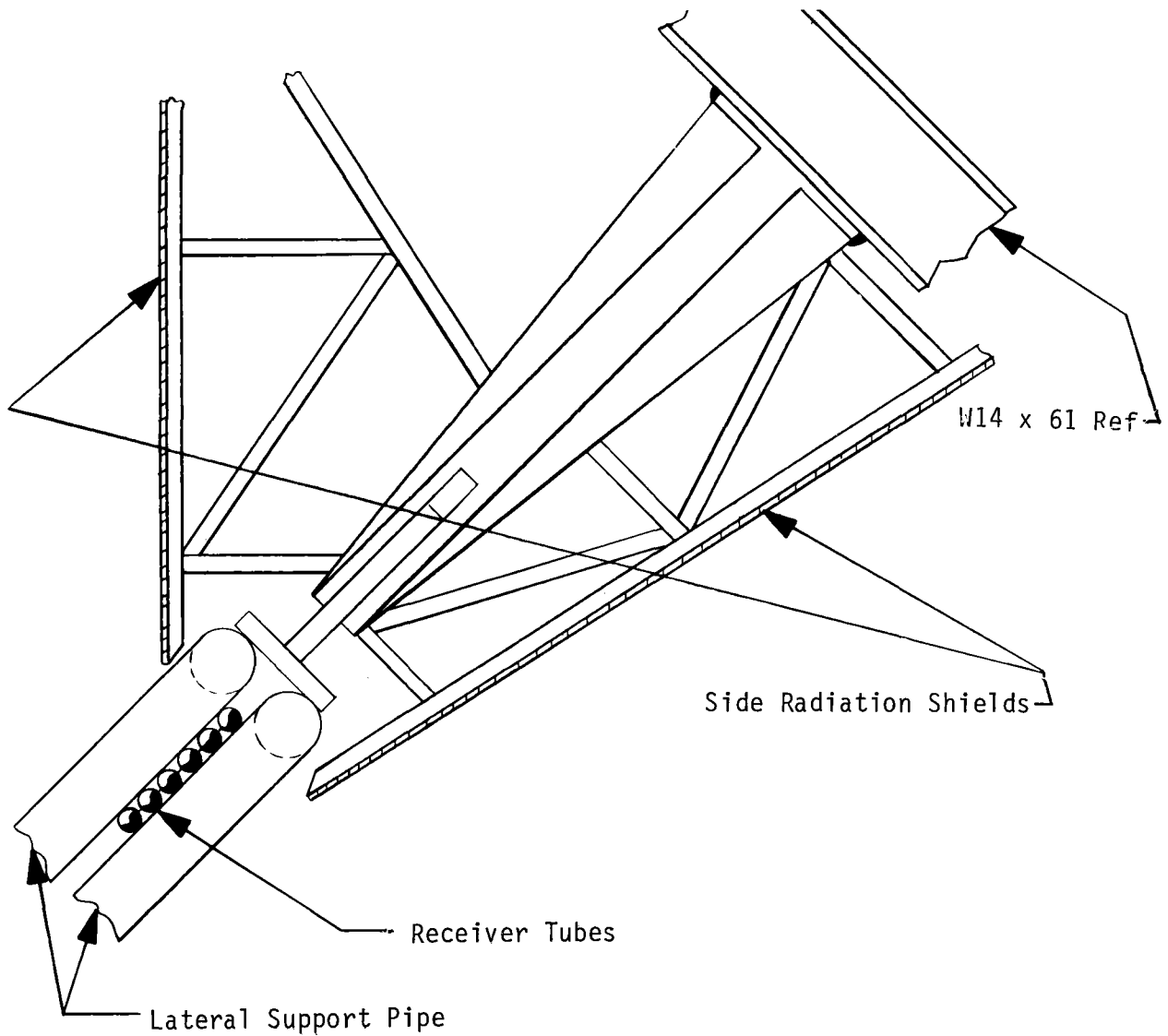


Figure 5.2-10 Outboard Lateral Support Attachment

For this support concept, cool salt flows through the support pipes to cool the pipe and to reduce the effect of the flux incident on its surface. A preliminary analysis of support pipe temperatures for the pipe supporting the north wall in the cavity is described in Paragraph 5.2.3.3. By painting the lateral support pipes white, the temperature increase in the salt was limited to less than 2.8°C (5 F) and the pipe external temperatures were less than 427°C (801°F). Four such pipe supports, e.g. one on each side of the northeast absorber and one on each side of the southeast absorber, are required in each symmetrical receiver half. Four pipes of this size are equivalent to a receiver panel in flow cross-sectional area. Because of the shorter length of the support pipes associated with the south cavity, restrictors will be provided to match flow rates, and thus salt velocities, in all eight support pipes. The connections to the lateral support pipes are shown in Figure 5.2-9.

An evaluation of pressure drops in the receiver at the design point was made with the results shown in Table 5.2-2. Most of the pressure drop can be seen to occur in the absorber tubes and the control valve. The control valve head was taken as a percentage of the dynamic head, and the margin was taken as a percentage of the first five items in Table 5.2-2.

Table 5.2-2 Receiver Pressure Drop Summary

Item	Equivalent Head of Salt, m (ft)
Absorber Tubes	49.4 (161.8)
Lateral Support Pipe	4.8 (15.7)
Tube Entrance/Exit	7.6 (24.8)
Connecting Pipe	3.7 (12.3)
Static Head (Morning Glory Spillway Crest over Cold Surge Tank)	1.7 (5.7)
Control Valve	22.6 (74.3)
Margin	6.7 (22.0)
Pressure in Morning Glory Spillway Tank	0 (0)
Total	96.5 (316.6)

5.2.2.5 Receiver Thermal Protection Considerations - Thermal protection methods were examined to (1) insulate the structure of the receiver from high temperatures, (2) minimize the cooldown of the receiver during overnight nonoperation, and (3) protect absorber tubes when a booster pump or power failure occurs with solar flux directed into the receiver. The first two items require the use of radiation shields within the receiver cavity to both redirect radiation within the receiver and also protect nonabsorber materials (structure, headers, instrumentation). The radiation shields are described in Section 5.2.2.2. Insulated doors on the receiver apertures are used to minimize cooldown during nonoperation. Protection of the absorber tubes during an unexpected salt flow stoppage required consideration of the potential causes of such a failure and methods to shield the absorber tubes from high energy flux.

Calculations were first performed to determine the absorber tube metal temperature rise rate with a salt flow stoppage and energy from the collector field into the receiver. Such an occurrence might happen due to one of the following:

- 1) Failure of the booster pumps;
- 2) Failure of the main circulation pumps;
- 3) Drag valve closure;
- 4) Salt piping blockage;
- 5) Receiver salt control valve failure in a closed position;
- 6) Electrical power failure;
- 7) Complete loss of high air pressure on the cold surge tank.

If such a salt flow stoppage should occur and power is available to the collector field, heliostats will be quickly defocused to reduce energy flux into the receiver. However a finite time period is involved in detecting the failure, deciding what action to take, and then acting. Therefore, in our evaluation the first step was to determine the time required to heat the absorber tubes to an upper temperature limit with complete salt flow stoppage. This temperature was determined to be approximately 927°C (1700°F) for Incoloy 800.

Results of these analyses, as given in Ref 1-2, clearly indicate that even a short-duration flow stoppage cannot be tolerated in a salt receiver with high solar flux levels on the receiver. Such an occurrence would lead to either absorber tube failure, tube warpage, or reduction of tube life. Therefore, in the receiver design, we have incorporated additional features that will ensure salt flow through the receiver (cold surge tank) and protection of absorber tube surfaces once salt flow through the receiver is exhausted (ablative covered door). A backup diesel generator will also be available that can provide 200 kW_e within 25 sec from start.

The primary approach for ensuring the availability of electric power is the provision of automatic power switching between the east and west 115-kV buses of the Saguaro switchyard. Upon loss of power on either bus, the solar system load would be immediately switched (within 8 cycles) to the other bus, and the diesel generator would be started. The solar system load is only switched to the diesel when both the east and west buses are lost. The worst case occurs when both the east and west 115-kV buses are lost at the same time, and then the diesel must be started. The diesel will be used to maintain power for the most important functions only. It does not have enough capacity to drive the salt booster pumps. However, it can be used to operate control valves, receiver doors, salt transfer pumps, or the collector field (only portions at any one time).

It is expected that any loss of cold salt surge tank pressure would be gradual. At the first sign of pressure loss, the heliostats would be quickly defocused. If salt flow dropped below a set limit before the cavity solar flux had dropped sufficiently, then the quick cavity door closing function would be exercised.

In case a booster pump stops due to a power failure, enough salt will be contained in the receiver cold salt surge tank to provide design flow through the receiver for at least 60 sec. During this time, the heliostats without power will be providing energy into the receiver. Even if power is available to the field, 1.1 MW_e is required to slew all 5,000 heliostats at the same time. Based on slew rates of 0.33r and 0.42r/min for the azimuthal and elevation directions, respectively, and heliostat control logic, 60 sec are required to get all heliostats off the receiver. Without power to the collector field, peak flux levels at the aperture higher than 315 kW_t/m² (100,000 Btu/hr-ft²) can last up to 4 min, and more than 6 min are required before all energy is off the receiver due to the apparent sun motion.

After a booster pump or power failure, the receiver door will be closed, with gravity assist, to shield incoming flux from the absorber tubes. The door mechanism discussed in paragraph 5.2.2.2 requires 7 sec to complete the cavity door closure. Once the door closes, the face of the door intercepts the incoming flux. Without thermal protection, the solar flux may damage the door by either creating thermal stresses that will warp it or burning a hole through the thin metal sheets. Therefore, various thermal protective systems were evaluated to protect the door.

Our evaluation of thermal protection methods considered the use of typical schemes for high-temperature applications. These methods included ablative, radiative, transpiration cooling, and heat-sink concepts. The concept selected for receiver door application was the use of an ablative material. The ablative provides the lowest cost and lowest weight of the options considered. The properties of the selected ablative material are given in Table 5.2-3.

Table 5.2-3 Material Properties of Martin Marietta ESA-3560 Ablator

Density	480 ₊₃₂ Kg/m ³ (30 ₊₂ lb/ft ³)
Thermal Conductivity	0.098 W/m-°C (0.68 Btu-in/hr-ft ² -°F)
Specific Heat at 24°C	1.55 J/Kg°C (0.37 Btu/lb-°F)
Emissivity	0.80
Ablation Temperature	443°C (830°F)
Effective Heat of Ablation	13491 kJ/kg (5800 Btu/lb) for 50 sec at 681 kW _t /m ² (60 Btu/ft ² -sec)
Storage Life	Indefinite below 66°C (150°F)

This ablative material has been used on flight test vehicles and the Viking spacecraft. A 0.076 m (3 in.) thickness of this ablative material was estimated to be sufficient to accept the peak solar flux and carry heat away from the receiver door as the material ablates. The material will be installed in small easily handled panels on the receiver door to minimize the expense of replacement. For design details, see Appendix A.

It now appears that such power failures leading to salt pump outages or collector field inoperation would occur infrequently, thus minimizing the need for replacement of ablative surfaces. However, the use of low cost thermal protection schemes alleviates the concern for absorber tube replacements due to excessive temperatures during potential failure modes.

5.2.2.6 Stress and Dynamic Analysis - The structural framework of the receiver module is designed to provide unobstructed entry for solar flux and protection for the absorber tube panels. The structure is symmetrical about the north-south axis and provides apertures of the following sizes:

- 1) North cavity - 12x12m (39 ft 4 in. by 39 ft 4 in.);
- 2) East-west cavities - 10x10m (32 ft 10 in. by 32 ft 10 in.);
- 3) South cavity - 7x7m (23 ft 0 in. by 23 ft 0 in.)

The most important receiver elements, the absorbing surfaces, are suspended from roof trusses in staggered "curtain" panels. Each panel consists of 46 tubes with 0.038-m (1-1/2-in.) OD of Incoloy 800 welded together with spacers between the tubes. Panel sizes are approximately 2.04 m (6.7 ft) wide and range from 10.8 m (35 ft 4 in.) to 17.9 m (58 ft 8 in.) long. The main structural framing offers no lateral or vertical restraint inhibiting thermal expansion and contraction of the tube panels; restraint systems of special design are discussed in Section 5.2.2.3.

The steel roof sections were designed to accommodate heavy-duty hoists for all cavity doors. Provisions were also made for a 9.1×10^3 kg (10-ton) lift crane on the central tower of the receiver. The lift crane can be used for hauling prefabricated panel sections into place. The construction crane will be removed when construction is complete. However, provisions have been made for rigging and supporting temporary hoists that can be used for component removal and replacement.

All structural elements of the receiver are standard A36 steel sections selected in accordance with AISC specifications (Ref 5-1). The siding is corrugated 14-gage steel siding and the roof is expanded metal. Standard long-span steel joists (18 LJ 02) are used on the roof. Open-web steel joists (J series) are used to carry the expanded metal floor deck.

Because of the heavy loads carried by the superstructure columns, the receiver loads were carried into the tower by a set of triangular trusses made up of standard I-beams. Diagonal I-beams were used to transfer torsional loads to the tower.

Loadings and design criteria have been cited in a number of reports and communications (Ref 2-1,5-2,5-3), in Section 5.2.1, and in the System Requirements Specification of the prior study (Ref 1-3). A brief summary of the design factors considered is useful.

- 1) Snow and ice - These conditions were assumed to include a layer of ice with a thickness of 25 mm (1 in.) and a snow cover with a weight of 240 Pa (5 lb/ft²).
- 2) Wind - For analysis a maximum wind condition that assumed winds up to 40 m/s (90 mph) with a gust factor of 1.05 at a reference height of 10 m (30 ft) was used. This value is used in the System Requirements Specification. However Reference 5-4 identifies a maximum wind speed at the 10-m (30-ft) level as being 33.5 m/s (75 mph) on a 100-yr recurrence level. The higher number was used as being conservative. The following model, as defined in the System Requirements Specification (Ref 1-3) was used for the extrapolation of wind speed to higher elevations.

$$V_H = V_1 (H/H_1)^c$$

where V_H = wind velocity at height H

V_1 = reference wind velocity

H_1 = reference height (10 m (30 ft))

c = 0.15

This formula results in a dynamic pressure of 2.50 kPa (52.3 psf) at the receiver centerline for a reference height velocity of 40 m/s (90 mph).

The location of Saguaro falls under Exposure C of ANSI A58.1-1972, which is defined as flat open country or flat coastal plains. When Exposure C data are taken from ANSI A58.1-1972, the resulting dynamic pressure at the receiver centerline is 2.50 kPa (52.3 psf) for a velocity of 40 m/s (90 mph). These two approaches give the same wind loading. However, the loads would be much lower if the 100-yr recurrence level of wind velocity had been used. A further discussion of wind loads is given as part of the analysis of lateral loads.

- 3) Earthquake conditions - Saguaro lies in Universal Building Code (UBC) Zone 2 that has low earthquake requirements (Ref 5-5). As the UBC requirements do not specify accelerations, another source is necessary. It is felt that the Nuclear Regulatory Commission requirements that were referenced in the prior study contract form of the System Requirements Specification were too stringent. Reference 5-6 gives an average survival value of $\ddot{X}_g = 0.07$ g for UBC seismic zone 2. During the design of the APS's Cholla station, a ground acceleration of 0.10 g was used. For the Saguaro design, \ddot{X}_g was taken as 0.10 g along with the methodology of Reference 5-6.

Lateral acceleration

$$(1) \quad \ddot{X}_{TT} = 1.05 \ddot{X}_g + \frac{1}{25} \left[H_t \sqrt{\frac{\ddot{X}_g}{W_R}} - 4.4 \right] \quad \text{and} \quad \ddot{X}_{TT} > \ddot{X}_g$$

where

\ddot{X}_{TT} = tower top acceleration,

\ddot{X}_g = ground acceleration,

H_t = height of tower, ft,

W_R = weight of tower, kips.

Vertical acceleration

$$(2) \quad \ddot{X}_{TT} = 3\ddot{X}_g$$

Peak accelerations for the top of the tower were obtained using these equations for both survival and operating conditions.

Survival

$$\ddot{X}_g = 0.10 \text{ g}$$

$$\text{Lateral acceleration } \ddot{X}_{TT} = 0.10 \text{ g,}$$

$$\text{Vertical acceleration } \ddot{X}_{TT} = 0.30 \text{ g.}$$

Operating

$$\ddot{X}_g = 0.07 \text{ g}$$

$$\text{Lateral acceleration } \ddot{X}_{TT} = 0.07 \text{ g,}$$

$$\text{Vertical acceleration } \ddot{X}_{TT} = 0.21 \text{ g.}$$

Structural design was based on maximum or survival conditions.

- 4) Live loads - In addition to the loading conditions outlined above, a live load of 4.8 kPa (100 psf) was used for sizing structural members for the receiver deck. This live load was used to represent special equipment loads or opening requirements for piping and auxiliary conduits that were not finalized during this conceptual design.
- 5) Combined loads - The following design criteria for combined loads were employed as a result of telephone conference communications with Sandia National Laboratories, Livermore (Ref 5-7).

Wind effects

$$(3) \quad 1.4 D + 1.7 W$$

Seismic effects

$$(4) \quad 1.0 D + 1.0 E, \text{ or}$$

$$(5) \quad 1.0 D - 1.0 E,$$

whichever is greater

where:

D refers to dead load,

W to wind load,

E to earthquake load.

These criteria are based on design procedures from ACI 318 (Ref 5-8). The wind and seismic loads of Equations (3) through (5) were not combined. Loading conditions obtained by using (3) were found to produce the most adverse set of loads on the receiver module.

A special analysis was performed for lateral loads (wind and seismic) acting against the receiver module to determine the most critical situation. This analysis was adapted from a similar analysis performed during the Martin Marietta Solar Central Receiver Hybrid Power System study. The four selected conditions were:

- 1) High wind at 40 m/s (90 mph) at 10 m (30 ft) reference height approaching the receiver from a direction 0.70 rad (40°) east of north, acting on the outside walls with all cavity doors closed;
- 2) Earthquake lateral forces acting against outside walls of receiver under same conditions as above;
- 3) High wind at 15.6 m/s (35 mph) again at a reference point of 10 m (30 ft), acting against the absorber tube panels with cavity doors open. Wind at an incident angle of 45° to north-south axis. This wind speed is used as it represents the speed at which heliostat stow must be initiated and the cavity doors closed.
- 4) Earthquake lateral forces acting on receiver absorber tube panels with conditions same as 3).

Condition 1) was found to superimpose the maximum loading condition and was used in conjunction with (3) previously mentioned.

Separate analyses were conducted on the strength of the receiver lateral support pipes and on the honeycomb-strengthened ablative material. In both cases, the structures were found to be conservatively designed.

Thermal stress and creep fatigue analyses were performed during the prior study (Ref 1-2) on the receiver absorber tubes and on the lateral support pipes. The design guidelines for creep-fatigue damage were based on the ASME Boiler Code, Code Case 1592. The results showed that the total projected damage due to creep and fatigue was 0.111 where the limit value is 1.0. The current design predicts more thermal cycles and thus more fatigue damage. It also predicts lower metal temperatures and thus less creep damage. When the large margin from the prior study is considered (0.111 vs 1.0) it is felt that an adequate creep-fatigue margin exists for the current design.

A combination of special factors served to offer a number of design constraints to obtaining the most effective and economical design for the receiver:

- 1) The geometry of the receiver offered symmetry only about the north-south axis. The north aperture was the largest opening; the east and west doors were 69% and the south door 34% as large as the north door. Additionally the depths of the cavities are different and the east and west apertures are not centered on the back wall. All of which means that the center support structure is not in the geometric center (north/south direction) of the receiver. Nor is the receiver center of gravity in the center of the receiver center structure. This loading is alleviated by the location of the heavy (when wet) cold surge tank over the south cavity. The morning glory spillway is not very heavy. The result is that the center structure loads introduce large moments into the receiver-to-tower supporting structure. A more careful consideration of this off-center loading could result in a decrease in weight of the receiver to tower supporting structure.
- 2) Limitations on deck space were imposed by the extensive number of pipes and tubes leading to and from the absorber panels.
- 3) Many factors remain unknown such as exact location of man-ways, personnel platforms, and elevator shaft openings. However, costs were estimated for such features.

During the design analysis, there were some concerns regarding the structural integrity of the steel in continuous contact with the high temperature environment within the receiver cavities. The operating temperatures of the molten salt within the tube panels will range from 277°C (530°F) to 566°C (1050°F). For ordinary structural steels such as the A36 used in this design at temperatures above 371°C (700°F), both yield and tensile strengths decrease with increasing temperatures (Ref 5-1). At 482°C (900°F), the modulus of elasticity for structural steel decreases to 172×10^6 kPa (25×10^6 psi) compared to a room temperature value of 200×10^6 kPa (29×10^6 psi). At 538°C (1000°F) the yield strength is approximately 70% of its room temperature value. The incorporation of "outdoor" construction into the design will provide better airflow patterns to cool the structure. The open structure will also be able to radiate its heat away to the earth and sky. The use of insulation and good airflow passages, however, will assure that temperatures of the structural steel sections will not rise more than 111°C (200°F) above ambient.

5.2.2.7 Weight - The results of the receiver weight study are summarized in Table 5.2-4. While the distribution of weights is somewhat different than prior quad-cavity molten salt receivers of comparable thermal capacity, the total weight on a per megawatt basis is comparable. Weight differences are due to (1) moving the insulation from the receiver outside wall to the cavity exterior, (2) smaller south cavity, (3) ablative material added to cavity doors, (4) redesign of the absorber tube lateral support structure, (5) addition of the cold surge tank, (6) replacement of floor structure with truss structure, (7) elimination of outside covering, and (8) addition of door counterbalances.

Table 5.2-4 Receiver Weight Summary

<u>Description</u>	<u>Weight</u>	
	<u>kg</u>	<u>lb</u>
Roof:		
Structure	42,928	94,640
Covering	<u>10,915</u>	<u>24,063</u>
	53,843	118,703
Walls:		
North Structure	42,284	93,220
South Structure	38,401	84,661
East Structure	42,739	94,224
West Structure	<u>42,739</u>	<u>94,224</u>
	166,163	366,329
Floor:		
Structure	25,437	56,080
Covering	<u>10,915</u>	<u>24,063</u>
	36,352	80,143
Support Structure:	27,612	60,874
Center Section:		
Structure	21,443	47,273
Insulation	<u>1,930</u>	<u>4,256</u>
	23,373	51,529
Radiation Shields:		
Structure and Facing		
Sides	7,643	16,849
Upper	24,854	54,794
Lower	21,192	46,720
Insulation		
Sides	3,099	6,832
Upper	3,549	7,825
Lower	<u>2,135</u>	<u>4,707</u>
	62,472	137,727
Doors:		
North		
Structure	10,380	22,885
Insulation	1,600	3,528
Ablative	6,001	13,230
Drive Mechanism	2,697	5,946
Counter Weight	21,656	47,743
Pulley Support Structure	7,163	15,791

Table 5.2-4 Receiver Weight Summary (cont)

<u>Description</u>	<u>Weight</u>	
	<u>kg</u>	<u>lb</u>
South		
Structure	4,189	9,236
Insulation	581	1,280
Ablative	2,178	4,801
Drive Mechanism	1,042	2,297
Counter Weight	5,684	12,532
Pulley Support Structure	4,259	9,390
East		
Structure	7,298	16,090
Insulation	1,111	2,450
Ablative	4,167	9,187
Drive Mechanism	1,886	4,159
Counter Weight	14,102	31,090
Pulley Support Structure	4,259	9,390
West		
Structure	7,298	16,090
Insulation	1,111	2,450
Ablative	4,167	9,187
Drive Mechanism	1,886	4,159
Counter Weight	14,102	31,090
Pulley Support Structure	4,259	9,390
	<u>133,080</u>	<u>293,391</u>
Piping:		
Absorber Tubes	26,944	59,401
Absorber Headers	3,434	7,571
Upper Interconnection Pipes w/Valves	5,147	11,347
Lower Interconnection Pipes w/Valves	4,211	9,284
Riser and Downcomer	3,186	7,024
Cold Surge Tank	20,342	44,847
Morning Glory Spillway	753	1,661
Lateral Support Pipes	11,284	24,877
	<u>75,301</u>	<u>166,012</u>
Piping Insulation:	30,210	66,602
Miscellaneous Insulation	3,039	6,700
Receiver Dry Weight:	<u>611,445</u>	<u>1,348,010</u>
Salt:		
Absorber Tubes and Headers	32,568	71,800
Upper Interconnection Piping	9,580	21,120
Lower Interconnection Piping	7,838	17,280
Riser and Downcomer	6,214	13,700
Cold Surge Tank	24,516	54,050
Morning Glory Spillway	3,674	8,100
Lateral Support Pipes	7,688	16,950
	<u>92,078</u>	<u>203,000</u>
Receiver Wet Weight:	<u>703,523</u>	<u>1,551,010</u>

5.2.3 Receiver Thermal Analyses

This section describes the receiver thermal analyses that were conducted and summarizes the resulting performance.

5.2.3.1 Aperture Sizing - Aperture size, shape, and cavity depth significantly influence the overall receiver size. The apertures must be large enough to allow the maximum amount of solar energy to enter the cavities (minimum spillage) while permitting a minimum amount of thermal losses. The aperture should be shaped so a good flux distribution can be achieved on the receiver absorbing surfaces. Depth and shape of the cavity also influence the absorber surface flux levels and distribution. Based on Phase I Advanced Water Steam Receiver (AWSR) work done by Martin Marietta, (Ref 2-4) square vertical apertures were selected for the repowering system receiver design. Tilted apertures show some reduced spillage advantage over vertical apertures but not a significant enough advantage to warrant the expected increased complexity and cost of receiver design. Square apertures were found to allow a heliostat aiming capability sufficient to provide reasonable flux distributions on the receiver absorbing walls. Heliostats are aimed (see Section 5.2.3.2) up and down at the aperture plane along its vertical centerline to distribute the solar flux within the cavity. Therefore the height of the aperture primarily depends on the desired peak flux. The width of the solar image from the heliostats in the corner of each cavity's collector field establishes the aperture width. Square apertures allow satisfactory peak flux limitations on the cavity absorbing surfaces for our collector field. If all heliostats were aimed at the center of each aperture and no limit were placed on peak flux values, a rectangular aperture with its long side horizontal would be optimum.

The apertures for the hybrid receiver were initially sized by an iterative approach using the Martin Marietta Thermal Radiation Analysis System (TRASYS) computer program. The spillage results as a percentage of the energy delivered to the aperture plane, were plotted against aperture size and summed with the corresponding cavity percentage thermal loss to indicate the optimum aperture sizes. The minimum point of the sum of the cavity losses and spillage losses determines the optimum aperture size. Figure 5.2-11 illustrates the sizing of the north aperture. As can be seen from the figure, the aperture size optimum is relatively flat near the selected cavity size. The east/west and south apertures were sized in the same manner. Thermal losses were calculated using correlations derived from detailed nodal computer models of solar cavities developed during the Martin Marietta Advanced Water/Steam Receiver Phase I project. These models were also used on the Martin Marietta Solar Central Receiver Hybrid Power System Phase I (Ref 2-3) study to determine the thermal losses from that receiver. For the north cavity, the optimum aperture size is 12x12 m (39.37x39.37 ft). The optimum aperture size for the east and west cavities is 10x10 m (32.81x32.81 ft), and that for the south cavity is 7x7 m (22.97x22.97 ft).

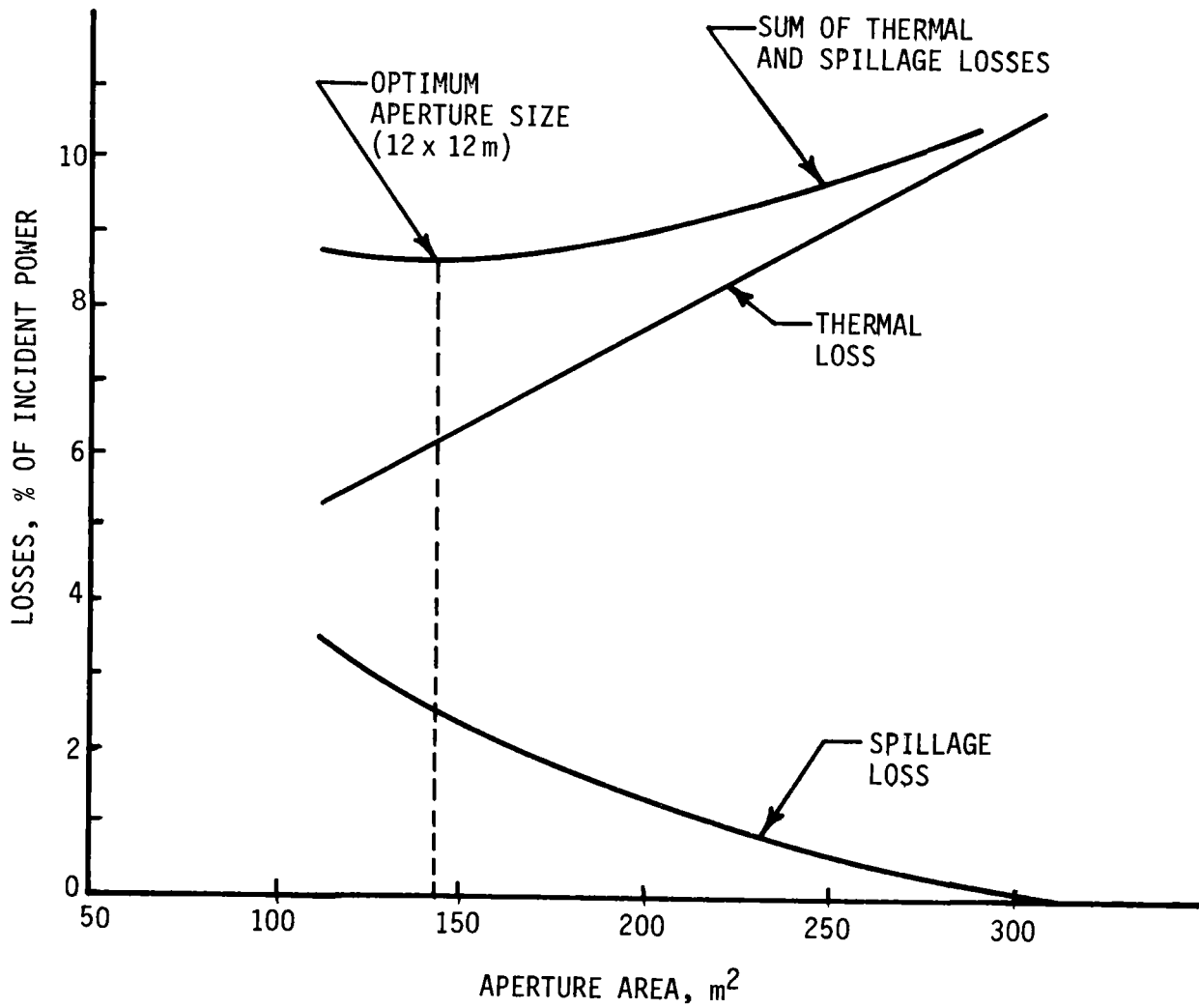


Figure 5.2-11 North Aperture Size Optimization

5.2.3.2 Flux Determination - Martin Marietta's TRASYS program was used to develop aiming strategies and flux distributions on the receiver surfaces. TRASYS is a computer program developed by Martin Marietta with the generalized capability to solve the radiation related aspects of thermal analysis problems. It has provided valuable, accurate data to support thermal analyses of a variety of space systems. The program has been expanded over several years to handle radiation problems associated with heliostat fields and solar central receivers by the addition of a "Mirror Field" library of subroutines. TRASYS-generated heliostat flux data have been compared with actual heliostat test data several times, most recently in the Martin Marietta Alternate Central Receiver Power System Phase II project (Ref 2-7). These comparisons indicated that TRASYS is fully capable of reproducing experimental measurements within a reasonable level of accuracy. Its particular advantage lies in its ability to determine radiant thermal interactions within a cavity receiver.

To calculate this information, TRASYS requires a geometric cavity surface description, along with the size and location of all the heliostats, the desired date, time, and solar beam strength. Each mirror on the heliostat is aimed directly at the aperture center unless otherwise specified, and the combined flux from all the heliostats is then totaled for each surface node.

The optimized collector field configuration described in Section 5.1 was used in the TRASYS model for repowering. The field was divided into north, south, east, and west quadrants, and separate TRASYS models were constructed for each quadrant. Figures 5.2-12 through 5.2-14 are computer generated plots of the north, east, and south cavities of the receiver, showing the nodal breakdown of the cavities. (Because of symmetry, it was not necessary to model the west cavity.)

Information calculated by TRASYS for each heliostat includes: the solar flux incident on that mirror, the flux reflected to the receiver (after allowing for atmospheric attenuation), the cosine of the half bounce angle, and the aperture and overall efficiencies. Results given for the entire field include the total power entering the aperture, the incident and absorbed fluxes on each receiver node, the field cosine of angle of incidence, aperture efficiency, and atmospheric attenuation.

An additional capability of the TRASYS program is the ability to simulate the effects of heliostat aiming. When the rows of heliostats are all aimed at the center of the aperture, their images strike the back wall of the receiver in a relatively tight group, resulting in a flux distribution with a sharp peak (Figure 5.2-15). Implementation of an aiming strategy to vertically spread the images from the various rows apart from each other can lower the maximum flux level as much as 32%, as shown in the figure.

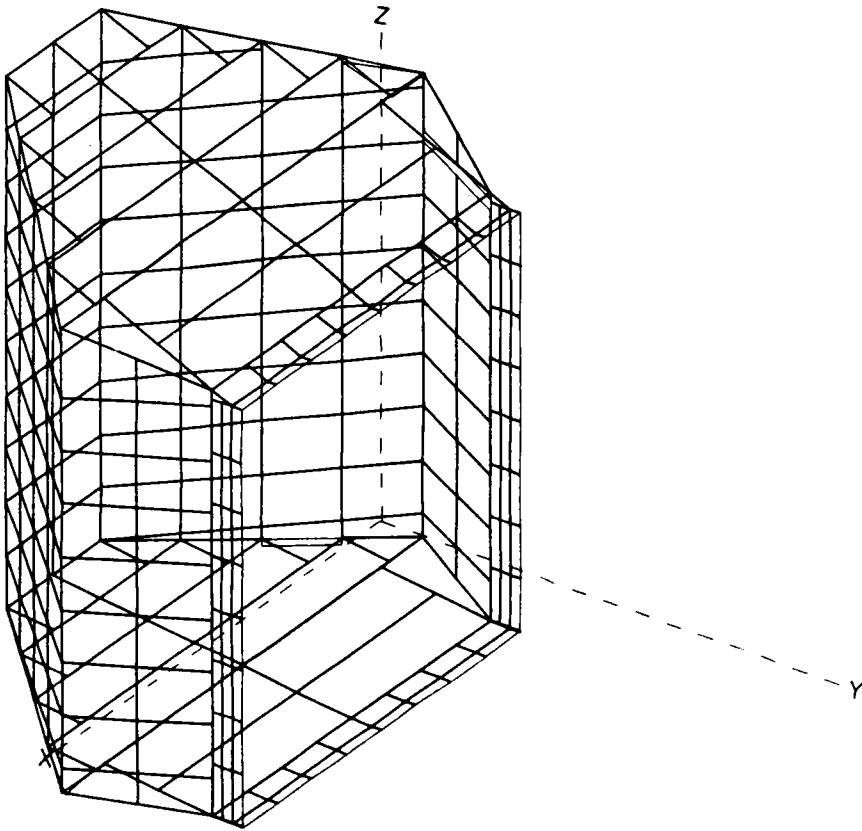


Figure 5.2-12 Receiver North Aperture

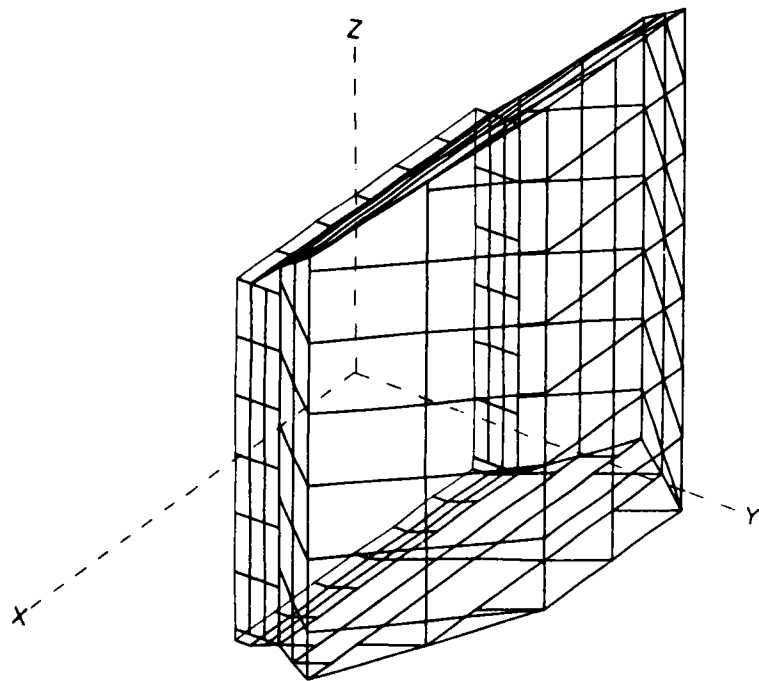


Figure 5.2-13 Receiver South Aperture

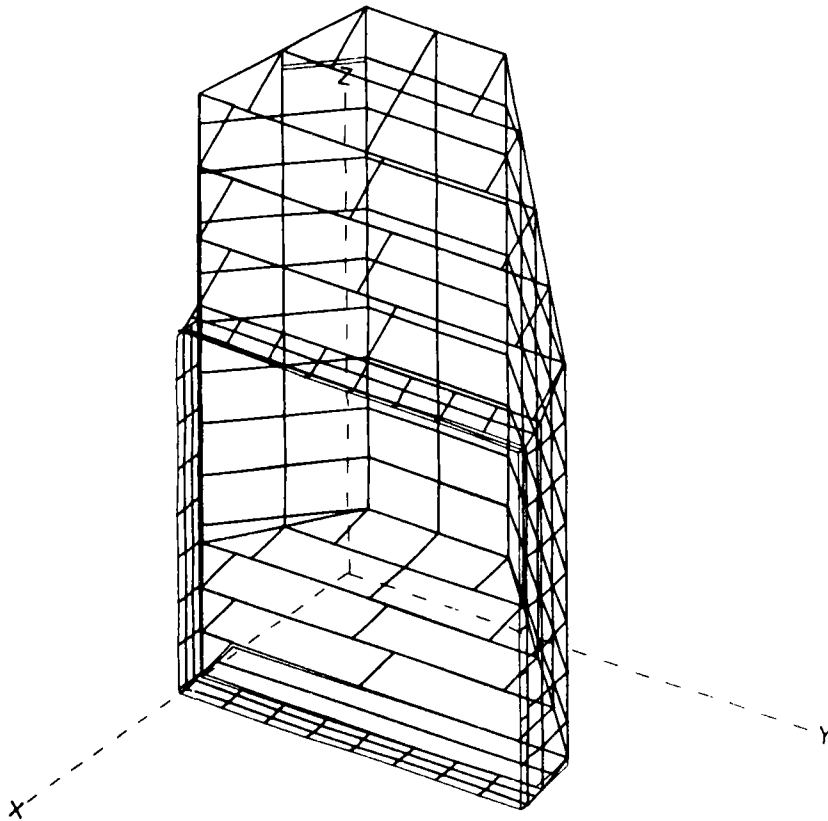


Figure 5.2-14 Receiver East Aperture

TRASYS was initially run for all cavities without any aiming strategy (all mirrors were aimed at the aperture center). Because of the low fluxes present, no further aiming was deemed necessary for the south cavity. However, the peak fluxes in the north and east/west cavities were well above the maximum allowable flux level of 63.1 W/cm^2 that was determined to be acceptable in Martin Marietta's prior work (Ref 2-3 and 2-5). Shifting the aimpoints horizontally and vertically was decided to be the best technique for reducing the peak fluxes. For simplicity, all the mirrors in a given heliostat row were aimed at the same point. The final aimpoints used to obtain the baseline receiver design fluxes are presented in Table 5.2-5.

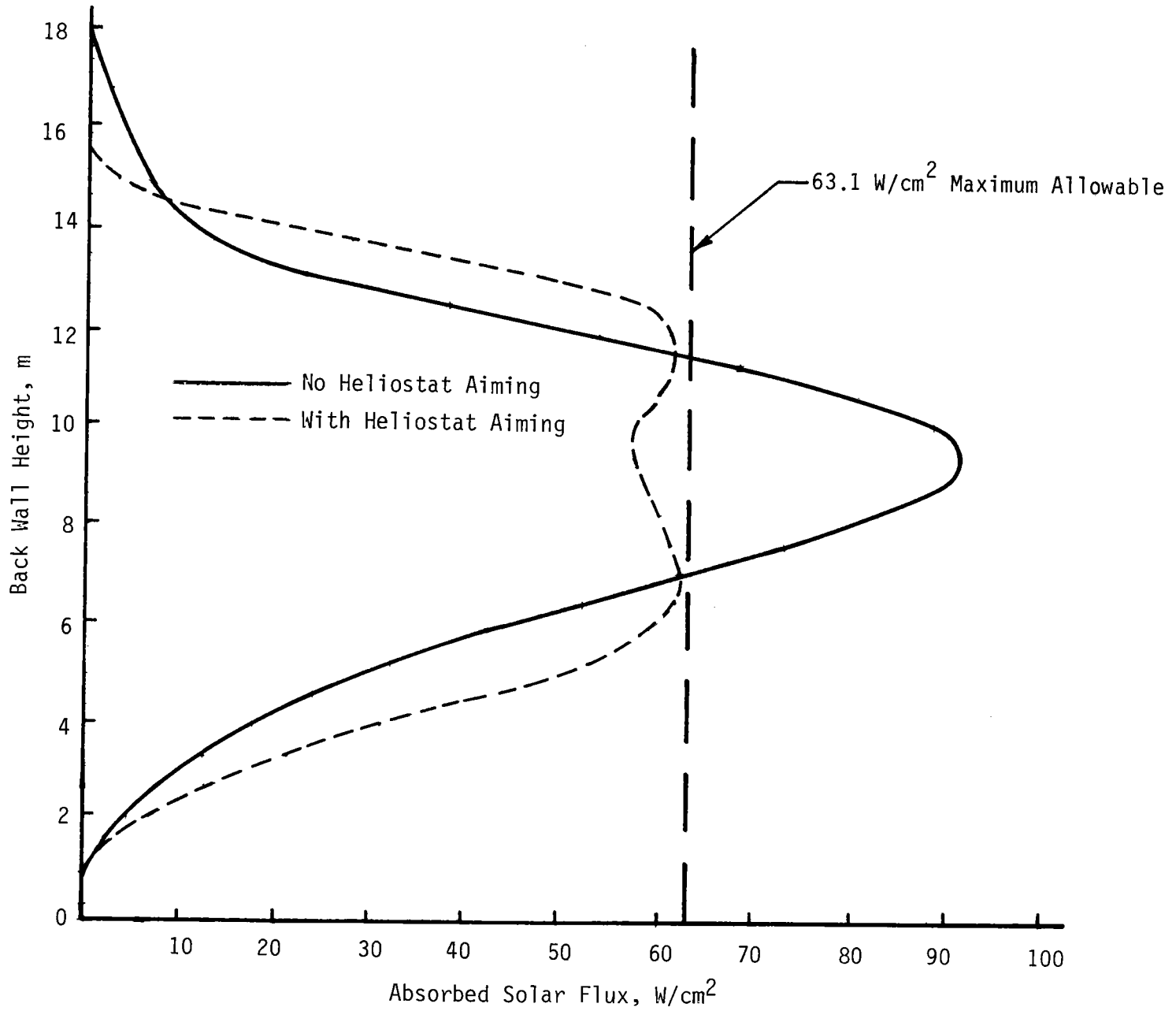


Figure 5.2-15 Effect of Heliostat Aiming on Peak Flux

Table 5.2-5 Heliostat Aiming Strategy

Rows	North Cavity,		Rows	East/West Cavity,	
	m	ft		m	ft
1-2	- 3.51	-11.52	1-5	1.22	4.0
3	- 3.03	- 9.94	6-8	1.07	3.5
4	- 2.59	- 8.5	9-14	0.91	3.0
5	- 1.34	- 4.4	15-20	0.76	2.5
6	- 0.64	- 2.1	21-45	0.00	0.0
7	0.61	2.0			
8	0.69	2.25			
9	0.76	2.5			
10	0.84	2.75			
19	0.91	3.0			
12	0.99	3.25			
13	1.07	3.5			
14	0.85	2.8			
15	2.08	6.84			
16	2.13	6.99			
17	2.17	7.13			
18	2.21	7.25			
19	1.31	4.3			
20	1.33	4.35			
21	1.34	4.4			
22	1.36	4.45			
23	1.37	4.5			
24	2.44	8.0			
25	2.41	7.9			
26	2.29	7.5			
27	2.26	7.3			
28-31	0.00	0.0			
32	- 1.84	- 6.04			
33	- 1.73	- 5.69			
34	- 1.62	- 5.30			
35	- 1.49	- 4.90			
36	- 1.37	- 4.48			
37	- 1.23	- 4.05			
38	- 1.09	- 3.59			
39	- 0.95	- 3.11			
40	- 0.80	- 2.62			
41	- 0.64	- 2.10			
42	- 0.48	- 1.57			
43	- 0.31	- 1.01			
44	- 0.15	- 0.50			
45-50	0.00	0.0			

Note: + Denotes distance above aperture center
- Denotes distance below aperture center

Having developed a viable aiming strategy, TRASYS runs were then made that calculated the absorbed flux on each receiver node for a given time of day and year. Figures 5.2-16 through 5.2-18 show flux data for noon, day 172, the system design point. Flux diagrams were also

Figure 5.2-16

Day: 172
 Time: 1200
 Insolation: 950 W/m²
 Aperture
 Efficiency: 0.9749
 Field Avg.
 Cosine: 0.8392

Absorbed Fluxes W/cm² (10³ Btu/hr-ft²)
 Incident Power: 77.450 MWt
 Absorbed Power: 75.596 MWt
 % Absorbed: 97.6

5-50

		3.80	4.35	5.55	5.55	4.35	3.80		
		(12.0)	(13.8)	(17.6)	(17.6)	(13.8)	(12.0)		
3.61	11.0	16.9	20.4	26.5	26.5	20.4	16.9	11.0	3.61
(11.4)	(35.0)	(53.6)	(64.6)	(84.4)	(84.4)	(64.6)	(53.6)	(35.0)	(11.4)
7.45	30.3	45.0	43.0	49.9	49.9	43.0	45.0	30.3	7.45
(23.6)	(96.1)	(143)	(136)	(158)	(158)	(136)	(143)	(96.1)	(23.6)
12.0	40.8	56.1	47.3	51.2	51.2	47.3	56.1	40.8	12.0
(38.1)	(129)	(178)	(150)	(162)	(162)	(150)	(178)	(129)	(38.1)
13.8	36.1	47.7	42.5	46.8	46.8	42.5	47.7	36.1	13.8
(43.8)	(114)	(151)	(135)	(148)	(148)	(135)	(151)	(114)	(43.8)
15.0	31.9	42.3	41.3	46.9	46.9	41.3	42.3	31.9	15.0
(47.4)	(101)	(134)	(131)	(149)	(149)	(131)	(134)	(101)	(47.4)
14.7	29.2	38.5	38.0	43.3	43.3	38.0	38.5	29.2	14.7
(46.5)	(92.5)	(122)	(121)	(137)	(137)	(121)	(122)	(92.5)	(46.5)
11.4	22.4	29.1	28.1	31.7	31.7	28.1	29.1	22.4	11.4
(36.1)	(71.0)	(92.3)	(89.2)	(101)	(101)	(89.2)	(92.3)	(71.0)	(36.1)
6.74	13.2	17.2	16.5	18.4	18.4	16.5	17.2	13.2	6.74
(21.4)	(41.8)	(54.4)	(52.2)	(58.5)	(58.5)	(52.2)	(54.4)	(41.8)	(21.4)
2.46	5.06	6.07	5.22	5.64	5.64	5.22	6.07	5.06	2.46
(7.81)	(16.0)	(19.2)	(16.5)	(17.9)	(17.9)	(16.5)	(19.2)	(16.0)	(7.81)
0.44	0.57	0.52	0.49			0.49	0.52	0.57	0.44
(1.38)	(1.80)	(1.66)	(1.56)			(1.56)	(1.66)	(1.80)	(1.38)

Figure 5.2-16 Absorbed Flux - North Cavity - Design Point

Figure 5.2-17

Day: 172
 Time: 1200
 Insolation: 950 W/m²
 Aperture Efficiency: 0.9846
 Field Avg. Cosine: 0.8221

Absorbed Fluxes W/cm² (10³ Btu/hr-ft²)
 Incident Power: 47.445 MWt
 Absorbed Power: 46.663 MWt
 % Absorbed: 98.4

	9.14	7.73	6.97	3.9			
	(29.0)	(24.5)	(22.1)	(12.4)			
4.33	12.7	12.8	12.9	7.7	5.63		
(13.7)	(40.4)	(40.6)	(40.8)	(24.5)	(17.8)		
6.54	20.8	23.0	23.8	15.9	15.5	10.9	5.0
(20.7)	(66.0)	(73.0)	(75.5)	(50.3)	(49.0)	(34.4)	(15.8)
13.3	32.6	38.3	42.4	30.3	36.6	33.7	10.2
(42.2)	(103)	(121)	(135)	(96.1)	(116)	(107)	(32.5)
17.9	38.4	46.3	53.4	40.3	55.0	54.6	20.9
(56.8)	(122)	(147)	(169)	(128)	(174)	(173)	(66.1)
18.9	37.2	45.2	53.0	40.4	57.6	58.8	26.3
(60.0)	(118)	(143)	(168)	(128)	(183)	(186)	(83.4)
15.8	29.0	35.3	41.6	31.7	45.6	46.9	23.2
(49.9)	(92.0)	(112)	(132)	(100)	(144)	(149)	(73.7)
10.3	17.9	21.5	25.3	19.2	27.9	28.6	15.0
(32.5)	(56.8)	(68.1)	(80.3)	(60.8)	(88.4)	(90.5)	(47.6)
5.39	8.78	10.1	11.5	8.27	12.2	12.9	6.56
(17.1)	(27.8)	(32.0)	(36.3)	(26.2)	(38.8)	(40.9)	(20.8)
2.25	3.05	3.05	3.31	2.39	3.32	3.16	1.73
(7.13)	(9.68)	(9.65)	(10.5)	(7.59)	(10.5)	(10.1)	(3.90)
0.47	0.35			0.45	0.55	(0.45)	0.30
(1.49)	(1.12)			(1.43)	(1.76)	(1.44)	(0.94)

5-51

Figure 5.2-17 Absorbed Flux - East Cavity - Design Point

Day: 172
 Time: 1200
 Insolation: 950 W/m²
 Aperture
 Efficiency: 0.9846
 Field Avg.
 Cosine: 0.8128

Absorbed Fluxes w/cm² (10³ Btu/hr-ft²)
 Incident Power: 22.018 MWt
 Absorbed Power: 20.757 MWt
 % Absorbed: 94.3

	4.07 (12.9)	3.04 (9.64)	2.27 (7.21)	2.41 (7.63)	
5.37 (17.0)	14.0 (44.5)	14.8 (46.8)	13.0 (41.2)	10.2 (32.5)	3.99 (12.6)
14.0 (44.3)	36.2 (115)	38.2 (121)	36.4 (116)	30.1 (95.3)	11.0 (35.0)
21.1 (67.0)	45.8 (145)	49.0 (155)	48.4 (154)	41.1 (130)	17.8 (56.5)
18.0 (57.0)	34.6 (110)	36.5 (116)	36.5 (116)	33.1 (105)	16.5 (52.2)
9.08 (28.8)	15.8 (50.1)	15.7 (49.9)	15.7 (49.9)	15.7 (49.8)	8.95 (28.4)
2.57 (8.14)	3.59 (11.4)	2.91 (9.24)	2.91 (9.23)	3.60 (11.4)	2.57 (8.16)
0.46 (1.45)	0.35 (1.10)			0.35 (1.12)	0.46 (1.47)

Figure 5.2-18 Absorbed Flux - South Cavity - Design Point

made for the time of year when the field quadrant delivers maximum energy to its particular cavity. In no cases were the design limits on incident or absorbed flux exceeded. Flux diagrams, for the design point, were also calculated for the area surrounding each aperture and for the absorbed solar fluxes on the sides of the aperture that are next to the aperture support beams. These absorbed fluxes are significantly lower than the cavity fluxes because of the shape of the reflected beams (spillage) and because the door frame will be painted white (Pyromark Series 2500) with an absorptivity of 0.32. The fluxes, both around the aperture and on the support beams, are sufficiently low to enable the use of simple radiation shields, insulation, and convective air flow to block the solar flux, without inducing excessive temperatures in load bearing structural members.

5.2.3.3 Receiver Performance - The receiver was designed to meet the subsystem requirements defined in section 5.2.1. The receiver will accept 195 MW_t of incident solar energy at the design environment and deliver 181 MW_t in the form of 409 kg/s (3.2 x 10⁶ lb/hr) of 566°C (1050°F) molten salt to the base of the tower. Salt enters the receiver at 277°C (530°F) and absorbs solar energy as it passes through tubes in the absorber panels to exit the receiver at 566°C (1050°F).

Throughout the receiver design the peak absorbed flux levels were minimized to obtain the required receiver life. This was accomplished by selectively locating the receiver absorbing panels within the cavity and through the use of various heliostat aiming strategies. The cyclic life of the receiver is a function of the absorbed flux, the fluid temperature and the resultant tube metal temperatures, both front and back. The temperatures were calculated for the 10 panels in the receiver east pass at the design point. This sequence of salt flow through the receiver (Fig. 5.2-6 and -19) was selected as the best compromise between allowing cool liquid to flow through panels with higher absorbed fluxes and maintaining a feasible piping configuration. Some additional improvement may be realized by changing the flow path through the receiver and adjusting the aiming to reduce the flux on the high salt temperature passes while increasing flux on the cooler salt passes. Alternatively, improvement might be made by decreasing the number of tubes in the hotter panels to obtain higher salt velocities and thus better convective heat transfer coefficients.

Results from the stress analysis discussed in section 5.2.2.6 were used to evaluate the cyclic life of the receiver based on the calculated salt and tube temperatures for each pass. To evaluate the cyclic life as a result of creep fatigue, an inelastic analysis (section 5.2.3.4 of Ref 1-2) was performed in the prior study recognizing that creep relaxation will occur. The prior study showed acceptable life requirements. As discussed in paragraph 5.2.2, the differences between conditions in the prior work and in this work indicate that acceptable creep and fatigue life will be obtained for the current design.

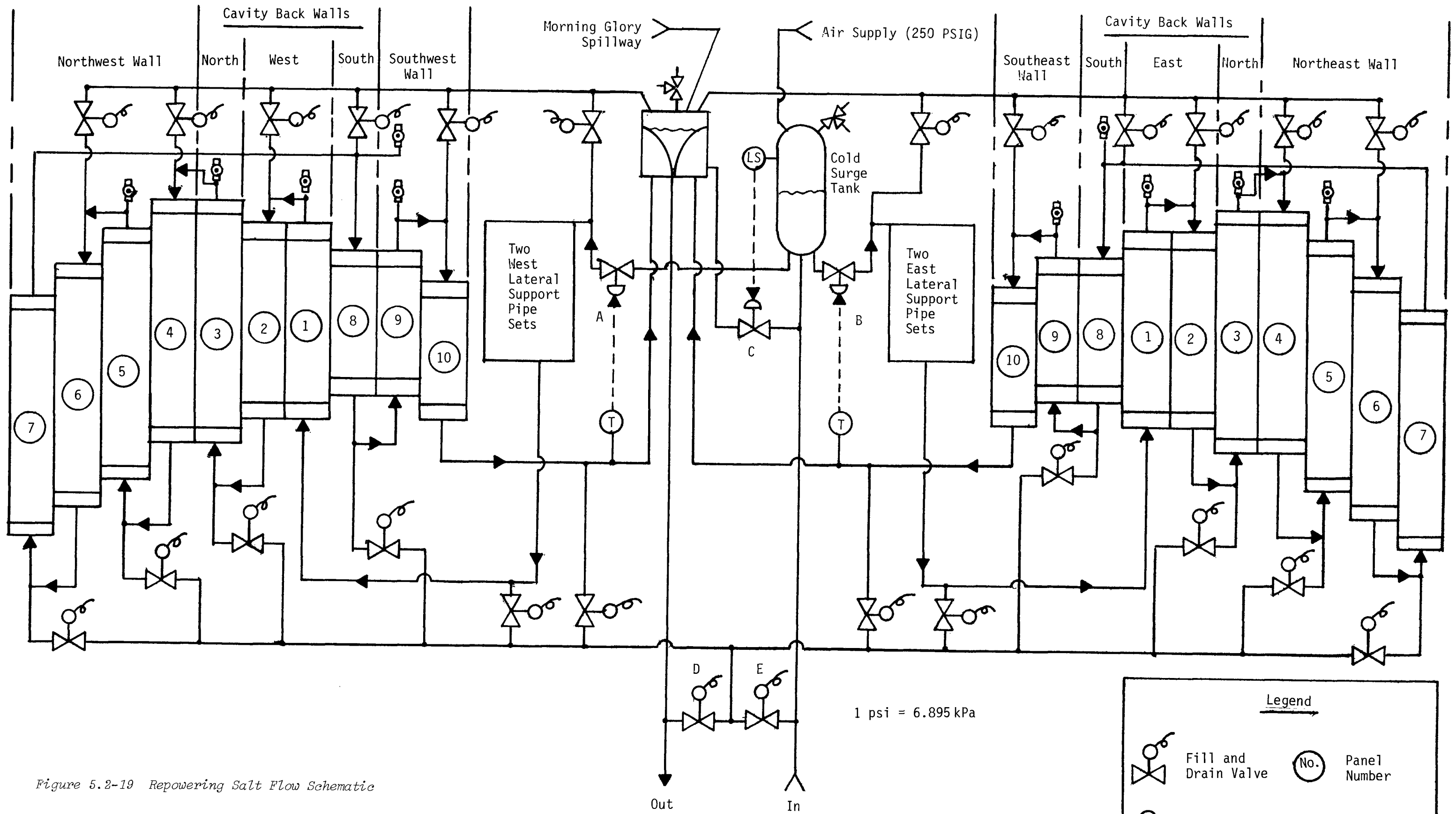
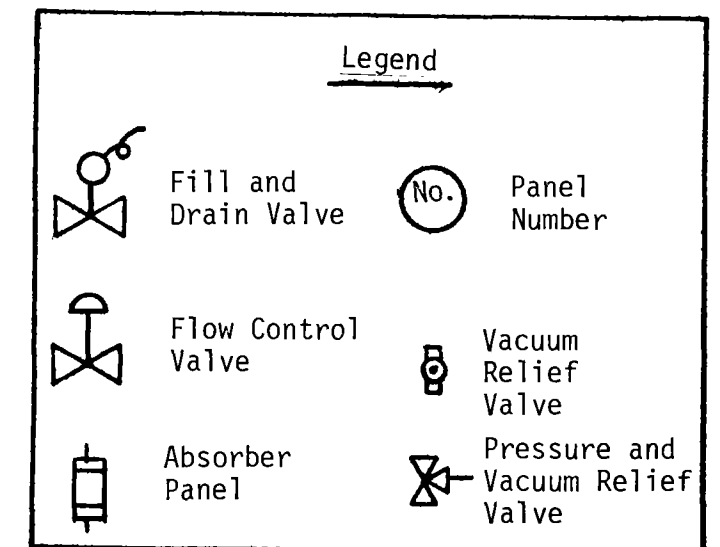


Figure 5.2-19 Repowering Salt Flow Schematic



The receiver is divided into two symmetrical flow zones about the north-south centerline as shown in Figures 5.2-6 and -19. Each zone is designed to produce one-half of the required thermal output at noon on day 172. Knowing the total heat output required from each zone of the receiver, 90.5 MW_t , and the required temperature rise, 289°C (520°F), establishes the mass flow rate of salt required through each zone as 204.5 kg/s ($1.6 \times 10^6 \text{ lb/hr}$). Paragraph 5.5.3 describes the fluid salt properties used.

The absorber tube size selected has a 38 mm (1.5 in.) OD with a 1.7 mm (0.065 in.) wall thickness. State-of-the-art superheaters and boilers of the size and operating temperatures required for molten salt receivers are generally designed with tubing in the range of 25.4 mm (1 in.) to 63.5 mm (2.5 in.) OD. The 38.1 mm (1.5 in.) OD tube selected is considered to be close to minimum fabrication and installation cost. The Babcock and Wilcox work on advanced molten salt receivers incorporates 50.8 mm (2 in.) tubing with $3 \times 6 \text{ mm}$ ($0.125 \times 0.25 \text{ in.}$) spacers between tubes. Similar spacers are used in the current design. A recent evaluation of the fabricability of this design by Babcock and Wilcox indicated that a slightly smaller web might be advisable. The use of the smaller web will not significantly change the overall design.

Based on a selected salt flow velocity of 2.567 m/s (8.42 fps), the number of tubes per panel can be determined from the mass flowrate through each zone:

$$N = \dot{m} / \rho v A$$

etc. where

N = number of tubes,

\dot{m} = mass flowrate, kg/s ,

ρ = salt density, kg/m^3 , at average salt temperature of 427°C (800°F)

v = velocity of salt, m/s ,

A = cross-sectional area of tube flow path, m^2

or

$$N = 204.5 / (1821.3)(2.567)(9.51 \times 10^{-4}) = 46$$

It was found that 46 tubes and 45 spacers were an excellent fit to the structural geometry of the receiver. This resulted in a panel width of 2.038 m (6.688 ft). The 0.06 m left at each corner of the back wall structure was filled with the end tube of the cavity side wall absorber panels. Each receiver pass was then divided into 10 panels. Panel lengths were established based on the absorbed flux diagrams shown in Figures 5.2-16 through 5.2-18. Where a panel receives heating from both sides, the panel length is determined by the larger

cavity. The upper and lower shields in each cavity are located approximately along a line on the absorber panels where the incident flux drops off to an acceptable level. Panel lengths are tabulated in Table 5.2-6.

Table 5.2-6 Tube Lengths Used for Receiver Pressure Drop Calculations

Panel Number	Tube Length, m (ft)
1, 2	15.14 (49.67)
3, 4	17.63 (57.83)
5	16.86 (55.33)
6	16.36 (53.67)
7	15.85 (52.00)
8	10.51 (34.50)
9	15.24 (50.00)
10	14.12 (46.33)
TOTAL	154.48 (506.83)

Cool salt coming into the receiver is split into two identical parallel flow passes, one path through each zone. Fluid flowing through a zone flows through the zone lateral support pipes and then through each of the 10 panels in series and then joins with flow from the other zone at the first morning glory spillway before exiting the receiver.

Tube lengths shown in Table 5.2-6 were used to calculate the pressure drops. Considering tube entrance and exit losses, the velocity head loss per pass, losses in the headers and interconnecting piping and valves, and a salt flow rate of 20% over design, the maximum pressure drop through the receiver due to salt flow is approximately 1.17 MPa (169.4 psi). The static head of salt in the receiver, the design pressure drop in the flow control valve, and a reasonable margin were added to establish a maximum operating pressure of 1.88 MPa (272 psi) for the receiver.

A MITAS thermal math model was constructed to calculate the salt and absorber tube steady-state temperature profiles in the receiver panels. One absorber tube was modeled to represent all of the tubes in a panel. This tube is divided into nine segments containing front and back outside tube surface nodes, front and back inside tube surface nodes and a salt node. A typical tube segment is shown in Figure 5.2-20.

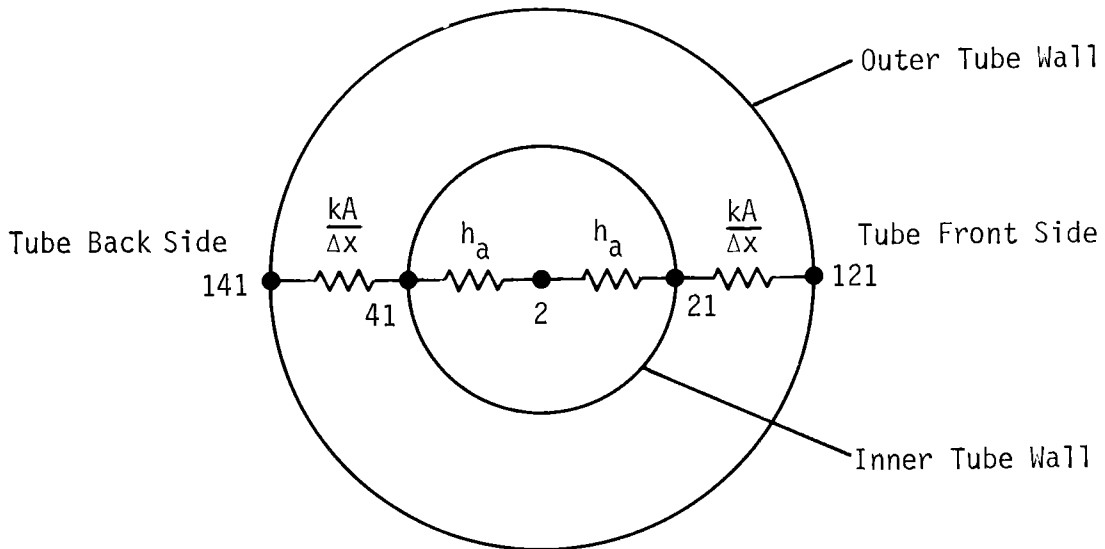


Figure 5.2-20 Typical Tube Segment in MITAS Model

The complete node and conductor diagram is shown in Figure 5.2-21. Fluid enters the tube at boundary temperature T_1 , receives heat inputs through the tube walls as it flows through the tube and exits at temperature T_{10} . By stacking MITAS runs, using the exit temperature from the preceding panel as the inlet temperature for the succeeding panel and applying the appropriate energy (Q) inputs for each panel, one can establish the receiver temperature profiles.

The MITAS model calculates the heat transfer coefficient between the fluid and tube inside surface nodes based on the node temperatures and fluid velocity. The fluid velocity is also calculated at each fluid node based on a constant mass flowrate through the tube and the fluid temperature. The heat transfer coefficient is calculated in MITAS using the following equation from W. H. McAdams Heat Transmission text:

$$h = 0.023 \frac{k}{d} (Re)^{0.8} (Pr)^{0.4}$$

where:

h = convective heat transfer coefficient of salt, $W/m^2\text{-}^\circ C$
 (Btu/h-ft²-°F)

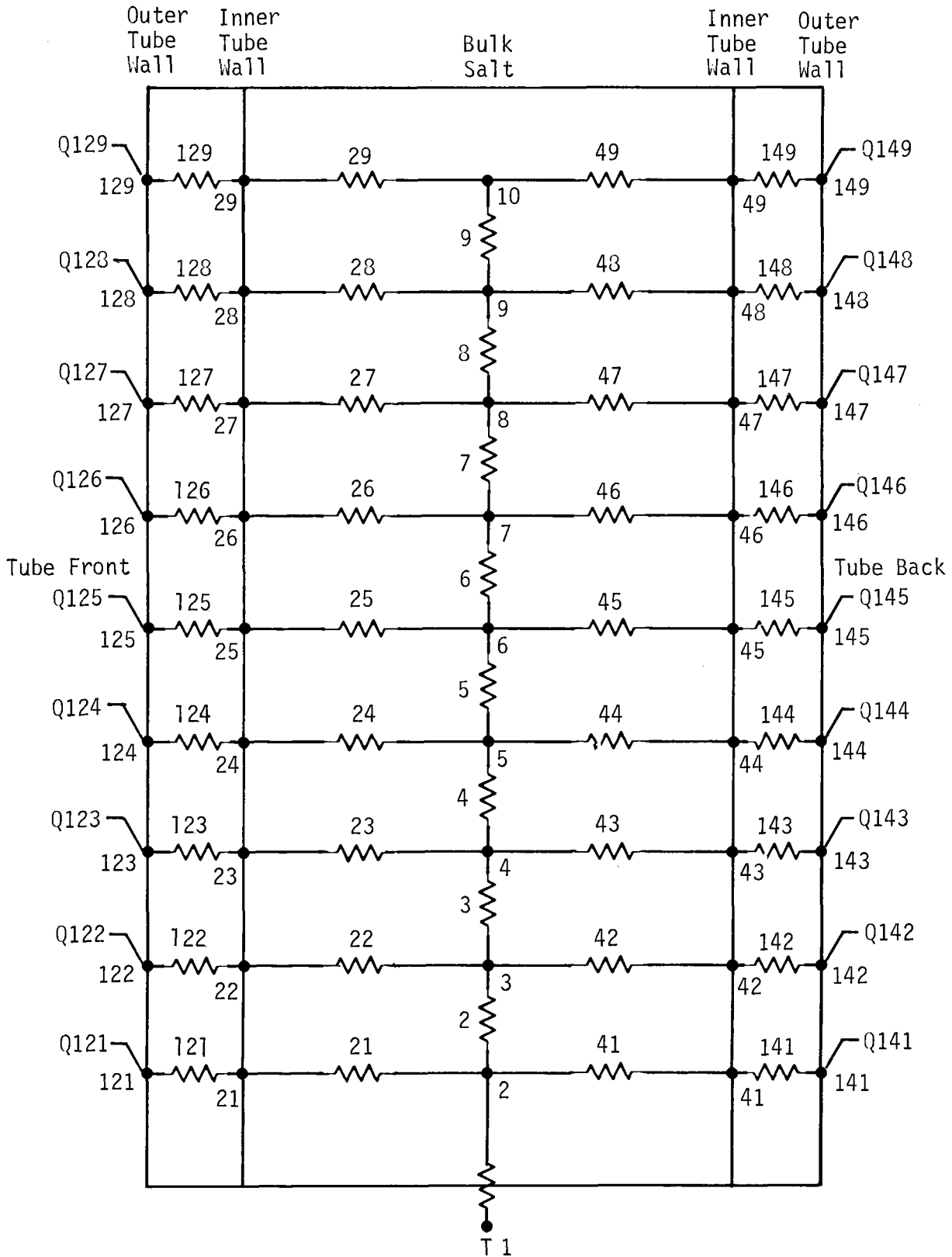


Figure 5.2-21 Absorber Tube MITAS Model Node Diagram

k = salt thermal conductivity, W/m°C (Btu/h-ft°F),

d = tube ID, m (ft),

$$Re = \frac{dv\rho}{\mu}$$

$$Pr = \frac{C_p u}{K}$$

v = flow velocity, m/s (fps),

ρ = salt density, kg/m³ (lbm/ft³),

C_p = specific heat of salt, J/kg-°C (Btu/lbm-°F),

μ = salt viscosity, kg/s-m (lbm/s-ft)

Heat inputs for the MITAS program described above were taken from the absorbed flux maps shown in Figures 5.2-16 through 5.2-18. Adjacent flux nodes were averaged to get 10 columns of fluxes corresponding to the 10 panels. These 10 columns of fluxes were then plotted against distance from the top of the receiver to represent the vertical flux distribution on each panel. The flux corresponding to the MITAS tube node point locations for each pass were selected from these plots and input to the MITAS program. The program further reduces these fluxes by an input loss fraction to account for the convection and radiation losses. The final flux used by MITAS to calculate the temperature profiles is the net flux absorbed by the tube nodes (incident minus reflected, convection and IR radiation losses).

Figure 5.2-22 is a graphic representation of the salt temperature rise as it travels through the receiver. This graph points out the fact that the greatest energy transfer to the salt occurs in panels 4 through 7, panels in which the salt temperature is still relatively low. This aids greatly in reducing both peak tube metal temperatures and thermal stresses. The maximum tube temperatures for each panel are given in Figure 5.2-23 for both the tube outside surface and the tube inside surface. The tube inside temperature is an upper bound on the salt temperature. As the temperatures shown in Figure 5.2-23 are the peaks that occur anywhere on the panel, one should not infer that the peak outside temperature and the peak inside temperature occur at the same point on the panel. The peak outside temperature is 589°C (1092°F) while the peak inside temperature is 579°C (1075°F). Thus the salt is always cooler than 600°C. Figure 5.2-24 shows the salt film convective heat transfer coefficient and salt velocity profiles through the receiver panels. This information was also calculated by MITAS for the same design point case.

Figure 5.2-22

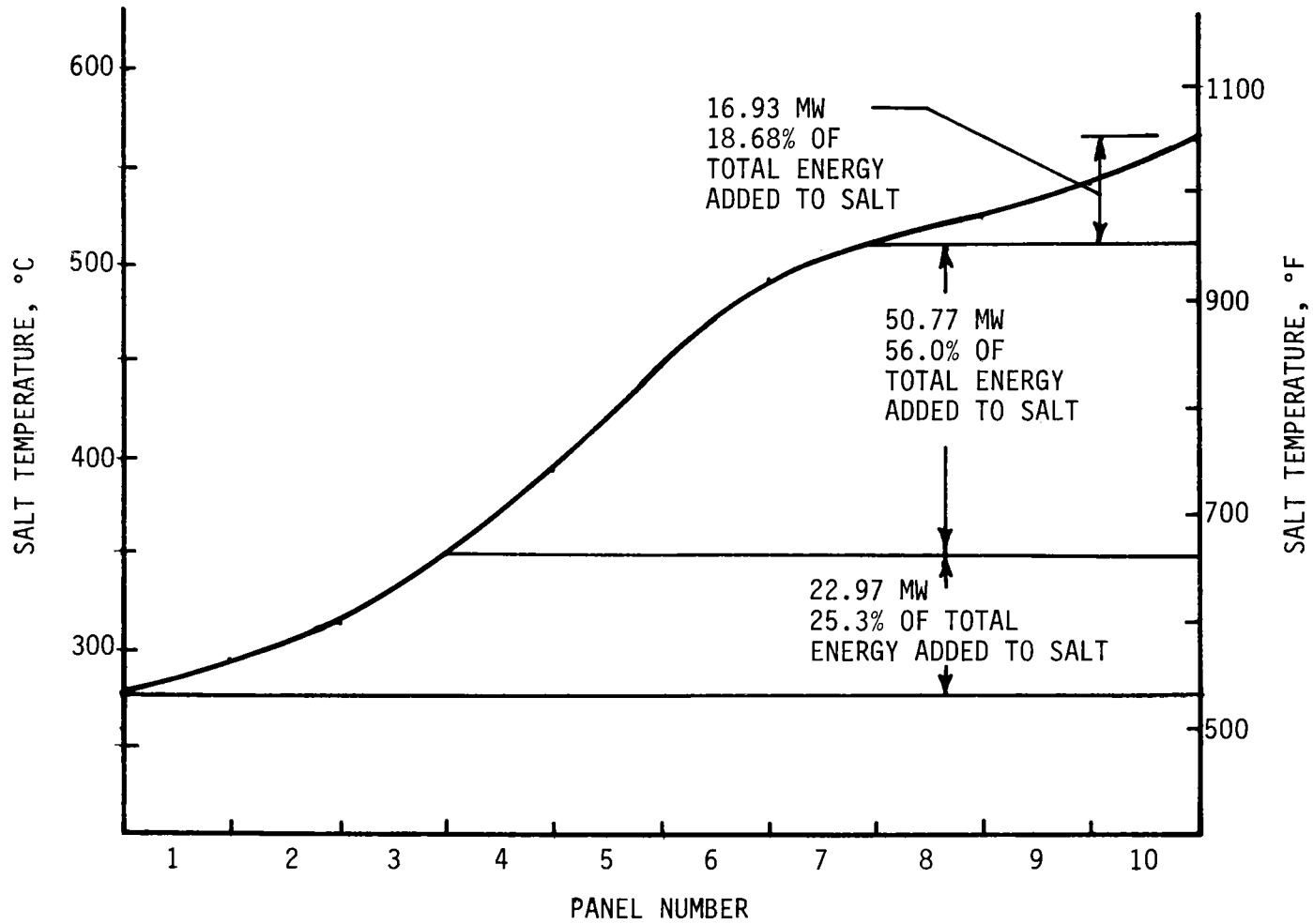


Figure 5.2-22 Bulk Salt Temperature Rise Across Receiver Panels

Figure 5.2-23

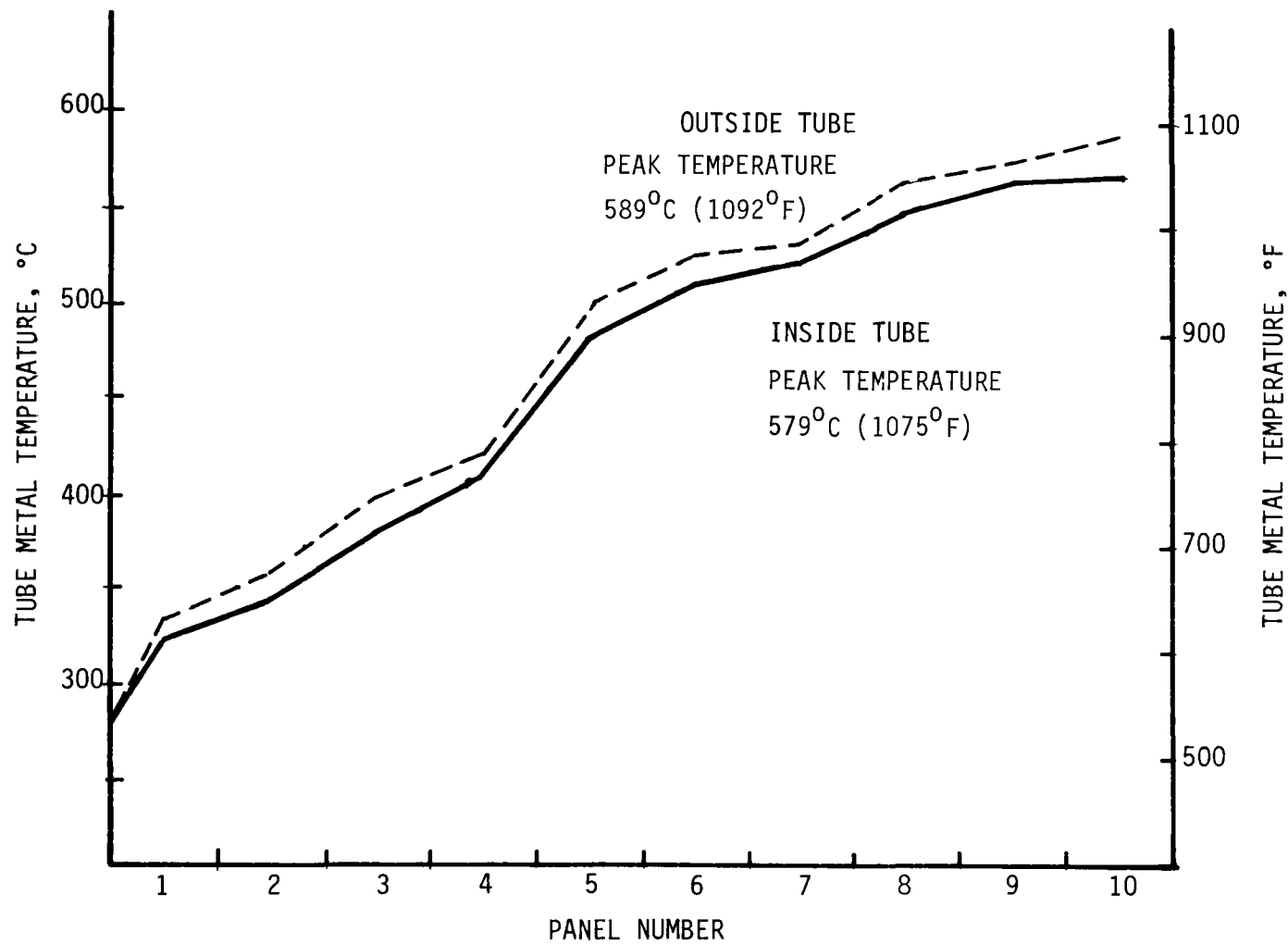


Figure 5.2-23 Receiver Maximum Tube Temperatures

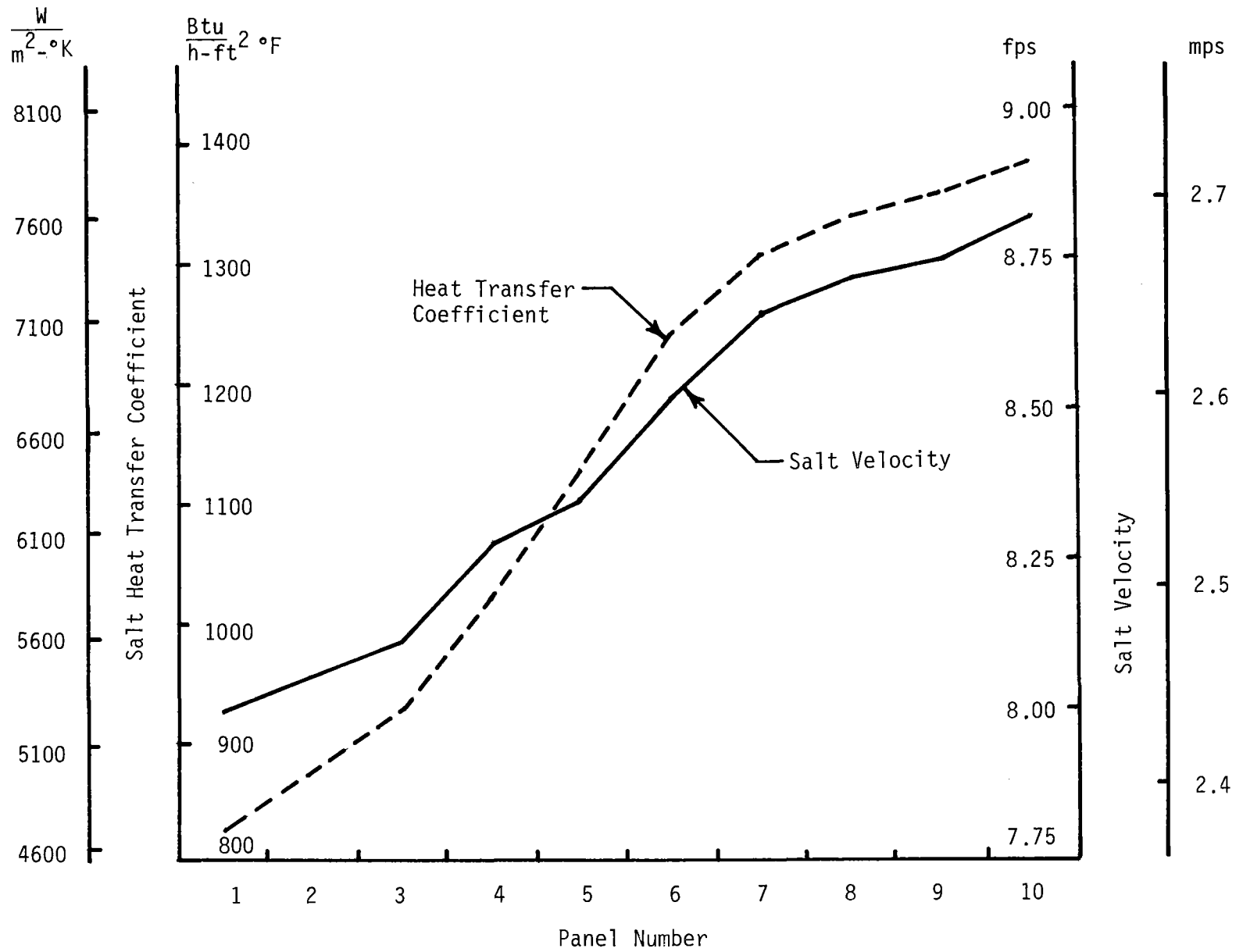


Figure 5.2-24 Absorber Tube Heat Transfer Coefficient and Salt Velocity Profiles

Temperature distributions on the lateral support pipes were also investigated using a slightly modified version of this MITAS model. As previously stated, heat inputs to the lateral support pipe model were obtained from the flux maps presented in Figures 5.2-16 through 5.2-18. The average flux data obtained from those maps was then adjusted to account for the lower absorptivity of the white-painted lateral support pipe. The lateral support pipe paint is the white Pyromark Series 2500, ($\epsilon_s = 0.32$, $\epsilon = 0.84$) used on the cavity inactive surfaces. As shown in Figure 5.2-25, the support pipe will not experience any severe heating. The salt temperature increase in the parallel lateral support pipes (e.g., north-east and south-east) was found to be less than 2.8°C (5°F) and thus is not significant. As the white paint on the lateral support pipes will reflect more of the incident energy than the black painted absorber tubes, the effect on overall cavity efficiency was addressed. This effect will be less than a 0.2% reduction in cavity efficiency.

5.2.3.4 Thermal Losses - Thermal losses from the solar central receivers consist of spillage, solar reflection, infrared radiation, convection, and conduction. The cavity receiver concept was selected primarily to minimize receiver thermal losses during operation and overnight or cloudy-day shutdown periods. Solar reflection, infrared radiation, and convection losses are minimized by the cavity enclosure during operation. Conduction is limited by a 0.1 m (4 in.) thick filmfrax ceramic fiber Duraback insulation (manufactured by the Carborundum Company of Niagara Falls, New York).

Spillage is defined as the amount of energy reaching the aperture plane that does not enter the cavity. Spillage losses depend on several factors including aperture size, aiming strategy, field configuration, and heliostat tracking errors. DELSOL II was used to calculate spillage, as this program considers more of the factors which affect spillage than does TRASYS and is, therefore, more realistic. For this cavity design, spillage losses were calculated to be 2.5% of the incident energy at the design point. Reflective losses are minimized by the cavity receiver concept because a large portion of the solar energy reflected from one panel is absorbed by the other panels and reflected by the inactive surfaces. Only that portion reflected directly back out the aperture is lost. This results in an effective cavity absorptivity of 0.980, using an absorber surface absorptivity of 0.950. Similarly, the infrared losses are also reduced by the cavity geometry. This reduction occurs because the aperture area is significantly less than the high temperature absorber area. These infrared losses were found to be 2.46% of the power incident on the receiver at the design point.

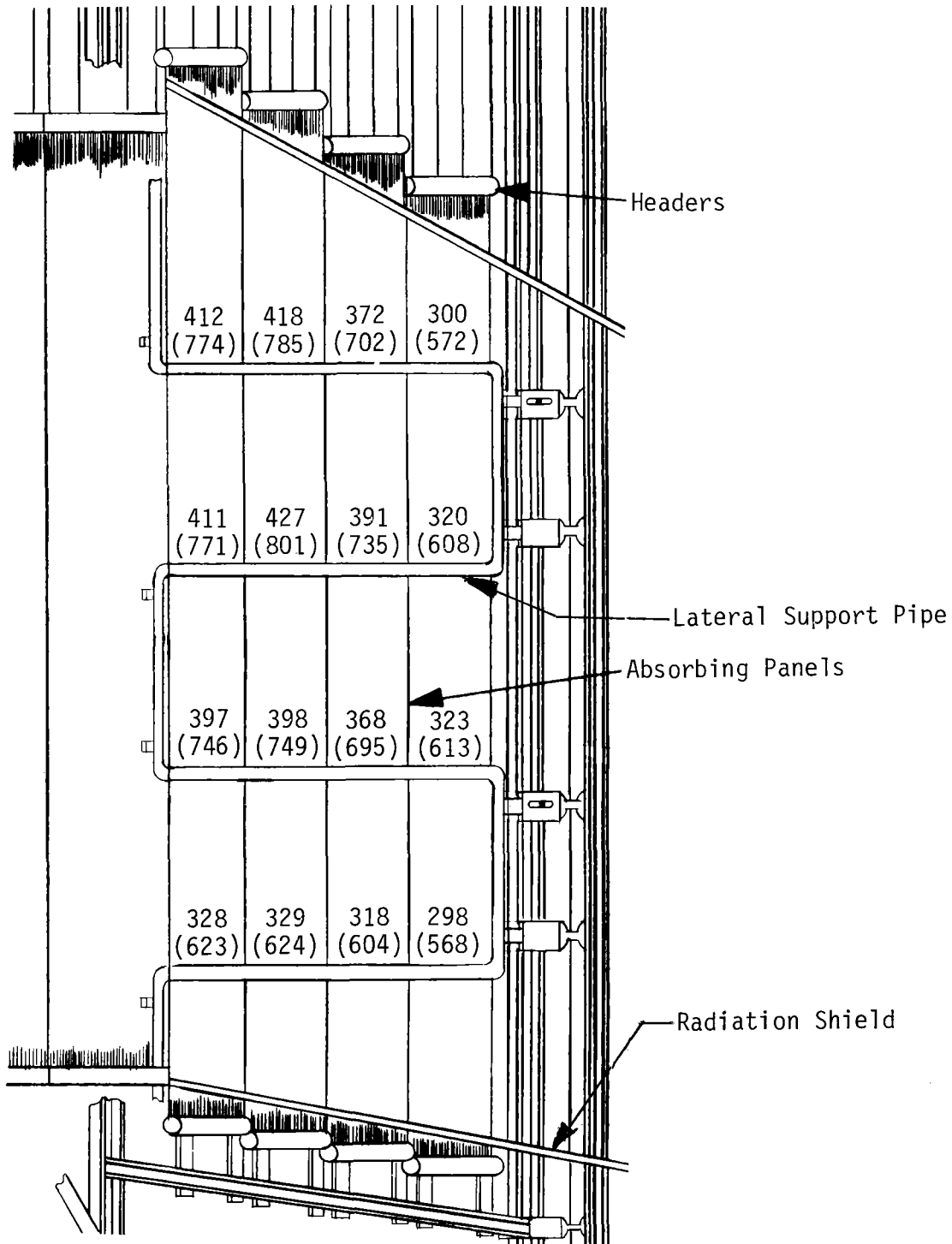


Figure 5.2-25 Temperature Profile for Lateral Support Pipe, °C (°F)

Convective heat losses for any type of a solar receiver are difficult to accurately calculate. The large physical dimensions of the heated surfaces as well as the high surface temperatures result in very high Reynolds and Grashof numbers, for which virtually no heat transfer data are available. A detailed MITAS nodal model of a cavity receiver was constructed for both the Martin Marietta Advanced Water Steam Phase I receiver (Ref 2-5), and for Martin Marietta Hybrid Phase I receiver (Ref 2-3 and 2-4), to calculate convective losses. The results of these programs agree well with the limited cavity test data available. Correlations derived from this model make use of an "effective heat transfer coefficient" (which is dependent on receiver geometry), the aperture area, and the average surface temperature in the cavity to product convective energy losses. For the repowering solar receiver, thermal losses due to convection are 2.16% of the incident energy at design point.

Conduction losses from the quad-cavity receiver were found to be 0.55% of the design point incident energy. It was assumed that the receiver interior is at the average salt temperature of 424°C (795°F) and that the exterior surfaces are at the ambient design point temperature of 39°C (102°F). A 25% additional loss was assumed to account for structural penetrations of the insulation. The design point thermal losses are summarized in Figure 5.2-26.

5.2.4 Receiver Supply and Return Piping

The receiver supply and return piping delivers molten salt to the receiver and returns it to the molten salt storage area. Based on Sandia's materials compatibility tests, the selection of type 304 stainless steel for hot salt piping and Al03 carbon steel for cold salt piping represent low risks for installation at the Saguaro repowering project. Discussed below are the requirements, design description, and performance and cost of this molten salt piping subsystem.

5.2.4.1 Requirements - The receiver supply and return piping as well as the pumps required to circulate molten salt through the receiver will be required to deliver molten salt at a flow rate which will allow a normal peak thermal rating of 181 MW_t (6.18×10^8 Btu/hr) at the base of the tower with a temperature differential of 289°C (520°F). The design salt flow will therefore be 409 kg/sec (3.25×10^6 lb/hr) or 0.213 m³/sec (3,380 gpm) of cold salt. The system of pumps, piping and controls will be capable of delivering molten salt at all flow rates from 5 to 110% of design. In every case, the pumps will need to overcome the static head of salt up to the liquid level in the cold salt surge tank plus the pressure in that drum above the liquid level as well as friction losses in the line. Return piping is designed to use the static head of salt from the morning glory spillway crest to the hot salt storage tank liquid inlet. The salt is to be pumped from the cold salt storage tank at 277°C (530°F) and returned to the hot salt storage tank at 566°C (1050°F). Provisions are made for temporary retention of salt that is too hot for return to the cold storage tank and too cold for storage in the hot tank. The piping is designed to accommodate thermal expansion (0.81% for Type 304 pipe, 0.49% for carbon steel) without exceeding allowable design stress limits. The piping is also designed to be drained to a tank provided for that purpose.

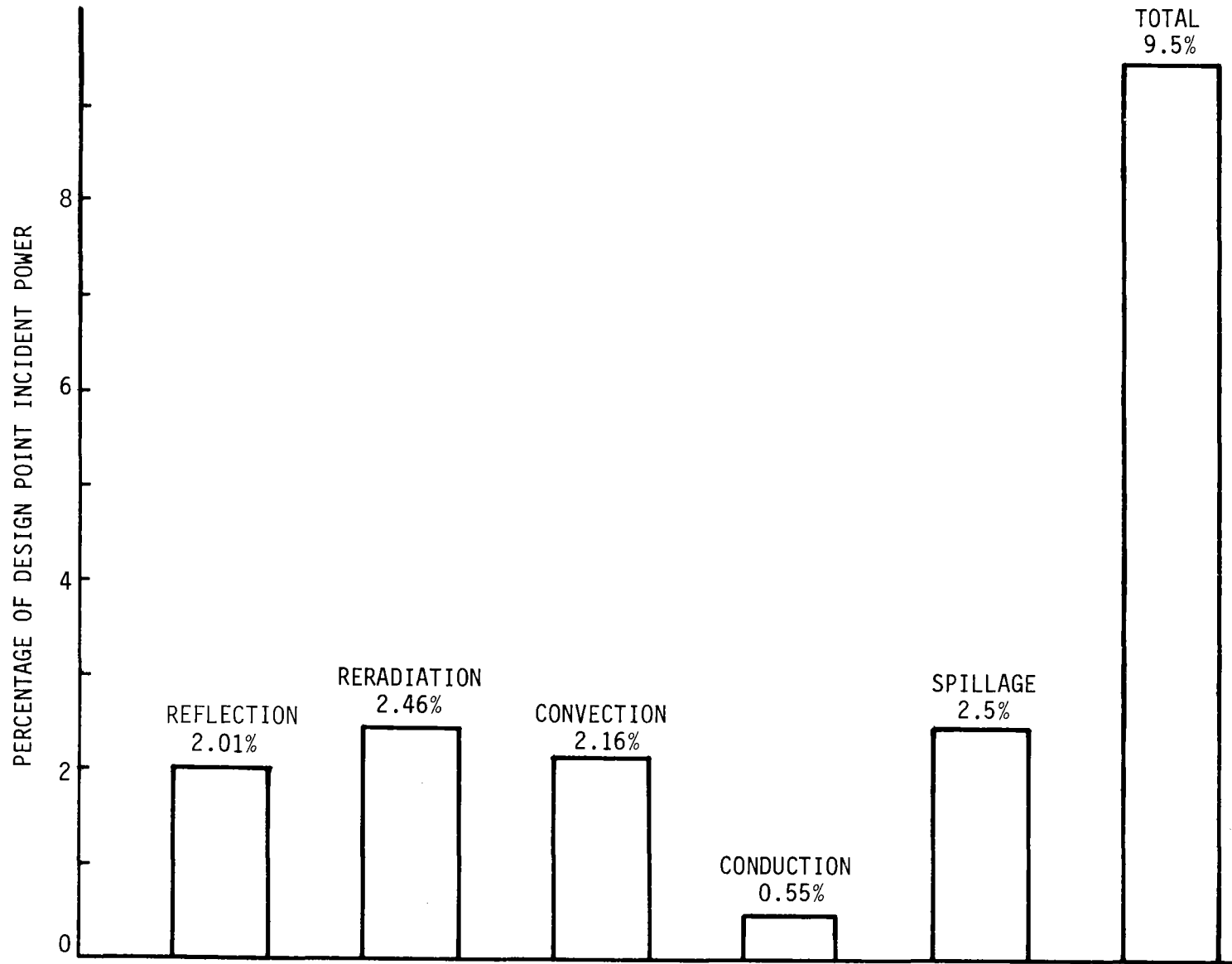


Figure 5.2-26 Receiver Design Point Losses

5.2.4.2 Design Description - The design of the salt piping system depends upon the location of each of the subsystems with respect to one another. Optimum pipe sizes for the selected configuration resulted from using a computer program and utilizing economic factors provided by Arizona Public Service in the prior study (Ref 1-2). The computer program calculated the optimum size by minimizing the total costs, which consisted of operating costs and capital investment costs. Investment costs increase with increasing pipe size, while the operating costs decrease with increasing pipe size. The nature of these cost relationships is dependent on such factors as type of material, installation costs, thickness of pipe, insulation type, pump type and efficiency, power costs, etc. The supply piping for the prior study was sized using this computer program.

The supply piping for the current study was sized by using the same salt flow velocity as for the prior study. The size was determined to be 305 mm (12 in.). The supply piping carries cold salt at 277°C (530°F) and will be made of carbon steel.

The return piping was sized differently. Pumping costs are independent of return piping size so long as the friction loss in the return piping does not exceed the head of salt available. The return piping is then only 254 mm (10 in. in diameter). The return piping carries hot salt at 566°C (1050°F) and will be made of Type 304 stainless steel. Since the pressure in the riser and downcomer vary considerably with the static head of salt, pipe wall thicknesses were selected based on the most critical requirement. Pipe wall thicknesses were calculated using standard methods. Allowable stresses for carbon steel and 304 stainless steel were taken from ANSI B31.1, the power piping code and from ASME, Section VIII, Boiler and Pressure Vessel code. Design pressures for the receiver loop were calculated by adding the salt head to the operating pressure in the appropriate salt surge drum and adding a 5% safety factor. For the header upstream of the booster pumps and downstream of the lowest plunge pool, 10% was added to the operating pressure at the design point to arrive at a design pressure.

A schematic of the receiver related salt piping is given in Figure 5.2-27. A complete description of the operation and control of the system is given in Section 5.3.2. Main circulation pumps provide only enough pressure for the working medium to reach the receiver tower, arriving at a pressure of 345 KPa(g) (50 psig) at the booster pump suction. The suction pressure was chosen to ensure sufficient net positive suction head at the booster pumps even with wide variation of flow through the system. The booster pumps provide sufficient head to overcome riser friction loss, salt head to the liquid level in the cold salt surge drum plus 1720 KPa(g) (250 psig), the cold salt surge drum operating pressure. Pressure in the morning glory spillway tank is at ambient to provide good venting in the downcomer. Provisions have been made for a twenty-to-one variation in salt flow rate. A recirculating loop including an air fin salt cooler is provided around the booster pumps. Recirculation from the main circulating pumps returns to the cold salt tank. Flow switches are provided to turn booster and main circulation pumps on and off as required. Valving

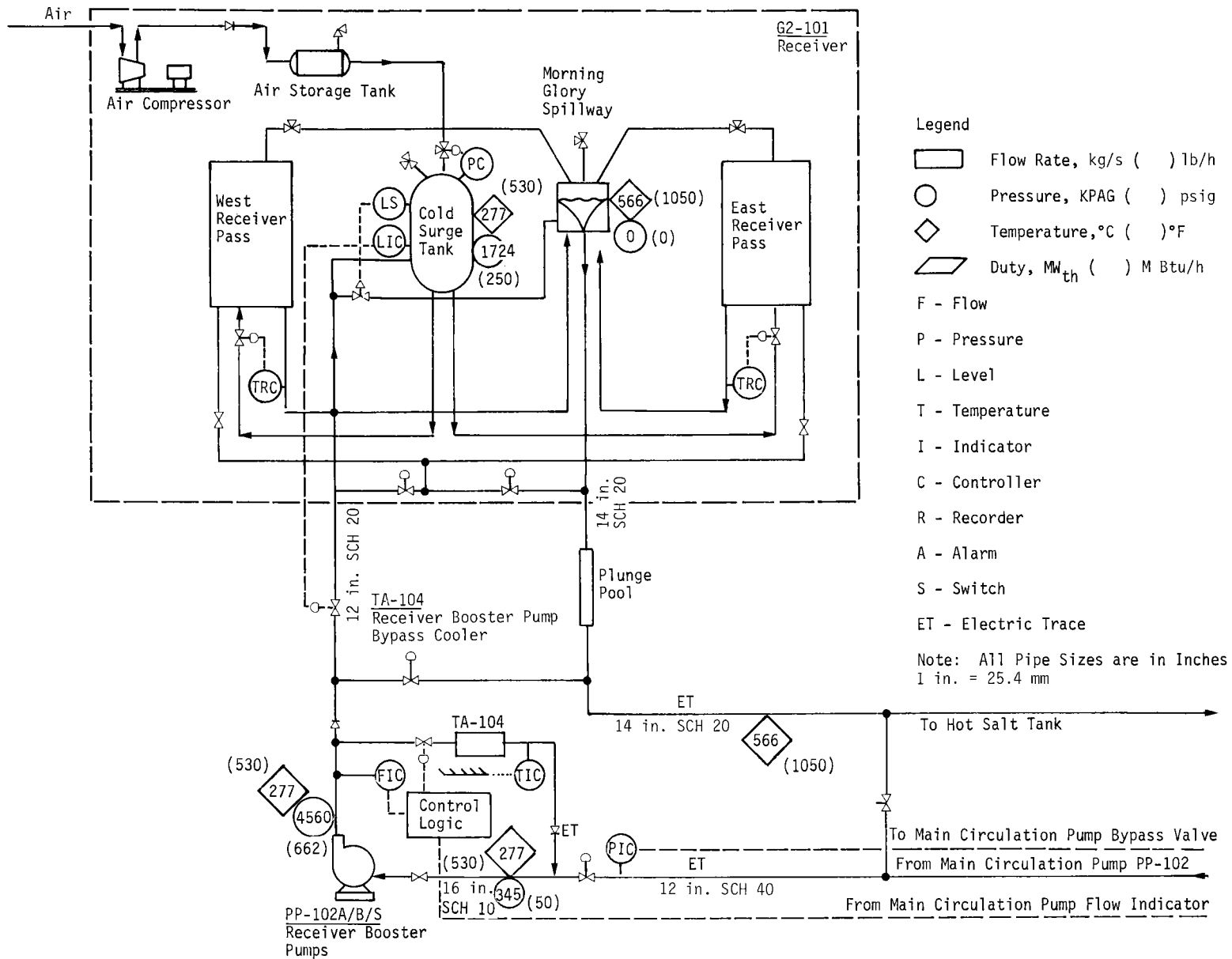


Figure 5.2-27 Receiver Supply and Return Piping

and piping is provided to allow salt from the receiver to flow to the drain tank in the case where the salt from the receiver is not sufficiently hot to introduce into the hot salt tank and is too hot for the cold tank. From the drain tank, this salt can be gradually worked off through the heat exchanger subsystem. Specifications for the pumps and the air-fin cooler can be found in Appendix C.

The receiver piping in the tower area is shown in Figure 5.2-28. Thermal expansion in the riser is accommodated by four expansion loops. The five sets of morning glory spillways and plunge pools used to control the descent of the salt from the top to the bottom of the tower are also shown. Each of the plunge pools is anchored so that the force of the falling salt as it enters the plunge pool can be transferred to the tower structure. The four lower morning glory spillways can move up and down to accommodate thermal expansion. The horizontal pipes will bend to accept this expansion. As the top spillway in the receiver has so many pipe connections, it also must be anchored. Thus expansion in the upper leg of the downcomer is accommodated by a bellows. The bellows has essentially zero pressure difference across it as the interior of the downcomer is vented to atmosphere.

The pressure head necessary to flow salt through the horizontal piping at 110% of design flow rate will cause the salt level in the downcomer to rise up to above the second (from the bottom) morning glory spillway. The relative location of the three booster pumps is also shown on the figure. Two pumps will provide 100% of design flow. The third pump is a spare that can be operated when it is needed.

All salt lines have been provided with an electric trace heating system for drying and preheating lines after long periods of shutdown and for emergency conditions when salt must be held in the lines for several days and circulation is not possible. Trace heating is not required during plant operation or for periods of diurnal shutdown. The tracers provided can supply over 100 watts per foot, more than enough for the required duty.

The optimum insulation thickness involves a tradeoff between the incremental cost of insulation over the minimum thickness required for personnel protection and the cost of heliostats that would be needed to replace the heat loss. The analysis is valid because the heat loss rate is a small fraction of the total plant heat rate. The optimum insulation thicknesses for 254 mm (10-in.) hot salt pipe and 305 mm (12-in.) cold salt pipes are 229 and 152 mm (nine and six inches) respectively. Total heat loss for this system with the specified insulation is 400 kW_t. The friction loss due to the high velocities in the hot salt line more than make up for thermal loss through the insulation of the hot salt line.

The general horizontal piping layout is depicted in Figure 5.2-29. An important item to note is that the horizontal piping from storage to the tower base has no expansion loops. Thermal expansion will be accommodated by the piping layout itself. This will permit as much as 12 m (40 ft) of expansion. The long sections of horizontal piping will be guided for most of their length so that motion is only axial. Near the elbows, the pipe will be allowed to bend. Most of the motion will be accommodated in the elbow near the tower. In that region, the two pipes will be suspended from trolleys that run on I beams.

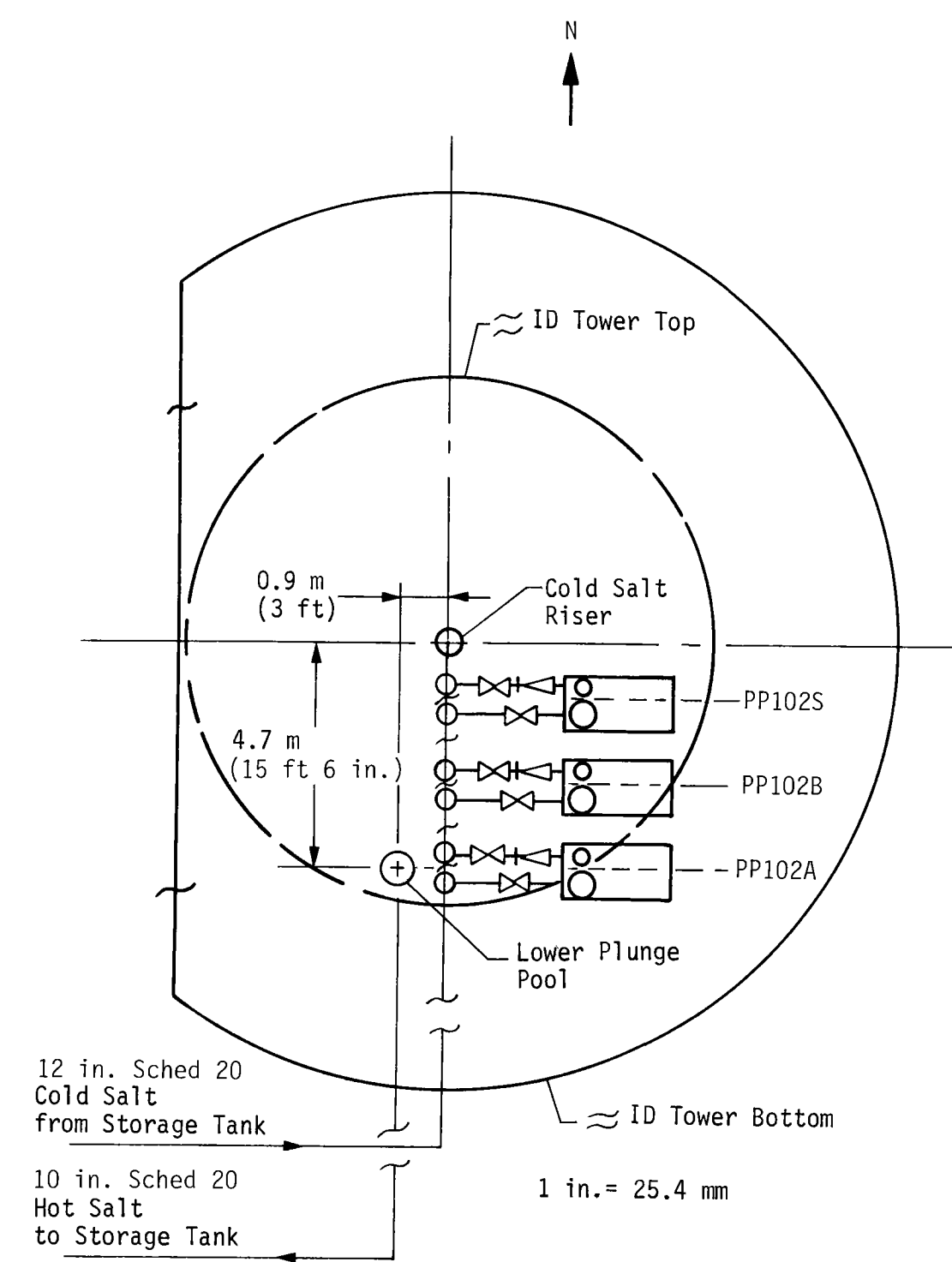
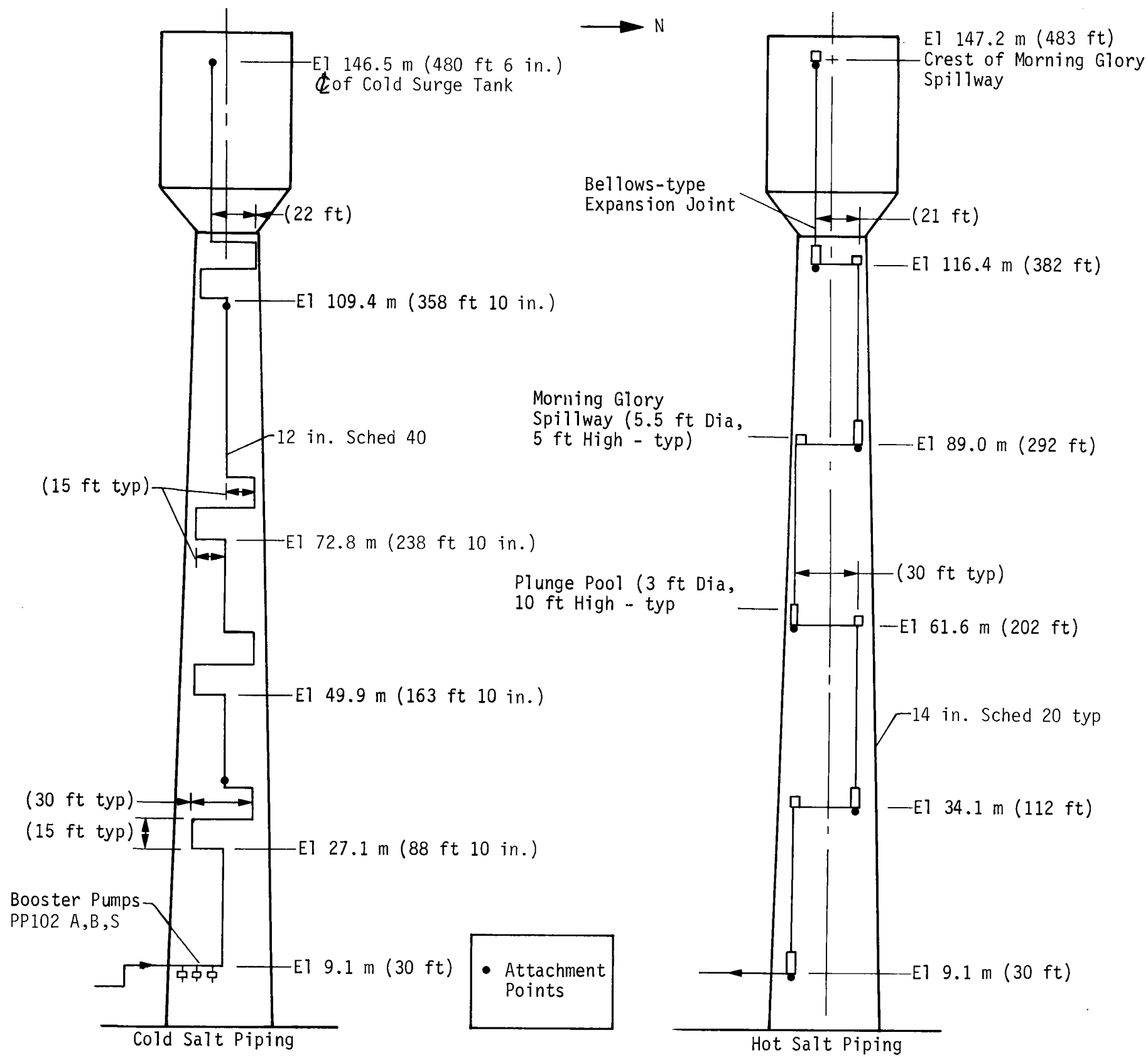


Figure 5.2-28 Tower Area Piping

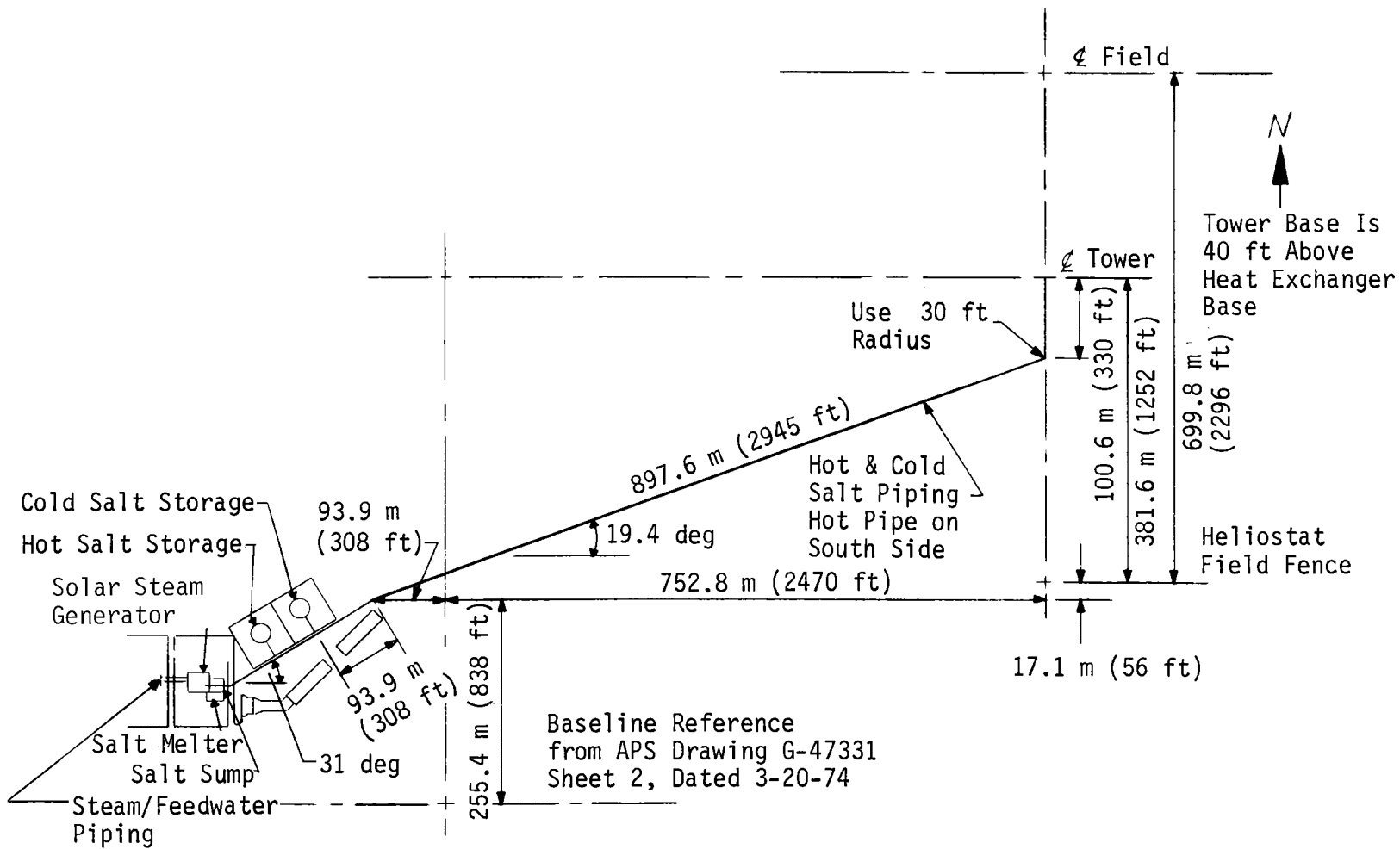


Figure 5.2-29 Salt Piping General Plot Plan

Vertical piping will include six conventional expansion loops. The booster pumps will be located 9 m (30 ft) above grade in the base of the tower. All lines are sloped to drain to the hot salt sump tank. From there, the salt is pumped to the drain tank. Fixed in-line pumps are provided at the low points around the main and booster pumps to drain the remnants of salt in the circuit.

- 5.2.4.3 Performance and Cost - The pumping and piping system has been designed with adequate controls and instrumentation to handle all flow rates between 5 and 110% of design capacity while minimizing operating costs. No difficulty is anticipated in meeting these requirements.

The estimated installed cost of the receiver circulating equipment and piping including instrumentation and controls, heat tracing, insulation and engineering is \$5,944,000 (1982\$). Details will be found in Chapter 6. Supporting data is in Appendix G.

5.2.5 Receiver Tower Design

This section describes the receiver tower design and discusses the supporting analyses influencing the tower design.

- 5.2.5.1 Receiver Tower Description - The reinforced concrete tower that supports the solar receiver, weighing 703,500 kg (1,551,000 lb) wet consists of a hollow truncated conical shaft integral with an octagonal mat foundation as shown in Figure 5.2-30. The conical shaft extends 121.5 meters (399 ft) above the top of foundation mat. Outside diameter of the concrete shaft is 16.75 m (55 ft) at the base and 9.96 m (32 ft-8 in.) at the top. Wall thickness of the concrete shaft at the base is 406 mm (16 in.) and it tapers uniformly to a thickness of 254 mm (10 in.) at the top. A large reinforced concrete ring beam which is integral with the shaft is provided at the top of the shaft in order to provide a seat for the receiver's steel support structure and base plates. A reinforced concrete floor slab is provided at the top of the shaft.

A room has been provided at the top of the tower for the air-compressor for the receiver cold surge tank and for the receiver control system air pressure compressor and storage tank. A smaller room at this level will contain the electronic equipment racks for the receiver controllers. The tower will be fitted with the appropriate lighting per Federal Aviation Administration requirements. An elevator has been provided for personnel and carrying smaller equipment to the top of the tower. The central area of the tower (near the vertical centerline) has been reserved for lowering and raising the larger receiver parts during repair operations. The three salt booster pumps will be mounted inside the tower, 9.14m (30 ft) above the foundation slab. The inside location will protect the pumps from the weather and the elevated location will simplify the fill and drain operations.

The reinforced concrete foundation mat, which is octagonal in plan, measures 33.5m (110 ft) between the parallel sides of the octagon. The mat is 3.0 m (10 ft) thick within and under the tower wall and tapers to 0.91 m (3 ft) at the perimeter. The bottom of the mat is located 4.6 m (15 ft) below the existing grade.

5.2.5.2 Receiver Tower Design Considerations - The receiver tower is designed to withstand the following lateral loads:

- 1) Wind loads corresponding to a maximum wind speed, including gust of 40 m/s (90mph). Wind loads are calculated in accordance with the requirements of ANSI A58.1 - 1972.
- 2) Seismic loads corresponding to the UBC Zone 2. Seismic loads are calculated in accordance with the procedure prescribed in the 1979 edition of the Uniform Building Code (UBC).

The tower bottom diameter, wall thickness and the mat plan dimensions and thicknesses are adequate to resist the maximum wind or seismic loads together with the gravity loads on the structure.

The size of the ring beam at the tower top is selected to suit the receiver support structure dimensions and to provide sufficient space for the elevator, piping, equipment and equipment hatch.

The calculated bearing pressure on the soil due to dead loads is approximately 143 kPa (3000 lb/ft²). From the site soil information available, it appears that the soil bearing capacity is adequate to support the tower loads.

The lateral displacement at the top of the tower under the operating wind speed of 14 m/s (31.5 mph) is expected to be less than the specified value of 12.5 cm (0.41 ft). The tower weight is 5.05×10^5 kg (1.11×10^7 lb) and the foundation weight is 6.03×10^5 kg (1.33×10^7 lb) for a total of 1.11×10^7 kg (2.44×10^7 lb) for the tower and foundation. These weights do not include the receiver weight.

5.2.6 Receiver Cost Summary

The cost of the various elements of the receiver subsystem are listed in Table 5.2-7. Further cost details may be found in Appendix G.

Table 5.2-7 *Receiver Subsystem Engineering and Construction Costs*
(1982 \$ x 10⁻³)

Cost Account	Element	Engr. Cost	Constr. Cost	Total Cost
5410	Receiver Unit	1,440	7,517	8,957
5420	Supply & Return Piping	648	5,296	5,944
5430	Heat Transport Fluid	negl.	249	249
5440	Tower	216	1,468	1,684
5450	Tower Foundation	252	1,594	1,846
5400	Total-Receiver s/s	2,556	16,124	18,680

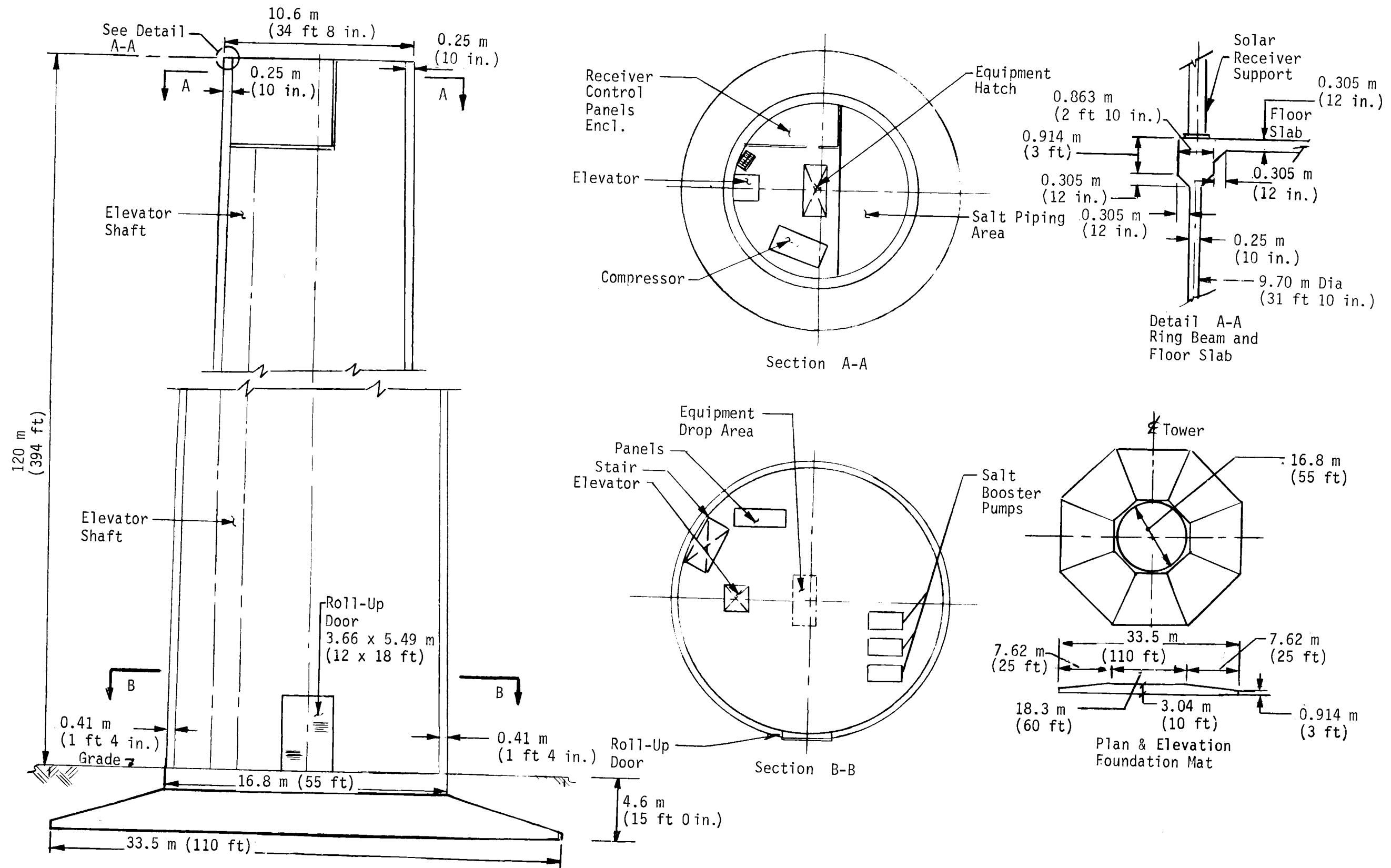


Figure 5.2-30 Receiver Tower

The master control subsystem (MCS) consists of an operational control subsystem, data acquisition subsystem, red-line units and a control subsystem for each of the major subsystems--collector, receiver, energy storage, fossil steam generator, electric power generation and solar steam generator. This general relationship is shown in Figure 5.3-1 where the APS dispatch center outline has been dashed to show that it is not a part of the master control subsystem. The man-machine interface (panel or CRT), computation type (analog or digital), method of performing computations (electronic or pneumatic) and communication method (electric, data bus, or pneumatic) are indicated for each of the control subsystem elements. The term data bus is used to include both the coaxial cable form and the optical fiber form. The arrangement shown for the data buses on the figure is only intended to show that data buses are used. The communication link arrangement is discussed further in paragraph 5.3.2. However, the detail specifics will be developed in the next contract phase. The figure shows the fossil steam generator and EPGS in the configuration recommended in paragraph 5.6.6. The fossil steam generator currently uses a pneumatic communications system, a panel board for display, and computations are done by analog pneumatics. The EPGS currently uses an electric communications system, a panel board for display, and the computation are performed by analog hydraulic and electric circuits.

It is recommended that APS upgrade the fossil steam generator and EPGS control systems to be compatible with the approach and specific equipment type used for the solar systems. This upgrading is not included as part of the repowering, costs. The discussion below assumes that APS will accept the recommendation and upgrade the two control systems. The red-line units are completely independent of the basic control and data acquisition subsystems. They are used to warn the operator of existing or impending emergencies. Corrective actions are taken through normal control channels.

The basic function of the master control subsystem is to sense, detect, monitor and control all system and subsystem parameters necessary to ensure safe and proper operation of the repowered Saguaro power plant. The emphasis in this study has been on the solar system related elements and their integration with the existing plant. Those parts of the existing plant that are to be upgraded are discussed in paragraph 5.6.6 with brief summaries of the existing systems included below. The master control system is applicable in all plant operating modes and transitions as discussed in paragraph 4.3. The basic philosophy used is supervisory control where the control system operates the plant automatically and the operator is only involved for out of tolerance operations and transitions between modes. The master control system is arranged so that it will fail safely and has redundancy. The distributed control heirarchy used means that each subsystem can be automatically controlled by itself if the operations control subsystem should fail, and each valve and actuator can be

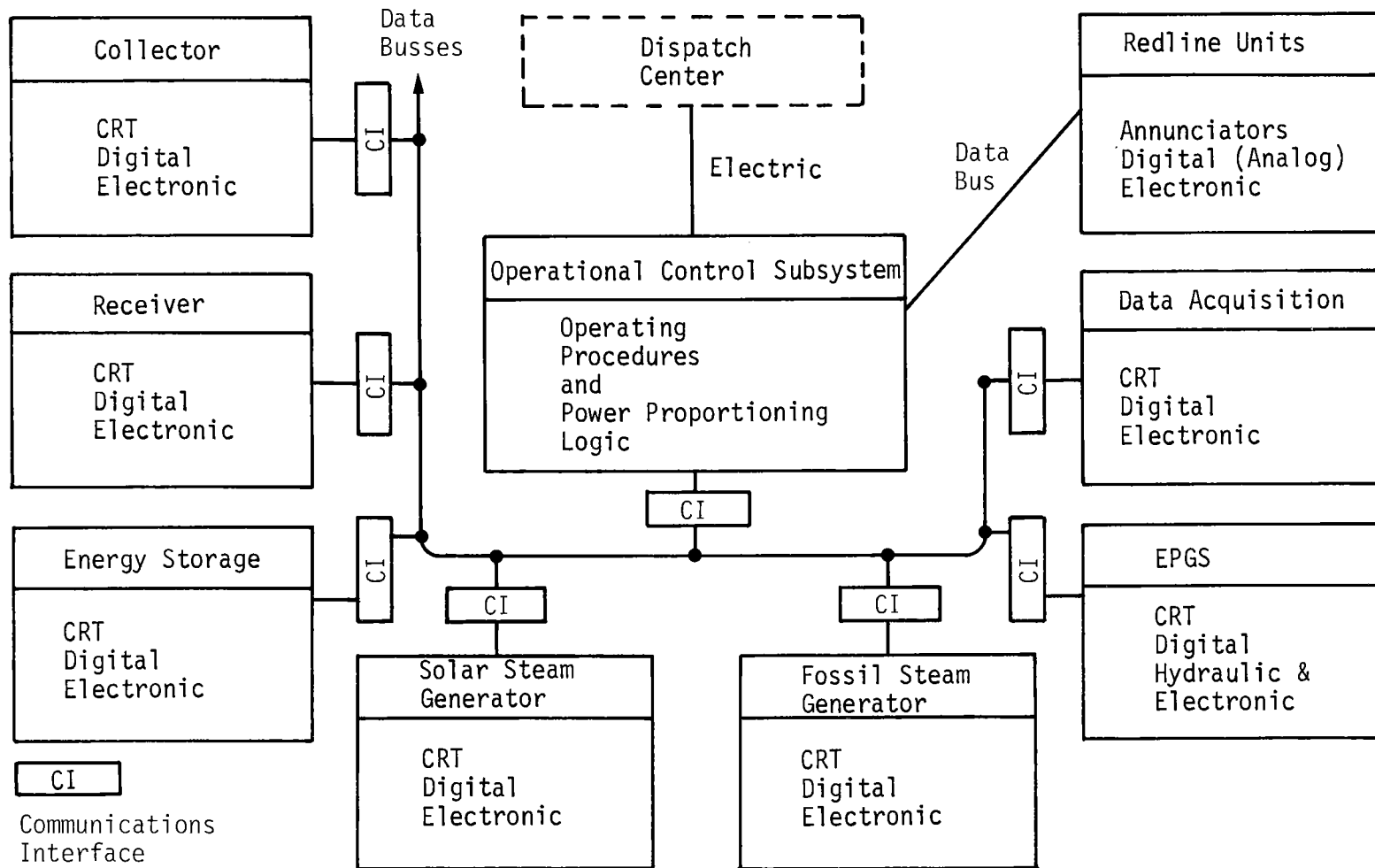


Figure 5.3-1 Master Control Subsystem Elements

positioned directly if the closed loop fails. Also each valve and actuator will have a selected fail safe position for when the pneumatic power, electric power, or the communication system fails.

Each control subsystem will consist of valves and actuators, sensors, communication lines, control elements, displays, operator input devices, interfaces with the equipments, and power supplies. The control elements will consist of microprocessors or minicomputers and will contain control logic, signal checking, transfer control (manual/automatic), output limiting, signal scaling, and signal conversion. Both electric and pneumatic valve actuators will be used. The operator interfaces will be located in an extension to the existing control room near the existing boiler, turbine, generator (BTG) panel for Saguaro Unit Two. The BTG board for Unit One will be removed. The collector subsystem displays and the CRT displays for the rest of the solar system, the fossil steam generator and the EPGS will be located on an L-shaped console array in the control room. The collector subsystem computer and the data acquisition subsystem, with computers and peripherals, will be located in a separate room adjacent to the control room. There will be separate subsystem control racks located near the sensors and actuators for the solar steam generator and for the energy storage subsystem. The control racks for the fossil steam generators and the EPGS can be located in part of the expanded control house as it is close to the equipment. The distributed nature of the receiver subsystem requires the use of three control racks-- near the main circulation pumps, near the receiver booster pumps, and in a room at the top of the tower adjacent to the receiver. Red-line units will be located in racks adjacent to the distributed subsystem control racks.

5.3.1 Master Control Subsystem Requirements

Requirements for the master control subsystem are divided into three classifications: (1) the general system requirements including those adapted from the original form of the Subsystem Requirements Specification, (2) environmental requirements, and (3) those requirements derived during the course of the two studies. All of the requirements can be met by the general master control subsystem configuration identified below. Emphasis has been placed on operability of the solar repowered plant and on maximizing the probability of successful operation.

5.3.1.1 General Requirements - These general requirements were established by the nature of the system, or were adapted from the original form of the System Requirements Specification.

- 1) Shall conform to the applicable codes and standards defined in Revision B of the System Requirements Specification (Reference 1-3) and with those IEEE standards, recommended practices, and application guides that are appropriate.
- 2) Shall provide safe and effective operation for all steady-state modes, transitions between modes, and emergency shutdowns.

- 3) Shall provide access for maintenance and inspection and shall provide for crew safety.
- 4) Shall be designed for a 30-yr operating life.
- 5) Shall have design simplicity, and the receiver, energy storage, and solar steam generator control systems shall resemble standard power plant or process heat control systems by use of:
 - a) Standard control practices;
 - b) Simple, well defined interfaces between the operational control subsystem and the other plant subsystem controls.
- 6) Shall have operational simplicity using the supervisory control philosophy (primary operation to be automatic with operator override capability) and have:
 - a) Centrally located control consoles for both automatic and manual operations;
 - b) Easily read displays;
 - c) Easily operated manual inputs.
- 7) Shall incorporate design reliability by:
 - a) Use of proven designs;
 - b) Elimination of single point failures through redundant elements whenever it is cost effective to do so.
- 8) Shall incorporate operational reliability:
 - a) Separation of plant operation controls from data acquisition and evaluation equipments and from peripheral controls within the master control subsystem and designing for independent operation of each subsystem control system;
- 9) The design shall be cost-effective based on:
 - a) Selection of off-the-shelf equipment;
 - b) Use of modularity among the major subsystems of the master control subsystem;
 - c) Use of generically similar equipment in the control systems for the receiver, energy storage, solar steam generator, fossil steam generator, and electric power generation subsystems.

5.3.1.2 Environmental Requirements - The applicable environmental requirements for operation and for survival of the master control subsystem are given in Chapter 4, Environmental Criteria, of Revision B of the System Requirements Specification. (Reference 1-3).

5.3.1.3 Derived Requirements - The following requirements were derived in the course of the study for the master control subsystem:

- 1) Sense, detect, monitor, and control all system and subsystem parameters.
- 2) Control all parts of the repowered plant in all steady-state operating modes and all transitions between modes.
- 3) Provide for steam generation from solar system alone, fossil system alone, or both systems together in selectable proportions.
- 4) Adapt the existing interface with the APS central dispatch system so the power level can be changed remotely.
- 5) Control of the collector subsystem shall be an extension and adaptation of the system being developed for Solar One at Barstow, CA.
- 6) The control system for Unit One may be different from the control system for Unit Two.
- 7) Control of the collection and storage of solar energy shall be decoupled from the control of the use of the stored thermal energy.
- 8) Provide the necessary sensors, communications, annunciators, and logic for proper and effective corrective actions.
- 9) The data acquisition subsystem shall interface with all elements of the master control system in a noninterfering manner.
- 10) The existing fossil steam generator subsystem and existing electric power generating subsystem controls shall be upgraded to be compatible with the solar system controls. Modifications of these controls to interface with the operational control subsystem is included in the repowering project. However, the upgrading of these control systems is not a part of the repowering project.
- 11) Control CRTs will display appropriate subsystem fluid flow diagrams when that display mode is selected.
- 12) CRT or video displays with keyboard controls shall be included for control of the collector, receiver, energy storage, solar steam generator, fossil steam generator, EPGS, and operational control subsystem.

- 13) Provide for additional data collection during the demonstration phase on a digital, computer-controlled basis.

5.3.2 Design Description

The master control subsystem is composed of seven subsystem control systems plus a data acquisition system and the red-line units. The specific subsystems being controlled are: (1) collector, (2) receiver, (3) energy storage, (4) fossil steam generator, (5) electric power generation, and (6) solar steam generator. These six are coordinated and interrelated by the operational control subsystem that also provides the interface with the APS central dispatch office. The red-line units are an alarm monitoring and reporting system. APS has considered a number of alternatives for control of Unit One as compared to Unit Two and has asked that a plan and cost estimate be prepared for upgrading of the Unit One control system only. The old Unit One control equipment could be used as spares for Unit Two, there will be less chance of unit misidentification, and the lifetime of the Unit One controls will be commensurate with the lifetime of the solar system controls.

A control subsystem has been developed for the collector field subsystem for Solar One at Barstow, CA. A review of the characteristics of that collector control subsystem (CCS) indicates that it will provide an excellent base for expanding to meet the needs of the Saguaro CCS. The heliostat array computer (HAC) at Solar One does not have the capacity to be extended from 1818 heliostats to 5000 heliostats. It is planned to add a new level, called a heliostat line controller, in the collector control hierarchy. Thus it was decided to use the extended Solar One CCS concept for Saguaro. The fossil steam generator and EPGS control system upgrading is discussed in paragraph 5.6.6. This leaves only the receiver, energy storage, solar steam generator, and operational control subsystems to be conceptualized, along with the data acquisition subsystem and the red-line units.

Table 5.3-1 summarizes the major characteristics of the elements of the master control subsystem. When the controls of the two existing subsystems are upgraded, then it is possible to use the same computational technique, communication method, and display and controls for all of the control systems and the DAS. The red-line units will use digital signals (mostly on/off), but will use separate hard lines for data communication and will display results on annunciators.

The overall design approach for the master control subsystem is the supervisory approach where normal control is completely automatic and the operator intervenes only for exceptions. In addition to the usual warning and emergency categories, the operator will be involved during start up and shutdown, and during the transitions between steady-state operating modes. When all equipment is operating properly, control will be from the control room. It will also be possible to do some control activities from the racks that contain the control electronics in the various parts of the plant.

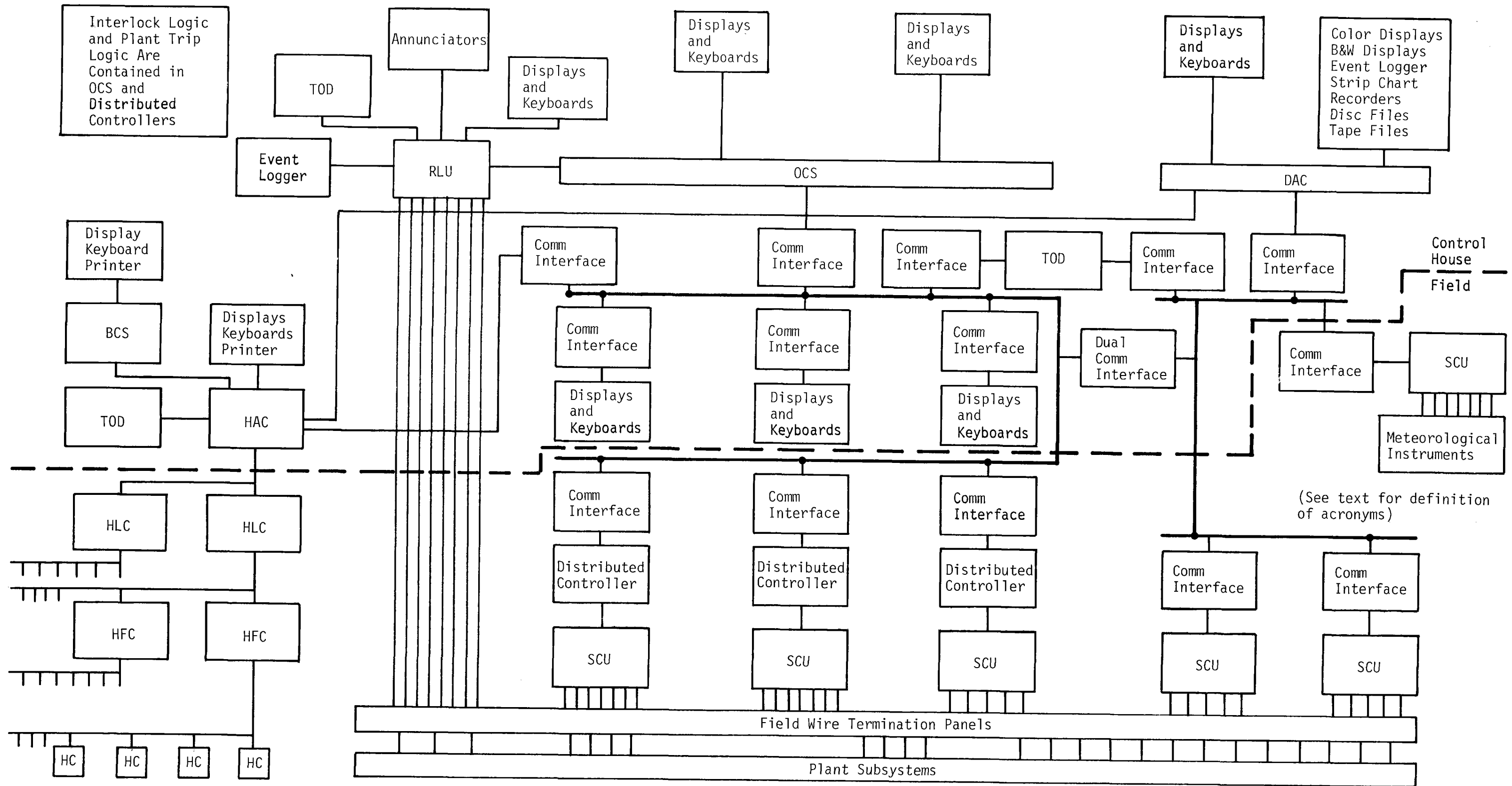


Figure 5.3-2 Master Control Subsystem Hierarchy

a special data bus because data is dumped from the HAC only once a day or on special request.

For critical function monitoring, the RLUs get data directly from the plant by hard lines. The RLUs primary output is to annunciator panels. However, warnings will also cause the OCS displays to flash and the event logger will print out the sequence of events. TOD is also used by the RLU. A number of monitoring activities will be undertaken by the distributed controllers and the DAS. Any alarms from these systems will appear on the OCS display and the DAS event logger.

Startup, shutdown, and other transition procedures will be stored in the OCS and presented on the OCS displays. The interlock logic, e.g. do not move heliostats onto the receiver until the cavity doors are open, will be incorporated in the OCS and the distributed controllers. Similarly, the plant trip logic, e.g. loss of feed water pump pressure trips the turbine and shuts off both the fossil fuel flow and salt flow, will be contained in the OCS and the distributed controllers.

The control and data acquisition systems will each have redundant data buses for greater reliability. While the data buses are considered to be coaxial cable, in our conceptual design, the commercial availability of fiber optics data buses should be considered during the detailed design. Fiber optics are immune to electromagnetic interference and their costs are dropping significantly. Effective connection methods for fiber optics are also being developed by industry. The Martin Marietta second generation heliostat control system uses fiber optics for all of its field communications. Communications on the data buses will be in a form that maximizes the likelihood of important messages being sent quickly. The data bus operating philosophy will be "masterless" or "peer-to-peer" to enhance the distributed aspects of the MCS and to increase overall reliability. Failures of control room equipments will cause control to revert to the distributed local controllers. The displays and keyboards shown towards the center of Figure 5.3-2 can be used to control specific subsystems through the data bus. Local controller failure will cause the system to switch automatically to a backup controller or to a shut down condition. All failures are reported back to the control room, recorded and printed. All control valves will be pneumatically or electrically controlled and will fail to a safe position. The local controllers can also be transferred from automatic to manual control for startup, shutdown, or other transitions.

The general layout of the control room, including the solar equipment, is shown in Figure 5.3-3. The existing control room layout has the Unit Two boiler-turbine-generator (BTG) board and the switchyard control panels in locations where they can be left in place. The Unit One BTG board has been removed and the control room will be expanded to 12.2m (40 ft) x 15.2m (50 ft). The new control console for all of the solar systems and the upgraded Unit One control system has been adapted from that used for Solar One. The EPGS controls are near the Unit Two BTG board and are flanked by the fossil and solar steam

Table 5.3-1 Master Control Subsystem Characteristics

Subsystem	Functions Being Controlled	Interfaces	Computation Technique	Communication Method	Display/Control Approach	Data Recording Method
Operational Control Subsystem (OCS)	Coordinates other subsystem controls, proportions power between solar and fossil, and interfaces with central dispatch	All other Control Subsystems, DAS, and Central Dispatch	Digital	Data bus	CRT Display and Keyboard Input	Strip Charts, DAS
Collector Control Subsystem (CCS)	Controls heliostats including activation, stow, washing, beam characterization	OCS RCS DAS	Digital	Data Bus	CRT Display and Keyboard Input	DAS Event Logger
Receiver Control Subsystem (RCS)	Main Circulation Pumps, Booster Pumps, Receiver, Salt Return	OCS CCS DAS	Digital	Data Bus	CRT Display and Keyboard Input	Strip Charts, DAS
Energy Storage Control Subsystem (ESCS)	Foundation Coolant Flow, Salt Reprocessing, Salt Melting, Drain Tank Level	OCS DAS	Digital	Data Bus	CRT Display and Keyboard Input	Strip Charts, DAS
Fossil Steam Generator Control Subsystem (FSGCS)	Feedwater Flow, Fuel Flow, Air Flow, Superheat Temperature, Blowdown Flow	OCS EPGCS	Digital	Data Bus	CRT Display and Keyboard Input	Strip Charts
Electric Power Generation Control Subsystem (EPGCS)	Fossil Steam Flow, Steam Admission, Circulating Water Flow, Condensate Flow	OCS FSGCS	Digital	Data Bus	CRT Display and Keyboard Input	Strip Charts
Solar Steam Generator Control Subsystem (SSGCS)	Solar Steam Flow, Feedwater Flow, Hot Salt Pump, Salt Recirculation Pump, Water Recirculation Pump, Solar Steam Temperature, Blowdown Flow	OCS EPGCS DAS	Digital	Data Bus	CRT Display and Keyboard Input	Strip Charts DAS
Red-line Units	Independently monitors all critical plant functions and warns operator	OCS DAS	Digital	Hard Lines	Annunciators	Event Logger
Data Acquisition Subsystem (DAS)	Data Collection and Processing	All Other Control Subsystems	Digital	Data Bus	CRT Displays and Keyboard Input	Magnetic Tape Disc Storage Event Loggers

The overall hierarchy of the master control subsystem is given in Figure 5.3-2. Only a few of some kinds of equipment, such as distributed controllers, are shown in order to keep the diagram from becoming excessively cluttered. Three basic hierarchies are shown: (1) control involving the operational control system (OCS), (2) data acquisition involving the data acquisition computer (DAC), and (3) critical function monitoring involving the red-line units (RLU). The control hierarchy starts with the man/machine interface with the OCS through CRT displays and keyboards. The OCS communicates with the distributed controllers (one or more for each subsystem) through a data bus that links the OCS, distributed controllers, displays and keyboards for each of the distributed controllers, time-of-day (TOD) clock, the heliostat array controller (HAC), and the data acquisition computer (DAC). Each component is connected to the data bus through a communications interface (CI) element. A separate data bus is used for the data acquisition system (DAS) to avoid overloading the controller data bus with all of the engineering data to be collected during the demonstration phase. The heliostat array computer (HAC) of the collector field can be thought of as a distributed controller. Each distributed controller except for the HAC communicates with its part of the solar or existing system through signal conditioning units (SCU) and the field using termination panels. Generally a single wire on the diagram corresponds to a data bus and multiple wires correspond to individual hard wires. The equipment shown above the heavy dashed line is in, or near, the control house and those below the line are distributed around the plant.

The collector subsystem hierarchy is arranged like a tree with the HAC at the top. The HAC feeds two heliostat line controllers (HLCs) which are an extension from the Solar One concept to permit handling the larger number of heliostats. The HLCs take some functions from the HAC, to relieve a timing condition. Each HLC feeds multiple (up to 128) heliostat field controllers (HFC). Each HFC in turn feeds up to 32 heliostat controllers (HC). There is an HC in each heliostat. The HAC also interfaces with the precision clock/receiver to obtain time of day (TOD) and with the beam characterization system (BCS). The BCS and the HAC each have their own CRT displays, keyboards and printers. All data buses in the collector control subsystem are dual redundant and all field buses use fiber optics. The CCS is unique in that it performs all three activities of control, data acquisition, and critical function monitoring. Both the HAC and each HLC are redundant with redundant communications to increase system availability.

Data is collected by the data acquisition system (DAS) using a number of SCUs located in the field, by indirect interfaces with the OCS and the RLU (through OCS) and by direct interface with the HAC. The DAS controlled SCUs collect data directly from the plant subsystems, indirectly from the distributed controllers, and directly from meteorological instruments. A variety of methods for processing, displaying, and archiving data will be included. A single TOD is used to feed both the OCS and the DAC. The DAS has its own data bus where each data collection area has an SCU and communications interface. A dual communications interface is used between the two primary data buses. The collector data is communicated directly to the DAC by

Figure 5.3-3

5-85

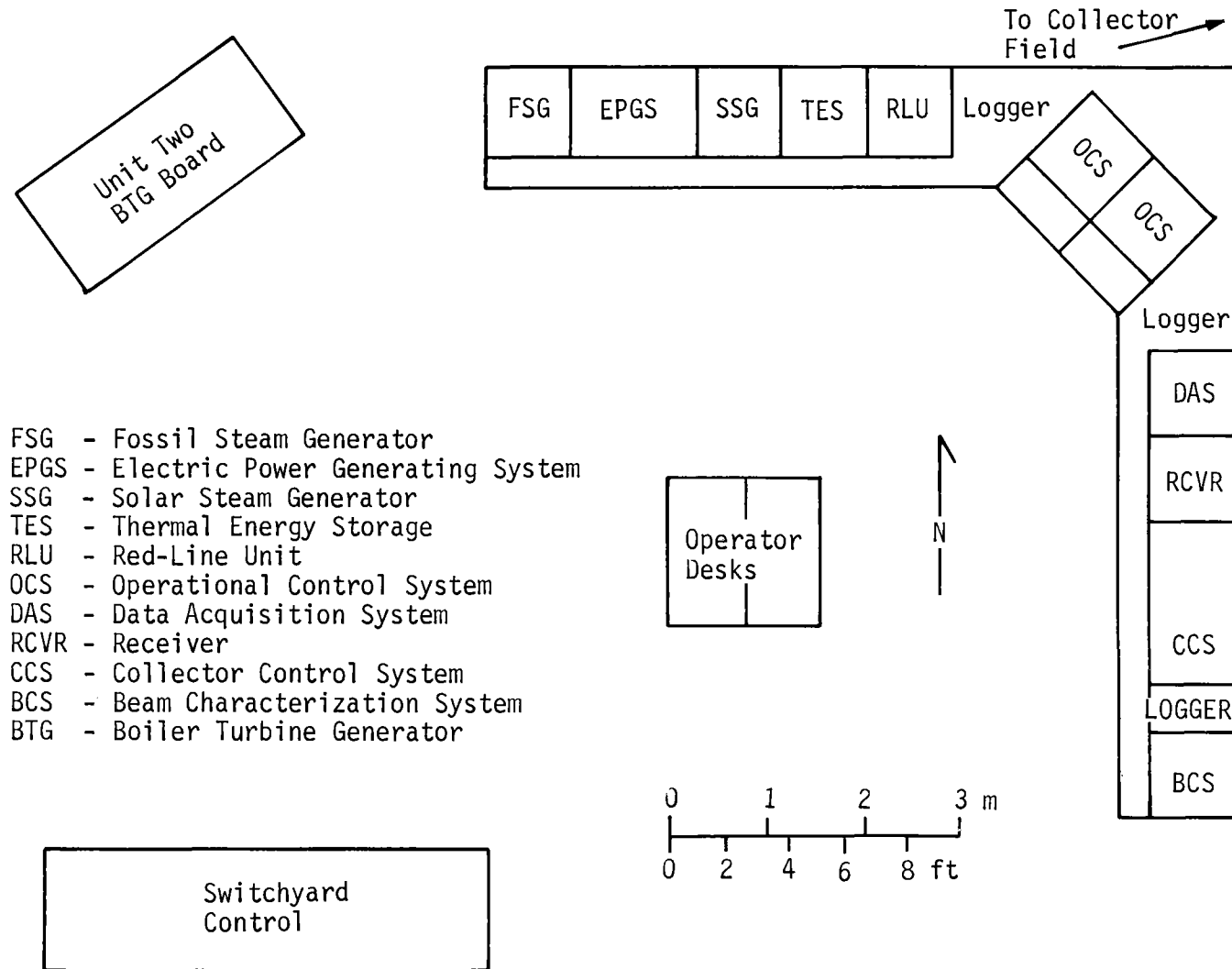


Figure 5.3-3 Control Room Layout

generator controls. The red-line unit displays are next to the OCS displays which are in the middle of the console as they are the primary control station. The DAS operator selectable displays are also located next to the OCS displays. The receiver controls are located next to the collector control system displays. The CCS has been allocated additional space for multiple displays. One display can be used to work with the BCS which is adjacent to the CCS. Three event loggers have been provided: RLU, DAS, and CCS/BCS. The open configuration of the console provides adequate room for multiple personnel during checkout, easy access to Unit Two and switchboard controls and good visibility from a visitors room that could be located just south of the region shown. There is adequate space for expanding the control room to the east and the south.

The data acquisition system, its console, and the computers in the master control subsystem will be located in an adjacent room. Space will also be provided in the adjacent room for DAS operator desks and DAS peripherals. Annunciators will be mounted as part of the RLU display and with other displays as appropriate. Trend chart recorders will be located with the DAS peripherals. The collector control subsystem console will have three color video displays with a keyboard input. Two of the displays will be used for status and one for communication with the heliostat array computer. Appropriately labeled individual keys are used for the more common control actions. Special annunciators will be located above the video displays. Warnings will also be flashed on the video screens.

Each of the consoles will be configured in the same general way in that they would have one or two color video displays. Operation would be on a menu basis where the machine displays a menu of options. The operator chooses one, such as receiver operation, the machine then presents another menu from which the operator selects the next activity. This way, the operator can go to any level of operation of any element of the solar system quickly and can display those ancillary functions that are most useful for the particular activity he is doing. While the OCS will be set up to display data from itself or any subsystem the individual subsystems will also be able to display only their own data. The two OCS displays and keyboards will provide the necessary redundancy for the OCS and the several subsystem displays and keyboards will provide redundancy for each other. It is also recommended that the startup, shutdown, and all transition procedures be stored in the minicomputer associated with the OCS. The machine can then lead the operator through any of these procedures and confirm the operator's verification that the desired actions happen in the desired order and if any unwanted actions occur. The ability of the video-console to present many and different kinds of displays is a powerful characteristic that should be used effectively.

The specific amount of redundancy to be used as well as the form of the redundancy will be determined in a later phase of the program. The use of "auctioneering" where the middle value of a set of three is used, or 1 of 2, or 1 of 3, redundancy considerations will be considered for application to critical functions. The number of redundant data buses, 1 or 2, and the way of using the redundancy

will also be addressed. However, as failures in a solar system do not always have severe penalties, the cost of establishing redundancy will also be considered.

In addition to the normal control operations described below, a number of other features will be included in the various control systems. These include items that fall under the heading of cutback control such as pump overtemperature, motor overtemperature, low pump suction pressure, high tank pressures, tank high levels, etc. These kinds of parameters will be measured and used to cut back system operation to a safe level and to warn the operator through the RLU or DAS systems. Dual power supplies will be used with battery/inverter supplies (uninterruptable power system) for critical elements. Critical parts of the master control subsystem can also be switched to the backup diesel generator when both of the basic electrical power systems have failed. Similar redundancy will be provided for the control valve compressed air supplies.

5.3.2.1 Operational Control Subsystem - The operational control subsystem (OCS) interconnects and interrelates all of the other control subsystems, the data acquisition subsystem and the APS dispatch center. Major characteristics of the operational control subsystem are listed in Table 5.3-2. While it would be difficult to identify the specific procedures and equipment that make up what we call the existing operational control system, the operational control functions are being performed. With the addition of the solar components, it is useful to formalize the body of equipments and procedures under the heading of "operational control subsystem."

Table 5.3-2 Operational Control Subsystem Characteristics

Extension of Existing Operating Equipment and Procedures
Determines Operating Mode/Transition for Each Subsystem
Contains Rules/Algorithms for Mode/Transition Selection
Configures Subsystems for Steady-State Operation in Various Modes
Contains Procedures for All Transitions between Modes, Startup, and Shutdown
Responds to Central Dispatch Requests for Power Changes
Proportions Requested Power between Solar and Fossil Steam Generators
Monitors Total System for Abnormal Conditions
Responds to Emergencies
Provides Data to Data Acquisition Subsystem

The existing OCS ties the boiler, turbine, generator, circulating water, condensate makeup, dispatch center, etc., into an operating entity. These functions are extended to the solar system elements. Because of this blend of the old and the new, the specific hardware expression of the OCS will be developed during the preliminary design phase. However, the functional capabilities of the OCS can be described here.

A set of rules, algorithms, and procedures will be developed that can be used to define what part of the system should be operated in what mode, and when. An example is the rules used to determine when the receiver should be shut down for the day. Considerations include: expectation of insolation above minimum operating level including cloud cover, hot storage tank salt level, expectation of continued solar steam generation for the day, equipment condition, and maintenance schedules. Rules will be developed based on similar considerations for each subsystem, for each mode and transition, and will be made a part of the OCS procedures. These procedures will be written and stored in a disk memory of the OCS.

The configuration of each subsystem for each steady-state mode, and the procedures for the transitions between modes as well as for start-up and shutdown will also be developed and made a part of the OCS. Preliminary operating procedures are presented in Appendix B. The diurnal nature of the solar resource makes transitions between modes a more common occurrence than the current practice for power plants. Normally a turbine is only started a few tens of times a year and is kept operating the rest of the year even if its level of operation may be changed several times a day. However, the solar receiver will be started and stopped at least once on most days. Thus the need for greater emphasis on transitions between steady-state operating modes.

The decision process on whether to attempt to collect, or to stop collecting, solar energy on a particular day is a part of the OCS. If the sky is clear of clouds near the sun, then energy should be collected. If the sky is overcast for a large region around the sun, then the receiver should be put into the standby mode. The decision is not so easy for intermittent clouds. The use of a solar coronagraph is suggested as an aid to the operator. The coronagraph could take the form of a sun-tracking TV camera with an opaque area in the center that would block out the sun's image and a small, 0.02rad, region around the sun. The overall field of view of the camera would be 0.52rad. The operator would view his display and determine if there were any clouds in the sky that were going to obscure the sun. A series of circular rings on the TV display and a stop watch would permit the operator to estimate the time interval before he would have to make a judgement about whether to shut down the receiver. The operator would also be able to switch the coronagraph from sun-tracking to a programmed path if the sun-sensor tended to lock onto bright clouds. It is likely that the operator would soon become skillful in establishing when to operate the receiver through intermittent clouds and when to put the receiver into standby.

The fact that the solar system is not operated at night or on cloudy days means that there are time periods when the normal controls and displays are not being used. It is suggested that the DAC be sized to permit it to include simple dynamic models of each subsystem. Then these models could be interconnected with the normal displays and controls to make an effective system trainer. The trainer could be used for initial operator training before plant start up as well as for new operator training. The only additional costs would be for some interface units to feed the simulated plant response signals to the various controllers and software programming. Motions of plant actuators could be inhibited by disconnecting the actuator or by shutting off power to the actuator.

The repowered plant is conceptualized to be able to operate in solar alone, fossil alone, or solar and fossil together in selectable proportions. The desire for combined operation means that the generation level requested by central dispatch must be proportioned between the solar and fossil systems. This proportioning is an OCS function and an example is shown in Figure 5.3-4. For this example it is assumed that the fossil system is operating on a 24-hr a day basis, and it is desired to share the steam generation load so at full load the fossil system provides 70 MW_e and the solar system provides 45 MW_e with the same proportion used over most of the operating range. Because the fossil system is the reference in this example and its minimum level is 30 MW_e , there is an exclusion zone from zero to 30 MW_e . The solar system has a minimum level of 25 MW_e , so it cannot be used until the total load is 55 MW_e . Thus only the fossil system is scheduled over region A to B. The solar system comes on at point B where the fossil system is cut back to 30 MW_e . The solar system is held constant at 25 MW_e from B to C while the fossil system picks up its share of the load until the desired proportion is obtained at point C. Between points C and D the load is shared in the desired proportions between solar and fossil. Different forms of this diagram on Figure 5.3-4 are obtained if solar is considered basic and dispatched first or if the proportioning level is changed, or if one steam source is held constant as the other is changed. All of these options will be provided in the OCS steam proportioning system.

- 5.3.2.2 Collector Control Subsystem - The collector control subsystem (CCS) will be based on the technology, philosophy, equipment and software being developed for the Solar One or Barstow 10- MW_e Pilot Plant Collector Subsystem. Modifications to this system for Saguaro will be in terms of more heliostats, larger heliostats, different field layout, addition of heliostat line controllers, and different interfaces with

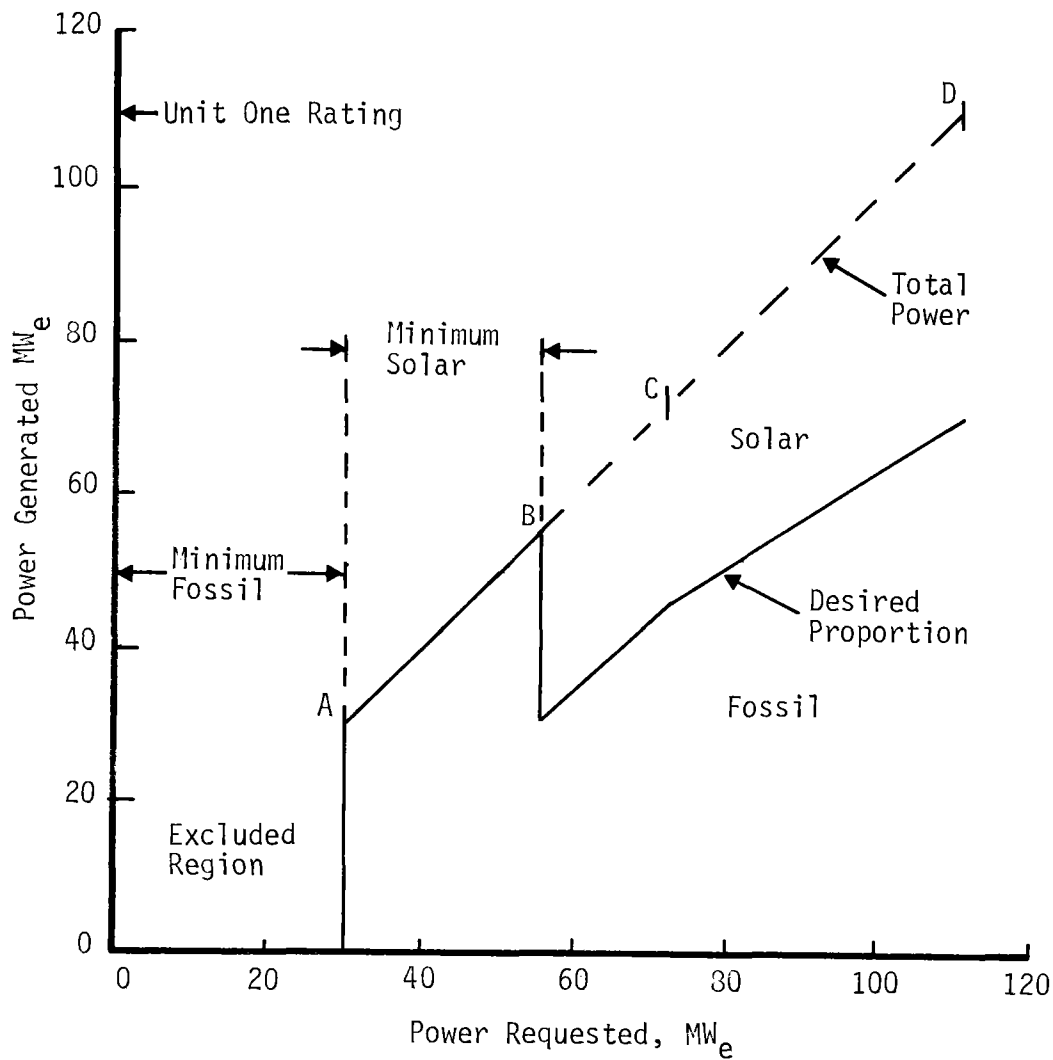


Figure 5.3-4 Example of Steam Generation Proportioning

the operational control subsystem. The CCS general characteristics are given in Table 5.3-3. The CCS control philosophy is automatic with direct control by exception, or supervisory; which is identical with the overall MCS control philosophy. The control console uses color video displays and keyboard inputs and the CCS uses all digital data bus communications. There are external displays, flashing displays on the video screen, and audio alarms for warning purposes.

Table 5.3-3 Collector Control Subsystem Characteristics

All Operator's Console Displays are Alpha-Numerics

Auxiliary Displays of Total Field Status and Selectable Field Segment Status

Collector Field Divided into Segments, Rings, and Wedges

Operator's Console Displays: Alarms, Warnings, Status, and Commands

Time Base is Included

Redundant Modcomp Computers

MAXNET IV Operating System

Asynchronous Data Links

Data Logging via Disk and Hard Copy

One Major Data Dump to Data Acquisition System Each Day

The interfaces with the OCS are in terms of defining which heliostats should be in use for what function. The OCS is also required to monitor wind velocity to initiate heliostat stow at a wind velocity of 15.6 m/s (35 mph). An interface with the RCS will also be established to initiate emergency heliostat stow as well as heliostat turn down when the insolation level exceeds receiver capability. Time of day is established by a quartz clock and a receiver that is tuned to station WWV. The WWV signals are used to correct the quartz clock. Similar time of day systems are used for the OCS, DAS, and RLU. Local (CCS console) modes include:

- 1) Field activation;
- 2) Stow;
- 3) Position for wash;

- 4) Position for beam characterization;
- 5) Position for maintenance;
- 6) Emergency actions.

The heliostats can also be controlled at their locations by a portable controller called a stimulator. This technique is used during maintenance. A beam characterization system is used to determine the geometric center and the dispersion of the reflected beams from each heliostat. The heliostats are evaluated one at a time by having them reflect their beam on a large flat target such as an open cavity door. An improper beam dispersion is corrected by realigning the heliostat's mirror facets. The location of the geometric center of the reflected beam is used to compute bias signals for that heliostat. To properly correct for the three components of pedestal alignment, three bias components must be determined. The bias computations are performed in the BCS controller and are stored in the HAC. After initial determination of the biases, they only need be verified once a year or after major maintenance activities.

5.3.2.3 Receiver Control Subsystem - The receiver control subsystem (RCS) involves control of the main salt circulation pump flow, the salt booster pump flow, salt flow through the receiver, and selection of hot, cold or drain storage tanks for return of hot or warm salt. The system is normally in a sun following mode so that the salt flow will be matched to the amount of available solar energy. The OCS will determine when solar energy should be collected. The collector field will be controlled to maximize the amount of energy reflected into the receiver cavities and the receiver will be controlled to absorb the incident energy safely. The OCS interfaces with the RCS for startup and shutdown, and the RCS interfaces with the CCS to initiate heliostat turn-down or defocus depending upon the degree to which the receiver cannot safely accept the incident energy.

A schematic of the control approach used for supply of cold salt to the receiver and the return of hot salt to energy storage is shown in Figure 5.3-5. A cold surge tank and a morning glory spillway are provided in the receiver. The cold salt surge tank decouples the supply of cold salt from the use of salt in the receiver. The morning glory spillway decouples the return of salt to energy storage from the flow of salt through the receiver. As the cold surge tank is charged to 2.72 kPa (380 psig) and the morning glory spillway is at atmospheric pressure a relatively constant pressure difference has been established for control of salt flow through the receiver. This decoupling approach has been taken because of the long horizontal pipe lines between the energy storage area and the receiver tower and the large inertia of the salt in these lines. A secondary advantage is the use of the cold salt surge tank pressure to maintain continuous salt flow through the receiver in spite of several different kinds of pump, valve, and electrical failures.

Figure 5.3-5

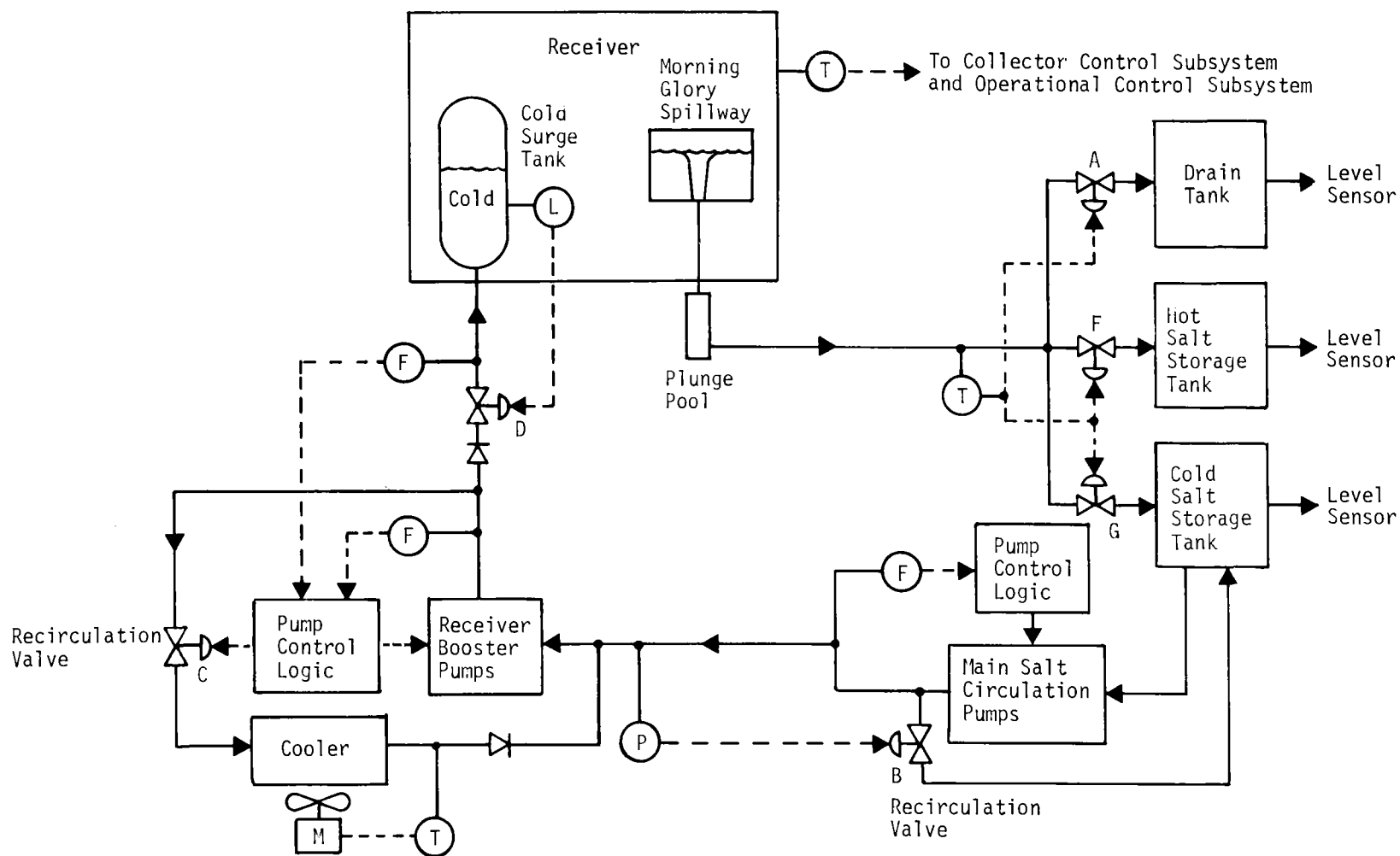


Figure 5.3-5 Control Diagram for Receiver Salt Supply and Return

Supply of salt to the receiver from the the cold salt storage tank is accomplished by two sets of pumps operating in series. The main circulation pumps are located near the cold salt storage tank and the receiver booster pumps are located near the base of the receiver tower. The primary controlled variable for the main salt circulation pumps is inlet pressure at the booster pumps. There are three main circulation pumps, any two of which can provide design flow. A flow sensor in the cold salt horizontal piping is used to select the number of pumps to be operated. Flow control is accomplished by measurement of booster pump inlet pressure and feeding that signal back to recirculation valve B. The excess salt flow is then bypassed back to the cold salt tank. This approach avoids the head loss associated with a series control valve. It also provides for flows well below the normal minimum flow point for centrifugal pumps. When centrifugal pumps are operated below one third of design flow they tend to overheat and to become unstable. The main salt circulation pump controllers will be located near the pumps. Air for the control valves will be obtained from a central supply near the energy storage area.

Control of the receiver booster pumps is different from control of the main salt circulation pumps. The primary controlled variable is cold salt surge tank level. This level signal is fed back to a controller and valve (D) located near the booster pumps. Valve D throttles the flow from the booster pumps. The series control valve approach is recommended for the booster pumps because the dynamic head (flow effects) and the control valve pressure head is a small part of the total pump head. The static head associated with tower height and the cold surge tank pressure is the large part of the booster pump head requirement. System flow is measured after flow control valve D and is used to control the number of pumps that are operating. At low flows, between 5 and 17% of design, a recirculation valve (C) is used to bypass part of the operating pump flow back through a cooler to the booster pump inlet rather than be returned approximately 1.2 km to the cold salt storage tank. The booster pump cooler outlet temperature is measured and used to control cooler fan and louver operation. Detailed considerations may permit removal of the fan and use of the chimney effect to establish cooler air flow. Recirculation valve C is enabled at system flows less than 17% of design flowrate and is operated to maintain single pump flow at one third of its design flow based on output of the pump flowmeter. The booster pump and cooler controllers will be located near the pumps at the base of the tower. An air compressor and storage tank for the control valves will also be located near the base of the tower. Flow of salt from the receiver is passively controlled by the morning glory spillway to maintain the desired elevation.

The salt returning to the energy storage area is directed to the hot or cold storage tanks or to the drain tank depending on its temperature. Valves F, G, and A are used for this function. The intermediate temperature salt in the drain tank will have cold salt added until its temperature is low enough for return to the cold salt tank. Several other alternatives to the use of the existing drain tank for the handling of the intermediate temperature salt were considered. The simplest in concept is to design a distribution device inside the cold salt tank so that the tank walls would never see the hot salt.

The difficulty is to be able to assure that this will not happen and to be able to justify the design in terms of storage vessel codes. A second approach is to put the salt into the hot salt pump sump and work the intermediate temperature salt off through the solar steam generator. This approach requires that the solar steam generator be working whenever intermediate temperature salt returns from the receiver. A third alternative is to mix cold salt with the intermediate temperature salt in a length of pipe and flow the mixture into the cold salt tank. This requires that the main cold salt circulation pump be designed to have excess capacity, which is not cost effective. The basic drain tank approach is preferred over the three alternatives. Preliminary estimates of the control temperatures are: if temperature is greater than 549°C (1020°F), the salt goes to the hot tank; if temperature is less than 343°C (650°F) the salt goes to the cold tank; all other salt goes to the drain tank. The controllers for valves F, G, and A will be located in the same electronics rack as the controllers for the main salt circulation pumps. Control valve air will be obtained from the central energy storage area supply.

The approach used for control of salt flow in the receiver itself is shown in Figure 5.3-6. As noted above, the inlet surge tank and morning glory spillway provide an almost constant pressure difference of 2.48 kPa (360 psi) across the receiver. Salt flow is divided into east and west passes that are similar. The salt in each pass flows through two parallel lateral support pipes (north and south) and then through ten absorber panels in series. Primary control is by feeding pass outlet temperature back to a control valve (A, B) and controlling salt flow to maintain outlet temperature near 566°C (1050°F). The large volume of salt implies large time constants (greater than 60 sec) and was initially thought to represent a difficult control problem when an outlet salt temperature tolerance of $+6^{\circ}\text{C}$ ($+10^{\circ}\text{F}$) and the variations in incident solar energy were considered. However, a significant analysis has been conducted regarding receiver control and several approaches have been shown to be useful.

The primary approach is to use a pseudo feedforward control system with feedback trim based on outlet temperature and its integral. The concept measures receiver salt inlet temperature, the outlet temperature of each panel and the salt flow rate. This data is then used to compute (estimate) the solar energy being absorbed in the receiver. If the absorbed solar energy could be measured instead of estimated, then a true feedforward system could be used. The estimate of absorbed solar energy is used to compute a desired salt flow to obtain the desired outlet salt temperature. If there were no measurement or computational errors or dynamic lags then the pseudo feedforward system would work well. In practice it is desirable to also feedback the outlet temperature and integral of the outlet salt temperature error. This system works well for moderate changes in level and distribution of the absorbed flux.

Intermittent cloud cover is the most serious challenge to the receiver control system. As clouds cover the field, the salt flow is reduced to keep outlet salt temperature up. Then when the cloud has passed, the high solar flux may not be absorbed by the salt due to its low velocity and corresponding low convective heat transfer coefficient.

Figure 5.3-6

5-96

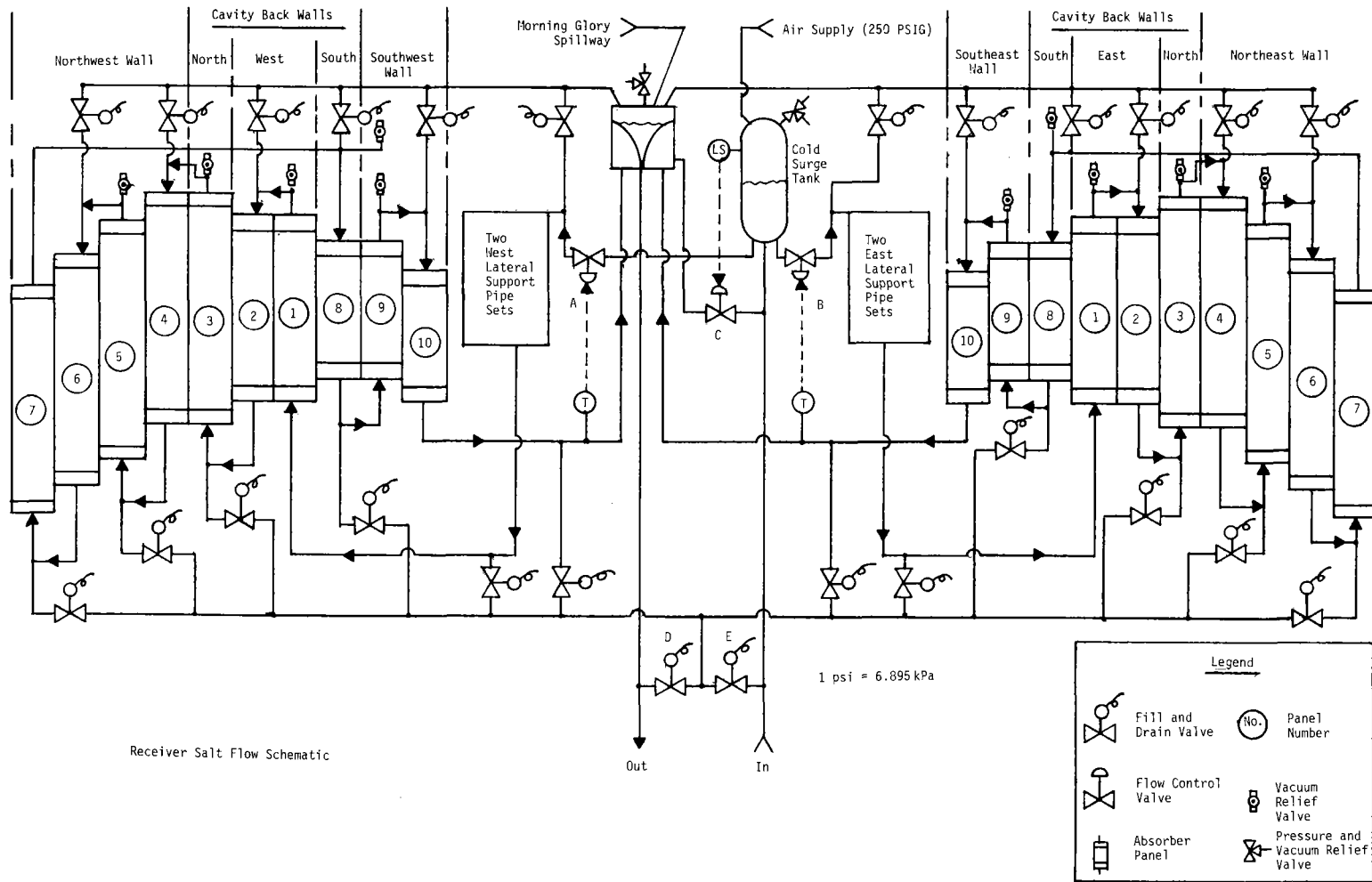


Figure 5.3-6 Repowering Salt Flow Schematic

The result is that the absorber tubes may overheat before the salt flow rate is increased. There are two ways out of this dilemma. They each are based on establishing a minimum salt flow rate, on the order of 50% of the design flow value, that will keep the salt convective heat flow coefficient high enough to prevent absorber tube damage. In the first approach, the outlet salt temperature is allowed to decrease. The off nominal temperature salt is then sent to the proper storage tank as shown on Figure 5.3-5. If there is a significant amount of off temperature salt then the storage tank temperatures will change from their design values and storage capacity will be reduced. The second approach is to add two recirculation pumps in the receiver, one for each pass. The pumps would take hot salt from the morning glory spillway tank and add it to the salt flowing into the first panel downstream from the flow control valve. The recirculation pump speed would be adjusted to provide some minimum flow, say 50% of design, through the panels. In this way, the temperature of the salt entering the panels would be raised and the salt flow would always be enough to maintain the desired convective heat transfer coefficient. The flow control valves (A and B of Figure 5.3-6) would be adjusted to maintain outlet salt temperature at the set point value using the pseudo-feedforward method described above. The second approach is preferred as it would avoid losing storage system capacity. The small pumping penalty and cost of the pumps is felt to be a worthwhile investment.

A number of receiver off-nominal control aspects have also been incorporated into the design (see also Appendix B.1). A high-level switch is included on the cold salt surge tank. This switch acts to open valve C and to bypass booster pump flow directly to the morning glory spillway tank and thus the downcomer. Another feature involves sending a signal to the collector control system to turn down heliostats if control valves A and B are almost full open and salt exit temperature is high. If the salt exit temperature goes above limit for any absorber panel then the heliostats will be commanded to defocus and the cavity doors will be shut within 7 sec.

The controller for valves A and B of Figure 5.3-6 will be located in a room inside the top of the receiver tower and protected from reflected sunlight. A control air compressor and receiver tank will also be located in this room at the top of the tower. The air compressor for the cold surge tank air will also be located in its own room in the top of the receiver tower. The associated air storage tank will be located on a lower level in the receiver (see Paragraph 5.2.2.4).

- 5.3.2.4 Energy Storage Control Subsystem - The energy storage control subsystem (ESCS) does not involve control of primary salt flow through either the receiver or the solar steam generator. Rather the level of salt in the hot storage tank, cold storage tank, and the drain tank are reported to the OCS for its use. There are a number of auxiliary control functions associated with the ESCS. These are: (1) control of storage tank foundation temperatures, (2) control of drain tank level, (3) control of salt melter when used for reheating, and (4) control of salt reprocessing.

A diagram of the energy storage control subsystem is shown in Figure 5.3-7. The foundation cooling control is shown on the lower part of the diagram. A single pump set is used to provide cooling water from the cooling tower sump. Each tank foundation has its own outlet water temperature sensor connected to an inlet control valve. Control of drain tank level involves two aspects. As drain tank salt temperature may be too hot for return to the cold tank, the equivalent of pump A is provided to transfer cold salt from the cold salt tank into the drain tank. The detail layout of the energy storage area resulted in the function of pump A being provided by the hot salt pump. The salt transfer pump B, is used to control the level of salt in the drain tank. The drain tank will be kept nearly empty so it is available for use when needed.

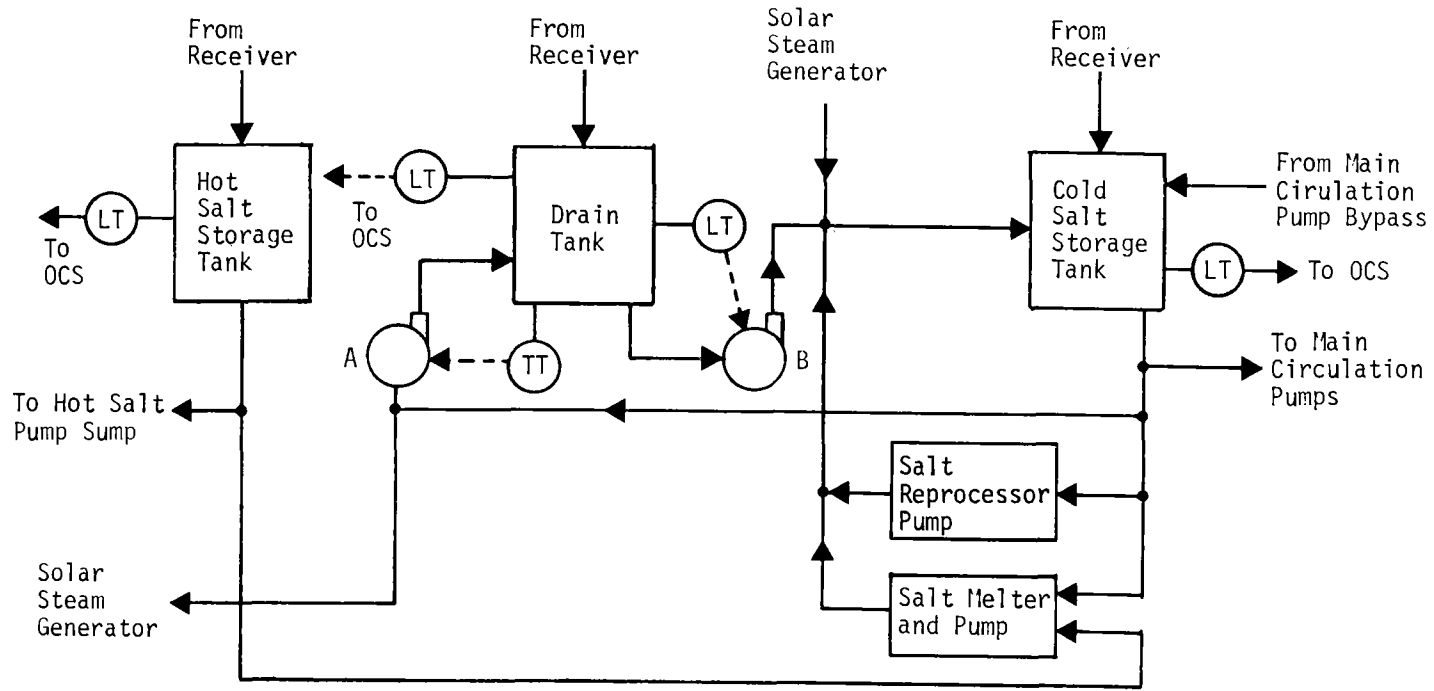
The salt reprocessor will contain its own controls. If the salt reprocessor is operated in a batch mode, then a pump will not be necessary. However, if salt reprocessing is continuous then a salt pump will be required. It basically will take salt from the cold salt tank, condition the salt to the proper purity and return the salt to the cold salt tank. The salt melter will also contain its own pumps and controls. The melter will be connected so it can be used in any of three ways:

- 1) To melt granular salt using a fossil fuel and transferring the melted salt to the cold salt tank.
- 2) To melt granular salt using hot salt and transferring the melted salt to the cold salt tank.
- 3) To add heat, using fossil fuel, to salt from the cold salt tank and returning the warmer salt to the cold salt tank.

The controllers associated with the ESCS will be located with the main salt circulation pump controllers and the control valves will use the same control air supply as the main salt circulation pumps.

A more complete discussion of the features of the piping in the energy storage area is given in Appendix B.3. The reverse salt flow function shown on Figure 5.3-7 is discussed fully in Appendices B.2 and B.3.

Figure 5.3-7



5-99

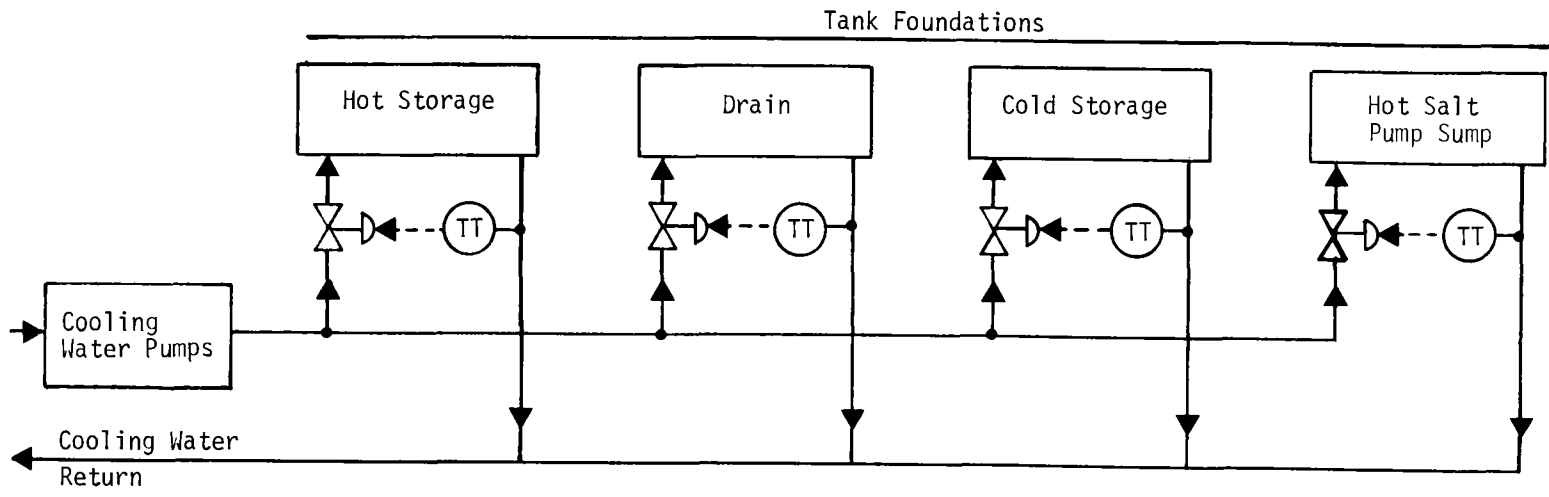


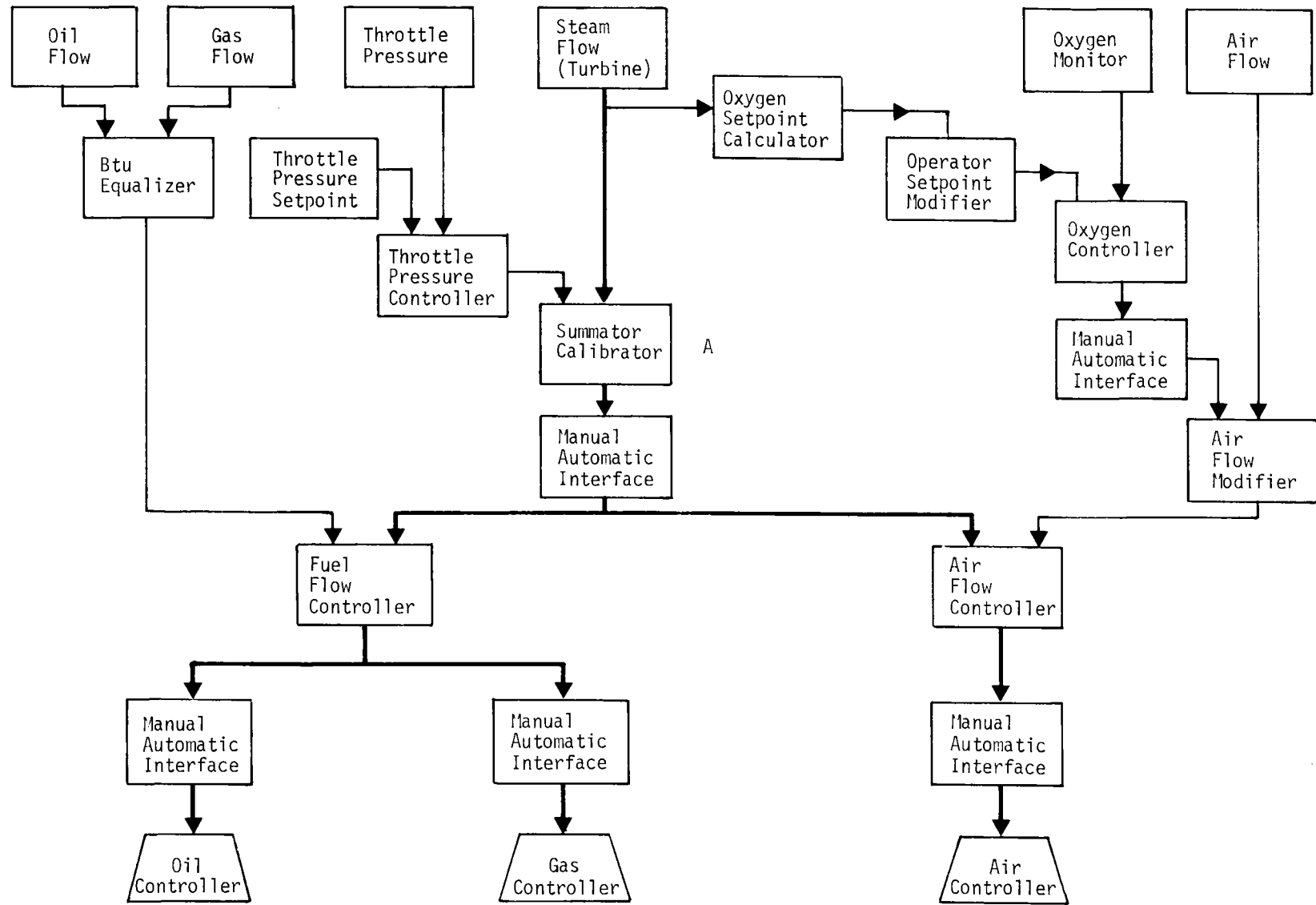
Figure 5.3-7 Energy Storage Control Subsystem Diagram

5.3.2.5 Fossil Control Subsystem - The fossil control subsystem will use the existing equipment or an upgraded version of the existing equipment. Any such updating is not considered to be a part of the repowering activity and has not been costed. The existing system is discussed here for reference and the recommended upgrading is discussed in paragraph 5.6.6. A large benchboard in the control room is used for operational controls and displays and for emergency functions. The functions controlled are gas flow, fuel flow, combustion air flow, feedwater flow, blowdown flow, and superheat temperature. The control approach is that of feeding the nominal demand forward and then trimming the control signals based on measured variables. Most of the controllers are pneumatically operated. The existing benchboard is the main OCS interface. An interface between the boiler controls and the turbine first stage steam pressure signal will be used in proportioning the requested steam demand between the solar and fossil systems. Data recording instruments are on the rear of the benchboard.

The combustion control system for Saguaro is illustrated in Figure 5.3-8. The feedforward lines are shown in boldface and are based on the fact that turbine first stage steam pressure is a measure of steam flow. Steam flow, at rated temperature and pressure, results from fuel flow and the associated air flow. Thus the feedforward of steam flow to fuel flow and air flow. Both oil and gas fuels are shown as the boiler can operate on either or both. The throttle pressure setpoint is established by dispatch control. The difference between throttle pressure setpoint and actual throttle pressure is used to trim the desired steam flow in summator, calibrator A. Fuel flow trimming involves the difference between the actual heating value of the fuels (oil or natural gas) as they are being used and the value originally designed into the feedforward controller. Oxygen in the flue gas is measured by the oxygen monitor and used with modified oxygen setpoint to trim the fuel/air ratio. Saguaro does not have, nor is required to have, any pollution control systems. The manual/automatic interface stations allow direct operator control of the setpoints on steam flow and fuel/air ratio.

Control of boiler feedwater is by a conventional three element feedwater regulator. The three elements are feedwater flow into the boiler, steam flow out of the boiler, and steam drum water level. All three elements are necessary because steam drum water level alone produces inadequate control due to swelling (apparent change in water density due to incipient boiling) of boiler water when drum pressure changes. Superheated steam temperature is controlled by tilting the burners in the boiler to change the proportion of heat going to the superheater as compared to the boiling sections of the steam generator.

Figure 5.3-8



5-101

Figure 5.3-8 Saguaro Combustion Control

The basic modification to the FCS for solar repowering has to do with the output of summator, calibrator A on Figure 5.3-8 that represents desired steam flow. For repowering, the desired steam flow signal will be proportioned by the OCS into desired fossil steam flow and desired solar steam flow. These two signals will then be sent to the appropriate controllers.

Fossil control subsystem equipments are located on or near the fossil steam generator. All of the controllers are pneumatic and a control air supply is available. The operator interface is through the BTG board.

- 5.3.2.6 Electric Power Generating Control Subsystem - The existing electric power generating control subsystem (EPGCS) uses the existing equipment on the boiler-turbine-generator (BTG) board in the control room. The recommended upgrading of the EPGCS is discussed in paragraph 5.6.6. The EPGCS controls and displays are integrated on the same board as those of the FCS. The primary function explicitly controlled is throttle pressure as shown on Figure 5.3-8 as the throttle pressure controller.

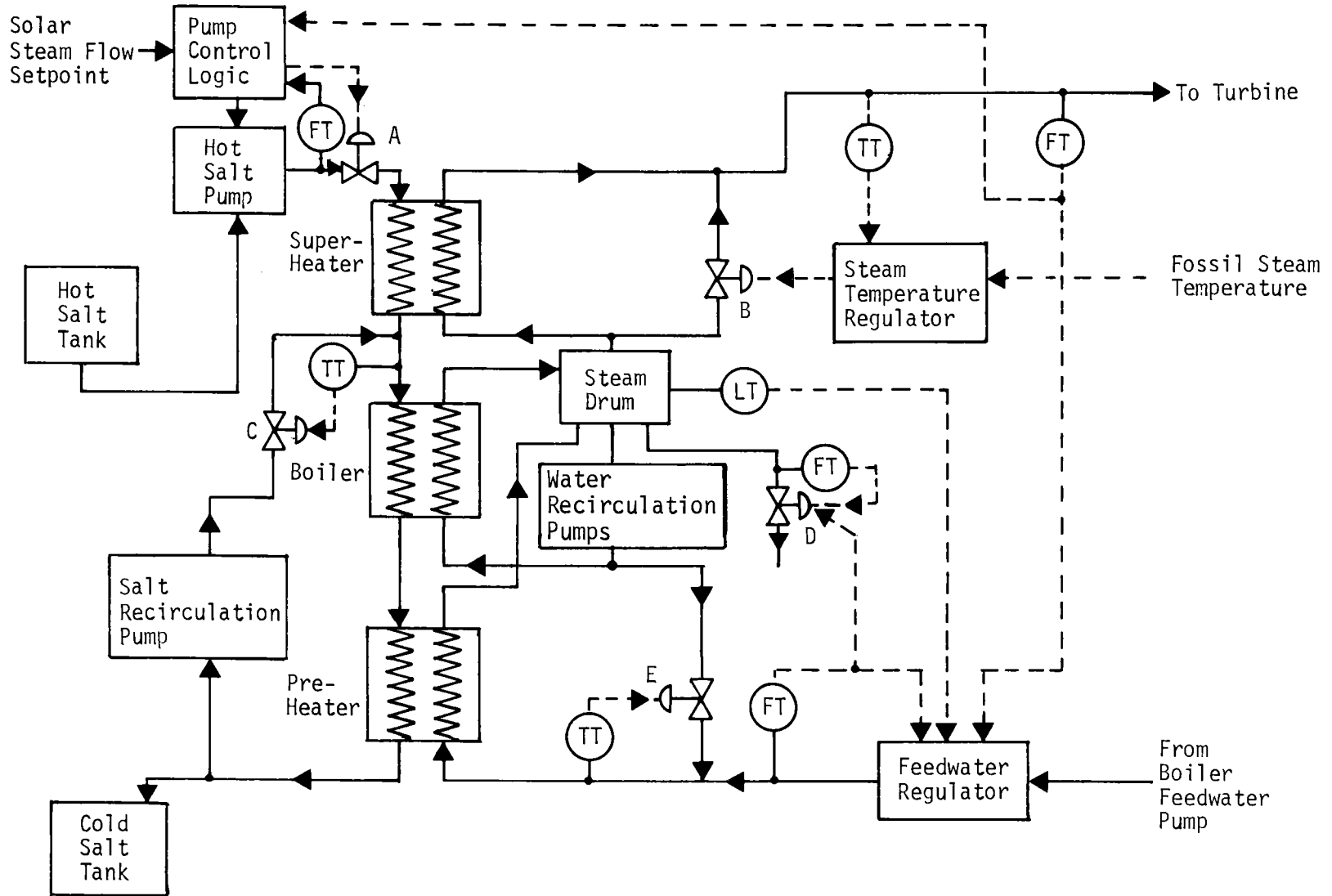
A full complement of the usual turbine controls is provided. These include: main steam stop valve, steam flow, admission control valves, turbine speed control, emergency trip, and the turbine-generator oil pumps. Additionally, a number of parameters are continually monitored such as turbine shell temperatures, bearing oil temperatures, thrust bearing temperature differences, sealing steam flow, and vibration and shaft eccentricity. Other functions being controlled are: circulating water flow, condenser back pressure, generator hydrogen pressure, generator output voltage, electrical auxiliaries, and switchyard functions.

All of these controls are located near the turbine, generator, or on the BTG board. A control air supply is available for the pneumatic controllers used.

5.3.2.7 Solar Steam Generator Control Subsystem - The solar steam generator control (SSGCS) involves control of the hot salt pump, solar steam flow, feedwater flow, solar steam temperature, salt recirculation pump flow, water recirculation pump flow, and steam blowdown flow. The solar steam generator control is patterned generally after the fossil steam generator control. For solar only steam generation, a signal will be taken from the output of summator, calibrator A (Figure 5.3-8) that represents the desired steam flow. The signal becomes the set point for solar steam flow. This set point is used as a feedforward to hot salt flow and then trimmed with a number of feedback parameters including the turbine throttle pressure error. When both the solar and fossil steam generators are operating, a slightly different logic is used. One of the two steam generators, say fossil, will be considered primary. The steam flow measurement from the turbine is sent to the OCS and proportioned into desired steam flows for solar and fossil. The desired steam flow for the primary generator (fossil) is fed to summator calibrator A (Figure 5.3-8), added to the throttle pressure processed error and sent to the primary steam generator's heat flow controller (fuel flow for the fossil system). The desired steam flow for the secondary generator (solar) is fed to the secondary generator's heat flow controller (salt flow for the solar system). As there are no control valves between the two steam drums the pressure in the primary drum will determine the pressure in the secondary drum. If throttle pressure error was sent to both steam generators, then dynamic instability could result. The SSGCS interfaces with the OCS to obtain the desired solar steam flow and requires fossil steam temperature for establishing the solar steam temperature setpoint. The approach suggested here is basically a steam generator following system. If faster system response is desired to satisfy the regulation reserve requirements, then additional feedforward terms based on turbine throttle position and central dispatch signals can be added to the salt flow control logic.

A schematic of the solar steam generator control subsystem is shown in Figure 5.3-9. The hot salt pumps and control valve A are used to control salt flow through the three heat exchangers--superheater, boiler, and preheater. Bypass control of the hot salt pumps is not necessary as the hot salt pumps have large clearances that result in internal bypass flows. Also the pumps are submerged in the hot salt sump which will tend to limit further increase in pump temperature. The solar steam flow setpoint is used to select the number of hot salt pumps that will be operated. Salt flow is adjusted, or trimmed based on superheated steam flow rate. The superheater is purposely overdesigned so its outlet steam temperature can be controlled. This permits blending some saturated steam from the steam drum (through valve B) to bring the steam delivered to the turbine to the same temperature as the steam being generated by the fossil subsystem. The two steam temperatures are compared in the steam temperature regulator and the difference used to set valve B and thus the flow of saturated steam. When the fossil steam generator is not operating, then a 538°C (1000°F) temperature will be used as the steam temperature regulator setpoint instead of the fossil steam temperature.

Figure 5.3-9



5-104

Figure 5.3-9 Solar Steam Generator Control Subsystem

A salt recirculation pump and flow control valve C are used to ensure that the temperature of salt entering the boiler heat exchanger does not exceed the boiler's corrosion limits. During increases in salt flow, there will initially not be enough superheated steam flow to drop the temperature of the salt exiting the superheater down to a low level to prevent boiler corrosion. However, blending of cold salt provided by the salt recirculation pump will insure safe salt temperatures.

The existing feedwater pump will be used for both the solar and fossil systems as it has adequate capacity. A conventional three element feedwater regulator will be used to control feedwater flow. This regulator measures feedwater flow, steam flow and drum water level and adjusts feedwater flow to keep drum water level constant. A steam drum blowdown control valve (D) is used to blow down approximately one percent of steam flow to help maintain water quality. A water recirculation pump and flow control valve (E) is used to ensure that the temperature of the water entering the preheater is sufficiently above the salt freezing point. The hot water source is the steam drum because it will always have water hotter than 304°C (580°F) whenever salt is flowing. The two water recirculation pumps operate at a constant speed. This approach maintains a nearly constant forced recirculation flow rate through the boiler as is desired. The recirculation ratio increases with decreasing feedwater flow rate.

A solar steam generator control system has been analyzed by Martin Marietta as part of the Babcock and Wilcox contract with Sandia National Laboratories Livermore, Ca on the Molten Salt Steam Generator Subsystem Research Experiment, Phase I. Control algorithms have been developed for each of the control loops shown on Figure 5.3-9 using the general approaches described above. The logic for valve A uses a thermal balance based on design conditions and measured steam flow as a feedforward term. A conventional PID (Proportional, Integral Derivative) controller is used on throttle pressure to trim the salt flow. For the Saguaro case, the PID would be applied to the difference between desired steam flow rate and measured steam flow rate from the solar system. The feedwater regulator was as described above except that auctioneer logic is used to select the median value of three steam drum level measurements. The preheater water, steam attemperator, and evaporator salt inlet temperature controllers all used the same configuration. Control was proportional with the proportioning factor being a function of measured steam flow-rate. The variation in proportional gain was necessary to compensate for variations in flow of the fluid whose temperature is being controlled. The subsystem research experiment (SRE) analysis did not require control of blowdown flow. However, control of blowdown flow only requires a simple ratio controller with proportional gain.

The molten salt steam generator SRE analysis included simulated load maneuvers over a range of loads at load changes of 10% per minute. The data showed that the controlled system was stable and steam outlet temperatures and pressure were well controlled. Variations in drum water level were well within acceptable limits. It may be concluded that control of the solar steam generator presents no unusual problems.

Further information on the solar steam generator operating procedures is given in Appendix B.2. The controllers for the solar steam generator control subsystem will be located in an electronics rack in the solar steam generator area. Compressed air for the control valves will be from the source in the energy storage area.

- 5.3.2.8 Red-Line Units - A red-line unit (RLU) system will be used to measure and monitor all plant critical parameters such as receiver outlet salt temperature and steam drum water level. When any parameter exceeds specified limits an annunciator at the RLU display console will light up, an alarm will sound, the displays on the OCS console will flash on and off and the event will be logged on the event logger with the time of day. In this way the operator will be made aware of any out of tolerance condition on critical parameters.

Inputs to this alarm monitoring and reporting system will be hard wired from separate sensors in the plant. It is intended to only select critical parameters for inclusion in the RLU system. The DAS, OCS and distributed controllers will also be monitoring plant parameters and will advise the operator when those parameters get to caution or warning levels. Television displays of the two steam drum water level sight gages (solar and fossil) will be included as part of the RLU system. To avoid unnecessary alarms, the RLU will monitor the desired plant configuration as established by the OCS so that only the pertinent critical parameters are enabled for alarming. RLU sensed parameters and established alarms will also be sent to the DAS for recording and display if appropriate.

The RLU microprocessor and its associated peripherals will be located in the control room. All responses to RLU established alarms will be through the OCS, distributed controllers, or by manual control of the actuators.

- 5.3.2.9 Data Acquisition Subsystem - A data acquisition subsystem (DAS) will be used to collect and process data during normal plant operations. The DAS does not include the strip chart recorders or other data recording systems in current use at Saguaro. The DAS will be sized for the normal plant operations activities and will be patterned after that being used at the APS Cholla station. It will have video displays and keyboard inputs for operation of the DAS. Data processing will be by a minicomputer with a standard set of output peripherals including line printers, disk, tape, and plotters. Communications with the rest of the master control subsystem will be through the DAS's own signal conditioning units and through direct connections to the heliostat array computer and the operational control computer.

It is anticipated that the DAS will be expanded for the demonstration phase of the program. If so, additional capacity will be provided to the DAS along with a range of additional sensors and adaptors to the existing plant instrumentation.

The DAS will be located in the control house in a room separate from the control room and separate from the computer room. A DAS CRT and keyboard will be included on the control console adjacent to the OCS so the operator can call up selected displays.

5.3.3 Performance and Cost

5.3.3.1 Operating Characteristics - The master control subsystem (MCS) has been conceptualized to satisfy all of the design requirements. It will provide effective control for fossil alone, for solar alone, and for combined solar and fossil operation in selectable proportions.

Each of the five steady-state operating modes (Section 4.3), has been examined and the MCS can control each and all of the subsystems in each mode. The operational control subsystem will provide integrated control for each of the five steady state modes.

The OCS provides the procedures for each of the five transitions (two way) between the steady-state modes. The various subsystem controls are adaptable to these transitions with some phases being accomplished by closed loop control and some parts by transferring valve control to manual from automatic. Automatic control and manual positioning of control valves are also used during normal start-up and shutdown. The normal start-up and shutdown procedures are a part of the OCS. Many emergency procedures will be made a part of the OCS. However, the receiver absorber tube overtemperature condition, and the response to it, has been made a part of the overall MCS operation. The sensors, communications, and actuators have been provided as part of the overall conceptual design.

Fail safe considerations have been included in the design criteria and are evidenced in the equipment. Dual power supplies are provided. Two transmission lines will be used as alternate power sources. Also, a diesel generator will provide power 25 sec after either transmission line power source is lost. All control valves are operated pneumatically or electrically. Air storage provides an air supply after the compressors have failed. The control valves will be selected to fail in a safe direction when electric power or the air supply is lost. All of these considerations will lead to a safe and effective master control subsystem design.

While cloud cover transients can be a major effect on some solar systems, their effect has been strongly mitigated by this repowering conceptual design. Because the turbine only gets energy from the hot salt storage tank, and not directly from the receiver, the turbine steam flow cannot be directly affected by cloud cover variations.

Within the receiver itself, the effect is not serious when insolation is reduced as it, at most, means production of some low temperature salt until salt flow is stabilized at a lower level. The off-nominal salt will be automatically handled by the temperature sensor at the storage tanks and sent to the proper storage tank.

When the cloud cover variations sharply increase the solar flux in the receiver, the penalty can be more serious if the salt flow is not quickly brought up to a level where the extra heat is removed. Several innovations have been introduced to permit rapid increases in salt flow. The cold surge tank and the morning glory spillway tank in the receiver provide a source and sink so that the salt hydraulic inertia is minimized. The receiver is effectively decoupled from the large inertia of the salt in the long lines between the storage tanks and the receiver. Receiver control systems have been analyzed and simulated that minimize the effects of cloud cover transients. A solar coronagraph has been suggested as a way to reduce the effect of cloud cover variations on absorber tube lifetime. Each of these considerations will lead to quick receiver response to cloud cover transients, minimization of absorber tube temperatures, and no effect on turbine steam conditions.

While the characteristics of the receiver and solar steam generator control systems have been examined using dynamic simulations of the process, the other subsystems and the total system will need to be simulated during a subsequent study phase. Important questions include: 1) use of Saguaro station as a regulation reserve for APS's southern area frequency control, 2) emergency operating transitions, 3) need to avoid steam generator or turbine following, 3) interactions of solar and fossil steam generators during trips, 4) where "auctioneering" of sensed signals should be used, and 5) need for initial fast valving on the turbine and two steam generators.

5.3.3.2 Costs - The hardware cost of the master control subsystem is \$1,968,000. Preliminary and detailed engineering costs for the master control system have been estimated at \$1,728,000. The total cost of implementing the system, then, is \$3,696,000. Further cost details may be found in Appendix G. Generally, the costs of control valves, instruments, and motor starters have been included in the costs for the particular subsystem. Similarly the cost of the control room modifications have been included as part of the site facilities. (All the above costs are quoted in 1982 dollars).

5.4 FOSSIL ENERGY SUBSYSTEM

The existing fossil energy subsystem at the Saguaro Steam Electric Station consists of the steam generator, manufactured by Combustion Engineering; the air supply system consisting of two forced draft fans and two induced draft fans; a 48.8 m (160 ft) tall smokestack and the fuel supply system. The steam generating unit consists of an economizer, boiler, superheater and air preheater. Most of the fossil energy subsystem equipment is located just to the north of the electric power generating subsystem equipment. Figure 4.1-3 shows the general arrangement of the equipment. The No. One boiler is south of the No. Two unit and is close to the solar steam generator. The main steam interface will be just to the south-east of the No. One boiler. The feedwater interface will be made near the exit piping from the No. 1 high pressure heater that is on the north-east corner of the heater deck adjacent to the No. One turbine generator. Natural gas fuel is supplied through a pipeline and a master meter. No. 6 fuel oil is brought to the Saguaro station by rail car and is stored in tanks to the northwest of the boiler and turbine generator equipment. Further information on the fossil steam generator is given in section 5.4 of Ref 1-2 including of the operating floor plan and elevation views.

The fossil energy subsystem concept is that fuel is burned in the furnace with release of heat. The outdoor designed furnace is configured to burn natural gas or oil or a combination of both and could be adapted to burning coal. However, compliance with presently applicable environmental laws makes this not feasible. The fuel is supplied through four burners located in the furnace corners. The burner tilt is adjustable in order to vary location of the flame front with respect to the superheater and thus to vary outlet steam temperature. The flow of combustion air and exhaust gas is maintained by the forced draft and induced draft fans. Feedwater enters the steam generator in the economizer, and passes to the boiler and superheater sections, then the superheated steam exits the steam generator and flows to the turbine. The boiler is designed to produce 126 kg/sec (1×10^6 lbm/hr) of steam at 10.7 MPa (1550 psig) and 541°C (1005°F) when supplied with feedwater at 232°C (450°F).

The existing combustion control system maintains the correct turbine inlet steam conditions by monitoring turbine inlet flow, pressure, and temperature and adjusting the various boiler parameters such as fuel and air flow, feedwater flow, and burner tilt.

The fossil energy subsystem requires little modification to incorporate repowering. The major modification will be made to the combustion control system which must be integrated with the solar steam generator control system to provide proper coordination of the two energy inputs to the cycle. The integration of the two subsystems will be done by the operational control subsystem (see Paragraph 5.3.2.1).

All modification costs have been included with the electric power generating subsystem modification cost (see Paragraph 5.6.7).

5.5 ENERGY STORAGE SUBSYSTEM

As described in Section 3.1, the selection of a two tank storage system (separate hot and cold tanks) is based on considerations of low cost containment, low risk, and the continuing progress of the Molten Salt Storage SRE at the CRTF. The storage system in our selected configuration is used to delay the start of the turbine to displace the most expensive fuels in the APS utility system. Because of the relatively large quantity of storage required for such purposes, the storage also serves as a very effective buffer between the solar collector/receiver operation and the solar steam generator. In the following discussion are described the requirements, design, performance, and cost of the molten salt energy storage subsystem.

5.5.1 Energy Storage Subsystem Requirements

The thermal energy storage subsystem is used to store thermal energy for use in operating a steam turbine at a nominal repowered capacity of 60 MW_e net. The storage medium is a molten mixture of 40% potassium nitrate and 60% sodium nitrate by weight. The capacity of the system is to be 688 MWh_t. This represents about 4.0 hr of storage while running the turbine at repowered capacity totally from storage. The operational and economic optimum configuration for a salt storage system of this size is a dual hot and cold tank system. Hot salt at 566°C (1050°F) is to be stored in one dedicated tank. A second dedicated tank is to store the cold salt at 277°C (530°F). The subsystem is to be capable of delivering the hot salt to the solar steam generator subsystem, of receiving cold salt from that subsystem, of delivering cold salt to the receiver circulating equipment, and of receiving hot salt from the receiver.

A drain tank is also included in this subsystem into which salt is piped when it is not within the operating temperature limitations of either the hot or cold salt tank. This tank will also contain the salt in the receiver and solar steam generator subsystems whenever it becomes necessary to drain these.

If required, provision may be made to minimize the degradation rate of the salt and to regenerate salt which has degraded.

The tanks are to be designed and insulated to optimize thermal losses, that is, to minimize the sum of insulation and excess heliostat costs. Tank foundations are to be cooled so that the underlying soil maintains its bearing strength and supports the tanks satisfactorily. The structural design parameters are: wind velocity, 40 m/s (90 mph); seismic UBC zone 2; snow load, 240 Pa (5 lb/ft²); maximum load on foundations, 192 kPa (4,000 lb/ft²).

The thermal energy storage subsystem will include all equipment, instrumentation, controls, piping, structures, civil work and electrical work necessary to meet these requirements. It will be designed to provide safe and reasonable access for proper inspection, maintenance, and repair of the structure, piping, utilities, instrumentation and controls.

5.5.2 Thermal Energy Storage Subsystem Design Description

The thermal energy storage subsystem is the interface between the receiver subsystem and the solar steam generator subsystem. It is designed not only to store thermal energy, but also to decouple the subsystems that interface with it. That is, storage acts also as a surge capacity which allows the receiver to operate independently from the solar steam generator and vice versa. This prevents insolation variations from affecting the EPGS power output. The recommended insulation materials and thicknesses for both the hot and cold tanks are presented in Table 5.5-1. The interconnections between the energy storage subsystem and the other subsystems are shown in Figure 5.5-1.

The equipment in this subsystem includes not only the hot and cold salt storage tanks, but also salt handling and treating equipment such as the salt reprocessing tower and scrubber, salt melter, conveyors, bins, salt transfer pumps, salt drain sump and sump transfer pumps. The specifications for this equipment can be found in Appendix C. A concept for the salt melter is shown in Figure 5.5-2. The information currently available on salt reprocessing is not sufficiently complete or detailed to permit preparation of a specification. Solids handling equipment was adapted from the work of Olin Chemical on Sandia Contract 84-3878. The initial loading of salt will be carried out in two phases. The salt melter will be used to melt 20% of the total inventory. It is a 1 MWt (3.5×10^6 BTU/hr) heater and would require 24 days (8 hrs/day) to melt the 1.42×10^6 Kg (3.13×10^6 lb) of salt. Then molten salt is pumped to the receiver and heated to 565.5°C (1050°F). The hot salt is mixed with prilled salt in the drain tank as shown in Figure 5.5-3. It requires 1.15 Kg of hot salt to melt 1 Kg of prilled salt. Due to the small size of the drain tank the excess hot salt will be stored in the hot tank. Depending on the insolation availability, this process should be completed within two weeks after the initial 20% is melted. The total salt inventory including storage fluid, 5% tank heel and salt in the receiver, heat exchangers and pipelines is 7.01×10^6 kg (15.63×10^6 lb).

Salt circulation and control are described in the report sections on the receiver circulating piping and equipment and the solar steam generator subsystem (Section 5.3 and Appendix B). The flow of hot salt from the hot salt storage tank is regulated by the level in the hot salt sump which, in turn, depends upon the salt demand from the solar steam generator subsystem. The vents of the hot and cold salt storage tanks are joined to minimize the interchange between the ullage gas in the vessels and the atmosphere. The purpose of this is to lessen the potentially deleterious effects of atmospheric water and

Table 5.5-1 Thermal Storage Tank Materials

Cold Salt Tank			
Component	Tank Side	Tank Top	Tank Bottom
Shell	A516 Grade 70 Carbon Steel	A516 Grade 70 Carbon Steel	A516 Grade 70 Carbon Steel
External Insulation	Holmes Flexwhite 1260 0.38m (1.25 ft)	Homes 1212 BLOCK 0.38m (1.25 ft)	JM 2100 Castable 0.38m (1.25 ft)
Sheathing	Aluminum with White Coating	Aluminum with White Coating	N/A
Hot Salt Tank			
Component	Tank Side	Tank Top	Tank Bottom
Liner	Incoloy 800 0.13 cm (0.05 in)	304 Stainless 0.13cm (0.05 in)	Incoloy 800 0.13 cm (0.05in)
Foil	304 Stainless 0.025cm (0.01in)	N/A	304 Stainless 0.025cm (0.01 in)
Internal Insulation	JM C22Z Brick 0.51m (1.687 ft) Zelie Mortar	Holmes Flexwhite 1260 0.76m (2.5 ft)	JM C22Z Brick 0.51m (1.687 ft) Zelie Mortar
Shell	A516 Grade 70 Carbon Steel	A516 Grade 70 Carbon Steel	A516 Grade 70 Carbon Steel
External Insulation	Holmes Flexwhite 1260 0.076m (0.25 ft)	Holmes 1212 BLOCK 0.23m (0.75 ft)	JM 2100 Castable 0.38m (1.25 ft)
Sheathing	Aluminum with White Coating	Aluminum with White Coating	N/A

MF-101
COLD SALT TANK

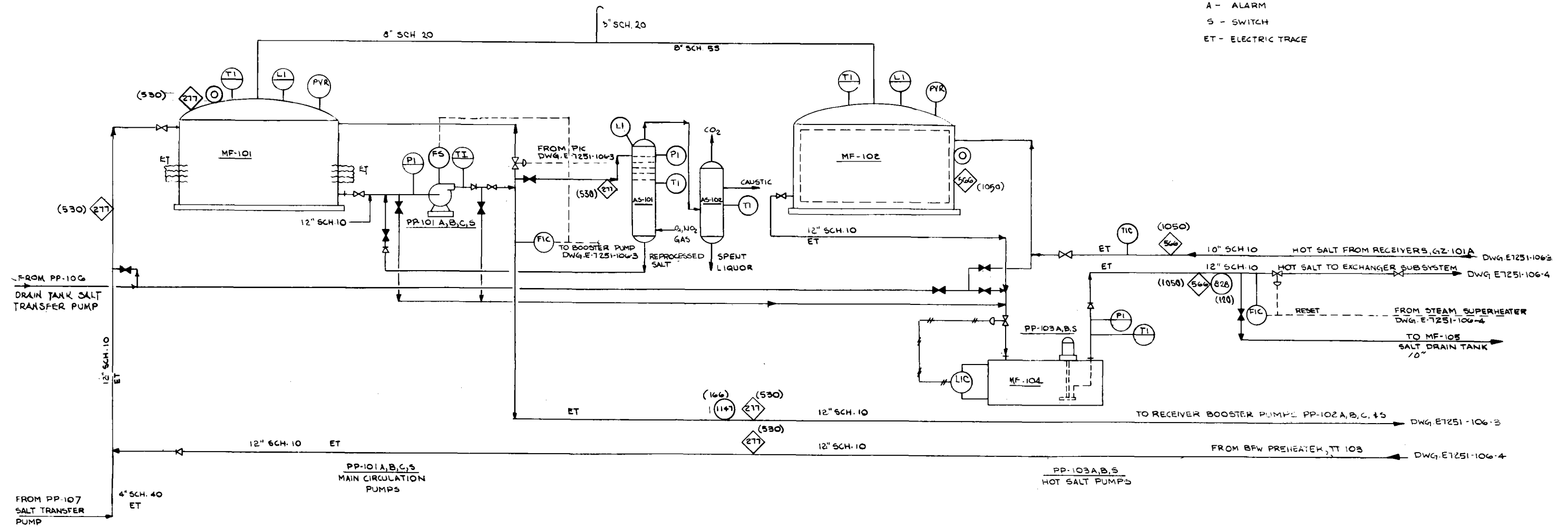
AS-101
SALT CONTACTOR

AS-102
CAUSTIC SCRUBBER

MF-102
HOT SALT TANK

MF-104
HOT SALT SUMP

- LEGEND**
- FLOW RATE, KG/S () LB./HR
 - PRESSURE, KPA(G) () PSIG
 - ◇ TEMPERATURE, °C () °F
 - ▭ DUTY, MWTH () MM BTU/HR
- F - FLOW
P - PRESSURE
L - LEVEL
T - TEMPERATURE
I - INDICATOR
C - CONTROLLER
A - ALARM
S - SWITCH
ET - ELECTRIC TRACE



NOTE
ALL PIPE SIZES ARE IN INCHES
1 IN. = 25.4 x 10⁻³ M

Figure 5.5-1 Energy Storage Area Flow Diagram

5-114

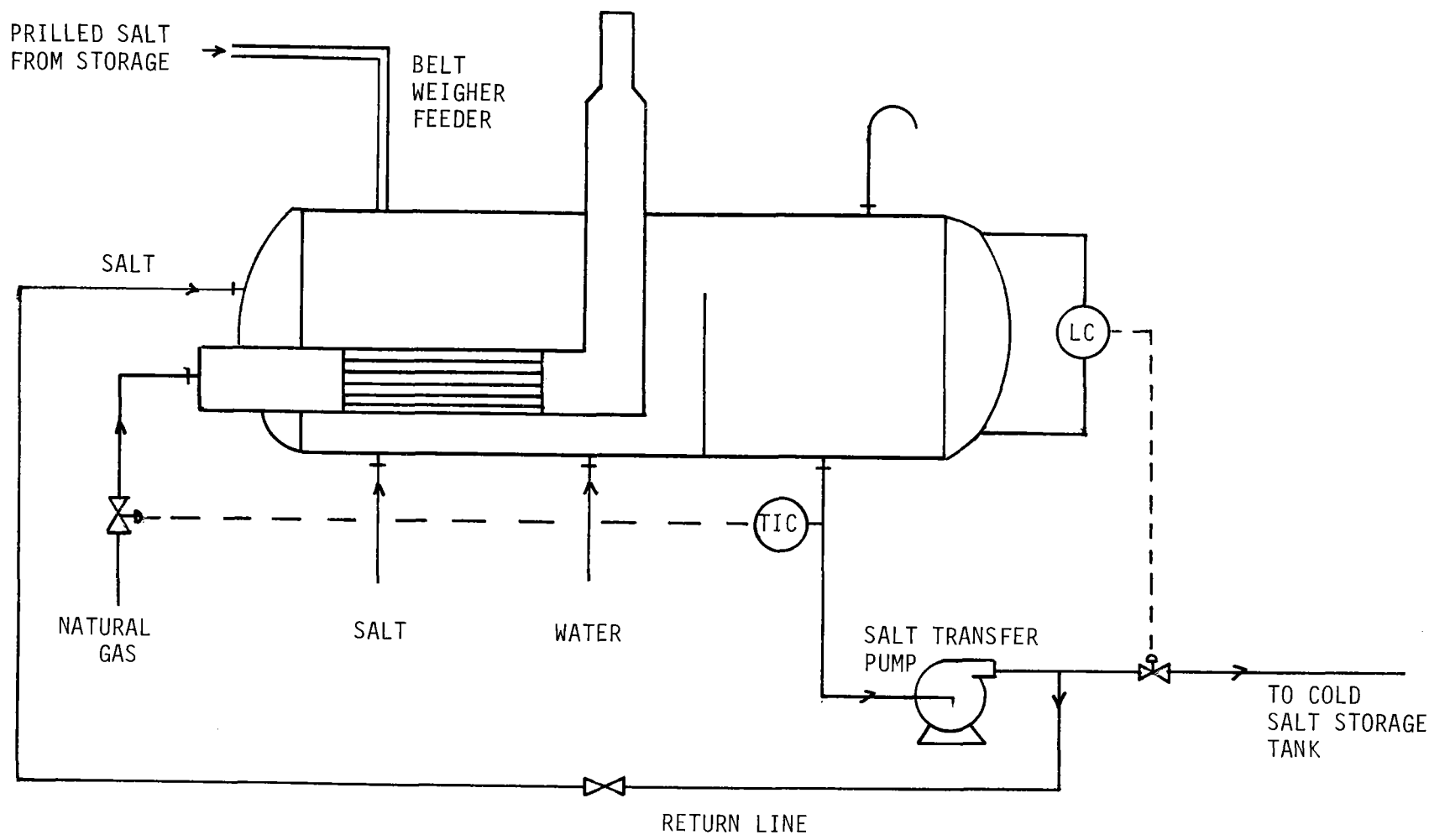


Figure 5.5-2 Salt Melting System

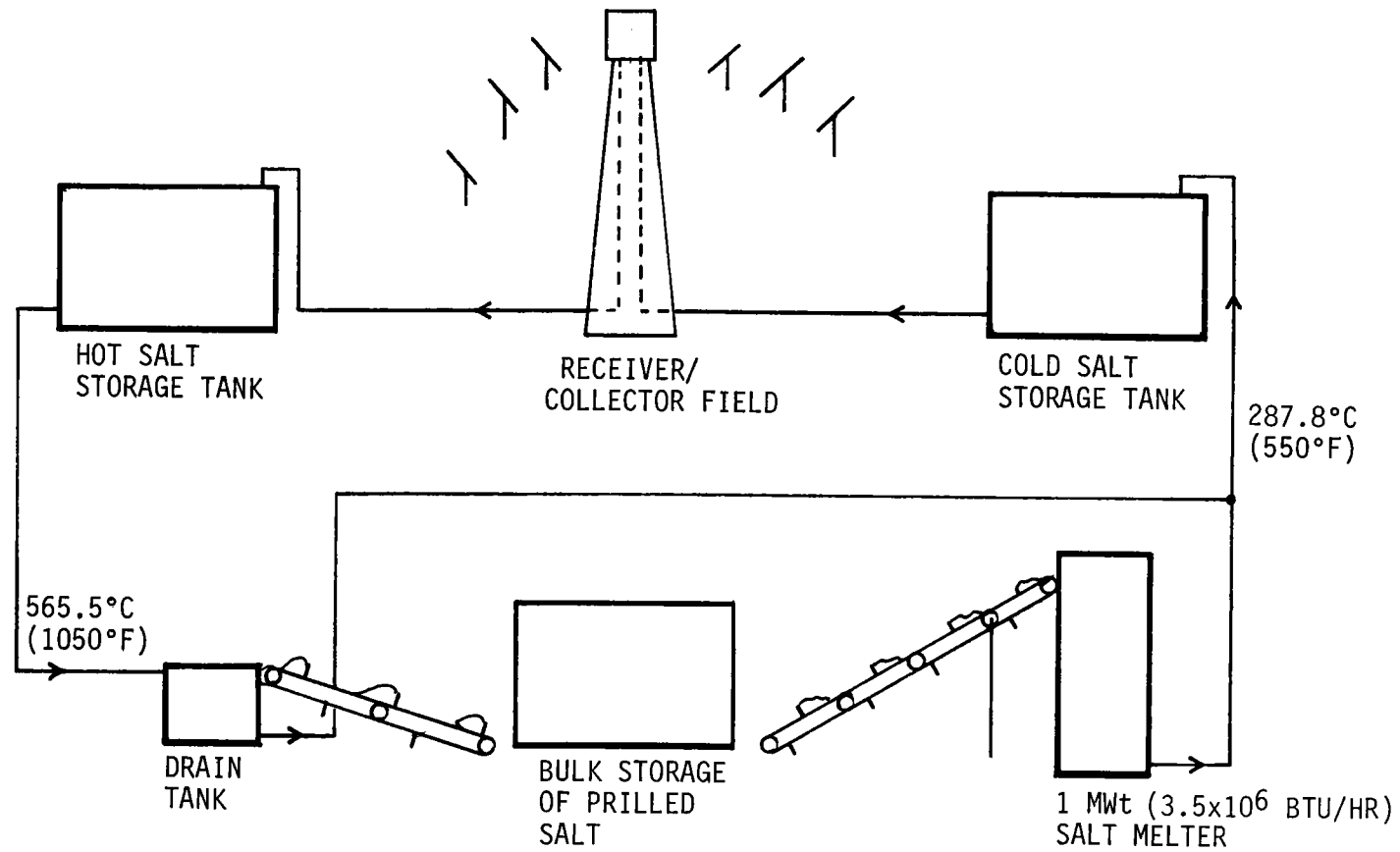


Figure 5.5-3 Initial Processing of Salt

carbon dioxide on molten salt composition. Treatment of the ullage gas was considered to be too expensive. Either a compressor would have to be provided to drive the make-up ullage air through drying and carbon dioxide removal beds, or the storage tanks would have to be designed for vacuum. Either alternative would be expensive. On the other hand, the quantities of water and carbon dioxide in atmospheric air are small and the reactions with molten salt are reversible. Therefore, water and carbon dioxide entering the tanks are allowed to react with the salt and a small portion of salt is removed from the system periodically and is either replaced or is treated with nitrogen dioxide and oxygen. Waste nitrogen dioxide from treatment is trapped in a caustic scrubber. The equipment needed to accomplish this is small and relatively inexpensive.

The hot and cold salt tanks are sized based on the required storage capacity, the total salt inventory, working temperature difference of the salt, salt density and heat capacity and allowable soil bearing load. The maximum salt height of both the hot and cold tanks is 8.65 m (28.4 ft) due to allowable soil bearing load limitations. Design includes allowance for the backpressure or vacuum created as the ullage gas flows through the vent as salt is pumped from one tank to the other. Pressure-vacuum relief valves are provided to safeguard against overpressuring the tanks. The tanks are designed to contain approximately 5.58×10^6 kg (12.3×10^6 lb) of storage salt plus about 8 to 10% excess capacity for a salt heel and overflowing protection.

The salt drain tank was sized to contain all the molten salt contained in the solar steam generator subsystem. The salt drain tank transfer pump was sized to provide about 10% of the flow of the hot salt pump so that salt in the drain tank could be gradually worked off through the heat exchangers. The height of the drain tank is limited by the allowable overhang of the cantilever pumps and it has been sized to the same height and diameter as the hot salt pump sump. The full capacity of the drain tank can be emptied by the sump transfer pump in one hour.

Carbon steel is resistant to corrosion from molten salt and maintains most of its strength at 316°C (600°F). Therefore, the cold salt storage tank is constructed of carbon steel and has external insulation only. Hot salt at 566°C ($1,050^{\circ}\text{F}$) attacks both carbon steel and many insulating refractory materials seriously. Carbon steel also loses much of its strength at these temperatures. Therefore, the hot salt storage tank, is provided with internal insulation as well as external and a protective, expandable, waffled membrane made of Incoloy 800. This membrane is similar to linings used in LNG storage tanks. The membrane protects the refractory from attack while the internal insulation maintains the carbon steel shell at a reasonable temperature. The hot salt pump sump and salt drain tank, because of their small size (8.8 m dia x 3.0 m high or 29 ft dia x 10 ft high), are made from type 304 stainless steel with external insulation.

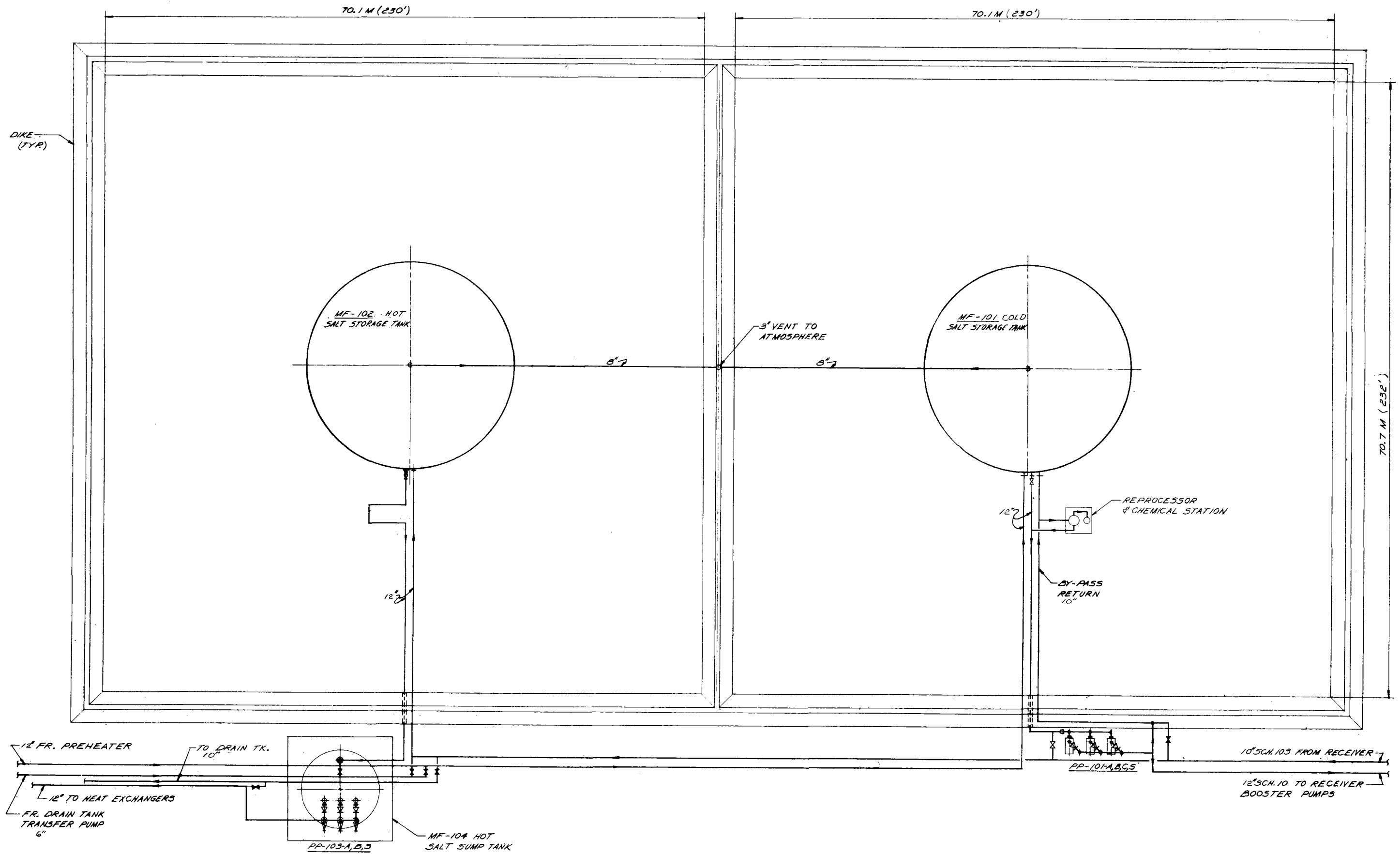
The concept of an internally insulated tank was investigated as part of a Thermal Energy Storage study funded by Sandia National Laboratory. A one cubic meter internally insulated tank was built and successfully fatigue tested. A small storage system (7 MWH_t) with an internally insulated hot tank was designed, built, and is being tested.

As part of the preliminary analyses of the storage subsystem, a trade study comparing internally and externally insulated hot tanks was made. Although the externally insulated tank costs less, an internally insulated tank was selected due to the soundness of the design. For larger size storage tanks, the internal insulation design is less costly than the externally insulated tank. Since Saguaro is a demonstration project, the technology to be used in commercial systems should be applied wherever possible.

The insulation thicknesses and types shown on the tank specifications (Table 5.5-1) were selected from recommendations of the storage contract. An additional constraint in hot tank insulation design is that the hot tank shell is designed for 277°C (550°F). Internal and external insulation thicknesses were adjusted to maintain this temperature.

The locations of the various equipments contained in the energy storage subsystem are shown on Figure 5.5-4. Although they resemble API tanks, none of the tanks fall under either the API or the ASME Pressure Vessel Codes. Quality standards from either of these codes may be adopted for convenience. Because of the unusual temperature and density of the contained material, a special design is required in each case. An example of this is the wall-to floor junction. Severe thermal stresses require a special junction design as depicted in the tank specifications (Appendix C). This design allows the tank wall to be supported while the differential thermal expansion between tank walls and bottom is accommodated. To minimize thermal shock and to prevent salt from freezing, the tanks are provided with electric resistance heaters. These will be used to preheat the tanks before filling.

Little is known about the behavior of soil and rock at high temperatures. Therefore, a foundation design that takes into consideration heat flow from the tank bottom and the variation in substrate bearing strength and other properties with temperature would require a fair amount of research. For the conceptual design, a foundation design is proposed that is expensive, yet safe. The tank sits on a pad of castable insulation, which affords thermal protection to a second pad of lightweight concrete. This second pad has cooling coils embedded in it. The heat flow out of the bottom of the tank is carried away in the cooling water, which is circulated through the cooling coils. The entire structure is supported on sand backfill, which is contained in a concrete ring-wall.



NOTES:
 1) ALL SALT LINES TO BE ELEC. TRACED.
 2) ALL PIPE SIZES ARE IN INCHES,
 (1) INCH = 25.4 x 10⁻³ M.

Figure 5.5-4 Energy Storage Plot Plan

5.5.3 Thermal Energy Storage Subsystem Performance and Cost Estimate

There are no limits to charging and discharging rates inherent in the thermal energy storage subsystem itself. This is because there is no functional heat exchange within the subsystem. The charge and discharge rates depend entirely upon the capabilities of the receiver and solar steam generator subsystems respectively. The maximum charge rate is the maximum thermal rating for the receiver, 199 MW_t ($0.68 \times 10^9 \text{ Btu/hr}$). The discharge rate is the rate at which salt is pumped and cooled in the solar steam generator subsystem, 172 MW_t ($0.59 \times 10^9 \text{ Btu/hr}$) at design point and 86 MW_t ($0.29 \times 10^9 \text{ Btu/hr}$) at reduced load.

The thermal losses from the tanks will be 200 kW_t ($0.68 \times 10^6 \text{ Btu/hr}$) from the hot tank and 75 kW_t ($0.25 \times 10^6 \text{ Btu/hr}$) from the cold tank. Both salt tanks are large enough to contain the entire inventory of salt including salt in the receiver, piping, heat exchangers, and cold salt tank at or below 315°C (600°F).

The construction cost of the storage subsystem is estimated to be \$8,794,000 (1982\$). The design engineering cost is estimated at \$972,000, yielding a total installed subsystem cost of \$9,766,000 (1982\$). The major cost elements of the storage subsystem are the storage tanks (29%) and the heat transport fluid (59%). The construction cost includes associated piping and pumps and salt loading and treating equipment. If one were willing to significantly increase the amount of time for loading salt to the system, some savings (perhaps \$0.5M) might be realized. The information currently available on salt treating is inadequate to arrive at an accurate cost estimate. Equipment was sized and costed based on the experience of Houdry in maintaining salt in cat-cracker heat transfer loops. The cost of this equipment is only an order-of-magnitude estimate. In any event, it has very little impact on the storage subsystem cost.

5.6 ELECTRIC POWER GENERATING SUBSYSTEM

The electric power generating subsystem (EPGS) at the Saguaro Steam Electric Station Unit One, which was completed in 1954, consists of the turbine, feedwater, heat rejection, and electrical subsystems. The 120 MW_e gross turbine generator set was manufactured by General Electric. The feedwater subsystem consists of five feedwater heaters and three boiler feed pumps (one spare). The heat rejection subsystem consists of a Westinghouse condenser, two circulating water pumps, three condensate pumps, (one spare) and Marley wet cooling towers. The electrical subsystem consists of the generator, main transformer, and auxiliary transformers. Further specifics on this equipment can be found in Appendix E of Ref 1-4 and section 5.6 of Ref 1-2.

All of the EPGS equipment has been operating satisfactorily for 28 years with the exception of the Unit One turbine high pressure shell. That shell was replaced in 1975 and the turbine was upgraded to a steam flow rate of 126 kg/sec (1x10⁶ lb/hr). The major part of the EPGS is located just to the south of the fossil energy subsystem (Fig. 4.1-3) with the cooling towers being located to the east.

5.6.1 EPGS Requirements

The requirement for the EPGS is to produce the rated electrical power of 120 MW_e when supplied with steam at the specified conditions. The EPGS was designed to operate in the environment at Saguaro and has done so.

5.6.2 EPGS Design Description

In the original fossil fuel fired plant, steam produced in the fossil energy subsystem is fed into the high pressure turbine. The steam expands through the 21 high and low pressure stages and exhausts to the condenser where the steam is condensed. The condensate is pumped through a series of five feedwater heaters where it is heated to successively higher temperatures by steam extracted at the 5th, 9th, 14th, 17th and 19th stages of the turbine. From the feedwater heaters, the condensate is pumped to the fossil energy subsystem. The heat rejection system provides the heat sink for the steam cycle. Cooling water flowing through the condenser absorbs heat from the steam exhausted from the turbine thereby condensing the steam. The heated cooling water from the condenser is circulated to the cooling tower where the cooling water gives up its heat to the atmosphere, after which it flows through an open channel to the pumps and is returned to the condenser. Makeup cooling water is provided by a set of wells at the plant site.

The electrical system of the plant takes the electrical energy produced by the generator at 15 kV and steps the voltage up in the main transformer to 115 kV from where the power is transmitted to the switchyard for interconnection to the utility's power grid. Auxiliary transformers use a portion of the generator's output for the powering of auxiliary equipment within the plant, such as, pumps, fans, heating, ventilating and air conditioning, etc.

5.6.3 EPGS Performance

Plant performance before repowering is given by the gross heat rates listed in Table 5.6-1 for various plant loads and condenser back pressures. The data in Table 5.6-1 are for the existing boiler characteristics with its pattern of superheated steam temperature variation with load (see Appendix E of Ref 1-4). The auxiliary electrical loads for the existing plant are given in Table 5.6-2. The auxiliary loads do not vary appreciably with condenser pressure, they only vary with generator load and thus steam rate.

Table 5.6-1 Gross EPGS Heat Rate (Fossil Steam), MW_t/MW_e (Btu/kWh)

Condenser Pressure, kPa (in. Hg)	Gross Power Output, MW_e				
	120	100	80	60	40
1.69 (0.5)	2.227 (7600)	2.236 (7631)	2.270 (7747)	2.333 (7960)	2.497 (8520)
3.38 (1.0)	2.321 (7921)	2.331 (7954)	2.364 (8067)	2.400 (8188)	2.565 (8752)
5.07 (1.5)	2.424 (8270.6)	2.434 (8305)	2.468 (8422)	2.549 (8699)	2.717 (9270.5)
6.75 (2.0)	2.541 (8670)	2.544 (8680)	2.580 (8803)	2.661 (9080)	2.830 (9655)
8.44 (2.5)	2.566 (8755)	2.577 (8792)	2.613 (8915)	2.694 (9194)	2.842 (9697)
10.13 (3.0)	2.583 (8814)	2.594 (8851)	2.631 (8976.5)	2.713 (9256)	2.881 (9830)

Table 5.6-2 Auxiliary Electrical Loads (Fossil Steam), MW_e

	Gross Power Output, MW_e				
	120	100	80	60	40
EPGS	3.93	3.45	2.99	2.51	2.03
Boiler	2.37	2.37	2.37	2.37	1.9

Heat balances for four levels of operation are given in Figures 5.6-3 through 5.6-6 of Ref 1-2. The EPGS performance after repowering is given in Table 5.6-3. This table reflects the fact that the solar steam generator will be able to hold superheated steam temperature higher at part load than the fossil boiler can. The solar powered performance of the EPGS is slightly better than the fossil performance. As presently operated, the fossil boiler efficiency at part load is lower than the efficiency at the design load. However, the fossil boiler could be operated at part load and at design point efficiency if the steam temperature is allowed to drop. In a fossil-solar mixed mode of operation the steam proportioning control will compensate by causing the solar steam temperature to track the fossil steam temperature and the performance of the turbine generator will remain unchanged.

Table 5.6-3 Gross EPGS Heat Rate (Solar Steam) at 6.77 kPa (2.0 in Hga) Backpressure

Gross Power Level MWe	Gross Heat Rate MWh/MWe (Btu/Kwh)	
120	2.541	(8670)
100	2.544	(8680)
80	2.569	(8767)
60	2.623	(8952)
40	2.742	(9356)
30	2.866	(9781)

5.6.4 EPGS to Solar Interfaces

The repowering of the plant consists mainly of the incorporation of the solar steam generator in parallel with the existing fossil energy subsystem to provide superheated steam to the turbine. The equipment and systems in the existing EPGS which will be affected by the repowering are listed in Table 5.6-4. Each piece of equipment or system in this table will require modifications except for the circulating water, feedwater, gland steam (turbine seals). The main steam lines will require modifications and the uninterruptible power system must be added. Table 5.6-5 lists that EPGS equipment and systems that do not require change. It can be said that all potential areas for change have been identified. The extent of the major changes are identified further in paragraph 3.8.3 of the System Requirements Specification of the prior Saguaro study (Ref 1-3).

5.6.5 EPGS Cyclic Performance

In section 2.6, Existing Plant Description, it was noted that the Saguaro Power Plant reached its 25th anniversary in 1979. By the year 1987, when solar repowering at Saguaro is planned to start, the plant will have passed its 30th anniversary. Based upon APS Engineering Generation Department recommendations, a tentative plant retirement date was set for 1995, provided no further improvements were implemented. The application of solar repowering, with an implied cyclic

Table 5.6-4 EPGS Elements That Require Changes

Main Steam	Low Voltage Auxiliary Power Systems, 480- and 120/208-V Auxiliary Systems (includes transformers, bus, switchgear, motor control centers, distribution panels, etc)
Plant Communications System	
Main Control Room System	
Circulating Water	
Station Batteries, Chargers, dc Distribution, and dc Emergency Lighting	Medium Voltage Auxiliary Power Systems, 13.8-, 6.9-, and 4.16-kV Auxiliary Systems (includes unit auxiliary transformers and reserve, house service, or startup transformers, bus, switchgear, etc)
Environmental Monitoring Systems	
Essential Service Power	
Fire Protection Systems (includes water, dry chemical systems and Halon systems)	Transmission Voltage System 765-, 345-, 161-, and 23.5-kV and other transmission or distribution levels)
Feedwater	
Grounding and Cathodic Protection	Plant Air (includes air compressors, receivers, and plant air piping, etc)
Gland Steam (turbine seals)	Uninterruptible Power (includes inverters and associated distribution equipment)
Hoists and Cranes	
Instrument Air	
Ventilating and Air Conditioning	

mode of operation being imposed upon Unit One, which has never operated in a daily cycling mode, established the necessity of examining what impacts such operation would impose and what possible modifications might be required.

The SERI "Solar Thermal Repowering Systems Integration" report (Ref 4-1) prepared by Sterns-Roger Services, served as a guideline and checklist to assess the Saguaro Unit One turbine generator's capabilities for cyclic operation. Both Saguaro Units One and Two, starting from the time of commissioning in 1954 and 1955, respectively, were operated as base loaded plants and only in the later years were they changed to intermediate loaded plants. In the latter mode of operation, the units were loaded at a minimum level of 30 MW_e out of 100 MW_e, ready to be brought up to full capacity if system demand so dictated. Unit One, by operator choice, was selected to swing with

Table 5.6-5 EPGs Elements That Do Not Require Changes

Blowdown	Heater Drains and Vents
Burners	Hydrogen Gas System
Boiler Drains and Vents	Hydrogen Seal Oil (turbine-generator)
Combustion Air and Seal Air and Air Heaters	Ignition Fuel
Condensate	Lube Oil (includes main turbine generator, turbine drives, and turbine oil conditioning equipment only)
Condenser Evacuation	
Chemical Feed and Handling for Steam Boiler Water Control	Turbine Control
Chlorination	Turbine Drains and Vents
Plant Cooling Water	Turbine Generator Auxiliaries and Miscellaneous Devices (turning gear, noncontrolling instrumentation, etc)
Extraction Steam	
Flue Gas	
Fuel Oil	Turbine Lube Oil, Storage and Transfer
Generator Voltage System (includes generator, exciter, main power transformer, isolated phase bus duct, potential transformer and surge protection cubicles, etc)	

system load, imposing a more severe loading condition on the turbine generator. This type of operation was ascertained as the cause of cracking of the high pressure turbine shell, leading to its replacement in 1975. In addition to replacing the high pressure shell, modifications were implemented to upgrade the turbine. These modifications were compared to the SERI report recommendations to ascertain whether any further upgrading would be necessary to meet cyclic operating requirements. It was decided that the turbine manufacturer (General Electric) was far more qualified to make an evaluation, resulting in recommendations and costs to effect modifications.

A cycling study for Saguaro Unit One was contracted with General Electric to arrive at recommendations regarding possible modifications to make the unit more suitable for cyclic duty. Rather than consider the unit operating as solar repowered, GE elected to take the approach that the unit would be cycled in the more conventional manner, wherein turbine inlet temperature falls off with load, thus representing a more severe cyclic duty.

GE recommendations are divided into five general categories with specifics for each:

- 1) Improved instrumentation and controls - Additional thermocouples and other instrumentation are recommended to provide the operators with sufficient guidance during starting, loading and shutting down periods and to record effects of the start-ups and shut-downs on the turbine parts.
- 2) Improved means of turbine temperature control - The aim in controlling temperature is to reduce the total temperature change the turbine parts experience when going from turning gear to full load and back to turning gear again. The temperature changes can be significantly reduced if control valves are cammed to open together instead of sequentially. New control valve cams are needed for this modification. Along with single admission cams it is recommended that the stop valve bypass valve be converted such that it is used for pre-warming only. New valve seats were installed in the stop valve bypass valve during the major outage in the fall of 1980.
- 3) Replacement and modification of turbine parts - Replacement of turbine parts is recommended where it is judged that there is significant risk of serious failure or otherwise unsatisfactory service in exposing them to repeated thermal stressing, or additional duty involved in frequent cycling. Recommendations were made for inspection, which is normally performed during a major maintenance outage, of the following items: turbine rotor, shells, exhaust hoods, diaphragms and clearances. A recommended list of replacement parts or modifications was made: Convert 3 and 4 water seals to steam, modify couplings with fitted studs and replace elliptical bearings with tilt pad bearings. New fitted studs for the turbine-generator couplings were installed during the fall 1980 major outage.
- 4) Cyclic life expenditure curves - For cyclic duty, it is recommended that Arizona Public Service Company select a cyclic life expenditure curve that is commensurate with the increased number of cycles anticipated and consistent with the expectations of life of the turbine parts. This may result in Arizona Public Service Company operating for cycling on a lower life expenditure than was used for base load operation.
- 5) Generator - Two areas of concern arose due to cyclic duty, one is the possibility of top turn breaks in the field windings, and the other is stator winding girth cracks. In either case partial rewinds are called for with new type insulation. Neither of the problems have yet been detected to date. Incipient girth cracking can be identified by hipotting, which is a recommended procedure.

Should Arizona Public Service Company elect to implement all of GE's recommendations, their quotation amounts to \$322,200 (1982 \$) for material without installation cost. Not all of these costs can be charged to the impact of repowering since some of the items will be done in the course of routine maintenance.

5.6.6 EPGS Control System Upgrading Recommendation

The existing Saguaro Unit One control system operates as a regulation reserve and area frequency support for the southeastern part of the APS grid. Thus, the main functional requirements for the upgrading of this control system are as follows:

- 1) The response time of the fossil fuel boiler and turbine should be short and, together with the voltage regulator, should provide rapid and stable response to load changes.
- 2) Measures should be taken to improve the response of the boiler, superheater and turbine to load changes.
- 3) The control system upgrading should feature the high level of automation that can be provided by a reliable and sophisticated control technology.
- 4) It should be possible to easily integrate the fossil fuel control system with the master control system of the solar repowering system. Instruments and controllers, as well as spare parts, should be identical for all subsystems of the repowered plant.
- 5) The two segments of the plant, solar and fossil, should be able to work together or independently and each should be able to start when the other is on line. Consequently, the connection between the two steam generators should be such that cross coupling is minimized.

5.6.6.1 Control Philosophy of the Fossil Fuel Power Plant - The Saguaro Power Plant fossil steam generator was built by Combustion Engineering in 1954. It can be fired by either natural gas or No. 6 oil, or a combination of both. As the most used fuel is natural gas, soot blowers were not provided.

Combustion Control - The combustion control system for the Saguaro Unit One is illustrated in Figure 5.3.8 where the feedforward lines are shown in boldface and are based on the fact that turbine first stage steam pressure is a measure of steam flow. Steam flow, at rated temperature and pressure, results from fuel flow and the associated air flow. Thus the feedforward signal of the steam flow goes to the fuel flow and air flow controllers. Both oil and gas fuels are shown as the boiler can operate on either or both. The throttle pressure setpoint is established by dispatch control. The difference between throttle pressure setpoint and actual throttle pressure is used to trim the desired steam flow in summator, calibrator A. Fuel flow trimming involves the difference between the actual heating value of the fuel (oil or natural gas) as it is being used and the value originally designed into the feedforward controller. Oxygen in the flue gas is measured by the oxygen monitor and used with a modified oxygen setpoint to trim the fuel/air ratio.

The Saguaro Power Plant does not have, nor is it required to have, any pollution control systems. The manual/automatic interface stations allow direct operator control of the setpoints on steam flow and fuel/air ratio.

The combustion control system on both units at the Saguaro Power Plant is an analog computer which uses air-powered computing elements and pneumatic control devices. Pneumatic systems are characterized by simplicity and reliability but lack the computational power and easy on-line diagnosis of electronic systems.

The hardware which comprises the combustion control system was manufactured primarily by Westinghouse. However, there also is equipment manufactured by Bailey, Republic, Fisher and Brooks.

Signal ranges include: 1) 3 to 15 psig; 2) 0 to 30 psig; 3) 0 to 60 psig; and 4) 3 to 27 psig. This not only reflects the different manufacturers represented but also hints at the numerous changes to the system over the years.

The combustion control system can be upgraded by introducing more transducers and control loops. When the EPGS is being controlled from the APS dispatch center, the L&N 11401 dispatch unit controller will send signals to the turbine governor valve controller and to the summator, calibrator function (see Figure 5.3-8) as a feedforward signal to increase/decrease combustion. In constant load operation, the turbine governor valve and the combustion control system are disconnected electrically and linked only via the steam pressure and steam flow rate. For rapid load increases, the megawatt setpoint of the turbine governor valve controller is switched by the operational control unit (OCU) to the steam pressure controller. The output signal of the main fuel controller forms the setpoint of the gas/oil flow rate controller.

Should the boiler feed pump or a forced or induced draft blower fail, or a turbine trip occur, or when the generator is switched over to the auxiliaries load, the fuel feed must be quickly reduced to about 30 MWe. The actual valve signal of the fuel controller will be reduced within about 10 seconds following a ramp curve. To avoid rapid raising of the fuel feed rate, the fuel set point will be lowered via an automatic load reduction device. This is designed to automatically take into account long-term variations in the calorific value of the fuel.

A flue gas oxygen analyzer will automatically correct the air-fuel ratio. The combustion control system will have two inputs from current air and fuel temperature readings.

There will be appropriate hardwired and software interlocks, limit actions, and runback actions to maintain the unit within the capabilities of the equipment.

Steam Drum and Throttle Pressure Control - A steam by-pass station should be added for the following reasons:

- 1) To provide a short start-up period with the least possible wear on plant components,
- 2) To provide a fast hot re-start capability,
- 3) To obtain low start-up and shut-down losses, and
- 4) For start-up when the solar system is already on line.

The by-pass station will dump steam into the condenser during start-up until the correct steam temperature is reached for the turbine to be started. If a turbine trip or a transfer of load to the auxiliaries occurs, the by-pass station will provide a steam route to the condenser. This will permit maintaining the steam generator operational for a fast hot re-start of the turbine. Partial load rejection can take place with the assistance of the by-pass station, thus reducing the impact on the steam generator.

The by-pass station is controlled by a tracking device which follows the steam pressure with a certain positive threshold. If the steam pressure rises faster than is allowed, the combined high-pressure safety and by-pass valves open and partially limit the rate of pressure increase. Excessively rapid pressure drops are also detected and the turbine control is enabled to change over to inlet pressure control. The turbine governor valve is controlled by the steam pressure controller of the high-pressure safety and bypass valve station instead of the megawatt setpoint. The OCU will supply a feedforward signal to control the by-pass station in accordance with the unit load demand. Besides the electronic digital steam pressure control, a separate safety system, with pressure switches, connected to a "1 out of 3" selector will be installed.

Steam Temperature Control - The hardware used for controlling the superheat temperature control was manufactured by: Bailey, Hagan (Westinghouse), Fisher, and Bell & Howell. The control signals in use are both electronic and pneumatic and include the following signals: millivolts, milliamps, 3-27 psig, and 0-30 psig. The superheater consists of a primary and a secondary section. Temperature is controlled by two means: 1) shunt & series dampers, and 2) burner tilts. The shunt dampers bypass hot boiler gases around the superheaters to lower the steam temperature and the series dampers pass hot gases over the superheaters to raise the steam temperature. The shunt and series dampers are controlled remotely by the operator - there is no automatic control.

The burners are tilted up to lift the fireball closer to the superheater section and to increase the steam temperature. The burners are tilted down to decrease the steam temperature.

Steam temperature is sensed at the turbine inlet by a thermocouple. The millivolt level signal from the thermocouple is converted to a pneumatic signal. This is compared to an operator-adjusted setpoint by the steam temperature controller which then tilts the burners appropriately. An additional input from the combustion controls gives a temporary kick to the burner tilt whenever airflow is suddenly changed.

Steam temperature control is not satisfactory for the following reasons:

- 1) The furnace is sized for gas which tends to produce higher steam temperatures. When firing oil, rated steam temperature of 541°C (1005°F) is seldom reached.
- 2) When firing gas, rated temperature is not reached until approximately 60 percent load. Since these units are constantly being moved above and below 60 percent load, the steam temperature varies with load.
- 3) Using burner tilting to control steam temperature is a slow method. This means that temperature excursions tend to be larger and longer than they would be if spray valves in an attemperator were used.
- 4) Sensing temperature at the turbine instead of at the boiler adds a time delay to an already slow process and magnifies temperature excursions.

The following measures are recommended for upgrading Saguaro Unit One steam temperature control:

- 1) An investigation should be conducted to establish how the rated superheated steam temperature can be easily reached when burning either No. 6 fuel oil or natural gas by improving the fuel flow, the combustion and the heat exchange processes.
- 2) A spray attemperator should be installed between the two sections of the superheater.
- 3) A by-pass valve should be installed around the finishing superheater.
- 4) The usefulness of soot-blowers should be considered in order to improve heat exchange efficiency.
- 5) The shunt and series damper positions should be automatically controlled.
- 6) The steam temperature sensors should be installed at locations that satisfy control requirements.
- 7) An integrated and coordinated control system should be provided that uses the most efficient methods to control steam temperature and avoid control cross-coupling. The OCU should supply a feedforward signal commensurate with unit load demand.
- 8) The air heater cold-end temperature should be controlled by modulating temperature control valves in the air preheater steam coil supply lines. The supply pressure should be kept constant by modulating valves in each supply line.

Feedwater Control - The feedwater control consists of a 3-element drum level control system. The control hardware is pneumatic and is manufactured entirely by Bailey. There is a chronic problem with the particular generation of hardware used. The problem would be best solved by switching to electronic equipment.

Steam drum water level (compensated for density changes) is compared to the drum level setpoint by the drum level controller. The controller opens or closes the feedwater valve to maintain drum level at its setpoint. During rapid load changes, erroneous drum level readings are sensed. This is because the water in the drum swells when pressure decreases on a sudden load pickup. The drum level controller will act to lower the level by decreasing the feedwater flow at a time when it should be increasing. The opposite effect occurs on a rapid load decrease. To counteract this effect, feedwater flow and steam flow are measured and compared. The error signal is used to cancel the drum level error.

The feedwater control system should be reviewed with emphasis on the effects which will result from using the same feedwater system for both fossil and solar steam generators. Any interference between the two feedwater control systems should be avoided. Oscillations in flow rate and pressure are possible. An investigation involving both analysis and computer simulation should be performed to avoid boiler/turbine trip caused by feedwater control system interactions.

The current steam flow rate transducer (the turbine first stage pressure) should be retained as a feedforward signal. Another feedforward signal should be supplied by the OCU based on unit load demand. Both signals should be ratioed according to the operating mode of both steam generators. Separate steam flow rate transducers are to be installed in each steam stream (solar and fossil). Three steam drum level transducers should be used with a "1 out of 3" selector and the signals should be processed for use by other master control subsystems.

Turbine Generator Control - The current turbine generator (TG) controls consist of: main steam stop valve, steam flow, governor control valves, turbine speed control, emergency trip, and the turbine generator oil pumps. Additionally, a number of parameters are continually monitored such as turbine shell temperatures, bearing oil temperatures, thrust bearing temperature differences, sealing steam flow, and vibration and shaft eccentricity. Other functions being controlled are: circulating water flow, condenser back pressure, generator hydrogen pressure, and generator output voltage. The current governor valve control is based on a mechanical system, and does not work well.

The upgrading of the turbine control should start by changing the current governor valve and actuator to a high speed electro-hydraulic actuator, and modern governor valve. The mechanical control should be replaced by a hybrid microprocessor-based controller that has the following advantages:

- 1) Operational flexibility for startup, load cycling, short term operation, and recovery from load rejection,
- 2) Protection of the turbine-generator unit against overspeed, loss of oil, overheating, and excessive heat rate of change, and
- 3) A full arc to partial arc transfer capability.

Microprocessors will be used to calculate critical thermal quantities in the turbine and to make and implement decisions on starting and loading. Closed loop controls and automatic sequencing, as well as provisions for automatic and manual supervision, will be supplied. Processing of temperature data and mechanical criteria (such as rotor stress) will be performed automatically. An admission mode selection (AMS) program will determine the way the control valves are used to allow rapid startup and load changes. Steam will be admitted to the first stage of the turbine over either a full or a partial arc. The AMC program will respond to changes induced by load variations, as well as by changes in boiler output temperature. This program will permit faster load changes without turbine damage.

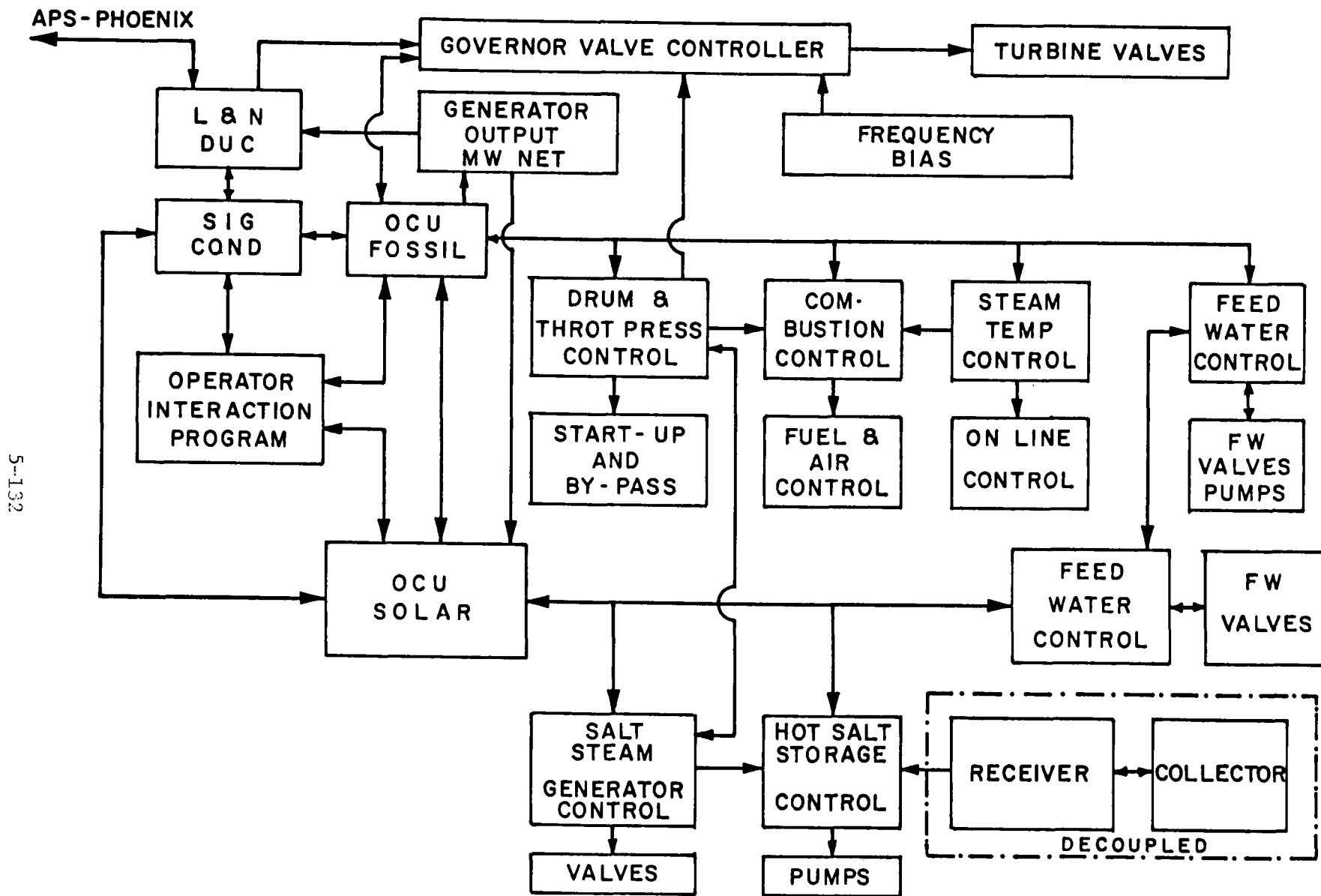
5.6.6.2 Integration and Coordination Control Recommendations - The operational control unit (OCU) provides the important integration and coordination control functions. Some general functions of this unit are described under the title "Operational Control Subsystem," paragraph 5.3.2.1. In the following paragraphs, specific functions related to the EPGS and the FSGCS are described.

Integration means a superimposed control function, which interrelates the actions of several local controllers that control elements of the generation process which are in series; e.g., drum level control and steam temperature control.

Coordination means a superimposed control function, which interrelates the actions of several local controllers that control elements of the generation process which are in parallel, e.g., the fossil steam generator controls and the solar steam generator controls.

Figure 5.6-1 shows the integration and coordination control philosophy. The figure does not represent the interconnections between computers, rather it illustrates the feedforward signal paths between the control units, which are considered control functions. The figure does not represent all signal exchanges necessary for control and data acquisition.

The operator will choose the operational mode and will program it onto an Operator Interaction program keyboard. The operator can choose the following operational modes:



5-132

Figure 5.6-1 Integration Control Schematic

- 1) Constant generation level determined remotely by APS-Phoenix dispatch center with only the fossil steam generator operational. In this case, the L&N Dispatch Unit Controller (DUC) will receive the required constant load. DUC will set up the governor valve controller according to the required generation and will receive back a signal proportional to the MW net output. At the same time, a signal will be sent through the signal conditioning unit to the OCU FOSSIL which will distribute it to all the other control units, such as drum and throttle pressure control, firing rate demand, steam temperature control and feedwater control. This signal will anticipate the control action required by the change of a generation level. Some regular exchanges of control signals are also shown on the figure, such as the drum and throttle pressure control and the steam temperature control, which will interact with the firing rate demand control.

We recommend that a frequency bias be added to the constant generation level operational mode. This addition will better support a constant frequency with better results for the APS interconnected grid.

- 2) Locally determined constant generation level. The operator will disable the DUC control and will set up an MW net output. This procedure is the same as in the previous case, except that the OCU will provide the functions which were provided by the DUC in mode 1), as well as its own control functions.
- 3) Load following operational mode. The operator will disable any constant generation level which was set up, either by the DUC or by the OCU. The governor controller will operate under speed and frequency bias control. The feedforward signals will continue to provide anticipation for the local controls to minimize their interactions.
- 4) Run-back operational mode. The operator can override all other controls and set up a lower level of generation in an emergency. This operational mode can be initiated by the drum and throttle pressure control and feedwater control as was described in a previous section.
- 5) Run-back operational mode (parallel operation). Each steam generator, solar or fossil, can initiate a run-back operational mode, which will be implemented either automatically or manually. The criticality and location of the upset which initiated a run-back call will determine whether both or only one of the generators would be run back.
- 6) Constant generation level with both fossil fuel and solar steam generators operating. The operator will establish the proportion of steam between the two steam generators. The constant output electric generation level can be set up by either the DUC or locally by the operator. Each OCU will proportion the constant generation setup and the measured MW net output in accordance with the operator imposed ratio. Each OCU will control its units so that its required share of steam is provided.

- 7) Constant locally determined generation level for the solar steam generator and remotely imposed generation level for the fossil steam generator. The operator sets up the constant generation level for the solar steam generator. The SOLAR OCU receives the order and converts the imposed level to a calculated MW net output equivalent to a steam pressure and flow rate. These calculated values are used as set points for all solar control components and are compared with real measured values for error correction. The fossil control assembly will operate in the operational mode described in item 1).

The OCU FOSSIL will receive the measure of the MW net output produced by both the solar and fossil generators and will supply the remainder of the total required constant power.

- 8) Constant locally determined generation level for the solar steam generator and load following mode for fossil fuel steam generator. In this mode of operation, the solar generator will work identically to item 6). The load demand variations will be compensated for by the fossil generator under its OCU control.
- 9) The solar steam generator operating as the fossil steam generator was in items 1), 2), 3) and 4). The fossil steam generator is shut-down.

The transitions between operating modes such as startup, normal shutdown, and emergency shutdown will be addressed in subsequent contract phases. These should include a detailed study and computer simulation for all normal modes and transitions between operational modes.

5.6.6.3 Physical Implementation Recommendations - Digital controls and data communications systems have used a centralized computer topology termed master to remote control/ communication system. The time-sharing technique of the mainframe computer has been applied to process computers, minicomputers and even microcomputers. The "dumb" (hardwired) terminals, which were used by the central computer, have been turned into "intelligent" data acquisition remote stations by using microprocessors. The electronic microtechnology has brought about more sophisticated control and data communications systems, i.e., the distributed, decentralized systems (multi control stations - multi access media systems).

The advantages of the distributed control technique as compared to the centralized digital control technique are well known. Some of these advantages are: better and simpler software structure, easier expandability and reconfiguration, better calibration at site location (including self-tuning capability), stand alone capability, and more sophisticated control algorithms. Even if the control functions are performed by application programs in a distributed way, the data communications structure may have a centralized or a decentralized configuration.

The commercially available distributed control systems are based on what is now called local computer networks. Such control systems have been developed into a third generation of sophistication.

The first generation has a centralized configuration, mainly a star configuration, with a master computer-controller at the center of the structure. The master computer controls the message traffic using a polling technique. The remote substations, based either on hard-wired logic or on microcomputers, are dedicated only to data collection functions.

Several centralized configurations are represented in ANSI C37.1-1979 (now under revision). Centralized configurations, either with a star topology or with a party line topology, have been used for SCADA and local control networks.

The advantage of a centralized communications configuration is that it is well established. However, the disadvantages are numerous. The centralized communications system is prone to a catastrophic failure mode. If the master station fails, the entire system is down. If a physical channel is cut off, one or more remotes remain isolated. A direct exchange of protocol data units between two remotes is not accommodated by such a configuration. The communications media access control is handled by the master station through polling one remote station at a time. This means that only one data unit can be signaled onto the entire deployment of physical channels at a certain time. Although the dedicated links between master and remote stations seem to favor an exchange of messages between them, the situation is similar to only one bus carrying messages because in both cases only one message is signaled at a time. Regularly, the priority of messages is not serviced in both cases. The alarming reports and the data batch messages wait in line for their polling time in a regular star network based on a half duplex communications system. The cost of long dedicated links is very high.

A centralized communications system represents a constrained configuration. This means that the carrier of a data unit between any two stations of the network has only one physical path to go; there is no alternative circuit. A constrained network configuration does not provide adequate reliability. At the same time, the throughput of the costly channels is not efficient. Such systems are represented by the Beckman MV 8000, Fisher, and Porter DCI 4000. The first phase of the solar repowering study of the Saguaro Power Plant appeared to use a centralized communications configuration.

The second generation of control networks is built as a multi-drop structure, with a common data communication link, called "data-highway." A centralized arbitration module controls the message traffic. The second generation of distributed systems makes use of distributed microcomputers, but the data-highway is mastered by an administration center, which represents the weakest point of these systems (e.g. Honeywell TDC 2000 and Foxboro Spectrum).

The modern control and data communications systems, either restrained to a local area or spread over a wide area, should comply with the International Standard Organization (ISO)-Open Systems Intercommunication (OSI) Reference Model (ISO document ISO/TC97/SC16N719 and DP 7498, Data Processing-Open Systems Interconnection Reference Model). Electronic microtechnology makes it possible to build cost-effective and technically effective networks, which comply with the above-mentioned model.

The third generation of distributed controls complies with the above-mentioned standard. They are called local control networks, or, for short, control networks. Local control networks are based on so-called local area networks or local computer networks, which are communications networks confined within a limited geographical area. The relatively short distances covered by these networks (0.1 to 10 km) allows high data rates with small mean bit error rates (MBER of, at most, 10 exp. ^{-9} at the link level). The life time of a protocol data unit is short. The media access control should be simple. The baseband signaling, using a Manchester code, is less expensive than the analog modulating technique.

The advantages of local computer networks brought about the development of many commercially available networks and standardization activities. Both the IEEE Local Area Network, Standard 802 Draft Oct. 19, 1981, and the International Purdue Workshop Proway (Technical Committee 5A of the IEC/SC65A/Working Group 6), have eliminated centralized media control access or other central administration control of the packet traffic, and both comply with the ISO-OSI reference model.

The third generation distributed control systems feature distributed control over the message traffic. For that reason, they are called "no-master, no-slave" networks. Some of these systems exhibit a "ring" configuration with a "store and forward" mechanism of controlling message traffic. Other systems are based on a "bus" configuration with a "token passing" or "master for a moment" mechanism for controlling the message traffic. Other control networks use the so-called carrier sense, multiple access/collision detection (CSMA/CD) technique for media access control. Such networks are completely "masterless" or "peer-to-peer" communicating control stations.

The third generation is represented by Bailey 90, Siemens Teleperm M, Westinghouse WDPF, Modcomp-Modway, Bailey-Bristol, etc. They are more reliable and fit much better for this application because they are easily expandable and reconfigurable. Only the third generation is in accordance with the new standards IEEE LAN 802, and Proway, IEC.

- 5.6.6.4 Distributed Control Network Recommendation - A distributed control network (third generation) is recommended for the Saguaro Power Plant repowering. The most modern and best control system, i.e., a totally distributed system of the third generation, is the network recommended

for the following reasons: the main function performed by the fossil fuel plant is as a regulation reserve for the APS grid; the control sophistication required by the hybrid concept; the expected changes and reconfigurations necessary during the demonstration phase; and the potential expansion of the control system to Unit Two.

The following description and Figure 5.6-2 are based on a unique concept, which takes advantage of the best features of all commercially available control networks. Although the depicted concept is not identical to any of the commercial networks, it can be implemented with some non-essential changes by any of the previously cited commercial networks. The concept has the advantage that the specification, which will be derived from this concept, will be a "neutral" specification, without giving advantage to any potential supplier. The evaluation process will be more impartial and the equipment offered by the vendors will be improved. The following description is detailed sufficiently for cost estimating.

Figure 5.6-2 illustrates three triple bus configurations: 1) a triple-bus for the fossil steam generator, which includes all control segments of the generation process as they are described above and in Figure 5.6-1; 2) a triple-bus for the solar power plant, which goes around the closely located segments of this plant (solar steam generator and salt tanks); and 3) a triple-bus for the common turbine/generator and auxiliaries (EPGS).

The recommended media access control is the CSMA/CD. For each of the three configurations, one bus is dedicated to data acquisition purposes, one bus is dedicated to control purposes, and one bus to priority messages. The system is built in such a way that any bus can replace the other. The dedicated buses are supposed to be loaded with many messages. That is why they are discontinued in the control room (or the spray cable room). But the discontinued buses can exchange necessary messages between them through the bridges, mounted at each discontinuity and also through the priority message bus according to the importance of the messages. Distributed stations take care of controls and data acquisition. They are built identically. Their software can be changed mutually so they are functionally redundant. All remote stations are linked to signal conditioners, sensors, transducers and actuators through selectors "1 out of 3," "1 out of 2," or directly for the less critical points. Hard-wired protection devices are connected to each remote station. The protection devices can be automatically released or released by the operator's override control. By this means, there is complete redundancy at all levels, and, for the critical points, a triple redundancy in data acquisition and protection actuation.

The solar steam generator and the fossil steam generator each have their own OCU, as described in paragraph 5.6.6.2. All three triple buses have separate supervising facilities in the control room. In other words, the two steam generators and the turbine/generator each have a supervising facility. The supervising facility is endowed with

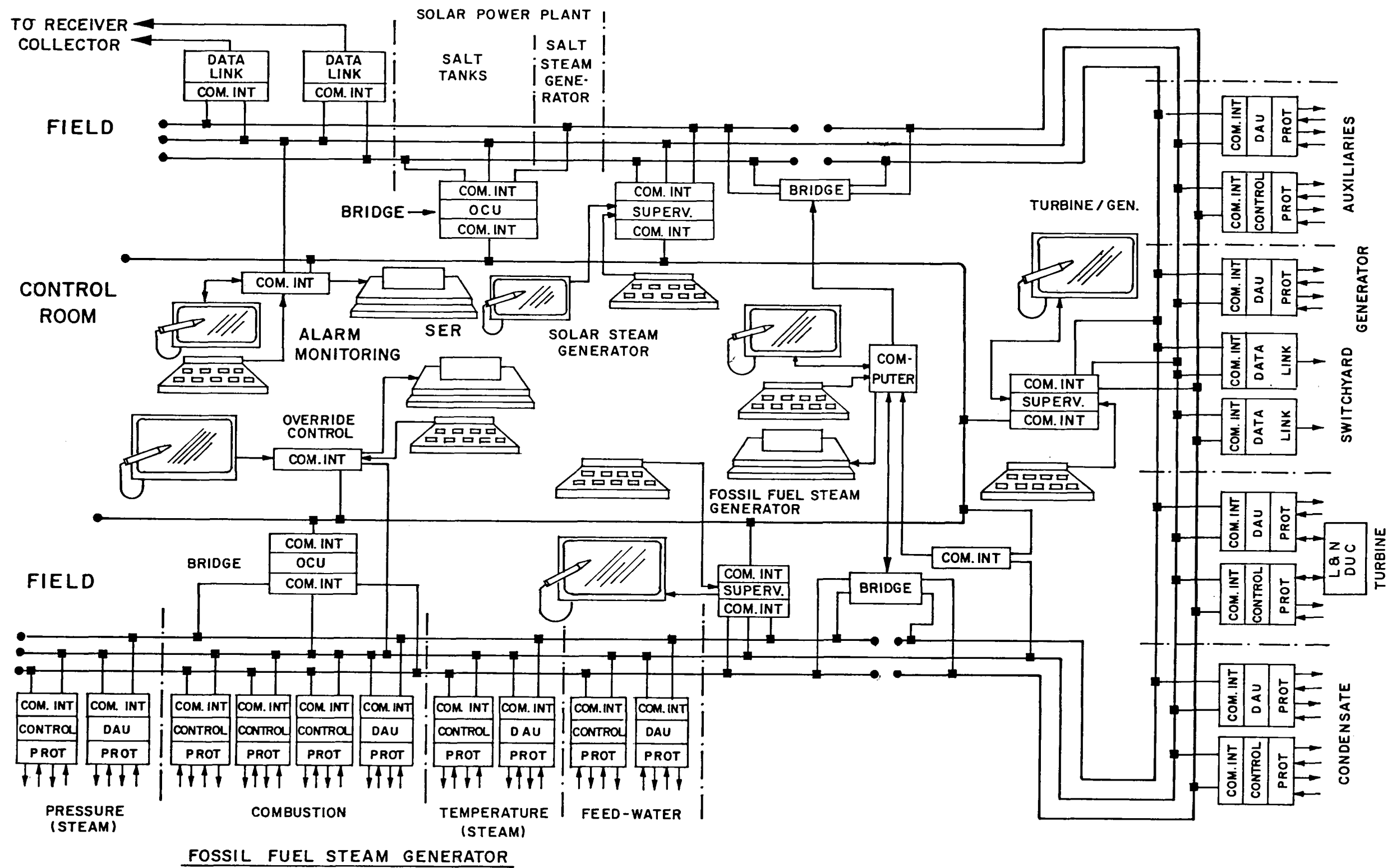


Figure 5.6-2 Distributed Control Arrangement

a CRT with a lightpen, a keyboard and a computer facility for intelligent monitoring, network management services, reconfigurations, software changes, etc.

A computer is linked to both bridges so that it has a connection with all triple buses. The computer performs optimization, computation, supervising and recording functions.

A special single bus was introduced only in the control room. This special bus is linked to all the other buses through the bridges used for other purposes such as OCU or supervising facilities. If only one bridge is still in good working condition, the special bus is linked to all other buses. The special bus services the alarm monitoring, override control and sequence of events recorder. These emergency facilities are interchangeable. Each can perform all functions. They are linked to two buses: the special bus and the priority bus (which is not discontinued). This means that a very high level of redundancy, in-depth computer-aided supervision, and very effective control has been recommended.

5.6.6.5 Cost Estimate for EPGS Control System Upgrading

A cost estimate was prepared for the equipment required to upgrade the existing EPGS and fossil steam generator to the level recommended above. Replacement of the governor valve and its controller are not included. The prices include installation and testing, but do not include preparation of a purchase specification.

Summarizing the control system upgrading costs (1982 \$) results in the following:

Sensors and transducers	\$ 64,500
Actuators	\$ 329,000
Control and intermediate stations	\$ 336,000
Data acquisition units	\$ 168,000
Control room equipment	\$ 550,000
Miscellaneous (including software)	\$ 355,000
Subtotal	<u>\$1,802,500</u>
Freight	\$ 108,150
Total	<u>\$1,910,650</u>

5.6.7 EPGS Modification Costs

General Electric's cyclic study recommended modifications to the turbine-generator to meet cyclic operation. These modifications were discussed in Section 5.6.5 along with a quotation for materials costs. APS Operations Department has reviewed the recommendations, and as indicated in the previous section, implemented some of the modifications during the planned major outage in the fall of 1980. The remaining modifications to the turbine will be performed at the next planned major outage, which is scheduled for the fall of 1984. Also, at this time a portion of the generator field will be rewound per GE recommendations.

Summarizing the EPGS modification costs (1982 \$) results in the following:

Turbine parts and labor	\$395,000
Generator field rewind parts and labor	\$152,000
NASH vacuum pump, parts and labor (for use with turbine steam seals)	\$ 82,000
Total EPGS modification cost	<hr/> \$629,000

This is an installed cost, including all wiring, controls, motors, piping and valves. Note that stator rewind has not been included. Regular 18 month inspections will be performed to ascertain status of the stator insulation. Costs for the EPGS control system upgrading are given in paragraph 5.6.6.5, but are not included in these EPGS modification costs.

5.7 SOLAR STEAM GENERATOR SUBSYSTEM

This section describes the requirements, design, performance and costs of the solar steam generator subsystem (SSGS).

The SSGS is a forced recirculation system employing a separate preheater, evaporator, superheater and steam drum. Within the subsystem, four functions are accomplished: the feedwater is preheated to the evaporation temperature, the water is evaporated to steam, the steam is separated from the recirculating fluid, and the steam is superheated for delivery to the turbine. Recirculating systems are used exclusively throughout the power industry where frequent startups and load swings must be accommodated. It is uniquely suited to the diurnal cycle service required in solar power plants. The arrangement of major components is shown in Figure 5.7-1.

5.7.1 Subsystem Requirements

The SSGS is designed to generate superheated steam at 10.0 MPa (1450 psig) and 538°C (1000°F) when supplied with feedwater at 216°C (420°F) from the high pressure feedwater heater from the Unit One turbine. The SSGS will be rated at a maximum power level of 172 MWt which is the thermal output requirement to produce a turbine generator gross electrical output of 66 MWe. The subsystem must also be designed to be compatible with the existing plant equipment, design and operating conditions. The repowered plant will have the capability to operate on fossil alone, solar alone, or combined in selectable proportions.

The design feedwater flow is 68.46 Kg/sec (543,370 lb/hr). The steam flow rate from the superheater is 67.8 Kg/sec (538,000 lb/hr) and the steam drum blowdown is 1% or 0.677 Kg/sec (5327 lb/hr). The inlet salt temperature from the hot salt storage tank is 566°C (1050°F) at 388.6 Kg/sec (3,084,000 lb/hr). The salt exits the preheater at 277°C (530°F).

The SSGS will be required to supply rated conditions down to 50% of design capacity. Feedwater temperature will drop with decreasing turbine output. Therefore, a provision must be made to maintain the temperature of feedwater entering the preheater, thus preventing salt from solidifying on the preheater tubes.

All components will be designed in accordance with ASME Section VIII, Division 1. Supplementary rules for elevated temperature design (developed under Sandia Contract number 20-9909A) will be used for design of the superheater to account for creep-ratcheting, creep-fatigue and creep-buckling considerations. The design life of the plant is 30 years and construction materials have been selected to meet this service.

Figure 5.7-1

5-142

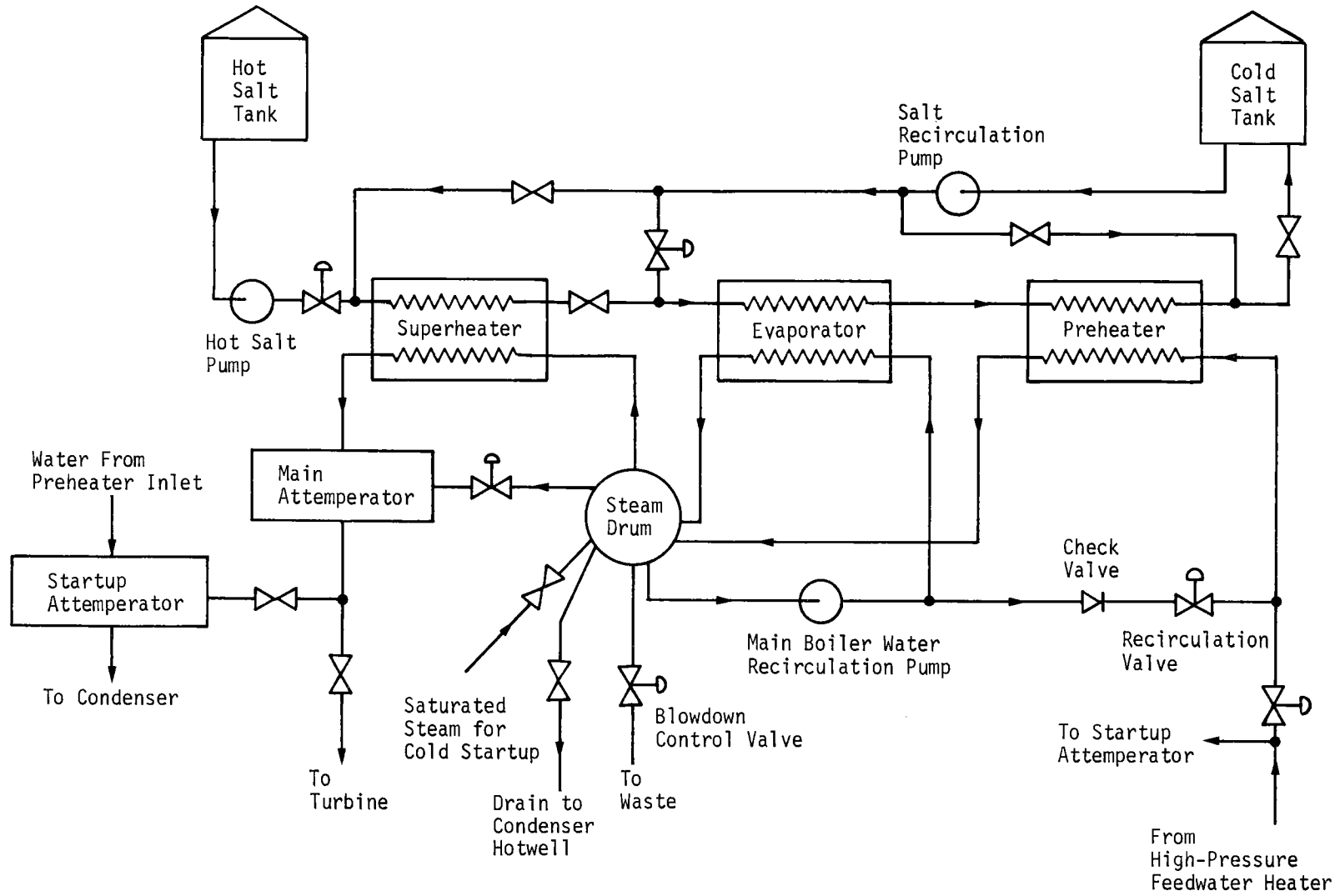


Figure 5.7-1 Solar Steam Generator Schematic

5.7.2 Subsystem Design Description

Figures 5.7-2 and 5.7-3 show the physical arrangement of the SSGS components. (Drain lines are not shown for clarity). The heat exchangers are oriented horizontally with nozzles arranged to facilitate venting and draining. The horizontal orientation also permits supporting the units on foundations at ground level. The steam drum arrangement is a standard fossil boiler design employing conventional cyclone steam separators and scrubbers. The steam drum is elevated to provide sufficient net positive suction head (NPSH) for the recirculation pumps. The routing of the salt and water/steam piping includes lengths necessary to connect the piping and provide sufficient flexibility for thermal expansion. The steam drum, superheater and piping are supported from a structural steel frame.

The SSGS will require a 21m x 30m (70 ft x 100 ft) plot of land adjacent to the salt drain tank area. The overall height of the systems is 7.6 m (25 ft). An earth berm will be built around the SSGS.

Figures 5.7-4, 5.7-5, 5.7-6 and 5.7-7 show the sectional arrangements for the preheater, evaporator, superheater, and steam drum respectively. The design philosophy for the SSGS components is consistent with that used for the 100 MWe Sandia SSGS design study (SANDIA: 20-9909A). The preheater and evaporator designs are U-tube bundles housed in a single straight shell. While U-tubes have also been used in the superheater, the large steam-side terminal temperature differences impose unacceptable thermal stresses on a single tubesheet. Therefore, a U-shell arrangement is used to house the superheater tube bundle.

The component designs include such features as:

- 1) Salt inlet/outlet distribution boxes
- 2) Tubesheet thermal shields (evaporator and superheater only)
- 3) Complete salt side drainage
- 4) Tube to tubesheet flush welds
- 5) Salt side inspection openings
- 6) Water/steam side inspection openings
- 7) U-bend tube supports
- 8) Differentially broached tube support plates (preheater and evaporator only)
- 9) Corrosion allowances based on available data
- 10) Salt side pressure relief in the event of a tube leak

Materials were selected to provide adequate strength and corrosion resistance in the operating environment. Carbon steel is used for the low temperature service of the preheater and steam drum. It provides favorable strength and acceptable corrosion resistance in both salt and steam/water at temperatures below 343°C (650°F). The evaporator operates in a higher temperature environment, normally as high as 452°C (845°F). Consequently, the increased mechanical strength and corrosion resistance of 2-1/4 Cr-1 Mo is considered necessary. The superheater operates in a temperature environment up to 566°C (1050°F). Therefore, 304 stainless steel is used to provide adequate strength and corrosion resistance.

Figure 5.7-2

5-144

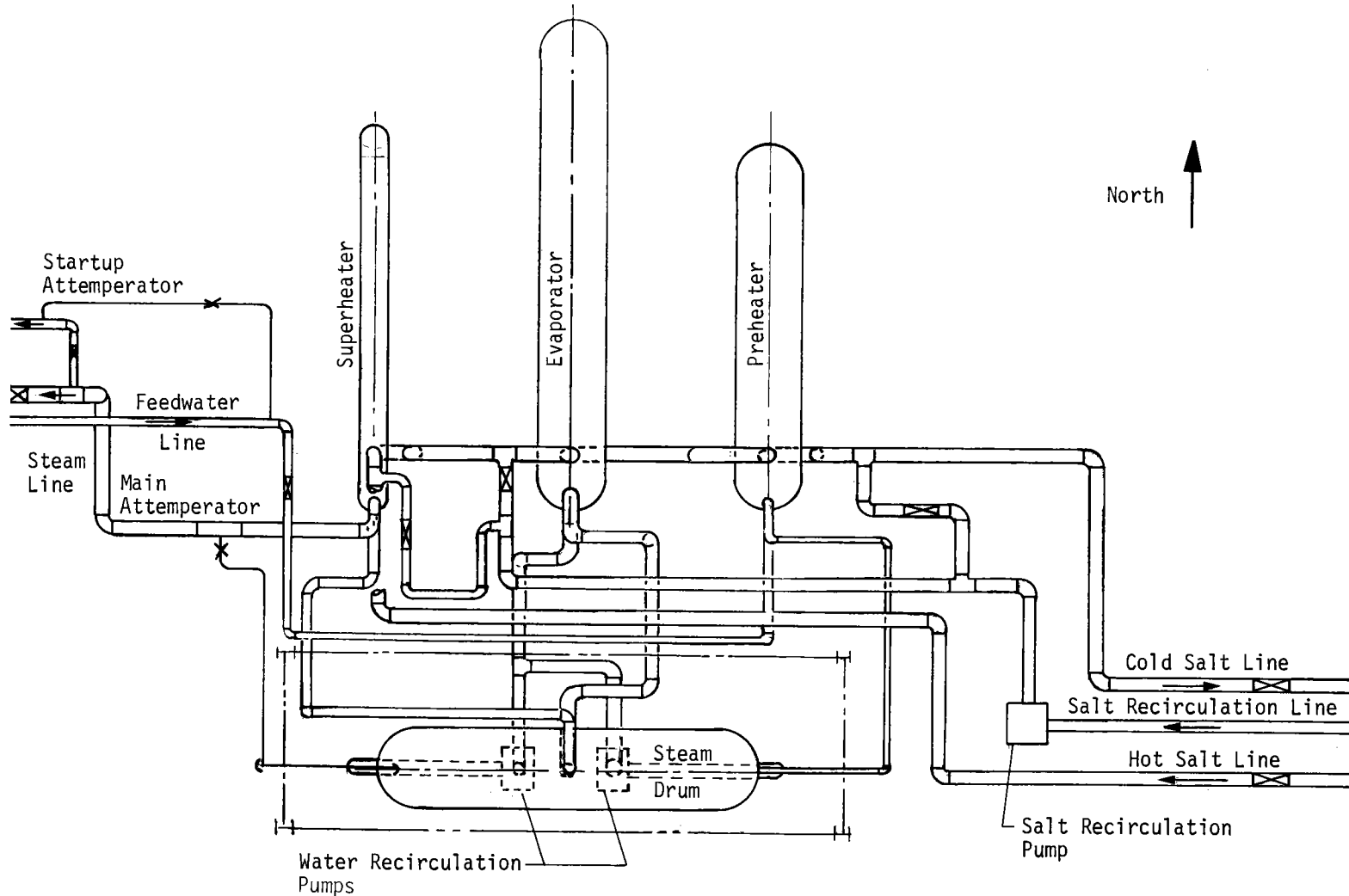
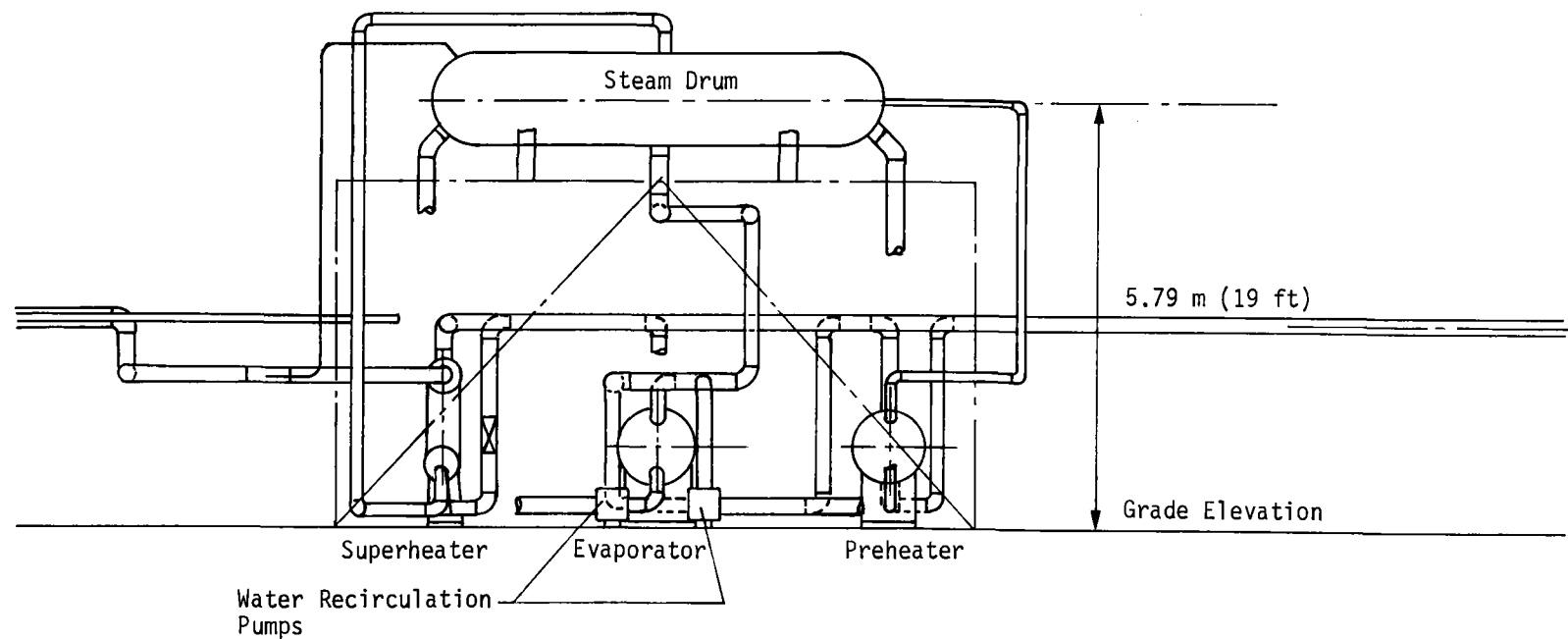


Figure 5.7-2 Solar Steam Generator Piping Plan View

Figure 5.7-3

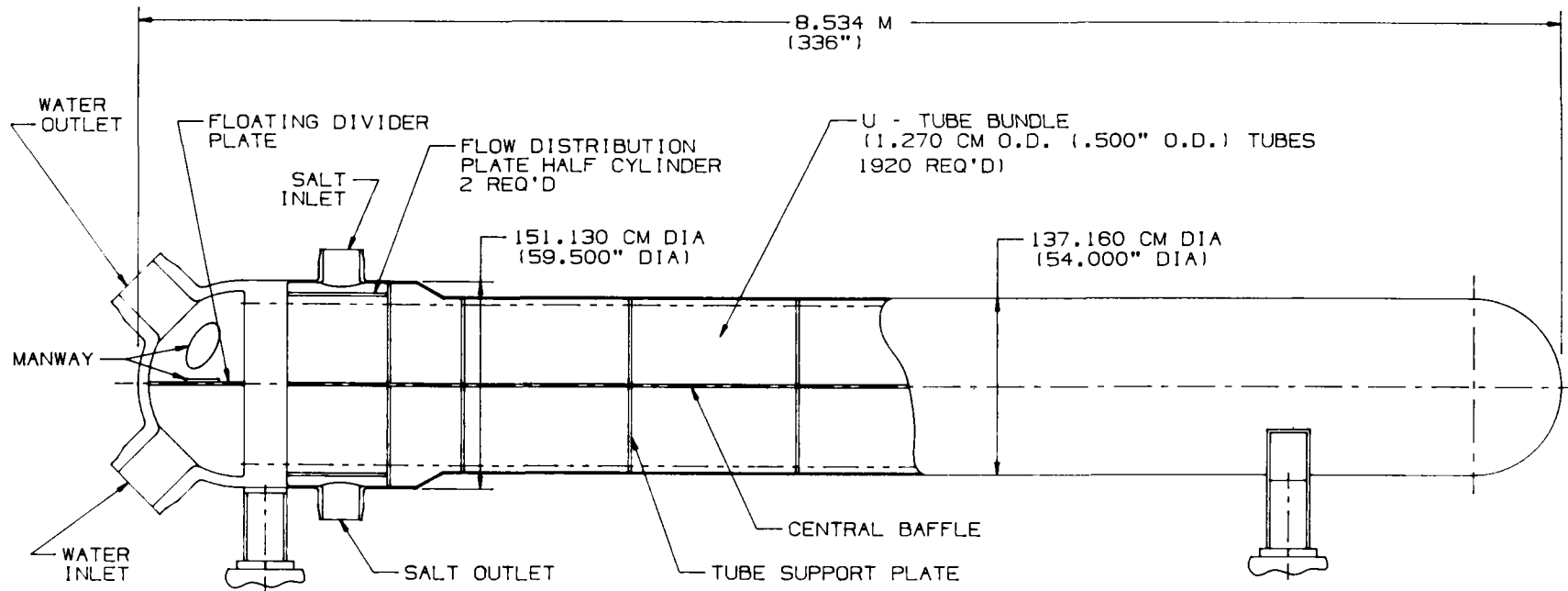


5-145

Figure 5.7-3 Solar Steam Generator Piping Elevation View

Figure 5.7-4

5-146

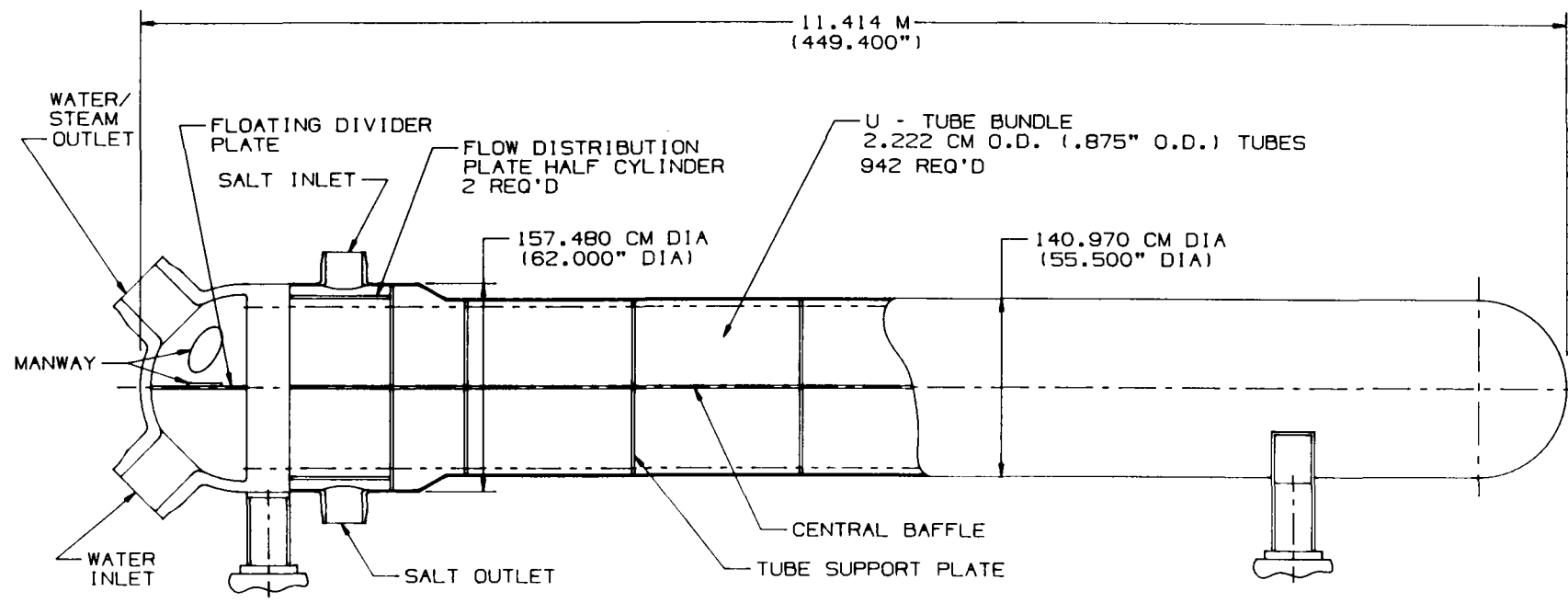


NOTE:
APPROX. DRY WEIGHT - 32000 KG (70560 LBS)
MATERIAL - CARBON STEEL

Figure 5.7-4 Preheater Sectional Arrangement

Figure 5.7-5

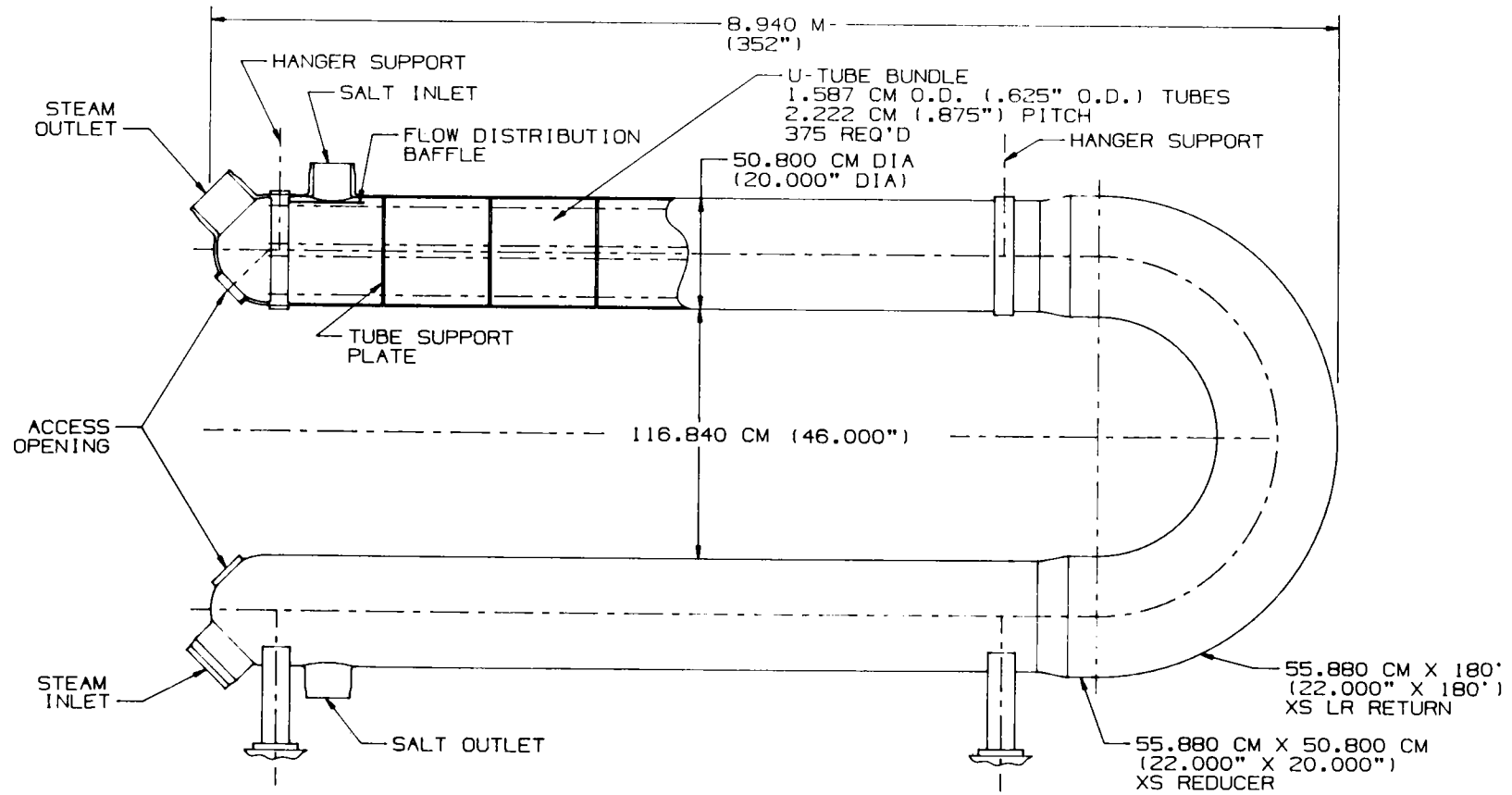
5-147



NOTE:
APPROX. DRY WEIGHT - 70,000 KG (154,000 LBS)
MATERIAL - 2 1/4 CR - 1 MO

Figure 5.7-5 Evaporator Sectional Arrangement

Figure 5.7-6



NOTE:
APPROX. DRY WEIGHT - 6,804 KG (15,000 LBS)
MATERIAL - TYPE 304 STAINLESS STEEL

Figure 5.7-6 Superheater Sectional Arrangement

5-148

Figure 5.7-7

NOTE:
APPROX. DRY WEIGHT = 24500 KG (54000 LBS)
MATERIAL = CARBON STEEL

5-149

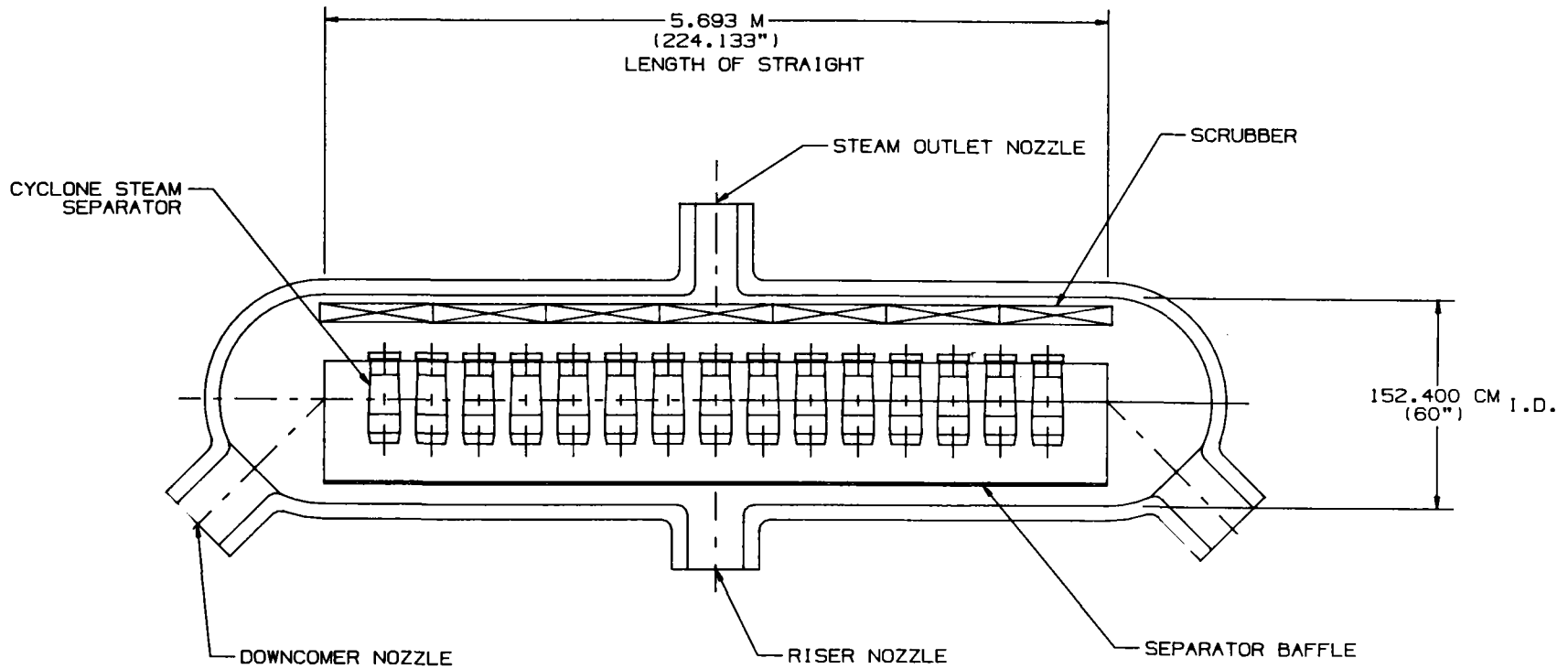


Figure 5.7-7 Steam Drum Sectional Arrangement

This forced recirculation system has been designed to preclude departure from nucleate boiling (DNB) in the evaporator. Typically, the fossil boiler circulation ratio is sufficiently high to maintain nucleate boiling in all circuits. In this design ribbed tubes have been used to allow the reduction of the circulation ratio to 1.5 thus reducing the necessary heat transfer surface area and recirculation pump power requirements. Additionally, the recirculating system is designed to operate with the existing fossil water quality specifications.

Sizing of the tube bundle for each heat exchanger has been accomplished using the Babcock & Wilcox VAGEN computer code. This code provides a determination of required heat transfer surface and number and length of tubes as a function of specified fluid flow rates and temperatures, tubeside pressure drop limitations, and tube material and configuration. Numerous fluid property and heat transfer subroutines are available enabling the code to be used with equal efficiency for subcooled, superheated, or two-phase steam/water mixtures. The physical properties of molten nitrate salts are included in the program library.

5.7.3 Subsystem Performance

At design conditions, hot salt at 566°C (1050°F) will be pumped from the hot salt storage tank to the superheater where saturated steam is heated to 538°C (1000°F). Heat exchanger design margins will result in an expected steam temperature above 538°C (1000°F). The steam temperature will be controlled by mixing saturated steam from the steam drum with the steam leaving the superheater in the main attemperator.

Salt then leaves the superheater, mixes with some recirculated cold salt (277°C, 530°F) and enters the evaporator. The recirculation of the cold salt ensures maintaining the evaporator salt inlet temperature below the maximum use temperature of the evaporator material (468°C, 875°F) during both steady-state and transient operation. A line from the salt recirculation pump also returns to the superheater inlet to reduce temperature gradients during plant startup. Steam generated in the evaporator enters the steam drum where separation takes place. Saturated steam goes to the superheater while saturated water, mixed with subcooled water from the preheater, is recirculated to the evaporator inlet. A circulation ratio of 1.5 is sufficient to prevent DNB. As the two evaporator recirculation pumps operate at constant speed, the water flow through the evaporator is nearly independent of steam generator duty or feedwater flow. A 1% blowdown from the steam drum has been assumed for design purposes.

Salt leaves the evaporator and enters the preheater at 326°C (618 F). Boiler feedwater is heated to 313°C (596°F) and piped to the steam drum. Feedwater comes from the high pressure feedwater heater at 216°C (420°F) and it is mixed with 317°C (602°F) water from the boiler recirculation pumps. This increases the water temperature to 238°C (460°F) before entering the preheater thus preventing solidification of salt on the preheater tubes. This temperature is maintained as the power level is reduced by increasing the recirculation ratio to feedwater flow (50% power is the minimum operating level). This offsets the reduction in feedwater temperature from the feed heaters as load is reduced. In the event of an upset condition where feedwater temperature would fall, the control system could further increase the recirculated flow through the preheater to maintain approximately a 266°C (510 F) preheater salt outlet temperature.

Figures 5.7-8 and 5.7-9 show the salt and steam/water temperature distributions through the SSGS components for both 100% and 50% power levels. The characteristics of the solar steam generator subsystem are given in Table 5.7-1. Additional characteristics are given in Appendix C.

Table 5.7-1 Heat Exchanger Characteristics

<u>Salt Side</u>	<u>100% duty</u>	<u>50% duty</u>
SH Inlet Temperature, °C (°F)	566 (1050)	566 (1050)
SH Outlet Temperature, °C (°F)	477 (891)	478 (892)
Evap Inlet Temperature, °C (°F)	452 (845)	452 (845)
Evap Outlet Temperature, °C (°F)	326 (618)	312 (594)
PH Inlet Temperature, °C (°F)	326 (618)	312 (594)
PH Outlet Temperature, °C (°F)	277 (530)	261 (502)
<u>Water/Steam Side</u>		
Feedwater Temperature, °C (°F) (from high pressure feedwater heater)	216 (420)	184 (364)
PH Inlet Temperature, °C (°F)	238 (460)	238 (460)
PH Outlet Temperature, °C (°F)	313 (596)	298 (568)
Evap Inlet Temperature, °C (°F)	317 (602)	307 (585)
Evap Outlet Temperature, °C (°F)	322 (611)	314 (598)
Steam Drum Pressure, MPa (psia)	11.5 (1670)	10.5 (1518)
SH Inlet Temperature, °C (°F)	322 (611)	314 (598)
SH Outlet Temperature, °C (°F)	543 (1010)	557 (1035)

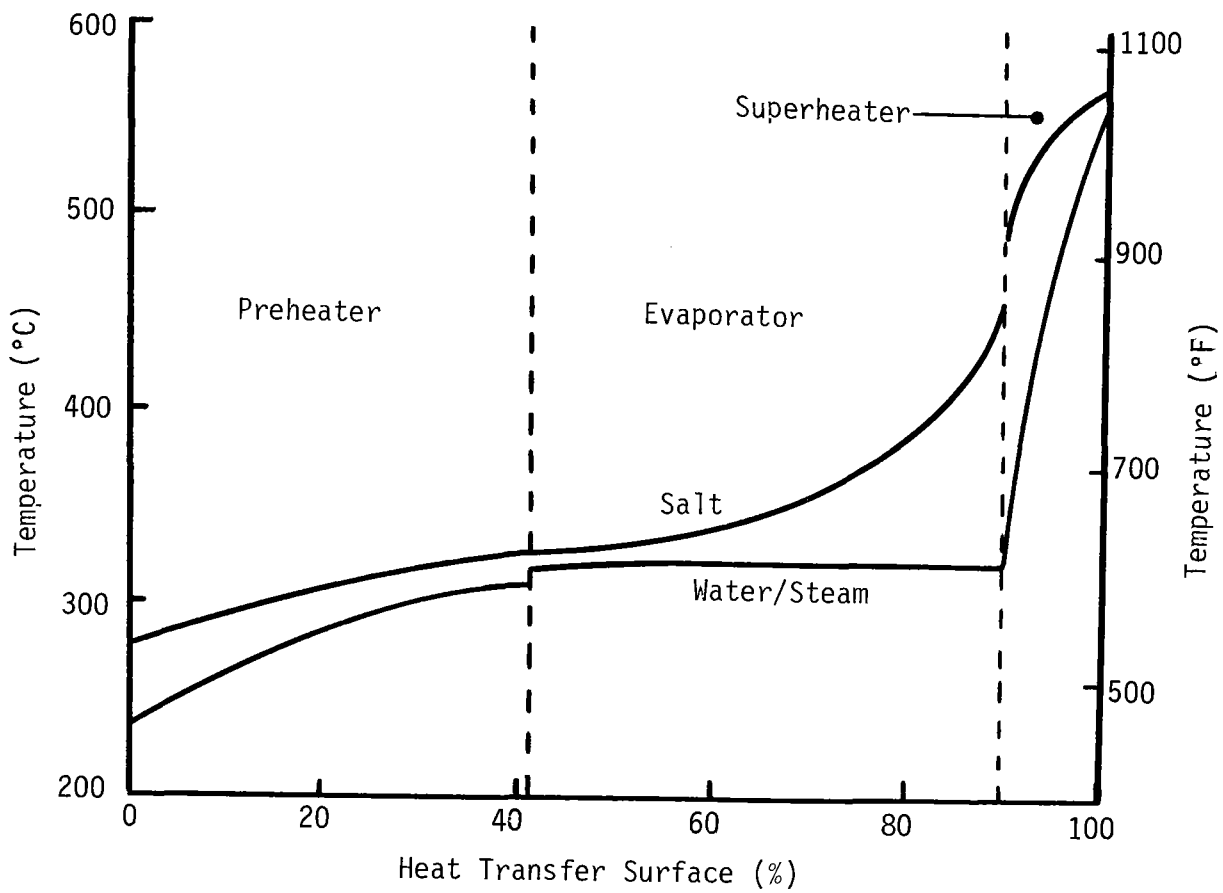


Figure 5.7-8 Fluid Temperature Distribution - 100% Power

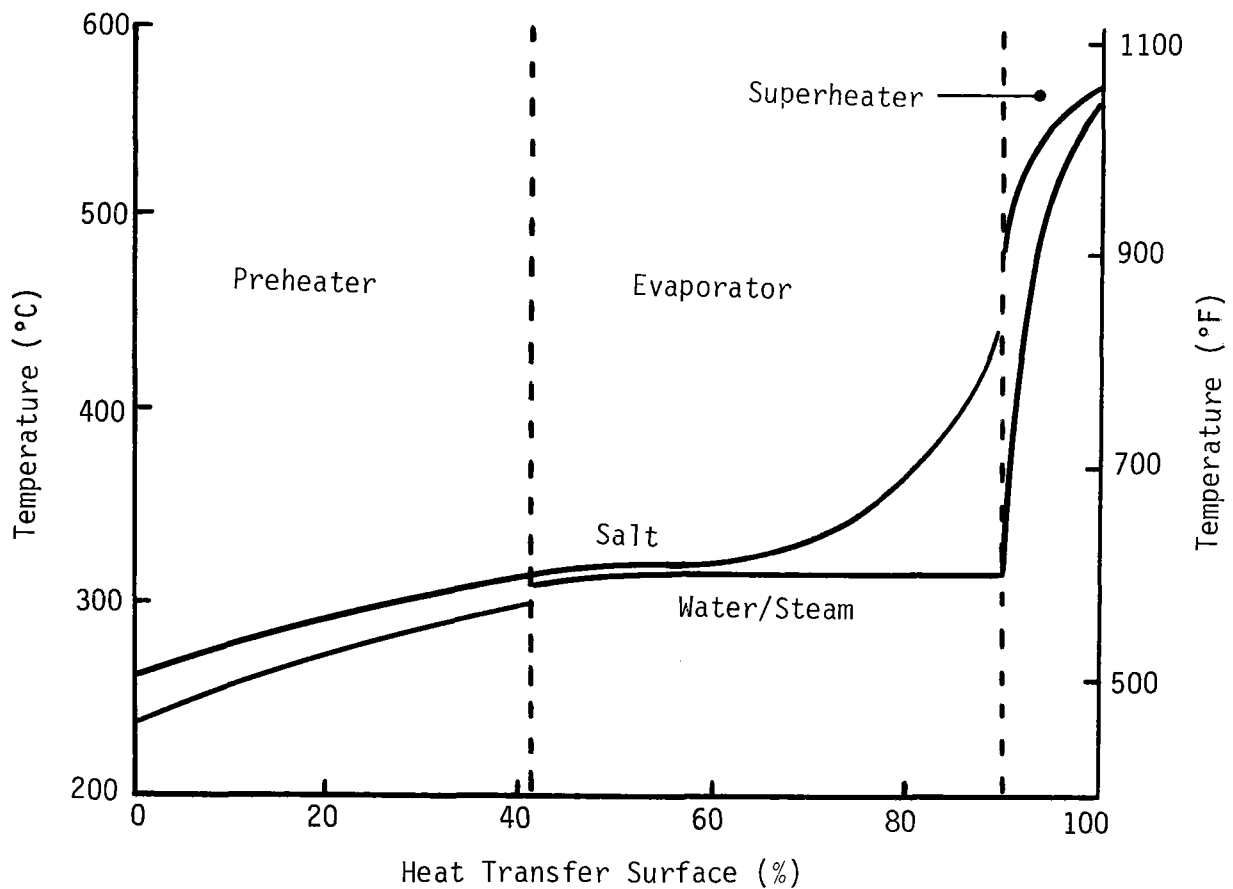


Figure 5.7-9 Fluid Temperature Distribution - 50% Power

5.7.4 Subsystem Cost Estimate

The construction of the solar steam generator subsystem including heat exchangers, vessels, pumps, valves, piping, instruments, electric heating, motors, power distribution, civil work, and salt is estimated to be \$8,428,000. Design engineering is estimated at \$1,044,000, giving a total installed cost of \$9,472,000.

6.0 ECONOMIC ANALYSIS

The objective of the economic analysis of the Saguaro repowering project was to examine the value of the project in comparison with the total project cost, which includes both project implementation costs (design, construction, owner's cost) and operating and maintenance costs. The costs of the project have been detailed in section 4.6 and are summarized in following paragraphs; the value determination will be the focus of this chapter.

The value of the Saguaro repowering project is comprised of two discrete benefits: predicted fuel displacement and savings on the APS system over the project demonstration period, and the future ratepayer benefits associated with demonstrating a cost-effective future utility generation alternative - Solar Thermal Central Receiver (STCR) technology. The fuel displacement analyses are detailed in section 6.3, with the demonstration value assessment discussed in section 6.4.

6.1 ECONOMIC ANALYSIS ASSUMPTIONS

A primary consideration in the economic analyses is to assess the value of this solar repowering project and future standalone STCR systems in the investor-owned utility environment. To provide realistic assessments, economic parameters currently used by the APS System Planning Department were used in this study as typical of Southwestern utilities. The major parameters describing the economic environment are shown in Table 6.1-1.

Table 6.1-1 Economic Parameters

Operating Period	10 years
Initial Year of Commercial Operation	1987
Construction Period	2.5 years
Performance Validation Period	0.5 years
Rate of Return (Present Worth Factor)	14.5%
Capital Escalation Rate	8%
Operating and Maintenance Cost Escalation Rate	8%
General Inflation Rate	8%

For the fuel displacement analyses, a 10-year Saguaro solar repowering demonstration period was baselined. The solar repowering plant has been designed for the normal 30-year life; however, several considerations were taken into account in baselining the 10-year operating period. A major factor is that the solar repowered plant would be the "first of a kind" plant, and thus would be considered a higher than normal risk. To account for the high risk, a shorter operating period is used. Another factor may be the age of the turbine; built in 1954 and renovated in 1975. Although many turbines have been in operation for periods much longer than 30 years, it would be unrealistic to assume 30 years of operation beyond 1987. Finally, the primary direct value of the solar plant will be realized from fuel displacement, the value of which is very difficult to estimate, particularly over 30 years.

The rate of return, also called the cost of money, has been calculated using the "Jeynes-EPRI" methodology, based on the average capital structure for the 1987-99 time frame. The rate of return is calculated as the weighted average of the return on the capital structure, ignoring income tax effects, as follows:

	<u>Fraction (%) x Cost of Money (%) = Composite Rate (%)</u>		
Common Equity	40.0	16.0	6.4
Preferred Stock	12.0	11.0	1.3
Long Term Debt	<u>48.0</u>	14.2	<u>6.8</u>
Total	100.0		14.5

This weighted cost of capital and the corresponding discount rate is used in discounting future cash flows to determine present worth in 1987, and in levelized busbar energy cost calculations in section 6.4.

The capital escalation rate shown in the table was used to calculate the total capital investment in 1987 dollars. To provide a realistic value for the total expenditures, the escalation rate was applied to the investment up to the year of expenditure, with an S-shaped construction spend plan over a 2.5-year period. The capital escalation rate (8%) was also used to escalate design engineering costs to the period of expenditure, as well as escalation on all owner's costs.

The fuel costs and escalation used in the fuel displacement analyses are shown in Table 6.1-2. The fuel costs and escalation rates shown in the table are those currently used by the APS System Planning Department. The APS coal cost varies over the wide range shown depending on when the coal contract was initiated. Typically, the high end of the range reflects future coal contracts in the 1985-1990 time frame de-escalated at 8% to 1982 dollars. The varying oil costs reflect a lower sulfur content for No. 6 combined cycle oil versus the \$7.06/MBtu cost for No. 6 oil for intermediate plants.

Table 6.1-2 APS Fuel Cost and Escalation Data (1982 \$)

Coal	
Coal Cost, \$/MBtu	\$0.65 - 2.33
Escalation Rate	8%
Oil	
Oil Cost, \$/MBtu	
#6 Oil	\$5.19
#6 Comb. Cycle Oil	\$7.06
#2 Oil	\$8.43
Escalation Rate	9%
Nuclear	
Fuel Cost, \$/MBtu	\$0.72
Escalation Rate	8%
Purchased Power	
Cost, \$/MBtu	\$5.10
Escalation Rate	9%

6.2 SAGUARO SOLAR REPOWERING PROJECT COST

As discussed in detail in section 4.6, the Saguaro solar repowering costs were estimated in four discrete elements: preliminary and detail design engineering costs, construction costs, owners costs, and operating and maintenance costs. The total project implementation cost (design, construction, and owners costs) was estimated at \$133.9M, in 1982 dollars. The annual operating and maintenance expense cost estimate was \$1,441,000 per year, again in 1982 dollars.

To arrive at a cost for use in the economic analyses, each component of the project implementation cost was escalated at the capital escalation rate of 8% to the period of expenditure as set forth in the development plan schedule. The result of this escalation is shown in Figure 6.2-1. The total project implementation cost is the sum of the escalated yearly expenditures, or \$171,126,000 (1987 \$).

A notable exclusion from the project implementation cost is Allowance for Funds Used During Construction (AFUDC), or interest costs on the design and construction costs from the period of expenditure to the year of commercial operation, when the plant is put into the rate base. The economic analysis of the Saguaro project excluded this cost due to the nature of the project. No AFUDC expenses would be incurred in either of two possible funding alternatives: government funding or APS funding. If the project were built entirely with APS funds, it would probably be considered a research and demonstration project, where APS could expense in the year of expenditure all costs, recovering those costs through ratepayer revenues. Thus, no AFUDC expense would be incurred.

COSTS IN THEN YEAR DOLLARS (\$000)

	1982	1983	1984	1985	1986	TOTAL
Preliminary Design	\$756	2,359				\$3,115
Detailed Design		\$1,637	5,105			6,742
Permits	\$320	327				647
Construction *			\$27,608	121,866	9,107	158,581
Checkout					\$2,041	2,041
TOTAL YEARLY OUTLAYS	\$1,076	4,323	32,713	121,866	11,148	\$171,126

* Not Including AFUDC

Figure 6.2-1 Total Escalated Project Implementation Cost

As the project implementation cost would not be capitalized as conventional generating capacity, the concept of annualized costs due to plant ownership (recovering the capital over the system life) does not apply. Therefore, the present worth of the project implementation cost is simply the total expenditures up to the time of commercial operation, or \$171,126,000 (1987 \$).

The only remaining element of cost associated with the solar repowering plant is the operating and maintenance expenses incurred over the operating period. Using the O&M estimate of \$1,441,000 per year, and 8% escalation rate, 14.5% discount factor, the present worth in 1987 of the 10 years of O&M expenses can be calculated, yielding a present worth cost of \$15.7M (1987 \$).

Thus, the total cost associated with the Saguaro solar repowering project for use in comparison with fuel displacement value and demonstration value is the sum of the implementation cost and the present worth of the O&M expenses, or \$186.8M (1987 \$).

6.3 FUEL DISPLACEMENT ANALYSIS

The objective of this analysis is to quantify the value of the fossil fuels displaced by the Saguaro solar repowering project. To accomplish this objective, the solar system design described in this report was evaluated on the projected APS generating system using APS system production cost computer programs to determine the types of fuel displaced and the value of those fuels.

This type of analysis also provides an evaluation as to the extent that this repowering design meets a larger, national objective--reducing the use of critical fuels (oil and natural gas) for the generation of electricity. If the Saguaro repowering project is capable of displacing these fuels in the APS generation mix, which is predominantly coal and nuclear plants, then significant oil and gas displacements can be expected from future solar repowering projects of this design on "less mature" (i.e., more oil/gas oriented) generation mixes currently existing in the southwestern U.S.

6.3.1 Fuel Displacement Analysis Methodology

The fuel displacement analysis used the APS detailed production costing model, PCOST, which simulates hourly operation of the forecasted future resources necessary to meet the projected electrical demand. The dispatch of generation resources is based on the incremental cost of each generation unit, with the lowest cost units being dispatched first. Incremental costs for a given generation unit are the fuel cost and variable operating and maintenance costs per unit of electrical output. Scheduled and forced outages are considered within the PCOST program.

Since PCOST does not have the capability to explicitly handle a solar repowered plant with its variable daily start-up, output and availability of solar-generated electricity, an evaluation sequence was developed to assess the impact of solar on the APS system. Figure 6.3-1 is a flow schematic of the methodology employed. The steps followed in the analysis are explained in the following paragraphs.

- 1) A "base case" was run with the PCOST model using APS forecasted loads (demands) and resources for the 1987-1999 time period. The projected loads and resources are forecasted by the APS System Planning Department on a semi-annual basis. Concurrent with the loads and resource forecasts are fuel cost and escalation estimates. The base case PCOST simulation provides the total yearly energy production by type of plant, as well as fuel costs and operating and maintenance costs.
- 2) The operation of a repowered plant operating from solar only is modeled with the Solar Thermal Electric Annual Energy Calculator (STEAEC) model, using insolation and weather data for Phoenix, AZ from the SOLMET Typical Meteorological Year (TMY) data base. The model provides the daily electric output from the repowered plant due to the collection and use of solar energy.

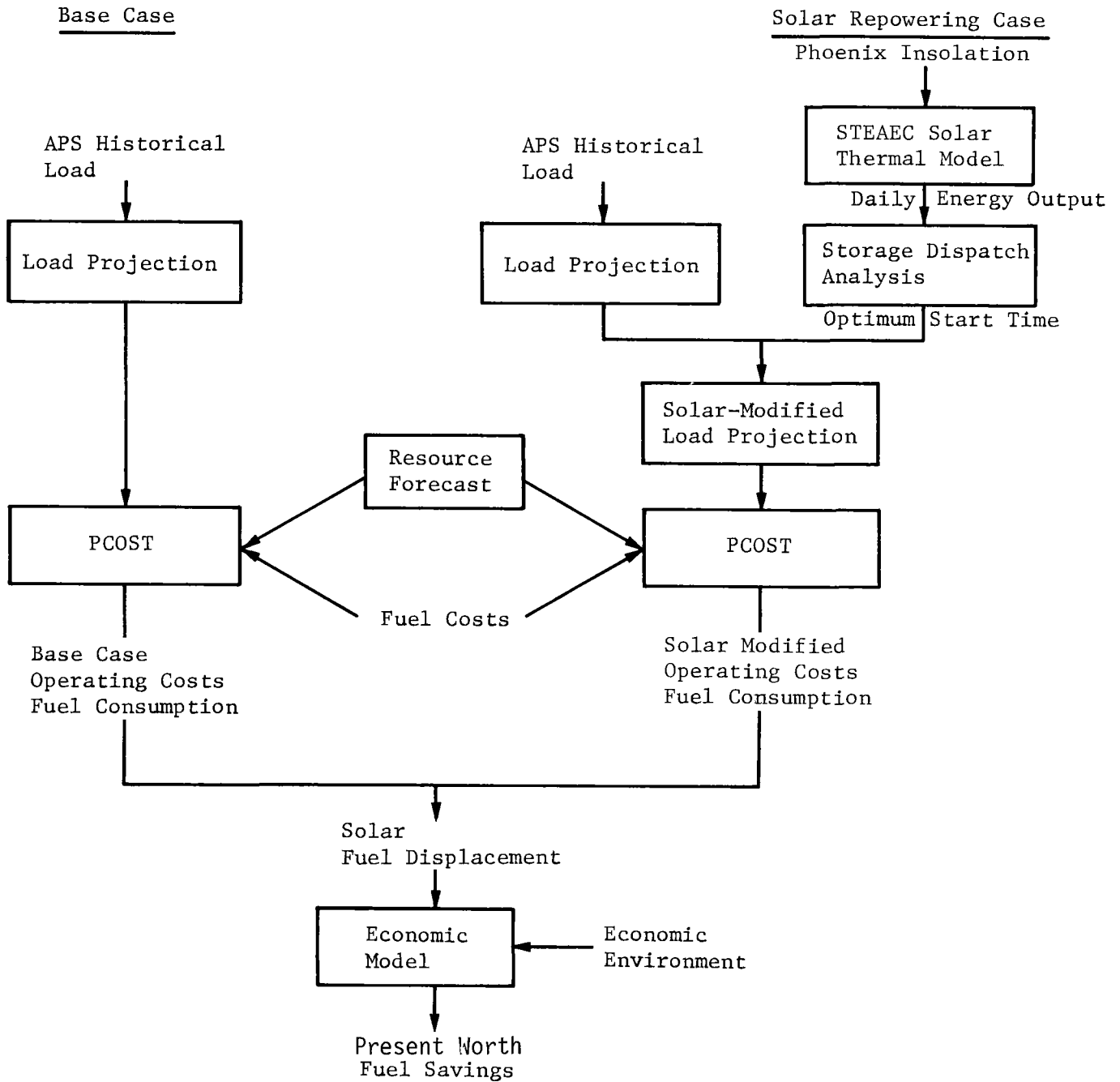


Figure 6.3-1 Fuel Displacement Analysis Method

- 3) As the STEAEC program cannot model the excess storage capacity (4.0 hours) for dispatch, the best start times for the use of collected solar energy at the repowered plant were calculated. This optimization of start time shifted the operation of the solar plant to center the solar project dispatch about 4:00 PM during the months of April through October. During the months of November through March, the solar project dispatch was centered about 9:00 AM and 7:00 PM in approximately equal amounts. This dispatch schedule closely approximated utilization of the solar output during the peak load demand times of the daily load cycle.
- 4) The hourly load projection used in the base case was then modified by subtracting the energy produced by solar from the projected demand based on the start time from step 3). This step essentially dispatches the solar-produced electricity in the same manner as PCOST, since the solar-produced electricity has the lowest incremental cost of all generating units and would be dispatched first by PCOST.
- 5) The solar-modified load demand is then input to PCOST, using the same resources and fuel costs as were used in the base case, with the exception that Saguaro Unit One (on oil) is derated from 115 MW_e to 55 MW_e. The unit is only derated and not removed from the system to avoid loss of capacity credit. The PCOST program then gives the total yearly operating costs and fuel consumption, again by fuel type, necessary to meet the solar-modified demand.
- 6) The energy displacement and fuel savings by type resulting from the solar repowering project for each year is calculated by subtracting the results of item 5) from the base case (item 1). These fuel savings are then properly discounted to find the present worth savings resultant from the solar repowering project.

This present worth fuel savings can then be compared with the present worth cost of the solar plant to arrive at a measure of the value (cost-effectiveness) to APS. This approach was exercised using the APS 3/6/81 resources plan and 7/81 Long Range Forecast Assumptions.

6.3.2 Plant and System Simulation Models

As discussed in paragraph 6.3.1, two separate simulation models were used in the economic analysis: STEAEC, a solar plant simulation model and PCOST, a generation system simulation model.

Solar Plant Simulation Model

The hourly output of the solar repowering plant due to collection of solar energy was simulated using the STEAEC program, developed by Sandia National Laboratories-Livermore (Ref 3-6). The model simulates the energy flow through the solar system on 15-minute increments, using insolation and weather data from the SOLMET TMY data tape as

input. The yearly net electrical output from the solar plant was calculated as 149,700 MWh_e. However, this value does not consider the normal scheduled maintenance outage for Saguaro from January 26 to February 15 each year. For purposes of fuel displacement analyses, the electric output that could be expected from the solar plant during this period was not considered, thus reducing the net electric output to 144,000 MWh_e (144 GWh_e). A further discussion of the performance modeling can be found in section 4.5.

System Simulation Model

The APS generation system and the fuel savings resultant from operation of the solar repowering plant was modeled using the APS PCOST production costing program. The PCOST program simulates the hourly operation of the generating mix, assigning generating units to meet the forecasted demand and reserve requirements. The dispatch is based on incremental costs for each generating unit, where the incremental cost is calculated based on fuel costs, net heat rates, and variable operating and maintenance costs. The dispatch priority dispatches the lowest cost units first (nuclear), followed by those with increasing incremental cost (coal, oil). An example of the load demand and resource dispatch is shown for the peak demand day in Figure 6.3-2, where the combustion turbines (No.2 oil) have the highest incremental costs. The SRP Territorial/Contingent resource represents power purchased by APS from the Salt River Project.

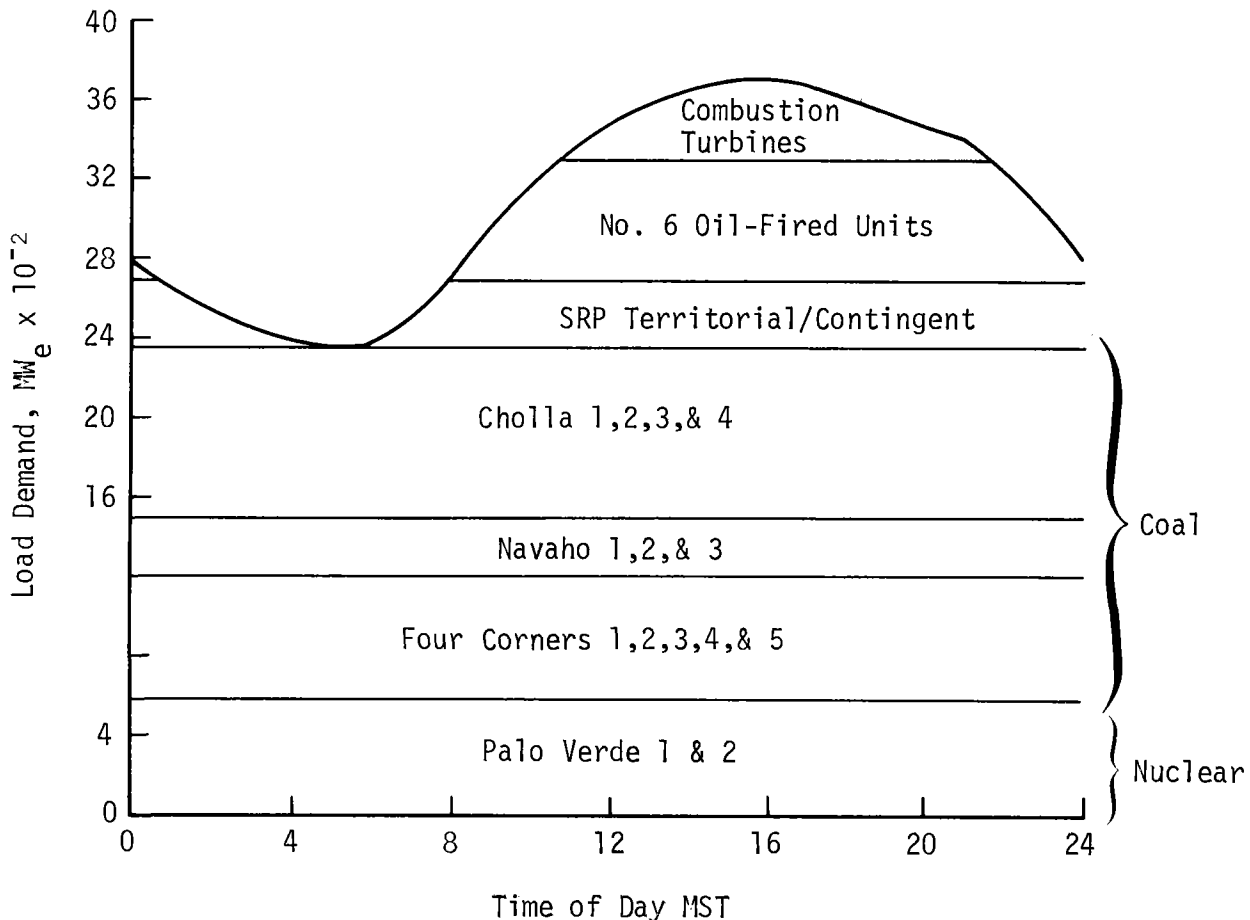


Figure 6.3-2 Peak Demand Day Load Demand and Resource Dispatch

6.3.3 Fuel Displacement Analysis Results

Using the methodology discussed in paragraph 6.3.1, the fuel displacement in terms of type of fuel, quantity and value were calculated by placing the solar repowering plant on the APS system and using the PCOST production costing program. First, a simplified analysis was performed using APS fuel cost data and assuming that the solar repowering displaced (1) all oil and (2) all coal to provide an upper and lower bound for fuel savings. The results from this analysis are shown in Table 6.3-1. If 100% oil displacement is assumed, 2.7 million barrels of oil would be displaced in 10 years (at 5.8 MBtu/bbl oil).

Table 6.3-1 Simplified Fuel Displacement Results - Present Worth Savings (1987 \$)

	<u>10 years</u>
Assuming 100% oil displacement (\$5.19/MBtu, 9% esc)	\$ 92.2M
Assuming 100% coal displacement (avg. weighted coal cost)	\$ 17.8M

The average generation-weighted coal cost varies by year, since new coal contracts are projected to be much higher than current long-term contracts. In constant 1982 dollars, 1987 coal cost is \$1.00/MBtu, increasing to \$1.14/MBtu in 1989, and \$1.26/MBtu in 1990.

The all oil case is not particularly applicable to the APS system, especially in the 1987-1999 time frame, as the forecasted resource mix is predominantly coal and nuclear. The dominance of coal and nuclear is evident in Figure 6.3.3, which shows an example of the results from the base case (no solar) PCOST run, showing the annual load demand curve and tabulating the production forecast by fuel for 1990 based on the 3/16/81 loads and resources forecast. As shown in the figure, 93% of the energy production forecast is coal and nuclear, with only the remaining 7% oil and purchased power.

The baseline results from the PCOST analysis of the fuel displacement due to the solar repowering project are shown in Figures 6.3-4 and 6.3-5. The first figure shows the energy displaced by type, in GWh_e (MWh_e x10³) for each year of interest. As shown, the solar plant displaces on the average 43% coal, 47.5% intermediate oil and purchased power. Due to the internal mechanics of the PCOST program meeting reserve requirements, additional pumped storage, representing approximately 9% of the solar output, was dispatched. This reduced the fuel displacement due to solar to an average of 130 GWh_e/yr. The oil and purchase displacements represent a total displacement of approximately 1.2 million barrels of oil over the 10-year period. The value of these energy displacements are expressed in Figure 6.3-5, showing the cumulative present value in 1987 of the fuels displaced over the operating period of the solar plant. The cumulative present worth at 10 has been expressed as present worth savings in 1987 dollars, with 10-year present worth savings of \$33.0M

Figure 6.3-3

6-10

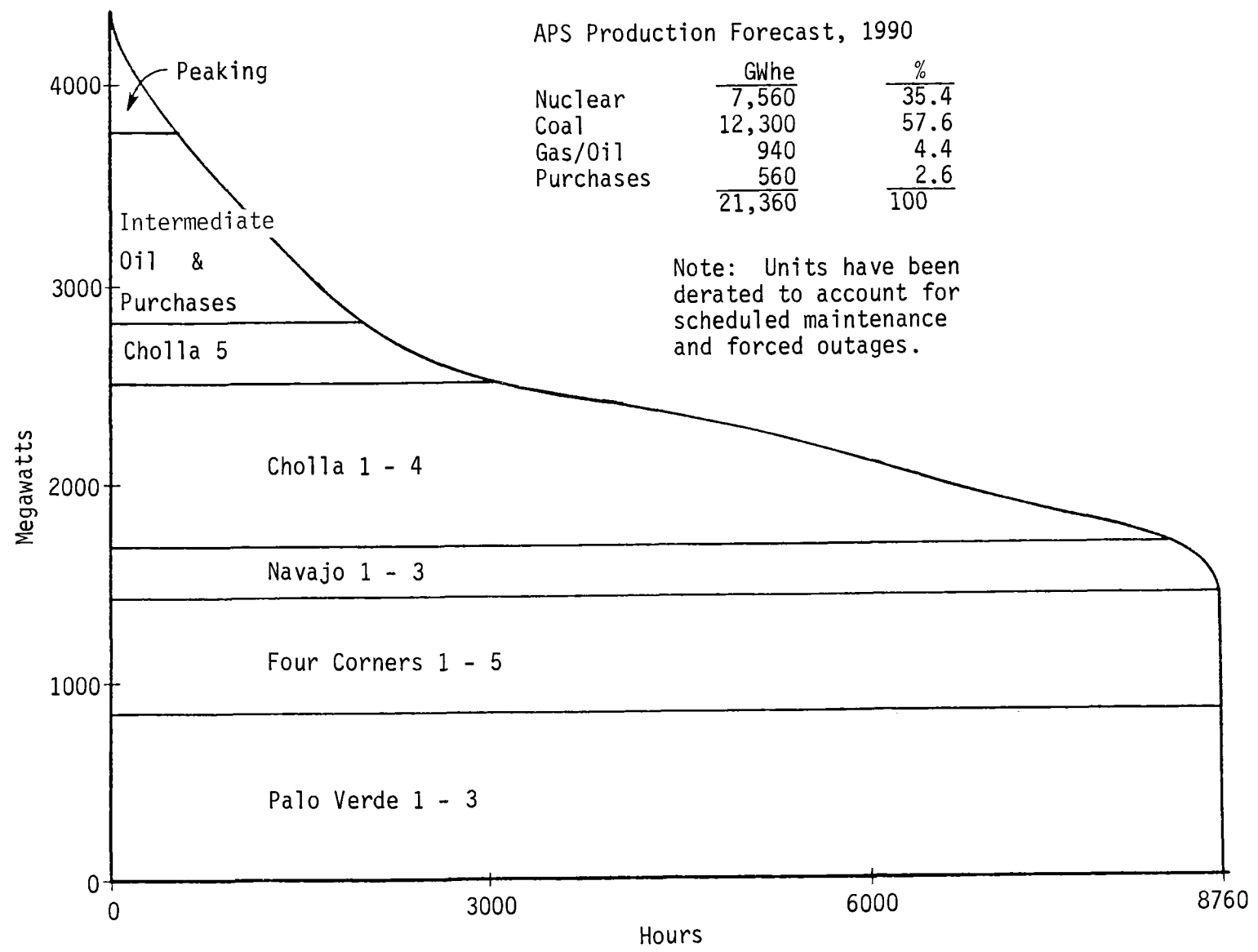


Figure 6.3-3 APS Load Resource Forecast, 1990, March 6, 1981 Forecast

Figure 6.3-4

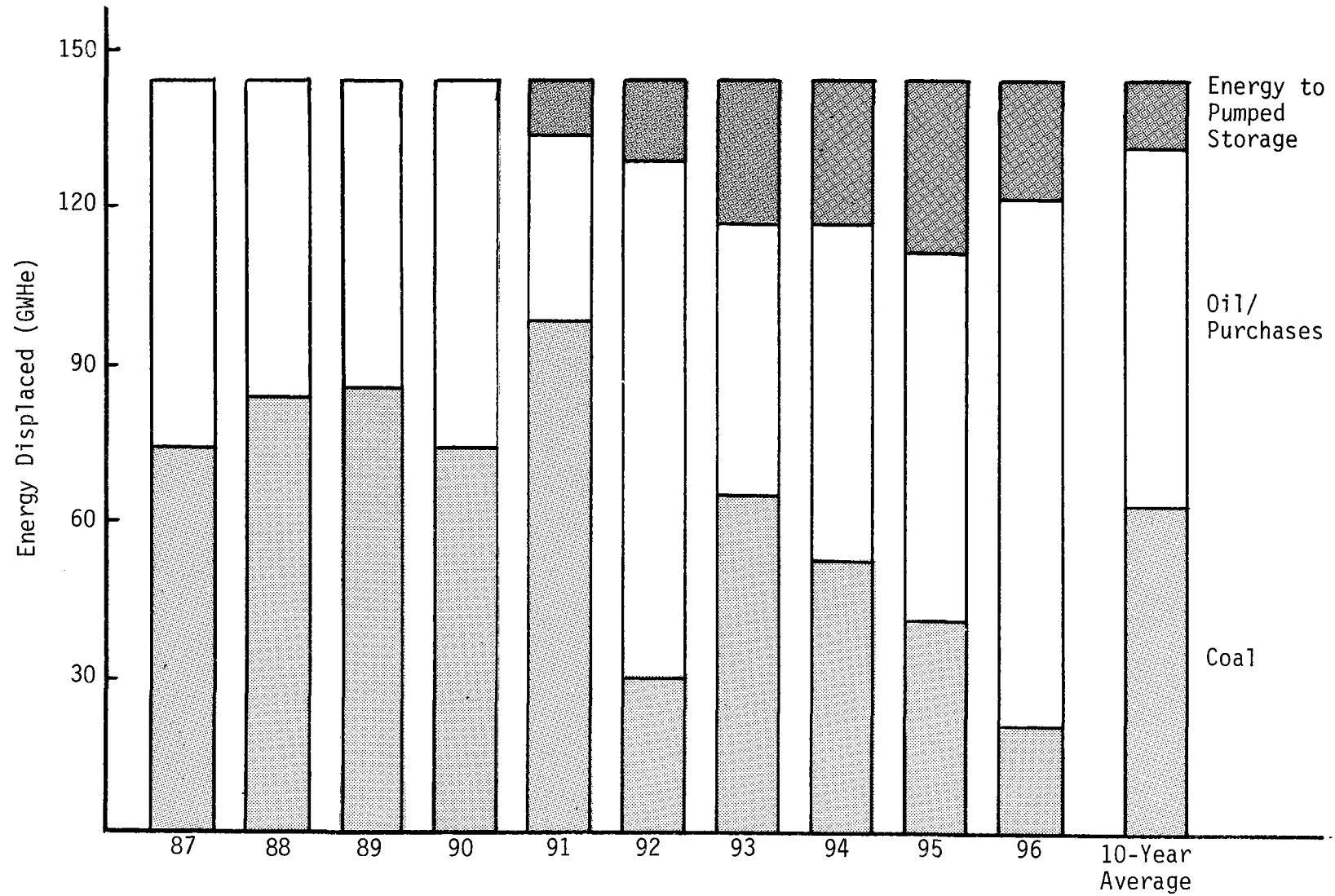


Figure 6.3-4 Yearly Fuel Displacement, March 6, 1981 Loads and Resources Forecast

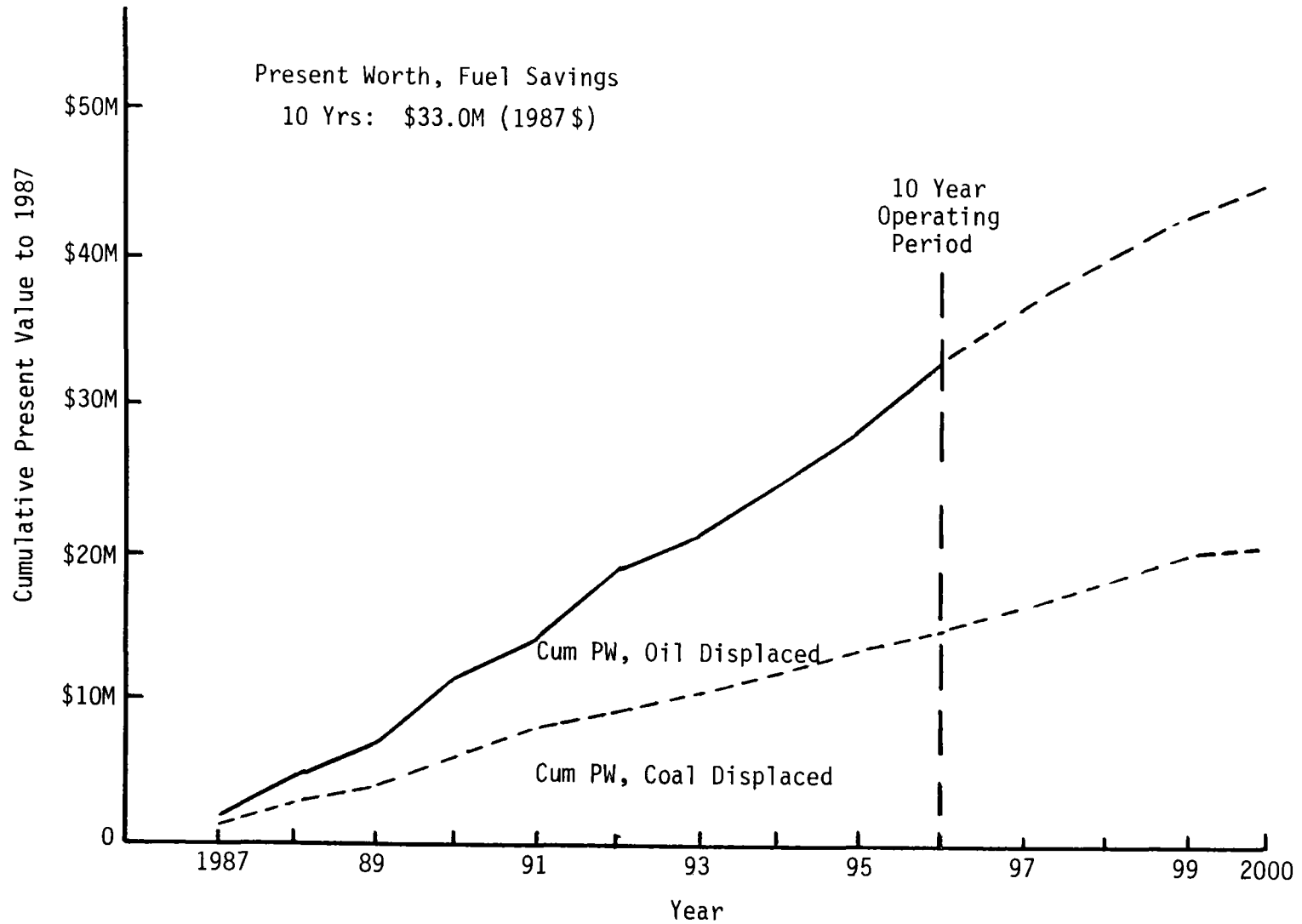


Figure 6.3-5 Cumulative Present Worth of Fuel Displaced, March 6, 1981 Forecast

6.3.4 Fuel Displacement Economics Summary

The economics of the Saguaro solar repowering project considering only the direct benefits of fuel savings on the APS system are summarized in Table 6.3-2. As defined earlier, the present worth of the total project cost is composed of the project implementation cost and the present worth of 10 years of O&M expenses, yielding a total project cost present worth of \$186.8M, in 1987 dollars. Three fuel displacement scenarios were examined, with a range of fuel savings from \$17.8M to \$92.2M. Combining the cost of the project and the fuel savings yields, in this case, the net project present worth in 1987 \$, ranging from \$-95M to \$-170M.

Table 6.3-2 Solar Repowering Economics - 10 Year Fuel Savings (1987 \$)

Saguaro Repowering Project Cost	
Implementation cost	\$171.1M
Present worth, O&M expenses	\$ 15.7M
Total project cost	<u>\$186.8M</u>
Saguaro Repowering Fuel Displacement	
100% oil displacement	\$ 92.2M
APS dispatch analysis	\$ 33.0M
100% coal displacement	\$ 17.6M
Net Saguaro Solar Repowering Present Worth	
100% oil displacement	(\$ 94.6M)
APS dispatch analysis	(\$153.8M)
100% coal displacement	(\$169.2M)

6.4 DEMONSTRATION VALUE ANALYSIS

In the preceding section, the direct economic benefits of the Saguaro solar repowering project--fuel cost savings--were assessed, with the conclusion that approximately \$33.0M in fuel savings result from the \$190M solar repowering project on the APS system. However, the repowering project will have a value in terms of satisfying the overall repowering program objectives, namely demonstrating the large-scale technical feasibility of STCR technology in a utility environment, thereby reducing the technical and economic uncertainty (risk) associated with a new technology. With a successful repowering demonstration, a cost-effective renewable technology (STCR) will be available as a central-station generation alternative to southwestern U.S. utilities. The following sections detail an approach used to quantify the benefits of the Saguaro repowering project, as well as results and conclusions that can be drawn from this analysis.

The primary objective of this analysis was to determine, for a given set of assumptions, the expected levelized busbar energy costs (BBEC) for 100 MWe-3hr standalone STCR systems operational in 1991 in the southwestern United States. Assuming that there is a quantifiable difference in the expected costs of electricity generated by standalone STCR plants when preceded by repowering and the cost of STCR-generated electricity without a repowering demonstration, the cost savings of the ratepayers should have a value directly attributable to the technology demonstration. The rationale behind expecting a lower BBEC from plants preceded by a repowering demonstration is that there should be lower cost and performance uncertainties for standalone STCR plants as well as some heliostat production capability in place from the repowering demonstration program.

The first step taken in this analysis was to develop a series of market scenarios that could define the number and cost of standalone 100 MWe-3hr STCR plants operational in 1991. The year of 1991 was chosen to allow a one-year operational period for the Saguaro repowering project to "prove" the technology, followed by a three year construction period for a standalone 100 MWe STCR plant. A total of seven market scenarios were developed, as summarized in Table 6.4-1.

Table 6.4-1 1991 STCR Market Scenarios

Scenario	Number of 100 MWe-3hr STCR Plants	Heliostat Production Capability	Heliostat Cost (1982 \$)	Scenario Probability
With Repowering				
A	1	4,000/yr	\$220/m ²	0.2
B	1	25,000/yr	\$150/m ²	0.2
C	4	25,000/yr (2 suppliers)	\$150/m ²	0.6
Without Repowering				
D	0	-	-	0.4
E	1	4,000/yr	\$260/m ²	0.4
F	1	25,000/yr	\$150/m ²	0.1
G	4	25,000/yr (2 suppliers)	\$150/m ²	0.1

Briefly, the three "with repowering" scenarios assumed that at least one standalone plant would be operational by 1991, with varying levels of heliostat production capability installed. The first scenario (A) assumes that the repowering demonstration does not stimulate the market to a very large degree, resulting in no further commitments to mass-production heliostat capability. Therefore, the heliostat cost is only reduced by the learning on the 5000 heliostats produced for the Saguaro project, or \$40 per sq. meter. Scenario B is essentially the same market projection as A, but a heliostat manufacturer

believes in the technology sufficiently to invest in some mass-production tooling, reducing the cost of heliostats to \$150 per sq. meter. Scenario C would be typical of a modest market stimulation due to repowering with 2 heliostat manufacturers committed, four plants built, and a corresponding slight (5-10%) reduction in balance-of-system (receiver, storage) costs.

The probabilities assigned to each scenario are necessarily extremely subjective in nature, and reflect only the judgement of the analyst responsible for this task. The probabilities were selected as fairly as possible, i.e., not weighting the results favorably towards or against the "with repowering" case.

The "without repowering" solar scenarios (E,F,G) are similar to scenarios A, B, and C, with the only difference being a higher heliostat cost associated with the low-production capability case, since the benefit of "learning" over the 5000 heliostats for Saguaro repowering has not occurred. The additional scenario, D, has been included to reflect the possibility that, without a repowering demonstration, no STCR plants will be built. In this case, any solar electrical generation that may have been provided in the "with repowering" scenarios will be generated with new coal generating capacity and existing oil-fired units in equal amounts. As shown in the table, a 40% chance of no STCR plants being built has been assumed.

The next step in the analysis is to determine the effects of a repowering demonstration on the cost and performance of the 100 MWe-3hr STCR plants in the market scenarios. To provide a baseline upon which the reduction in technical and cost uncertainty resulting from a repowering demonstration can be assessed, estimates of the cost and performance of a "typical" 100 MWe-3hr standalone STCR plant were made. The basis of these estimates is a 100 MWe-3hr molten salt conceptual design derived by Martin Marietta, consisting of 10,900 heliostats, a single quad-cavity molten salt receiver and an internally insulated salt storage system. A summary of the plant costs associated with the various market scenarios is given in Table 6.4-2. The balance-of-plant costs vary between with and without repowering due to levels of design engineering required. An arbitrary 10% reduction in balance of plant costs was assumed in both scenarios involving the building of four plants.

Other pertinent parameters estimated were operating and maintenance expenses of \$3.7 M/year for all cases and a 38% capacity factor for the solar plants, or 337 GWh/year net electrical output, including scheduled outages.

Table 6.4-2 Standalone 100 MWe-3Hr STCR Plant Costs (1982 \$)

Market Scenario	With Repowering			Without Repowering		
	A	B	C	E	F	G
Number of Plants	1	1	4	1	1	4
Heliostat Cost	\$220/m ²	\$150/m ²	\$150/m ²	\$260/m ²	\$150/m ²	\$150/m ²
Collector S/S Cost	\$138M	\$ 94M	\$ 94M	\$153M	\$ 94M	\$ 94M
Balance of Plant Cost Total	<u>\$ 93M</u>	<u>\$ 93M</u>	<u>\$ 83M</u>	<u>\$ 95M</u>	<u>\$ 95M</u>	<u>\$ 84M</u>
Plant Cost	\$231M	\$187M	\$177M	\$248M	\$189M	\$178M

To determine the impact of a repowering demonstration in terms of reducing technical and cost risk associated with the standalone STCR plants, probability assessments were made on each of the cost and performance parameters discussed in the preceding paragraphs. A summary of these assessments is given in Table 6.4-3.

Table 6.4-3 Probability Assessments for 100 MWe-3Hr Standalone STCR Plants

	<u>With Repowering</u>	<u>Without Repowering</u>
Construction Cost		
+10% of Estimate	0.75	0.5
>25% Overrun	0.25	0.5
O&M Cost		
+10% of Estimate	0.8	0.5
200% of Estimate	0.2	0.5
Electric Output		
+10% of Prediction	0.9	0.6
20% Outage Rate	0.1	0.4
Operating Life		
30 Years	0.8	0.5
15 Years	0.2	0.5

The probability assessments given in the table were again made subjectively, and are representative of the analyst's estimate on the effect of a repowering demonstration on the uncertainties associated with estimates for

any new technology. The categories are fairly self-explanatory, with a clarification that the 25% overrun referred to in the construction cost is only on the balance-of-system; that is, the heliostat costs are not increased.

With the definition of the standalone plant costs and performance, the levelized busbar energy costs can be calculated, considering the variations in the individual parameters shown in the previous table. For these calculations, the Martin Marietta Solar Central Receiver Economic Analysis Model (SCREAM) was utilized, with the economic environment given in section 6.1. For each market scenario, with its associated plant costs, a probability "tree" was constructed to consider all combinations of the variables in Table 6.4-3. Examples of these "trees" are shown in Figures 6.4-1 and 6.4-2, where Figure 6.4-1 is representative of the "with repowering" scenario A (1 plant, \$220/m² heliostat cost), and Figure 6.4-2 is the "without repowering" scenario E.

For each branch of the tree, the \overline{BBEC} resultant from that combination of variables was calculated using the SCREAM program, and tabulated to the right of the branch. Concurrently, the probability associated with the individual branch of the tree can be calculated by multiplying the individual probabilities for the path taken. By multiplying the individual branch \overline{BBEC} by the associated probability, and summing across all branches, an expected value of the \overline{BBEC} for the scenario can be found, as shown on the figures. In this manner, the expected \overline{BBEC} for each of the solar scenarios (A,B,C,E,F, and G) were calculated.

A similar approach was taken for Scenario D, where no STCR plants are built and the balance of electrical generation was assumed to be provided by new coal capacity and existing oil-fired units. In this case, 50% of the cost of energy was provided by a new intermediate coal-fired unit with a capital cost of \$1100/KWe and coal cost of \$1.86/MBtu (1982 \$). The other 50% of the cost of energy was due to the fuel cost in existing oil-fired units, with equal probabilities of oil costs escalating at 9%, 10%, and 11% per year.

Thus, at this point, the expected busbar energy cost for each market scenario has been determined, as shown in Figure 6.4-3. For the "with repowering" scenarios, the expected \overline{BBEC} ranges from 12.4 cents/kwh to 15.5 cents/kwh; as opposed to a range of 14.3 cents to 18.9 cents/kwh in the "without repowering" cases, with all costs given in 1982 dollars. By multiplying the individual scenario expected \overline{BBEC} by the probability assigned to the scenario, and again summing across scenarios, the expected busbar energy cost resulting from either repowering decision can be found.

As shown in the figure, the expected \overline{BBEC} for the "with repowering" decision is 13.1 cents/kwh, and increases to 16.2 cents/kwh with a negative repowering decision.

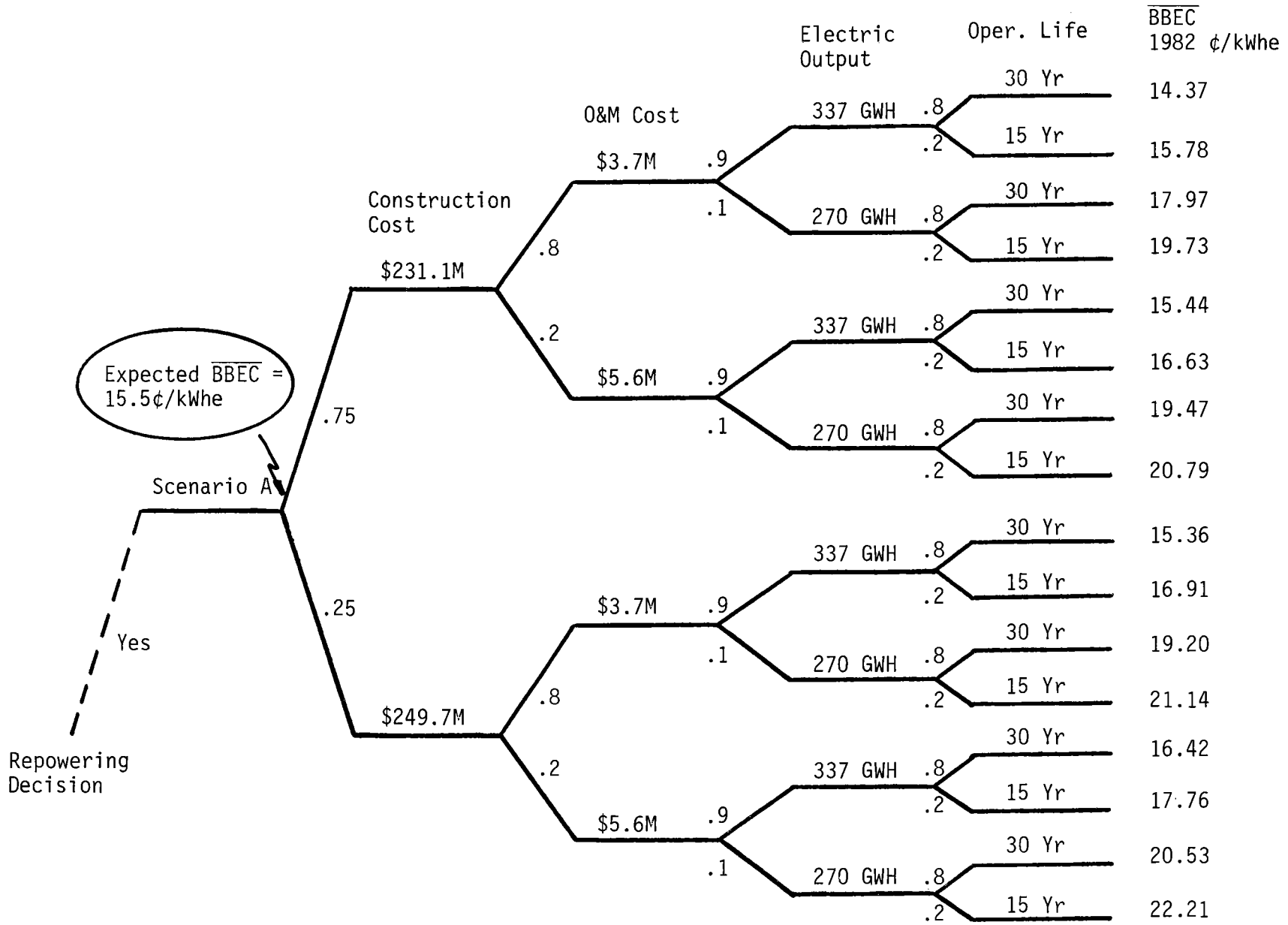


Figure 6.4-1 Expected \overline{BBEC} , Scenario A (1-100 MWe - 3 hr STCR Plant, \$220/m²)

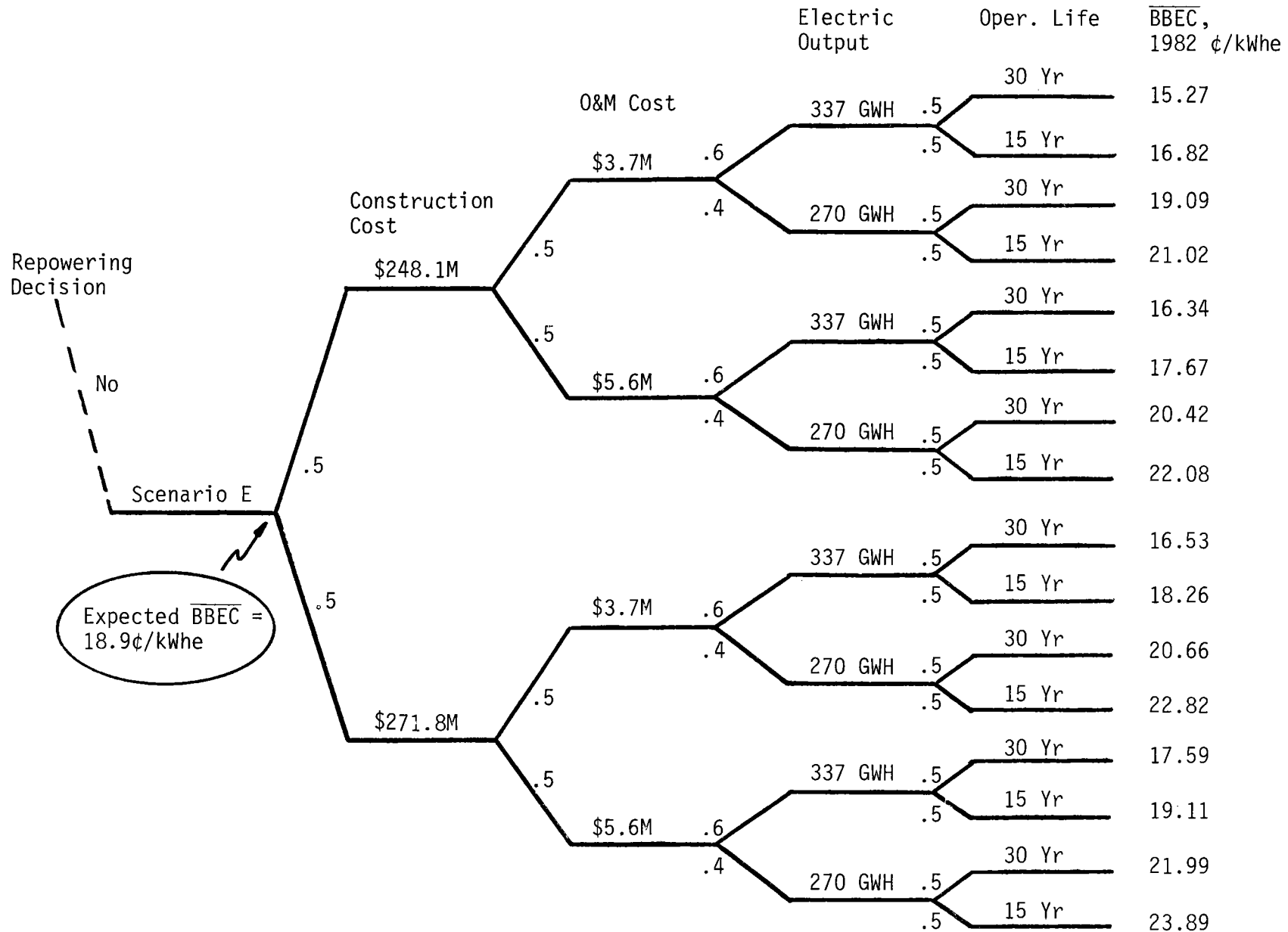


Figure 6.4-2 Expected \overline{BBEC} , Scenario E (1-100 MWe - 3 hr STCR Plant, \$260/m²)

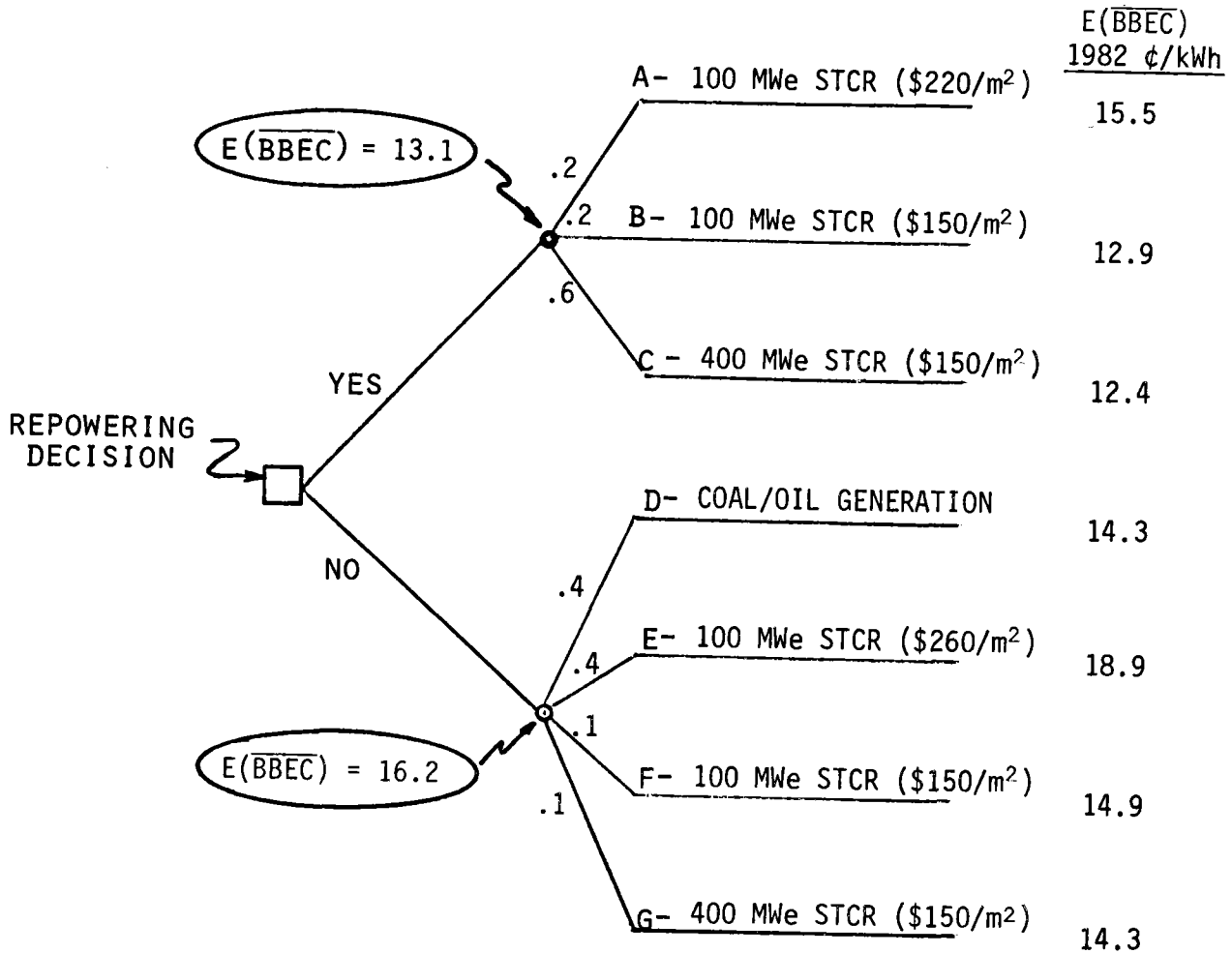


Figure 6.4-3 Expected \overline{BBEC} , With and Without Repowering Demonstration (1991 Plant Start-up)

Taking the analysis one step further, the expected solar capacity installed in 1991 with a favorable repowering decision can also be calculated. As with the \overline{BBEC} calculation, by multiplying the scenario capacity by the scenario probability and summing, $(0.2)(100\text{MWe}) + (0.2)(100\text{MWe}) + 0.6(400\text{MWe}) = 280\text{MWe}$ of solar capacity can be expected in this analysis. At a 0.38 capacity factor, this translates into 943 GWh/yr of solar generated electrical output.

The final step in this assessment is to translate the difference in expected levelized busbar energy costs into a single value for comparison with the solar repowering project cost. Specifically, the difference in energy costs times the solar generation is the 30 year levelized savings in 1982 \$ to the ratepayers due to repowering, or

$$(16.2 \text{ cents} - 13.1 \text{ cents}) \times (943 \times 10^9 \text{ kwh/yr}) = \$30\text{M/yr savings.}$$

By dividing the levelized savings by the appropriate capital recovery factor (0.1475), the present worth in 1991 of these levelized savings can be found:

$$\text{Present Worth in 1991} = \frac{\$30\text{M}}{0.1475} = \$200 \text{ M (1982 \$)}.$$

The final calculation is to escalate 1982 dollars at 8% per year to 1991, which is the year of commercial operation, and then discount that value at 14.5% per year to 1987, yielding:

$$\text{Present Worth in 1987} = \frac{(\$200\text{M})(1.08)^9}{(1.145)^4} = \$230\text{M}.$$

This value of \$230M, then, is the present worth of future ratepayer savings that can be attributed to the repowering project.

6.5 ECONOMIC ANALYSIS SUMMARY

In the preceding sections, the costs associated with the Saguaro solar repowering project were compiled, and two separate measures of the value of the project were determined -- direct fuel savings and a "demonstration value", measured by future ratepayer savings. In present worth terms, the economics of the repowering project are summarized in Table 6.5-1.

Table 6.5-1 Saguaro Solar Repowering Project Economics Summary (1987 \$)

Saguaro Repowering Project Cost	(\$190M)
Present Worth, APS Fuel Displacement	<u>\$ 30M</u>
Net Direct Present Worth, Saguaro Project	(\$160M)
Present Worth, Future Ratepayer Savings	<u>\$230M</u>
Net Present Worth, Saguaro Project	\$ 70M

Several points should be amplified. First, there are many uncertainties associated with attempting to quantify the future STCR market, and the impact of repowering on those uncertainties. Probabilities were assigned to market scenarios, and being subjective probabilities, they are certainly subject to debate. Although detailed sensitivity analyses were not performed, the net result of \$70M, is sufficiently large to require significant changes in the assumptions for the net present worth to become negative.

Second, only a very small STCR market was considered, since only the first increment of STCR plant(s) after repowering was included in the analysis. If a longer range view of the market was taken, the value results would be much greater than those shown. Third, the benefits from the repowering demonstration accrue not just to the APS ratepayers, but to the ratepayers of any utility that might, at some time in the future, build a STCR plant that uses the molten salt technology. Thus the costs of the Saguaro demonstration should be born by a larger constituency than the APS ratepayers.

The overriding conclusion is that the Saguaro solar repowering project should not be evaluated only in relationship to the fuel displaced during operation, but in the larger context of being a demonstration of a viable renewable utility generation alternative.

- 1-1 "Saguaro Power Plant Solar Repowering Project", Final Report, Executive Summary, DOE/SF 10739-1, Arizona Public Service Company, Phoenix, AZ, July 1980.
- 1-2 "Saguaro Power Plant Solar Repowering Project", Final Report, Vol. I, Conceptual Design, DOE/SF 10739-2, Arizona Public Service Company, Phoenix, AZ, July 1980.
- 1-3 "Saguaro Power Plant Solar Repowering Project," Final Report, Vol. II, System Requirements Specification, DOE/SF 10739-3, Arizona Public Service Company, Phoenix, AZ, July 1980.
- 1-4 "Saguaro Power Plant Solar Repowering Project," Final Report, Vol. III, Appendices, DOE/SF 10739-4, Arizona Public Service Company, Phoenix, AZ, July 1980.
- 2-1 Conceptual Design of Advanced Central Receiver Power System, Phase I. EG-77-C-03-1724, Martin Marietta Aerospace, Denver, CO, September 1978.
- 2-2 "Technical and Economic Assessment of Solar Hybrid Repowering," Final Report, SAN/1608-4-1, Public Service Company of New Mexico, Albuquerque, NM, September, 1978.
- 2-3 "Solar Central Receiver Hybrid Power System," Final Report, Vol II, DOE-ET-21038-1, Martin Marietta Aerospace, Denver, CO, September 1979.
- 2-4 "Solar Central Receiver Hybrid Power System," Final Report, Vol III, DOE-ET-21038-1, Martin Marietta Aerospace, Denver, CO, September 1979.
- 2-5 "Advanced Water/Steam Receiver Phase 1: Conceptual Design," Final Report, MCR-79-1370, Martin Marietta Aerospace, Denver, CO, January 1980.
- 2-6 "Alternate Central Receiver Power System, Phase II", Final Report, Vol. I, Executive Summary, MCR-81-1707, Martin Marietta Denver Aerospace, Denver, CO, May, 1981.
- 2-7 "Alternate Central Receiver Power System, Phase II", Final Report, Vol. II, Molten Salt Receiver, MCR-81-1707, Martin Marietta Denver Aerospace, Denver, CO, May, 1981.
- 2-8 "Alternate Central Receiver Power System, Phase II", Final Report, Vol, III, Molten Salt Materials Tests, MCR-81-1707, Martin Marietta Denver Aerospace, Denver, CO, May, 1981.

2-9 "Corrosion of 304SS by Molten NaNO_3 - KNO_3 in a Thermal Convection Loop", R.W. Bradshaw, SAND 80-8858, Sandia National Laboratories, Livermore, CA, December, 1980.

2-10 "Molten Salt Safety Study," Final Report, MCR-80-1305, Martin Marietta Corporation, Denver, CO, January 1980.

2-11 "Saguaro Steam Plant Station Job Summary for Arizona Public Service," Ebasco Services Inc., New York, NY, March 1955.

2-12 "Climatic Atlas of the United States," U.S. Department of Commerce, Washington, D.C., June 1968.

3-1 Spencer, R. C., K. C. Cotton, and C. N. Cannon, "A Method for Predicting the Performance of Steam Turbine Generators," Journal of Engineering for Power, ASME, October 1963, p 249 ff.

3-2 "An Assessment of Feasibility, Economics, and Market Potential for a Molten Salt System at 1000°F Reheat Steam," ATR-79(7773-01)-06, The Aerospace Corporation, El Segundo, CA, June 1979.

3-3 Wetz, N. H. and Sergent, B. D., "Soil and Foundation Investigation Report for Saguaro Station," Job No. E75-37, Sergent, Hauskins, and Beckwith letter dated April 29, 1975.

3-4 "Internally Insulated Thermal Storage System Development Program," Martin Marietta Aerospace, Sandia Contract No. 83-3638, December 1979.

3-5 Randall, C.M., Johnson, B.R. and Whitson, M.E. Jr, "Measurements of Typical Insolation Variation at Daggett, California", Vol. I, Methodology and Sample Data, and Vol. II, Appendices Including Data Sets, ART-80(7747)-1, The Aerospace Corporation, El Segundo, CA, March, 1980.

3-6 Miller, G. J. and Woodward, J. B., "STEAEC - Solar Thermal Electric Annual Energy Calculator Documentation," SAND77-8278, Sandia Laboratories, Livermore, CA, January 1978.

4-1 "Solar Thermal Repowering Systems Integration," Final Report, SERI/TR8037-1, Stearns Rodger Services, Inc., Denver, Colorado, August 1979.

4-2 APS Transmission (location and impact evaluation) Cholla to Saguaro. Phase I (November 1972), Phase II (May 1983), and "Exhibit V-2," a final environmental report. Prime consultants, Wirth Associates, Billings, MT, and Dames and Moore, Phoenix, AZ.

4-3 Draft, Environmental Statement, "Cholla Project," Including Transmission Line. USDA, Forest Service, August 1974.

- 4-4 Palo Verde Nuclear Generating Station Units 1, 2, 3, Environmental Report, Construction Phase. Sec 3.9 and 4.2.
- 4-5 Final Environmental Statement, PVNGS Units 1, 2, 3. U.S.N.R.C., September 1975.
- 4-6 PVNGS "Project 2, "Environmental Analysis, 500 kV Transmission System (Saguaro-Winchester). Westinghouse Electric Corporation Environmental Systems Department, February 1975.
- 4-7 Palo Verde Nuclear Generating Station Units 1, 2, 3 Environmental Report, Operating License State. Sec. 3.9.
- 4-8 Phase I Environmental Analysis, Vista-Saguaro 115 kV Transmission Line. Envista, Inc., September 1977.
- 4-9 Santa Rosa-Saguaro 230 kV Transmission Line Application for Certificate of Environmental Compatibility. April 1979, Sec. 6.
- 4-10 1978 Air Quality Data for Arizona. Arizona Department of Health Services, Air Quality Control Monitoring Section of the Division of Environmental Health Services.
- 4-11 WEST Associates (Insolation data): Solar Resource Evaluation Project (project managed by Southern California Edison), Solar Energy Measurements During 1976, 1977, and 1978.
- 4-12 Kevin P. Golden and Ronald L. Peterson: Final Report on Wind Climatological Study at Ocotillo & Saguaro Power Plants. September 1975.
- 4-13 Paper dealing with effects of artificial shading in a Sonoran Desert environment, based on work done by Stanley D. Smith and Duncan T. Patten (Oecologia, 1980).
- 4-14 Stanley D. Smith and Duncan T. Patten: Ecological Society of America and AIBS annual meeting, August 1979. Abstract published, Bulletin of the Ecological Society, Vol 60, p 81.
- 4-15 Annual reports and progress reports to Nuclear Medicine and Radiation Biology Laboratory. The DOE-funded lab at UCLA contracted work for Barstow Project, but data collected is more appropriate for Saguaro Project.
- 5-1 Manual of Steel Construction. American Institute of Steel Construction (AISC), Seventh Edition, New York, NY, 1973.
- 5-2 Solar Central Receiver Hybrid Power Systems Requirements Definition Document A 10621, Issue C. November 6, 1978.

5-3 Interim Report: Solar Central Receiver Hybrid Power System - Phase I. Martin Marietta Aerospace, Denver, CO, June 1979, pp 3-13.

5-4 Building Code Requirements for Minimum Design Loads in Buildings and Other Structures. ANSI A58.1-1972, American National Standards Institute (ANSI), New York, NY, 1972.

5-5 Uniform Building Code, 1976 Edition. International Conference of Building Officials (ICBO), Whittier, CA.

5-6 Solar Utility Powering/Industrial Retrofit Technical Information. Memo Number 5, V. V. Bartel, Sandia National Laboratories, Livermore, Livermore, CA, January 11, 1980.

5-7 Telcon from J. Grant, Sandia Laboratories to C. Bolton, Martin Marietta Corporation, July 24, 1979.

5-8 Building Code Requirements for Reinforced Concrete. ACI 318-71, American Concrete Institute, Detroit, Sections 9.3.1-9.3.7.

